



UNIVERSITY OF  
LIVERPOOL

**NOVEL IRON-PYBISULIDINE CATALYSTS FOR THE  
SELECTIVE AEROBIC OXIDATION AND C-O/C-C  
CLEAVAGE OF ORGANIC SUBSTRATES**

Thesis submitted in accordance with the requirements of  
the University of Liverpool for the degree of Doctor in  
Philosophy

by

**Angela Gonzalez de Castro**

January 2014

*“Do not go where the path may lead;  
Go instead where there is no path and leave a trail”*

*(Anonymous)*

*“Logic will take you from A to B;  
Imagination will take you everywhere”*

*(Albert Einstein)*

## ACKNOWLEDGEMENTS

I would like to take this opportunity to express my gratitude to all the people that have contributed to make this Thesis possible. Firstly, I would like to show my gratitude to my supervisor Prof Jianliang Xiao for giving me the opportunity to join his research group as a Ph D student. I would like to thank Jianliang for all his help and supervision during my 4 years in his group. His encouragement and passion for chemistry have been an angular support and source of motivation throughout my Ph D. I also want to thank all the freedom I have received from him for the exploration of a completely new area of research in his group and his encouragement to follow my own thinking and instinct in investigating and interpreting interesting results.

I will like to thank Dr Craig Robertson for his help and valuable lessons in X-ray diffraction experiment and analyses. He has shown great enthusiasm in the project and provided high-quality X ray diffraction analyses at lightning speed. My thanks also go to Dr. John Bacsa who provided X-ray analyses for compounds shown in Chapter 2 and taught me a lot about X ray techniques. Thanks also go to Dr Konstantin Luzyanin and Dr Jon Iggo for his suggestions and discussions in NMR experiments and for his help with the NMR facilities of the department. I will like to show gratitude to the Analytical staff of the Chemistry department and the members of the MS service of the University of Swansea for all the analytical data they have provided and their help.

Many thanks go to the past and present members of the Xiao group, who have helped me during my time in Liverpool. I am particularly grateful to Dinesh, whose advice and suggestions have contributed to improve the chemistry presented in this thesis and who gave me a hand in synthesising some of the isochromans shown in Chapter 5. I also want to thank him for his help in many aspects of my life, for his unconditional friendship and for our four hours long debates in Bold St. cafes. I would like to thank Weijun for his support and friendship and all the questions he has helped me answering. I really miss our debates about

Chemistry, food and life. My thanks go to Jianjun and Steven for their support, enthusiasm and participation in our daily discussions. I would like to thank the ladies of the Xiao group: Zhijun, Jen and Barbara who have contributed to make my time in this group more enjoyable. I additionally want to thank Noemi, Antonio, Ed, John Li, Xiaofeng, Yi, Felix, Ory, Sergio, Maria, Carlos and Susanna for their help and friendship through all these years.

Many thanks go to my “scouse” family: Marta, Ben, Gita, Naser, Natalia, Alejandro, Angela, Paula, Rocio and Barbara-Gisela. You have truly made me feel at home and you are the best friends anyone could ask for. A special mention goes to the “gastro-club” meetings in the Kazimier Garden on Thursdays which have made my time in Liverpool truly enjoyable. I also want to thank my friends from Spain, especially Nuria, Rafa, Marta C., Agueda, Maria T. and Martita among others for their support and love no matter the distance between us.

Finally, I will like to thank everyone who has helped me to get where I am now. My thanks go to Prof. Jose M. Gonzalez from the University of Oviedo for his valuable lessons in Organic Chemistry and for sparking my interest in research and Organic Chemistry. I will also want to thank Dr. Maria Jesus Gonzalez Castanon and Prof. Alfredo Sanz Medel for their lessons in Analytical Chemistry. I want to express my gratitude to Dr. Juan Felix Espinosa and Dr. Paloma Vidal from Lilly Laboratories in Alcobendas for all their help and lessons in advance NMR spectroscopy and in chemical research in general. Finally, I would like to give my deepest thanks to my ever-loving parents and sister for their huge emotional and economical support. You have always had a strong faith in my capabilities and have helped me in very difficult moments. You have shown me unconditional support in everything I do and provided great advice and guidance. Such support has been my biggest source of inspiration for making possible the chemistry that is presented in this Thesis and therefore, it is to you I dedicate this Thesis.

## ABSTRACT

The selective oxidation of organic compounds is one of the most attractive transformations for both, industry and academia. Industrial interest stems from the potential application of such oxidation methodologies in the economic, greener synthesis of valuable products, whereas academic research is challenged by the difficulties in achieving specific, direct functionalisation of the “inert” CH bonds in complex molecules. In this Ph. D. thesis, our contribution to the selective oxidation of organic substrates using a novel class of iron catalysts is presented.

A general introduction covering the major challenges in the area of iron-catalysed selective oxidation of organic compounds is described in Chapter 1. Chapter 2 covers the design, synthesis and coordination properties of the novel PyBisulidine type ligands, which we have conceived for their potential use in selective oxidation, attempting to overcome some of the limitations of current methods.

The efficiency of such PyBisulidine ligands is demonstrated in Chapter 3, where iron-PyBisulidine complexes are used for catalysing the aerobic  $\alpha$ -oxidation of functionalised ethers. High catalytic efficiency, very good mass balance and excellent functional group tolerance were achieved with these catalysts under mild conditions. Such advantages stem from an unconventional reaction mechanism, involving the dehydrogenative oxygenation of the ether substrate to give a peroxobisether, followed by the cleavage of the peroxy bond to form two ester molecules. Unlike metalloenzymes and biomimetic iron complexes,  $H_2$  is released as the sole byproduct during the catalytic cycle. The oxidation mechanism is discussed in Chapter 4.

Like natural dioxygenases, iron-PyBisulidine catalysts were found capable of promoting the aerobic cleavage of aliphatic C-C and C-O bonds. Even though biomimetic complexes are often seen as simplified models to study enzymatic processes, a more synthetic perspective

of the selective aerobic cleavage of ethereal C-C and C-O bonds is described in Chapter 5. The great potential of such cleavages in organic synthesis is well exemplified in the iron-PyBisulidine catalysed direct conversion of natural isochromans into biologically active isochromanones with excellent selectivity.

The ability of the iron-PyBisulidine complexes in catalysing aerobic C-C cleavages is further expanded in Chapter 6, where the oxidative cleavage of olefinic C=C bonds to carbonyl compounds is demonstrated. The catalytic reactions proceeded efficiently, showing a broad scope and a mechanism that involves the formation of dioxetane intermediates is postulated. Chapter 7 is an extension of Chapter 6, in which iron-PyBisulidine complexes were found to catalyse  $\alpha$ -methylstyrene linear dimerisation under an inert atmosphere. Moreover, control in the regioselectivity of the double bond in the dimers can be achieved by modifications in the PyBisulidine ligands.

Final conclusions and a perspective of the research covered in this Ph.D. thesis are provided in Chapter 8.

## ABBREVIATIONS

$\alpha$	alpha
$\delta$	chemical shift
Å	amstrong
AcOEt	ethyl acetate
AcOH	acetic acid
Ar	aryl
atm	atmosphere
°C	Celsius degree
<sup>13</sup> C	carbon 13
CI	chemical ionisation
<i>circa</i>	approximately
DCM	dichloromethane
DCE	1,2-dichloroethane
FAB	fast atom bombardment
EI	ionisation potential
equiv.	equivalent
ESI	electrospray ionisation

Et <sub>2</sub> O	diethyl ether
g	gram(s)
GC	gas chromatography
h	hour
<sup>1</sup> H	proton
H <sub>2</sub>	molecular hydrogen
HRMS	high resolution mass spectroscopy
HOMO	highest occupied molecular orbital
Hz	hertz
i.e.	<i>id est</i> (that is to say)
IR	infrared spectrometry
<i>J</i>	coupling constant value
LUMO	lowest occupied molecular orbital
MeCN	acetonitrile
MEMCl	2-methoxyethoxymethyl chloride
mg	milligram(s)
min	minute(s)
mL	millilitre
mmol	milimole(s)



MS	mass spectrometry
NEt <sub>3</sub>	triethylamine
NMR	nuclear magnetic resonance
O <sub>2</sub>	molecular oxygen
Ph-H	benzene
Ph-Me	toluene
ppm	parts per million
rsm	recovered starting material
r.t.	room temperature
S/C	substrate to catalyst ratio
THF	tetrahydrofuran
THP	tetrahydropyran
TMS	tetramethylsilane
TON	turnover number
t <sub>R</sub>	retention time
<i>vide infra</i>	see below
<i>vide supra</i>	see above
vs	versus

## CONTENTS

<b>ACKNOWLEDGEMENTS.....</b>	<b>I</b>
<b>ABSTRACT.....</b>	<b>III</b>
<b>ABBREVIATIONS.....</b>	<b>V</b>
<b>CONTENTS.....</b>	<b>VIII</b>
<b>CHAPTER 1: INTRODUCTION.....</b>	<b>1</b>
1.1. Iron: metal of the past, metal for the future.....	2
1.2. Iron catalysed selective oxidation of organic compounds.....	5
1.3. Major challenges in iron-catalysed selective oxidations.....	8
1.3.1. Alternatives to tetradentate ligands.....	8
1.3.2. Use of molecular oxygen as oxidant.....	11
1.3.3. Electron-rich substrates: aerobic oxidation of ethers.....	24
1.3.4. Aerobic C-C cleavage of organic substrates.....	32
1.4. Aims of the thesis.....	44
1.5. References.....	46
<b>CHAPTER 2: DESIGN, SYNTHESIS AND PROPERTIES OF NOVEL PYBISULIDINE TYPE LIGANDS.....</b>	<b>53</b>
2.1. Introduction.....	54
2.1.1. Ligand design in homogeneous iron catalysis.....	54
2.1.2. PyBox ligands: successes and challenges.....	56
2.2. Aims of the chapter.....	58
2.3. Results and discussion.....	58
2.3.1. Pentacoordinated designs.....	58
2.3.2. Tridentate ligands.....	62
2.3.2.1. Design and synthesis of PyBisulidines.....	62
2.3.2.2. Coordination properties of PyBisulidines.....	64
2.3.2.3. Ligand library.....	68
2.3.2.3.1. Sulfonamide substitution.....	68
2.3.2.3.2. Amino substitution.....	70
2.3.2.3.3. Pyridine substitution.....	74
2.3.2.3.4. Bidentate designs.....	76
2.3.2.3.5. Asymmetric versions.....	78
2.4. Conclusions.....	79
2.5. Experimental section.....	80
2.6. References.....	97
<b>CHAPTER 3: DISCOVERY, OPTIMISATION AND SCOPE OF THE Fe(OTf)<sub>2</sub>-PYBISULIDINE CATALYSED AEROBIC <math>\alpha</math>-OXIDATION OF ETHERS.....</b>	<b>100</b>
3.1. Introduction.....	101
3.1.1. Organic esters.....	101
3.1.2. Methods for ester syntheses.....	104

3.2. Aims of the chapter.....	111
3.3. Results and discussion.....	112
3.3.1. Discovery of the Fe(OTf) <sub>2</sub> L1 catalysed aerobic oxidation of THF.....	112
3.3.2. Optimisation of the iron-catalysed aerobic oxidation of THF.....	113
3.3.2.1. Effect of oxidant and water.....	113
3.3.2.2. Temperature effect.....	114
3.3.2.3. Control experiments.....	115
3.3.2.4. Optimisation of the S/C ratio.....	116
3.3.2.5. Ligand effect.....	118
3.3.2.6. Solvent effect.....	120
3.3.3. Substrate scope.....	121
3.3.3.1. Lactone oxidation.....	121
3.3.3.2. Oxidation of isochromans.....	122
3.3.3.3. Oxidation of phthalans.....	126
3.3.3.4. Oxidation of benzyl ethers.....	128
3.3.4. Product inhibition and catalyst reuse.....	130
3.4. Conclusions.....	131
3.5. Experimental section.....	132
3.6. References.....	155

**CHAPTER 4: MECHANISTIC INVESTIGATIONS OF THE Fe(OTf)<sub>2</sub>-  
PYBISULIDINE CATALYSED AEROBIC  $\alpha$ -OXIDATION OF ETHERS..... 161**

4.1. Introduction.....	162
4.2. Aims of the chapter.....	163
4.3. Results and discussion.....	163
4.3.1. Radical trapping experiments.....	163
4.3.2. Oxidation of 3-methyl-3,4-dihydro-1 <i>H</i> -isochromene-5,8-dione.....	166
4.3.3. Effect of a radical initiator.....	166
4.3.4. Oxidation of a radical clock.....	168
4.3.5. Identification of a peroxide intermediate.....	170
4.3.6. Conversion of 1,1'-peroxyisochroman to chromanone.....	173
4.3.7. Ligand effect in the conversion of peroxidiisochroman to chromanone.....	176
4.3.8. Selective formation of the peroxide intermediate.....	177
4.3.9. Formation of hydroperoxides under high dilution conditions.....	178
4.3.10. Rate limiting step.....	180
4.3.11. Evidence of H <sub>2</sub> gas release during the oxidation reaction.....	181
4.3.12. Absence of water formation.....	182
4.3.13. Isotope labelling experiments.....	184
4.3.14. H/D exchange experiments.....	185
4.3.15. Postulated mechanism.....	186
4.3.16. Catalytic cycle.....	194
4.4. Conclusions.....	195
4.5. Experimental section.....	196
4.6. References.....	224

<b>CHAPTER 5: Fe(OTf)<sub>2</sub>-PYBISULIDINE CATALYSED AEROBIC CLEAVAGE OF ALIPHATIC C-O AND C-C BONDS.....</b>	<b>227</b>
5.1. Introduction.....	228
5.1.1. Selective cleavage of aliphatic C-C bonds.....	228
5.1.2. Iron-catalysed selective cleavage of aliphatic C-C bonds.....	229
5.1.3. Iron-catalysed selective cleavage of aliphatic C-O bonds.....	231
5.2. Aims of the chapter.....	233
5.3. Results and discussion.....	234
5.3.1. Selective cleavage of Csp <sup>3</sup> -O bonds.....	234
5.3.1.1. Discovery and scope of the Fe(OTf) <sub>2</sub> L1 catalysed aerobic cleavage of Csp <sup>3</sup> -O bonds.....	234
5.3.1.2. Mechanistic investigations of the Fe(OTf) <sub>2</sub> L1 catalysed aerobic cleavage of Csp <sup>3</sup> -O bonds.....	238
5.3.2. Selective cleavage of Csp <sup>3</sup> -Csp <sup>3</sup> bonds.....	239
5.3.2.1. Conversion of isochromans into isochromanones <i>via</i> selective aerobic cleavage of exocyclic Csp <sup>3</sup> -Csp <sup>3</sup> bonds.....	239
5.3.2.2. Mechanistic investigations of the selective exocyclic Csp <sup>3</sup> -Csp <sup>3</sup> cleavage.....	242
5.3.3. Combined Fe(OTf) <sub>2</sub> L1 catalysed selective Csp <sup>2</sup> -Csp <sup>3</sup> and Csp <sup>3</sup> -O cleavage	251
5.3.4. Combined Fe(OTf) <sub>2</sub> L1 catalysed selective Csp <sup>3</sup> -Csp <sup>2</sup> and Csp <sup>2</sup> -X (X = O, N) cleavage via decarboxylation.....	252
5.4. Conclusions.....	254
5.5. Experimental section.....	255
5.6. References.....	272
<b>CHAPTER 6: Fe(OTf)<sub>3</sub>-PYBISULIDINE CATALYSED AEROBIC C-C CLEAVAGE OF OLEFINS TO CARBONYL COMPOUNDS.....</b>	<b>275</b>
6.1. Introduction.....	276
6.1.1. Oxidative cleavage of olefins.....	276
6.1.1.1. Ozonolysis.....	276
6.1.1.2. Alternatives to ozonolysis.....	279
6.1.1.3. Additional strategies for transforming olefins into carbonyls.....	284
6.2. Aims of the chapter.....	286
6.3. Results and discussion.....	287
6.3.1. Optimisation of the Fe-catalysed aerobic cleavage of olefins.....	287
6.3.1.1. Model reaction for optimization studies.....	287
6.3.1.2. Effect of temperature and concentration.....	288
6.3.1.3. Solvent effect.....	289
6.3.1.4. Ligand effect.....	290
6.3.2. Substrate scope.....	292
6.3.2.1. Aerobic cleavage of monosubstituted styrenes.....	292
6.3.2.2. Aerobic cleavage of 1,1,-substituted styrenes.....	294
6.3.3. Mechanistic investigations.....	296
6.3.3.1. Radical trapping experiments.....	296
6.3.3.2. Coordination of the olefin to the catalyst.....	301
6.3.3.3. Competitive direct dehydrogenation of dienes.....	303
6.3.3.4. Dioxetane intermediate formation.....	306

6.3.3.5. Postulated catalytic cycle.....	308
6.4. Conclusions.....	309
6.5. Experimental section.....	309
6.6. References.....	321
<b>CHAPTER 7: Fe(OTf)<sub>3</sub>-PYBISULIDINE CATALYSED REGIOSELECTIVE OLEFIN DIMERISATION.....</b>	<b>327</b>
7.1. Introduction.....	328
7.1.1. Dimerisation of styrenes: importance and challenges.....	328
7.1.2. Catalytic methods for the dimerisation of $\alpha$ -methylstyrenes.....	328
7.2. Aims of the chapter.....	333
7.3. Results and discussion.....	333
7.3.1. Discovery and optimisation of the iron-catalysed olefin dimerisation.....	333
7.3.1.1. Solvent effect.....	333
7.3.1.2. Effect of the iron salt.....	335
7.3.1.3. Ligand effect.....	336
7.3.2. Substrate scope.....	339
7.3.2.1. Electron rich substrates.....	339
7.3.2.2. Electron deficient substrates.....	344
7.3.3. Mechanistic considerations.....	346
7.4. Conclusions.....	348
7.5. Experimental section.....	349
7.6. References.....	355
<b>CHAPTER 8: CONCLUSIONS AND PERSPECTIVES.....</b>	<b>357</b>
8.1. General perspective of the thesis.....	358
8.2. Future work.....	362

## APPENDIX

# *Chapter 1*

## **INTRODUCTION**

## **1.1. Iron: metal of the past, metal for the future**

### **1.1.1. Sustainable chemistry**

Global concern about sustainability is currently leading to a progressive change in economics, politics and science. In that regard, the role of chemists has been strongly criticised, quoting Terry Collins “*chemists have been focused on developing reactions that generate only the desired product by using simple process designs and involving almost every element of the periodic table instead of using a few more innocuous elements in more sophisticated designs*”.<sup>1</sup> However, chemists nowadays are well aware of the enormous potential and necessity of sustainable chemistry. Indeed, the development of more environmentally friendly transformations has become a new great challenge with a growing number of publications covering many chemical transformations under greener conditions. In addition, the attitude of companies and organizations towards sustainable processes is also evolving and nowadays the biggest question that arises is how to accomplish their implementation rather than questioning the necessity.<sup>2</sup> The design of new low-waste processes, such as click chemistry transformations<sup>3</sup> and the incorporation of catalysts to reduce the energy consumption have emerged as chief technologies for achieving more sustainable chemical processes.

### **1.1.2. Sustainable metal catalysis**

Because of their efficiency and lower environmental impact, catalytic transformations are of utmost importance in academia and industry. In fact, the industrial synthesis of about 80% of all chemicals and pharmaceutical products involves the utilization of catalysts and the figure rises up to a 90% in the case of more modern processes.<sup>4</sup> Catalysis can be generally divided in two main areas:

1. Heterogeneous catalysis in which the catalyst and substrates are in different phases
2. Homogenous catalysis in which catalyst and substrate are in the same phase

Even though heterogeneous catalysis is more applied in industrial transformations, homogenous catalysis offers certain advantages, such as higher regio-, chemo- and stereoselective control, and because the catalyst and the substrates are present in the same phase it is relatively easy to perform mechanistic investigations that allow a better understanding of the reaction and the possibility of improving the catalyst. Nevertheless, one of the biggest issues of homogeneous catalysis is that the vast majority of homogenous catalysts are based on platinum metals of limited abundance, high cost and significant toxicity (Figure 1). Therefore, transition metal catalysis is still far from satisfying sustainability.<sup>5</sup>



**Period average (\$US/troy oz)**

Pt: \$987.17

Rh: \$2673.61

Ir: \$349.21

Ru: \$171.72

Iron: 150.67 \$US/mt (0.00468\$/troy oz)

**Figure 1.** Comparison of market prices of transition metals and iron during the last decade.

(Values based on [www.platinum.mattey.com](http://www.platinum.mattey.com) data for platinum metals and [www.metalprices.com](http://www.metalprices.com) data for iron scrap).



In order to make catalytic processes more sustainable, three major strategies have merged and rapidly expanded during the last years:

1. Organocatalysis,<sup>6</sup> which is based on the utility of small organic molecules for accelerating chemical reactions and thus, it eliminates the use of toxic transition metals.
2. Bio-catalysis,<sup>7</sup> which aims to apply isolated enzymes or cells as catalysts in order to achieve the high efficiency and stereoselectivity of biological processes in laboratory and commercial scale transformations.
3. Sustainable metal catalysis which is focused on the use of highly active catalysts based on non expensive, abundant and metabolizable transition metals such as iron, copper, zinc and manganese.<sup>4</sup>

### 1.1.3. Iron in catalysis

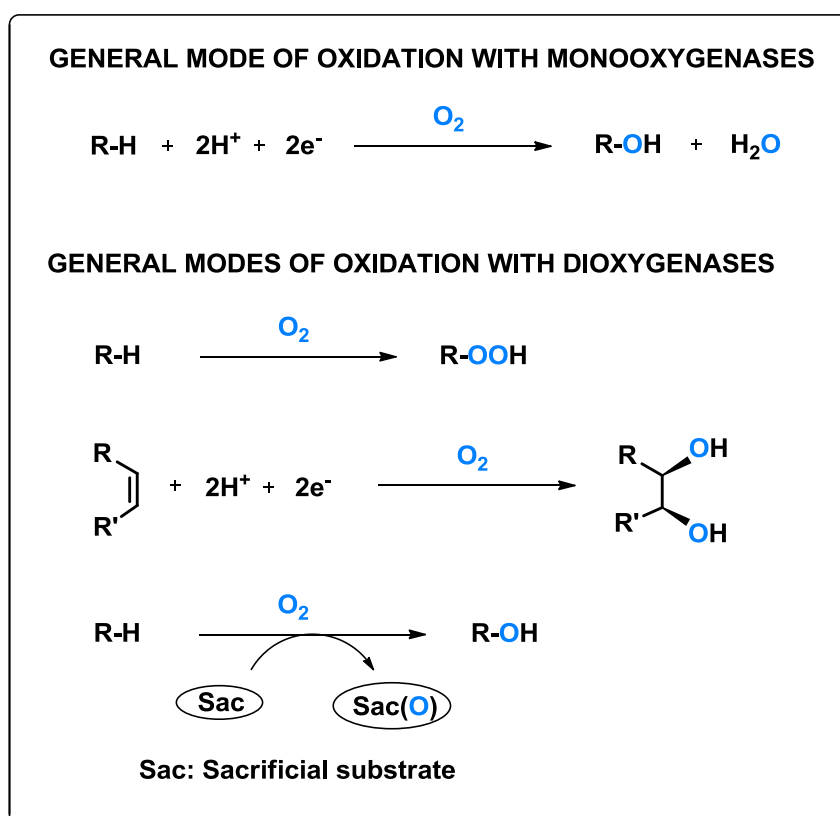
Among cheap metals, iron is particularly advantageous as it is very accessible due to its great abundance on the earth crust and thus, it is relatively cheap compared with precious metals (Figure 1). In addition, a large variety of iron salts are commercially available or can be easily synthesised and as iron is an essential element, its salts are relatively non-toxic for humans.<sup>4</sup> Furthermore, many oxidation states are accessible; so iron complexes exhibit a very ample organometallic chemistry allowing excellent versatility in catalysis.<sup>7</sup>

Despite all these advantages the impact of iron in the field of catalysis has been surprisingly modest compared with that of the other Group VIII metals, the Reppe synthesis and subsequent related processes being the most significant contributions in the area.<sup>8</sup> Only relatively recently the potential of iron has started to be explored and very efficient transformations that can compete with other platinum metal-catalysed ones have been reported<sup>9</sup>. In particular, many iron-based methodologies are being developed in the field of oxidation, reduction and coupling chemistry. Thus it can be foreseen that iron has an important role to play in future catalysis.

## 1.2. Iron catalysed selective oxidation of organic compounds

### 1.2.1. Natural metalloenzymes

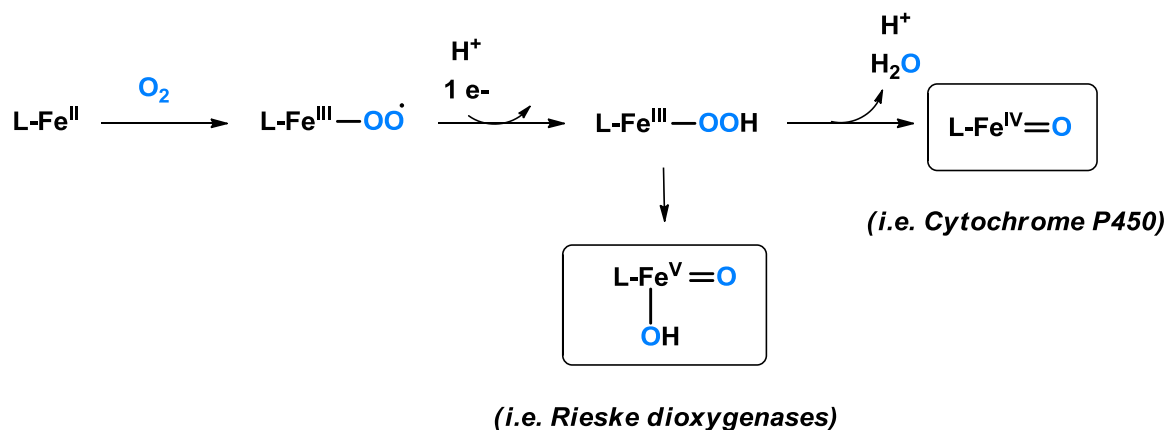
Nature has mastered the art of oxidation using metalloenzymes, which are capable of selectively oxidizing various substrates with O<sub>2</sub> under mild conditions showing excellent specificity and chemoselectivity.<sup>10</sup> Interestingly, most of these enzymes are metalloenzymes containing an iron-based active site. Depending on the nature of the prosthetic group, oxygenases are often classified as heme (or haem) if the metal centre is contained in a porphyrin ring, or non-heme when there is no porphyrin core.<sup>11</sup>



**Scheme 1.** Common natural modes of selective oxidation of organic substrates

Depending on the oxygenases used, different modes of O<sub>2</sub> activation are possible, leading to the insertion of one (monooxygenase activity) or both (dioxygenase activity) oxygen atoms of O<sub>2</sub> into a C-H bond<sup>10,12</sup> (Scheme 1). Although the reaction mechanism for different enzymes may differ in some aspects, mononuclear iron-metalloenzymes react with O<sub>2</sub> to generate a

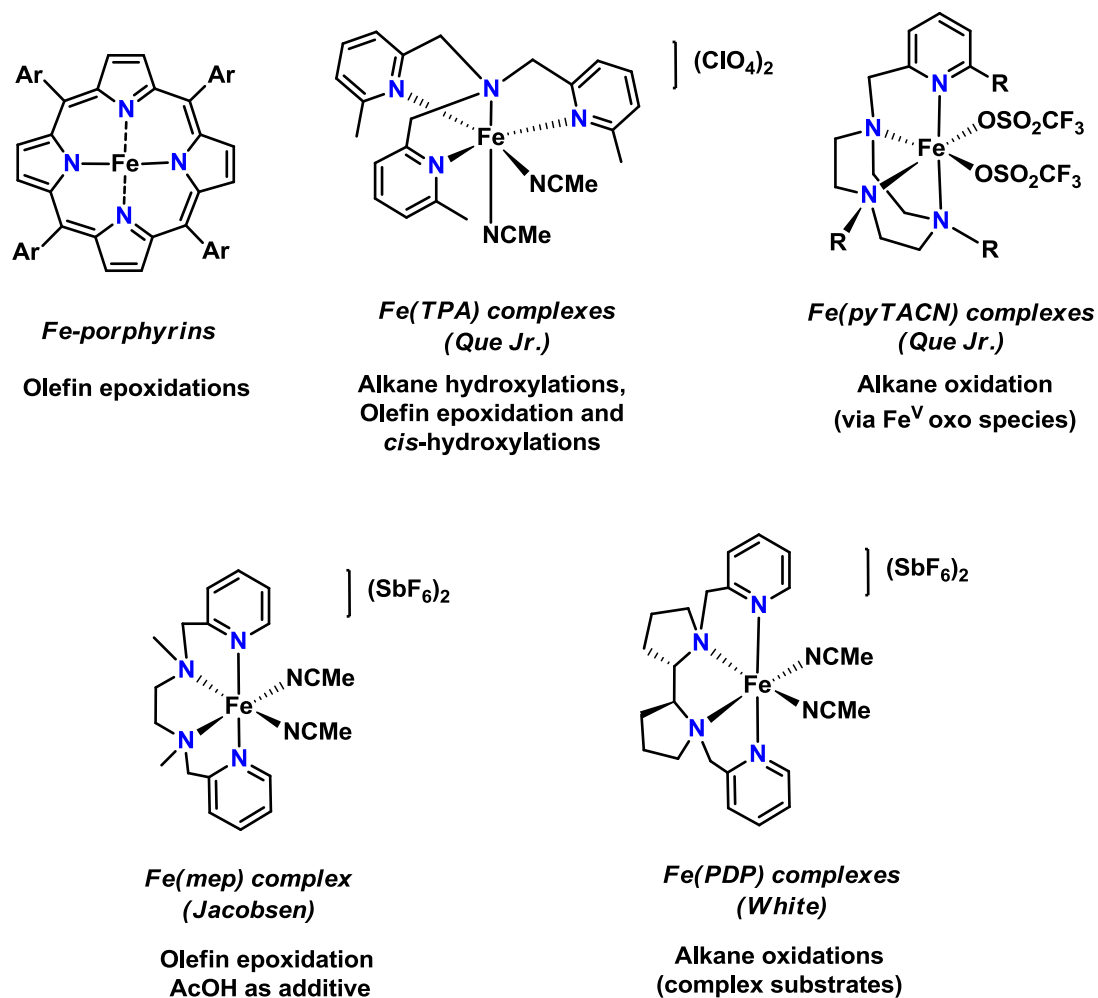
high valent  $\text{Fe}^{\text{IV}}=\text{O}$  or  $\text{Fe}^{\text{V}}\text{O}(\text{OH})$  species, which act as the oxidising agent of the reaction<sup>12</sup> (Scheme 2).



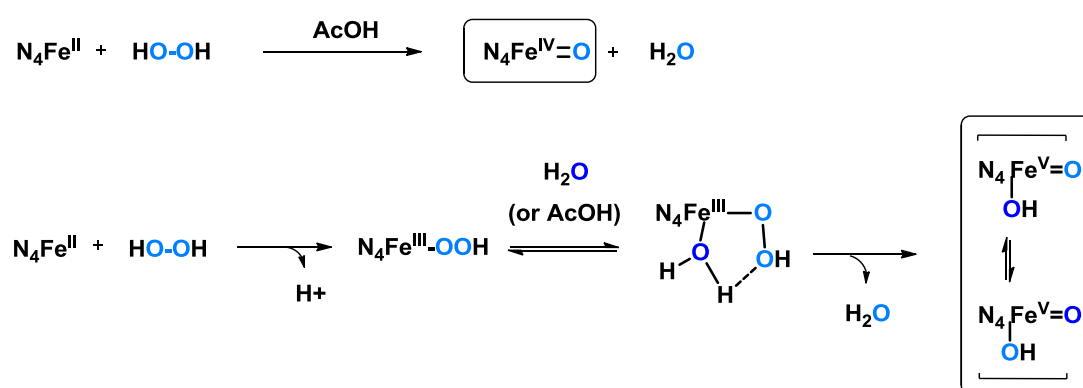
**Scheme 2.** Mononuclear iron-oxygenase mechanisms

### 1.2.2. Biomimetic iron catalysts

Inspired by nature, a great variety of iron-based biomimetic catalysts have been designed to replicate and expand naturally occurring oxidations. The groups of Que Jr.<sup>13</sup>, Jacobsen<sup>14</sup> and White<sup>15</sup> among others<sup>16</sup> have demonstrated that tetradentate *N*-donor ligands in combination with commercial iron salts are efficient catalysts for the selective oxidation of many organic substrates (Scheme 3). However, these biomimetic catalysts generally require the use of more active and expensive  $\text{H}_2\text{O}_2$  as oxidant and additives (AcOH) to generate the high valent iron-oxo species<sup>12</sup> (Scheme 4).



**Scheme 3.** Examples of biomimetic iron complexes bearing tetradentate *N*-donor ligands



**Scheme 4.** Formation of iron-oxo species from bioinspired iron catalysts

### 1.3. Major challenges in iron-catalysed selective oxidations

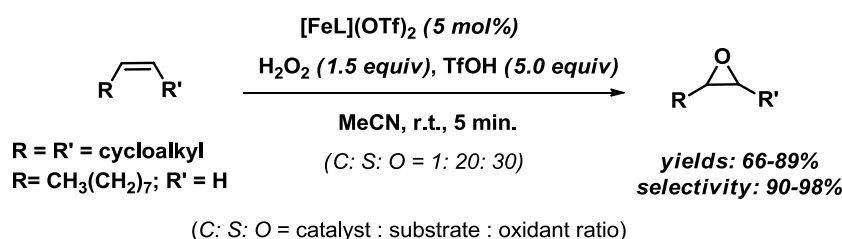
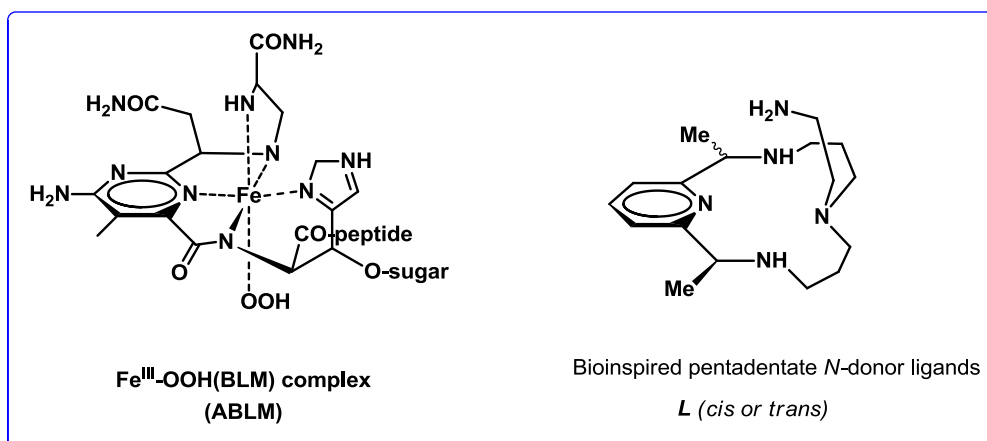
Even though the iron catalysed selective oxidation of organic substrates has expanded broadly with significant advances being reported in the field during the last decade, many issues remain unsolved. A summary of the most important challenges in the area is discussed herein, mainly covering: type of ligands, O<sub>2</sub> activation, oxidation of electron rich substrates and selective aerobic C-C cleavage.

#### 1.3.1. Alternatives to tetradentate ligands

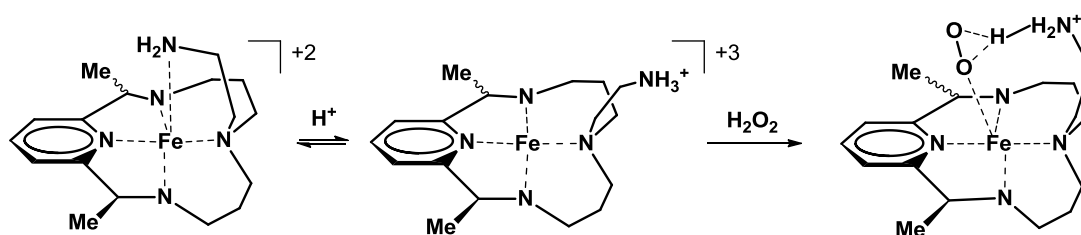
The application of tetradentate *N*-donor ligands for biomimetic oxidations has been extensively studied either as porphyrin type skeletons or as non-heme designs.<sup>17</sup> Such interest stems from the belief of catalyst decomposition and unselective Fenton-type side reactivity under oxidation conditions would be prevented by chelating the iron centre with a rigid, tetradentate ligand.<sup>18</sup> However, iron complexes bearing pentadentate or tridentate *N*-donor ligands are much less explored alternatives that might help overcoming some of the limitations associated to tetradentate complexes.

##### 1.3.1.1. Bioinspired pentadentate *N*-donor ligands

Inspired by the ability of natural iron<sup>II</sup>-bleomicyne (Fe-BLM) to react with O<sub>2</sub> and undergo oxidation reactions similar to heme proteins,<sup>19</sup> the group of Rybak-Akimova developed a library of pentadentate *N*-donor ligands which can complex with Fe<sup>II</sup> salts in a tetragonal-pyramidal geometry analogue to natural Fe-BLM. This family of iron complexes were found active for the epoxidation of aliphatic olefins with good yields and selectivity using H<sub>2</sub>O<sub>2</sub> as oxidant.<sup>20</sup> The protonation of the pendant amino-arm with non-coordinating triflic acid was considered crucial for achieving peroxide activation (Scheme 5). To the best of our knowledge, this is the only example in the literature of *N*-donor pentadentate-iron catalysts for oxidation reactions.



**Proposed peroxide activation:**

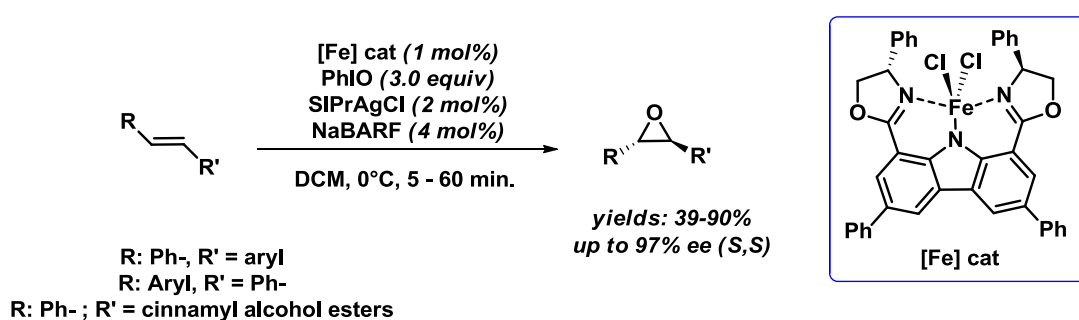


**Scheme 5.** Bioinspired  $N$ -donor pentadentate-iron catalysts for olefin epoxidation

### 1.3.1.2. Tridentate $N$ -donor ligands

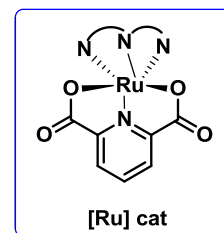
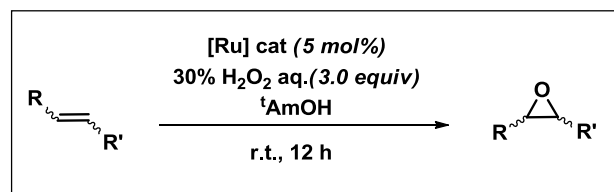
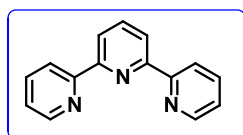
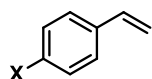
Tridentate  $N$ -donor ligands have been slightly more investigated for oxidations than pentadentate skeletons. However, their application has been surprisingly limited to asymmetric olefin epoxidation reactions. Very recently, Niwa and Nakada reported a family of  $\text{Fe}^{\text{III}}$  complexes bearing a tridentate 1,8-(bisoxazolyl)carbazole ligand and their application for the catalytic asymmetric epoxidation of ( $E$ )-alkenes using  $\text{PhIO}$  as oxidant<sup>21</sup> (Scheme 6). Such ligand design possesses the same structural aspects as porphyrines, i.e. a conjugated planar structure with donor  $N$  atoms, but it can be easily synthesised and stereoinductive moieties can be more facily introduced and modified than in chiral porphyrins.<sup>22</sup> Excellent enantioselectivity was achieved for the epoxidation of stilbenes and

cinnamyl alcohol derived alkenes with such iron complexes under mild conditions. However, more than stoichiometric amounts of the strong oxidant PhIO as well as additives were needed. Indeed, the use of sodium tetrakis[3,5-bis(trifluoromethyl)phenyl] borate (NaBARF) for abstracting the halogens from the iron pre-catalyst was essential for the oxidation to proceed and the addition of a SIPrAgCl (SIPr = N, N'-bis(2,6-diisopropylphenyl)-4,5-dihydro imidazol-2-ylidene) allowed to improve both the reaction yields and enantioselectivity.

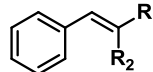


**Scheme 6.** Asymmetric olefin epoxidation catalysed by tridentate iron<sup>III</sup>-carbazole complexes

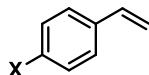
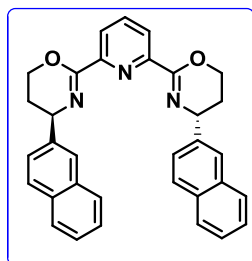
In addition, extensive research from the group of Beller demonstrated that ruthenium complexes with privileged tridentate ligands such as terpyridines (terpy), pyridinebisoxazolines (pybox), pyridinebisoxazines (pyboxazines), pyridine bisimidazolines (pybims) can be applied to enantioselective olefin epoxidations in the presence of pyridine-2,6-dicarboxylate using H<sub>2</sub>O<sub>2</sub> as oxidant<sup>23</sup> (Scheme 7). However, epoxidations attempted with analogue iron complexes showed poor results.

***N,N,N* ligands:****Substrate scope:**

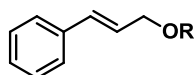
X	Yield
H	39%
Me	74%
F	39%
Cl	28%



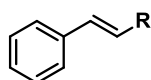
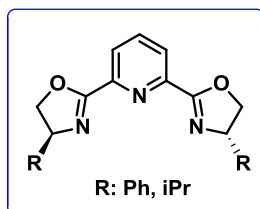
R <sub>1</sub>	R <sub>2</sub>	Yield
Me	H	95%
CH <sub>2</sub> OPh	H	92%
Me	H	67%
Me	Me	83%



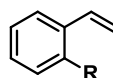
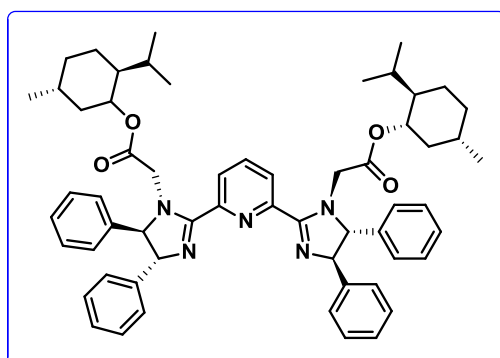
X	Yield	ee %
H	85%	59
Me	80%	58
F	82%	60
Cl	76%	54



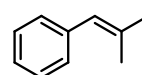
R	Yield	ee %
Ac	83	48
TBS	79	41
Me	72	49
Ph	77	6



R	Yield	ee %
Ph	100	67
Me	82	58



R	Yield	ee %
H	76%	42
Me	88%	43



Yield	ee %
82%	68

**Scheme 7.** Asymmetric olefin epoxidation catalysed by tridentate Ru complexes.

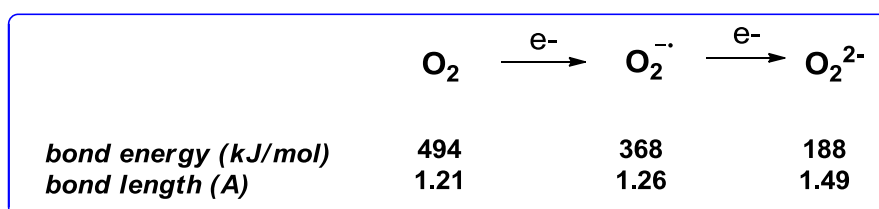
### 1.3.2. Use of molecular oxygen as oxidant

Even though dioxygen is the most desired oxidant in oxidation chemistry<sup>24</sup> and natural enzymes can readily activate it under very mild conditions, its catalytic activation by



synthetic iron complexes or salts has proven a significant challenge, because of two major reasons:

1. The reaction of an organic substrate with O<sub>2</sub> is thermodynamically favoured as it is linked to high energy release. However, the spin mismatch between ground-state O<sub>2</sub> (triplet) and most organic substrates (singlet) makes the reaction kinetically unfavoured.<sup>10</sup> As a consequence, reactions with O<sub>2</sub> tend to proceed slowly.
2. The O=O bond is relatively strong with a bond dissociation energy (BDE) of 494 kJ/mol. Having two unpaired electrons on its ground state, O<sub>2</sub> can be classified as a diradical. Most of its reactions proceed via one-electron steps, with the addition of electrons weakening the O-O bond and resulting in more reactive superoxo and peroxy species<sup>25</sup> (Scheme 8). As biomimetic iron catalysts usually rely on the formation of an iron-oxo species, the use of H<sub>2</sub>O<sub>2</sub> is widespread, given that the cleavage of the O-O bond is easier than in molecular oxygen.



**Scheme 8.** BDE and length differences between dioxygen, superoxo and peroxy species.

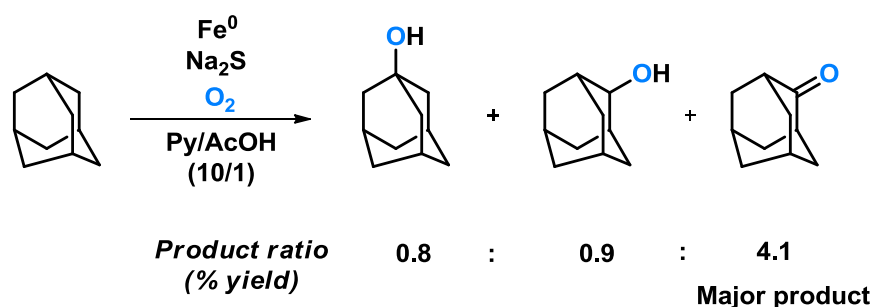
Although most of the synthetic iron complexes rely on the use of hydrogen peroxide as an oxidant, a few selected iron catalysts have been proven capable of activating O<sub>2</sub>. However, poor selectivities and a strong need of additives are major drawbacks associated to these catalysts.

### 1.3.2.1. Oxidations in the presence of a reductant

#### 1.3.2.1.1. Gif Chemistry

In 1983, Barton reported a protocol for the mild oxidation of C-H bonds in alkanes using metallic iron under aerobic atmosphere. The use of a source of sulfide anions (H<sub>2</sub>S or Na<sub>2</sub>S) in combination with pyridine and acetic acid as a solvent mixture was found crucial to

accomplish the oxidation of adamantane<sup>26</sup> (Scheme 9). Since this pioneering report, many variations of the initial reactive mixture have been reported with a significant contribution from the group of Barton himself. As most of their work was developed in Gif-sur-Yvette, the name “Gif chemistry” has been coined for such oxidations. The major resemblances and limitations<sup>27</sup> of Gif systems are summarised in Table 1.



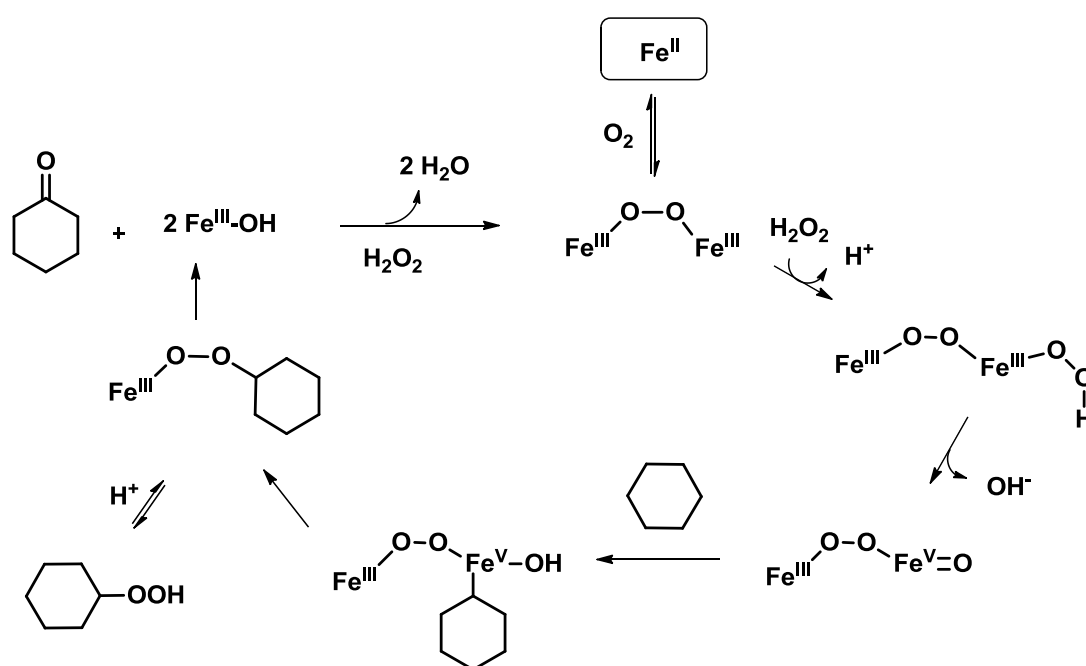
**Scheme 9.** Oxidation of adamantane using  $\text{Na}_2\text{S}$  as a sulphide source

Resemblances	Limitations
Ketones are obtained as major products Alcohols are byproducts, not intermediates Reactions are not suppressed in the presence of alcohols or aldehydes. Olefins are not epoxidised. Selectivity in the CH bond oxidation : <i>sec</i> > <i>tert</i> > <i>prim</i> Alkyl derivatives are formed in the presence of trapping agents (i.e. alkyl bromide with $\text{BrCCl}_3$ )	Slow reaction rates in comparison with some autoxidation processes High catalyst loadings and facile deactivation via iron oxide and peroxide formation Use of toxic pyridine in large amounts

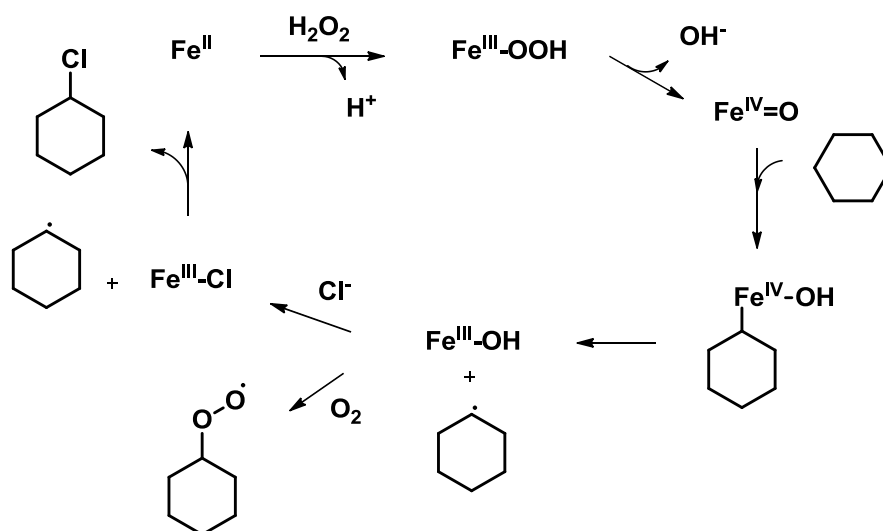
**Table 1.** Resemblances and limitations of Gif systems

Despite its limitations some relevant industrial applications of Gif systems have been disclosed. For instance, the oxidation of cyclohexane or cyclododecane to their keto/alcohol form is used for the industrial production of adipic acid and 1,12-dodecanedioic acid, which are important precursors in the manufacture of Nylon.<sup>28</sup> Due to its high complexity, the mechanistic understanding of Gif systems has been quite controversial. Barton hypothesised that the predominant formation of the ketone product and the preferential oxidation on secondary CH bonds stemmed from the formation of an electrophilic  $\text{Fe}^{\text{V}}=\text{O}$  species undergoing a concerted addition to the CH bond. The preference for oxidising secondary CH

bonds was interpreted as a compromise between bond strength (*prim* > *sec* > *tert*) and steric hindrance (*tert* > *sec* > *prim*). Such process is known as “non-radical Fe<sup>III</sup> - Fe<sup>V</sup> manifold”<sup>29</sup> (Scheme 10). However, formation of hydroperoxide species was also demonstrated, with the oxygen content of such peroxide species derived from O<sub>2</sub> and suggesting radical side reactions.<sup>30</sup> Moreover, the competitive formation of a Fe<sup>IV</sup>=O species capable of generating alkyl radicals was also hypothesised by Barton and co-workers as the “radical Fe<sup>II</sup> - Fe<sup>IV</sup> manifold”<sup>30,31</sup> (Scheme 11). Evidence of such manifold is based on the detection of alkyl chloride byproducts.

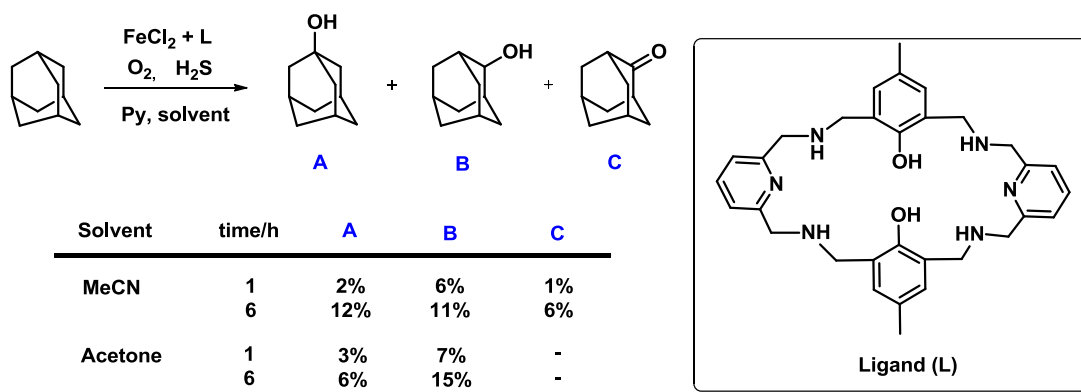


**Scheme 10.** Non radical Fe<sup>III</sup> - Fe<sup>V</sup> manifold

Scheme 11. Radical  $\text{Fe}^{\text{II}} - \text{Fe}^{\text{IV}}$  manifold

### 1.3.2.1.2. Greener alternatives to Gif systems: macrocyclic iron catalysts

Dinuclear  $\text{Fe}^{\text{II}}$  complexes resulting from the combination of iron chlorides with poly(azadiphenol) macrocyclic ligands were found to catalyse the aerobic oxidation of adamantane to its alcohol or keto form<sup>32</sup> (Scheme 12). Such catalysts are similar to Gif systems, requiring the use of hydrogen sulfide as a reductant but affording preferentially a mixture of alcohol products. Lower catalysts loadings and much reduced amounts of pyridine were used to achieve catalytic activity, resulting in a more environmentally friendly protocol. In addition, these macrocyclic complexes are compatible with different solvents, with the product distribution being affected by the choice of solvent and reaction time (Scheme 12).



Scheme 12. Macrocyclic Fe complexes for the aerobic oxidation of adamantane

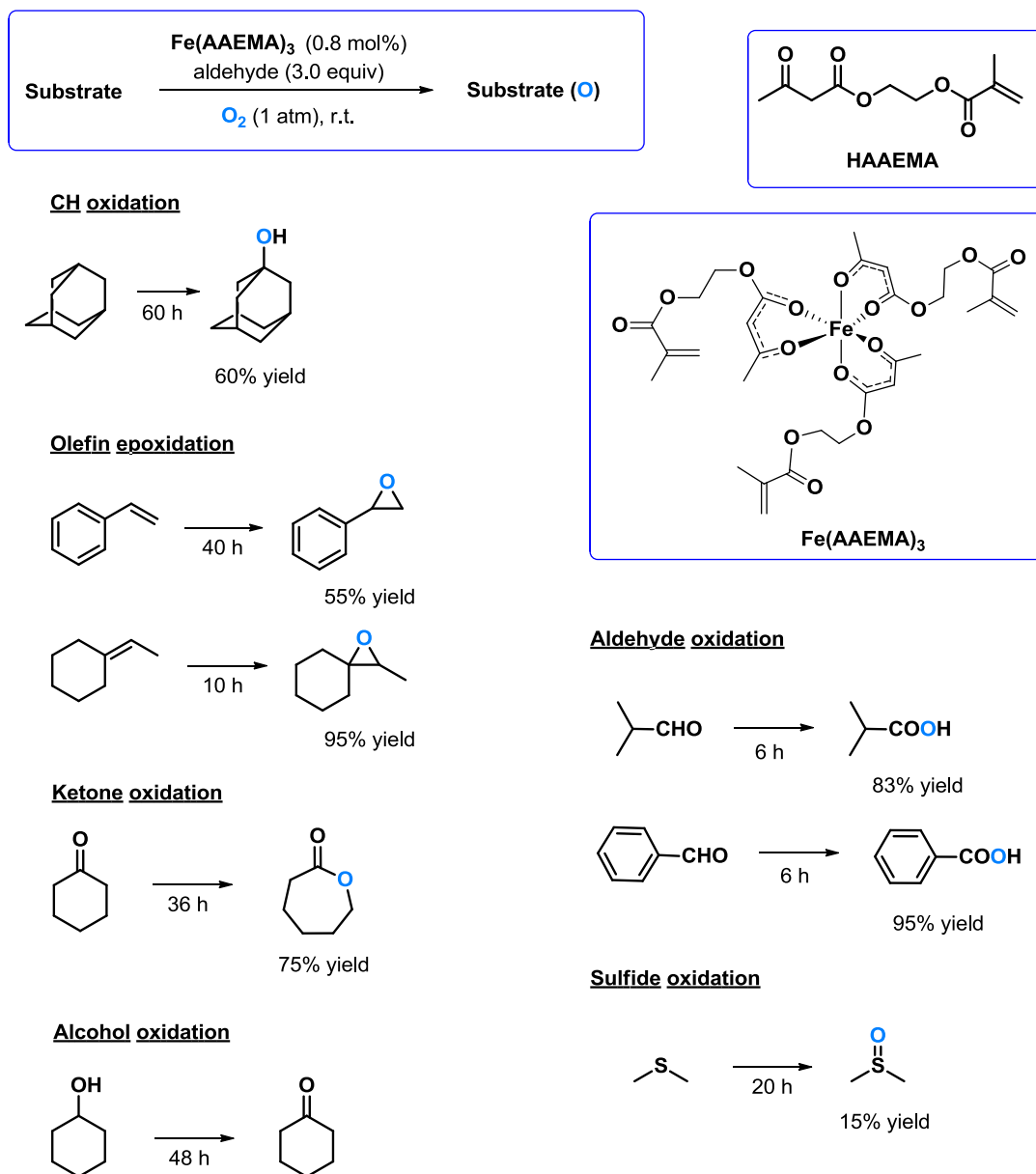
---

### 1.3.2.2. Oxidations in the presence of sacrificial substrates

#### 1.3.2.2.1. Mukaiyama's oxidation reactions

The catalytic aerobic oxidation of an ample variety of organic substrates in the presence of a large excess of an aldehyde or an acetal was demonstrated by Mukaiyama and co-workers in the early 90's.<sup>33</sup> Because many transition metal complexes can serve as active catalysts for such transformations and because of its wide scope, the atmospheric aerobic oxidations of organic substrates in the presence of a sacrificial aldehyde are known as oxidations under Mukaiyama's conditions.

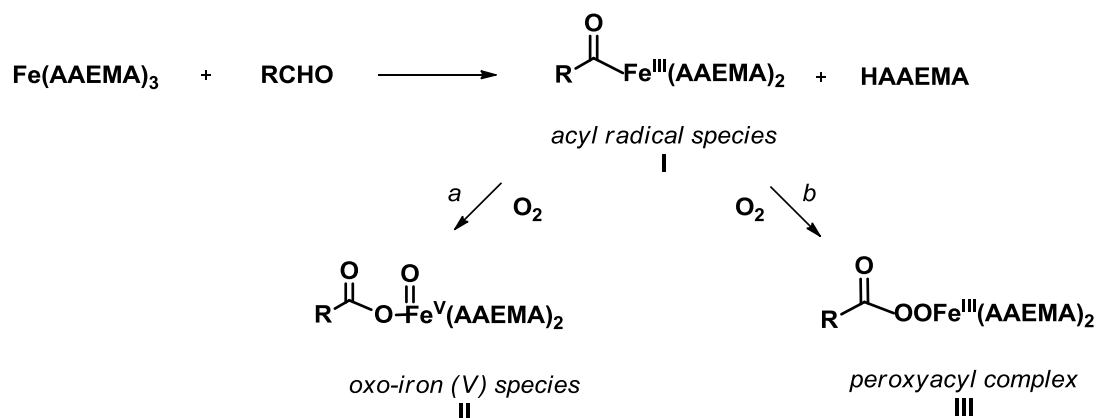
In particular, complexes of deprotonated 2-(acetoxy)ethyl methacrylate (AAEMA<sup>-</sup>) with cheap metals such as Fe, Cu or Ni have shown catalytic activity for the oxidation of alkanes, alkenes, alcohols, aldehydes, sulfides and cyclic ketones albeit in each case the investigated substrate scope is limited to only one or two examples<sup>34</sup> (scheme 13).



**Scheme 13.** Scope of the oxidation reactions catalysed by the Fe(AAEMA)<sub>3</sub> complex using *iso*-butyraldehyde as a sacrificial substrate

Although not much mechanistic evidence has been reported, variations on the reaction efficiency with different metals suggest that different mechanisms for oxygen activation and different oxygen transfer species may be in operation.<sup>35</sup> Participation of radical species is suggested in all cases as inhibition of different oxidation reactions was detected in the presence of radical scavengers. In addition, the isomerisation of the C-C double bond observed in *cis*- and *trans*-octenes during their Fe(AAEMA)<sub>3</sub> catalysed epoxidation

reactions is also consistent with the formation of radical intermediates.<sup>35</sup> The hypothetical mechanism for the Fe(AAEMA)<sub>3</sub> catalysed oxidation reactions involves the formation of a Fe<sup>III</sup> acyl radical species **I** by replacement of a AAEMA ligand with a molecule of aldehyde. Further reaction of this species with dioxygen would result in the formation of the Fe<sup>V</sup>-oxo species **II** and/or a Fe<sup>III</sup> peroxyacyl complex **III** (Scheme 14). Both intermediates could serve as the active oxidising agents of the Fe-catalysed Mukaiyama's reactions.<sup>35</sup>

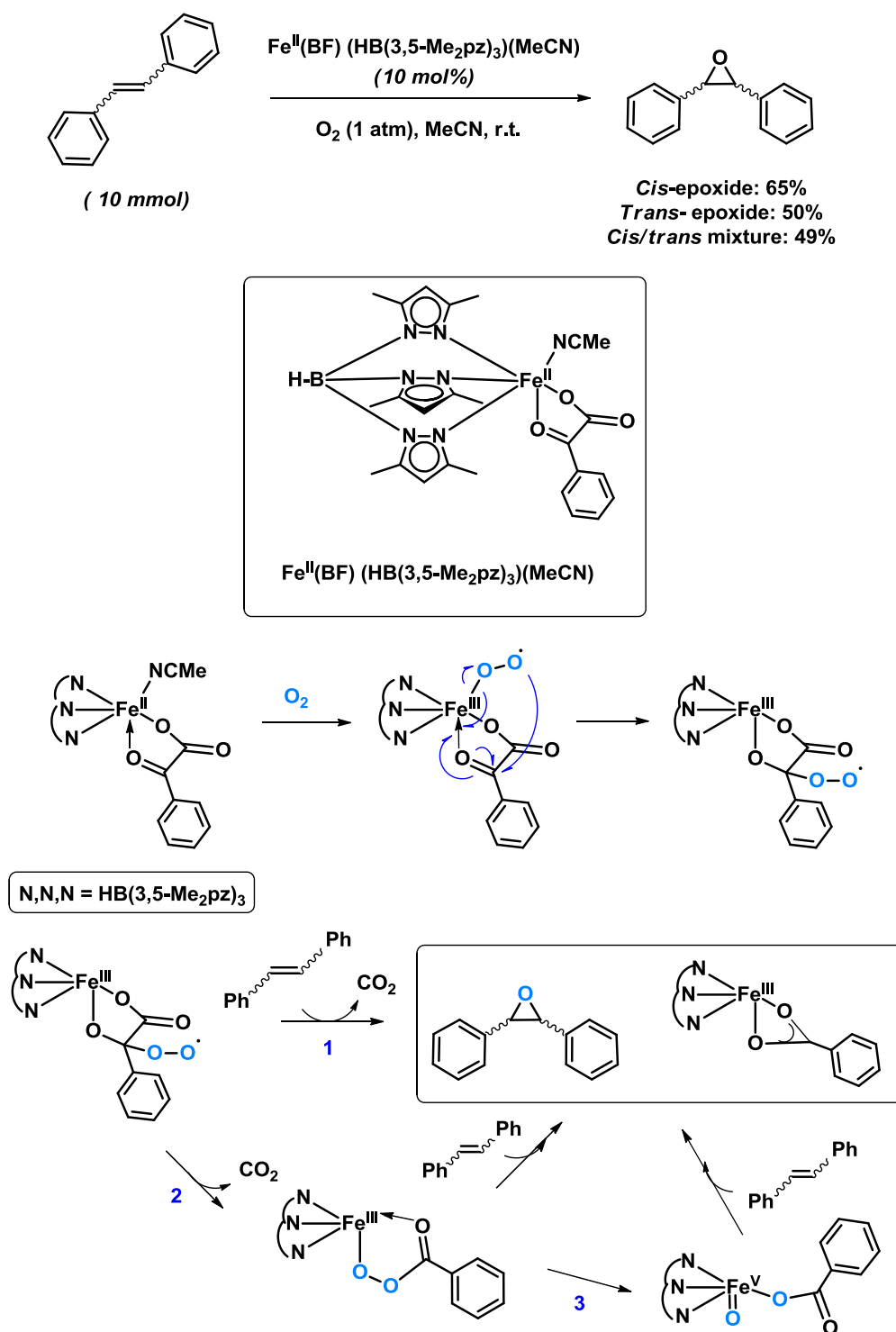


**Scheme 14.** Proposed mechanism for the Fe(AAEMA)<sub>3</sub> catalysed oxidation reactions

#### 1.3.2.2.2. Biomimetic designs

Natural  $\alpha$ -ketoglutarate-dependent Fe<sup>II</sup> dioxygenases are known to catalyse the aerobic oxygenation of organic substrates with additional oxidation and decarboxylation of a cofactor, releasing CO<sub>2</sub> and succinate.<sup>36</sup> Inspired by this natural system, Valentine and co-workers reported a Fe<sup>II</sup> complex of benzoylformate (BF) and tris-(3,5-dimethyl-1-pyrazolyl)borohydride (HB(3,5-Me<sub>2</sub>pz)<sub>3</sub>) capable of catalysing the aerobic epoxidation of *cis* and *trans*-stilbenes with additional oxidation of the BF ligand to give benzoate<sup>37</sup> (Scheme 15). The reaction proceeded with good yields under mild conditions and it is the first reported biomimetic catalyst capable of oxygenating both an organic substrate and a cofactor.

Mechanistic investigations revealed that a free radical autoxidation pathway is not involved as no *cis/trans* isomerisation was detected in stilbene epoxidations and no competitive allylic oxidation of cyclohexene was observed. A reaction mechanism involving the formation of a



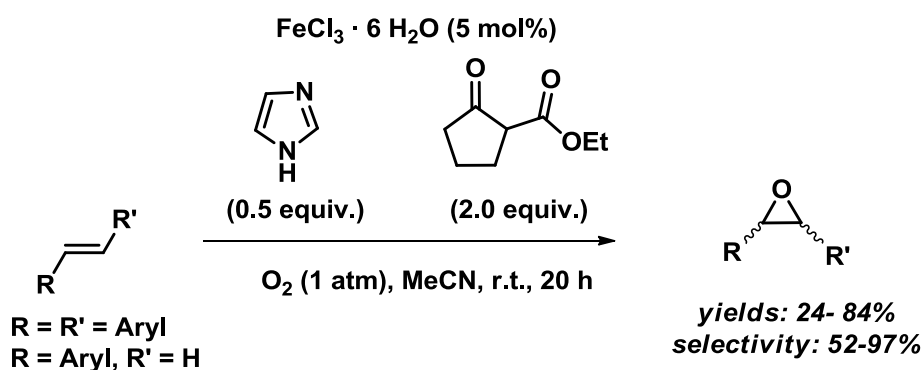
**Scheme 15.** Fe-catalysed epoxidation of stilbenes catalysed under aerobic conditions and its postulated mechanism.

ferric superoxide that can react with the BF ligand generating a peroxy adduct was postulated. This peroxy adduct can react with the stilbene, giving the epoxide product,  $\text{CO}_2$  and the benzoate. However, the initial decarboxylation of the peroxy adduct with



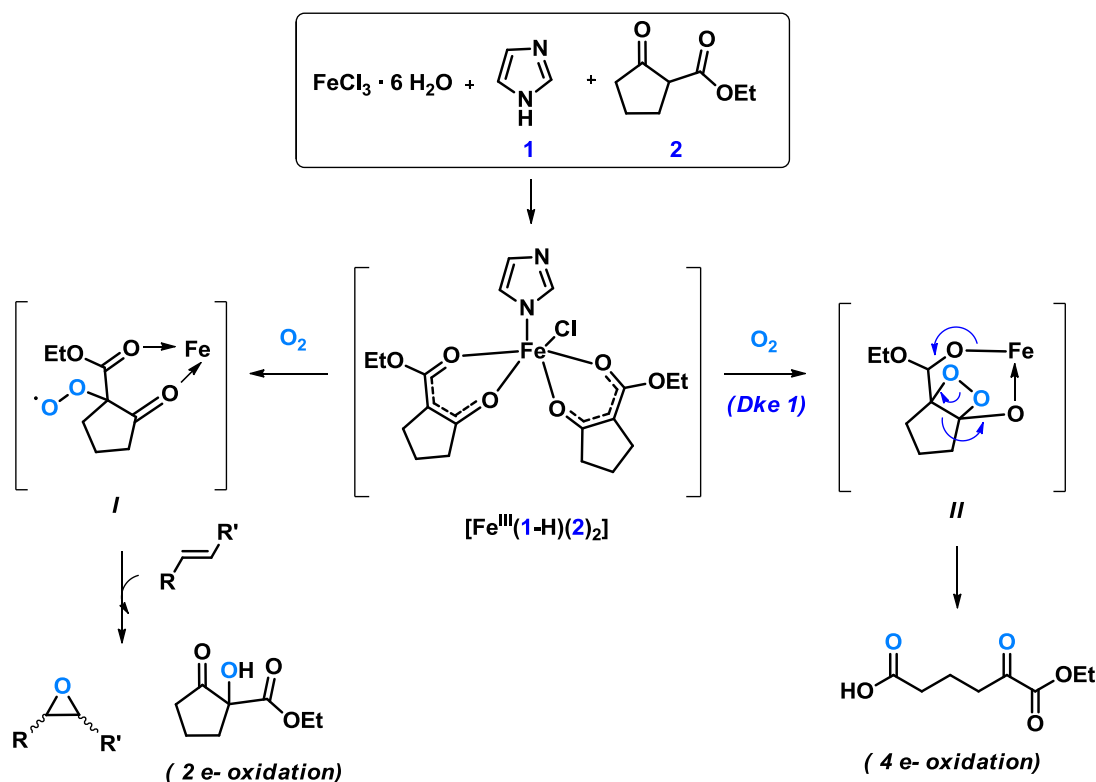
concomitant formation of other oxo-iron species as oxidizing agents cannot be ruled out (Scheme 15).

The iron-catalysed aerobic epoxidation of olefins using a bioinspired sacrificial substrate was further expanded by the groups of Costas and Beller, who demonstrated that catalytic amounts of iron chloride with an excess of imidazole **1** and ethyl 2-oxocyclohexane carboxylate **2** could epoxidise a variety of stilbenes and styrenes with moderate yields and selectivity under mild conditions<sup>38</sup>(Scheme 16).



**Scheme 16.** Iron-catalysed aerobic epoxidation of olefins with a bioinspired sacrificial substrate

Mechanistic investigations showed consistency with the formation of a dicarboxylate, monoimidazole  $\text{Fe}^{\text{III}}$  complex ( $[\text{Fe}^{\text{III}}(\text{1-H})(\text{2})_2]^+$ ) as the catalytic active species. Under aerobic atmosphere, formation of a superoxide species **I** was proposed. The superoxide species can be radically added to the olefinic substrate and after O-O cleavage, formation of the epoxide product and hydroxylation of the sacrificial keto-ester was postulated (Scheme 17). However, a competitive four electron oxidation of the sacrificial substrate was also observed. Its formation is suspected to stem from the formation of the organic peroxide species **II**, in a similar fashion as the iron-dependent acetylacetonate dioxygenase (Dke 1) oxygenates 2,4-pentadione.<sup>39</sup>

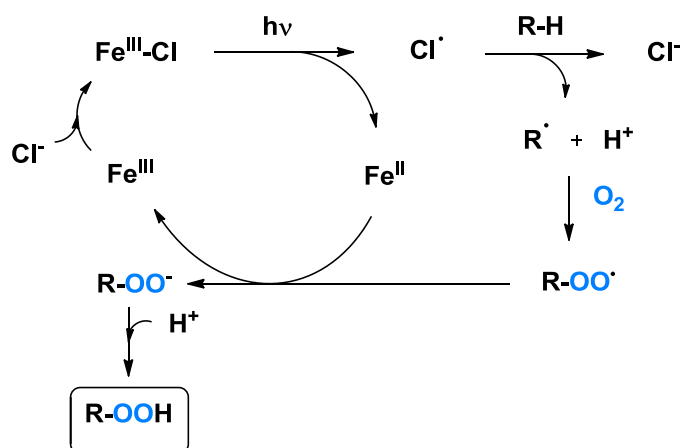
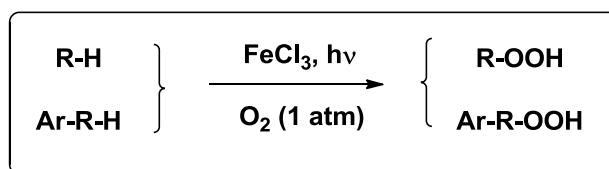


**Scheme 17.** Proposed mechanism for the iron-catalysed olefin epoxidation with a bioinspired sacrificial substrate

### 1.3.2.3. Photoinduced aerobic oxidations

#### 1.3.2.3.1. Reactions catalysed by simple iron salts

In the early 90's the group of Shul'pin developed a novel methodology for the photocatalytic ( $h\nu > 300 \text{ nm}$ ) aerobic oxygenation of alkanes and arylalkanes into hydroperoxides using  $\text{FeCl}_3$  as catalyst.<sup>40</sup> The catalyst is compatible with different solvents such as acetic acid, acetonitrile or alcohols; however, the scope of the method is limited to simple alkanes such as cyclohexane and toluene.  $\text{FeBr}_3$  was also found catalytically active for the oxidation of the more activated arylalkanes.<sup>41</sup> The proposed mechanism involves the photoinduced homolytic cleavage of the Fe-Cl bond releasing a chloride radical. The chlorine radical initiates the formation of carbon-centred radicals that undergo subsequent oxygenation to form the final peroxyalkyl species<sup>42</sup> (Scheme 18). The reduced catalytic efficiency of the  $\text{FeBr}_3$  can be understood on the basis of the lower reactivity of the bromine radical.

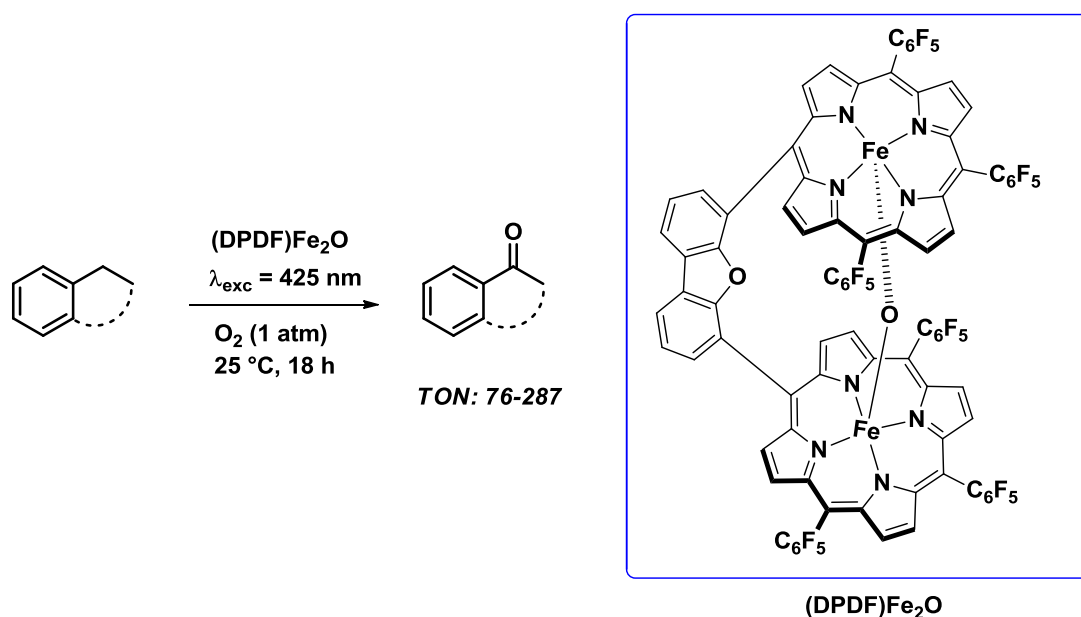


**Scheme 18.** Photoinduced oxygenation of alkanes into alkylhydroxides catalysed by  $\text{FeCl}_3$

### 1.3.2.3.2. Bioinspired catalysts

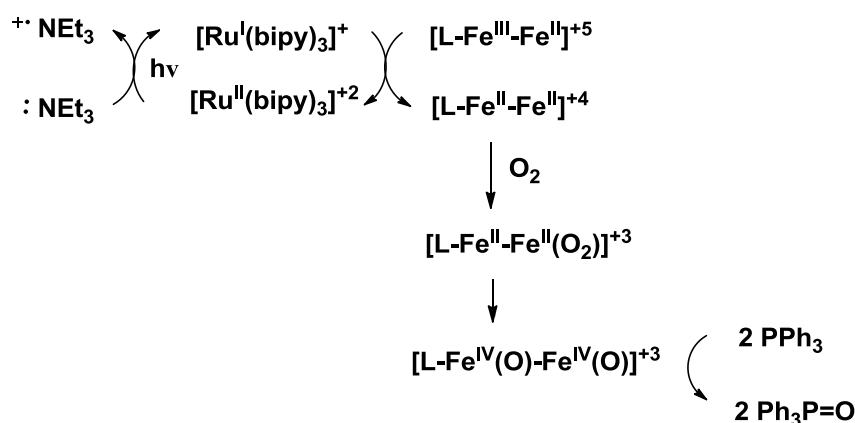
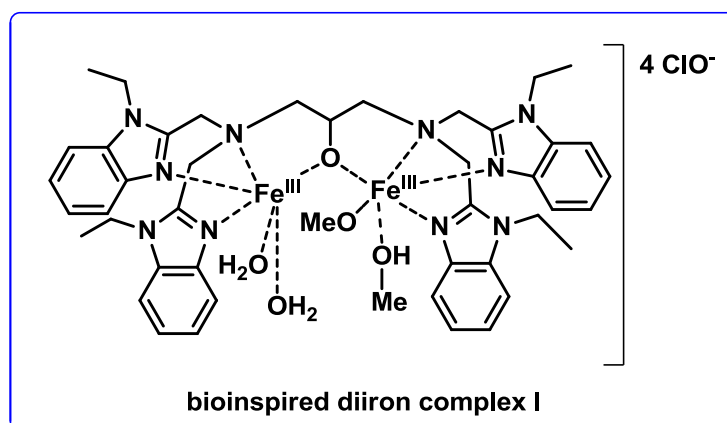
Inspired by the capability of iron-porphyrines in oxidising organic substrates under aerobic conditions via the formation of an electrophilic  $\text{Fe}^{\text{IV}}=\text{O}$  species, the group of Nocera investigated the use of iron bisporphyrine skeletons for undergoing similar aerobic oxidations. Extensive studies showed that bis- $\text{Fe}^{\text{III}}\text{-}\mu\text{-oxo}$ -Pacman porphyrin complexes were effective for the oxidation of olefins<sup>43</sup> and activated unfunctionalised aryl hydrocarbon CH bonds<sup>44</sup> under aerobic atmosphere and visible light irradiation (Scheme 19). Even though the scope of the CH oxidation is very limited, good TONs were achieved for substrates displaying lower CH ionisation energies (EI). The catalytic cycle for such transformation is under current investigation; however, the formation of a  $\text{Fe}^{\text{IV}}=\text{O}$  species capable of undergoing hydrogen atom abstraction from the substrate is postulated. In addition, a small kinetic isotopic effect ( $k_{\text{H}}/k_{\text{D}}$ ) of 1.55 at 25 °C obtained by comparing the oxidation of toluene with deuterated toluene suggests that the oxidation reaction occurs via an asynchronous proton coupled electron transfer (PCET) mechanism,<sup>45</sup> according to which the

abstraction of a hydrogen radical from the organic substrate takes place. Subsequent oxidation of the carbon-based radical species would afford the reaction product.



**Scheme 19.** Photoinduced oxidation of hydrocarbons catalysed by bis-iron<sup>III</sup>- $\mu$ -oxo-Pacman porphyrin complexes

More recently, the groups of Mahy and Auckauloo reported the sophisticated generation of a diiron<sup>III</sup> peroxo species via photoactivation of the bioinspired diiron<sup>II</sup> complex **I** under aerobic atmosphere. The resulting oxygenated diiron<sup>III</sup> peroxide was found capable of oxidising  $\text{PPh}_3$  to  $\text{Ph}_3\text{P}=\text{O}$  via oxygen atom transfer.<sup>46</sup> In addition, triethylamine was used as a sacrificial electron donor in the presence of a Ru-pyridine photosensitizer that ultimately reduces the initial diiron<sup>III</sup> species to its diiron<sup>II</sup> form (Scheme 20).



**Scheme 20.** Photoinduced oxygen activation at a diiron<sup>III</sup> complex followed by oxygen transfer to PPh<sub>3</sub>.

### 1.3.3. Electron-rich substrates: aerobic oxidation of ethers

The selective catalytic oxidation of C-H bonds has evolved rapidly in the last decade, with many iron-based catalysts being now available for the oxidation of complex substrates. However, the development of chemoselective catalysts capable of undergoing CH oxidations in the presence of electron rich functionalities is a remaining challenge. For such substrates, poor selectivity, limited substrate scope and undesired substrate decomposition are often encountered limitations, partly because of the harsh reaction conditions required.<sup>47</sup>

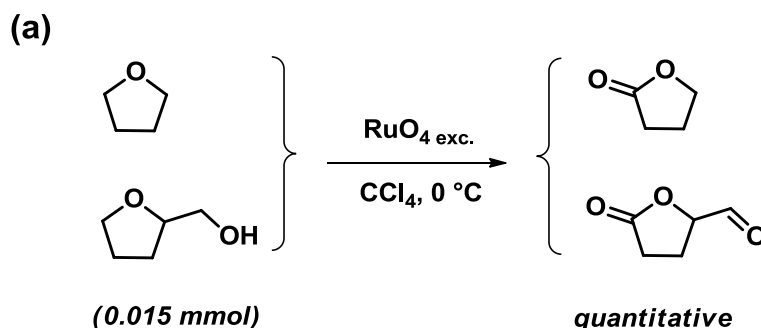
The selective  $\alpha$ -oxidation of ethers under aerobic conditions is a long time pursued transformation of industrial interest. Efficient methods for the aerobic oxidation of functionalised ethers would in principle, facilitate the synthesis of natural products and biologically active molecules in an industrial scale.<sup>48</sup> Because of the aforementioned issues, a green and efficient catalytic version of this reaction remains to be developed.

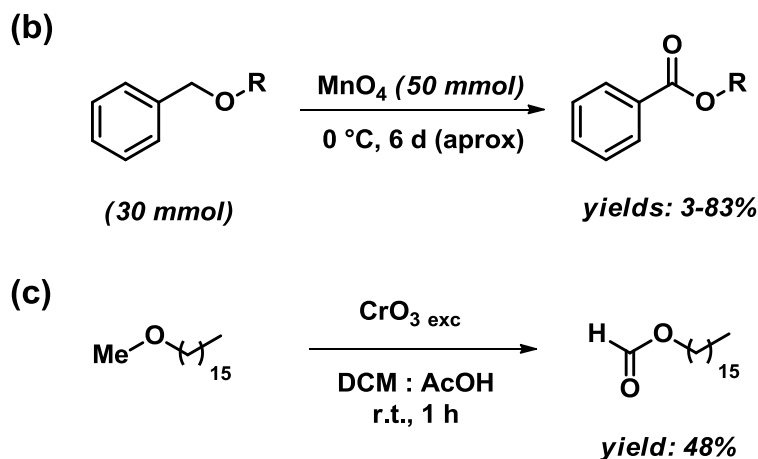
### 1.3.3.1. Stoichiometric metal oxides as oxidising agents

Early attempts on the selective  $\alpha$ -oxidation of ethereal substrates to esters were based on the use of transition metal oxides as oxidising agents. In this regard, ruthenium tetroxide ( $\text{RuO}_4$ ) was found to selectively oxidise tetrahydrofuran (THF) to  $\gamma$ -butyrolactone with quantitative yields<sup>49</sup> (Scheme 21(a)). More than stoichiometric amounts of oxidising agent were needed and the scope of the reaction was not explored further, probably because the oxidation of tetrahydrofurfuryl alcohol afforded the aldehyde lactone, suggesting poor functional group tolerance. In addition, aryl ethers cannot be oxidised as  $\text{RuO}_4$  is known to degrade aryl groups.<sup>50</sup>

The reaction scope was slightly improved by the group of Schaeffer, who demonstrated that benzyl(triethylammonium) permanganate in stoichiometric amounts could undergo the chemoselective oxidation of unfunctionalised alkyl and phenyl ethers to esters<sup>51</sup> (Scheme 21(b)). However, the reactions were slow (*circa* 6 days), low temperatures were needed and the scope was mainly limited to few benzyl ethers.

The selective oxidation of methyl ethers to formates was demonstrated using an excess of toxic chromium trioxide ( $\text{CrO}_3$ ) in acetic acid.<sup>52</sup> Non-functionalised aliphatic methyl ethers were oxidised with moderate yields under mild conditions. However, the high reactivity of such strong oxidant limited the reaction scope, and additional synthetic steps for group protection and deprotection were required (Scheme 21(c)).

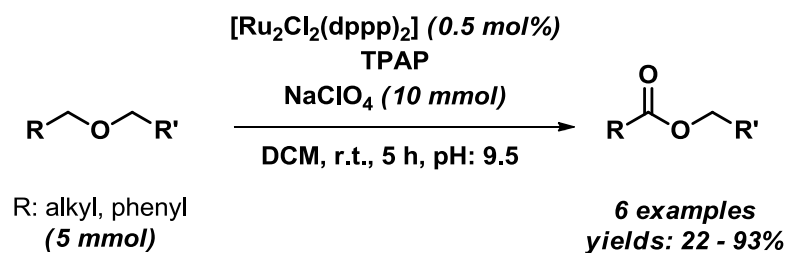




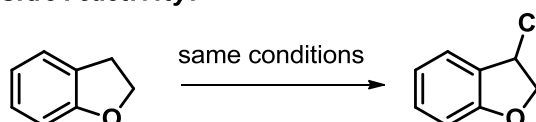
**Scheme 21.** Selective  $\alpha$ -oxidation of ethers to ester using stoichiometric transition metal oxides

### 1.3.3.2. Catalytic methods using strong oxidants

Since its introduction in 1958, classical ether oxidation with  $\text{RuO}_4$  has been exhaustively improved. More modern methods allow the *in situ* preparation of the oxidant from commercial Ru salts such as  $\text{RuCl}_3$  or  $\text{RuO}_2$  and a strong inorganic oxidant such as  $\text{NaIO}_4$ .<sup>53</sup> In addition, Sharpless and co-workers demonstrated that such oxidations could proceed using catalytic amounts of Ru by incorporating MeCN in the biphasic  $\text{CCl}_4/\text{H}_2\text{O}$  solvent mixture.<sup>54</sup> Under such conditions, deactivation of the Ru catalysts via insoluble species generation is prevented due to the coordinating properties of MeCN. In addition, Sheldon and co-workers demonstrated that the efficiency of the ether oxidation can be significantly improved by controlling the reaction pH values.<sup>55</sup> Under basic conditions, aliphatic and some benzyl ethers were oxidised to esters at r.t. using small loadings of  $\text{RuCl}_2$  complexes (typically 0.5 mol%). Because the method still requires an excess of  $\text{NaClO}_4$  as an oxidant, undesired side-reactivity such as chlorination in some benzylic positions was observed, limiting the reaction scope (Scheme 22).

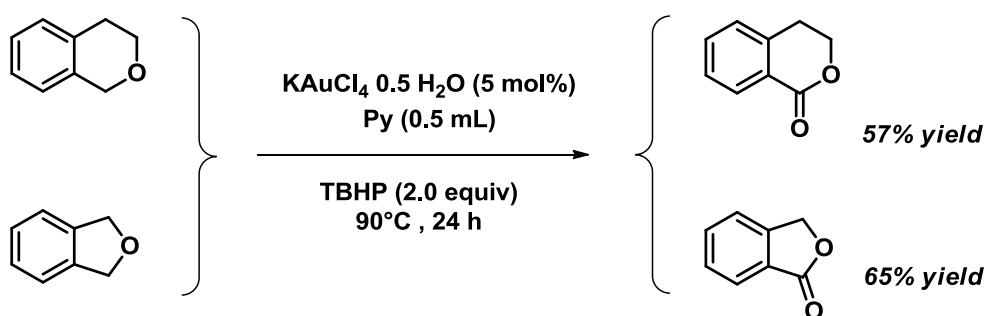


**Side reactivity:**



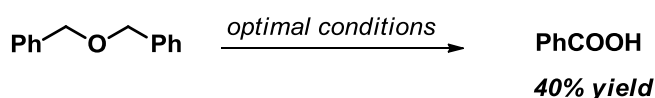
**Scheme 22.** Ru-catalysed  $\alpha$ -oxidation using NaOCl under controlled pH

Less toxic gold-based catalysts have also been explored for oxidation reactions. The combination of catalytic amounts of  $\text{KAuCl}_4$  with an excess of pyridine was found to be an active catalyst for oxidising benzylic CH bonds, including ethereal examples such as phthalan and isochroman<sup>56</sup> (Scheme 23). The reactions proceeded with moderate yields; however, the structure of the *in situ* generated catalyst was not elucidated and high catalyst loading (5 mol%), harsh reaction conditions (90 °C) and an excess of tertbutylhydroperoxide (TBHP) as the oxidising reagent were required. Moreover, the scope of the reaction is limited to two substrates, as oxidative cleavage of open chain benzylic ethers to form benzoic acid occurred under optimal reaction conditions.



**Only 2 examples**

**Side reactivity:**



**Scheme 23.** Gold-catalysed  $\alpha$ -oxidation of esters to esters

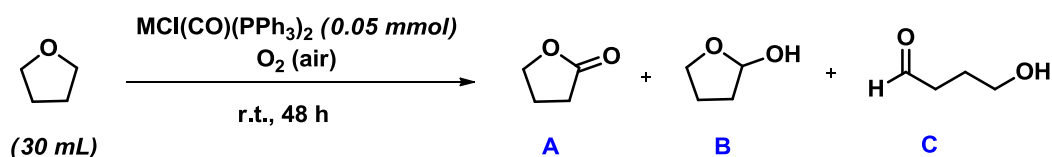


### 1.3.3.3. Catalytic aerobic oxidations

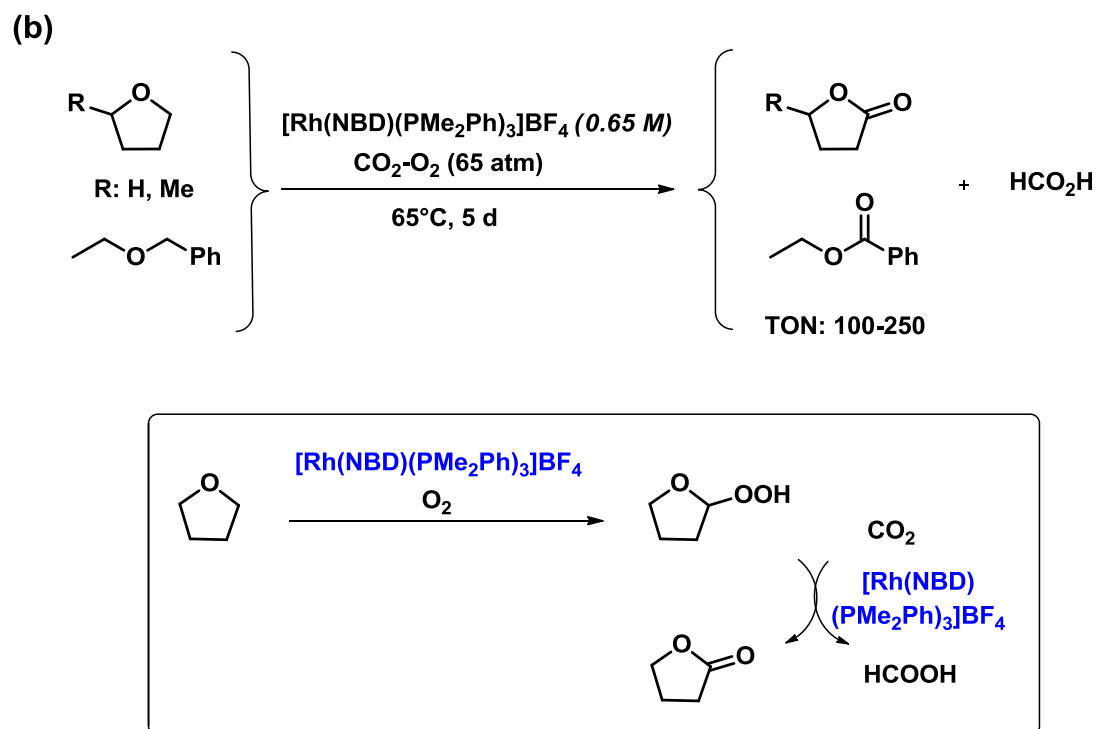
Vaska-type complexes of Ir and Rh were found active for the aerobic oxygenation of THF to  $\gamma$ -butyrolactone at r.t.<sup>57</sup> (Scheme 24 (a)). Undesired byproduct formation occurred, with lactol and 4-hydroxybutyraldehyde detected with low yields. Although the reaction required low catalysts loading, THF was used in solvent amounts affording the lactone product with a maximum TON of 150. Further reaction scope and the reaction mechanism were not investigated.

The use of Rh-based catalysts for the oxygenation of ethers to esters was further explored by the group of Nicholas, who coupled the oxidation of ethers to esters with the reduction of CO<sub>2</sub> to formic acid using catalytic amounts of [Rh(NBD)(PMe<sub>2</sub>Ph)<sub>3</sub>][BF<sub>4</sub>], (NBD= 2,5-norbornadiene), in a pressurised O<sub>2</sub>-CO<sub>2</sub> atmosphere.<sup>58</sup> Cyclic ethers and benzyl ethyl ether were oxidised with TONs of 100-250 after 6 days at 60 °C (Scheme 24 (b)). Mechanistic investigations using isotopically labelled gas mixtures revealed that the oxygen of the lactone products was derived from O<sub>2</sub> whereas the formic acid was generated from the CO<sub>2</sub> reduction and ether degradation. Even though the reaction mechanism has not been investigated in detail, exposure of THF to the Rh catalyst under O<sub>2</sub> atmosphere resulted in the formation of tetrahydrofuran hydroperoxide. Addition of CO<sub>2</sub> to the reaction mixture allowed the formation of  $\gamma$ -butyrolactone and formic acid, probably via Rh-mediated hydride transfer from the hydroperoxide to the CO<sub>2</sub>, as Rh-H species have been detected in solution by <sup>1</sup>H NMR.

(a)



M	A (TON)	B (TON)	C (TON)
Ir	150	4	3
Rh	94	4	5



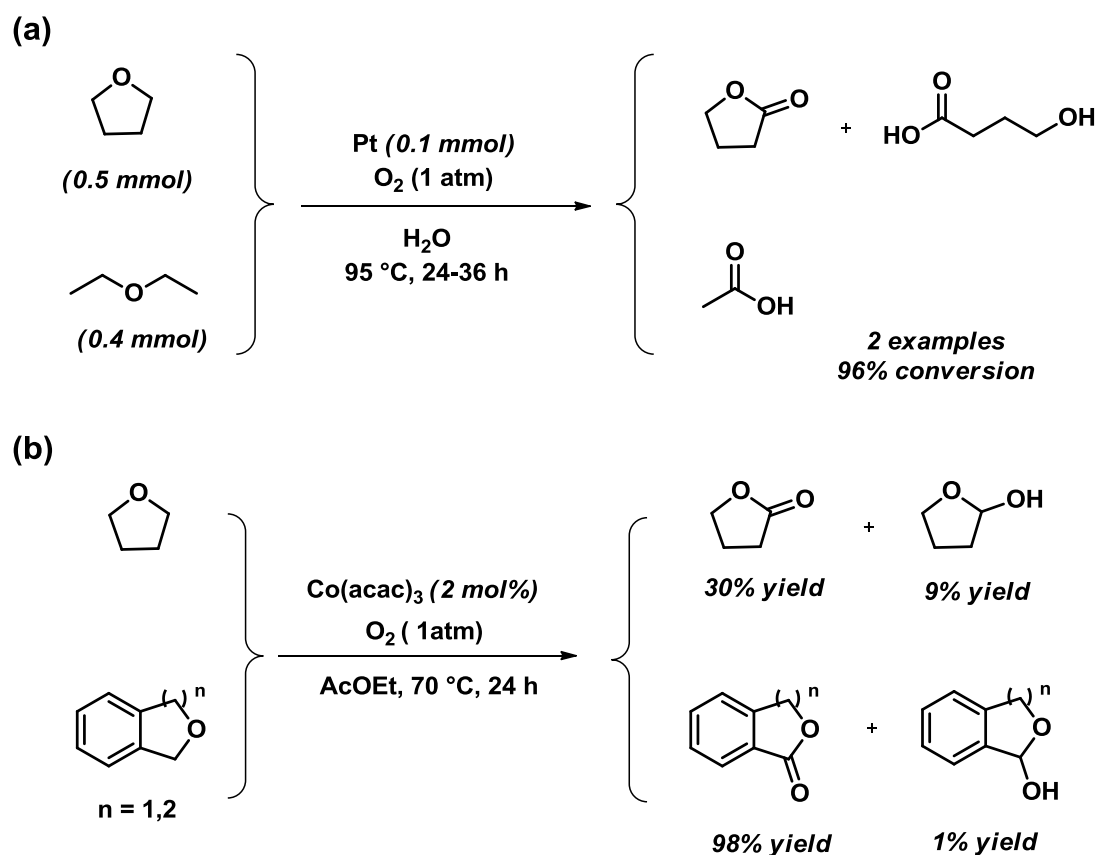
**Scheme 24.** Aerobic oxidation of ethers catalysed by Ir and Rh-based complexes

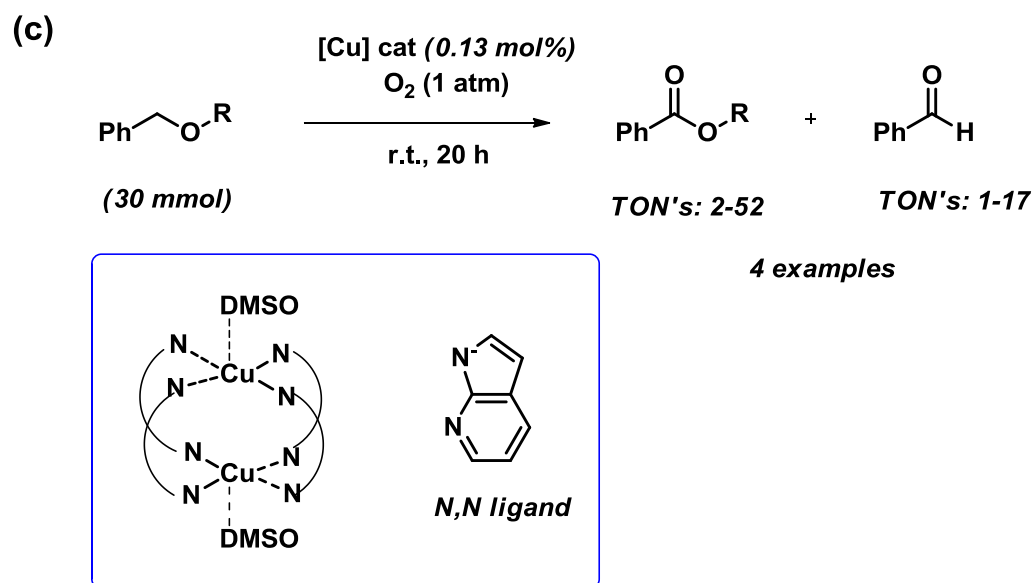
Metallic Pt was also investigated as catalyst for the aerobic oxidation of THF and diethyl ether to esters in water at high temperature<sup>59</sup> (Scheme 25 (a)). The catalyst showed high efficiency in the oxidation of THF affording the lactone product with very good yields and small amounts of 4-hydroxybutanoic acid that resulted from the ring opening oxidation. However, acetic acid was obtained exclusively in the oxidation of diethyl ether due to the ester hydrolysis easily occurring in the aqueous phase. The proposed mechanism involves the activation of the C-H bond  $\alpha$  to the oxygen atom *via* oxidative addition on the metallic Pt surface followed by the aerobic oxidation of the hydrocarbonyl moieties.

Because the replacement of precious metals with cheap metal catalysts is highly desirable, the group of Reetz reported the use of a simple  $\text{Co(acac)}_3$  complexes as potential catalysts for the  $\alpha$ -oxygenation of cyclic ethers to lactones under aerobic atmosphere<sup>60</sup> (Scheme 25 (b)). Moderate to very good yields were achieved with minor formation of lactol byproducts; however, the scope of the reaction was surprisingly limited to three substrates. *In situ*

formation of an ether hydroperoxide as the real oxidant has been postulated; but the reaction mechanism is unclear.

In addition, the bioinspired binuclear  $\text{Cu}^{\text{II}}$ -1*H*-pyrrolo[2,3-*b*]pyridine (7-azaindole) complex was found catalytically active for the aerobic oxidation of benzylic ethers at 80 °C<sup>61</sup> (Scheme 25 (c)). The reaction proceeded with high TON but low yields for benzylic ethers, with benzaldehyde being formed as a byproduct. However, the catalyst was found inactive for the oxidation of alkyl ethers. The efficiency of the reaction was improved upon increasing the steric bulkiness of the alkyl chain. Thus, the coordination of the catalyst to the substrate seemed not essential during the oxidation reaction. However, a good correlation between the TON and the calculated ionization potentials was observed. Although further mechanistic evidence was not provided, an outer sphere electron transfer was suggested to explain the influence of the EI.



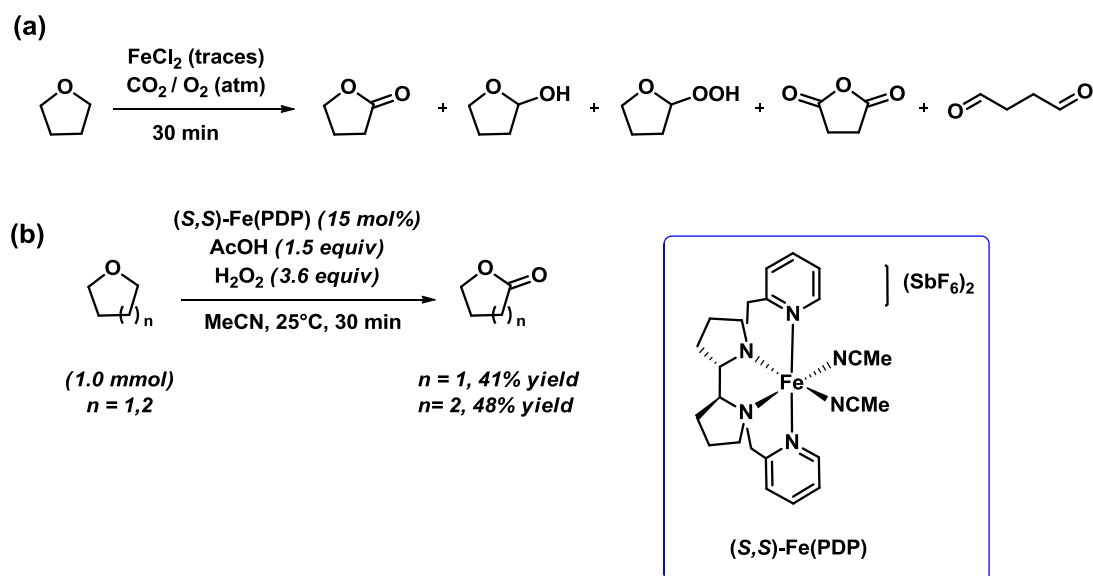


**Scheme 25.** Aerobic oxidation of ethereal substrates using Pt and cheap metal-based complexes

#### 1.3.3.4. Iron-catalysed oxidations

The use of environmentally friendly iron catalysts for the oxidation of ethers is surprisingly limited to the example of a  $\text{FeCl}_2$  catalyzed oxidation of THF under  $\text{CO}_2/\text{O}_2$  pressure, which yields a variety of species mostly derived from THF ring openings<sup>62</sup> (Scheme 26 (a)). The substrate scope is limited to THF and different product distributions were obtained under  $\text{CO}_2/\text{O}_2$  atmosphere and pure  $\text{O}_2$ . Both metal assisted and radical processes were proposed under the explored reaction conditions.

Chen and White demonstrated that the biomimetic  $\text{Fe(PDP)}$  catalyst can oxidise THF and tetrahydropyran (THP) with  $\text{H}_2\text{O}_2/\text{AcOH}$ , yielding a turnover number (TON) of 1-2<sup>63</sup> (Scheme 26 (b)). Byproducts resulting from the ring opening were also detected due to undesired Fenton chemistry and/or side reactivity of the highly electrophilic iron-oxo species. Further investigations of the substrate scope were not reported probably because the catalyst decomposed substrates containing aromatic rings.



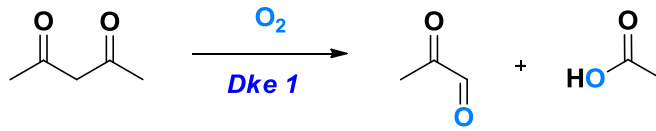
**Scheme 26.** Iron-catalysed aerobic oxidations of ethers to lactones

#### 1.3.4. Aerobic C-C cleavage in organic substrates

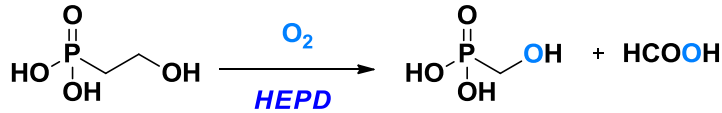
Non-heme iron enzymes capable of activating dioxygen can serve as versatile catalysts for an ample spectrum of reactions. Apart from selective oxidation of complex molecules, such enzymes are capable of selectively cleaving C-C bonds of organic substrates with incorporation of two oxygen atoms into the final product.<sup>64</sup> Aromatic<sup>65</sup> and aliphatic<sup>66</sup> C-C bonds can be oxidatively cleaved by different types of dioxygenases with excellent specificity and thus, high complexity can be introduced and/or significant structure modifications can be effected in the starting substrate (Scheme 27). As a consequence, these types of enzymatic transformations are often encountered in bacteria or metabolic processes.

## Aliphatic C-C cleavage

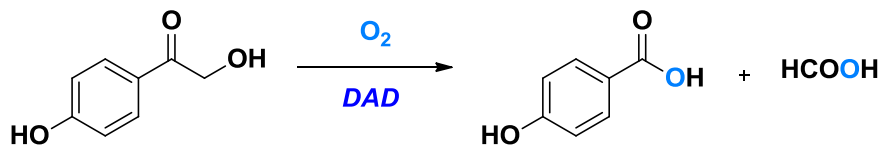
### Acetylacetonone 2,3-dioxygenases



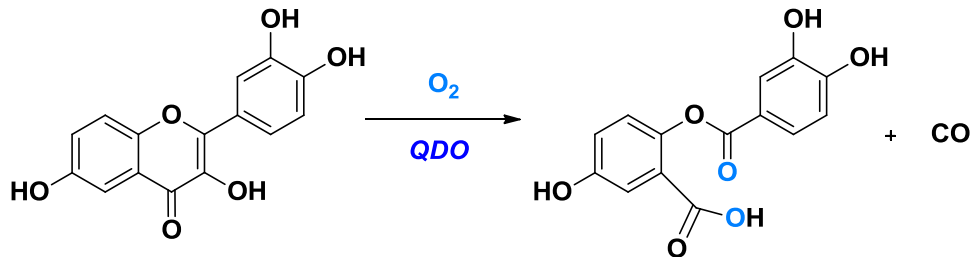
### Hydroxyethylphosphonate dioxygenase



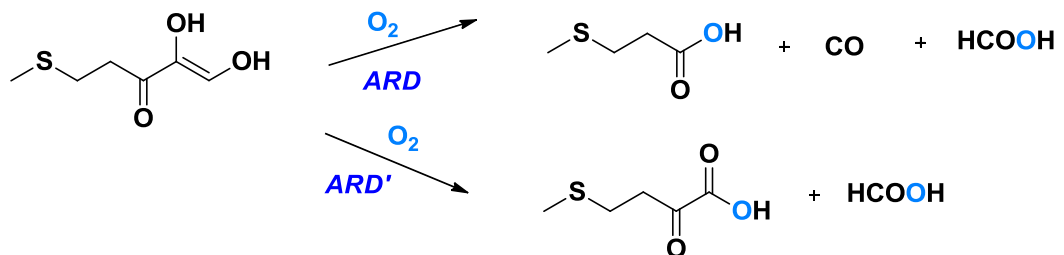
### 2,4'-Dihydroxyacetophenone dioxygenase



### Quercetin dioxygenases

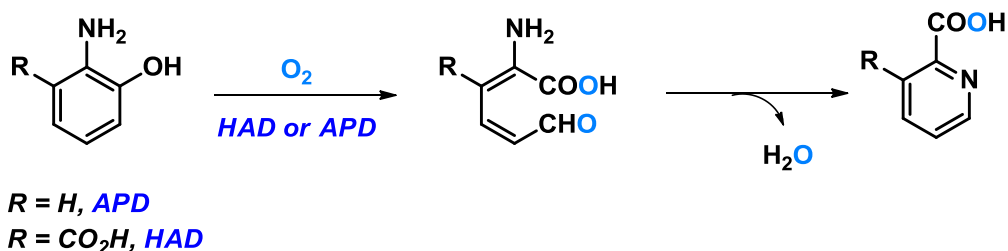


### Acireductone dioxygenases

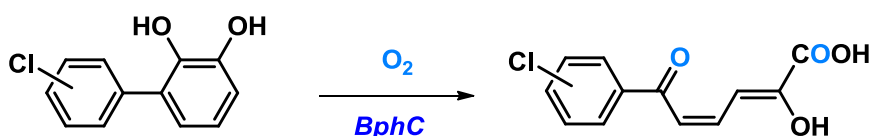


### Aromatic C-C cleavage

#### 3-Hydroxyantranilate-3,4-dioxygenase and 2-aminophenol-1,6-dioxygenase



#### 2,3-Dihydroxyphenyl dioxygenase



**Scheme 27.** Modes of enzymatic aerobic C-C cleavages

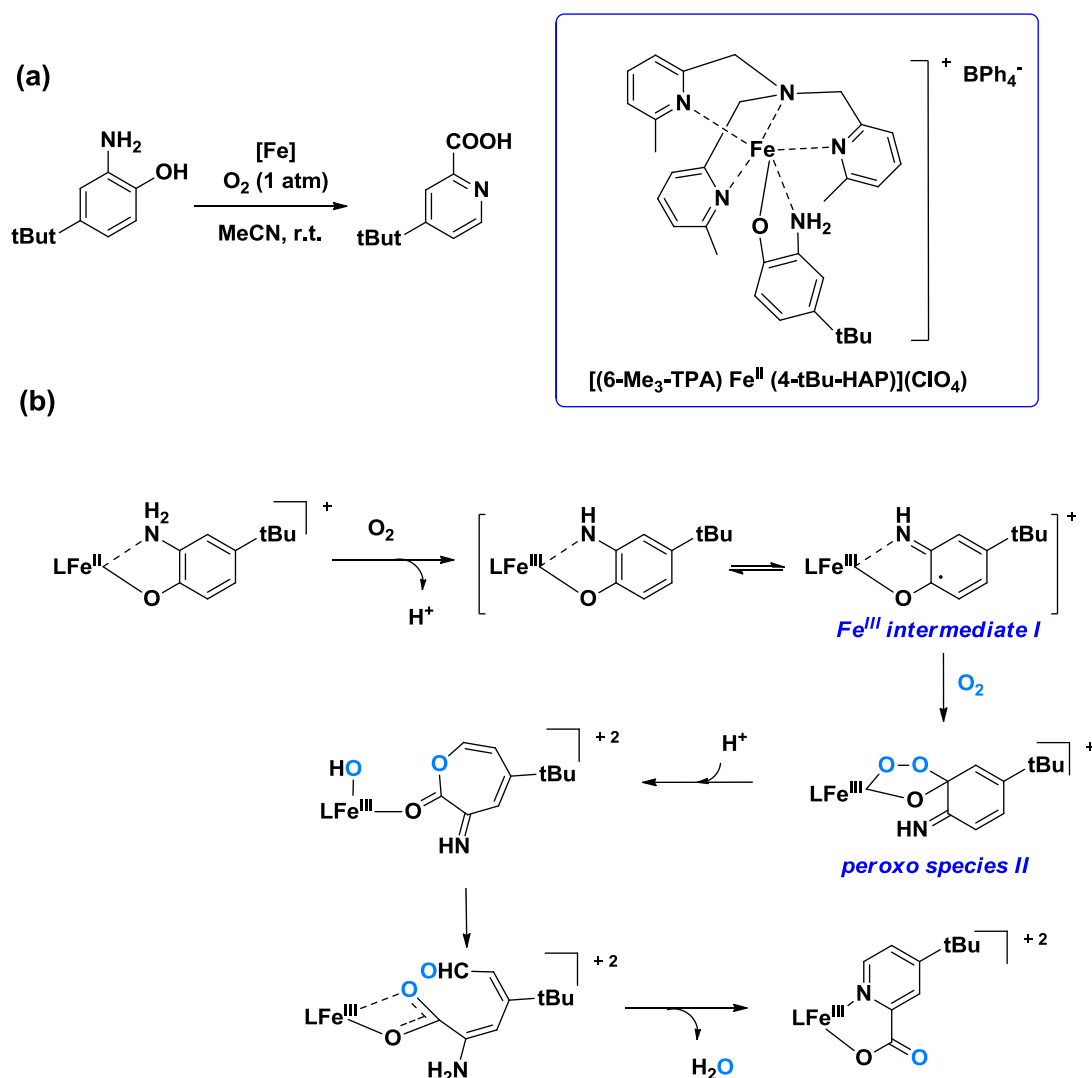
#### 1.3.4.1. Bioinspired iron complexes for the aerobic cleavage of aromatic C-C bonds

2-Aminophenol-1,6-dioxygenase<sup>67</sup> (APD) and 3-hydroxyantranilate-3,4-dioxygenase<sup>68</sup> (HAD) are iron-containing metalloenzymes found in bacteria that catalyse the degradation of aminoaryl compounds into pyridines via aerobic C-C cleavage. The non heme Fe<sup>II</sup> complex [(6-Me<sub>3</sub>-TPA)Fe<sup>II</sup>(4-tBu-HAP)](ClO<sub>4</sub>), where 6-Me<sub>3</sub>-TPA = tris(6-methyl-2-pyridylmethyl) amine and 4-tBu-HAP = monoanionic 2-amino-4-tert-butylphenolate, reported by the group of Paine, was conceived as a mimic of the active site of HAD enzymes and it was found capable of oxidising the C-C bond of 2-amino-4-tert-butylphenolate under mild conditions<sup>69</sup> (Scheme 28 (a)).

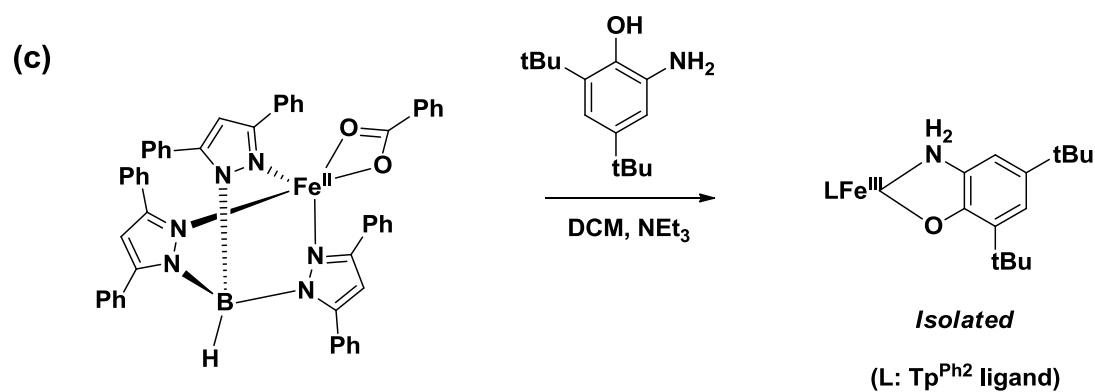
The proposed reaction mechanism is similar to the natural metalloenzyme, with the initial Fe<sup>II</sup> complex reacting with O<sub>2</sub> to generate the Fe<sup>III</sup> intermediate **I** via one electron oxidation. Further reaction of this radical Fe<sup>III</sup> intermediate with O<sub>2</sub> results in the formation of a peroxo species **II** that undergoes the C-C cleavage of the 2-aminophenol, generating the

semialdehyde intermediate. By dehydration, the semialdehyde is facily converted into the final 4-tert-butyl-2-picolinic acid (Scheme 28 (b)).

Independently, the group of Fiedler reported the reaction of the Fe<sup>II</sup> 2-aminophenolate complex [(Tp<sup>Ph2</sup>) Fe<sup>II</sup> (<sup>tBu</sup>APH)], where Tp<sup>Ph2</sup> = tris(pyrazolyl) borate ligand and <sup>tBu</sup>APH = 2-amino-4,6-ditertbutylphenol, which upon exposure to aerobic atmosphere resulted in the formation of the proposed Fe<sup>III</sup> radical intermediate<sup>70</sup> (Scheme 28 (c)). Such findings are consistent with the formation of radical Fe<sup>III</sup> intermediates during natural and bioinspired aerobic C-C cleavages.







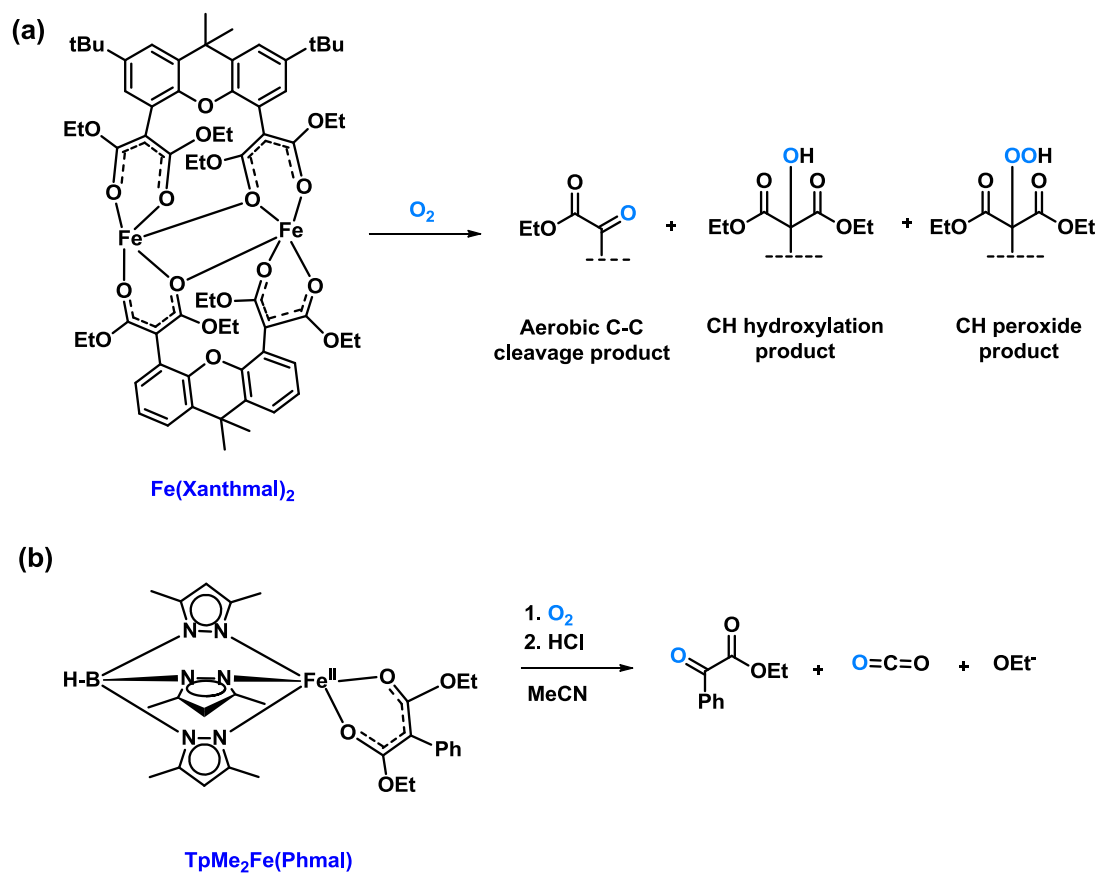
**Scheme 28.** Biomimetic iron complexes capable of undergoing aromatic C-C cleavage

### 1.3.4.2. Bioinspired iron complexes for the aerobic cleavage of aliphatic C-C bonds

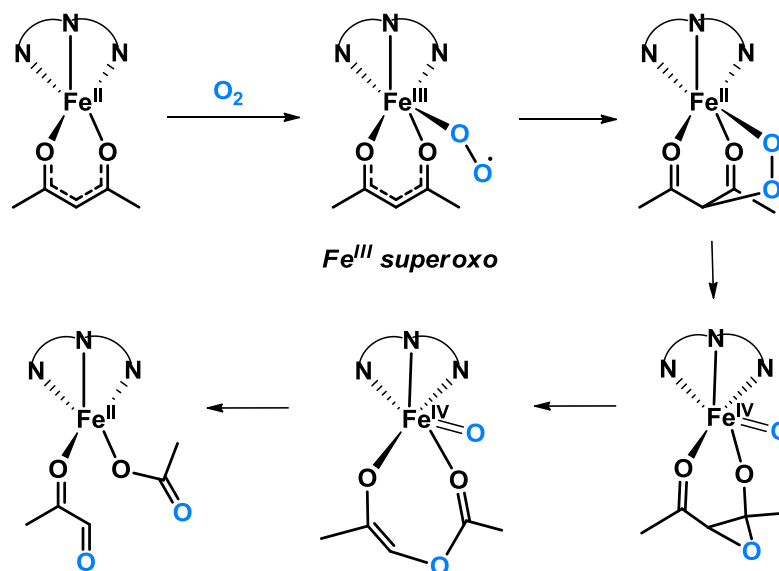
#### 1.3.4.2.1. Iron complexes that mimic acetylacetonate-2,3-dioxygenase (Dke 1)

Dke 1 enzymes catalyse the decomposition of several  $\beta$ -diketones,<sup>71</sup> including toxic acetylacetonate,<sup>72</sup> into acetate and methyl glyoxal under aerobic conditions. Current interest in understanding the mechanism of this transformation stems from the potential application of biomimetic complexes in bioremediation processes. Tripodal chelating ligands incorporating heterocyclic *N*-donors have been exploited for the development of iron biomimetics due to the resemblance of such structure with the 2-histidine-carboxylate moieties present in the active site of the natural enzyme.<sup>71a, 73</sup>

In 2008, Siewert et al. reported that the Fe(Xanthmal)<sub>2</sub> complex was capable of undergoing aerobic C-C cleavage of the malonate part of the ligand, affording an  $\alpha$ -ketoester product. Additional hydroxylated and peroxyalkyl species were also generated.<sup>74</sup> Interestingly, the Tp<sup>Me2</sup>Fe(Phmal) complex with Phmal = 3-phenylmalonate, exhibited similar reactivity as it decomposed the initial malonate into ethyl benzoylformate and ethylcarbonate in a catalytic fashion (Scheme 29). Iron-centered activation of O<sub>2</sub> with concomitant formation of a Fe<sup>III</sup> superoxo species was proposed as the initial step of the reaction (Scheme 30).

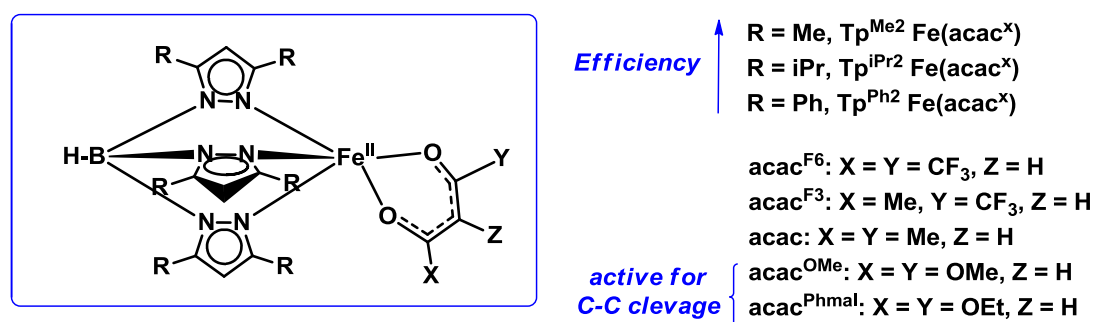


Scheme 29. Biomimetic iron complexes for aerobic C-C cleavage of malonates



Scheme 30. Proposed reaction mechanism

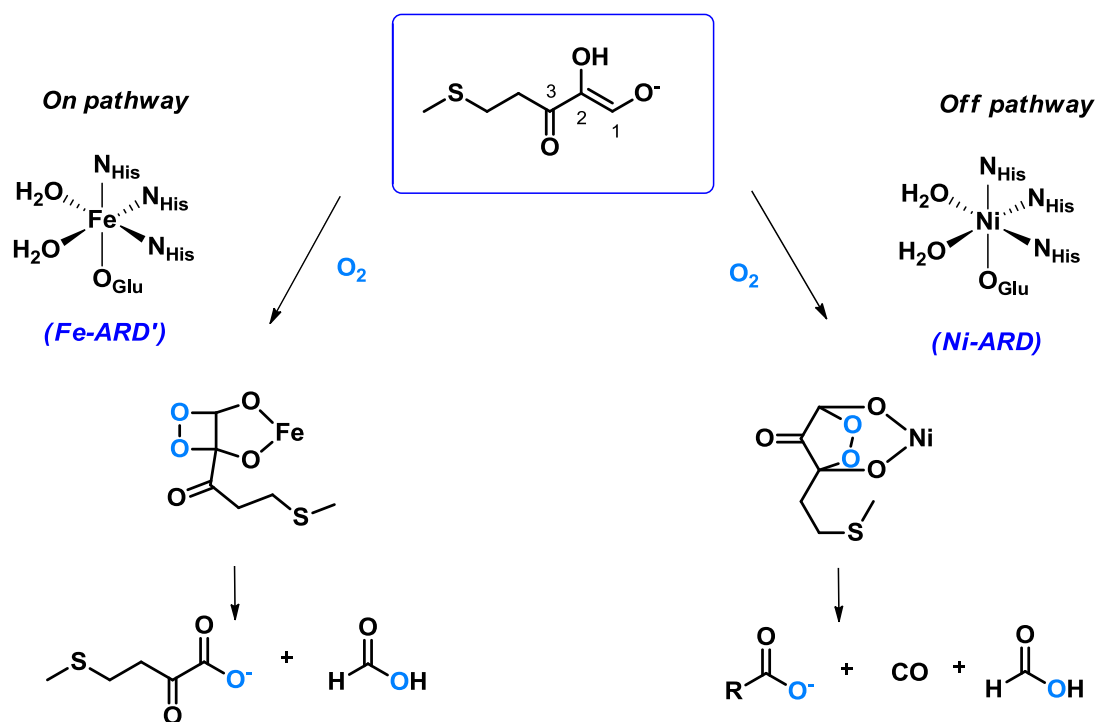
A series of  $\text{Tp}^{\text{R}2}\text{Fe}(\text{acac}^{\text{x}})$  complexes<sup>75</sup> reported by the group of Fiedler exhibited activity comparable to the Siewert system. The nature of the substituents was found to affect the rate with which the complexes react with  $\text{O}_2$  to form the proposed  $\text{Fe}^{\text{III}}$  peroxo intermediate, with bulkier substituents such as Ph resulting in much slower reactions. Moreover, among all the series of acetylacetonates investigated, only activated electron rich malonates could be cleaved (Scheme 31).



**Scheme 31.** Different reactivity of Fiedler's iron biomimetic complexes

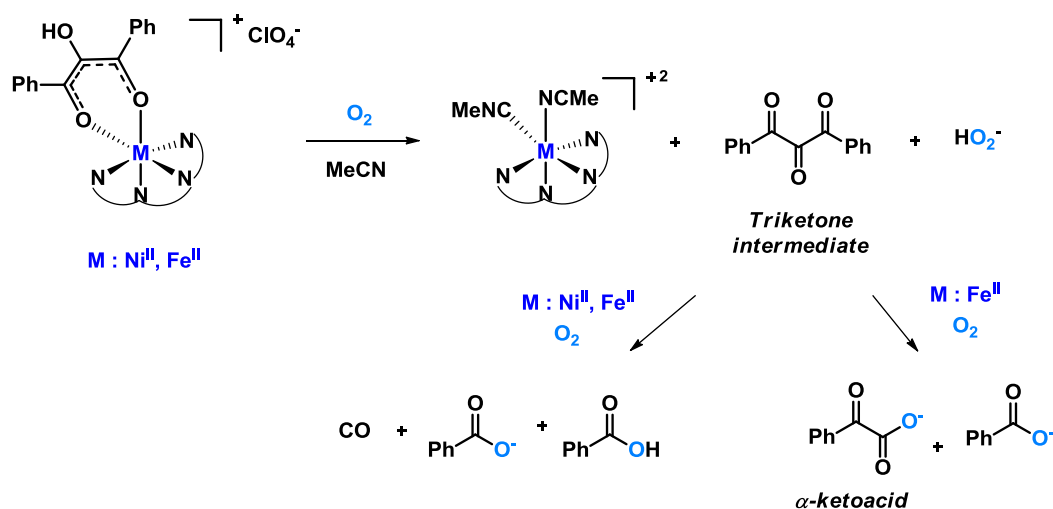
#### 1.3.4.2.2. Iron complexes that mimic acireductone dioxygenases (ARD)

ARD enzymes are found in the methionine salvage pathway, an omnipresent pathway in biological systems for the regeneration of methionine from 5'-methylthioadenosine.<sup>76</sup> Interestingly, two pathways for the degradation of the 1,2-hydroxy-3-oxo-(S)-methyl thiopentene intermediate, which are catalysed by different dioxygenases, have been discovered in aerobic systems.<sup>77</sup> In the on-pathway, the iron-containing dioxygenase (Fe-ARD) catalyses the regioselective aerobic C(1)-C(2) cleavage of the intermediate releasing formic acid and an  $\alpha$ -ketoacid, which is further reacted to generate methionine. In the off-pathway, the nickel-containing dioxygenase (Ni-ARD) cleaves both the C(1)-C(2) and C(2)-C(3) bonds, generating formic acid, CO and a carboxylic acid (Scheme 32).

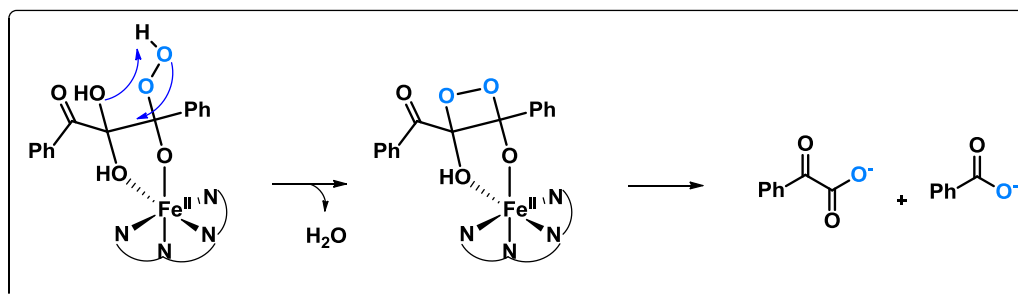


**Scheme 32.** Methionine salvage On and Off pathways

In order to understand the origins behind the different regioselectivity exhibited by such Fe and Ni dioxygenases, the group of Berreau reported the mononuclear  $[(6-Ph_2TPA)Fe(PhC(O)C(R)C(O)Ph)X]$  complexes, where  $6-Ph_2TPA = N,N$ -bis((6-phenyl-2-pyridyl)methyl)- $N$ -(2-pyridylmethyl)amine,  $R = H, OH$  and  $X = OTf, ClO_4$ , bound to a  $\beta$ -diketonate ligand, and explored their reactivity under dry and wet aerobic conditions<sup>78</sup> (Scheme 33). Surprisingly, the oxidation of a triketone intermediate species facily occurred in the presence of the Fe complex, followed by its C-C cleavage that afforded the ketoacid product. However, such oxidative dehydration was not efficient with an analogue Ni-based complex. Thus, the dehydration of an intermediate appears to be the major reason behind the different regioselectivity between the Fe and Ni-based ARDs.



**Proposed C-C cleavage of the triketone intermediate:**



**Scheme 33.** Biomimetic Fe and Ni TPA complexes showing different reactivity towards the oxidation of a triketone intermediate

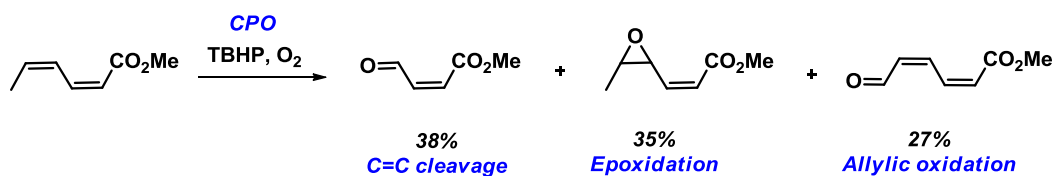
### 1.3.4.3. Aerobic cleavage of olefins

The selective C=C cleavage of alkenes using biocatalysts has become a growing area of research due to the excellent chemo- and regioselectivity with which heme and nonheme enzymes can cleave olefins under very mild conditions (r.t., atmospheric O<sub>2</sub>, aqueous media).<sup>79</sup> As biocatalysts do not suffer from the harsh conditions and safety issues associated with chemical C-C cleavages, they have gained popularity for the production of costly natural flavour compounds.<sup>80</sup>

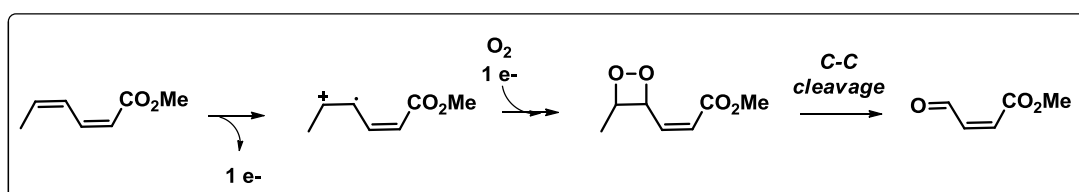
#### 1.3.4.3.1. Olefin cleavage with heme peroxidases

Conjugated dienoic esters were cleaved to  $\alpha,\beta$ -unsaturated aldehydes using natural chloroperoxidase (CPO) as catalysts and TBHP as oxidant.<sup>81</sup> The aldehyde product was formed mainly from the trans-dienes under aerobic atmosphere. However, *cis*-dienes mainly

afforded the allylic oxidation product. The postulated reaction mechanism invokes the formation of an intermediate radical cation via electron transfer from the olefin to a  $\text{Fe}^{\text{V}}=\text{O}(\text{OH})$  species. Reaction of the radical cation with  $\text{O}_2$  results in the formation of a dioxetane intermediate that is cleaved to generate the aldehyde product (scheme 34).

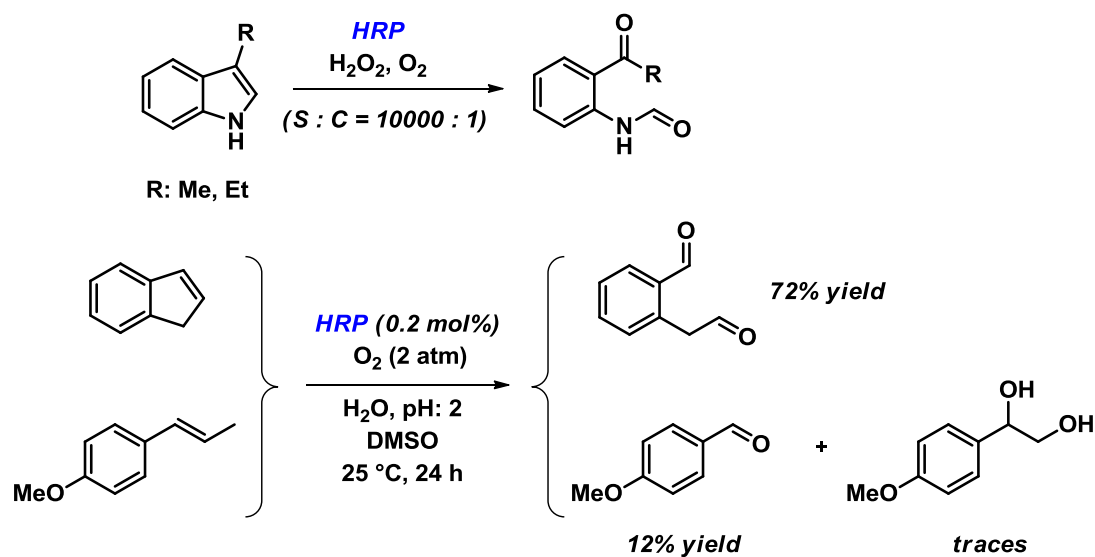


**Proposed mechanism:**



**Scheme 34.** Oxidative cleavage of methyl-(2Z, 4Z)-hexadecanoate catalysed by CPO

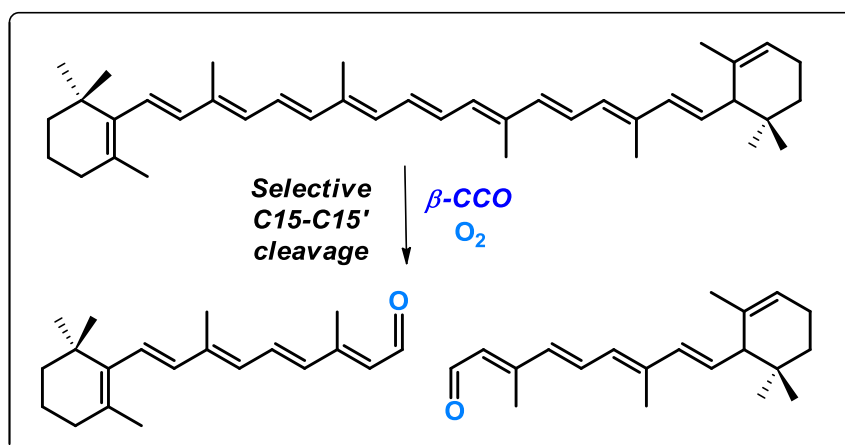
Horseradish peroxidase (HRP) is a very versatile peroxidase enzyme that has shown catalytic activity for the oxidative cleavage of 3-alkylindoles to acylformanilides in the presence of catalytic amounts of  $\text{H}_2\text{O}_2$  under aerobic atmosphere.<sup>82</sup> Additionally, conjugated C=C bonds of substrates such as indene and *trans*-anethole were also cleaved with good yields under pressurised aerobic atmosphere (2 atm  $\text{O}_2$ ) and acidic aqueous conditions<sup>83</sup> (Scheme 35).

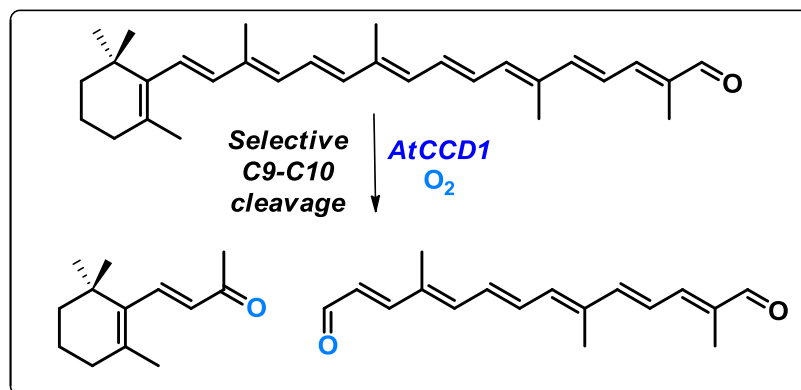


**Scheme 35.** Aerobic cleavages of allylic olefins catalysed by HRP

#### 1.3.4.3.2. Olefin cleavage with heme and nonheme oxygenases

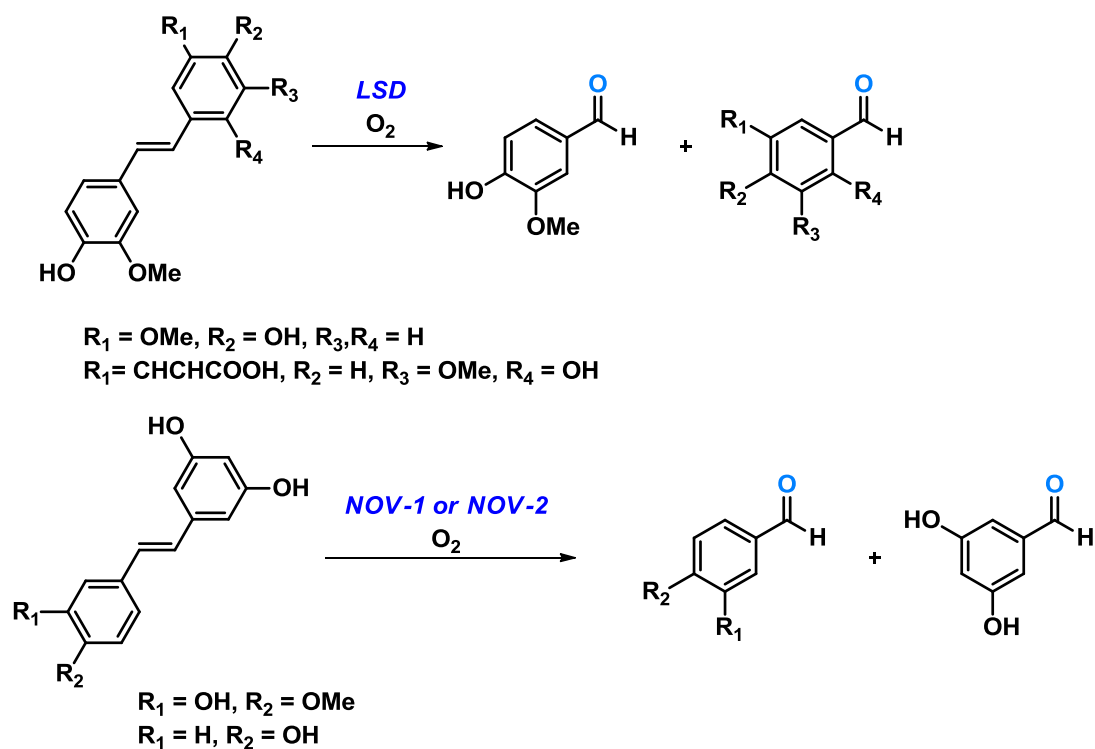
Carotenoid Cleavage Oxygenases (CCOs) were found to catalyse the selective C=C bond cleavage of carotenoids, affording valuable apocarotenoids as products.<sup>84</sup> The cleavage occurs with exquisite specificity, with different enzymes of this family being capable of oxidatively cleaving C=C bonds at different positions<sup>85</sup> (Scheme 36). Even though the reaction mechanism are still unclear, some of this enzymes are been investigated as biocatalysts for industrial and academic purposes due to the importance of apocarotenoids in the aroma industry.<sup>86</sup>





**Scheme 36.** Selective C=C cleavage of carotenoids catalysed by different CCO enzymes

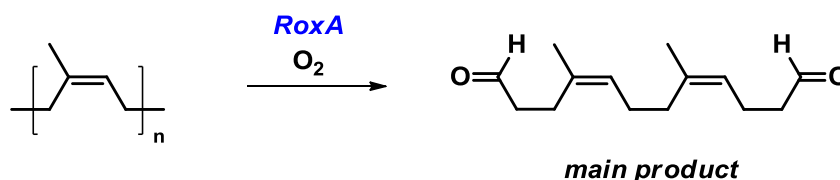
Stilbene- $\alpha$ -oxygenases constitute a family of enzymes capable of cleaving stilbene type substrates into carbonyl compounds. Such enzymes specifically react with stilbenes in a *trans*-configuration and incorporating a hydroxyl or a methoxy group in *para*-position to the C=C bond<sup>87</sup> (Scheme 37).



**Scheme 37.** C=C cleavage of stilbene substrates catalysed by various stilbene oxygenases



Finally, a purified protein isolated from *Xanthomonas sp.* was found capable of cleaving C=C bonds of natural rubbers, such as poly-(*cis*-1,4-isoprene).<sup>88</sup> Such protein, known as rubber oxygenase (RoxA), exhibited high specificity, cleaving C=C bonds at regular intervals of three isoprene units (Scheme 38). Mechanistic investigations are consistent with a dioxygenase mode of reactivity.



**Scheme 38.** C=C cleavage of poly-(*cis*-1,4-isoprene) catalysed by RoxA

#### 1.4. Aims of the thesis

Catalytic selective oxidation of organic chemicals is identified as the most important area to impact the future chemical industry.<sup>89</sup> Biomimetic iron-based complexes with tetradentate *N*-donor ligands have been extensively studied and applied for the oxidation of complex organic substrates using H<sub>2</sub>O<sub>2</sub> as the oxygen source. Despite the advances achieved in the area during the last decade, significant limitations are still unresolved. For instance, the development of catalyst capable of dioxygen activation and compatible with electron rich functionalities are highly desirable.

This thesis covers our efforts and possible solutions for many of the limitations that affect iron-catalysed selective oxidations, with the main objectives being:

- 1) To investigate new ligand designs aiming for more efficient iron-catalysed aerobic oxidations.
- 2) To gain some mechanism understanding of the oxidation processes developed with such catalysts.

This thesis is mainly concerned with the application of a novel class of iron complexes for the oxidation of two major classes of substrates: oxidation of ethers and olefins. While ether oxidation has been studied for a long time, catalysts capable of activating O<sub>2</sub> for such reactions are few. It was hoped that with a novel class of catalysts such oxidations could be performed in a greener, more selective manner and applied for organic syntheses.

Even though the selective oxidation of organic substrates using biologically-inspired Fe catalysts has become an extensive area of research, the development of iron-based catalysts for the selective aerobic cleavage of organic compounds has received much less attention. In fact, such catalysts are often seen either as tools to investigate enzymatic processes or as alternatives for the usage of biomass in fuel production or bioremediation processes<sup>66</sup>. However, we envisioned that catalysts capable of undergoing selective aerobic cleavage of C-C bonds in organic substrates would facilely become an attractive new tool for synthesising valuable organic compounds. Thus, this thesis also includes our investigations in the area of selective aerobic cleavage of aliphatic and olefinic C-C bonds and aliphatic C-O bonds, with the major goals being:

- 1) To provide an alternative for the synthesis of complex oxygenated products, which cannot be obtained by current oxidation methodologies but can be accessed by selective oxidative cleavage.
- 2) To replace less environmentally benign oxidative protocols employed in organic synthesis with greener aerobic cleavages.
- 3) To ultimately develop novel synthetic methodologies.

---

## 1.5. References

- [1] Collins, T. *Science* **2001**, *291*, 48
- [2] Poliakkof, M.; Fitzpatrick, M.J.; Farren, T.R.; Anastas, P.T. *Science* **2002**, *297*, 807. In the case of pharmaceutical industry, see for instance: (a) Davies, I.W.; Welch, C.J. *Science* **2009**, *325*, 701. (b) Warner, J.C. *Abstracts of papers, 239<sup>th</sup> ACS National Meeting*, San Francisco CA USA, March 21-25 (2010).
- [3] Selected examples: (a) Kolb, H.C.; Finn, M.G.; Sharpless, K.B. *Angew. Chem. Int. Ed.* **2001**, *40*, 2004. (b) Moses, J. E.; Moorhouse, A. D. *Chem. Soc. Rev.* **2007**, *36*, 1249. (c) Hein, C. D.; Liu, X.-M.; Wang, D. *Pharmaceutical research* **2008**, *25(10)*, 2216.
- [4] Enthaler, S.; Junge, K.; Beller, M. *Angew. Chem. Int. Ed.* **2008**, *47*, 3317.
- [5] Holzwarth, M. S.; Plietker, B. *Chem. Cat. Chem.* **2013**, *5*, 1650.
- [6] List, B.; Yang, J.W. *Science* **2006**, *313*, 1584. An example of its potential: Northrup, A.B.; Mac Millan, D.W.C. *Science* **2005**, *305*, 1752.
- [7] Bommarius, A.S.; Riebel, B.R. *Biocatalysis* (Wiley-VCH Chapter 1, 2004) In industry: Schoemaker, H.E.; Mink, D.; Wubbolts, M. G. *Science* **2003**, *299*, 1694.
- [8] Plietker, B. *Iron catalysis in Organic Chemistry* (Wiley-VCH, 2008).
- [9] Bolm, C.; Legros, J.; Le Paih, J.; Zani, L. *Chem. Rev.* **2004**, *104*, 6217.
- [10] Abu-Omar, M. M.; Luaiza, A.; Hontzeas, N. *Chem. Rev.* **2005**, *105*, 2227.
- [11] Kikuchi, G.; Yoshida, T.; Noguchi, M., *Biochem. Biophys. Res. Commun.* **2005**, *338*, 558.
- [12] Que Jr., L.; Tolman, W. B. *Nature* **2008**, *455*, 333.
- [13] Selected examples: (a) Kim, C.; Chen, K.; Kim, J.; Que Jr., L. *J. Am. Chem. Soc.* **1997**, *119*, 5964. (b) Chen, K.; Que Jr., L. *J. Am. Chem. Soc.* **2001**, *123*, 6327. (c) Chen, K.; Costas, M.; Kim, J.; Tipton, A. K.; Que Jr., L. *J. Am. Chem. Soc.* **2002**, *124*, 3026. (d) Suzuki, K.; Oldenburg, P. D.; Que Jr., L. *Angew. Chem. Int. Ed.* **2008**, *47*, 1887. (e) Wang, D.; Farquhar, E. R.; Stubna, A.; Munck, E.; Que Jr., L. *Nat. Chem.* **2009**, *1*, 145.

- (f) Mukherjee, A.; martinho, M.; Bominar, E. L.; Munck, E.; Que Jr., L. *Angew. Chem. Int. Ed.* **2009**, *48*, 1780.
- [14] White, M. C.; Doyle, A. G.; Jacobsen, E. N. *J. Am. Chem. Soc.* **2001**, *123*, 7194.
- [15] Selected examples: (a) Chen, M. S.; White, M. C. *Science* **2007**, *318*, 783. (b) Chen, M. S.; White, M. C. *Science* **2010**, *327*, 566. (c) White, M. C. *Science* **2012**, *335*, 807. (d) Bigi, M. A.; Reed, S. A.; White, M. C. *J. Am. Chem. Soc.* **2012**, *134*, 9721. (e) Gorminsky, P. E.; White, M. C., *J. Am. Chem. Soc.* **2013**, *135*, 14052.
- [16] Examples of iron-porphyrin complexes: (a) Nam, W.; Oh, S.-Y.; Sun, Y. J.; Kim, J.; Kim, W.-K.; Woo, S. K.; Shin, W. *J. Org. Chem.* **2007**, *68*, 7903. (b) Srivinas, K. A.; Kumar, A.; Chauhan, M. S. *Chem. Commun.* **2002**, 2456. (c) Stephenson, N. A.; Bell, A. T., *J. Am. Chem. Soc.* **2005**, *127*, 8635. (d) Grinstaff, M. W.; Hill, M. G.; Labinger, J. A.; Gray, H. B. *Science* **1994**, *264*, 1311.
- [17] See section 2.
- [18] England, J.; Britovsek, G. J. P.; Rabadia, N.; White, A. J. P. *Inorg. Chem.* **2007**, *46*, 3752.
- [19] (a) Solomon, E. I.; Brunold, T. C.; Davis, M. I.; Kemsley, J. N.; Lee, S.-K.; Lehnert, N.; Neese, F.; Skulan, A. J.; Yang, Y.-S.; Zhou, J. *Chem. Rev.* **2000**, *100*, 235. (b) Dekker, A.; Chow, M. S.; Kemsley, N. J.; Lenhert, N.; Solomon, E. I. *J. Am. Chem. Soc.* **2006**, *128*, 4719.
- [20] Taktak, S.; Ye, W.; Herrera, A. M.; Rybak-Akimova, E. V. *Inorg. Chem.* **2007**, *46*, 2929.
- [21] Niwa, T.; Nakada, M. *J. Am. Chem. Soc.* **2012**, *134*, 13538.
- [22] (a) Groves, J. T.; Myers, R. S. *J. Am. Chem. Soc.* **1983**, *105*, 5791. (b) Rose, E.; Ren, Q.-Z.; Andrioletti, B. *Chem. Eur. J.* **2004**, *10*, 224.
- [23] (a) Tse, M. K.; Bhor, S.; Klawonn, M.; Döbler, C.; Beller, M. *Tetrahedron Lett.* **2003**, *44*, 7479. (b) Tse, M. K.; Bhor, S.; Klawonn, M.; Anilkumar, G.; Jiao, H.; Döbler, G.; Spannenberg, A.; Magerlein, W.; Hugl, H.; Beller, M. *Chem. Eur. J.* **2006**, *12*, 1855. (c)

- Tse, M. K.; Bhor, S.; Klawonn, M.; Anilkumar, G.; Jiao, H.; Döbler, G.; Spannenberg, A.; Magerlein, W.; Hugl, H.; Beller, M. *Chem. Eur. J.* **2006**, *12*, 1875. (d) Tse, M. K.; Jiao, H.; Anilkumar, G.; Bitterlich, B.; Gelalcha, F. G.; Beller, M. *J. Organomet. Chem.* **2006**, *691*, 4419. (e) Bhor, S.; Anilkumar, G.; Tse, M. K.; Klawonn, M.; Döbler, G.; Bitterlich, B.; Grotevendt, A.; Beller, M. *Org. Lett.* **2005**, *7*, 3393.
- [24] Stahl, S. S. *Science* **2005**, *309*, 1824.
- [25] Clerici, M. G.; Ricci, M.; Strukul, G. *Oxidation reactions in industry* (Wiley, Chapter 2, p. 23, 2007).
- [26] Barton, D. H. R.; Gastiger, M. J.; Motherwell, W. B. *J. Chem. Soc., Chem. Commun.* **1983**, 41.
- [27] Schuscharadt, U.; Carvalho, W. A.; Spinace, E. V. *Synlett* **1993**, 713.
- [28] Stavropoulos, P.; Celenligil-Cetin, R.; Tapper, A. E. *Acc. Chem. Res.* **2001**, *34*, 745.
- [29] Barton, D. H. R.; Hu, B.; Taylor, D. K.; Rojas Wahl, R. U. *J. Chem. Soc., Perkin Trans.* **1996**, *2*, 1031.
- [30] Barton, D. H. R.; Beviere, S. D.; Chavasiri, W.; Csuhai, E.; Doller, D.; Liu, W.-G. *J. Am. Chem. Soc.* **1992**, *114*, 2147.
- [31] Barton, D. H. R. *Tetrahedron* **1998**, *54*, 5805.
- [32] Kong, D.; Martell, A. E.; Motekaitis, R. J. *Ind. Eng. Chem. Res.* **2000**, *39*, 3429.
- [33] Selected examples of Mukaiyama's reactions: (a) Mukaiyama, T.; Takai, T.; Yamada, T.; Rhode, O. *Chem. Lett.* **1990**, 1661. (b) Yamada, T.; Takai, T.; Rhode, O.; Mukaiyama, T. *Bull. Chem. Soc. Jpn.* **1991**, *64*, 2109. (c) Murahashi, S.; Oda, Y.; Naota, T. *J. Am. Chem. Soc.* **1992**, *114*, 7913. (d) Yoroazu, K.; Takai, T.; Yamada, T.; Mukaiyama, T. *Bull. Chem. Soc. Jpn.* **1994**, *67*, 2195.
- [34] (a) Mastroilli, P.; Nobile, F. C. *Tetrahedron Lett.* **1994**, *35*, 4193. (b) Mastroilli, P.; Nobile, F. C., *J. Mol. Catal.* **1994**, *99*, 19. (c) Giannandrea, R.; Mastroilli, P.; Nobile, F. C.; Suranna, G. P., *J. Mol. Catal.* **1994**, *99*, 27.
- [35] Mastroilli, P.; Nobile, F. C.; Suranna, G. P.; Lopez, L. *Tetrahedron* **1995**, *51*, 7943.

- [36] Feig, A. L.; Lippard, S. J. *Chem. Rev.* **1994**, *94*, 759.
- [37] Ha, E. H.; Ho, R. Y. N.; Kisiel, J. F.; Valentine, J. S. *Inorg. Chem.* **1995**, *34*, 2265.
- [38] Schroeder, K.; Join, B.; Amali, A. J.; Junge, K.; Ribas, X.; Costas, M.; Beller, M. *Angew. Chem. Int. Ed.* **2011**, *50*, 1425.
- [39] (a) Straganz, G. D.; Glieder, A.; brecher, L.; Ribbons, D. W.; Steiner, W. *Biochem. J.* **2003**, *369*, 573. (b) Straganz, G. D.; Nidetzky, B. *J. Am. Chem. Soc.* **2005**, *127*, 12306.
- [40] Shilov, A. E.; Shul'pin, G. B. *Activation and Catalytic Reactions of Saturated Hydrocarbons in the Presence of Metal Complexes* (Kluwer Academic Publishers, Dordrecht/Boston/London, 2000).
- [41] Shul'pin, G. B.; Kats, M. M. *Petrol. Chem.* **1991**, *31*, 647.
- [42] Shul'pin, G. B.; Nizova, G. V.; Kozlov, Y. N. *New J. Chem.* **1996**, *20*, 1243.
- [43] Rosenthal, J.; Pistorio, B. J.; Chng, L. L.; Nocera, D. G. *J. Org. Chem.* **2005**, *70*, 1885.
- [44] Rosenthal, J.; Luckett, T. D.; Hodgkiss, J. M.; Nocera, D. G. *J. Am. Chem. Soc.* **2006**, *128*, 6546.
- [45] a) Cukier, R. I.; Nocera, D. G. *Annu. Rev. Phys. Chem.* **1998**, *49*, 337. b) Reece, S. Y.; Nocera, D. G. *Annu. Rev. Biochem.* **2009**, *78*, 673.
- [46] Avenier, F.; Herrero, C.; Leibl, W.; Desbois, A.; Guillot, R.; Mahy, J.-P.; Aukauloo, A. *Angew. Chem. Int. Ed.* **2013**, *52*, 1.
- [47] White, M. C. *Science* **2012**, *335*, 807.
- [48] See Chapter 3, section 3.1. Introduction
- [49] Berkowitz, L. M.; Rylander, P. N. *J. Am. Chem. Soc.* **1958**, *80*, 6682.
- [50] Smith III, A. B.; Scarborough Jr. R. M. *Synth. Commun.* **1980**, *10*, 205.
- [51] Schmidt, H.-J.; Schafer, H. J. *Angew. Chem. Int. Ed.* **1979**, *18*, 69.
- [52] Harrison, I. T.; Harrison S. *J. Chem. Soc., Chem. Commun.* **1966**, *20*, 752.
- [53] (a) Stevens, C. L.; Bryant, C. P. *Methods Carbohydr. Chem.* **1972**, *3*, 337. (b) Baker, D. C.; Horton, D.; Tindall, G. C. *Methods Carbohydr. Chem.* **1976**, *7*, 3. (c) Giddings, S.; Mills, A. *J. Org. Chem.* **1998**, *53*, 1103.

- [54] Carlsen, P. H. J.; Katsuki, T.; Martin, V. S.; Sharpless, K. B. *J. Org. Chem.* **1981**, *46*, 3936.
- [55] Gonzsalvi, L.; Arends, I. W. C. E.; Moilanen, P.; Sheldon R. A. *Adv. Synth. Catal.* **2003**, *345*, 1321.
- [56] Li, H.; Li, Z.; Shi Z. *Tetrahedron* **2009**, *65*, 1856.
- [57] Shi, M. *J. Chem. Research* **1998**, *9*, 592.
- [58] Fazlur- Rahman, A. K.; Chai, J.-C.; Nicholas, K. M. *J. Chem. Soc., Chem. Commun.* **1992**, 1334.
- [59] Sen, A.; Lin, M.; Kao, L.-C.; Hutson, A. C. *J. Am. Chem. Soc.* **1992**, *114*, 6385.
- [60] Reetz, M. T.; Tollner, K. *Tetrahedron Lett.* **1995**, *36*, 9461.
- [61] Minakata, S.; Imai, E.; Ohshima, Y.; Inaki, K.; Ryu, I.; Komatsu, M., Ohshiru, Y. *Chem. Lett.* **1996**, *25*, 19.
- [62] Aresta, M.; Fragale, C.; Quaranta, E.; Tomáís, I. *J. Chem. Soc., Chem. Commun.* **1992**, 315.
- [63] Chen, M. S.; White, M. C. *Science* **2010**, *327*, 566.
- [64] Lange, S. J.; Que Jr., L. *Curr. Opin. Chem. Biol.* **1998**, *2*, 159.
- [65] (a) Bugg, T. D. H.; Ramaswamy, S. *Curr. Opin. Chem. Biol.* **2008**, *12*, 134. (b) Broderick, J. B. *Essays Biochem.* **1999**, *34*, 173.
- [66] Allpress, C. J.; Berreau, L. M. *Coord. Chem. Rev.* **2013**, *257*, 3005.
- [67] Takenaka, S.; Murakami, S.; Shinke, R.; Hatakeyama, K.; Yukawa, H.; Aoki, K. *J. Biol. Chem.* **1997**, *272*, 14727.
- [68] Colabroy, K. L.; Zhai, H.; Li, T.; Ge, Y.; Zhang, Y.; Liu, A.; Ealick, S. E.; McLafferty, F. W.; Begley, T. P. *Biochemistry* **2005**, *44*, 7623.
- [69] Chakraborty, B.; Paine, T. K. *Angew. Chem. Int. Ed.* **2012**, *52*, 920.
- [70] Bittner, M. M.; Lindeman, S. V.; Fiedler, A.T. *J. Am. Chem. Soc.* **2012**, *134*, 5460.
- [71] (a) Straganz, G. D.; Glieder, A.; Brecker, L.; Ribbons, D. W.; Steiner, W. *Biochem. J.* **2003**, *369*, 573. (b) Straganz, G. D.; Nidetzky, B. *J. Am. Chem. Soc.* **2005**, *127*, 12306.

- [72] (a) Ballantyne, G.; Cawley, T. J. *J. Appl. Toxicol.* **2001**, *21*, 165. (b) Thurston, R. V.; Gilfoil, T. A.; Meyn, E. L.; Zajdal, R. K.; Aoki, T. I.; Veith, G. D. *WaterRes.* **1985**, *19*, 1145. (c) Bringmann, G.; Kühn, R. *Water Res.* **1980**, *14*, 231.
- [73] Straganz, G.; Brecker L.; Weber, H. J.; Steiner, W.; Ribbons, D.W. *Biochem. Bio-phys. Res. Commun.* **2002**, *297*, 232.
- [74] Siewert, I.; Limberg, C.; Demeshko, S.; Hoppe, E. *Chem. Eur. J.* **2008**, *14*, 9377.
- [75] (a) Park, H.; Baus, J. S.; Lindeman, S. V.; Fiedler, A. T. *Inorg. Chem.* **2011**, *50*, 11978. (b) Bittner, M. M.; Baus, J. S.; Lindeman, S. V.; Fiedler, A. T. *Eur. J. Inorg. Chem.* **2012**, 1848. (c) Park, H.; Bittner, M. M.; Baus, J. S.; Lindeman, S. V.; Fiedler, A. T. *Inorg. Chem.* **2012**, *51*, 10279.
- [76] Albers, E. *IUBMB Life* **2009**, *61*, 1133.
- [77] Pochapsky, T. C.; Ju, T.; Dang, M.; Beaulieu, R.; Pagani, G. M.; OuYang, B. In *Metal Ions in Life Sciences* (Sigel, A., Sigel, H., Sigel, R. K. O., Eds.; Wiley-VCH: Weinheim, Germany, 2007; Vol. 2, pp 473–500).
- [78] Allpress, J.P.; Grubel, K.; Szajna-Fuller, E.; Arif, A. M.; Berreau, L. M. *J. Am. Chem. Soc.* **2013**, *135*, 659.
- [79] Mutti, F. G. *Bioinorg. Chem. Appl.* **2012**, doi: 10.1155/2012/626909
- [80] Schrader, J.; Etschmann, M. M. W.; Sell, D.; Hilmer, J. M.; Rabenhorst, J. *Biotechnology Lett.* **2004**, *26*, 463.
- [81] Bougioukou, D. J.; Smonou, I. *Tetrahedron Lett.* **2002**, *43*, 339. (b) Bougioukou, D. J.; Smonou, I. *Tetrahedron Lett.* **2002**, *43*, 4511.
- [82] Ling, K. Q.; Sayre, L. M. *Bioinorg. Med. Chem.* 2005, **13**, 3543.
- [83] Mutti, F. G.; Lara, M.; Kroutil, M.; Kroutil, W. *Chemistry* **2010**, *16*, 14142.
- [84] Auldridge, M. E.; McCarthy, D. R.; Klee, H. J. *Curr. Opin. Plant. Biol.* **2006**, *9*, 315.
- [85] (a) Marasco, E. K.; Vay, K.; Schmidt-Dannert, C. *J. Biol. Chem.* **2006**, *281*, 31583. (b) Leuenberger, M. G.; Engeloch-jarret, C.; Woggon, W. D. *Angew. Chem.* **2001**, *40*, 2614.
- [86] Nacke, C.; Schrader, J. *J. Mol. Catal. B.* **2012**, *77*, 67.



[87] (a) Kamoda, S.; Saburi, Y. *Bioscience, Biotechnology and Biochemistry* **1993**, *57*, 931.

(b) Kamoda, S.; Terada, T.; Saburi, Y. *Bioscience, Biotechnology and Biochemistry* **1993**, *63*, 1394. (c) Makoto, A.; Niwa, S.; Kamoda, S.; Saburi, Y. *Bioscience, Biotechnology and Biochemistry* **2001**, *11*, 884.

[88] Braaz, R.; Armbruster, W.; Jendrossek, D. *Applied Environmental Microbiology* **2005**, *71*, 2473.

[89] Technology Vision 2020: Catalyst technology roadmap report,

<http://www.osti.gov/scitech/biblio/544046>

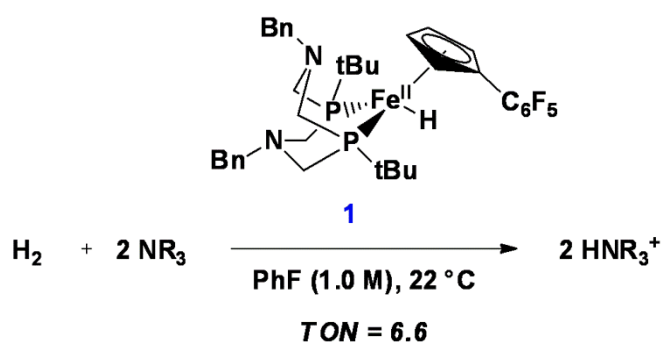
## *Chapter 2*

# **DESIGN, SYNTHESIS AND PROPERTIES OF NOVEL PYBISULIDINE TYPE LIGANDS**

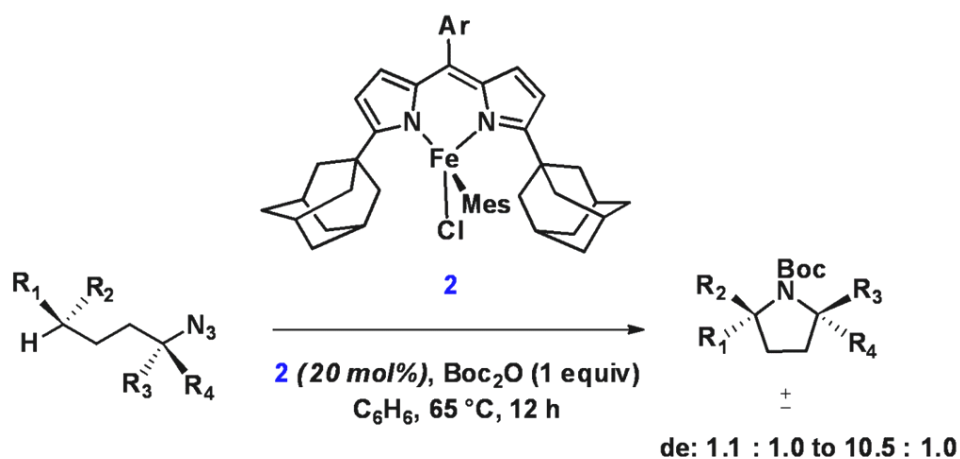
## 2.1. Introduction

### 2.1.1. Ligand design in homogeneous iron catalysis

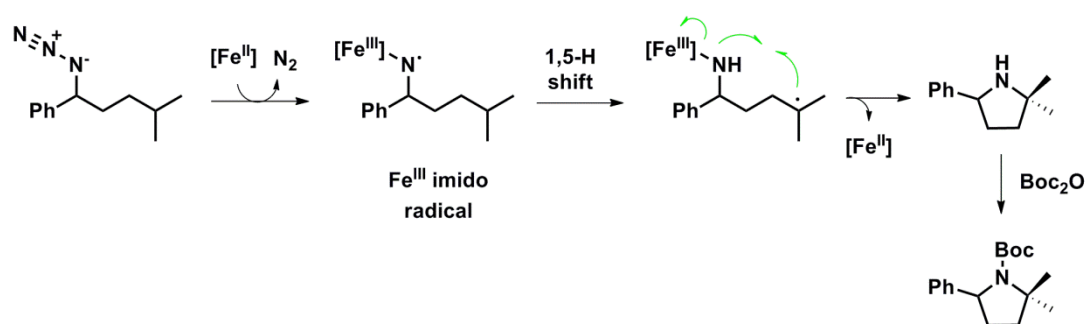
Very sophisticated catalytic reactions are being developed nowadays in the area of iron catalysis by introducing new ligand designs. For instance, Bullock and co-workers have reported the novel  $\text{Cp}^{\text{C}_6\text{F}_5}\text{Fe}(\text{P}^{\text{tBu}}_2\text{N}^{\text{Bn}})_2\text{H}$  complex as an electrocatalyst for the oxidation of  $\text{H}_2$ .<sup>1</sup> A rational ligand design introducing pendant amino groups and bulky phosphines favours the coordination and splitting of the  $\text{H}_2$  molecule. The presence of the  $\text{C}_6\text{F}_5$  group in the Cp moiety increases the acidity of the iron-dihydrogen complex, allowing a faster proton transfer during the catalytic cycle (Scheme 1). In addition, iron-dipyrrinato complexes developed by the group of Betley can serve as catalysts for the direct amination of aliphatic C-H bonds.<sup>2</sup> These dipyrrinato ligands provide the perfect electronic environment for the formation of an iron-imido radical intermediate in which both Fe and N- atoms have radical character which facilitates H-abstraction from the substrate and a radical recombination process that enables the formation of the amine product (Scheme 2). Therefore, state-of-the-art ligand design is crucial to achieve catalytic activity in such iron-catalysed transformations.



**Scheme 1.** Iron electrocatalyst for  $\text{H}_2$  oxidation

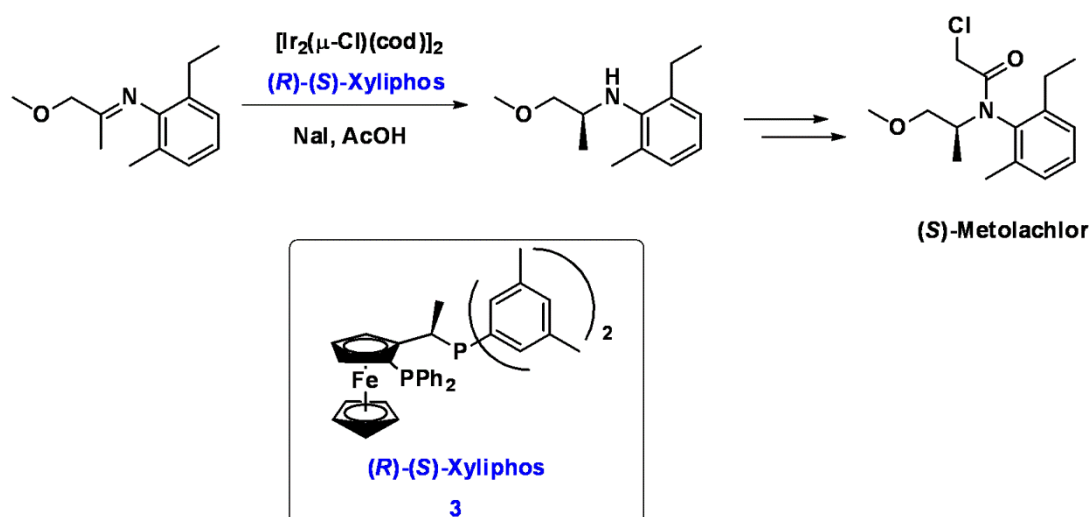


Postulated mechanism:



**Scheme 2.** Iron-dipyrinato catalyst for CH amination

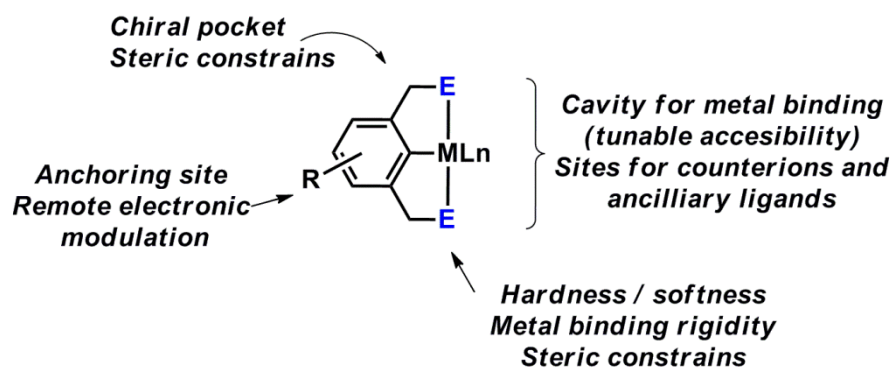
From these examples it can already be intuited that the design of a new good catalyst is a difficult art that pursues a perfect balance between activity and selectivity: the catalyst must achieve good activity in a specific transformation without generating an undesired myriad of byproducts. Additionally, the catalyst must be relatively stable under the reaction conditions so the efficiency of the transformation is not compromised.<sup>3</sup> The tremendous difficulty behind new catalyst design is well represented in the Ir-Xyliphos catalyst for the industrial production of (*S*)-metolachlor, with fourteen years of intense research invested on its design and implementation<sup>4</sup> (Scheme 3). A careful ligand design, capable of modulating the electronic and steric properties of the metal centre, is often viewed as the best strategy to create a good homogeneous catalyst.<sup>5</sup> A cost effective synthetic route and the stability of the pre-catalyst and active catalytic species are other important aspects that influence ligand design, especially for industrial applications.<sup>4</sup>



**Scheme 3.** Industrial synthesis of (*S*)-metolachlor using an Ir-Xyliphos catalyst

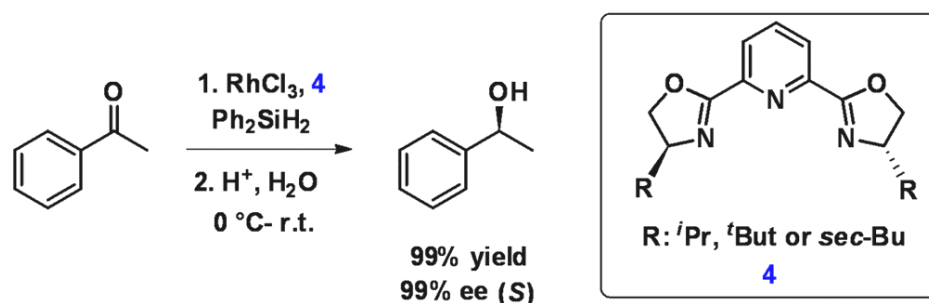
### 2.1.2. PyBox ligands: successes and challenges

Since the late 1990's, pincer ligands have been widely explored in homogeneous catalysis due to the high activity, stability and variability of the resulting metal complexes.<sup>6</sup> These tridentate ligands are based on an aromatic backbone tethered by two electron donor groups (E) with different spacers such that they can be easily modified at different sites allowing control of the steric and electronic properties of the metal centre<sup>7</sup> (Scheme 4). For these reasons, an ample variety of applications have emerged for pincer type complexes in the areas of catalysis, molecular recognition and supramolecular chemistry.<sup>6</sup>

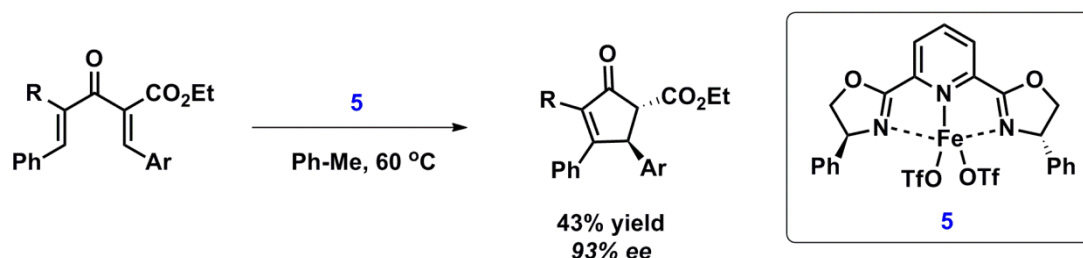


**Scheme 4.** Potential sites for pincer type ligand modifications

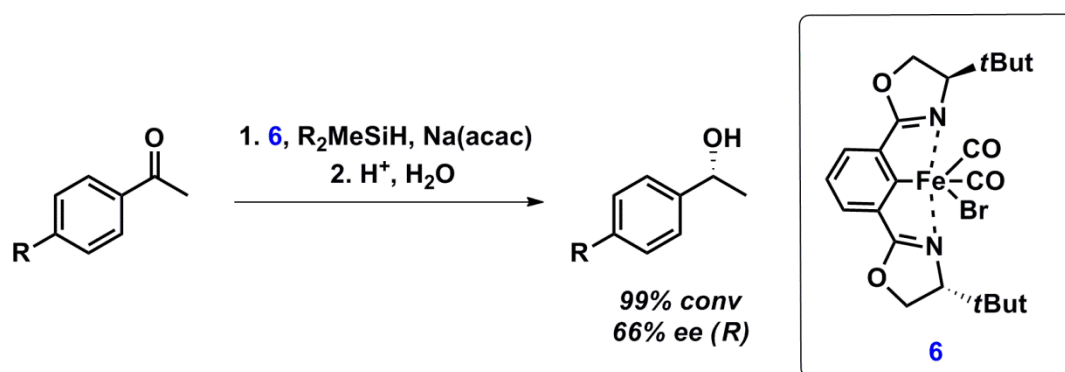
Among pincer ligands, *N*-donor based pyridine bis(oxazolanyl) (PyBox) ligands have become popular in catalysis since their introduction by the group of Nishiyama in 1989 for the asymmetric hydrosilylation of ketones<sup>8</sup> (Scheme 5). The facile and cost effective preparation of this type of ligands<sup>9</sup> in conjunction with their exceptional stereoinductive effects derived from their  $C_2$ -symmetry<sup>10</sup> have turned them into widely applied ligands in catalysis. Nonetheless, PyBox ligands in combination with commercially available iron salts have shown limitations in terms of both activity and stereinduction. For instance, the enantioselective Nazarov cyclization of divinyl ketones using  $Fe(OTf)_2$ -PyBox complexes has been achieved with low yields (43%) due to the limited solubility and activity of the iron complex in the reaction solvent<sup>11</sup> (Scheme 6). Additionally, Nishiyama and co-workers reported a Fe-Phebox complex for the enantioselective hydrosilylation of ketones with good activity (99%) but only moderate enantioselectivity (63% ee) (Scheme 7), whereas excellent enantioselectivity (99%) was achieved with a similar Rh complex<sup>12</sup> (Scheme 5).



**Scheme 5.** Asymmetric hydrosilylation of ketones using Rh-PyBox complexes



**Scheme 6.** Iron-PyBox complexes as catalyst in Nazarov cyclizations



**Scheme 7.** Iron-PheBox complex for asymmetric hydrosilylation of ketones

## 2.2. Aims of this chapter

The application of tetradentate *N*-donor ligands for biomimetic oxidations has been extensively studied as porphyrine type skeletons or as non-heme designs<sup>13</sup> (Chapter 1). However, tridentate or pentadentate skeletons are much less explored alternatives. PyBox derived ligands have showed good activity for olefin epoxidation in combination with Ru salts, whereas poorer results were achieved with their iron counterparts.<sup>14</sup> Because a careful ligand design is a key factor in activating iron for catalytic transformations (*vide supra*), the development of a new family of ligands for its application in iron catalysed oxidation reactions is attempted in this chapter. Two main strategies will be described in order to overcome the limitations of iron-PyBox complexes:

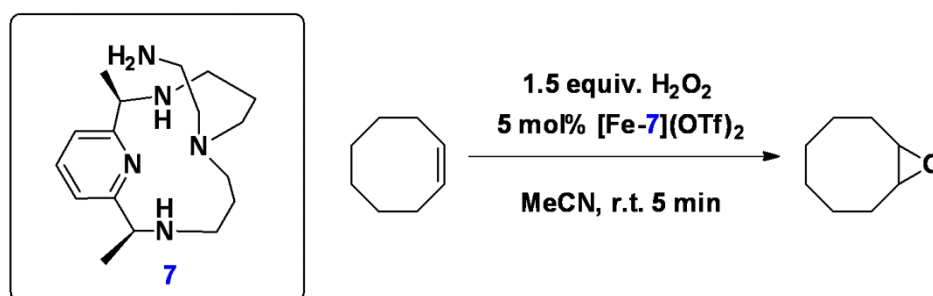
- The design of pentadentate *N*-donor skeletons by combining PyBox type and bidentate ligands
- The design of new tridentate *N*-donor skeletons capable of overcoming the limited solubility and activity of Fe-PyBox complexes.

## 2.3. Results and discussion

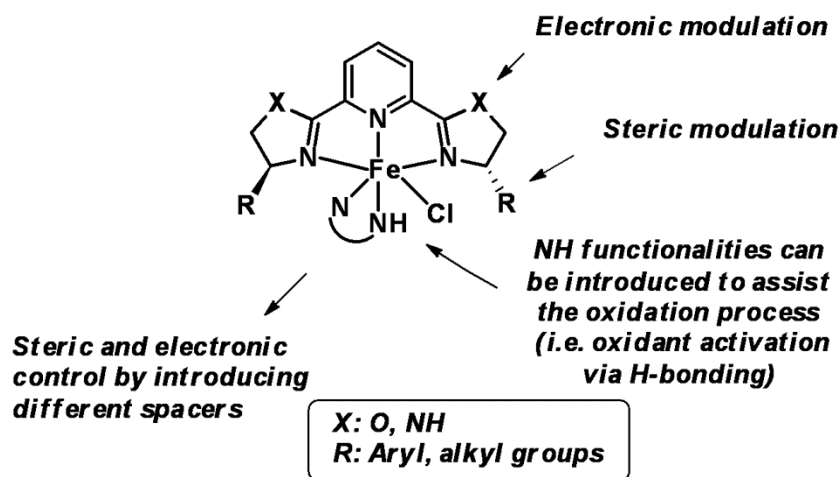
### 2.3.1. Pentacoordinated designs

Pentacoordinated  $Fe^{II}$  complexes are rare in iron-catalysed oxidation reactions. However, the bioinspired ligand **7** was applied in the Fe-catalysed olefin epoxidation reactions with good efficiency<sup>15</sup> (Scheme 8). This seminal work prompted us to further investigate pentadentate

*N*-donor skeletons for their application in iron catalysed selective oxidation reactions. Initially, we hypothesised that a pentadentate *N*-donor ligand core could also be achieved by combining two independent *N*-donor ligands: a tridentate PyBox type one and an additional bidentate ligand. With this modular design, we expected to gain more versatility and fine tuning of the electronic and steric properties of the final iron complexes (Scheme 9). For instance, the NH functionalities would be capable of assisting the O-O cleavage via H-bonding.



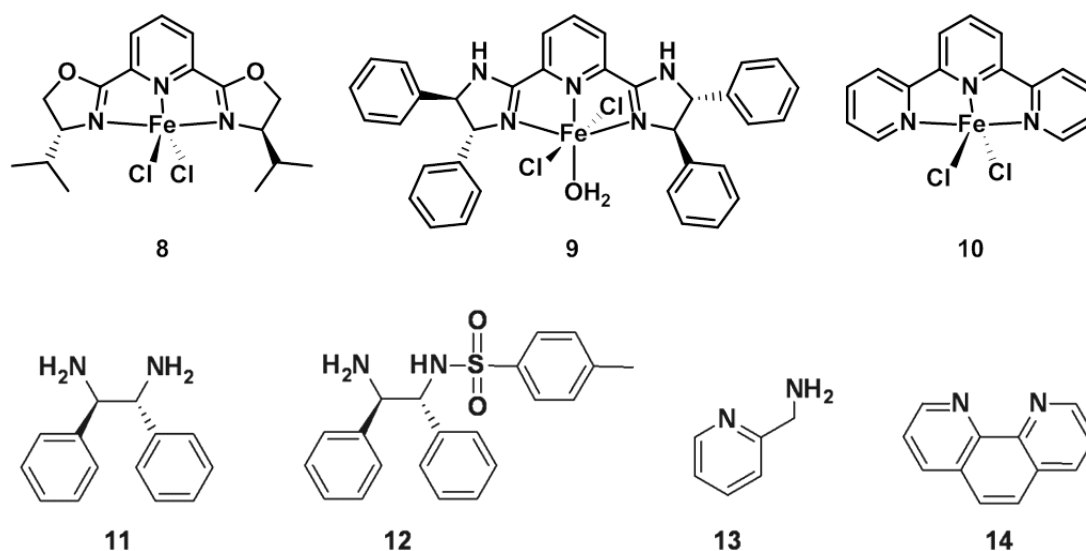
**Scheme 8.** Pentadentate *N*-donor ligands for iron catalysed epoxidation of olefins



**Scheme 9.** Modular *N*-donor pentacoordinated iron complex design

Preformed iron complexes **8** and **9** were initially tested for their further derivatisation with diamine type ligands **11**, **12**, **13** and **14**. However, the related iron complex **10** was discarded due to its poor solubility in common organic solvents.





Discouragingly, no coordination of the diamine ligands to the preformed iron complexes was achieved after screening different organic solvents,<sup>16</sup> temperatures and additives (Table 1). Nonetheless, the addition of ligand **12** and  $\text{AgPF}_6$  to the initial dark blue solution of complex **8** showed color evolution to bright dark pink, suggesting reactivity (Table 1, entry 6). Isolation and crystallisation of the resulting species in DCM/hexane allowed the formation of crystals suitable for X-ray diffraction analysis. Surprisingly, X-ray diffraction analysis revealed a complex cluster formation with a P21 asymmetric unit cell composed of four  $[\text{FeL}_2]^{2+}$  (L: PyBox ligand in **8**) complexes, eight  $\text{PF}_6^-$  counterions and eight DCM molecules (Fig. 1).

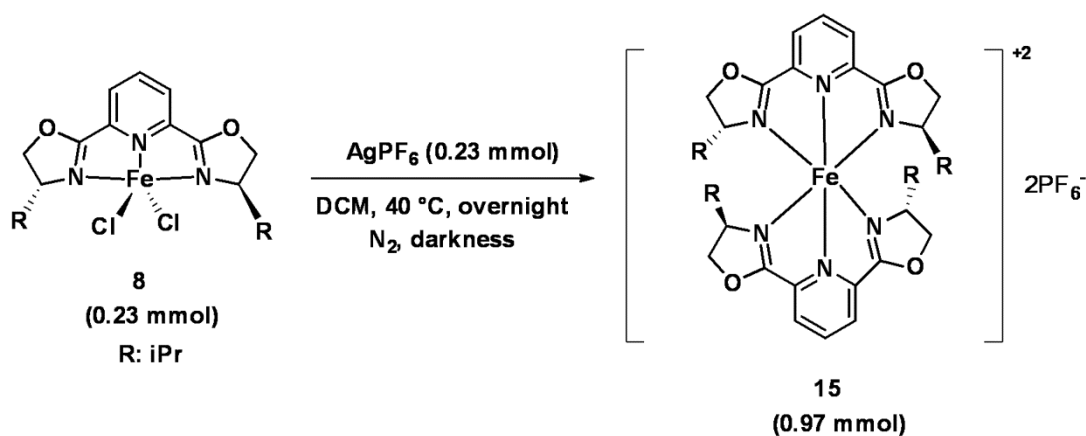
Even though the formation of **15** was not expected under the explored conditions,  $\text{Fe}^{\text{II}}$  salts have a strong tendency to form octahedral ( $O_h$ ) complexes with a coordination number of six.<sup>17</sup> Indeed, distorted  $O_h$  complexes of the formula  $[\text{Fe}(\text{NNN})_2]^{2+}$  are well studied and can be easily synthesised with conjugated (and rigid) tridentate ligands such as terpyridine (terpy) and even with PyBox type ligands.<sup>18</sup> Because these ligands are good  $\sigma$  and  $\pi$  donors and  $\pi$  acceptors they can chelate easily to metal ions and the resulting  $[\text{M}(\text{N},\text{N},\text{N})_2]^{n+}$  complexes tend to be very stable.<sup>19</sup>



Entry	Iron complex	Ligand	Solvent	Temperature / °C	Base	Additive	Conversion
1	8	12	DMF	25	NEt <sub>3</sub>	-	n.d.
2	8	12	MeCN	25	NEt <sub>3</sub>	-	n.d.
3	8	12	acetone	25	NEt <sub>3</sub>	-	n.d.
4	8	12	DCM	25	NEt <sub>3</sub>	-	n.d.
5	8	12	DCM	40	NEt <sub>3</sub>	-	n.d.
6	8	12	DCM	40	-	AgPF <sub>6</sub>	pink solution
7	8	12	DCM	40	NEt <sub>3</sub>	AgPF <sub>6</sub>	n.d.
8	8	12	DCM	40	<sup>t</sup> ButOK	-	n.d.
9	8	12	DCM	40	<sup>t</sup> ButOK	AgPF <sub>6</sub>	n.d.
10	8	11	DCM	40	-	AgPF <sub>6</sub>	n.d.
11	8	13	DCM	40	-	AgPF <sub>6</sub>	n.d.
12	8	14	DCM	40	-	AgPF <sub>6</sub>	n.d.
13	9	11	DCM	40	-	AgPF <sub>6</sub>	n.d.
14	9	12	DCM	40	-	AgPF <sub>6</sub>	n.d.
15	9	13	DCM	40	-	AgPF <sub>6</sub>	n.d.
16	9	14	DCM	40	-	AgPF <sub>6</sub>	n.d.

Reaction conditions: 0.116 mmol Fe complex, 0.116 mmol ligand, 0.116 mmol Ag salt, 0.16 mmol base, 12 mL freshly distilled solvent, overnight, under N<sub>2</sub> atmosphere in darkness.

**Table 1.** Screening of the conditions for the coordination of different diamine ligands to preformed iron complexes



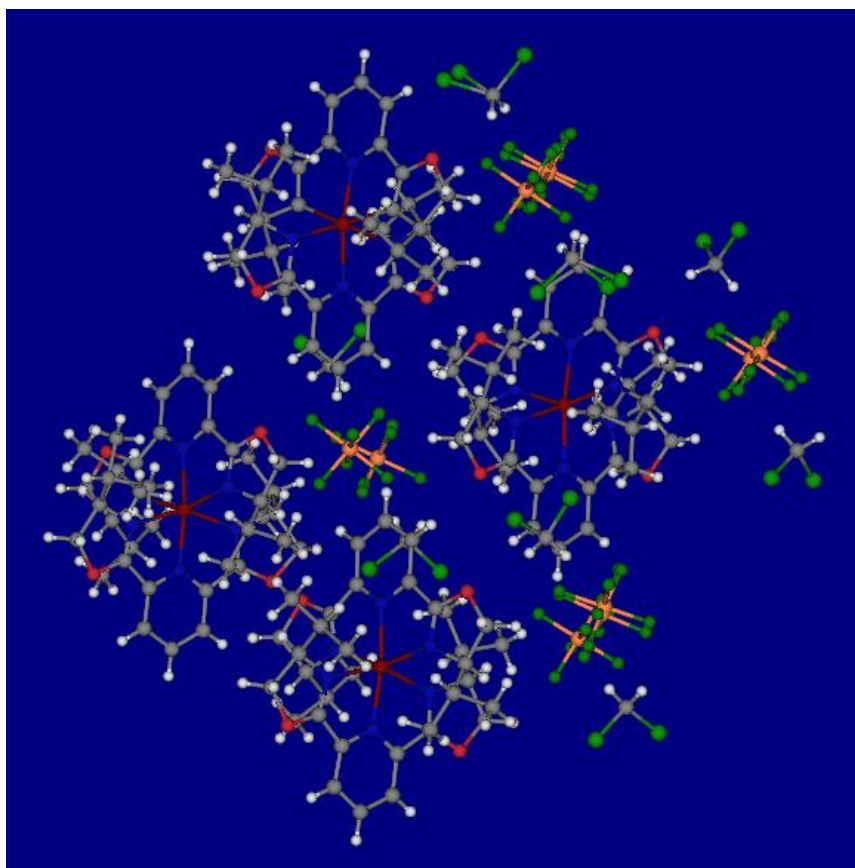


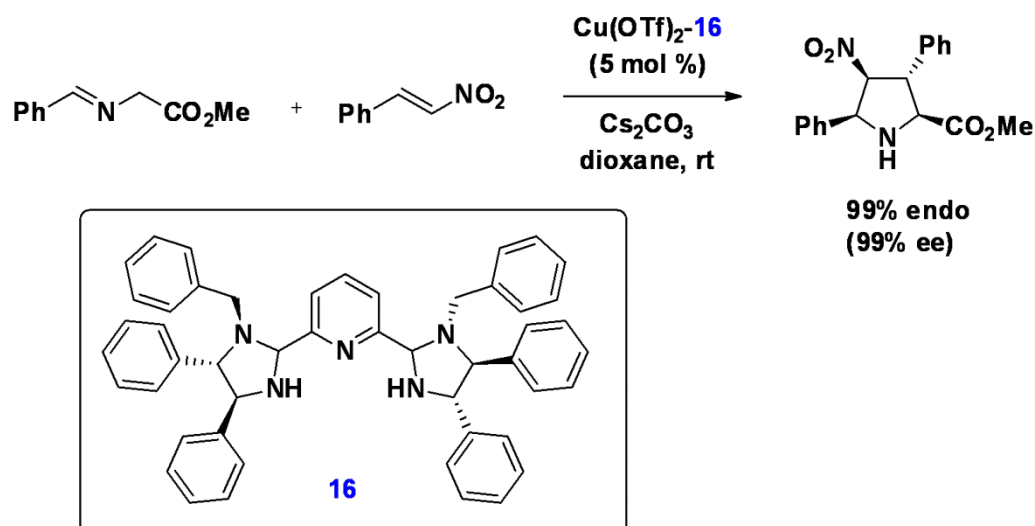
**Figure 1.** Dicationic Fe-(PyBox)<sub>2</sub> formation: reaction conditions and X-ray diffraction structure of the half unit cell.

### 2.3.2. Tridentate ligands: design, synthesis and properties of PyBisulidines

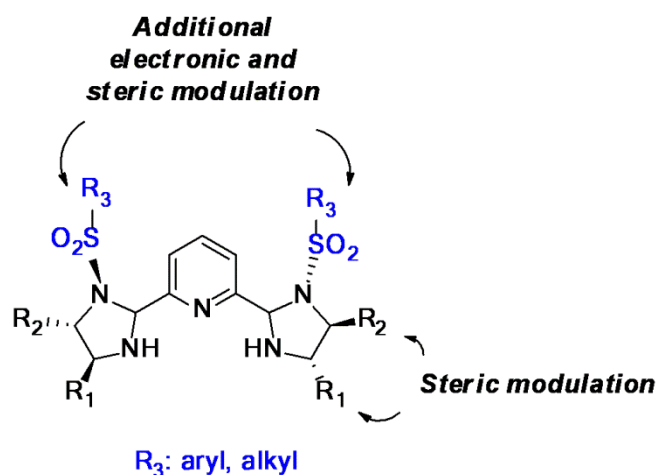
#### 2.3.2.1. Design and synthesis of PyBisulidines

Inspired by the limitations found in the pentacoordination strategy, the design of a new pincer type skeleton was attempted to ultimately overcome the double chelate formation, limited solubility and poor stereospecificity associated to the previous iron-PyBox complexes. To enhance the solubility and gain more flexibility in the final iron pincer complex, a bulky and non-conjugated tridentate *N*-donor skeleton analogous to the recently reported pyridine bisimidazolidine (PyBidine) ligand **16** was initially selected<sup>20</sup> (Scheme 10). In particular, we envisioned that replacement of the initial imidazolidine moieties with the more electron withdrawing sulfonamides could give rise to a new family of ligands with interesting coordinating properties, which might confer tunable Lewis acidity on the iron

centre and enhance the ability of iron for O<sub>2</sub> activation, allowing for better catalytic activity and selectivity. Additionally, an ample variety of sulfonamides can be facily synthesised and amended at different positions so that the steric hindrance around the iron centre could be tuned by simple modification of the sulfonamide moiety (Scheme 11).



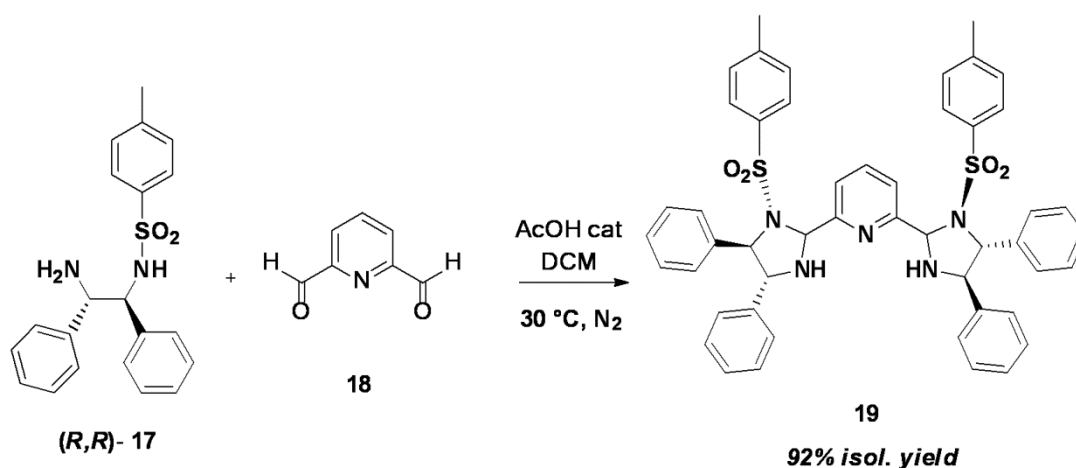
**Scheme 10.** Structure of the PyBidine ligand and its application for asymmetric endo-selective [3+2] cycloadditions



**Scheme 11.** General Pyridine bis(sulfonylimidazolidine) skeleton.

Initially, the optimal synthetic conditions for this class of pyridine bis(sulfonylimidazolidine) (PyBidine) ligands were investigated. The compound **19** was

synthesised by condensation of (*R, R*)-*N*-(2-amino-1,2-diphenylethyl)-4-methylbenzene sulfonamide **17** with pyridine-2,6-dicarboxaldehyde **18** (Scheme 12). The reaction proceeded with excellent yields under acidic catalytic conditions (AcOH) and very mild temperatures under inert atmosphere. Additionally, the synthesis was easily scaled up to the gram level (*circa.* 10 g) with excellent efficiency (isolated yields of 90%).

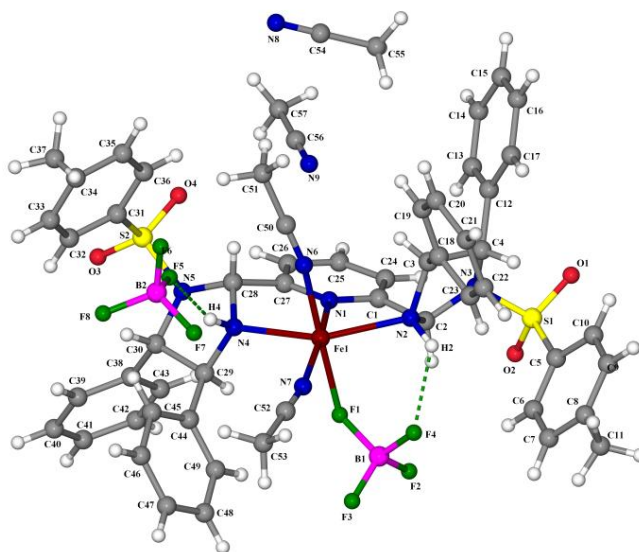
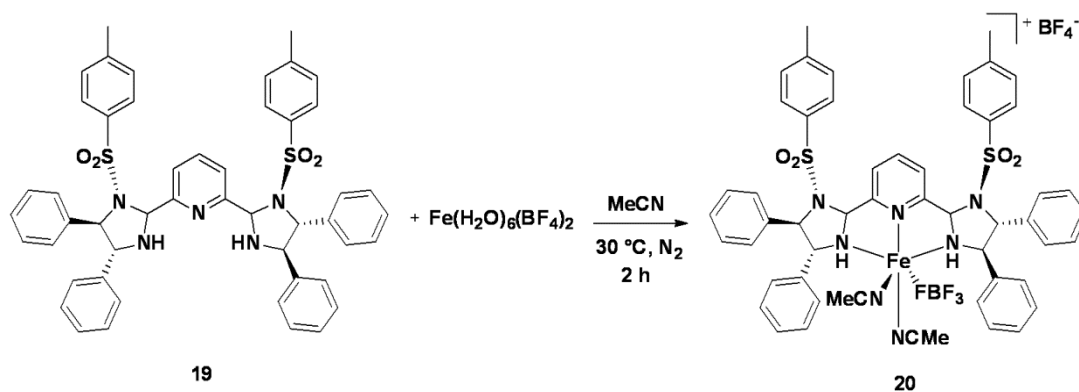


**Scheme 12.** General procedure for the synthesis of PyBisulidine ligands.

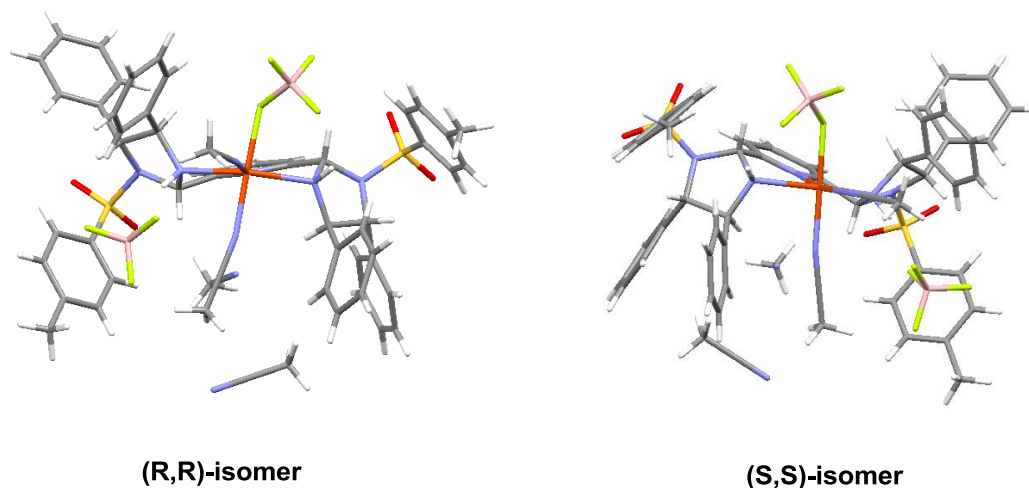
### 2.3.2.2. Coordination properties of PyBisulidines

When ligand **19** was combined with equimolar amounts of  $\text{Fe}(\text{H}_2\text{O})_6(\text{BF}_4)_2$  in MeCN, the initial colorless solution rapidly evolved to pale orange, indicating some type of reactivity (Scheme 13). In an attempt to identify whether the iron metal had successfully coordinated to ligand **19**, large quality crystals suitable for X ray diffraction were grown in MeCN/Et<sub>2</sub>O. The X ray diffraction analysis revealed a well-defined molecular complex in which the iron centre is coordinated to a single PyBisulidine ligand (Scheme 13). The complex exhibits a distorted O<sub>h</sub> geometry, with the ligand coordinated to the iron centre in a tridentate mode with a N<sup>2</sup>-Fe-N<sup>4</sup> angle of 148.92°. The initial stereochemistry of the ligand was retained in the final structure of the complex and the absence of conjugation provides more flexibility with two new stereocentres of opposite configuration being created in C2 and C28 in a similar fashion as in the reported Cu-PyBidines complex. Moreover, the spatial orientation of the sulfonamide groups in the crystalline complex is also pre-established by

the stereochemistry of the dpen moiety as it can be appreciated by comparing the x-ray structures of the (*R,R*) and the (*S,S*)-isomers of complex **20** (Scheme 14). Remarkably, the monocationic complex  $[\text{Fe}(\text{BF}_4)(\text{NNN})(\text{CH}_3\text{CN})_2](\text{BF}_4)$  **20** was formed exclusively under these reaction conditions with two molecules of acetonitrile and one of the  $\text{BF}_4^-$  counter ions directly coordinating to the iron metal. Because of its innate flexibility, the complex formed almost a bowl shaped cavity in which these acetonitrile molecules reside (Scheme 15).

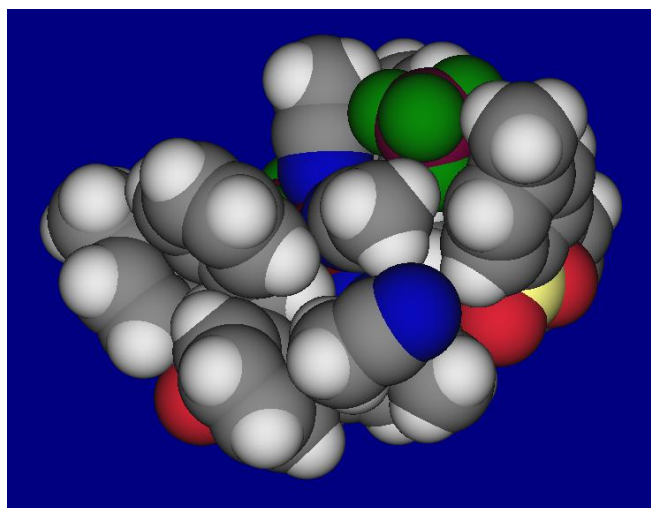


**Scheme 13.** Complexation of the PyBisulidine ligand to a commercially available iron salt.



**Scheme 14.** X-ray structures of the (*R, R*) and (*S, S*)- isomers of complex **20**. Note that the spatial orientation of the sulfonamide is determined in the crystalline structure of the complex.

Nonetheless, the coordination of the  $\text{BF}_4^-$  counterion was particularly surprising with a short  $\text{Fe-F}(\text{BF}_3)$  distance of 2.163 Å, indicating a strong bonding between the two atoms. This coordinated  $\text{BF}_4^-$  ion exhibited nearly tetrahedral geometry [F-B-F 107.5(1)-110.4(2), mean 109.4°] with the F-B distance [1.445(2) Å] of the coordinated fluorine being longer than the other B-F distances [1.377(2)-1.386(2), mean 1.381 Å]. The uncoordinated  $\text{BF}_4^-$  ion also presented angles close to tetrahedral [F-B-F 108.4(2)-110.0(2), mean 109.4°] but longer B-F distances [1.383(3)- 1.391(3), mean 1.387 Å]. The Fe-N bond of the acetonitrile molecule *trans* to the coordinated  $\text{BF}_4^-$  was longer than that in the *cis* (2.114(2) and 2.099(3) Å respectively) possibly due to the *trans* effect of the electronegative fluorine atom. Thus, a stretching difference of 0.015 Å between the two Fe-NCMe bonds in the *Oh* complex suggests that the coordination of the  $\text{BF}_4^-$  counterion to the iron centre labilises (i.e. destabilises) the bond between the iron centre and the MeCN in *trans* position to the  $\text{BF}_4^-$ .



**Scheme 15.** A sphere type model of the complex showing the almost bowl shaped cavity in which the acetonitrile molecules reside.

Coordination of “weakly coordinating”  $\text{BF}_4^-$  ions to other metal complexes have also been reported. However, such coordination often occurs in solvents of low dielectric constant.<sup>21</sup> To the best of our knowledge, complex **20** is the only example in the literature in which coordination of the  $\text{BF}_4^-$  to an iron centre is achieved in the presence of strong donor solvents (MeCN) and  $\text{H}_2\text{O}$  coordination molecules. Unfortunately, **20** is a high spin complex and thus a study of the coordination of the  $\text{BF}_4^-$  counterion in solution by NMR techniques could not be performed.

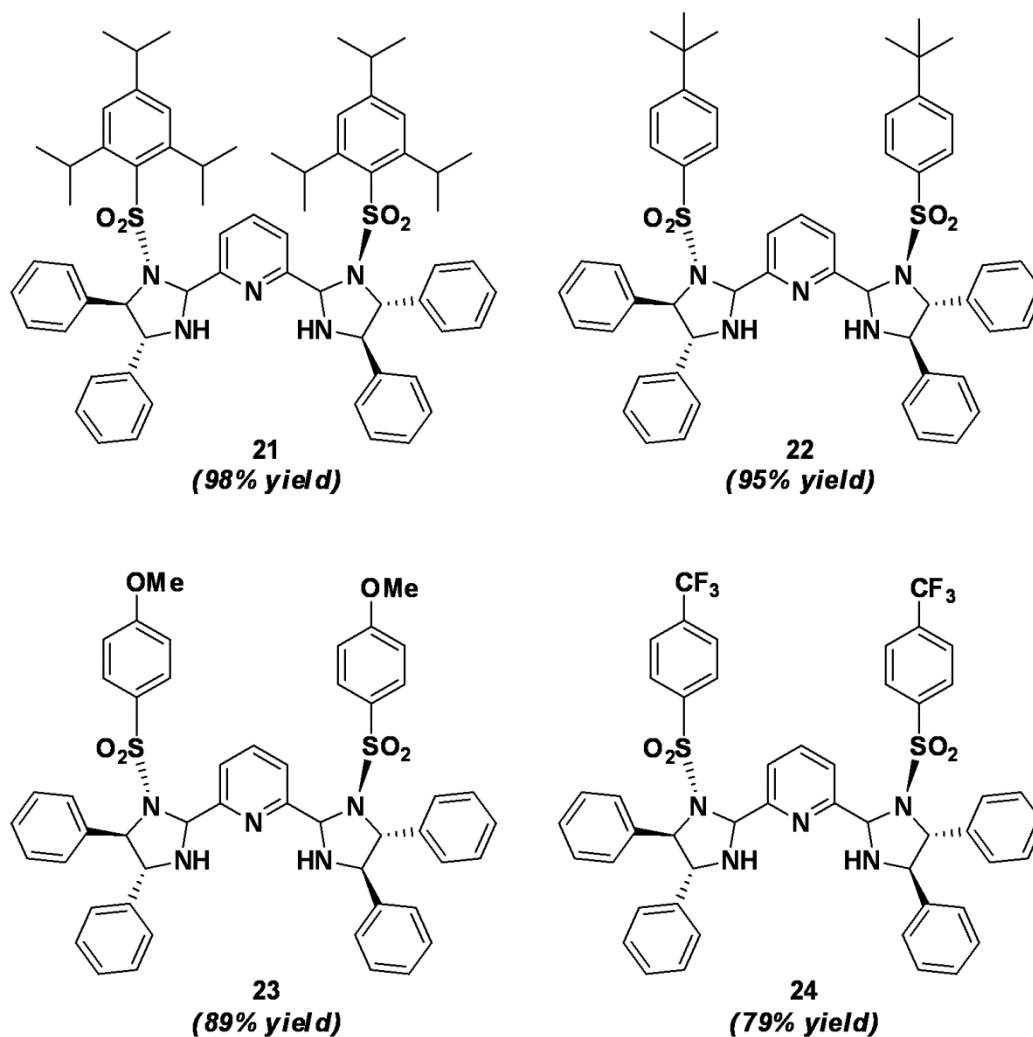
The protons of the sulfonylimidazolidine moiety were retained in the structure of the complex and characteristic IR absorptions for  $\nu_{\text{NH}}$  were detected at 3625 and 3727  $\text{cm}^{-1}$ , whereas the NH stretching bands in the uncoordinated ligand **19** were detected at 3125-3390  $\text{cm}^{-1}$ . This bathochromic shift reflects that the acidity of the amine protons is increased upon complexation of the amine to the iron centre and upon hydrogen bonding to the  $\text{BF}_4^-$  counterions (Scheme 13). These significantly high  $\nu_{\text{NH}}$  values and the unusual Fe-FBF<sub>3</sub> coordination indicate that the iron centre in **20** has a remarkable Lewis acid character.

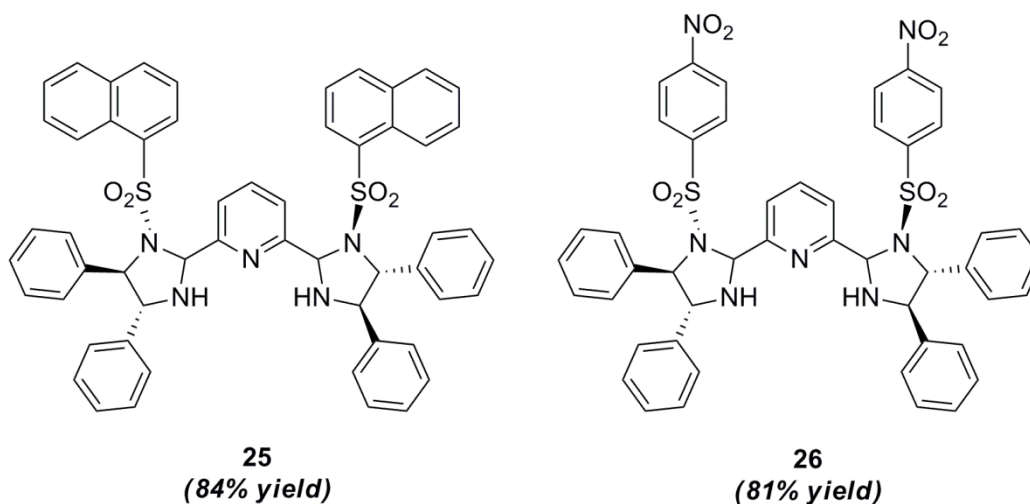


### 2.3.2.3. Ligand library

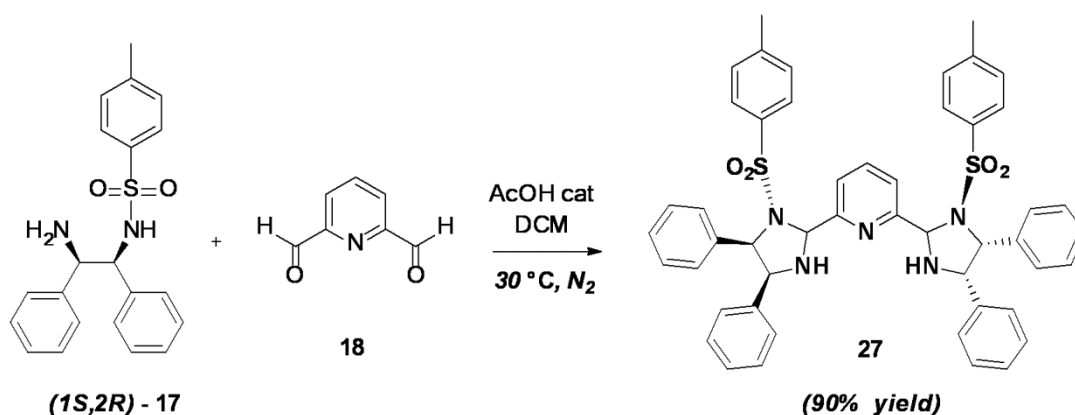
#### 2.3.2.3.1. Sulfonamide substitution

An ample variety of PyBisulidines incorporating aryl sulfonyl groups of different electronic and steric properties were synthesised with excellent yields by simple replacement of the initial sulfonamide (Scheme 16). In addition, ligand **27** possessing  $C_2$  symmetry was also synthesised with excellent yields by replacement of the initial (*R,R*)-**17** sulfonamide with its *meso* form (Scheme 17).



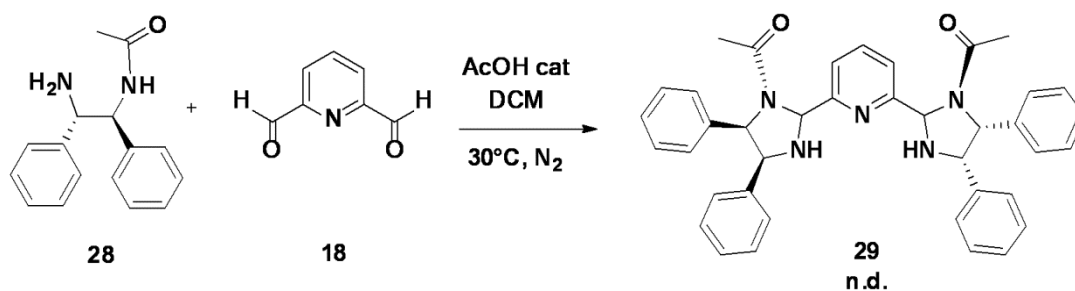


**Scheme 16.** Library of PyBisulidines synthesised by modification of the sulfonyl group of the initial sulfonamide.

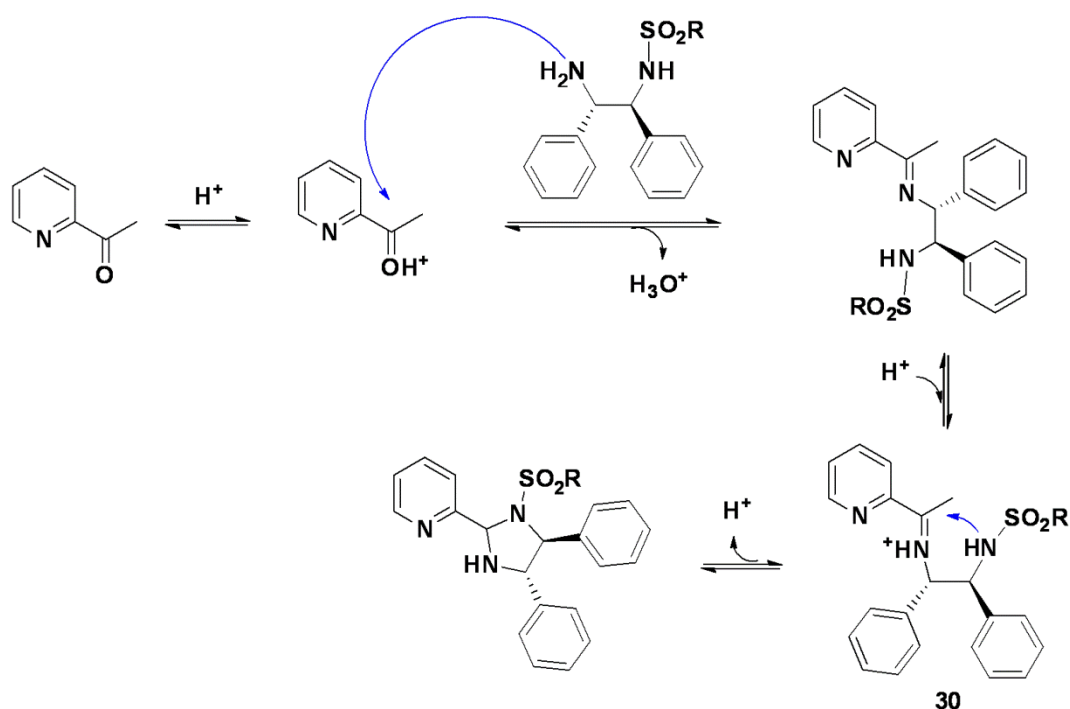


**Scheme 17.** Procedure for the synthesis of the C<sub>2</sub> symmetric PyBisulidine **27**.

However, replacement of the aryl sulfonyl moiety with a less bulky *N*-acetyl group in (*1R,2R*)-*N*-acetyl-1,2-diphenyl-1,2-ethylenediamine **28**, gave no reaction under optimal conditions or at reflux in several organic solvents (Scheme 18). This lack of reactivity was attributed to the electrophilicity of the carbonyl group in **28**, which reduces the nucleophilicity of the partial *sp*<sup>2</sup>-hybridised N of the amide, hampering the cyclization of the iminium salt **30** to forward the imidazolidine product (Scheme 19).



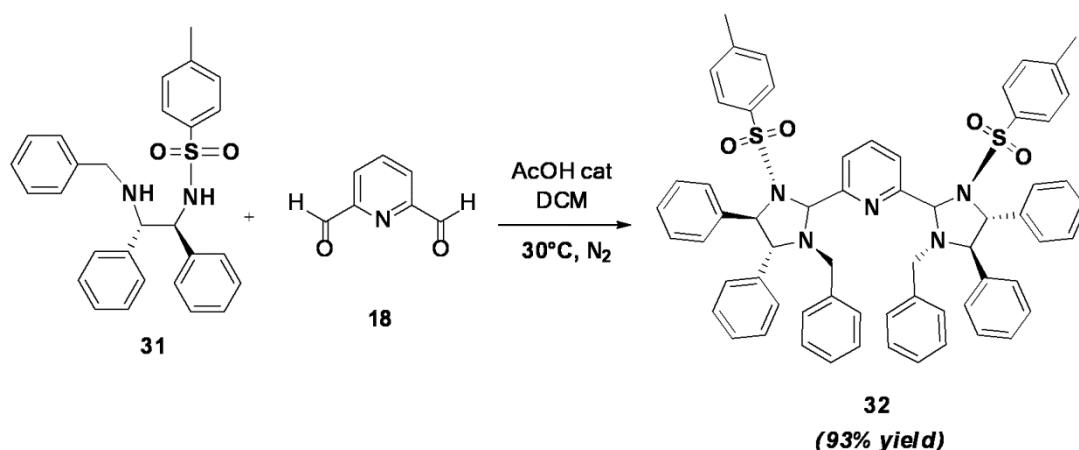
**Scheme 18.** Replacement of the sulfonamide with a  $\beta$ -amino amide gave no reactivity.



**Scheme 19.** Proposed mechanism of the acid catalysed synthesis of Pyridine sulfonylimidazolidines.

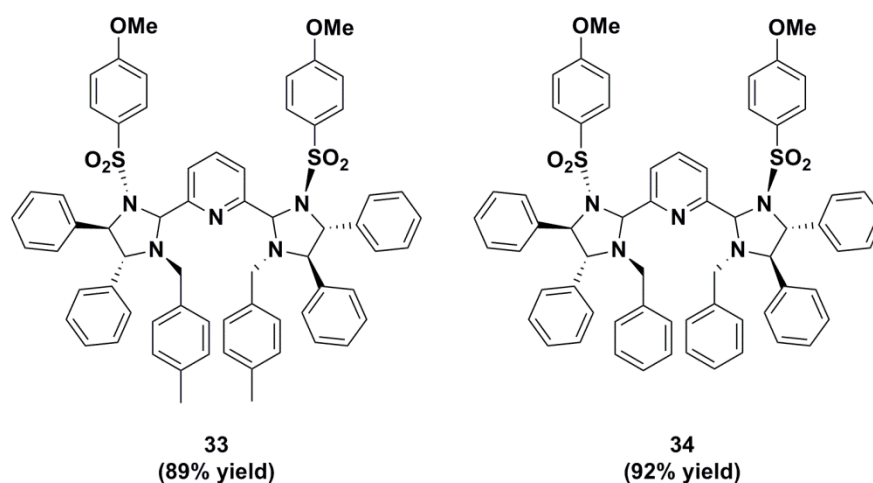
### 2.3.2.3.2. Amino substitution

The effect of substitution in the  $sp^3$ -N of the PyBisulidine skeleton was investigated in order to evaluate the impact of steric bulkiness and to explore additional tunability of the ligand. When compound **31**, was subjected to standard cyclisation conditions, the bulkier PyBisulidine **32** was obtained with excellent yield (Scheme 20).

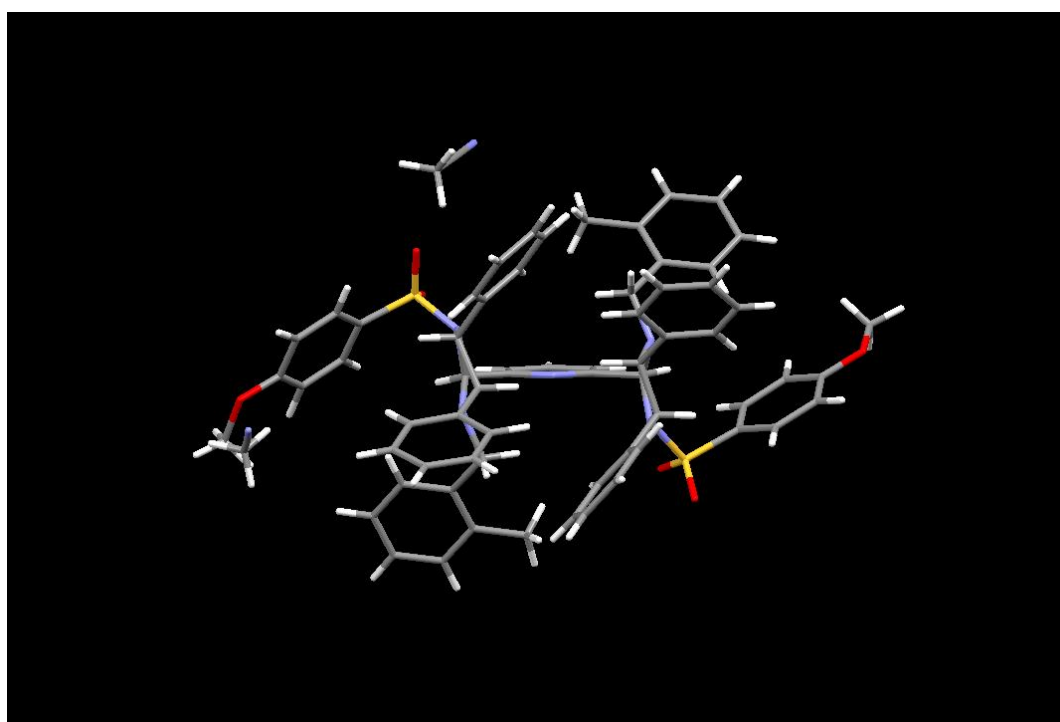
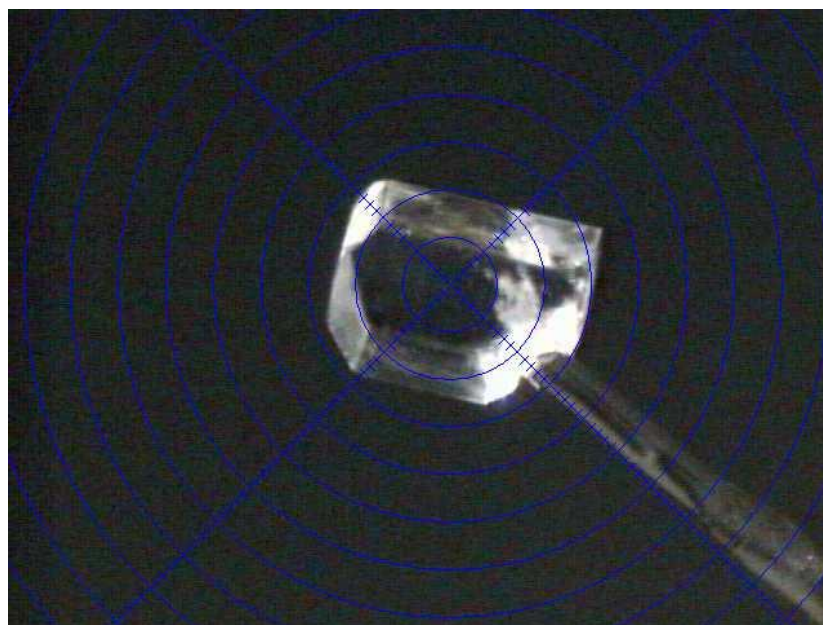


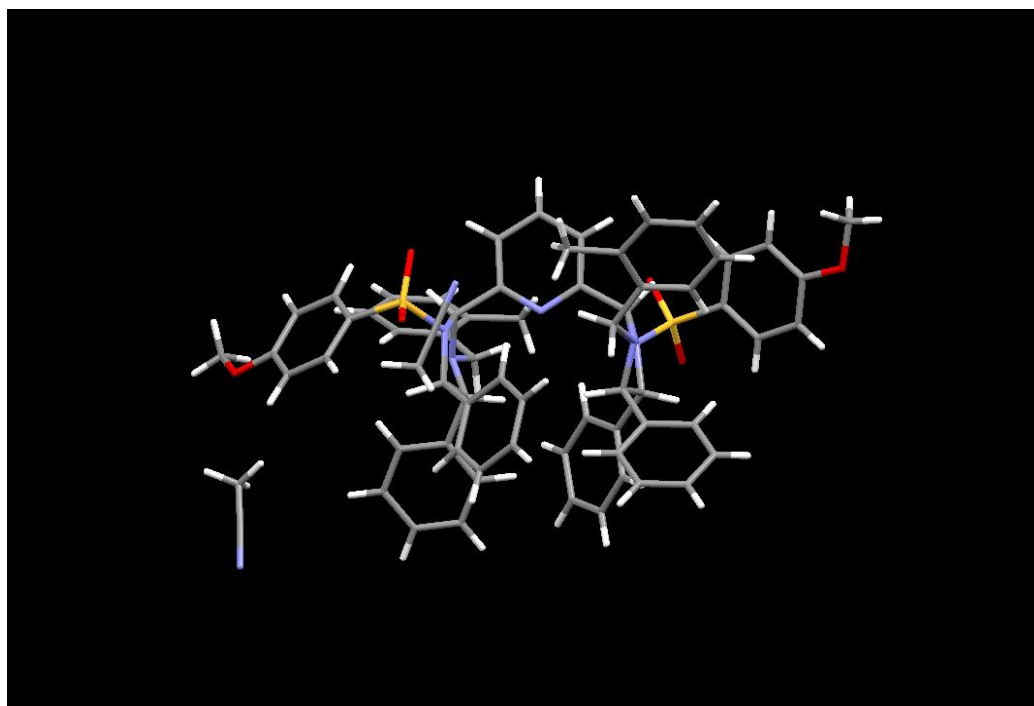
**Scheme 20.** General procedure for the synthesis of  $sp^3$ -N substituted PyBidine ligands.

A variety of  $sp^3$ -N-substituted PyBisulidines were obtained with excellent yields by simple modification of the arylsulfonyl group or the *N*-benzyl substituents of the initial *N*-(benzylamino-1,2-diphenylethyl) arylsulfonamide (Scheme 21). In an attempt to visualise these  $sp^3$ -N-substituted PyBisulidines of increased molecular complexity, beautiful gemstone-type crystals of **33** were grown in MeCN/hexane and subjected to X-ray diffraction analyses. Ligand **33** showed a bowl shaped geometry with the  $sp^2$  N of the pyridine being in the centre of the bowl (Scheme 22). In addition, the steric crowding pre-determines the spatial orientation of the *N*-benzyl substituents in the crystalline compound too.



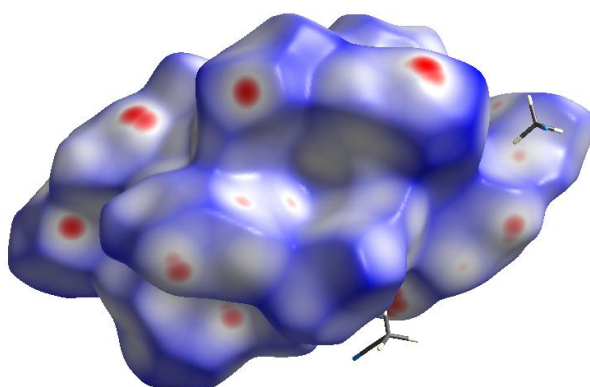
**Scheme 21.** Library of  $sp^3$ -N-substituted PyBisulidines including modifications in the sulfonamide moiety and the *N*-benzyl substituent.



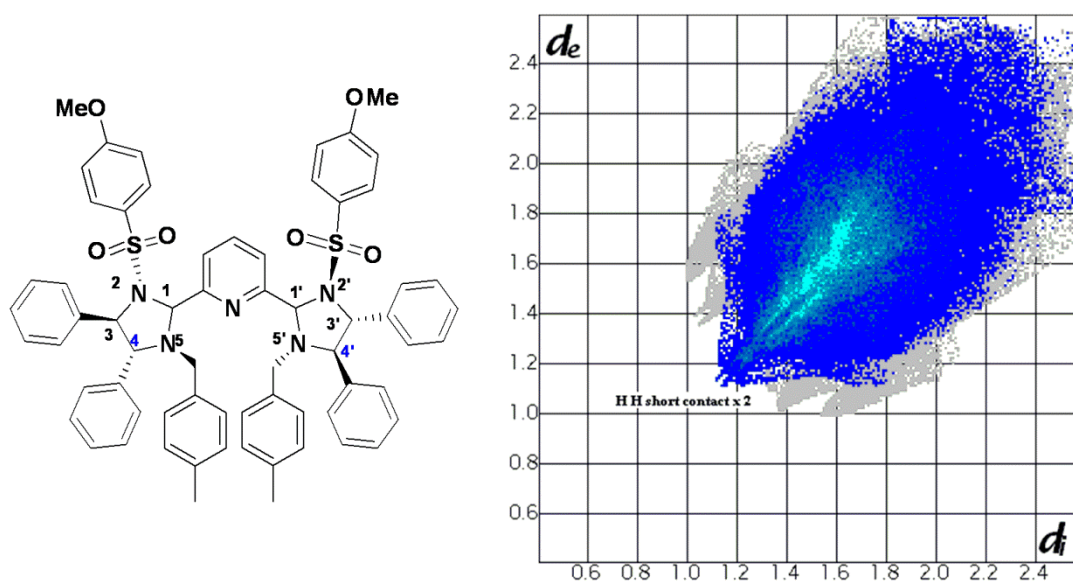


**Scheme 22.** A zoomed image of the crystal shape and two perspectives of the X-ray diffraction analysis of  $sp^3$ -*N*-substituted PyBisulidine **33**

This bowl shape structure is generated by the interaction among the four phenyl groups surrounding the central N atom of the pyridine as shown in the Hirshfeld surface (Scheme 23). Additionally, the 2D fingerprint of the Hirshfeld surface showed that there is a short contact between hydrogen atoms in positions 4 and 4', consequence of this bowl shape structure (Scheme 24).



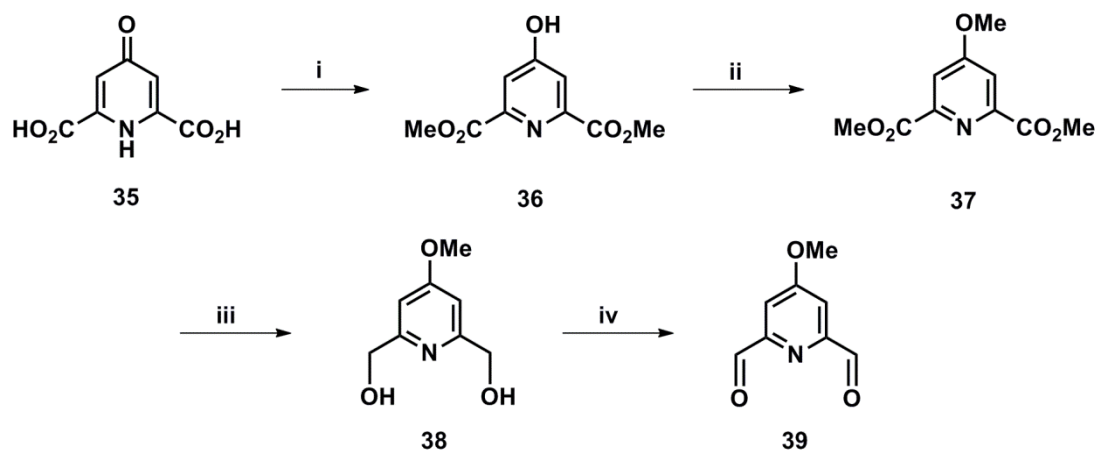
**Scheme 23.** Hirshfeld surface of **33** showing a bowl shape structure. The red surfaces represent short interatomic distances whereas the blue ones represent long distances.



**Scheme 24.** 2D-Fingerprint of the Hirshfeld surface of PiBisulidine **33**. The plot is a representation of  $d_e$  (distance from the surface to external atom) vs  $d_i$  (distance from the surface to internal atom) summarising the interactions in the Hirshfeld surface. The features along the diagonal ( $d_e = d_i$ ) are indicative of a short H-H distance between H4 and H4'.

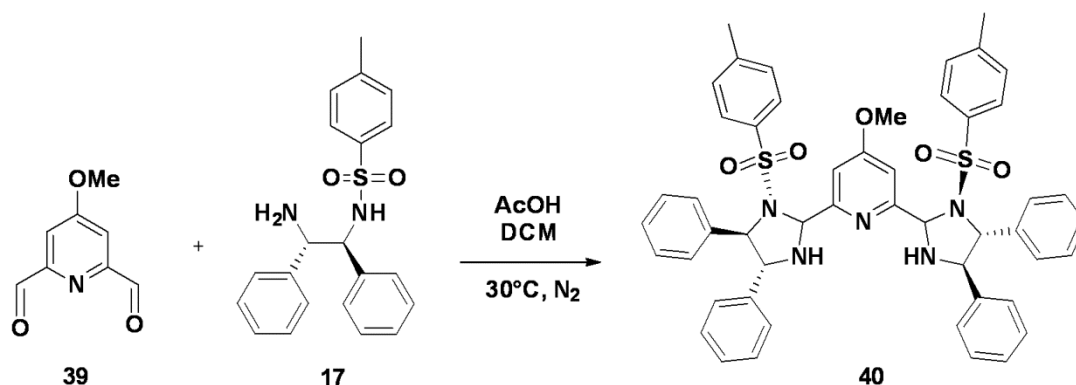
### 2.3.2.3.3. Pyridine substitution

Even though *N*-(benzylamino-1,2-diphenylethyl) arylsulfonamides can be easily modified and synthesised in one pot, derivatisation of the pyridine moiety turned out to be more complicated. A multistep synthetic pathway was followed to generate the 4-methoxypyridine-2,6-dicarbaldehyde **39** from commercially available chelidamic acid monohydrate **35** (Scheme 25).



**Scheme 25.** Reaction conditions for the synthesis of substituted pyridine **38**: (i)  $\text{H}_2\text{SO}_4$  (98%) in MeOH, reflux 2 h, then  $\text{NaHCO}_3$  (aq.) up to pH= 8.00 (80% yield). (ii)  $(\text{CH}_3\text{O})_2\text{SO}_2$ ,  $\text{K}_2\text{CO}_3$  in DMF at r.t. for 24 h (90% yield). (iii)  $\text{NaBH}_4$  in THF reflux, 1 h, then anhydrous MeOH, reflux 3 h (80% yield). (iv)  $\text{SeO}_2$  in xylene, reflux 24 h (96% yield).

Condensation of **39** with the standard sulfonamide **17** under optimal conditions afforded PyBisulidine **40** with excellent yields, indicating that further functionalisation of the central pyridine moiety of the PyBisulidine skeleton can also be achieved (Scheme 26). Nonetheless, the longer and more complex synthetic routes needed to perform such functionalisation stopped us from making more analogues of **40** unless future catalytic performance revealed strong necessity to introduce functionalisation at this specific position.

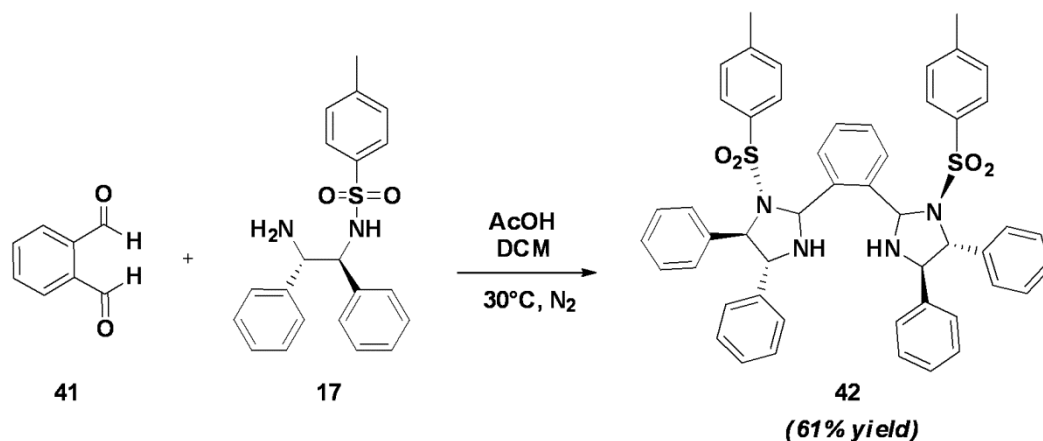


**Scheme 26.** Procedure for the synthesis of PyBidines bearing a functionalised pyridine linker.



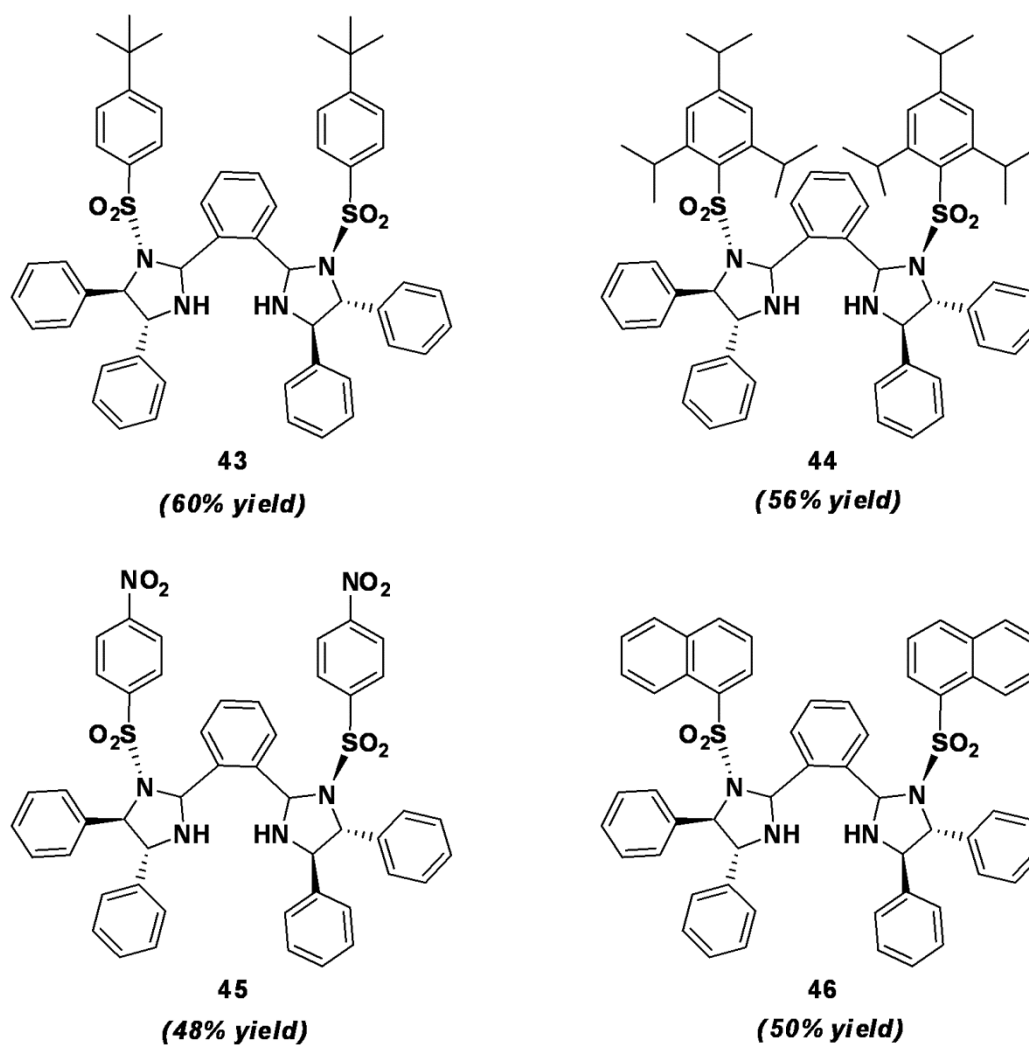
## 2.3.2.3.4. Bidentate designs

Inspired by the many successful applications of Box ligands as bidentate versions of PyBox skeletons, bidentate versions of the PyBisulidine ligands were next attempted. The Bis(sulfonylimidazolidine) (Bisulidine) **42** was obtained in good yields upon catalytic acidic condensation of phthalaldehyde **41** and the initial sulfonamide **17** (Scheme 27).

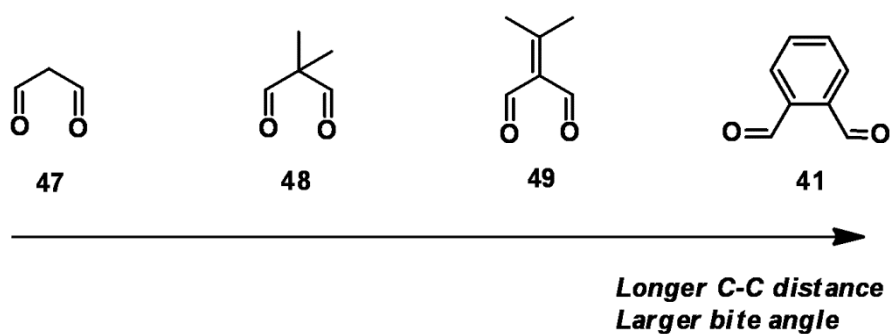


**Scheme 27.** Procedure for the synthesis of Bisulidine type ligands.

A small library of Bisulidine ligands incorporating aryl sulfonyl groups of different electronic and steric properties was created by facile replacement of the initial sulfonamide **17** (Scheme 28). In comparison with the tridentate PyBisulidines, the yields of the bidentate Bisulidines were slightly lower probably due to the steric hindrance resulting from positioning the two flexible sulfonylimidazolidine rings in close spatial proximity. Indeed, phthalaldehyde **40** was chosen as a linker because of the longer distance separating the two terminal aldehydes in comparison with malonaldehyde type linkers **47-49** that are commonly used in Box ligands. Moreover, Box ligands are compatible with different type of linkers, with modifications of the bite angle on the resulting Box-metal complex being the main reason to select a specific linker<sup>22</sup> (Scheme 29). However, the innate flexibility of the Bisulidine ligands limited the type of linkers that can be used to those resulting in larger bite angles, as no Bisulidine formation occurs when smaller malonaldehydes **47** and **48** were used as linkers.



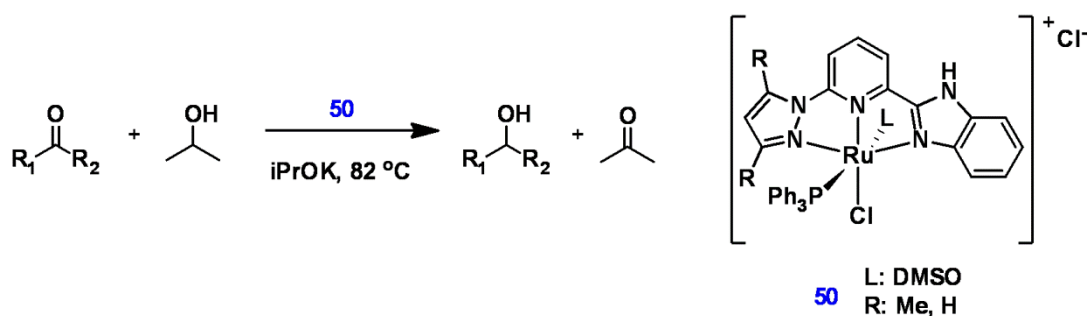
**Scheme 28.** Bisulidene type ligands incorporating different aryl sulfonyl substituents.



**Scheme 29.** Common linkers used in the synthesis of bidentate ligands.

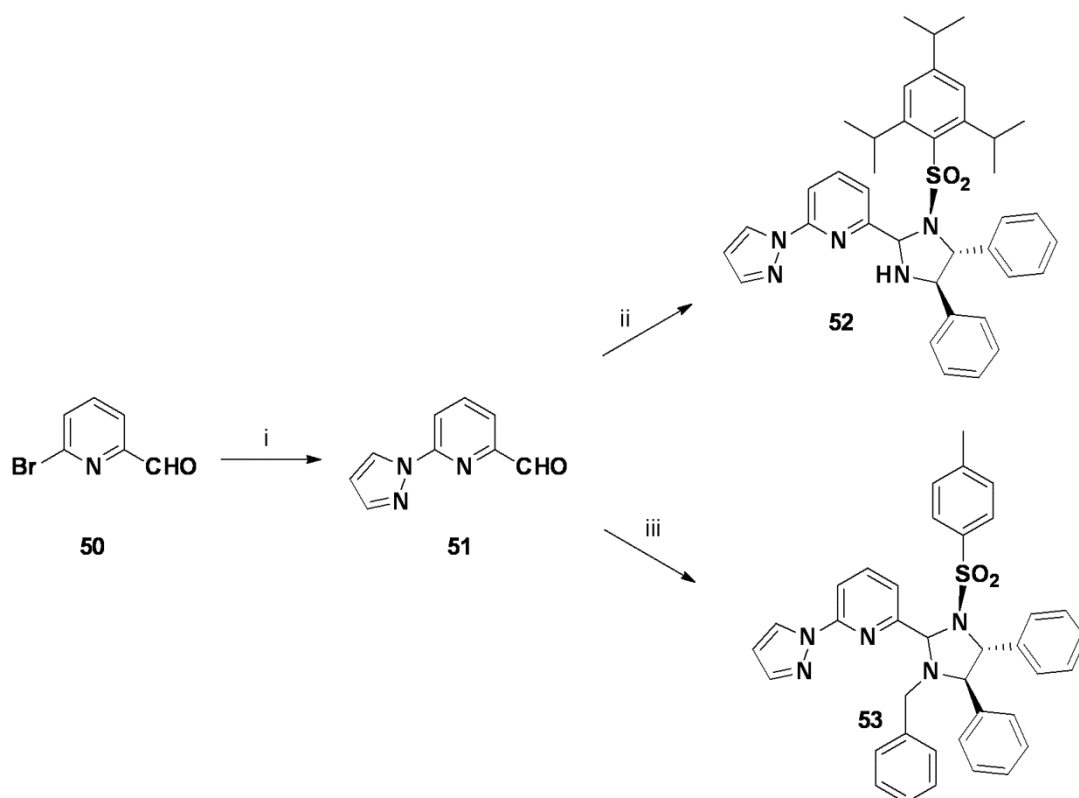
## 2.3.2.3.5. Asymmetric versions

Asymmetric tridentate NNN ligands have recently drawn some attention for catalytic applications as they can potentially provide an *on* and *off* chelating effect during the catalytic cycle.<sup>23</sup> Indeed, the asymmetric Ru<sup>II</sup>-Pyrazolyl-imidazolyl-pyridine complex **50** was found exceptionally active in the transfer hydrogenation (TH) of ketones<sup>24</sup> (Scheme 30).



**Scheme 30.** Asymmetric Ru<sup>II</sup>-NNN complex as an active catalyst for TH.

As pyrazoles have been used as ligands in oxidation processes and as they are present in the active centre of oxidases, an asymmetric pyrazolyl-pyridine-sulfonylimidazolidine ligand was constructed in order to investigate the potentially beneficial effects of asymmetry in PyBisulidine ligands. The asymmetric Pyrazolyl-pyridine-sulfonylimidazolidine ligands **52** and **53** were prepared in very good yields according to a facile two step synthesis (Scheme 31).



**Scheme 31.** Two step synthesis of asymmetric PyBisulidine ligands: (i) **50** (1 equiv), pyrazole (1.3 equiv), phenanthroline (0.25 equiv), CuI (0.12 equiv),  $K_2CO_3$  (1 equiv), toluene, 120 °C, 24 h. (ii) **51** (1.0 mmol), (*R, R*)-sulfonamide (1.0 mmol), acetic acid (1.0 mmol), DCM, 30 °C, 24 h (98% yield). (iii) **51** (1.0 mmol), *N*-(2-(arylamino)-1,2-diphenylethyl) aryl sulfonamide (1.0 mmol), acetic acid (1.0 mmol), DCM, 30 °C, 24 h (97% yield).

## 2.4. Conclusions

A new library of tridentate *N*-donor ligands based on a pyridine bis(sulfonylimidazolidine) skeleton was developed. The initial ligand design allowed modifications of the sulfonamide, amino moiety, pyridine linker and denticity, giving rise to an ample variety of ligands. Commercially available iron salts can readily coordinate the PyBisulidine skeleton, forming a well-defined molecular complex of high flexibility and unusual Lewis acidity.

## 2.5. Experimental section

### 2.5.1. General techniques

Experiments involving air or moisture sensitive reagents were performed under an atmosphere of purified N<sub>2</sub> using standard Schlenck techniques. Solvents used in these experiments were reagent grade or better. MeCN, DCM and CHCl<sub>3</sub> were refluxed over CaH<sub>2</sub> and THF and Et<sub>2</sub>O were refluxed over Na/benzophenone and distilled under purified N<sub>2</sub> atmosphere. Commercial grade solvents used in the synthesis of non air or moisture sensitive components were used without further purification. Chemicals employed in the synthesis of ligands were purchased from commercial suppliers and used without further purification. PyBox and terpyridine ligands and iron salts were purchased from commercial suppliers and used without further purification. Analytical thin-layer chromatography (TLC) was conducted with TLC Silica gel 60 F254 (Merck) and plates were revealed under UV irradiation, iodine, potassium permanganate or vanillin staining. Flash column chromatography was performed using Aldrich Silica Gel 60 and columns were packed according to the dry method and equilibrated with the appropriate eluent prior to use. HPLC grade solvents were used and the solvent mixtures used as eluent are understood as volume/volume. <sup>1</sup>H NMR spectra were recorded on a Bruker Advance 400 (400 MHz) NMR spectrometer and reported in units of parts per million (ppm) relative to tetramethyl silane ( $\delta = 0$  ppm) or CDCl<sub>3</sub> ( $\delta = 7.26$  ppm). Multiplicities are given as: bs (broad singlet), s (singlet), d (doublet), t (triplet), q (quartet), dd (doublets of doublet), dt (doublets of triplet) or m (multiplet). <sup>13</sup>C NMR spectra were recorded on a Bruker Advance 400 (100 MHz) NMR spectrometer and reported in ppm relative to CDCl<sub>3</sub> ( $\delta = 77.0$  ppm). Coupling constants were reported as a J value in Hz. Mass spectra were obtained by electrospray ionisation (EI) or fast atom bombardment (FAB) at the Analytical Services of the Chemistry Department, University of Liverpool and EPSRC National Mass Spectrometry Service Centre, College of Medicine, Swansea University. IR spectra were recorded on a Jacso FT/IR-4200 type A spectrometer.

## 2.5.2. Synthesis of the iron complexes with previously reported tridentate *N,N,N*-donor ligands

### 2.5.2.1. $\text{FeCl}_2(\text{PyBox})$ complex<sup>25</sup> (**8**)

In a 100 mL two-necked round bottom flask,  $\text{FeCl}_2 \times 4\text{H}_2\text{O}$  (2.0 mmol, 395.8 mg) and 2,6-bis((*R*)-4-isopropyl-4,5-dihydrooxazol-2-yl)pyridine (2.0 mmol, 600.0 mg) were added. The flask was degassed and placed under a  $\text{N}_2$  atmosphere. Freshly distilled THF (20 mL) was added by syringe and the reaction immediately turned dark blue. The reaction was stirred for 2h at 25 °C and then, the solvent was removed slowly under vacuo. The dark blue precipitate was washed with cold, freshly distilled  $\text{Et}_2\text{O}$  to afford the complex almost quantitatively (97% yield, 830.2 mg). **Anal Calc'd** for  $\text{C}_{17}\text{H}_{23}\text{Cl}_2\text{FeN}_3\text{O}_2$  : C, 47.69, H, 5.41, N, 9.81; found: C, 47.53, H, 5.32, N, 9.76.

### 2.5.2.2. $\text{FeCl}_2(\text{Pyridineimidazolidine})(\text{H}_2\text{O})$ complex<sup>25</sup> (**9**)

This complex was synthesised in a similar fashion as for **8** from  $\text{FeCl}_2 \times 4\text{H}_2\text{O}$  (1.15 mmol, 227.50 mg) and 2,6-bis((*4R,5R*)-4,5-diphenyl-4,5-dihydro-1H-imidazol-2-yl)pyridine (1.15 mmol, 600.00 mg). **Anal Calc'd** for  $\text{C}_{35}\text{H}_{31}\text{Cl}_2\text{FeN}_5\text{O}$  : C, 63.27, H, 4.70, N, 10.54; found: C, 63.36, H, 4.81, N, 10.46.

### 2.5.2.3. $\text{FeCl}_2(\text{terpy})$ complex<sup>26</sup> (**10**)

In a two-necked round bottom flask equipped with a reflux condenser, terpyridine (0.45 mmol, 100.00 mg) was added, degassed and placed under a  $\text{N}_2$  atmosphere. Freshly distilled  $\text{CHCl}_3$  (18 mL) was added by syringe and the mixture was heated to 40 °C. In a separated two necked round bottom flask, anhydrous  $\text{FeCl}_2$  (0.58 mmol, 73.80 mg) was added, degassed and placed under a  $\text{N}_2$  atmosphere. Freshly distilled MeOH (6.0 mL) was added by syringe and the mixture was heated to 50 °C until a clean yellow solution was observed. The hot solution of terpyridine was added by syringe to the metal solution resulting in the almost immediate formation of the dark purple crystalline metal complex. The crystals were filtered

off and washed with hot  $\text{CHCl}_3$ , then with methanol and finally with ether. The crystals were dried in vacuo and characterised as the mono-ligand metal complex by microanalysis (65% yield). **Anal Calc'd** for  $\text{C}_{15}\text{H}_{11}\text{Cl}_2\text{FeN}_3$  : C, 50.04, H, 3.08, N, 11.67; found: C, 50.34, H, 3.11, N, 11.78.

### **2.5.3 General procedure for the attempted functionalisation of the preformed iron-PyBox type complexes.**

In a 50 ml two-necked round bottom flask, **8** (0.11 mmol, 1.0 equiv., 50.00 mg), a bidentate ligand (0.16 mmol, 1.0 equiv.) and  $\text{AgPF}_6$  (0.11 mmol, 1.0 equiv., 29.50 mg) were added. The mixture was degassed and placed under a  $\text{N}_2$  atmosphere. The flask was kept in darkness by using kitchen foil and then, 12.0 mL of freshly distilled DCM (or the corresponding solvent) were added by syringe. The reaction mixture was stirred overnight.

### **2.5.4. Procedure for the synthesis of the dicationic bis(PyBox) $\text{Fe}^{\text{II}}$ complex (15)**

In a 50 mL two-necked round bottom flask, **8** (0.11 mmol, 1.0 equiv., 50.00 mg), **12** (0.16 mmol, 1.0 equiv., 60.80 mg) and  $\text{AgPF}_6$  (0.11 mmol, 1.0 equiv., 29.50 mg) were added, degassed and placed under a  $\text{N}_2$  atmosphere. The flask was kept in darkness by using kitchen foil and then, 12 mL of freshly distilled DCM (or the corresponding solvent) were added by syringe. Next morning, the pink coloured solution was filtered over Celite under inert atmosphere to remove the white precipitate. The clear solution was concentrated to a small volume (0.75 mL approx) and crystals of the complex were grown by slow addition of distilled hexane (1.0 ml approx) to the concentrated DCM solution.

### **2.5.5. General procedure for the synthesis of sulfonyl DPEN derivatives**

Sulfonyl DPEN derivatives were obtained by reaction between DPEN and the corresponding sulfonyl chloride as previously reported in the literature.<sup>27</sup> A representative synthetic procedure is described below.

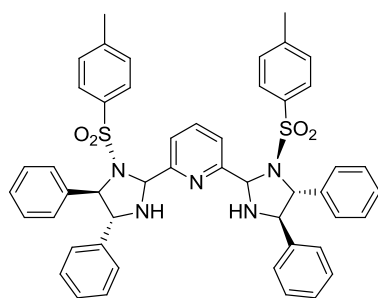
**(*R,R*)-*N*-(2-Amino-1,2-diphenylethyl)-4-methylbenzenesulfonamide ((*R,R*)-17)**

(*R,R*)-DPEN (2.8 mmol, 600.0 mg) was dissolved in freshly distilled DCM (20 mL) and cooled to 0 °C. NEt<sub>3</sub> (4.2 mmol, 585 μL) was added followed by a solution of 4-methylbenzenesulfonyl chloride (2.8 mmol, 538 mg) in DCM (8 mL) and the reaction mixture was stirred overnight at rt. The system was washed with distilled water (20 mL) and the organic phase was extracted, dried over MgSO<sub>4</sub>, filtered and evaporated under vacuum to give a crude product that was purified by column (1/1 hexane/AcOEt) affording the product as a white solid (85% yield, 880 mg).

Analytical data for the sulfonamides used in these syntheses has been reported in the literature and thus it is not included in this thesis.

**2.5.6. General Procedure for the synthesis of PyBisulidine ligands**

Pyridine-2,6-dicarbaldehyde (1.0 mmol, 135.0 mg) and (*R,R*)-*N*-(2-amino-1,2-diphenylethyl)-4-*t*-butylbenzenesulfonamide (2.1 mmol, 860.0 mg) were added to a double necked round bottom flask, degassed and placed under a N<sub>2</sub> atmosphere. Freshly distilled DCM (30 mL) and acetic acid (1.0 mmol, 60 μL) were added and the reaction mixture was stirred at 30 °C for c.a. 48 h. The reaction mixture was washed with NaHCO<sub>3</sub> (aq) solution and the organic layer extracted with DCM, dried over MgSO<sub>4</sub>, filtered and evaporated in vacuo. The residue was purified by silica gel column chromatography or crystallisation to afford the product.

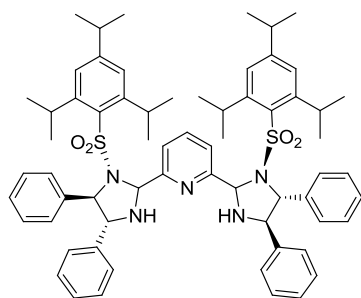
**Analytical data****2-((2*R*,4*R*,5*R*)-4,5-Diphenyl-1-tosylimidazolidin-2-yl)-6-((2*S*,4*R*,5*R*)-4,5-diphenyl-1-tosylimidazolidin-2-yl)pyridine (19)**

White solid (92% yield, 761.8 mg). Purification by flash chromatography (Hexane/EtOAc, 3/2). <sup>1</sup>H NMR (400 MHz, CDCl<sub>3</sub>): δ (ppm) = 8.01-7.96 (m, 3H), 7.53 (d, J = 8.3 Hz, 4H), 7.18-7.20 (m, 20H), 7.00-6.96 (d, J = 7.0 Hz, 4H), 4.71 (d, J = 5.3 Hz, 2H), 4.25 (d, J = 5.3 Hz, 2H), 2.39 (s, 6H). <sup>13</sup>C NMR (100 MHz, CDCl<sub>3</sub>): δ (ppm) = 158.3, 144.1, 140.0, 139.5, 138.5, 134.5, 129.9, 128.9, 128.6, 128.1, 127.8, 127.7, 127.3, 127.1, 124.5, 78.7, 71.8, 69.6, 31.4. IR (neat) ν = 3307, 2933, 2888, 1596, 1578, 1496, 1474, 1445, 1348, 1307, 1163, 1093, 1033, 982, 922, 886, 811, 729, 700, 667, 600, 586 cm<sup>-1</sup>. HRMS (FAB, [M+H]<sup>+</sup>) calc'd for



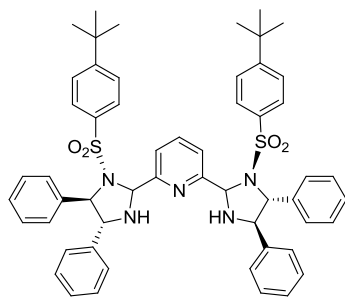
$[\text{C}_{49}\text{H}_{47}\text{N}_5\text{O}_4\text{S}_2]^+$ : 832.2986, found: 832.2980. **Anal Calc'd** for  $\text{C}_{49}\text{H}_{46}\text{N}_5\text{O}_4\text{S}_2$ : C, 70.73, H, 5.45, N, 8.42, found: C, 70.97, H, 5.36, N, 8.24. **mp**: 157-158 °C.

**2-((2R,4R,5R)-4,5-Diphenyl-1-((2,4,6-triisopropylphenyl)sulfonyl)imidazolidin-2-yl)-6-((2S,4R,5R)-4,5-diphenyl-1-((2,4,6-triisopropylphenyl)sulfonyl)imidazolidin-2-yl)pyridine (21)**



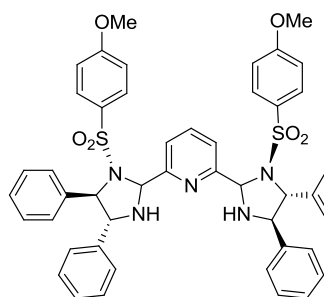
White solid (98% yield, 1031.1 mg). Purification by flash chromatography (Hexane/EtOAc, 3/1).  **$^1\text{H}$  NMR** (400 MHz,  $\text{CDCl}_3$ ):  $\delta$  (ppm) = 7.61 (t,  $J$  = 7.6 Hz, 1H), 7.26-7.14 (m, 6H), 7.06-7.04 (m, 5H), 6.90-6.85 (m, 15H), 6.30 (s, 2H), 4.84 (t,  $J$  = 7.2 Hz, 4H), 3.81 (septet,  $J$  = 6.8 Hz, 4H), 3.52 (s, 2H), 2.75 (septet,  $J$  = 6.8 Hz, 2H), 1.14 (d,  $J$  = 6.8 Hz, 12H), 0.96 (d,  $J$  = 6.8 Hz, 24H).  **$^{13}\text{C}$  NMR** (100 MHz,  $\text{CDCl}_3$ ):  $\delta$  (ppm) = 159.9, 154.0, 151.8, 139.0, 137.3, 131.3, 128.8, 128.2, 128.1, 127.7, 127.6, 127.5, 123.8, 123.5, 78.3, 72.1, 71.0, 34.5, 29.7, 25.2, 25.1, 23.9. **IR** (neat)  $\nu$  = 3333, 2959, 2904, 1604, 1566, 1455, 1429, 1385, 1363, 1311, 1289, 1148, 930, 886, 848, 815, 755, 697, 685, 674  $\text{cm}^{-1}$ . **HRMS** (FAB,  $[\text{M}+\text{H}]^+$ ) calc'd for 1056.5490, found: 1056.5487. **Anal Calc'd** for  $\text{C}_{65}\text{H}_{77}\text{N}_5\text{O}_4\text{S}_2$ : C, 73.90, H, 7.35, N, 6.63, S, 6.07; found: C, 73.81, H, 7.35, N, 6.66, S, 5.86. **mp**: 181-184 °C.

**2-((2R,4R,5R)-1-((4-*tert*-Butyl)phenyl)sulfonyl)-4,5-diphenylimidazolidin-2-yl)-6-((2S,4R,5R)-1-((4-*tert*-butyl)phenyl)sulfonyl)-4,5-diphenylimidazolidin-2-yl)pyridine (22)**



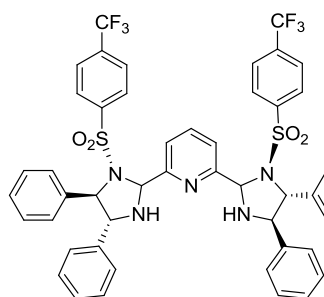
White solid (95% yield, 866.5 mg). Purification by flash chromatography (Hexane/EtOAc, 3/1).  **$^1\text{H}$  NMR** (400 MHz,  $\text{CDCl}_3$ ):  $\delta$  (ppm) = 7.94 (m, 3H), 7.53 (d,  $J$  = 8.5 Hz, 4H), 7.30 (d,  $J$  = 8.5 Hz, 4H), 7.12-7.00 (m, 16H), 6.88 (d,  $J$  = 6.8 Hz, 2H), 5.84 (s, 2H), 4.58 (d,  $J$  = 6.0 Hz, 2H), 4.17 (d,  $J$  = 5.9 Hz, 2H), 3.48 (bs, 2H), 1.27 (s, 18H).  **$^{13}\text{C}$  NMR** (100 MHz,  $\text{CDCl}_3$ ):  $\delta$  (ppm) = 158.5, 157.1, 139.8, 139.5, 134.4, 128.8, 128.6, 128.2, 128.1, 127.8, 127.3, 127.2, 126.3, 124.1, 78.5, 72.0, 69.8, 35.5, 31.5. **IR** (neat):  $\nu$  = 3296, 2963, 2907, 2866, 1596, 1574, 1496, 1448, 1400, 1348, 1167, 1111, 1085, 1029, 834, 808, 755, 700, 630  $\text{cm}^{-1}$ . **HRMS** (FAB,  $[\text{M}+\text{H}]^+$ ) calc'd for  $[\text{C}_{56}\text{H}_{59}\text{N}_5\text{O}_4\text{S}_2]^+$ : 916.3925, found: 916.3923. **Anal Calc'd** for  $\text{C}_{56}\text{H}_{58}\text{N}_4\text{O}_4\text{S}_2$ : C, 72.10, H, 6.27, N, 7.64, found: C, 71.69, H, 6.45, N, 7.42. **mp**: 185-187 °C.

**2-((2*R*,4*R*,5*R*)-1-((4-Methoxyphenyl)sulfonyl)-4,5-diphenylimidazolidin-2-yl)-6-((2*S*,4*R*,5*R*)-1-((4-methoxyphenyl)sulfonyl)-4,5-diphenylimidazolidin-2-yl)pyridine (23)**



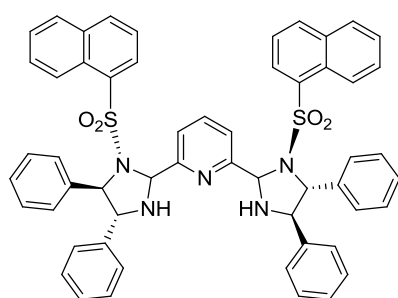
White solid (89% yield, 765.3 mg). Purification by crystallization in DCM/MeOH.  $^1\text{H NMR}$  (400 MHz,  $\text{CDCl}_3$ ):  $\delta$  (ppm) = 8.01-7.95 (m, 3H), 7.56 (dt,  $J$  = 8.8, 2.8 Hz, 4H), 7.19-7.02 (m, 20H), 6.80 (dt,  $J$  = 8.8, 2.9 Hz, 4H), 5.81 (s, 2H), 4.70 (d,  $J$  = 5.2 Hz, 2H), 4.25 (d,  $J$  = 5.3 Hz, 2H), 3.85 (s, 6H), 3.56 (s, 2H).  $^{13}\text{C NMR}$  (100 MHz,  $\text{CDCl}_3$ ):  $\delta$  (ppm) = 163.4, 158.4, 140.1, 139.5, 138.4, 130.2, 129.3, 128.8, 128.6, 127.9, 127.8, 127.3, 127.1, 124.4, 114.4, 78.6, 71.8, 69.6, 55.9. **IR** (neat)  $\nu$  = 3300, 2926, 2888, 1592, 1574, 1496, 1467, 1448, 1345, 1304, 1260, 1152, 1093, 1023, 985, 892, 837, 804, 749, 729, 700, 630, 608, 564  $\text{cm}^{-1}$ . **HRMS** (FAB,  $[\text{M}+\text{H}]^+$ ) calc'd for : 864.2884; found: 864.2887. **Anal Calc'd** for  $\text{C}_{49}\text{H}_{45}\text{N}_5\text{O}_6\text{S}_2$ : C, 68.11, H, 5.25, N, 8.11, S, 7.42; found: C, 67.85, H, 5.27, N, 8.08, S, 7.20. **mp**: 194-197  $^\circ\text{C}$ .

**2-((2*R*,4*R*,5*R*)-4,5-Diphenyl-1-((4-trifluoromethyl)phenyl)sulfonylimidazolidin-2-yl)-6-((2*S*,4*R*,5*R*)-4,5-diphenyl-1-((4-(trifluoromethyl)phenyl)sulfonylimidazolidin-2-yl)pyridine (24)**



Colourless crystals (79% yield, 739.2 mg). Purification by crystallization in DCM/MeOH.  $^1\text{H NMR}$  (400 MHz,  $\text{CDCl}_3$ ):  $\delta$  (ppm) = 7.99 (d,  $J$  = 7.8 Hz, 1H), 7.86 (d,  $J$  = 7.6 Hz, 2H), 7.55 (d,  $J$  = 8.4 Hz, 4H), 7.45 (d,  $J$  = 8.4 Hz, 4H), 7.17-7.09 (m, 20H), 5.79 (s, 2H), 4.91 (d,  $J$  = 3.1 Hz, 2H), 4.42 (d,  $J$  = 3.0 Hz, 2H), 3.58 (s, 2H).  $^{13}\text{C NMR}$  (100 MHz,  $\text{CDCl}_3$ ):  $\delta$  (ppm) = 157.1, 141.4, 140.0, 139.5, 138.5, 134.7 (d,  $^2J_{\text{C-F}}$  = 32.7 Hz), 129.1, 128.7, 128.2, 128.1, 127.9, 127.6, 127.1, 126.5, 126.3, 126.2, 125.7, 124.9 (t,  $^1J_{\text{C-F}}$  = 271.2 Hz), 79.4, 71.1, 69.3. **IR** (neat)  $\nu$  = 3289, 1604, 1579, 1457, 1403, 1353, 1321, 1162, 1135, 1095, 1058, 1012, 983, 887, 840, 811, 736, 711, 620. **HRMS** (FAB,  $[\text{M}+\text{H}]^+$ ) calc'd for  $[\text{C}_{49}\text{H}_{40}\text{F}_6\text{N}_5\text{O}_4\text{S}_2]^+$ : 940.2420, found: 940.2419. **mp**: 154-155  $^\circ\text{C}$ .

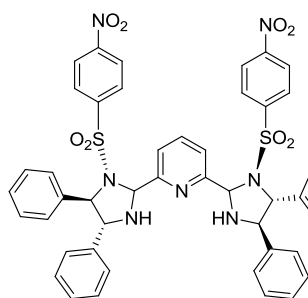
**2-((2*R*,4*R*,5*R*)-4,5-Diphenyl-1-(naphthalene-1-ylsulfonyl)-4,5-diphenylimidazolidin-2-yl)-6-((2*S*,4*R*,5*R*)-4,5-diphenyl-1-(naphthalene-1-ylsulfonyl)-4,5-diphenylimidazolidin-2-yl)pyridine (25)**



White solid (84% yield, 759.4 mg). Purification by flash chromatography (Hexane/EtOAc, 3/1).  $^1\text{H NMR}$  (400 MHz,  $\text{CDCl}_3$ ):  $\delta$  (ppm) = 8.58 (d,  $J$  = 8.6 Hz, 2H), 7.97 (d,  $J$  = 8.2 Hz, 2H), 7.91 (d,  $J$  = 7.6 Hz, 2H), 7.82 (dd,  $J$  = 7.3, 1.2 Hz, 4H), 7.64-7.61 (m, 2H), 7.59-7.57 (m, 2H), 7.34 (t,  $J$  = 8.0 Hz, 2H), 7.00-6.94 (m, 10H), 6.77-6.71 (m, 12H), 5.81 (s, 2H), 4.76 (d,  $J$  = 6.8 Hz, 2H), 4.60 (d,  $J$  = 6.8 Hz, 2H), 3.21 (bs, 2H).  $^{13}\text{C NMR}$  (100 MHz,  $\text{CDCl}_3$ ):  $\delta$  (ppm)

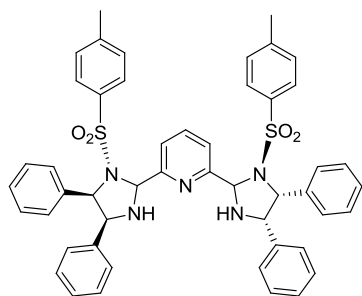
= 158.3, 142.2, 138.4, 136.2, 134.1, 131.6, 130.8, 128.5, 127.8, 127.0, 126.6, 126.4, 124.5, 121.2, 79.8, 70.9, 66.7. **Anal Calc'd** for  $C_{55}H_{45}N_5O_4S_2$ : C, 73.07, H, 5.02, N, 7.75, found: C, 72.94, H, 5.09, N, 7.89.

**2-((2*R*,4*R*,5*R*)-4,5-Diphenyl-1-((4-nitrophenyl)sulfonyl)imidazolidin-2-yl)-6-((2*S*,4*R*,5*R*)-4,5-diphenyl-1-((4-nitrophenyl)sulfonyl)imidazolidin-2-yl)pyridine (26)**



Colourless crystals (81% yield, 724.1 mg). Purification by crystallisation in DCM/MeOH.  $^1\text{H NMR}$  (400 MHz,  $\text{CDCl}_3$ ):  $\delta$  (ppm) = 8.01 (t,  $J$  = 7.6 Hz, 1H), 7.97 (d,  $J$  = 7.1 Hz, 4H), 7.82 (d,  $J$  = 8.0 Hz, 2H), 7.56 (m, 4H), 7.09-7.28 (m, 20H), 5.72 (d,  $J$  = 5.2 Hz, 2H), 4.91 (s, 2H), 4.46 (m, 2H), 3.54 (t,  $J$  = 3.1 Hz, 2H).  $^{13}\text{C NMR}$  (100 MHz,  $\text{CDCl}_3$ ):  $\delta$  (ppm) = 156.6, 150.2, 139.9, 139.6, 129.2, 129.0, 128.8, 128.6, 128.2, 128.1, 128.0, 127.9, 127.2, 127.1, 126.6, 126.4, 126.2, 124.2, 124.1, 79.6, 70.9, 69.2. **HRMS** (FAB,  $[\text{M}+\text{H}]^+$ ) calc'd for  $[\text{C}_{47}\text{H}_{36}\text{N}_7\text{O}_8\text{S}_2]^+$ : 889.1989, found: 889.1987.

**Meso-2-(4,5-diphenyl-1-tosylimidazolidin-2-yl)-6-(4,5-diphenyl-1-tosylimidazolidin-2-yl)pyridine (27)**



White solid (90% yield, 748.6 mg). Purification by flash chromatography (Hexane/EtOAc, 3/2).  $^1\text{H NMR}$  (400 MHz,  $\text{CDCl}_3$ ):  $\delta$  (ppm) = 8.12 (d,  $J$  = 7.5 Hz, 2H), 8.08 (t,  $J$  = 7.0 Hz, 1H), 7.52 (d,  $J$  = 8.2 Hz, 4H), 7.17 (d,  $J$  = 8.2 Hz, 4H), 7.05 (t,  $J$  = 7.5 Hz, 2H), 6.72-6.84 (m, 25H), 6.51 (d,  $J$  = 7.4 Hz, 2H), 6.08 (d,  $J$  = 10.6 Hz, 2H), 5.19 (d,  $J$  = 6.8 Hz, 2H), 4.51 (q,  $J$  = 6.8 Hz, 2H), 4.30 (t,  $J$  = 11.5 Hz, 2H), 2.35 (s, 6H).  $^{13}\text{C NMR}$  (100 MHz,  $\text{CDCl}_3$ ):  $\delta$  (ppm) = 154.2, 144.1, 136.9, 136.3, 134.9, 129.9, 128.3, 128.2, 128.0, 127.8, 127.7, 127.5, 127.2, 78.9, 67.6, 67.5, 31.3. **IR** (neat):  $\nu$  = 3289, 3032, 1597, 1495, 1452, 1430, 1334, 1306, 1289, 1187, 1161, 1088, 1048, 1029, 1003, 967, 941, 887, 858, 800, 762, 707, 691, 662, 623, 580, 565  $\text{cm}^{-1}$ . **HRMS** (FAB,  $[\text{M}+\text{H}]^+$ ) calc'd for  $[\text{C}_{49}\text{H}_{47}\text{N}_5\text{O}_4\text{S}_2]^+$ : 832.2986, found: 832.2982. **Anal Calc'd** for  $\text{C}_{49}\text{H}_{46}\text{N}_5\text{O}_4\text{S}_2$ : C, 70.73, H, 5.45, N, 8.42, found: C, 70.84, H, 5.48, N, 8.36. **mp**: 156-157  $^\circ\text{C}$ .

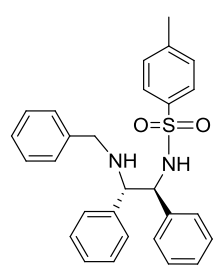
**2.5.7. General Procedure for the synthesis of N-(2-(arylamino)-1,2-diphenylethyl)arylsulfonamides<sup>28</sup>**

(*R,R*)-*N*-(2-amino-1,2-diphenylethyl)-4-methylbenzenesulfonamide (4.9 mmol, 1.8 g) was added in a two necked flask, degassed and placed under a  $\text{N}_2$  atmosphere. Freshly distilled THF (12 mL) and *p*-tolylbenzaldehyde (5.4 mmol, 649.0 mg) were subsequently added and the reaction mixture was stirred at r.t. for 2 h under inert atmosphere. Then, anhydrous EtOH (18 mL) was added to the solution and  $\text{NaBH}_4$  (7.8 mmol, 297.0 mg) was added portionwise.

The reaction system was stirred overnight at r.t. Water was added dropwise until no gas evolution was observed and then DCM (20 mL) was added. The solution was filtered and the organic phase was washed with water, extracted, dried over MgSO<sub>4</sub>, filtered and evaporated under vacuum to give a crude product that was purified by column (hexane/ethyl acetate) affording the pure product.

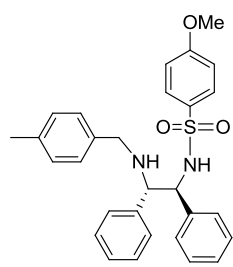
### Analytical data

#### *N*-((1*R*,2*R*)-2-(benzylamino)-1,2-diphenylethyl)-4-methylbenzenesulfonamide<sup>28</sup> (31)



White solid, (93% yield, 1.146 g). Purification by flash column chromatography (Hexane/EtOAc, 3/1). <sup>1</sup>H NMR (400 MHz, CDCl<sub>3</sub>) δ (ppm) = 7.4 (d, J = 8.3 Hz, 2H), 7.3 (m, 3H), 7.2 (m, 3H), 7 (m, 9H), 6.9 (d, J = 6.7 Hz, 2H), 6.1 (bs, 1H), 4.3 (d, J = 7.8 Hz, 1H), 3.7 (d, J = 7.8 Hz, 1H), 3.6 (d, J = 13.0 Hz, 1H), 3.4 (d, J = 13.1 Hz, 1H), 2.2 (s, 3H), 1.7 (bs, 1H). <sup>13</sup>C NMR (100 MHz, CDCl<sub>3</sub>): δ (ppm) = 143.1, 138.6, 137.3, 129.5, 128.9, 128.8, 128.5, 128.3, 128.0, 127.9(8), 127.9(0), 127.7, 127.6, 127.5, 67.1, 63.4, 51.2, 21.8. HRMS (CI, [M+H]<sup>+</sup>) calc'd for C<sub>28</sub>H<sub>28</sub>N<sub>2</sub>O<sub>2</sub>S: 457.1950, found 457.1949. Anal Calc'd for C<sub>28</sub>H<sub>28</sub>N<sub>2</sub>O<sub>2</sub>S: C, 73.65, H, 6.18, N, 6.14, found: C, 73.81, H, 6.15, N, 6.05.

#### 4-Methyl-*N*-((1*R*,2*R*)-2-((4-methylbenzyl)amino)-1,2-diphenylethyl)benzene sulfonamide

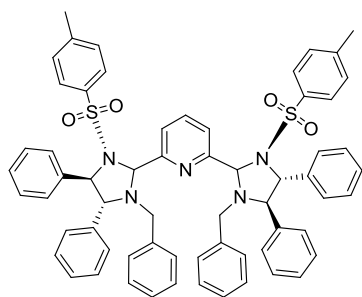


White solid, (96% isol. yield, 2.218 g). Purification by flash column chromatography (Hexane/EtOAc, 3/1). <sup>1</sup>H NMR (400 MHz, CDCl<sub>3</sub>) δ (ppm) = 7.3-6.8 (m, 18H), 6.0 (bs, 1H), 4.3 (d, J = 7.4 Hz, 1H), 3.6 (d, J = 7.6 Hz, 1H), 3.5 (d, J = 13.0 Hz, 1H), 3.3 (d, J = 13.0 Hz, 1H), 2.2 (s, 3H), 2.1 (s, 3H), 1.7 (bs, 1H). <sup>13</sup>C NMR (100 MHz, CDCl<sub>3</sub>): δ (ppm) = 143.1, 138.7, 137.5, 137.3, 136.8, 130.8, 129.5, 128.8, 128.4, 128.2, 128.0, 127.9, 127.8, 127.7(4), 127.7(1), 127.5, 126.5, 126.3, 67.6, 63.5, 49.3, 21.8, 19.2. HRMS (CI, [M+H]<sup>+</sup>) calc'd for C<sub>29</sub>H<sub>30</sub>N<sub>2</sub>O<sub>2</sub>S: 471.2106, found: 471.2104. Anal Calc'd for C<sub>29</sub>H<sub>30</sub>N<sub>2</sub>O<sub>2</sub>S: C, 74.01, H, 6.43, N, 5.95, found: C, 73.72, H, 6.55, N, 5.57.

### 2.5.8. General procedure for the synthesis of *sp*<sup>3</sup>-*N*-benzyl substituted PyBisulidine ligands.

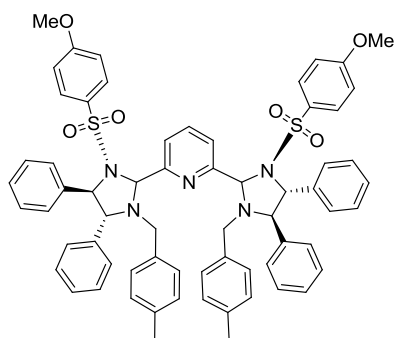
Prepared according to the general procedure, using pyridine-2,6-dicarbaldehyde (0.6 mmol, 81.0 mg), (*R,R*)- *N*-(2-amino-1,2-diphenylethyl)-4-methylbenzenesulfonamide (1.3 mmol, 483.8 mg), acetic acid (1.2 mmol, 60 μL) and DCM (24 mL).

## Analytical data

**2-((2R,4S,5S)-1-Benzyl-4,5-diphenyl-3-tosylimidazolidin-2-yl)-6-((2S,4S,5S)-1-benzyl-4,5-diphenyl-3-tosylimidazolidin-2-yl)pyridine (32)**

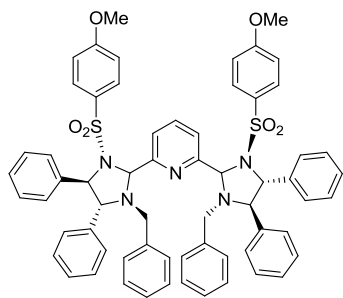
Colourless crystals (93% isol. yield, 607.0 mg). Purification by crystallization in DCM/MeOH.  $^1\text{H NMR}$  (400 MHz,  $\text{CDCl}_3$ ):  $\delta$  (ppm) = 7.67 (t,  $J$  = 7.7 Hz, 1H), 7.58 (d,  $J$  = 8.1 Hz, 4H), 7.31-7.10 (m, 22H), 6.96 (d,  $J$  = 2.4 Hz, 6H), 6.78 (d,  $J$  = 6.3 Hz, 4H), 6.61 (d,  $J$  = 7.3 Hz, 4H), 5.78 (s, 2H), 4.86 (d,  $J$  = 7.9 Hz, 2H), 4.63 (d,  $J$  = 8.6 Hz, 2H), 3.35 (m, 4H), 2.51 (s, 6H).  $^{13}\text{C NMR}$  (100 MHz,  $\text{CDCl}_3$ ):  $\delta$  (ppm) = 159.1, 144.2, 138.5, 138.0, 137.8, 134.2, 129.9, 129.2, 128.8, 128.7, 128.6,

128.5, 128.4, 127.9, 127.6, 127.5, 125.3, 79.6, 73.7, 72.4, 49.7, 22.1. **IR** (neat)  $\nu$  = 1594, 1494, 1454, 1346, 1160, 1091, 1070, 998, 811, 757, 736, 703, 661, 636. **HRMS** (FAB,  $[\text{M}+\text{H}]^+$ ) calc'd for  $[\text{C}_{63}\text{H}_{57}\text{N}_5\text{O}_4\text{S}_2]^+$ : 1012.3925, found: 1012.3923. **Anal Calc'd** for  $\text{C}_{63}\text{H}_{56}\text{N}_5\text{O}_4\text{S}_2$ : C, 74.75, H, 5.68, N, 6.92, found: C, 74.53, H, 5.68, N, 6.86. **mp**: 202-203  $^\circ\text{C}$ .

**2-((2R,4S,5S)-1-Benzyl-4,5-diphenyl-3-(methoxyphenyl)imidazolidin-2-yl)-6-((2S,4S,5S)-1-benzyl-4,5-diphenyl-3-(methoxyphenyl)imidazolidin-2-yl)pyridine (33)**

White solid (89% isol. yield, 607.0 mg). Purification by crystallisation in DCM/MeOH.  $^1\text{H NMR}$  (400 MHz,  $\text{CDCl}_3$ ):  $\delta$  (ppm) = 7.71 (t,  $J$  = 7.7 Hz, 1H), 7.62 (d,  $J$  = 7.1 Hz, 4H), 7.26-7.13 (m, 7H), 6.98-6.93 (m, 6H), 6.82 (d,  $J$  = 7.2 Hz, 4H), 6.67 (d,  $J$  = 7.1 Hz, 4H), 5.79 (s, 2H), 4.87 (d,  $J$  = 7.8 Hz, 2H), 4.65 (d,  $J$  = 7.8 Hz, 2H), 3.91 (s, 6H), 3.39 (d,  $J$  = 13.9 Hz, 2H), 3.32 (d,  $J$  = 13.9 Hz, 2H), 2.13 (s, 6H).  $^{13}\text{C NMR}$  (100 MHz,  $\text{CDCl}_3$ ):  $\delta$  (ppm) = 163.4, 158.9, 138.4, 137.3, 137.1, 136.5, 135.2, 130.5, 130.0,

128.8, 128.4, 128.2, 128.1, 127.5, 127.1, 126.8, 125.5, 124.7, 114.1, 79.5, 73.3, 71.9, 55.8, 46.8, 29.7. **IR** (neat)  $\nu$  = 2923, 2852, 1593, 1575, 1495, 1453, 1382, 1311, 1266, 1246, 1179, 1158, 1091, 1074, 1011, 970, 895, 833, 747, 699, 673, 653, 628, 569, 551  $\text{cm}^{-1}$ . **Anal Calc'd** for  $\text{C}_{65}\text{H}_{57}\text{N}_5\text{O}_6\text{S}_2$ : C, 73.08, H, 5.38, N, 6.56, found: C, 73.18, H, 5.32, N, 6.44. **mp**: 232-233  $^\circ\text{C}$ . **X-ray diffraction** of this compound is provided in pages 72-73.

**2-((2R,4S,5S)-1-Benzyl-4,5-diphenyl-3-(methoxyphenyl)imidazolidin-2-yl)-6-((2S,4S,5S)-1-benzyl-4,5-diphenyl-3-(methoxyphenyl)imidazolidin-2-yl)pyridine (34)**

White solid (92% isol. yield, 576.4 mg). Purification by crystallisation in DCM/MeOH.  $^1\text{H NMR}$  (400 MHz,  $\text{CDCl}_3$ )  $\delta$  (ppm) = 7.68-7.66 (m, 1H), 7.64-7.59 (m, 4H), 7.22-7.14 (m, 20H), 6.98-6.93 (m, 4H), 6.66 (d,  $J$  = 7.4 Hz, 4H), 5.79 (s, 2H), 4.86 (d,  $J$  = 7.8 Hz, 2H), 4.63 (d,  $J$  = 7.7 Hz, 2H), 3.91 (s, 6H), 3.40 (d,  $J$  = 13.9 Hz, 1H), 3.32 (d,  $J$  = 13.9 Hz, 2H).  $^{13}\text{C NMR}$  (100 MHz,  $\text{CDCl}_3$ )  $\delta$  (ppm) = 163.2, 158.8, 138.1, 137.7, 137.3, 130.4, 128.7, 128.6, 128.5, 128.3, 128.2, 128.1, 128.0,

127.5, 127.2, 124.8, 114.0, 79.2, 73.3, 72.0, 55.7, 49.3. **Anal Calc'd** for  $C_{63}H_{57}N_5O_6S_2$ : C, 72.46, H, 5.50, N, 6.71, found: C, 72.23, H, 5.47, N, 6.61. **IR** (neat)  $\nu = 3102, 1592, 1576, 1493, 1454, 1346, 1313, 1264, 1241, 1157, 1090, 1075, 1055, 1018, 837, 820, 762, 743, 696, 674, 628, 589, 569, 541\text{ cm}^{-1}$ . **mp**: 209-210 °C.

### 2.5.9. General multistep procedure for the synthesis of 4-methoxypyridine-2,6-dicarboxaldehyde

#### 2.5.9.1. Synthesis of dimethyl-4-hydroxypyridine-2,6-dicarboxylate<sup>28</sup> (36)

Chelidamic acid monohydrate (8.00 mmol, 1.46 g) was suspended in MeOH (35 mL) and sulphuric acid (97%) was added slowly under vigorous stirring until complete solution of the starting acid. The resulting yellow solution was refluxed for 2 h and then solvents were removed in vacuo. Water was added (20 mL) and the solution was neutralised with saturated  $\text{NaHCO}_3$  to pH 8 and the aqueous solution was extracted with DCM (4 x 20 mL). The organic phase was dried over  $\text{MgSO}_4$ , filtered and evaporated under vacuo to afford the product as a white solid (80% yield, 1.41 g).

**<sup>1</sup>H NMR** (400 MHz,  $\text{CDCl}_3$ )  $\delta$  (ppm) = 7.8 (bs, 1H), 7.2 (s, 2H), 4.0 (s, 6H). **MS** (CI,  $[\text{M}+\text{H}]^+$ ) calc'd for  $\text{C}_9\text{H}_9\text{NO}_5$  : 212, found : 212. **Anal Calc'd** for  $\text{C}_9\text{H}_9\text{NO}_5$ : C, 51.19, H, 4.30, N, 6.63, found: C, 50.79, H, 4.70, N, 6.19.

#### 2.5.9.2. Synthesis of dimethyl 4-methoxypyridine-2,6-dicarboxylate<sup>29</sup> (37)

Dimethyl-4-hydroxypyridine-2,6-dicarboxylate (4.0 mmol, 900 mg),  $\text{K}_2\text{CO}_3$  (6.6 mmol, 990 mg) and dimethyl sulphate (4.4 mmol, 594 mg) were stirred in DMF (10 mL) at r.t. for 24 h (t.l.c. control). The solvent was removed under reduced pressure and the crude product was dissolved in DCM/water and the organic phase extracted with DCM, dried over  $\text{MgSO}_4$ , filtered and evaporated under vacuo to afford the product as a white solid (90% yield, 825.4 mg).

**<sup>1</sup>H NMR** (400 MHz,  $\text{CDCl}_3$ )  $\delta$  (ppm) = 7.8 (s, 2H), 4.0 (s, 6H), 3.9 (s, 3H). **<sup>13</sup>C NMR** (100 MHz,  $\text{CDCl}_3$ )  $\delta$  (ppm) = 167.7, 165.2, 149.8, 114.2, 56.1, 53.3. **MS** (CI,  $[\text{M}+\text{Na}]^+$ ) calc'd for  $\text{C}_{10}\text{H}_{11}\text{NO}_5\text{Na}$ : 248, found: 248. **Anal Calc'd** for  $\text{C}_{10}\text{H}_{11}\text{NO}_5$ : C, 53.33, H, 4.92, N, 6.22, found: C, 53.11, H, 4.84, N, 6.03.

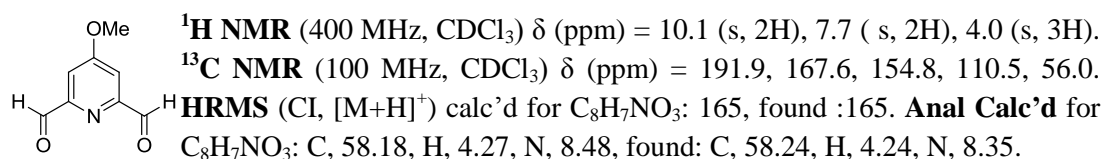
**2.5.9.3. Synthesis of dimethyl 2,4-dihydroxymethyl-4-methoxypyridine<sup>30</sup> (38)**

4-Methoxypyridine-2,6-dicarboxylate (2.5 mmol, 560 mg) and NaBH<sub>4</sub> (3.75 mmol, 469 mg) were refluxed in freshly distilled THF (22 mL) and anhydrous MeOH (6 mL) was added slowly dropwise to the boiling mixture over a period of 1 h. The mixture was allowed to reflux for an additional 2 h and then cooled to r.t. Water (12 mL) was added slowly and the organic solvent was removed in vacuo and the solution was extracted with ethyl acetate (3 x 12 mL). The organic phase was evaporated to dryness and the residue was purified by silica gel column chromatography (9/1 DCM/MeOH) to afford the product as a white solid (80% yield, 338 mg).

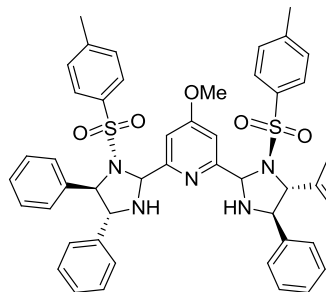
<sup>1</sup>H NMR (400 MHz, DMSO-d<sub>6</sub>) δ (ppm) = 6.9 (s, 2H), 5.4 (d, J = 5.9 Hz, 4H), 4.4 (d, J = 5.9 Hz, 2H), 3.8 (s, 3H). <sup>13</sup>C NMR (100 MHz, DMSO-d<sub>6</sub>) δ (ppm) = 167.1, 163.4, 104.6, 64.5, 56.1. MS (CI, [M+H]<sup>+</sup>) calc'd for C<sub>8</sub>H<sub>11</sub>NO<sub>3</sub> 170, found 170.

**2.5.9.4. Synthesis of 4-methoxypyridinedicarbaldehyde<sup>31</sup> (39)**

Dimethyl 2,4-dihydroxymethyl-4-methoxypyridine (1.8 mmol, 300 mg) and SeO<sub>2</sub> (1.8 mmol, 200 mg) were heated overnight in xylene at 110 °C. The hot reaction mixture was filtered through Celite and the solvent was removed under vacuo. The resulting red-pink solid was purified by silica gel column chromatography (3/1 ethyl acetate/DCM) to afford the final product as cream needles (96% yield, 385.0 mg).

**2.5.10. General procedure for the synthesis of Pyridyl-substituted PiBisulidine ligands.**

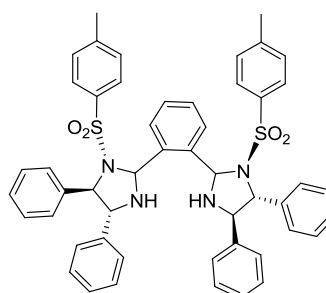
Prepared according to the general procedure, using 4-methoxypyridine-2,6-dicarbaldehyde (0.5 mmol, 165 mg) and (*R,R*)-*N*-(2-amino-1,2-diphenylethyl)-4-methylbenzenesulfonamide (1.1 mmol, 806.5 mg), acetic acid (1.0 mmol, 50 μL) and DCM (24 mL).

**Analytical data****2-((2*R*,4*R*,5*R*)-4,5-Diphenyl-1-tosylimidazolidin-2-yl)-6-((2*S*,4*R*,5*R*)-4,5-diphenyl-3-tosylpyrrolidin-2-yl)-4-methoxypyridine (40)**

Transparent crystals (90% isol. yield, 775.2 mg). Purification by crystallisation in DCM/MeOH.  $^1\text{H NMR}$  (400 MHz,  $\text{CDCl}_3$ )  $\delta$  (ppm) = 7.57 (d,  $J = 8.0$  Hz, 4H), 7.50 (s, 2H), 7.17-7.14 (m, 20H), 6.96 (d,  $J = 7.1$  Hz, 4H), 5.76 (s, 2H), 4.65 (d,  $J = 5.9$  Hz, 2H), 4.20 (d,  $J = 5.4$  Hz, 2H), 4.02 (s, 3H), 3.53 (bs, 2H), 2.41 (s, 6H).  $^{13}\text{C NMR}$  (100 MHz,  $\text{CDCl}_3$ )  $\delta$  (ppm) = 167.4, 159.9, 143.7, 139.4, 139.0, 134.1, 129.5, 128.4, 128.2, 127.8, 127.4, 127.1, 126.7, 109.7, 78.1, 71.6, 69.1, 55.7, 21.6. **IR** (neat)  $\nu = 3286, 1599, 1573, 1493, 1472, 1446, 1345, 1319, 1274, 1161, 1135, 1091, 1055, 1035, 888, 853, 846, 798, 730, 697, 664, 600, 587, 551, 530$   $\text{cm}^{-1}$ . **HRMS** (FAB,  $[\text{M}+\text{H}]^+$ ) calc'd: 1056.5490, found: 1056.5467. **Anal Calc'd** for  $\text{C}_{55}\text{H}_{54}\text{N}_6\text{O}_5\text{S}_2$ : C, 70.04, H, 5.77, N, 8.91, found: C, 70.28, H, 5.46, N, 8.94. **mp**: 138-139  $^\circ\text{C}$ .

**2.5.11. General procedure for the synthesis of Bisulidine ligands**

Prepared according to the general procedure, using phthaldehyde (1.0 mmol, 134.1 mg) and (*R,R*)-*N*-(2-amino-1,2-diphenylethyl)-4-*t*-butylbenzenesulfonamide (2.05 mmol), acetic acid (1.0 mmol, 50  $\mu\text{L}$ ) and DCM (24 mL).

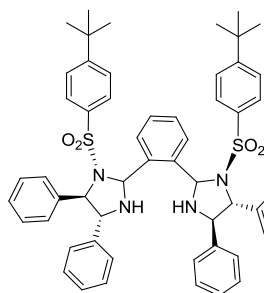
**Analytical data****1-((2*R*,4*R*,5*R*)-1-((4-(Methyl)phenyl)sulfonyl)-4,5-diphenylimidazolidin-2-yl)-2-((2*S*,4*R*,5*R*)-1-((4-(methyl)phenyl)sulfonyl)-4,5-diphenylimidazolidin-2-yl)benzene (42)**

White solid (60% yield, 498.7 mg). Purification by flash chromatography (Hexane/EtOAc: 3/1).  $^1\text{H NMR}$  (400 MHz,  $\text{CDCl}_3$ ):  $\delta$  (ppm) = 6.95-7.78 (m, 32H), 6.56 (d,  $J = 7.1$  Hz, 1H), 5.51 (d,  $J = 7.1$  Hz, 1H), 5.23 (d,  $J = 11.4$  Hz, 1H), 4.97 (d,  $J = 7.1$  Hz, 1H), 4.71 (d,  $J = 11.2$  Hz, 1H), 4.00 (d,  $J = 12.2$  Hz, 1H), 2.40 (s, 3H), 2.34 (s, 3H).  $^{13}\text{C NMR}$  (100 MHz,  $\text{CDCl}_3$ ):  $\delta$  (ppm) = 157.8, 154.2, 153.9, 140.8, 140.6, 138.7, 137.6, 136.6, 136.5, 129.4, 128.8, 128.7, 128.3, 128.1, 127.4, 127.1, 126.9, 126.3, 124.9, 113.4, 77.7, 66.5, 59.7, 23.4. **HRMS** (FAB,  $[\text{M}+\text{H}]^+$ ) calc'd for  $[\text{C}_{50}\text{H}_{46}\text{N}_4\text{O}_4\text{S}_2]^+$ : 830.2960, found: 830.2958. **mp**: 181-182  $^\circ\text{C}$ .



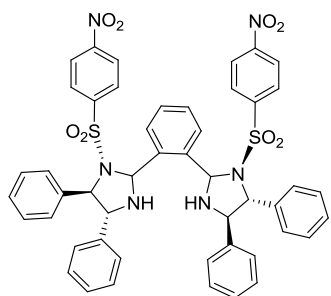
**1-((2*R*,4*R*,5*R*)-1-((4-*tert*-Butyl)phenyl)sulfonyl)-4,5-diphenylimidazolidin-2-yl)-2-((2*S*,4*R*,5*R*)-1-((4-*tert*-butyl)phenyl)sulfonyl)-4,5-diphenylimidazolidin-2-yl)benzene**

(43)



White solid (60% yield, 548.9 mg). Purification by flash chromatography (Hexane/EtOAc, 3/1).  $^1\text{H NMR}$  (400 MHz,  $\text{CDCl}_3$ ):  $\delta$  (ppm) = 7.78 (d,  $J=7.6$  Hz, 1H), 7.59 (d,  $J=7.6$  Hz, 2H), 7.52 (d,  $J=7.6$  Hz, 2H), 7.19-6.94 (m, 27H), 6.57 (bs, 3H), 5.36 (d,  $J=7.4$  Hz, 1H), 5.12 (d,  $J=11.3$  Hz, 1H), 4.86 (m, 2H), 4.06 (d,  $J=16.2$  Hz, 1H), 1.23 (d,  $J=7.6$  Hz, 18H).  $^{13}\text{C NMR}$  (100 MHz,  $\text{CDCl}_3$ ):  $\delta$  (ppm) = 157.7, 154.0, 153.8, 140.9, 140.5, 137.2, 136.6, 136.4, 136.3, 129.3, 128.4, 127.5, 127.0, 126.8, 126.4, 126.3, 126.2, 126.1, 125.8, 125.7, 125.4, 125.3, 124.6, 123.9, 123.8, 121.7, 75.9, 64.8, 57.9, 33.4, 29.6. **IR** (neat)  $\nu = 3257, 2958, 1629, 1454, 1400, 1321, 1211, 1157, 1110, 1087, 1058, 1027, 927, 829, 754, 700, 636$ . **HRMS** (FAB,  $[\text{M}+\text{H}]^+$ ) calc'd for  $[\text{C}_{56}\text{H}_{59}\text{N}_4\text{O}_4\text{S}_2]^+$ : 915.3972, found: 915.3958. **Anal Calc'd** for  $\text{C}_{56}\text{H}_{58}\text{N}_4\text{O}_4\text{S}_2$ : C, 73.49, H, 6.39, N, 6.12, S, 7.01; found: C, 72.99, H, 6.55, N, 6.13, S, 6.95. **mp**: 190-191 °C.

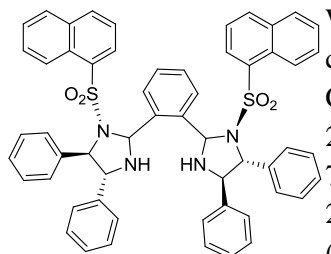
**1-((2*R*,4*R*,5*R*)-1-(4-Nitrophenyl)sulfonyl)-4,5-diphenylimidazolidin-2-yl)-2-((2*S*,4*R*,5*R*)-1-(4-nitrophenyl)sulfonyl)-4,5-diphenylimidazolidin-2-yl)benzene** (45)



White solid (48% yield, 428.4 mg). Purification by flash chromatography (Hexane/EtOAc, 5/2).  $^1\text{H NMR}$  (400 MHz,  $\text{CDCl}_3$ ):  $\delta$  (ppm) = 7.75 (m, 4H), 7.57 (m, 4H), 7.43 (d,  $J=6.3, 1.1$  Hz, 2H), 7.32 (dd,  $J=6.3, 1.2$  Hz, 2H), 7.24-7.12 (m, 16H), 6.92-6.89 (m, 4H), 5.87 (s, 2H), 5.24 (bs, 2H), 4.54 (d,  $J=5.6$  Hz, 2H), 4.06 (d,  $J=5.7$  Hz, 2H).  $^{13}\text{C NMR}$  (100 MHz,  $\text{CDCl}_3$ ):  $\delta$  (ppm) = 151.4, 145.9, 138.3, 128.6, 128.3, 127.9, 127.7, 127.1, 124.2, 78.9, 71.8, 65.8. **IR** (neat)  $\nu = 3262, 1678, 1523, 1349, 1311, 1225, 1211, 1163, 1154, 967, 946, 887, 794, 764, 732, 589, 569$   $\text{cm}^{-1}$ . **HRMS** (FAB) calc'd for  $[\text{C}_{42}\text{H}_{38}\text{N}_5\text{O}_5\text{S}]^+$ : 724.2588, found: 724.2588. **mp**: 192-193 °C.

**1-((2*R*,4*R*,5*R*)-1-(Naphthalene-1-ylsulfonyl)-4,5-diphenylimidazolidin-2-yl)-2-**

**((2*S*,4*R*,5*R*)-1-(naphthalene-1-ylsulfonyl)-4,5-diphenylimidazolidin-2-yl)benzene** (46)



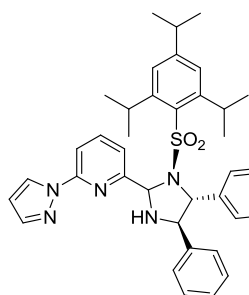
White solid (50% yield, 451.1 mg). Purification by flash chromatography (Hexane/EtOAc, 5/2).  $^1\text{H NMR}$  (400 MHz,  $\text{CDCl}_3$ ):  $\delta$  (ppm) = 8.42 (d,  $J=8.5$  Hz, 2H), 7.92 (d,  $J=8.6$  Hz, 2H), 8.73 (d,  $J=7.8$  Hz, 2H), 8.68 (d,  $J=8.0$  Hz, 2H), 8.54 (d,  $J=7.9$  Hz, 2H), 7.42-7.29 (m, 12H), 7.21-7.03 (m, 12H), 6.87 (m, 2H), 6.72 (m, 2H), 5.22 (d,  $J=4.5$  Hz, 2H), 5.14 (bs, 2H), 4.56 (d,  $J=5.6$  Hz, 2H), 3.96 (d,  $J=5.6$  Hz, 2H).  $^{13}\text{C NMR}$  (100 MHz,  $\text{CDCl}_3$ ):  $\delta$  (ppm) = 142.5, 138.3, 136.7, 134.0, 131.6, 131.0, 128.5, 128.3, 127.9, 127.7, 127.1, 126.8, 126.3, 124.6, 78.8, 71.5, 65.9. **Anal Calc'd** for  $\text{C}_{56}\text{H}_{46}\text{N}_4\text{O}_4\text{S}_2$ : C, 74.48, H, 5.13, N, 6.20; found: C, 74.65, H, 5.22, N, 6.17.

### 2.5.12. General procedure for the synthesis of asymmetric ligands

Prepared according to the general procedure using 6-(1H-pyrazol-1-yl)picolinaldehyde<sup>24</sup> (1.0 mmol, 134.1 mg) and (*R,R*)-*N*-(2-amino-1,2-diphenylethyl)-2,4,6-triisopropylbenzene sulfonamide (1.05 mmol), acetic acid (1.0 mmol, 50  $\mu$ L) and DCM (24 mL).

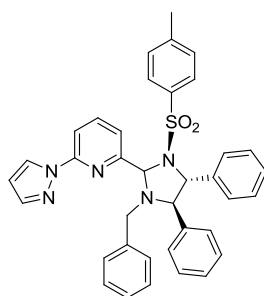
#### Analytical data

#### 2-((2*S*,4*R*,5*R*)-4,5-Diphenyl-1-((2,4,6-triisopropylphenyl)sulfonyl)imidazolidin-2-yl)-6-(1H-pyrazol-1-yl)pyridine (53)



White solid (98% yield, 620.9 mg). Purification by flash chromatography (Hexane/EtOAc, 3/1). <sup>1</sup>H NMR (400 MHz, CDCl<sub>3</sub>):  $\delta$  (ppm) = 8.32 (d, *J* = 2.5 Hz, 1H), 8.02 (d, *J* = 8.2 Hz, 1H), 7.82 (t, *J* = 7.5 Hz, 1H), 7.77 (d, *J* = 1.5 Hz, 1H), 7.43-7.28 (m, 5H), 7.22 (d, *J* = 7.5 Hz, 1H), 7.09-6.94 (m, 7H), 6.43 (dd, *J* = 2.5, 1.6 Hz, 1H), 6.28 (s, 1H), 5.05 (d, *J* = 7.4 Hz, 1H), 4.95 (d, *J* = 7.3 Hz, 1H), 3.90 (septet, *J* = 6.6 Hz, 2H), 3.51 (bs, 1H), 2.79 (septet, *J* = 6.6 Hz, 1H), 1.17 (d, *J* = 6.7 Hz, 6H), 0.99 (d, *J* = 6.7 Hz, 18H). <sup>13</sup>C NMR (100 MHz, CDCl<sub>3</sub>):  $\delta$  (ppm) = 158.5, 153.9, 152.0, 151.8, 142.6, 139.8, 139.4, 138.7, 131.6, 129.1, 128.6, 128.3, 127.8, 127.7, 127.6, 127.4, 123.9, 120.7, 112.3, 108.2, 78.2, 72.6, 70.9, 34.5, 29.7, 25.1, 23.9. IR (neat)  $\nu$  = 3355, 2955, 2870, 1600, 1578, 1455, 1389, 1307, 1293, 1200, 1148, 1133, 1041, 944, 889, 837, 811, 749, 700, 671, 596 cm<sup>-1</sup>. HRMS (EI) *m/z* calc'd C<sub>38</sub>H<sub>43</sub>N<sub>5</sub>O<sub>2</sub>SNa [M + Na]<sup>+</sup> : 656.3035, found, 656.3057. Anal Calc'd for C<sub>38</sub>H<sub>43</sub>N<sub>5</sub>O<sub>4</sub>S: C, 72.01, H, 6.84, N, 11.05, found: C, 71.92, H, 6.89, N, 11.07. mp: 134-135 °C.

#### 2-((4*R*,5*R*)-1-Benzyl-4,5-diphenyl-3-tosylimidazolidin-2-yl)-6-(1H-pyrazol-1-yl)pyridine (54)



White solid (97% yield, 593.1 mg). Purification by flash chromatography (Hexane/EtOAc, 3/1). <sup>1</sup>H NMR (400 MHz, CDCl<sub>3</sub>):  $\delta$  (ppm) = 8.37 (d, *J* = 2.0 Hz, 1H), 8.04 (m, 2H), 7.77 (d, *J* = 8.0 Hz, 2H), 7.55 (d, *J* = 8.0 Hz, 2H), 7.35-7.12 (m, 13H), 6.45 (q, *J* = 1.8 Hz, 1H), 5.95 (s, 1H), 4.85 (d, *J* = 5.7 Hz, 1H), 4.48 (m, 1H), 3.65 (m, 1H), 2.40 (s, 3H). <sup>13</sup>C NMR (100 MHz, CDCl<sub>3</sub>):  $\delta$  (ppm) = 158.7, 151.1, 142.2, 139.7, 138.8, 138.3, 137.5, 129.3, 128.9, 128.8, 128.6, 127.9, 127.3, 121.6, 110.5, 107.8, 78.6, 72.7, 70.7, 49.8, 22.3.

### 2.5.13. General procedure for the synthesis of [Fe(BF<sub>4</sub>)(NNN)(MeCN)<sub>2</sub>](BF<sub>4</sub>) (20)

In an Schlenk tube equipped with a stirring bar, ligand **19** (0.12 mmol, 100 mg) and Fe(BF<sub>4</sub>)<sub>2</sub> x 6H<sub>2</sub>O (0.12 mmol, 40.5 mg) were added. The tube was degassed and placed under a N<sub>2</sub> atmosphere. Freshly distilled MeCN ( 5 mL) was added by syringe and the initial

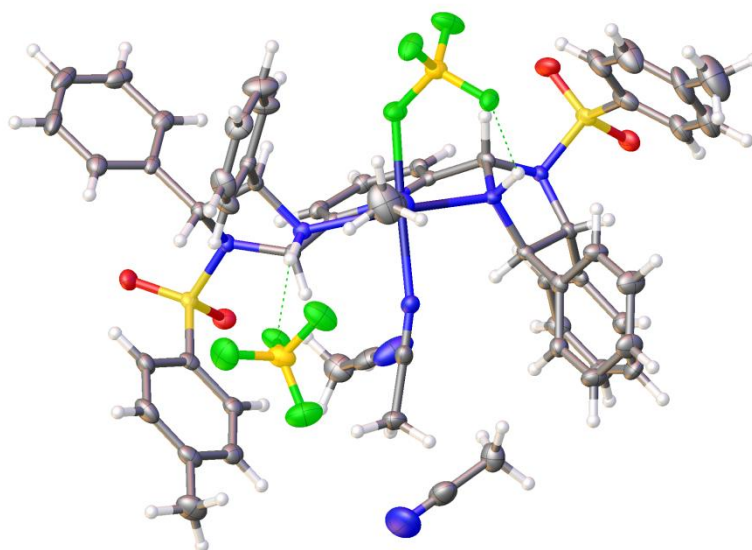
transparent solution rapidly turned orange. The reaction mixture was stirred at 30 °C for 2 h and then filtered over Celite under a N<sub>2</sub> atmosphere. The bright orange solution was concentrated to a small volume (*circa* 2.0 mL) and freshly distilled hexane (2.0 mL) was subsequently added dropwise over the MeCN layer. The biphasic mixture was left under a N<sub>2</sub> atmosphere until well shaped crystals formed. The crystals were filtered and washed with distilled hexane and stored under a N<sub>2</sub> atmosphere, where they were found to be stable for months (68% yield, 96.8 mg).

### Crystallographic data of 20

The structure determination was performed by the Chemistry Department X-ray Crystallographic Service.

Single crystals of each reported compound were mounted on a MiTeGen MicroMount using Fomblin oil. The data were measured at 100 K on a Bruker D8 diffractometer using Mo wavelengths and observed with an Apex II CCD detector. Data collection and processing were completed inside the APEX2 software suite<sup>33</sup>. Data integration and global cell refinement were performed with the program SAINT<sup>34</sup> and data were corrected using SADABS<sup>35</sup>. Structural solutions and least-squares refinements were conducted using the OLEX2 interface<sup>36</sup> to the SHELX suit of packages.<sup>37</sup>

### (*R,R*)-20

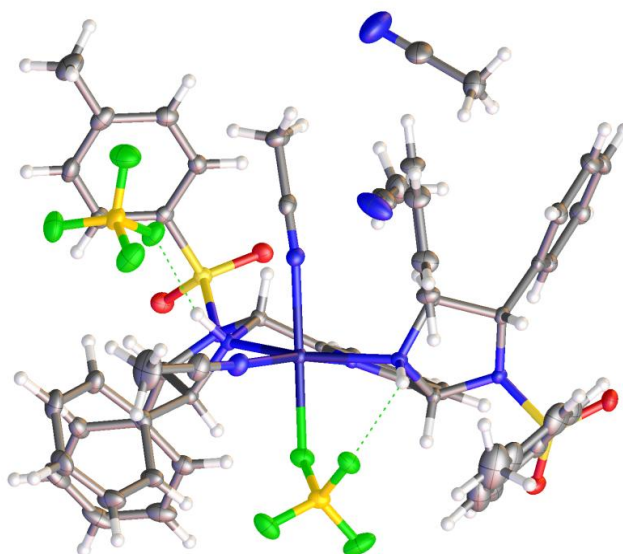


CCDC 1005139 contains the supplementary crystallographic data for this compound. This data can be obtained free of charge from The Cambridge Crystallographic Data Centre via [www.ccdc.cam.ac.uk/data\\_request/cif](http://www.ccdc.cam.ac.uk/data_request/cif).

**Crystal structure determination of CCDC 1005139.** Crystal Data for  $C_{57}H_{57}B_2F_8FeN_9O_4S_2$  ( $M=1225.71$ ): orthorhombic, space group  $P2_12_12_1$  (no. 19),  $a = 10.4974(5)$  Å,  $b = 14.7463(8)$  Å,  $c = 37.618(2)$  Å,  $V = 5823.2(5)$  Å<sup>3</sup>,  $Z = 4$ ,  $T = 110(2)$  K,  $\mu(\text{MoK}\alpha) = 0.411$  mm<sup>-1</sup>,  $D_{\text{calc}} = 1.398$  g/mm<sup>3</sup>, 38429 reflections measured ( $2.96 \leq 2\theta \leq 52.04$ ), 11119 unique ( $R_{\text{int}} = 0.0329$ ,  $R_{\text{sigma}} = 0.0394$ ) which were used in all calculations. The final  $R_1$  was 0.0398 ( $>2\sigma(I)$ ) and  $wR_2$  was 0.0886 (all data).

**Table 1 Crystal data and structure refinement for CCDC 1005139.**

Identification code	gon429bm
Empirical formula	$C_{57}H_{57}B_2F_8FeN_9O_4S_2$
Formula weight	1225.71
Temperature/K	110(2)
Crystal system	orthorhombic
Space group	$P2_12_12_1$
$a/\text{\AA}$	10.4974(5)
$b/\text{\AA}$	14.7463(8)
$c/\text{\AA}$	37.618(2)
$\alpha/^\circ$	90.00
$\beta/^\circ$	90.00
$\gamma/^\circ$	90.00
Volume/Å <sup>3</sup>	5823.2(5)
Z	4
$\rho_{\text{calc}}/\text{mg/mm}^3$	1.398
$m/\text{mm}^{-1}$	0.411
F(000)	2536.0
Crystal size/mm <sup>3</sup>	$0.39 \times 0.32 \times 0.19$
Radiation	MoK $\alpha$ ( $\lambda = 0.71073$ )
$2\theta$ range for data collection	2.96 to 52.04°
Index ranges	$-12 \leq h \leq 12, -17 \leq k \leq 17, -41 \leq l \leq 46$
Reflections collected	38429
Independent reflections	11119 [ $R_{\text{int}} = 0.0329, R_{\text{sigma}} = 0.0394$ ]
Data/restraints/parameters	11119/417/811
Goodness-of-fit on $F^2$	1.084
Final R indexes [ $I > 2\sigma(I)$ ]	$R_1 = 0.0398, wR_2 = 0.0864$
Final R indexes [all data]	$R_1 = 0.0432, wR_2 = 0.0886$
Largest diff. peak/hole / e Å <sup>-3</sup>	0.44/-0.26
Flack parameter	-0.002(12)

**(S,S)-20**

**Crystal structure determination of (S,S)-20. Crystal Data** for  $C_{57}H_{57}B_2F_8FeN_9O_4S_2$  ( $M=1225.71$ ): orthorhombic, space group  $P2_12_12_1$  (no. 19),  $a = 10.4888(5)$  Å,  $b = 14.7280(7)$  Å,  $c = 37.5951(18)$  Å,  $V = 5807.7(5)$  Å<sup>3</sup>,  $Z = 4$ ,  $T = 100(2)$  K,  $\mu(\text{MoK}\alpha) = 0.412$  mm<sup>-1</sup>,  $D_{\text{calc}} = 1.402$  g/mm<sup>3</sup>, 51590 reflections measured ( $3.52 \leq 2\theta \leq 54.96$ ), 13288 unique ( $R_{\text{int}} = 0.0284$ ) which were used in all calculations. The final  $R_1$  was 0.0309 ( $>2\sigma(I)$ ) and  $wR_2$  was 0.0714 (all data).

**Table 1 Crystal data and structure refinement for  $[\text{Fe}(\text{BF}_4)(\text{NNN})(\text{MeCN})_2](\text{BF}_4)$**

Identification code	$[\text{Fe}(\text{BF}_4)(\text{NNN})(\text{MeCN})_2](\text{BF}_4)$
Empirical formula	$C_{57}H_{57}B_2F_8FeN_9O_4S_2$
Formula weight	1225.71
Temperature/K	100(2)
Crystal system	orthorhombic
Space group	$P2_12_12_1$
$a/\text{Å}$	10.4888(5)
$b/\text{Å}$	14.7280(7)
$c/\text{Å}$	37.5951(18)
$\alpha/^\circ$	90.00
$\beta/^\circ$	90.00
$\gamma/^\circ$	90.00
Volume/Å <sup>3</sup>	5807.7(5)
$Z$	4
$\rho_{\text{calc}}/\text{mg}/\text{mm}^3$	1.402
$\mu/\text{mm}^{-1}$	0.412
$F(000)$	2536.0

---

Crystal size/mm <sup>3</sup>	0.25 × 0.19 × 0.09
2 $\theta$ range for data collection	3.52 to 54.96°
Index ranges	-11 ≤ h ≤ 13, -19 ≤ k ≤ 19, -48 ≤ l ≤ 48
Reflections collected	51590
Independent reflections	13288[R(int) = 0.0284]
Data/restraints/parameters	13288/0/811
Goodness-of-fit on F <sup>2</sup>	1.025
Final R indexes [I ≥ 2σ (I)]	R <sub>1</sub> = 0.0309, wR <sub>2</sub> = 0.0701
Final R indexes [all data]	R <sub>1</sub> = 0.0340, wR <sub>2</sub> = 0.0714
Largest diff. peak/hole / e Å <sup>-3</sup>	0.37/-0.25
Flack parameter	0.011(8)

## 2.6. References

- [1] Liu, T.; DuBois, D. L.; Morris Bullock, R. *Nat. Chem.* **2013**, *5*, 228.
- [2] Hennessy, E. T.; Betley, T. A. *Science* **2013**, *340*, 591.
- [3] Pfaltz, A.; Drury III, W. J. *P.N.A.S.* **2004**, *101*, 5723.
- [4] Blaser, H. U. *Adv. Synth. Catal.* **2002**, *344*, 17.
- [5] Shibasaki, M.; Matsunaga, S. *Chem. Soc. Rev.* **2006**, *35*, 269.
- [6] Benito-Garagorri, D.; Kirchner, K. *Acc. Chem. Res.* **2008**, *41*, 201.
- [7] Van der Boom, M. E.; Milstein, D. *Chem. Rev.* **2003**, *103*, 1759.
- [8] Nishiyama, H.; Sakaguchi, H.; Nakamura, T.; Horihata, M.; Kondo, M.; Itoh, K. *Organometallics* **1989**, *8*, 846.
- [9] (a) Gant, T.; Meyers, A. I. *Tetrahedron* **1994**, *50*, 2297. (b) Ager, D. J.; Prakash, I.; Schaad, D. R. *Chem. Rev.* **1996**, *96*, 835. (c) Schwekendrek, K.; Glorius, F. *Synlett* **1996**, *18*, 2996. (d) Sayama, S. *Synlett* **2006**, *10*, 1479. (e) Takahashi, S.; Togo, H. *Synthesis* **2009**, *14*, 2329.
- [10] (a) Evans, D. A.; Kozlowski, M. C.; Murry, J. A.; Burgey, C. S.; Campos, K. R.; Connell, B. T.; Staples, R. J. *J. Am. Chem. Soc.* **1999**, *121*, 669. (b) Evans, D. A.; Wu, J. *J. Am. Chem. Soc.* **2005**, *127*, 8006. (c) Evans, D. A.; Aye, Y. *J. Am. Chem. Soc.* **2006**, *128*, 11034. (d) Zhao, J. F.; Tsui, H. Y.; Wu, P. J., Lu; J., Loh, T. P. *J. Am. Chem. Soc.*

- 2008, 130, 16492. (e) Zhao, Y. J.; Li, B.; Tan, L. J. S.; Shen, Z. L.; Loh, T. P. *J. Am. Chem. Soc.* **2008**, 132, 10242.
- [11] Kawatsura, M.; Kajita, K.; Hayase, S.; Itoh, T. *Synlett* **2010**, 8, 1243.
- [12] Hosokawa, S.; Ito, J. I.; Nishiyama, H. *Organometallics* **2010**, 29, 5773.
- [13] Que Jr., L.; Tolman, W. B. *Nature* **2008**, 455, 333.
- [14] See Chapter 1
- [15] See Chapter 1
- [16] Complexes 8 and 9 are partially soluble in common organic solvents such as THF, MeCN and chlorinated solvents. Dilution was found to enhance the solubility in DCM.
- [17] Bauer, I., Knolker, H.-J. in *Iron Catalysis in Organic Chemistry* (Wiley – V.H.C., Weinheim, 2008, Chapter 1, pg 1-3).
- [18] Examples of Fe(terpy)<sub>2</sub> complexes : (a) Machan, C. W.; Adelhardt, M.; Sarjeant, A. A.; Stern, C. L.; Sutter, J.; Meyer, K.; Mirkin, C. A. *J. Am. Chem. Soc.* **2012**, 134, 16921. (b) Henderson, I. M.; Hyward, R. C. *J. Mater. Chem.* **2012**, 22, 21366. Examples of Fe(PyBox)<sub>2</sub> complexes: Cabort, A. *Inorganica Chimica Acta* **2004**, 350, 193.
- [19] Constable, E. C. *Advances Inorg. Chem.* **1986**, 30, 69.
- [20] (a) Arai, T.; Mishiro, A.; Yokoyama, N.; Suzuki, K.; Sato, H. *J. Am. Chem. Soc.* **2010**, 132, 5338. (b) Arai, T.; Mishiro, A.; Matsumura, E.; Awata, A.; Shirasugi, M. *Chem. Eur. J.* **2012**, 18, 11219.
- [21] Beck, W.; Suenkel, K. *Chem. Rev.* **1988**, 88, 1405.
- [22] Desimoni, G.; Faita, G.; Jorgensen, K. A. *Chem. Rev.* **2006**, 106, 3561.
- [23] (a) Zeng, F. L.; Yu, Z. K. *J. Org. Chem.* **2006**, 71, 5274. (b) Sun, X. J.; Yu, Z. K.; Wu, S. Z.; Xiao, W.-J. *Organometallics* **2005**, 24, 2959. (c) Deng, H. X.; Yu, Z. K.; Dong, J. H.; Wu, S. Z. *Organometallics* **2005**, 24, 4110.
- [24] Zheng, F.; Yu, Z. *Organometallics* **2009**, 28, 1855.
- [25] Redlich, M.; Hossain, M. M. *Tetrahedron Lett.* **2004**, 45, 8987.
- [26] Livingstone, S. E.; Nolan, J. D. *J. Chem. Soc., Dalton Trans.* **1972**, 217.
- [27] Martins, J. E. D.; Wills, M. *Tetrahedron* **2009**, 65, 5782.

- 
- [28] Gelalcha, F. G.; Bitterlich, B.; Anilkumar, G.; Tse, M. K.; Beller, M. *Angew. Chem. Int. Ed.* **2007**, *46*, 7293.
- [28] Lundgren, S.; Lutsenko, S.; Jonsson, C.; Moberg, C. *Org. Lett.* **2003**, *5*, 3663.
- [29] Howath, G.; Rusa, C.; Kontos, Z.; Gerencser, J.; Huszthy, P. *Synthetic Commun.* **1999**, *29*, 3719.
- [30] Pellegatti, L.; Zhang, J.; Drahos, B.; Villette, S.; Suzenet, F.; Guillaumet, G.; Petroud, S.; Toth, E. *Chem. Commun.* **2008**, *48*, 6591.
- [31] Lunning, U.; Baumstark, R.; Peters, K.; Von Schnering, H.G. *Liebigs Ann. Chem.* **1990**, *2*, 129.
- [32] Movassaghi, M.; Jacobsen, E. N. *J. Am. Chem. Soc.* **2002**, *124*, 2456.
- [33] Bruker (2010).APEX2. Version 2010.1-2. Bruker AXS Inc., Madison, Wisconsin, USA.
- [34] Bruker (2001). SAINT. Version 7.68a. Bruker AXS Inc., Madison, Wisconsin, USA
- [35] Sheldrick, G. M. (2003). SADABS. Version 2.10. University of Göttingen, Germany.
- [36] Dolomanov, O. V.; Bourhis, L. J.; Gildea, R. J.; Howard, J. A. K.; Puschmann, H. J. *Appl. Cryst.* **2009**, *42*, 339.
- [37] XL, Sheldrick, G.M. *Acta Cryst.* **2008**, *A64*, 112.



## *Chapter 3*

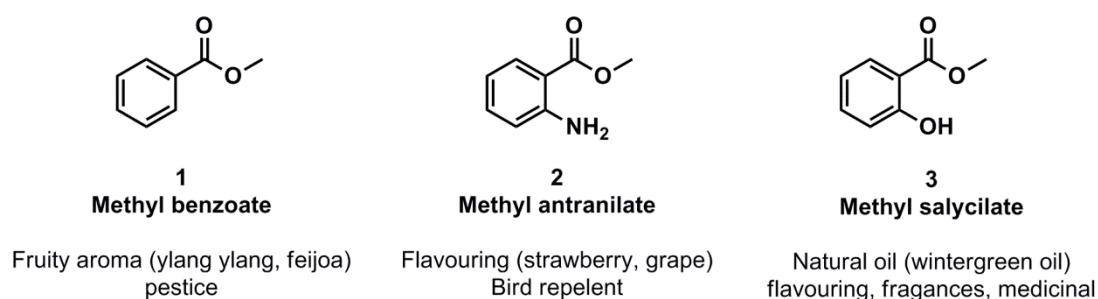
# **DISCOVERY, OPTIMISATION AND SCOPE OF THE Fe(OTf)<sub>2</sub>- PYBISULIDINE CATALYSED AEROBIC $\alpha$ -OXIDATION OF ETHERS**

### 3.1. Introduction

#### 3.1.1. Organic esters

In 1848, the German chemist Leopold Gmelin introduced the concept of ester functionality for naming a carboxylic acid derivative in which the carbonyl group is bonded with an ether.<sup>1</sup> Indeed, the name ester is a contraction of the German word *essigäther* (acetic ether) and is commonly used nowadays instead of the old terms *oxy-acid ethers* or *ethers of the third class* that were also coined for this type of functionality.<sup>1</sup> Both inorganic and organic esters are ubiquitous functionalities in nature and are present in molecules essential for life itself, such as phosphoesters which act as linkers between nucleosides in DNA molecules,<sup>2</sup> or in different types of lipids which constitute natural lipid bilayers.<sup>3</sup>

Among organic esters, aryl esters are particularly relevant due to their natural properties and industrial applications. For instance, many benzoates have sweet flavours and strong pleasant aromas and/or are derived from natural oils and therefore they have industrial uses in perfumery or as pesticides or bird repellents<sup>4-6</sup> (Scheme 1).

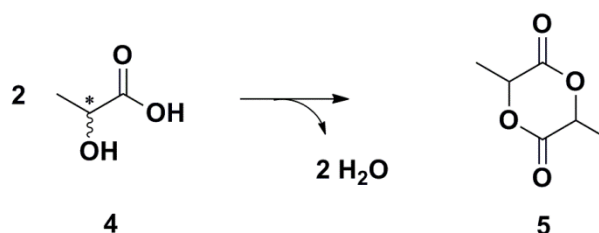


**Scheme 1.** Examples of simple aryl esters and their applications

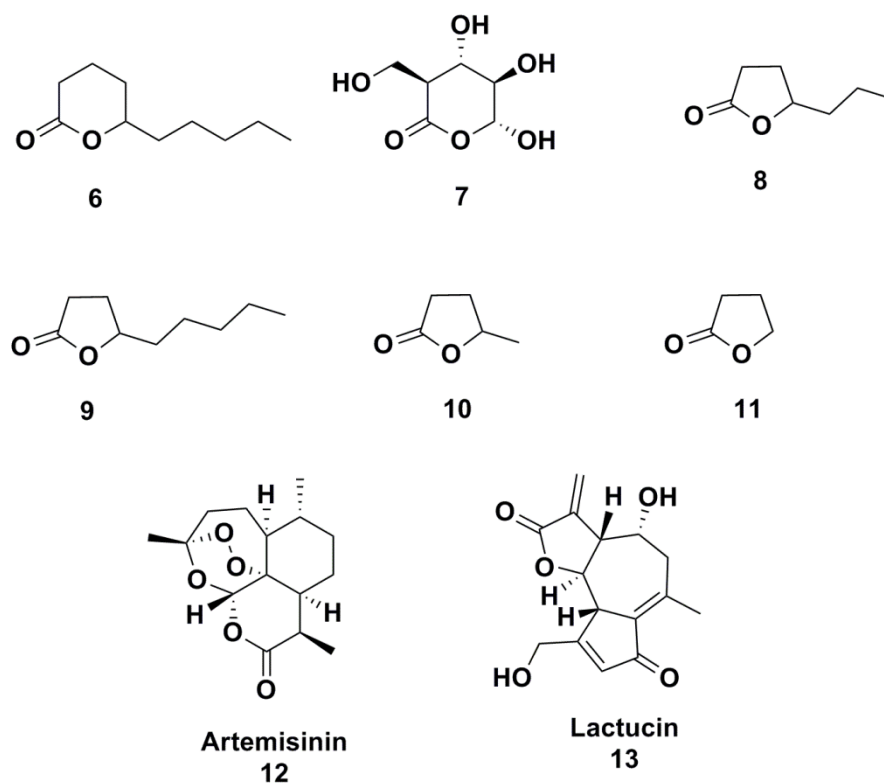
Cyclic esters are commonly named lactones, a term that comes from the cyclic compound lactide **5** that is derived from the dehydration of lactic acid **4**<sup>7</sup> (Scheme 2). As its name suggests (from latin *lactic*: milk), many aliphatic lactones have important applications in dairy products industries, such as delta-decalactone **6** or glucono-delta-lactone **7**, which are often employed as acidifiers or pH regulators in milk and cheeses.<sup>8</sup> Additionally, many aliphatic lactones have fruity or sweet flavours and aromas, such as  $\gamma$ -heptalactone **8** or  $\gamma$ -

nonalactone **9** which are frequently used in food industries due to their strong coconut flavour.<sup>9</sup> Other applications include potential fuel and green solvent uses,<sup>10</sup> such as  $\gamma$ -valerolactone **10** and  $\gamma$ -butyrolactone **11**, or prodrugs<sup>11</sup> or natural products of medicinal applications,<sup>12</sup> such as **11** and lactones of the sesquiterpene family **12-13** respectively (Scheme 3).

**Dehydration of lactic acid to lactide:**



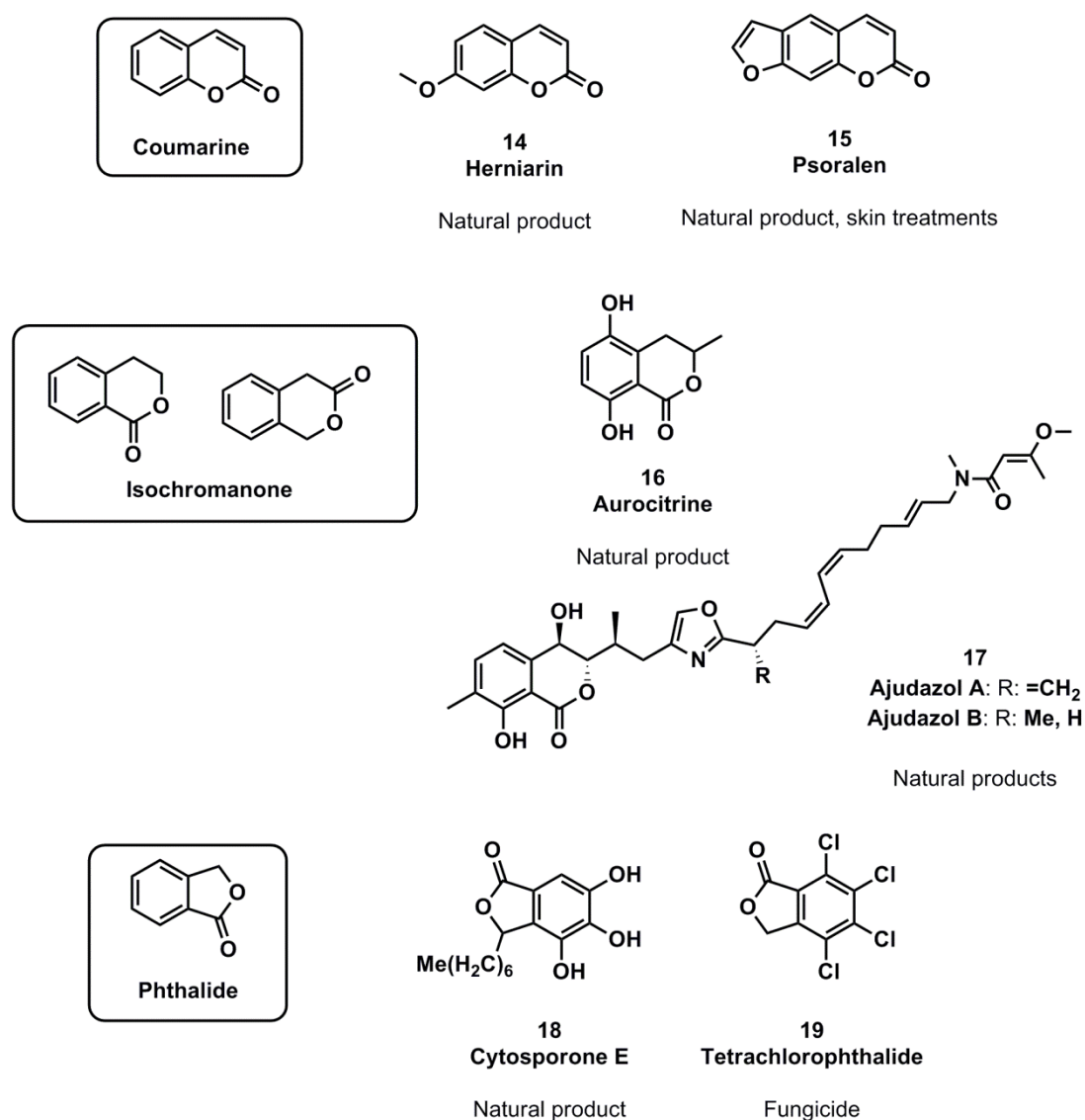
**Scheme 2.** Formation of lactide from lactic acid



**Scheme 3.** Examples of aliphatic lactones

From a synthetic point of view, aryl lactones are particularly interesting due to the many natural products and biologically active compounds that contain this type of skeleton.

Coumarines,<sup>13</sup> isochromanones<sup>14</sup> and phthalides<sup>15</sup> are three major families of aryl lactones that have been found in an ample variety of natural products and whose derivatives are of widespread use in pharmaceutical and agrochemical industries due to their biological properties. Scheme 4 illustrates some significant examples of these families, such as natural product **15**, which is applied in skin diseases treatments, natural products of the ajudazol family **17** which exhibit antibacterial properties and the industrially relevant fungicide **19**.

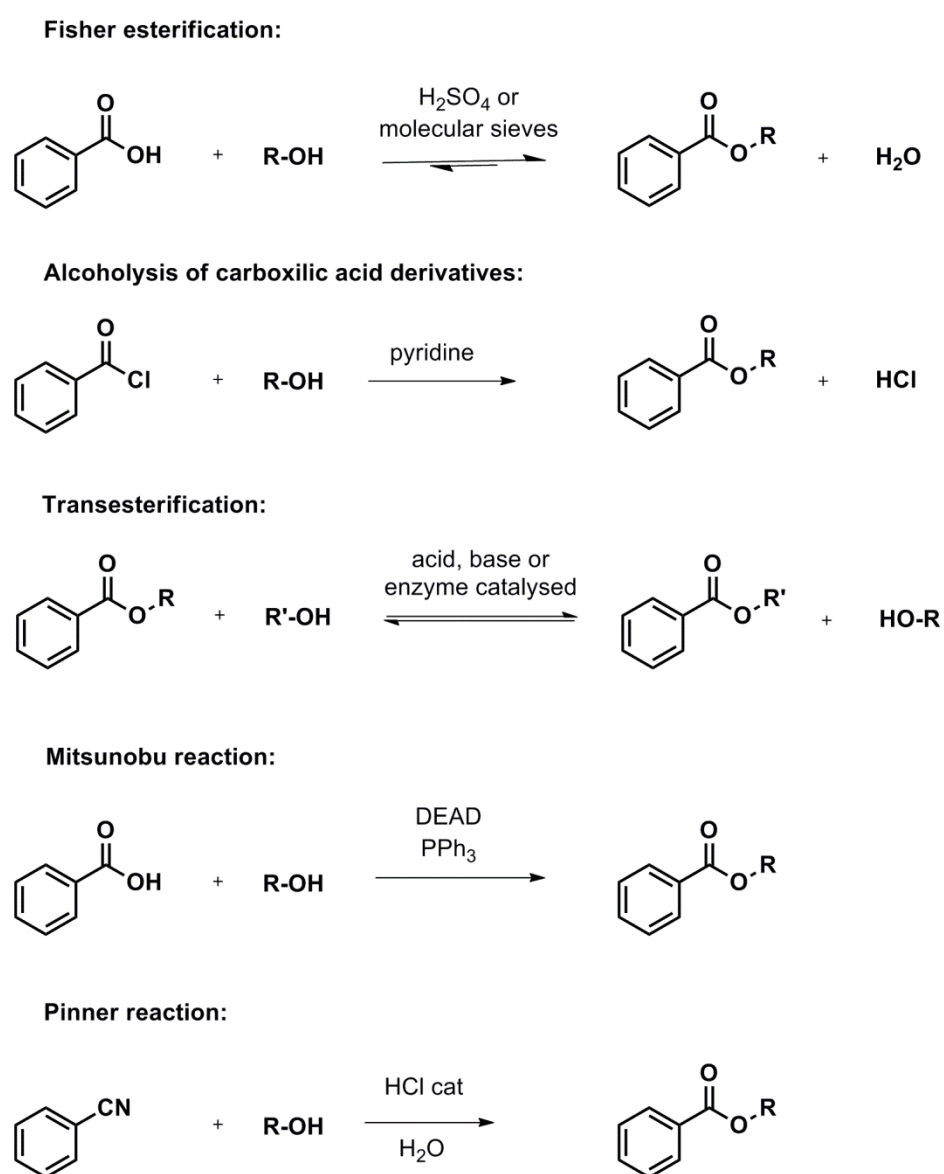


**Scheme 4.** Examples of natural products and biologically active cyclic aryl esters

### 3.1.2. Methods for ester syntheses

#### 3.1.2.1. Benzylic esters

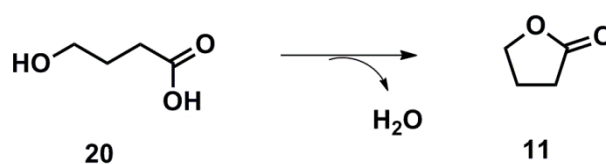
Because of their simple structure and industrial properties, many methodologies have been described for synthesising benzyl esters. Traditional and widely employed methods include the synthesis of benzyl esters from carboxylic acids (Fisher esterification) or its derivatives such as acyl chlorides, anhydrides or even esters via transesterification.<sup>16</sup> Other commonly applied methods include Mitsunobu reaction<sup>17</sup> and Pinner reaction<sup>18</sup> (Scheme 5).



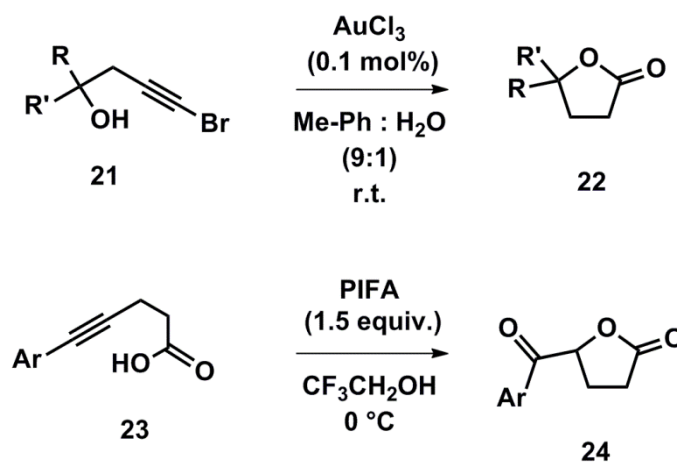
**Scheme 5.** Frequent methods for synthesising aryl esters

## 3.1.2.2. Aliphatic lactones

Generally, aliphatic lactones can be synthesised from hydroxyacids by water removal or distillation.<sup>19</sup> Such method is employed in the industrial production of **11** from  $\gamma$ -hydroxybutyric acid **20** (Scheme 6). Nonetheless, a vast collection of methodologies have been reported for producing these valuable lactones from different organic precursors. Alkyne derivatives such as **21** and **23** can undergo electrophilic cyclisation to afford  $\gamma$ -butyrolactones in good yields with specific alpha alkyl-substitution patterns<sup>20,21</sup> (Scheme 7).



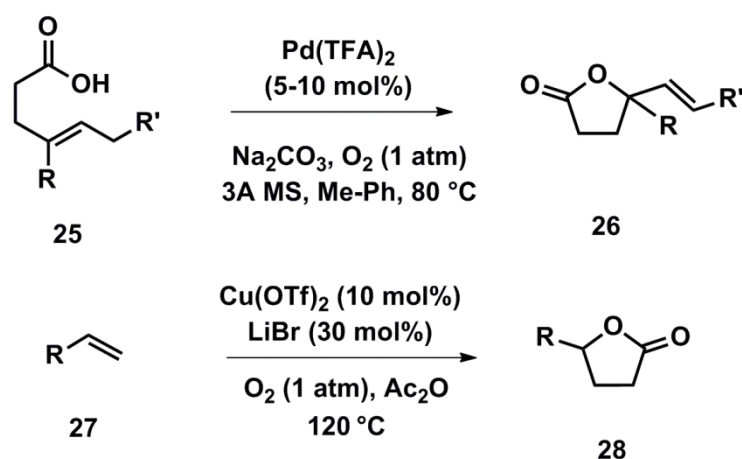
Scheme 6. Synthesis of lactones from hydroxyacids



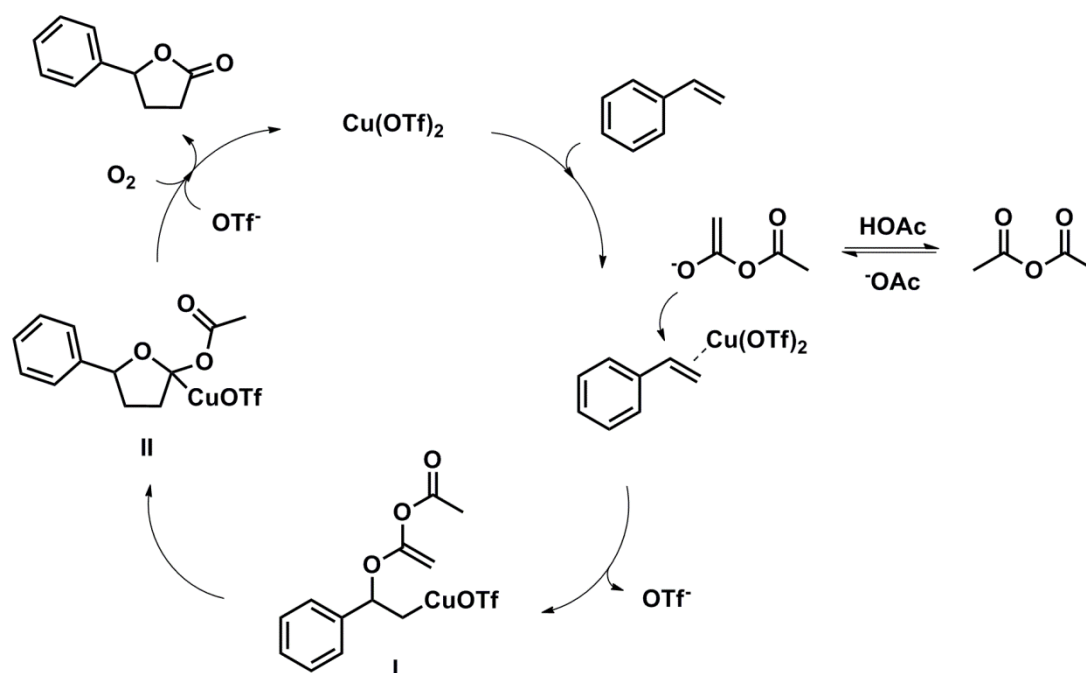
Scheme 7. Lactone synthesis from alkyne derivatives via electrophilic cyclisation

Additionally, alkenes can be used as precursors for lactones syntheses by means of different synthetic methodologies such as oxidative cyclisation,<sup>22</sup> although high catalyst loadings, large amounts of additives and harsh conditions are often required for achieving good yields in these transformations (Scheme 8). In addition, the oxidative [3+2] cycloaddition of styrenes to anhydrides furnished  $\gamma$ -arylbutyrolactones in good yields albeit with high catalyst loadings and harsh reaction conditions<sup>23</sup> (Scheme 8). A plausible reaction mechanism would

involve the nucleophilic attack of the enol of the anhydride to the Cu-coordinated styrene generating intermediate I. Intramolecular insertion into the enol would furnish intermediate II from which the  $\gamma$ -butyrolactone results (Scheme 9).



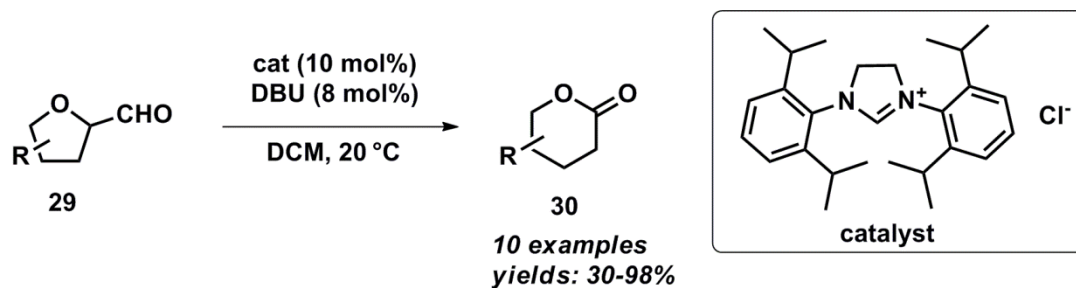
**Scheme 8.** Alkenes as precursors for lactone production



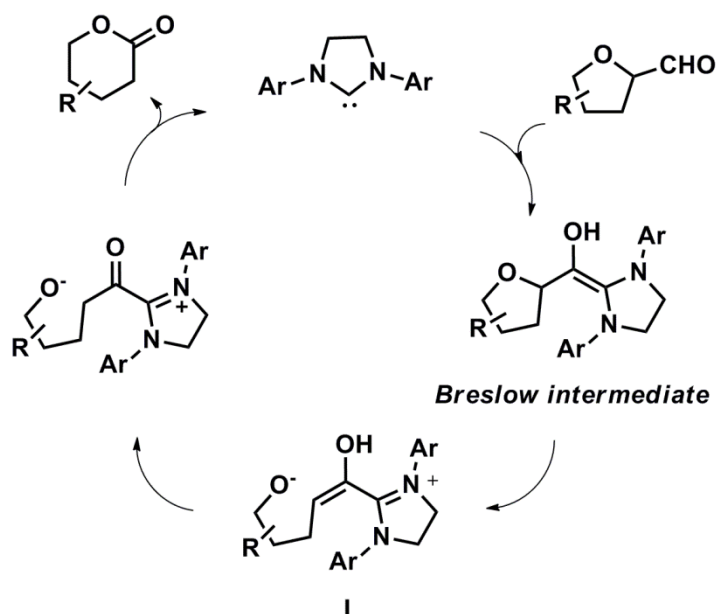
**Scheme 9.** Postulated formation of **28** via Cu-mediated carboesterification of styrenes

Other less widely applied methods for synthesising butyrolactones include carbene-catalysed ring expansion and subsequent lactonisation.<sup>24</sup> From a mechanistic perspective, the hypothetical formation of Breslow-type intermediates by reaction of *N*-heterocyclic carbenes

with tetrahydrofuran 2-carbaldehydes would promote the ether ring opening. The resulting acyclic intermediate I would easily furnish the expanded lactone *via* initial enol tautomerisation and subsequent lactonisation (Scheme 10). Additionally, hetero-Diels –Alder reactions<sup>25</sup> have been reported to successfully provide specific lactone type products under mild conditions but with significantly high catalyst loadings (Scheme 11).

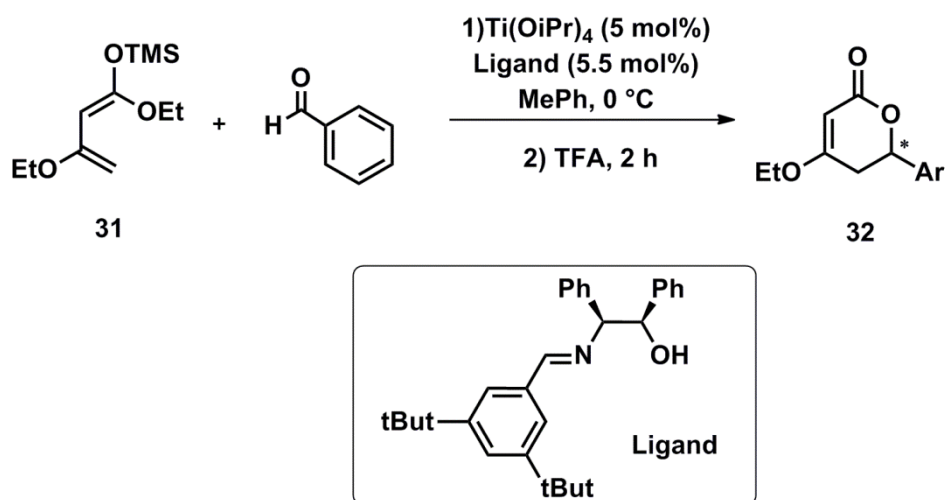


#### Postulated mechanism



**Scheme 10.** Synthesis of lactones via ring expansion

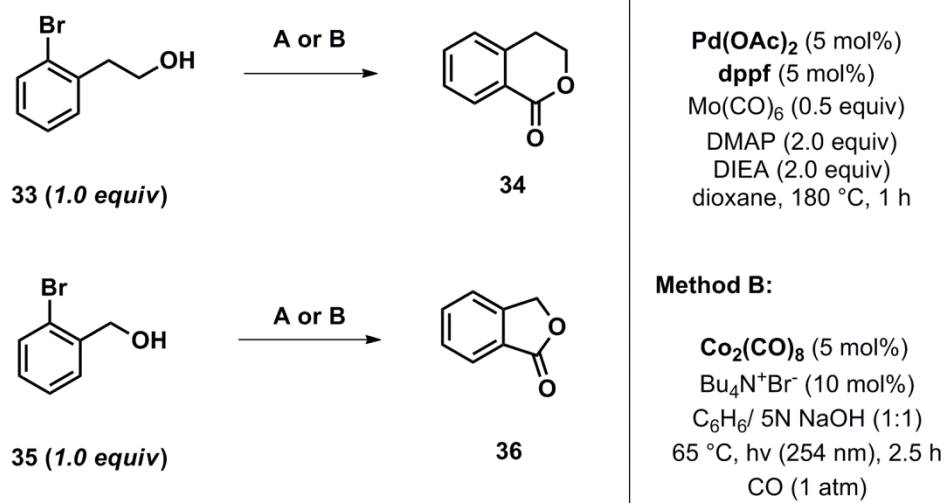




**Scheme 11.** Synthesis of lactones by hetero Diels-Alder reaction

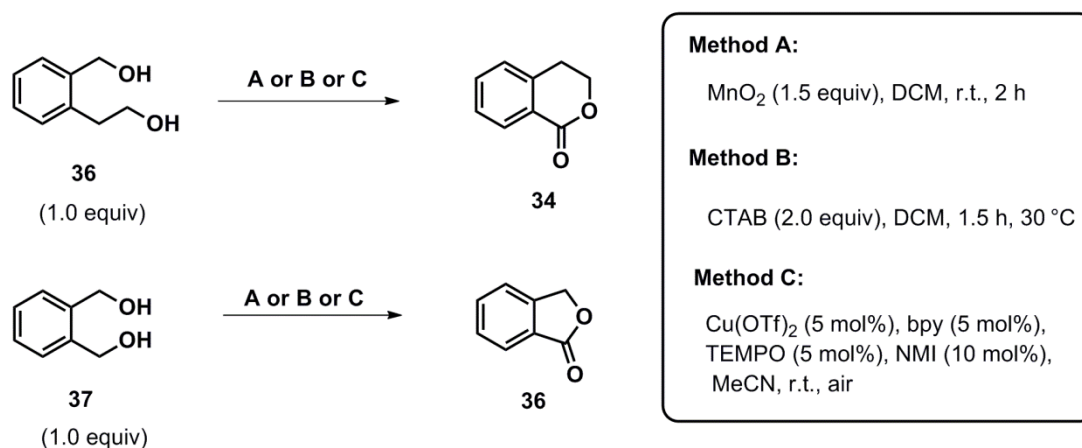
### 3.1.2.3. Isochromanones and phthalides

Due to the importance of isochromanones and phthalides, several synthetic methods have been developed for their preparation. Transition metal catalysed carbonylation of aryl halides is probably one of the most widely employed procedures as it allows the construction of regioselective isochromanones.<sup>26</sup> However, this method often requires harsh reaction conditions (high temperatures, basic conditions) and toxic metal catalysts such as Pd or Co. Solid and relatively easy to handle Mo carbonyls can be used as a carbonylation source, albeit almost stoichiometric amounts are required to achieve good yields.<sup>26a</sup> Co carbonyls can be used in a catalytic fashion although the reactions needed to be placed under 1 atm of CO.<sup>26b</sup> Multistep syntheses are required for obtaining more complex derivatives of the starting alcohols **33** and **35** which often limits the usefulness of the aryl halide carbonylation strategy for synthesising substituted isochromanones and phthalides (Scheme 12).



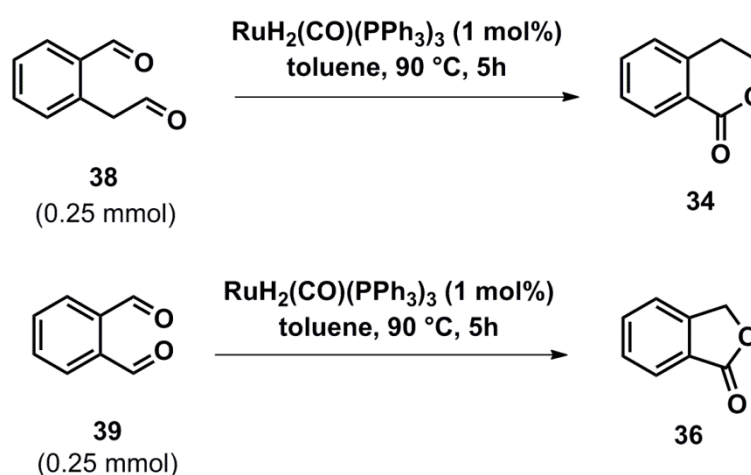
**Scheme 12.** Synthesis of isochromanones and phthalides via carbonylation of aryl halides

Additionally, isochromanones and phthalides can be obtained from 2-(2-(hydroxymethyl)phenyl)ethanol **36** or 1,2-phenylenedimethanol **37** respectively, via selective benzylic oxidation followed by intramolecular cyclisation (Scheme 13). Several oxidants such as MnO<sub>2</sub>,<sup>27</sup> cetyltrimethylammonium permanganate<sup>28</sup> and Cu(bpy)<sub>2</sub>/TEMPO<sup>29</sup> have been reported for undergoing this transformation. Nonetheless, stoichiometric amounts of oxidants are often required and the substrate scope is limited to isochromanone and phthalide themselves, suggesting poor functional group compatibility.



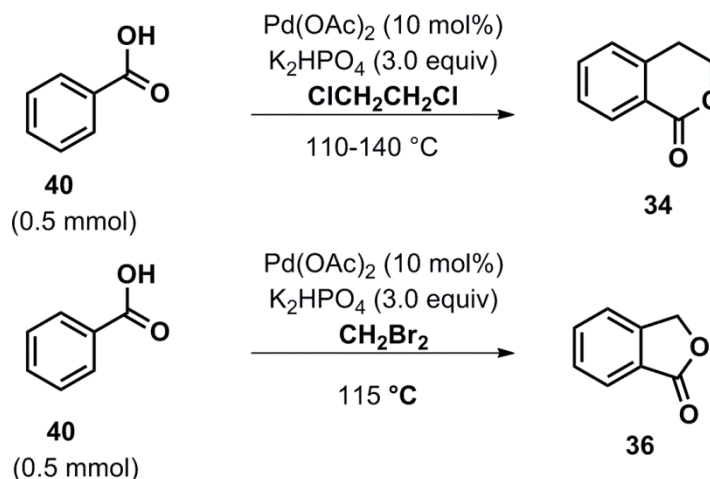
**Scheme 13.** Synthesis of isochromanone by benzylic oxidation followed by intramolecular cyclisation

Similarly, dialdehydes can be directly converted to aryl lactones (intramolecular Tishchenko reaction) such as isochromanone and phthalide. Traditionally, strongly basic metal alkoxides, amphoteric aluminium alkoxides or strong acids used to be employed for both inter and intramolecular Tishchenko reactions.<sup>30</sup> Nonetheless, the use of Ru hydrides as catalysts has become a greener alternative to afford these products by direct lactonization of aldehydes (Scheme 14).<sup>31</sup>



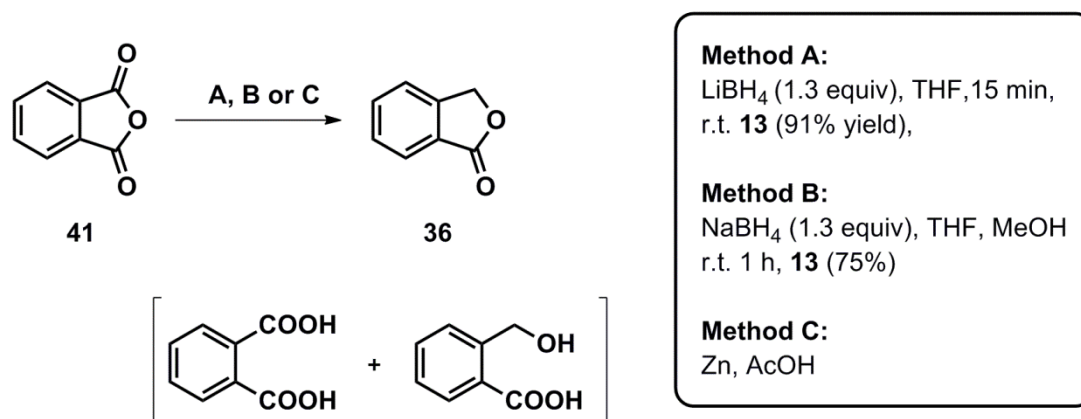
**Scheme 14.** Conversion of dialdehydes to lactones via hydorruthenation

The more recent Pd-catalysed *ortho*-alkylation of benzoic acids with haloalkanes is a much more efficient and versatile method for the synthesis of isochromans and phthalides than the aforementioned procedures. Although this method still relies on the use of toxic transition metals in relatively high catalyst loadings and requires a high reaction temperature, it can be applied to the construction of an ample variety of isochromans and phthalides with good yields and good regioselectivity<sup>32</sup> (Scheme 15).



**Scheme 15.** Pd-catalysed alkylation of benzoic acids to afford isochromanones and phthalides

Additionally, phthalides can be directly synthesised by reducing phthalide anhydrides with metal borohydrides. Nonetheless, these methods require more than stoichiometric amounts of borohydrides or reductants and they often result in some byproduct formation derived from undesired ring opening reactions<sup>33</sup> (Scheme 16).



**Scheme 16.** Synthesis of phthalides from phthalic anhydrides

### 3.2. Aims of this chapter

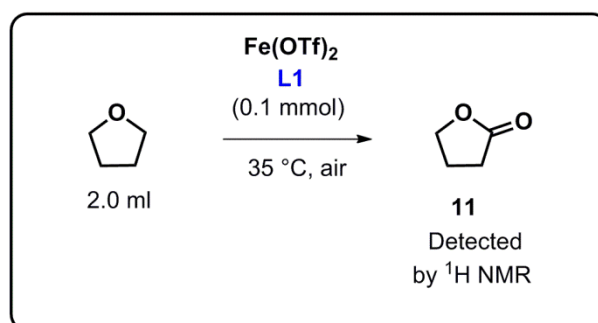
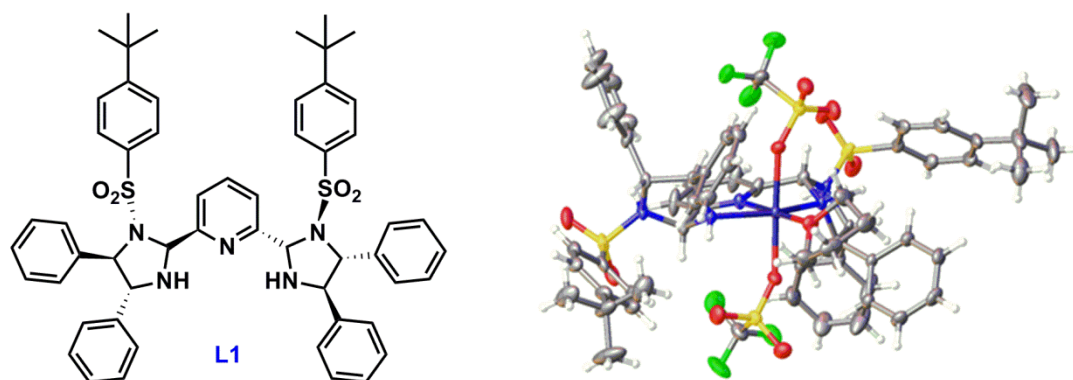
The direct oxidation of ethers to esters and/or lactones is viewed as an excellent alternative for the synthesis of these industrially valuable products.<sup>34</sup> Nonetheless, very important limitations such as limited substrate scope, lack of chemoselectivity and the current need of

additives in more than stoichiometric amounts limit the implementation of these transformation on industrial and laboratory scales. Therefore, the development of novel catalysts capable of overcoming these limitations would be of great interest. This chapter covers the discovery and the subsequent application of Fe(OTf)<sub>2</sub>-PyBisulidine complexes as powerful catalysts for the selective alpha oxidation of ethers to ester under aerobic conditions.

### 3.3. Results and Discussion

#### 3.3.1. Discovery of the Fe(OTf)<sub>2</sub>-L1 catalysed aerobic oxidation of THF

PyBisulidine type ligands covered in Chapter 2 can easily coordinate to commercially available iron salts under mild conditions in different organic solvents. Reacting **L1** with Fe(OTf)<sub>2</sub> in THF led to a THF-ligated complex [Fe**L1**(THF)(OTf)<sub>2</sub>], the structure of which has been determined by X-ray diffraction (Scheme 17). The complex shows a distorted octahedral geometry with two axial OTf ligands and an equatorial THF. Although surrounded by the sterically demanding **L1**, the Fe-O distance of 2.042 Å is considerably shorter than those found in the iron porphyrine [Fe(TPP)(THF)<sub>2</sub>] type complexes,<sup>35</sup> suggesting a highly electrophilic Fe<sup>II</sup> centre. Surprisingly, when investigating possible catalytic reactions with the complex, small amounts of  $\gamma$ -butyrolactone were detected in the bright orange THF solution of [Fe**L1**(THF)(OTf)<sub>2</sub>]. Prompted by this observation, we set out to explore this complex as a potential catalyst for the aerobic oxidation of THF.



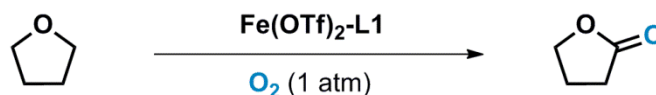
**Scheme 17.** PyBisulidone ligand **L1**, X-ray structure of  $[\text{FeL1}(\text{THF})(\text{OTf})_2]$  and unexpected oxidation of THF to **11**

### 3.3.2. Optimisation of the iron-catalysed aerobic oxidation of THF

#### 3.3.2.1. Effect of oxidant and water

Exposing a stirred THF solution of the  $[\text{FeL1}(\text{THF})(\text{OTf})_2]$  complex to 1 atm of  $\text{O}_2$  indeed led to the isolation of  $\gamma$ -butyrolactone, with a TON of 98 in 24 h at  $40^\circ\text{C}$ . The in situ prepared complex  $\text{Fe(OTf)}_2\text{-L1}$  showed similar behaviour to the preformed complex under identical reaction conditions (Table 1, entries 1,2). Initially, the in situ prepared  $\text{Fe(OTf)}_2\text{-L1}$  complex showed improved efficiency under a pure molecular oxygen atmosphere rather than under air at different temperatures (Table 1, entries 2,6 and 4,7). But more importantly, higher efficiency and excellent reproducibility were achieved when anhydrous (freshly distilled) THF was used as a solvent (Table 1, entries 2 and 3). We suspect that the superior catalytic performance in anhydrous THF is due to the detrimental effect of water during

complex formation as iron triflates are known to be highly hygroscopic and can allow the formation of undesired iron hydroxides. Additionally, when the reaction was performed with dry THF and an excess of activated 4 Å MS, no product formation was detected and no bright orange colour evolution was observed, suggesting that the complex formation may be hampered in the presence of activated molecular sieves.



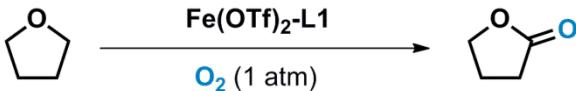
Entry	Oxidant	Temperature /°C	butyrolactone /TON <sup>a</sup>
1	O <sub>2</sub>	40	98 <sup>b</sup>
2	O <sub>2</sub>	40	98
3	O <sub>2</sub>	40	62 <sup>c</sup>
4	air	40	63
5	air	40	21 <sup>b</sup>
6	O <sub>2</sub>	60	240
7	air	60	101

Reaction conditions: anhydrous THF (2.0 mL), *in situ* prepared Fe(OTf)<sub>2</sub>L1 (5.71 × 10<sup>-3</sup> mmol), O<sub>2</sub> (1 atm), 24 h. All reactions were run twice. [a] TON referred to mmol of product per mmol of catalyst. [b] Premade [FeL1(OTf)<sub>2</sub>(THF)] complex was used. [c] non-distilled THF (commercial grade) was used.

**Table 1.** Effect of the oxidant and water traces in the iron catalysed aerobic oxidation of THF to  $\gamma$ -butyrolactone

### 3.3.2.2. Temperature effect

The catalytic activity of Fe(OTf)<sub>2</sub>L1 in anhydrous THF was significantly affected by the reaction temperature, with the catalytic efficiency being boosted at higher temperatures and reaching a maximum TON of 240 at 60 °C (Table 2, entry 4). Nonetheless, the catalytic efficiency started to diminish at temperatures higher than 60 °C (Table 2, entry 5) and it was drastically reduced at temperatures closer to THF's boiling point (Table 2, entry 6).



Entry	Temperature /°C	butyrolactone /TON <sup>a</sup>
1	30	23
2	40	98
3	50	153
4	<b>60</b>	<b>240</b>
5	65	192
6	72	10

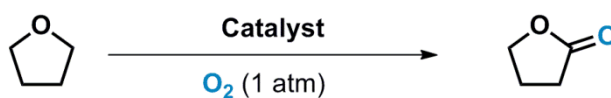
Reaction conditions: anhydrous THF (2.0 mL), *in situ* prepared Fe(OTf)<sub>2</sub>L1 (5.71 x10<sup>-3</sup> mmol), O<sub>2</sub> (1 atm), 24 h. [a] TON referred to mmol of product per mmol of catalyst.

**Table 2.** Effect of the reaction temperature in the iron catalysed aerobic oxidation of THF to  $\gamma$ -butyrolactone

### 3.3.2.3. Control experiments

At the optimal temperature of 60 °C, no oxidation reaction occurred in the absence of PyBisulidine ligand **L1**, Fe(OTf)<sub>2</sub> or molecular oxygen (Table 3, entries 1,2,3), which highlights that the three components are indispensable for the oxidation of THF. Additionally, when the oxidation reaction was performed in analogous conditions but using limited amounts of molecular oxygen (Table 3, entry 4) the same lactone product **11** was formed with lower conversion with no trace of any alcohol intermediate formation. These data clearly show that molecular oxygen is the real oxidising agent of the process and suggest that the lactone product formation does not occur via an initial alcohol formation followed by its overoxidation to afford the ketone product.





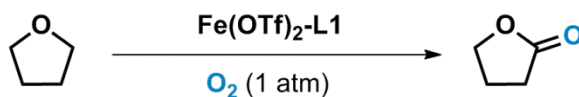
Entry	Oxidant	Temperature /°C	Catalyst	butyrolactone /TON <sup>a</sup>
1	O <sub>2</sub>	60	None	NR
2	O <sub>2</sub>	60	Fe(OTf) <sub>2</sub>	NR
3	O <sub>2</sub>	60	L1	NR
4	N <sub>2</sub>	60	Fe(OTf) <sub>2</sub> -L1	NR <sup>b</sup>
5	O <sub>2</sub>	60	Fe(OTf) <sub>2</sub> -L1	25 <sup>c</sup>

Reaction conditions: anhydrous THF (2.0 mL), Catalyst ( $5.71 \times 10^{-3}$  mmol), O<sub>2</sub> (1 atm), 60 °C, 24h. [a] TON referred to mmol of product per mmol of catalyst. [b] Reaction run under N<sub>2</sub> (1 atm). [c] Reaction run under limiting oxidant conditions (tube degassed and charged with oxygen but no oxygen balloon added)

**Table 3.** Control reactions

#### 3.3.2.4. Optimisation of the S/C ratio

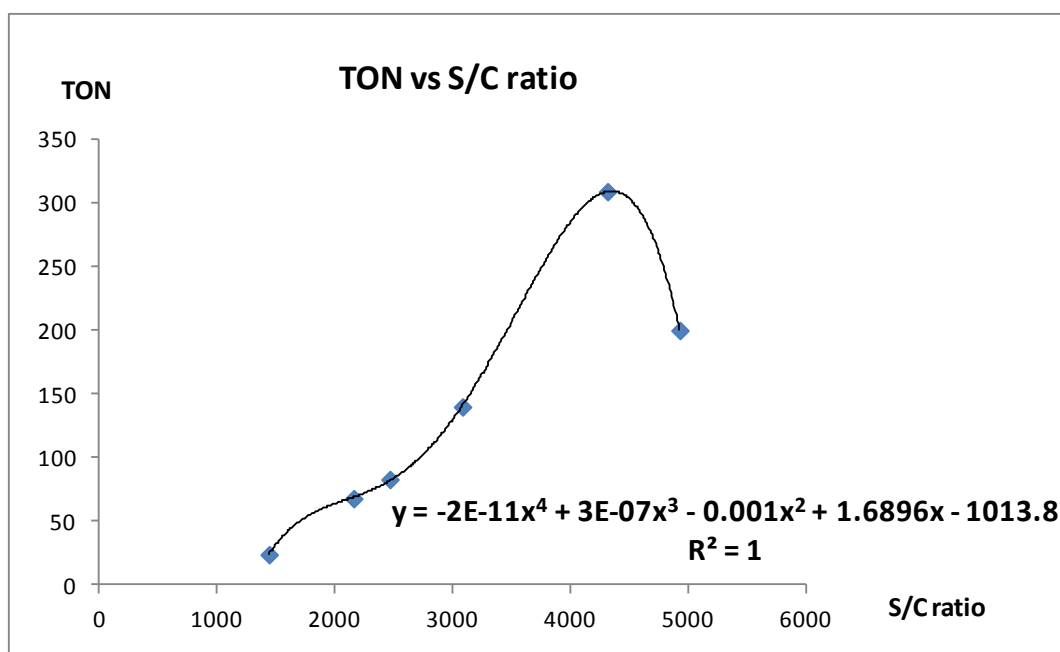
Further optimisation of the substrate-to-catalyst ratio (S/C) showed an increase of the catalyst efficiency at lower catalyst loading until reaching a maximum TON of 309 at a S/C of 4315 (Table 4, entries 3,4). However, a further increase of the S/C ratio resulted in detrimental effect for the catalytic activity (Table 4, entry 5). The variation of the S/C vs the catalytic efficiency (TON) showed a polynomial trend line distribution of 4<sup>th</sup> order (with a Gauss bell shaped curve similitude), with a clear maximum at 4315 (Scheme 18).



Entry	S/C ratio (ml THF/ mmol cat)	butyrolactone /TON <sup>a</sup>
1	2465 (2.0/0.01)	83
2	3082 (2.5/0.01)	140
3	<b>4315 (3.5/0.01)</b>	<b>309</b>
4	<b>4315 (2.0/5.71 x 10<sup>-3</sup>)</b>	<b>309</b>
5	4930 (4.0/0.01)	200
6	2157 (3.5/0.02)	68
7	1438 (3.5/0.02)	24

Reaction conditions: anhydrous THF, *in situ* prepared Fe(OTf)<sub>2</sub>L1 catalyst, O<sub>2</sub> (1 atm), 60 °C, 24h. [a] TON referred to mmol of product per mmol of catalyst.

**Table 4.** Effect of the S/C ratio in the iron catalysed aerobic oxidation of THF to  $\gamma$ -butyrolactone

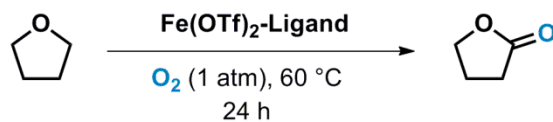


**Scheme 18.** Polynomial distribution of the variation of the S/C ratio vs the TON of the aerobic oxidation of THF to  $\gamma$ -butyrolactone

### 3.3.2.5. Ligand effect

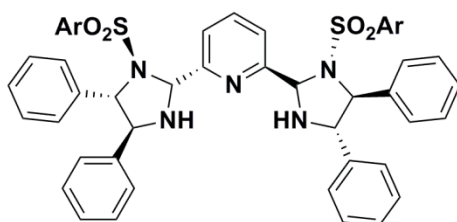
Further optimisation revealed that modification of the ligand structure resulted in the most significant oscillations in the catalytic activity. Among all the *N*-donor ligands investigated, PyBisulidine type ligands showed the highest efficiency under optimal reaction conditions, especially when electron donating groups are present in the sulfonamide skeleton (Table 5, entries 3-7). Nonetheless, replacement of **L1** with the more electron rich but much more sterically demanding PyBisulidine **L5** resulted in a 2.5 fold reduction of the TON (Table 5, entry 7) and the sterically very congested **L6**, in which the NH proton is replaced with a benzyl group, afforded no activity at all (Table 5, entry 8), indicating that both electronic and steric effects are important factors in modulating the catalyst activity. Using the conjugated **L7** or **L8** as ligands resulted in a significant TON reduction and lower selectivity; the undesired autooxidation product tetrahydrofuran  $\alpha$ -hydroperoxide was also observed (Table 5, entries 9, 10). Additionally, replacement of **L1** with the previously reported PyBidine ligand **L9** significantly lowered the catalytic activity, showing the beneficial effect of the sulfonyl group (Table 5, entry 11). Interestingly, the asymmetric ligand **L10**, in which a sulfonamide moiety is replaced by a *N*-donor pyrazole moiety, and bidentate ligands **L11-L13** with no central pyridine linker were all found inactive (Table 5, entries 9-12).

Finally, prolonging of the reaction time resulted in a further improvement of the catalytic efficiency of Fe(OTf)<sub>2</sub>-**L1** giving a final TON of 412 after 48 hours of reaction (Table 5, entries 1- 3). Further increase in the reaction time showed no improvement in the catalyst efficiency, however.

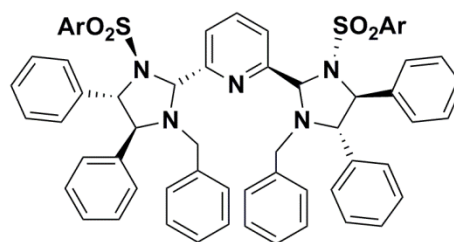


Entry	Ligand	butyrolactone /TON <sup>a</sup>
1	L1	312
2	L1	348 <sup>b</sup>
3	L1	412 <sup>c</sup>
4	L2	283
5	L3	207
6	L4	194
7	L5	121
8	L6	NR
9	L7	20 <sup>d</sup>
10	L8	68 <sup>e</sup>
11	L9	50
12	L10	NR
13	L11	NR
14	L12	NR
15	L13	NR

Reaction conditions: anhydrous THF (2.0 mL), *in situ* prepared Fe(OTf)<sub>2</sub>-Ligand complex (5.71 × 10<sup>-3</sup> mmol), O<sub>2</sub> (1 atm), 60 °C, 24 h. [a] TON referred to mmol of product per mmol of catalyst. [b] Reaction run for 36 h. [c] Reaction run for 48 h. [d] Tetrahydrofuran hydroperoxide was formed predominantly. (peroxide/lactone) = 4/1. [e] Tetrahydrofuran hydroperoxide was also formed. (peroxide/lactone) = 0.4/1.



- L1:** Ar = 4-tButylC<sub>6</sub>H<sub>4</sub>  
**L2:** Ar = 4-MeOC<sub>6</sub>H<sub>4</sub>  
**L3:** Ar = 4-MeC<sub>6</sub>H<sub>4</sub>  
**L4:** Ar = 4-CF<sub>3</sub>C<sub>6</sub>H<sub>4</sub>  
**L5:** Ar = 2,4,6-triisopropylC<sub>6</sub>H<sub>2</sub>



- L6:** Ar = 4-MeC<sub>6</sub>H<sub>4</sub>

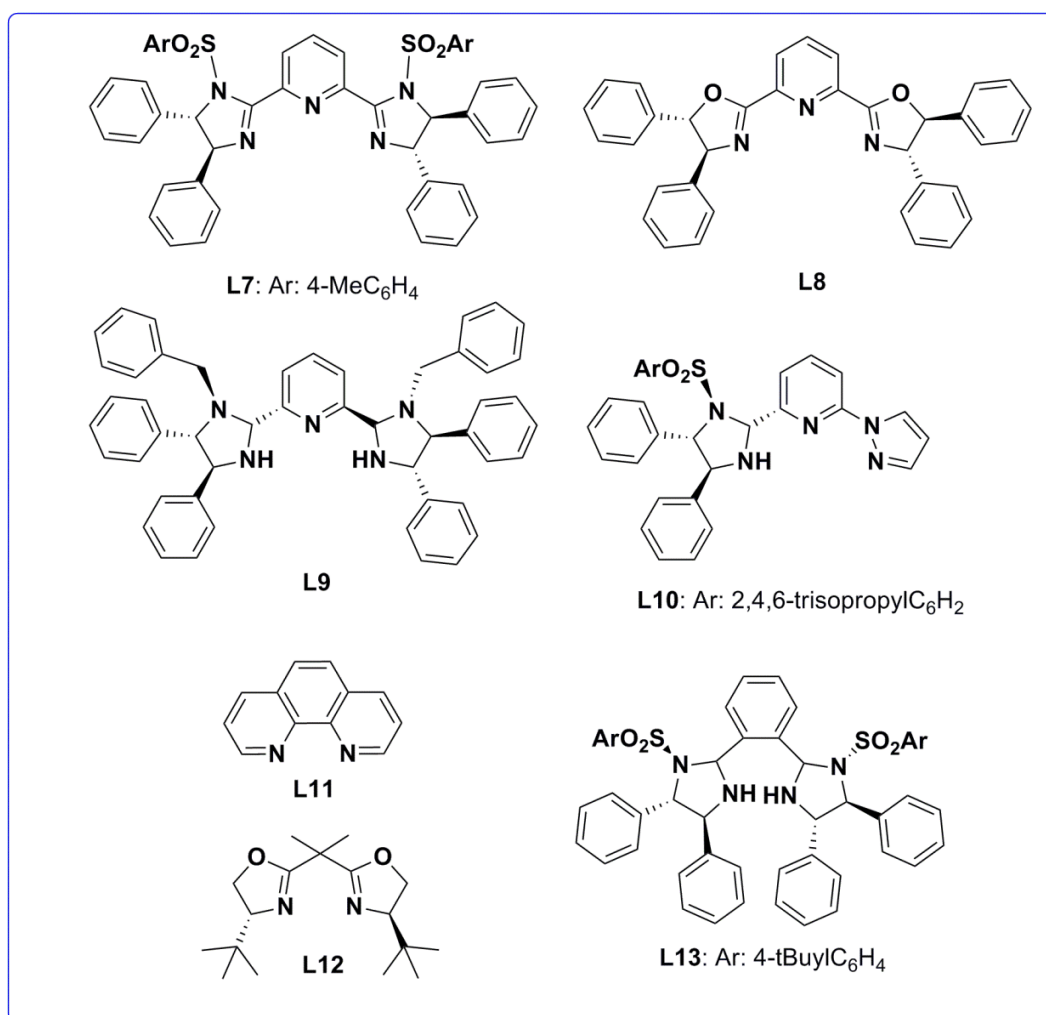
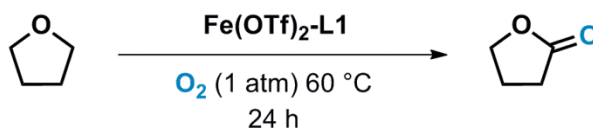


**Table 5.** Effect of the *N*-donor ligand in the iron catalysed aerobic oxidation of THF to butyrolactone

### 3.3.2.6. Solvent effect

The Fe(OTf)<sub>2</sub>L1 catalysed aerobic oxidation of THF to  $\gamma$ -butyrolactone was found to be compatible with arene type solvents (Table 6, entries 1-6) which are not oxidised under the reaction conditions. Nonetheless, a much higher efficiency is obtained in a neat reaction and a significant reduction in the catalyst efficiency is manifested when using larger solvent amounts (Table 6, entries 1,2,3). In addition, halogenated (Table 6, entries 7,8) or coordinating solvents (Table 6, entry 9) were found to be incompatible with this reaction. We suspect this is because of the catalyst being capable of strongly coordinating to different organic solvents as shown and discussed in Chapter 2.



Entry	Solvent (ml THF: ml solvent)	butyrolactone /TON <sup>a</sup>
1	THF:Ph-H (1.0:2.0)	NR
2	THF:Ph-H (1.5:1.5)	5
3	THF:Ph-H (2.0:1.0)	100
4	THF:Ph-H (2.5:1.0)	185
5	THF:Ph-Me (2.0:1.0)	77
6	THF:Ph-Me (2.5:0.5)	135
7	THF:DCM (2.0:1.0)	NR
8	THF:DCE (2.0:1.0)	NR
9	THF:MeCN (2.0:1.0)	NR

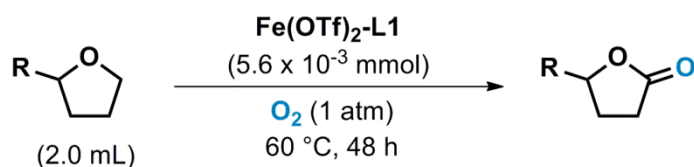
Reaction conditions: anhydrous THF and anhydrous solvent (ml:ml) , *in situ* prepared Fe(OTf)<sub>2</sub>-L1 (5.71 × 10<sup>-3</sup> mmol), O<sub>2</sub> (1 atm), 60 °C, 24 h. [a] TON referred to mmol of product per mmol of catalyst.

**Table 6.** Effect of different solvents in the iron-catalysed aerobic oxidation of THF to  $\gamma$ -butyrolactone

### 3.3.3. Substrate scope

#### 3.3.3.1. Lactone oxidation

Using the *in situ* prepared Fe(OTf)<sub>2</sub>-L1 as catalyst, a wide range of cyclic ethers were subjected to the oxidation at 1 atm of O<sub>2</sub> and 60 °C. THF type substrates were first examined, which afforded  $\gamma$ -butyrolactones, a structural unit found in many natural products.<sup>14</sup> Moderate efficiencies together with good functional group tolerance were achieved (Table 7). However, the product yields were diminished in the presence of substituents (Table 7, entries 2-5). The oxidation is characterized with excellent mass balance with few by-products observed. The catalyst selectivity towards the lactone product formation was excellent, with no trace of tertiary alcohol product formation and no competitive oxidation occurring in the methylene positions of the substituents.



Entry	Starting material (% rsm <sup>a</sup> )	Ester product (TON <sup>b</sup> ; mmol)
1	 42 (76%)	 43 (412; 2.33)
2	 44 (88%)	 45 (371; 2.10)
3	 46 (87%)	 47 (133; 0.75)
4	 48 (90%)	 49 (123; 0.70)
5	 50 (93%)	 51 (94; 0.53)

<sup>a</sup> rsm: % recovered starting material (unoxidised). <sup>b</sup> TON refers to the mmol of isolated product per mmol of catalyst.

**Table 7.** Substrate scope and functional group tolerance in the  $\text{Fe(OTf)}_2\text{L1}$  catalysed aerobic alpha oxidation of THF type substrates

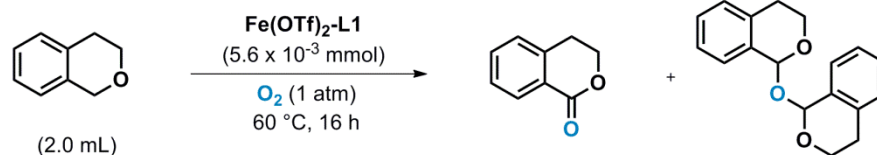
### 3.3.3.2. Oxidation of isochromans

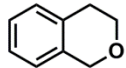
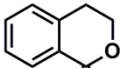
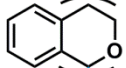
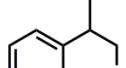
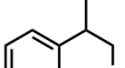
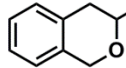
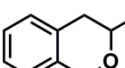
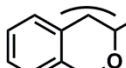
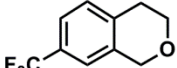
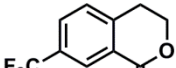
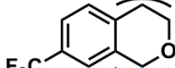
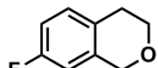
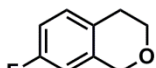
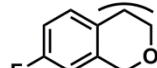
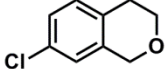
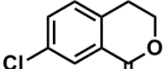
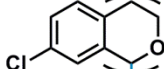
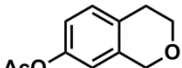
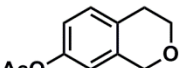
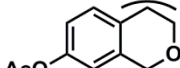
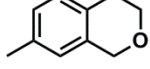
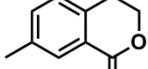
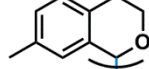
Next, we started investigating the  $\alpha$ -oxidation of isochromans to isochromanones which, like  $\gamma$ -butyrolactones, are common motifs in natural products and bioactive molecules,<sup>14</sup> and bearing in mind that reported iron catalysts fail to undergo oxidation reactions in the presence of aromatic rings and electron rich functionalities.<sup>36</sup>

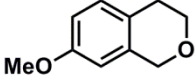
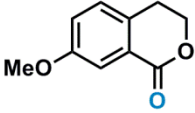
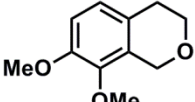
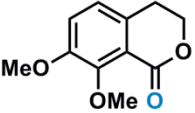
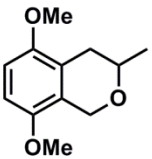
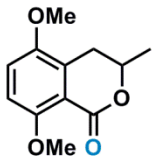
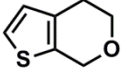
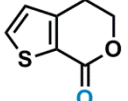
To our delight, isochromanone **53** was obtained from **52** in a 30% isolated yield with TON reaching 844 in an overnight reaction (Table 8, entry 1). No trace of isochroman-1-ol **83** (*vide infra*) was detected even as an intermediate under conditions of limiting oxidant. Nonetheless, the unexpected 1,1'-oxidiisochroman product **54** was generated in low yield. Even though the formation of this oxygenated dimer as byproduct has not been observed with other catalysts capable of undergoing aerobic  $\alpha$ -oxidation of ethers, some authors have reported the formation of such product upon exposure of isochroman to radical catalysts,<sup>37</sup> radical oxidants<sup>38</sup> or stoichiometric oxidants<sup>39</sup> (Scheme 19).

The catalyst operates with excellent chemoselectivity even in the presence of tertiary benzyl (Table 8, entry 2) or O-alkyl substituents (Table 8, entry 3) with no trace of any tertiary alcohol byproduct formation. In addition, the reactions proceed with excellent mass balance with no substrate decomposition and with the unreacted starting material being easily recovered upon purification by flash chromatography. Although the presence of substituents in the alkyl chain barely affects the reaction yields, substitution in the aromatic ring revealed a dramatic electronic effect, with electron withdrawing groups inducing higher TONs while electron donating groups exerting the opposite effect (Table 8, entries 4-12). Nonetheless, very electron rich isochromans can still be oxidized, albeit with reduced TONs but with very good mass balance (Table 8, entry 10-11). Indeed, the protected form of the natural product *aurocitrine*<sup>40</sup> was isolated in 5% yield (Table 8, entry 11), indicating the potential applicability of our catalyst in natural product synthesis. Additionally, the scope of the reaction can be extended to a thiophene derivative with moderate yield (Table 8, entry 12). Excellent chemoselectivity towards the formation of the isochromanone product and excellent mass balances were again observed for all the substrates independently of the electronic properties of the aromatic rings.



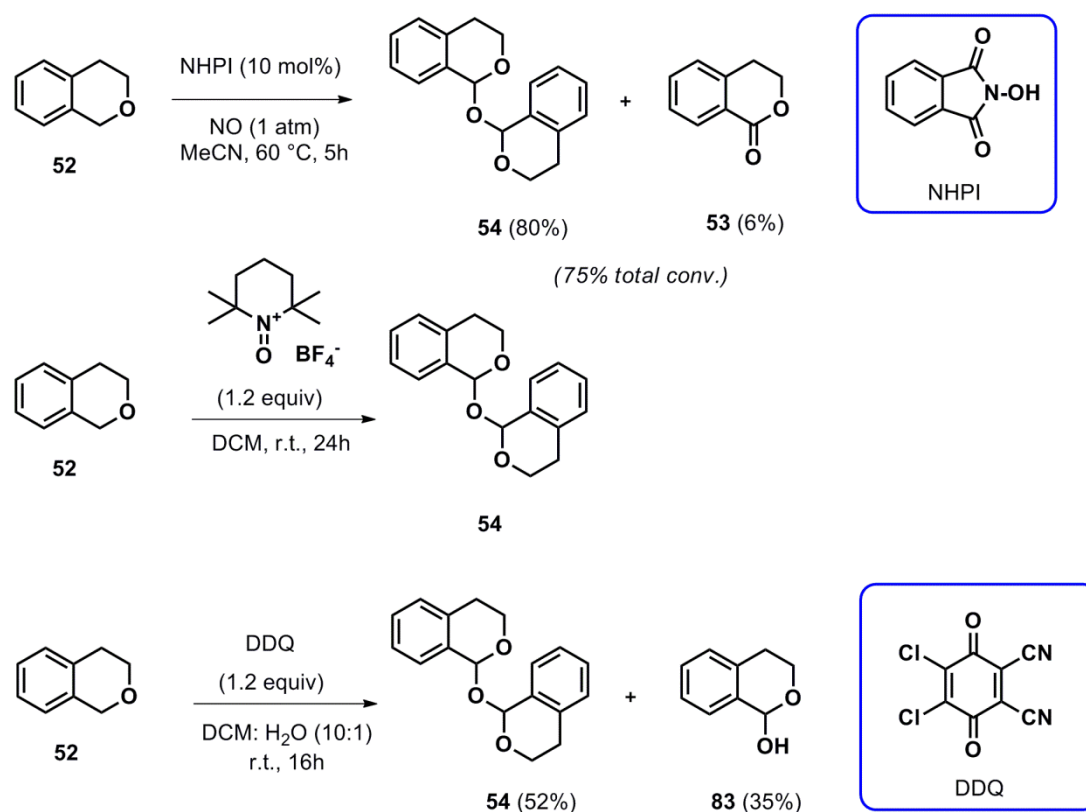


Entry	Starting material (% rsm <sup>a</sup> )	Chromanone (% isol. yield; TON <sup>b</sup> )	1,1'-Oxydiisochroman (% isol. yield; TON <sup>b</sup> )
1	 <b>52</b> (59%)	 <b>53</b> . 30%; 844	 <b>54</b> . 11%; 153
2	 <b>55</b> (71%)	 <b>56</b> . 24%; 573	ND
3	 <b>57</b> (61%)	 <b>58</b> . 28%; 668	 <b>59</b> . 10%; 118
4	 <b>60</b> (16%)	 <b>61</b> . 67%; 1173	 <b>62</b> . 17%; 147
5	 <b>63</b> (30%)	 <b>64</b> . 54%; 1256	 <b>65</b> . 16%; 184
6	 <b>66</b> (44%)	 <b>67</b> . 43%; 902	 <b>68</b> . 13%; 135
7	 <b>69</b> (47%)	 <b>70</b> . 41%; 552*	 <b>71</b> . 12%; 82*
8	 <b>72</b> (64%)	 <b>73</b> . 25%; 597	 <b>74</b> . 10%; 118

9	 75 (88%)	 76. 18%; 388	ND
10	 77 (92%)	 78. 8%; 109 <sup>c</sup>	ND
11	 79 (95%)	 80. 5%; 63 <sup>c</sup>	ND
12	 81 (82%)	 82. 18%; 454	ND

<sup>a</sup> rsm: % recovered starting material (unoxidised). <sup>b</sup> TON refers to the mmol of isolated product per mmol of catalyst. <sup>c</sup> 1.5 g of substrate were used with the catalyst made in situ in 0.5 mL benzene upon stirring at 35 °C for 30 min. ND = Not Detected

**Table 8.** Steric and electronic effects in the Fe(OTf)<sub>2</sub>L1 catalysed aerobic oxidation of isochromans

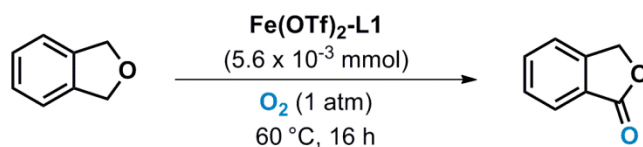


**Scheme 19.** Formation of byproduct **54** in the presence of radical species or stoichiometric oxidants

### 3.3.3.3. Oxidation of phthalans

Next, we turned our attention to the oxidation of phthalans to phthalides, important building blocks for more complex chemicals, such as dyes,<sup>41</sup> natural oils,<sup>42</sup> fungicides<sup>43</sup> and biologically active compounds.<sup>44</sup> A similar strong electronic effect was observed for these substrates, with higher yields obtained for substrates containing electron withdrawing groups (Table 9). Interestingly, this electronic effect can now be harnessed to direct the regioselectivity of the oxidation. Thus, with a strong *meta* directing effect ( $\sigma_m = 0.34$  vs  $\sigma_p = 0.06$ ), the fluorine substitute induced exclusive oxidation of the *meta* methylene unit to afford the ester **85** in 60% isolated yield and 1533 TON. Similarly, dihydrofuro[3,4]pyridines were regioselectively oxidized at the *ortho* or *meta* position, leading to pyridinone skeletons of pharmaceutical interest (Table 9, entries 5-6). The higher TON observed for **93** than **95** is consistent with a stronger inductive effect by the nitrogen

on the *ortho* methylene. In the case of the heavier halogens, their significantly stronger *para* directing effect ( $\sigma_m = 0.37$  for Cl and 0.39 for Br vs  $\sigma_p = 0.23$  for both) and larger size might result in the observed *para* oxidation (Table 9, entries 2-3). The regioselectivity of the products was determined by 2D NMR (see appendix).



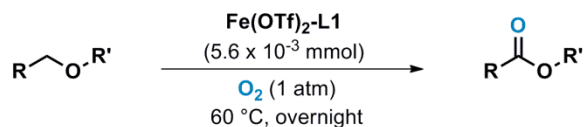
Entry	Starting material (% rsm <sup>a</sup> )	Ester product (% isol. yield; TON <sup>b</sup> )
1	 84 (40%)	 85. 60%; 1533
2	 86 (49%)	 87. 51%; 1164
3	 88 (60%)	 89. 40%; 711
4	 90 (83%)	 91. 17%; 500
5	 92 (48%)	 93. 52%; 1517
6	 94 (81%)	 95. 19%, 555

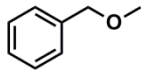
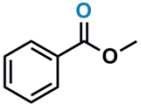
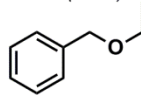
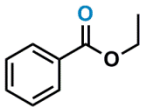
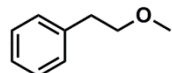
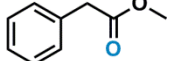
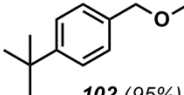
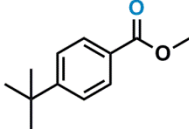
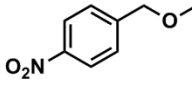
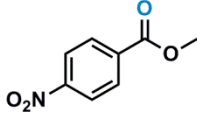
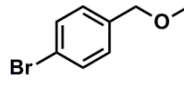
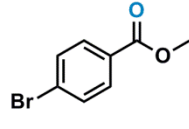
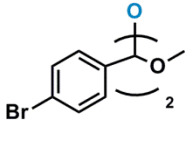
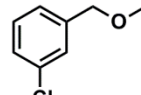
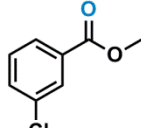
<sup>a</sup> rsm: % recovered starting material (unoxidised). <sup>b</sup> TON refers to the mmol of isolated product per mmol of catalyst.

**Table 9.** Chemo- and regioselective oxidation of phthalans catalysed by  $\text{Fe(OTf)}_2\text{L1}$ .

#### 3.3.3.4. Oxidation of benzyl ethers

Aerobic oxidation of open chain benzyl ethers was also evaluated. Lower TONs were obtained in comparison with isochroman type substrates (Table 10). This is probably because of increased steric hindrance around the ether oxygen atom, which inhibits the oxygen coordination to the iron. In support of this view, the benzyl <sup>t</sup>butyl ether afforded no oxidation. In addition, the hyperconjugative effect in the  $\alpha$ -methylene is weakened in comparison to the cyclic ethers due to the free rotation of the alkyl chain. For those acyclic ethers that reacted, a clear electronic bias was again observed, with electron-withdrawing substituents inducing higher TONs (Table 10, entries 5-7). The catalyst showed excellent chemoselectivity affording the benzoates as sole products; however, traces of the oxidation dimer **108** were also detected during the oxidation of **106**.



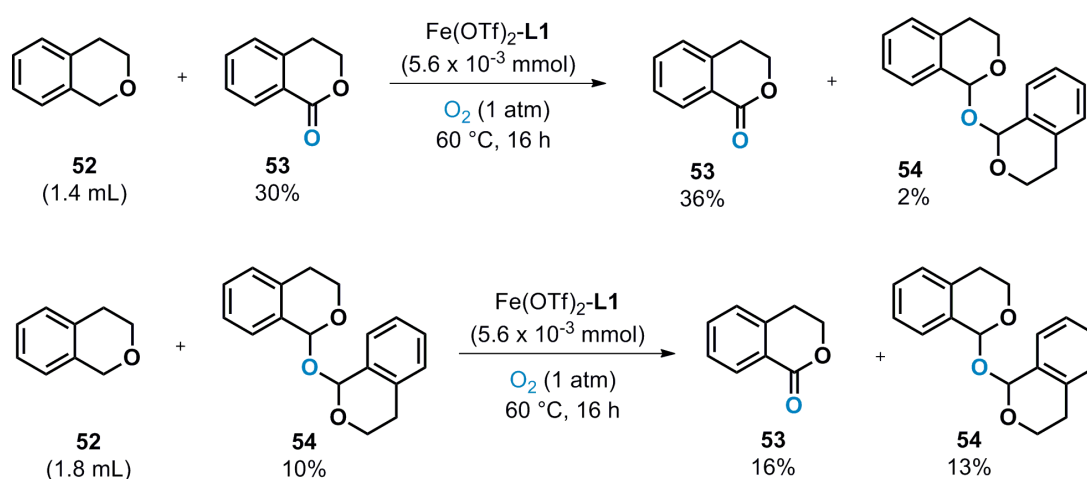
Entry	Starting material (% rsm <sup>a</sup> )	Ester product (% isol. yield; TON <sup>b</sup> )	Byproducts (% isol. yield)
1	 <b>96</b> (91%)	 <b>97.4%</b> ; 116	ND
2	 <b>98</b> (93%)	 <b>99.2%</b> ; 52	ND
3	 <b>100</b> (95%)	 <b>101.2%</b> ; 52	ND
4	 <b>102</b> (95%)	 <b>103.2%</b> ; 40	ND
5	 <b>104</b> (87%)	 <b>105.8%</b> ; 127	ND
6	 <b>106</b> (76%)	 <b>107.15%</b> ; 266 <sup>c</sup>	 <b>108.1%</b>
7	 <b>109</b> (78%)	 <b>110.14%</b> ; 319	ND

[a] rsm: % recovered starting material (unoxidised). [b] TON referred to the mmol of isolated product per mmol of catalyst. [c] 1.5 g of starting material were used for the reaction with the *in situ* prepared Fe(OTf)<sub>2</sub>L1 complex in 0.5 mL of C<sub>6</sub>H<sub>6</sub>.

**Table 10.** Steric, electronic and hyperconjugative effects in the Fe(OTf)<sub>2</sub>L1 catalysed aerobic oxidation of benzyl ethers

### 3.3.4. Product inhibition and catalyst reuse

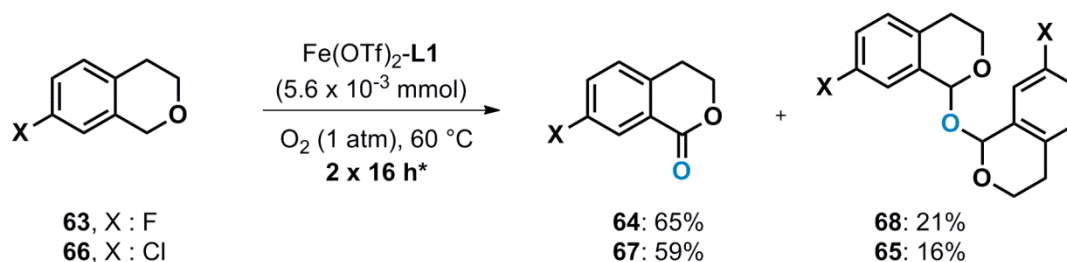
Although the  $\text{Fe}(\text{OTf})_2\text{-L1}$  catalyst showed high chemoselectivity and TONs, the oxidations above generally displayed relatively low conversions. In an attempt to increase the efficiency of the  $\text{Fe}(\text{OTf})_2\text{-L1}$  catalyzed aerobic oxidations, higher catalyst loadings were tested. However, no significant improvement was observed in the oxidation of **42** and **52** when the catalyst loading was increased under otherwise the same conditions. Further experiments revealed, surprisingly somehow, that the loss of catalytic activity at a certain level of conversion results from product inhibition, rather than catalyst decomposition. Thus, in the presence of the ester product **53** (30%, chosen according to the yield obtained under the normal conditions; Table 8, entry 1), the  $\text{Fe}(\text{OTf})_2\text{-L1}$  catalyzed oxidation of **52** afforded only 6% of additional **53** (Scheme 20), in stark contrast with the isolated yield of **53** shown in Table 3. The oxidation was also inhibited by the ether byproduct **54**. Most likely, the inhibition arises from the carbonyl coordination in the case of **53**, or the ether chelation in the case of **54**, to the iron centre, preventing the coordination of **52** and hence its oxidation. This is in line with the detrimental effect exerted by coordinating solvents mentioned above.



**Scheme 20.** Product inhibition during the aerobic oxidation of **52**

Realizing the inhibition effect of product, it became possible to increase the overall yield of the oxidation with  $\text{Fe}(\text{OTf})_2\text{-L1}$ , particularly when the product could be readily separated

from the reaction mixture. This is demonstrated in the oxidation of isochromans **63** and **66** (Scheme 21). After the initial oxidation under the same conditions as those in Table 8, the resulting solid products were removed, enabling the oxidation to continue for another 16 h to give **64** and **67** in a total isolated yield of 65% (1503 TON) and 59% (1282 TON), respectively, with no product over-oxidation. These results highlight the robustness of the iron catalyst and point to a strategy for addressing the conversion issue in question, i.e. run the oxidation in a continuous flow reactor.



\*Following the first 16 h, the product was removed and the oxidation continued for another 16 h.

**Scheme 21.** Improvement in the efficiency of the aerobic oxidation by catalyst reuse

### 3.4. Conclusions

Selective  $\alpha$ -oxidation of ethers under aerobic and additiveless conditions is a long-pursued transformation of industrial interest; however, a green and efficient catalytic version of this transformation has been challenging. We have found that our family of iron-PyBisulidine complexes are capable of catalysing the chemoselective  $\alpha$ -oxidation of functionalized ethers with excellent mass balance and high catalytic turnover numbers under 1 atm of  $\text{O}_2$  with no need for any additives. Unlike other biomimetic iron catalysts, our system shows excellent functional group tolerance even in the case of electron rich substrates. In addition, the catalyst is sensitive to electronic effects and such electronic bias can be applied for regioselective oxidation of certain substrates such as phthalans. The operational simplicity of this method combined with its environmental friendliness and high efficiency results in a useful alternative for performing selective oxidation.



### 3.5. Experimental section

#### 3.5.1 General techniques

Experiments involving air or moisture sensitive reagents were performed under an atmosphere of purified N<sub>2</sub> using standard Schlenck techniques. Solvents used in these experiments were reagent grade or better. MeCN, DCM and CHCl<sub>3</sub> were refluxed over CaH<sub>2</sub>/benzophenone and THF and Et<sub>2</sub>O were refluxed over Na/benzophenone and distilled under purified N<sub>2</sub> atmosphere. Anhydrous benzene 99.9% was purchased from Aldrich and stored over CaH<sub>2</sub> under N<sub>2</sub> atmosphere. Commercial grade solvents used in the synthesis of non air or non moisture sensitive components were used without further purification. Chemicals employed in the synthesis of ligands and substrates were purchased from commercial suppliers and used without further purification. Previously reported ligands PyBox and Box and iron salts were purchased from commercial suppliers and used without further purification.

#### 3.5.2. Ligand syntheses

PyBisulidine type ligands were synthesised according to the procedures provided in Chapter 2 of this Thesis. Ligand **L7** (Table 5, entry **9**), **L9** (Table 5, entry **11**) and the 6-(1H-pyrazol-1-yl)picolinaldehyde from ligand **L10** ( Table 5, entry **12**) were synthesised according to the literature.<sup>45,46,47</sup> Ligands **L8** (Table 5, entry **10**), **L11** (Table 5, entry **13**) and **L12** (Table 5, entry **14**) were purchased from commercial suppliers.

#### 3.5.3. Substrate syntheses and characterisation

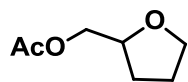
##### 3.5.3.1. Tetrahydrofuran substrates

Tetrahydrofuran type substrates were purchased from commercial suppliers apart from (tetrahydrofuran-2-yl) methyl acetate which was synthesised via acetylation of tetrahydrofurfuryl alcohol.<sup>48</sup>

## Analytical data

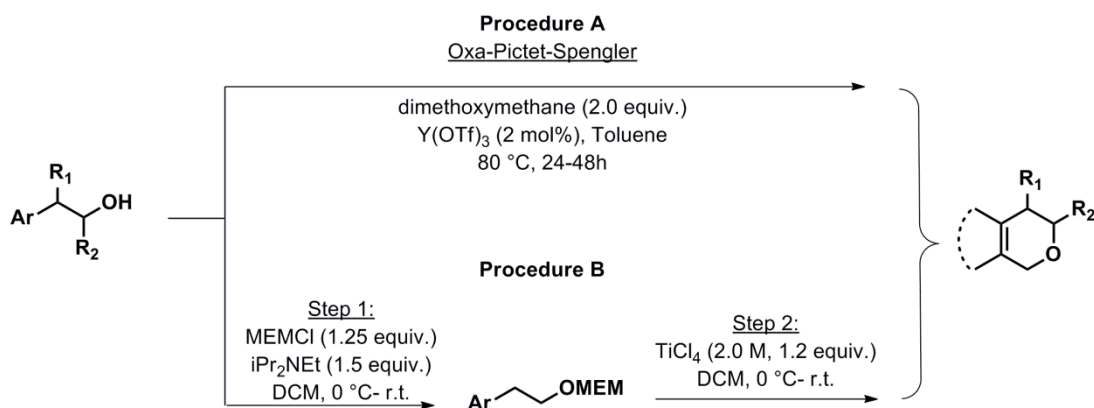
(Tetrahydrofuran-2-yl)methyl acetate<sup>48</sup>

Colourless liquid. Yield: 97%. <sup>1</sup>H NMR (400 MHz, CDCl<sub>3</sub>): δ (ppm) = 4.20-4.10 (m, 2H), 3.99 (dd, J = 11.1 Hz, 6.8 Hz, 1H), 3.94-3.88 (m, 1H), 3.84-3.79 (m, 1H), 2.15 (s, 3H), 2.06-1.87 (m, 3H), 1.65-1.57 (m, 2H). <sup>13</sup>C NMR (100 MHz, CDCl<sub>3</sub>): δ (ppm) = 171.1, 75.7, 68.5, 65.1, 27.6, 25.6, 20.3.



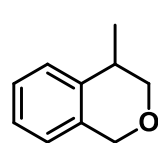
## 3.5.3.2. Isochromans

Isochroman derivatives were synthesised according to previous procedures described in the literature:

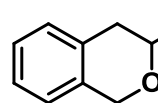
Procedure A: Acid catalysed oxa-Pictet-Spengler reaction<sup>49</sup>

In a round bottom flask equipped with a stirring bar and a reflux condenser, toluene (40 mL) and dimethoxymethane (6.0 mL, 2.0 equiv) were added. The corresponding β-arylethanol (4.0 mL, 1.0 equiv) and Y(OTf)<sub>3</sub> (2 mol%) were subsequently added and the reaction mixture was allowed to stir at 80 °C for 24-48h (t.l.c. monitoring) under inert atmosphere. The solvents were evaporated and the liquid residue was dissolved in DCM (30 mL) and washed with aqueous NaHCO<sub>3</sub> and water and dried over MgSO<sub>4</sub>. The solvents were removed in vacuo and the residue purified by flash column chromatography (Hexane:AcOEt 95:5) to afford the desired isochroman in good yields (74-97% isol. yield).

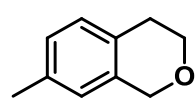
## Analytical data of substrates synthesised according to procedure A:

**4-Methylisochroman<sup>50</sup> (55)**

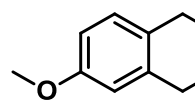
Pale yellow oil, 65% yield. <sup>1</sup>H NMR (400 MHz, CDCl<sub>3</sub>): δ (ppm) = 7.35-7.31 (m, 2H), 7.25-7.14 (m, 2H), 4.62 (dd, J = 10.0, 6.4 Hz, 2H), 3.70 (dd, J = 6.9, 2.0 Hz, 1H), 3.62 (dd, J = 7.1, 2.3 Hz, 1H), 3.06 (m, 1H), 1.33 (d, J = 6.8 Hz, 3H). <sup>13</sup>C NMR (100 MHz, CDCl<sub>3</sub>): δ (ppm) = 144.7, 128.7, 126.9, 126.4, 96.8, 71.8, 68.8, 32.3, 19.6. HRMS (EI) m/z calc'd C<sub>10</sub>H<sub>13</sub>O [M + H]<sup>+</sup>: 149.0961, found: 149.0960.

**3-Methylisochroman<sup>50</sup> (57)**

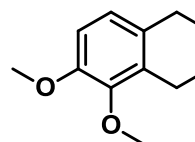
Colourless oil, 74% yield. <sup>1</sup>H NMR (400 MHz, CDCl<sub>3</sub>): δ (ppm) = 7.16 (m, 2H), 7.10, (m, 1H), 7.00 (m, 1H), 4.83 (d, J = 15.2 Hz, 2H), 3.81 (sextuplet, J = 6.8 Hz, 1H), 2.71 (d, J = 6.8 Hz, 2H), 1.35 (d, J = 6.4 Hz, 3H). <sup>13</sup>C NMR (100 MHz, CDCl<sub>3</sub>): δ (ppm) = 135.0, 133.9, 129.1, 126.7, 126.3, 124.6, 71.4, 68.6, 36.2, 22.0. HRMS (EI) m/z calc'd C<sub>10</sub>H<sub>13</sub>O [M + H]<sup>+</sup>: 149.0961, found: 149.0958.

**7-Methylisochroman<sup>50</sup> (72)**

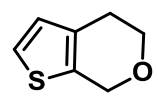
Colourless oil, 68% yield. <sup>1</sup>H NMR (400 MHz, CDCl<sub>3</sub>): δ (ppm) = 7.08 (m, 1H), 6.93 (m, 1H), 6.72 (s, 1H), 4.66 (s, 2H), 3.88 (t, J = 5.6 Hz, 2H), 2.74 (t, J = 5.6 Hz, 2H), 2.22 (s, 3H). <sup>13</sup>C NMR (100 MHz, CDCl<sub>3</sub>): δ (ppm) = 135.9, 135.1, 130.5, 129.6, 129.1, 128.7, 68.3, 65.9, 28.3, 21.4. HRMS (EI) m/z calc'd C<sub>10</sub>H<sub>13</sub>O [M + H]<sup>+</sup>: 149.0961, found: 149.0959.

**7-Methoxyisochroman (75)**

White solid, 42% yield. <sup>1</sup>H NMR (400 MHz, CDCl<sub>3</sub>): δ (ppm) = 7.00 (d, J = 8.4 Hz, 1H), 6.66 (dd, J = 8.0, 2.8 Hz, 1H), 6.46 (d, J = 2.4 Hz, 1H), 4.71 (s, 2H), 4.69 (s, 3H), 3.95 (t, J = 6.0 Hz, 2H), 2.78 (t, J = 5.8 Hz, 2H). <sup>13</sup>C NMR (100 MHz, CDCl<sub>3</sub>): δ (ppm) = 154.0, 136.6, 130.4, 114.2, 111.1, 68.3, 66.0, 55.7, 27.9. HRMS (EI) m/z calc'd C<sub>9</sub>H<sub>11</sub>O<sub>2</sub> [M + H]<sup>+</sup>: 151.0754, found: 151.0751.

**7,8-Dimethoxyisochroman<sup>50</sup> (77)**

White solid, 74% yield. <sup>1</sup>H NMR (400 MHz, CDCl<sub>3</sub>): δ (ppm) = 6.54 (s, 1H), 6.40 (s, 1H), 4.63 (s, 2H), 3.88 (t, J = 5.6 Hz, 2H), 3.80 (s, 3H), 3.77 (s, 3H), 2.70 (t, J = 5.6 Hz, 2H). <sup>13</sup>C NMR (100 MHz, CDCl<sub>3</sub>): δ (ppm) = 148.0, 147.9, 127.0, 125.4, 112.0, 107.7, 68.0, 65.8, 56.3, 28.2. HRMS (EI) m/z calc'd C<sub>11</sub>H<sub>15</sub>O<sub>3</sub> [M + H]<sup>+</sup>: 195.1016, found: 195.1017.

**4,5-Dihydro-4H-thieno[2,3c]pyran (81)**

Yellow oil, 65% yield. <sup>1</sup>H NMR (400 MHz, CDCl<sub>3</sub>): δ (ppm) = 7.08 (d, J = 5.2 Hz, 1H), 6.76 (d, J = 5.2 Hz, 1H), 4.76 (s, 2H), 3.88 (t, J = 5.6 Hz, 2H), 2.69 (t, J = 5.6 Hz, 2H). <sup>13</sup>C NMR (100 MHz, CDCl<sub>3</sub>): δ (ppm) = 133.1, 133.1, 127.4, 122.9, 66.0, 65.4, 26.5. IR ν (neat) = 2962, 2908, 2837, 1675, 1460, 1442, 1431, 1392, 1379, 1282, 1233, 1213, 1154, 1094, 1083, 1066, 1020, 985, 971, 895, 848, 821, 755, 700, 645, 611, 574 cm<sup>-1</sup>. HRMS (EI) m/z calc'd C<sub>7</sub>H<sub>9</sub>OS [M + H]<sup>+</sup>: 141.0369, found: 141.0366.

## Procedure B: intramolecular oxonium cyclisation of MEM-protected phenethyl alcohols

### Synthesis of the MEM ethers <sup>51</sup>

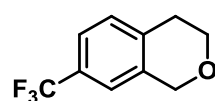
In a round bottom flask equipped with a stirring bar, the corresponding  $\beta$ -arylethanol (0.8 equiv) was dissolved in freshly distilled DCM (30 mL) and the reaction mixture was cooled to 0 °C. Diisopropylethylamine (1.2 equiv) was subsequently added to the flask and finally MEMCl (1.0 equiv) was added dropwise to the reaction mixture which was allowed to stir overnight at r.t. The reaction was washed with aqueous HCl solution and water and dried over MgSO<sub>4</sub>. After filtration, the volatiles were evaporated and the residue was purified by flash column chromatography (Hexane: EtOAc 8:1) to afford the MEM ether in excellent yields (94-98% isol. yield).

### TiCl<sub>4</sub> promoted acetal cyclisation <sup>51</sup>

A two necked round bottom flask equipped with a stirring bar was placed under inert atmosphere on an ice bath. TiCl<sub>4</sub> (1.0 M in DCM solution, 1.2 equiv) was added by syringe and the corresponding MEM ether was subsequently added dropwise at 0 °C. The reaction was allowed to stir for 4 h before being quenched with 1.0M HCl solution. The organic phase was extracted in DCM and washed with diluted NaHCO<sub>3</sub> solution and water. The organic phase was dried over MgSO<sub>4</sub>, filtrated and volatiles evaporated in vacuo. The residue was purified by silica gel column chromatography (Hexane: AcOEt 8:1) to afford the desired isochroman substrate with high yield (75-92%).

### Analytical data of substrates synthesised according to procedure B

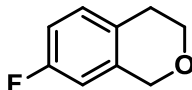
#### 7-(Trifluoromethyl)isochroman (60)



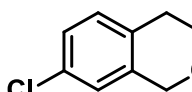
Colourless liquid, 45% abs. yield. <sup>1</sup>H NMR (400 MHz, CDCl<sub>3</sub>):  $\delta$  (ppm) = 7.41 (d,  $J$  = 8.0 Hz, 1H), 7.24 (m, 3H), 4.80 (s, 2H), 3.99 (t,  $J$  = 6.0 Hz, 2H), 2.91 (t,  $J$  = 5.8 Hz, 2H). <sup>13</sup>C NMR (100 MHz, CDCl<sub>3</sub>):  $\delta$  (ppm) = 137.7, 136.0, 129.8 (d, <sup>2</sup>J<sub>C-F</sub> = 31.9 Hz), 125.1 (t, <sup>1</sup>J<sub>C-F</sub> = 127.6 Hz), 123.5 (d, <sup>3</sup>J<sub>C-F</sub> = 3.6 Hz), 121.8 (d, <sup>3</sup>J<sub>C-F</sub> = 3.9 Hz), 68.1, 65.4, 28.7. IR  $\nu$  (neat) = 1626, 1432, 1380, 1330, 1307, 1277,

1250, 1228, 1187, 1161, 1115, 1073, 1036, 990, 960, 895, 823, 784, 749, 718, 670, 660, 630, 603  $\text{cm}^{-1}$ . **HRMS** (EI)  $m/z$  calc'd  $\text{C}_{10}\text{H}_{10}\text{F}_3\text{O}$   $[\text{M} + \text{H}]^+$ : 203.0678, found: 203.0679.

### 7-Fluoroisochroman<sup>50</sup> (63)

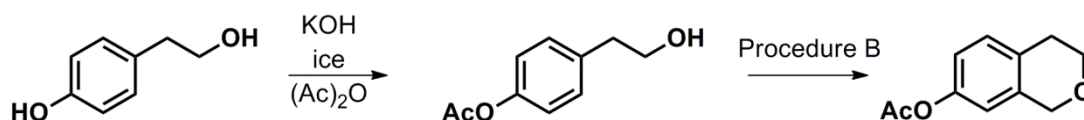
 Colourless liquid, 78% abs. yield. **<sup>1</sup>H NMR** (400 MHz,  $\text{CDCl}_3$ ):  $\delta$  (ppm) = 7.07 (dd,  $J = 8.4, 5.6$  Hz, 1H), 6.86 (dt,  $J = 8.6, 2.6$  Hz, 1H), 6.70 (dd,  $J = 9.2, 2.6$  Hz, 1H), 4.74 (s, 2H), 3.96 (t,  $J = 6.8$  Hz, 2H), 2.81 (t,  $J = 6.8$  Hz, 2H). **<sup>13</sup>C NMR** (100 MHz,  $\text{CDCl}_3$ ):  $\delta$  (ppm) = 161.2 (d,  $^1J_{\text{C-F}} = 242.9$  Hz), 137.0 (d,  $^3J_{\text{C-F}} = 6.9$  Hz), 130.7 (d,  $^3J_{\text{C-F}} = 7.6$  Hz), 129.1 (d,  $^4J_{\text{C-F}} = 3.0$  Hz), 114.0 (d,  $^2J_{\text{C-F}} = 21.2$  Hz), 111.4 (d,  $^2J_{\text{C-F}} = 21.4$  Hz), 68.1, 65.8, 28.0. **HRMS** (EI)  $m/z$  calc'd  $\text{C}_9\text{H}_{10}\text{FO}$   $[\text{M} + \text{H}]^+$ : 153.0711, found: 153.0713.

### 7-Chloroisochroman<sup>50</sup> (66)

 Colourless liquid, 68% abs. yield. **<sup>1</sup>H NMR** (400 MHz,  $\text{CDCl}_3$ ):  $\delta$  (ppm) = 7.15 (m, 1H), 7.05 (m, 1H), 6.98 (m, 1H), 4.72 (s, 2H), 3.97 (t,  $J = 6.4$  Hz, 2H), 2.87 (t,  $J = 6.8$  Hz, 2H). **<sup>13</sup>C NMR** (100 MHz,  $\text{CDCl}_3$ ):  $\delta$  (ppm) = 136.6, 131.6, 131.5, 130.2, 126.5, 124.4, 67.5, 65.2, 27.7. **HRMS** (EI)  $m/z$  calc'd  $\text{C}_9\text{H}_{10}\text{ClO}$   $[\text{M} + \text{H}]^+$ : 169.0415, found: 169.0415.

### Synthesis of isochroman-7-yl acetate

Isochroman-7-yl acetate was synthesised according to the following previously reported steps.<sup>52</sup>



### Synthesis of 3-acetoxybenzyl alcohol

To a stirred solution of 3-hydroxybenzyl alcohol (3.72 g, 30 mmol) in 6.4N aqueous KOH (7 mL) at room temperature was added ice (15 g) followed by acetic anhydride (3.55 mL, 1.25 equiv.). After stirring for 45 min, water (250 mL) was added and the mixture was stirred for a further 30 min before extracting with dichloromethane (3×100 mL). The combined extracts were washed with water, brine and dried over  $\text{MgSO}_4$ . Evaporation of the solvent gave a brown oil which was purified by flash column chromatography (Hexane: AcOEt 6:1) to give the desired product as a colourless oil (3.24 g, 65%).

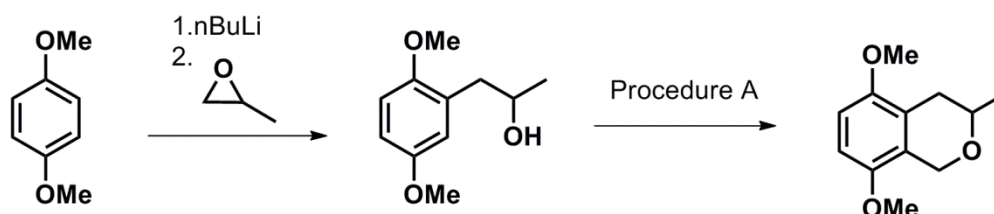
## Analytical data

Isochroman-7-yl acetate<sup>52</sup> (69)

Colourless oil, 74% yield. <sup>1</sup>H NMR (400 MHz, CDCl<sub>3</sub>): δ (ppm) = 7.13 (d, J = 8.4 Hz, 2H), 6.88 (dd, J = 8.0, 2.0 Hz, 2H), 6.72 (d, J = 2.2 Hz, 1H), 4.75 (s, 2H), 3.96 (t, J = 5.6 Hz, 2H), 2.84 (t, J = 5.6 Hz, 2H), 2.28 (s, 3H). <sup>13</sup>C NMR (100 MHz, CDCl<sub>3</sub>): δ (ppm) = 170.1, 149.0, 136.5, 131.2, 130.3, 120.0, 117.7, 68.1, 65.7, 28.2, 21.5. HRMS (EI) m/z calc'd C<sub>11</sub>H<sub>13</sub>O<sub>3</sub> [M + H]<sup>+</sup>: 193.0860, found: 193.0859.

## Synthesis of 5,8-dimethoxy-3-methylisochroman

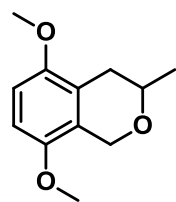
5,8-Dimethoxy-3-methylisochroman was synthesised as reported in the literature.<sup>53</sup>



## Synthesis of (±)-1-(2,5-dimethoxyphenyl)-2-propanol

In a two necked round bottom flask equipped with a magnetic bar and placed under inert atmosphere, 1,4-dimethoxybenzene (7.0 g, 68.5 mmol) was added to freshly distilled THF (20 mL) and placed on an ice bath. N-butyllithium (5.7 mL, 59.8 mmol, 10.5 M in hexanes) was added dropwise and the reaction mixture was refluxed for 48 h under inert atmosphere. Then, the dark reddish solution was cooled to 0 °C and propylene oxide (4.2 mL, 29 mmol) was added dropwise. The reaction mixture was stirred at 0 °C (1 h), then warmed to 25 °C (50 min) and refluxed for 2.5 h. The reaction mixture was cooled to r.t. and quenched with water (15 mL) forming a white suspension that was diluted with THF (25 mL) and then water (50 mL). The THF was evaporated in vacuo and the organic phase was extracted with DCM. The extract was washed with brine and water and dried over MgSO<sub>4</sub>. The solution was filtered and the solvent eliminated in vacuo to afford a crude oil that was purified by flash column chromatography (Hexane /AcOEt, 5/1) to afford the desired product as a clear oil in good yield (60%).

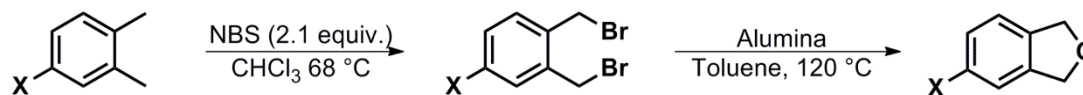
## Analytical data

5,8-Dimethoxy-3-methylisochroman<sup>53</sup> (79)

White solid, 73% yield. <sup>1</sup>H NMR (400 MHz, CDCl<sub>3</sub>): δ (ppm) = 6.56 (dd, J = 16.0, 8.8 Hz, 2H), 6.55 (d, J = 8.8 Hz, 1H, overlapped), 4.85 (d, J = 16.0 Hz, 1H), 4.53 (d, J = 16.0 Hz, 1H), 3.72 (s, 3H), 3.71 (s, 3H), 3.67-3.58 (m, 1H), 2.71 (dd, J = 2.8, 1.2 Hz, 1H), 2.66 (dd, J = 3.2, 1.6 Hz, 1H), 2.28 (d, J = 6.4 Hz, 3H). <sup>13</sup>C NMR (100 MHz, CDCl<sub>3</sub>): δ (ppm) = 151.3, 149.8, 125.1, 124.4, 107.8, 107.2, 70.5, 64.9, 60.8, 56.0, 55.8, 30.7, 22.0. HRMS (EI) m/z calc'd C<sub>12</sub>H<sub>17</sub>O<sub>3</sub> [M + H]<sup>+</sup>: 209.1172, found, 209.1173.

## 3.5.3.3. Synthesis of phthalans

1,3-dihydroisobenzofurans derivatives (phthalans) were synthesised following the same procedure described for the synthesis of 4-nitro-1,3-dihydroisobenzofuran.<sup>54</sup>



X: halogen

## Synthesis of 1,2-bis(bromomethyl)-4-halobenzenes

A two necked round bottom flask equipped with a stirring bar and a reflux condenser was placed under inert atmosphere. CHCl<sub>3</sub> (40 mL), 1,2-dimethyl-4-halobenzene (1.0 equiv), NBS (2.1 equiv) and benzoyl peroxide (1 mol%) were added sequentially. The reaction was heated up to 65 °C and small amounts of benzoyl peroxide (50 mg) were added every 30 min for a period of 2 h. The reaction was heated up for another 4 h and then cooled to r.t. The reaction was filtered to remove the white precipitate and washed with CHCl<sub>3</sub>. The solvent was evaporated in vacuo to afford the desired product as a yellowish oil (87% isol. yield).

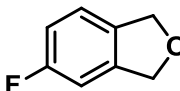
## Synthesis of the 1,3-dihydroisobenzofurans

In a round bottom flask equipped with a stirring bar, the corresponding 1,2-bis(bromomethyl)-4-halobenzene (1.0 equiv) was dissolved in toluene (40 mL). Alumina (40 equiv) was added and the mixture was heated up to 120 °C overnight. The reaction mixture

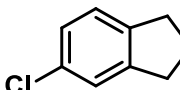
was filtered to remove the alumina and washed with AcOEt. The solvents were evaporated and the residue was purified by flash column chromatography (Hexane /AcOEt 100/0 to 94/6) to afford the desired product as a bright oil (67-88% isol. yields).

### Analytical data

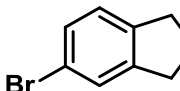
#### 5-Fluoro-1,3-dihydroisobenzofuran<sup>55</sup> (84)

 Pale yellow liquid, 45% yield. <sup>1</sup>H NMR (400 MHz, CDCl<sub>3</sub>): δ (ppm) = 7.28-7.23 (m, 1H), 7.00 (d, J = 7.6 Hz, 1H), 6.93 (t, J = 8.0 Hz, 1H), 5.17 (s, 2H), 5.13 (s, 2H). <sup>13</sup>C NMR (100 MHz, CDCl<sub>3</sub>): δ (ppm) = 156.4, 143.3, 130.0 (d, <sup>3</sup>J<sub>C-F</sub> = 6.5 Hz), 126.1, 117.0 (d, <sup>2</sup>J<sub>C-F</sub> = 13.5 Hz), 114.4 (d, <sup>2</sup>J<sub>C-F</sub> = 19.8 Hz), 74.2, 71.4. HRMS (EI) m/z calc'd C<sub>8</sub>H<sub>8</sub>FO [M + H]<sup>+</sup>: 139.1464, found: 139.1462.

#### 5-Chloro-1,3-dihydroisobenzofuran<sup>56</sup> (86)

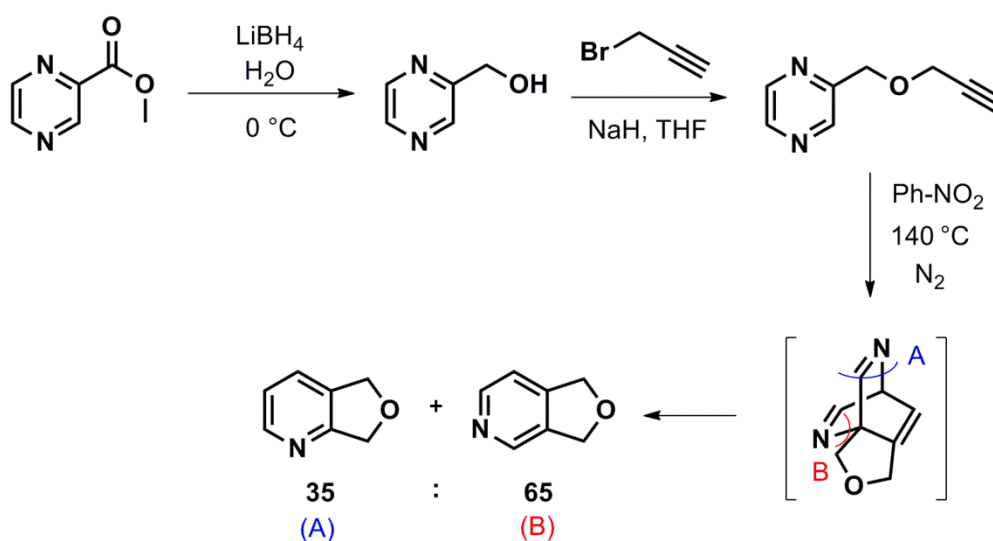
 White wax, 46% yield. <sup>1</sup>H NMR (400 MHz, CDCl<sub>3</sub>): δ (ppm) = 7.25-7.22 (m, 2H), 7.17 (d, J = 8.0 Hz, 1H), 5.08 (s, 4H). <sup>13</sup>C NMR (100 MHz, CDCl<sub>3</sub>): δ (ppm) = 141.6, 137.9, 133.5, 127.8, 122.4, 121.7, 73.5. HRMS (EI) m/z calc'd C<sub>8</sub>H<sub>8</sub>ClO [M + H]<sup>+</sup>: 155.0259, found: 155.0262.

#### 5-Bromo-1,3-dihydroisobenzofuran<sup>55</sup> (88)

 White wax, 44% yield. <sup>1</sup>H NMR (400 MHz, CDCl<sub>3</sub>): δ (ppm) = 7.4 (d, J = 7.2 Hz, 1H), 7.17-7.06 (m, 2H), 5.10 (s, 2H), 5.08 (s, 2H). <sup>13</sup>C NMR (100 MHz, CDCl<sub>3</sub>): δ (ppm) = 138.5, 130.7, 124.7, 122.8, 121.4, 73.5, 73.4. HRMS (EI) m/z calc'd C<sub>8</sub>H<sub>8</sub>BrO [M + H]<sup>+</sup>: 198.9754, found: 198.9751.

### 4.4.3. 4. Synthesis of 1,3-dihydrofuro-pyridines

1,3-Dihydrofuro-pyridines were synthesised in a similar fashion as reported in the literature.<sup>57</sup>





---

**Alternative procedure for the reduction of methyl 2-pyrazinecarboxylate to pyrazin-2-yl methanol**

In a 500 mL round bottom flask equipped with a magnetic stirring bar, methyl 2-pyrazinecarboxylate (8.5 g) was added and dissolved in distilled water (200 mL). The flask was cooled to 0 °C and LiBH<sub>4</sub> (6.7 g) was added constantly in small portions (20 mg) over a period of approximately 1.5-2 h. (**Note:** this process must be performed **extremely carefully** as it is a very exothermic reaction and the addition should be done constantly and in very small portions. A single portion addition of the borohydride is **extremely dangerous** and should not be done under any circumstance). Once the addition is finished, the reaction mixture was allowed to stir for additional 30 min. EtOH (80 mL) and K<sub>2</sub>CO<sub>3</sub> sat solution (150 mL) were then added to the reaction mixture which was stirred for an additional 30 min period. The reaction was extracted with AcOEt (5 x 150 mL) and DCM (5 x 150 mL) and the organic extracts combined and dried over MgSO<sub>4</sub>. The extract was filtered and the solvents removed in vacuo to afford the product as a yellow oil.

**O-propargylation of pyrazin-2-yl methanol**

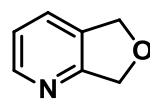
Pyrazin-2-yl methanol (1.0 equiv) was slowly added into a suspension of NaH (1.1 equiv) in dried THF (30 mL) at 0 °C. The mixture was stirred until the evolution of hydrogen ceased (*circa* 10-15 min). Then propargyl bromide (2.0 equiv) was added and the reaction mixture was refluxed for 3 h. The reaction was quenched with water (50 mL) and extracted with diethyl ether. The organic layer was dried over MgSO<sub>4</sub>, filtered and the solvents removed in vacuo. The residue was purified by flash column chromatography (Hexane/Et<sub>2</sub>O 2/1) to afford the desired product as a light oil (89% yield).

**Cyclisation of the 5-(2-propynyloxymethyl)pyrimidine**

In a round bottom flask equipped with a stirring bar and a reflux condenser, 5-(2-propynyloxymethyl)pyrimidine (10 equiv) was dissolved in nitrobenzene (5 mL). There

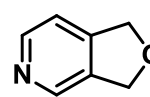
action mixture was heated up to 140 °C overnight under inert atmosphere. The reaction products were isolated by flash column chromatography (Hexane/Et<sub>2</sub>O 3/1 to 2/1) to afford both regioisomers in good yields (65 and 35%).

#### 5,7-Dihydrofuro[3,4b]pyridine<sup>57</sup> (92)



White solid, 35% isol. yield. <sup>1</sup>H NMR (400 MHz, CDCl<sub>3</sub>): δ (ppm) = 8.53 (m, 2H), 7.22 (d, J = 4.8 Hz, 1H), 5.16 (s, 2H), 5.11 (s, 2H). <sup>13</sup>C NMR (100 MHz, CDCl<sub>3</sub>): δ (ppm) = 161.0, 148.1, 142.7, 116.2, 72.7, 71.5. HRMS (EI) m/z calc'd C<sub>7</sub>H<sub>8</sub>NO [M + H]<sup>+</sup>: 122.0597, found: 122.0600.

#### 1,3-Dihydrofuro[3,4-c]pyridine<sup>57</sup> (94)

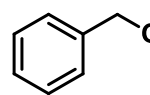


White solid, 65% isol. yield. <sup>1</sup>H NMR (400 MHz, CDCl<sub>3</sub>): δ (ppm) = 8.48 (d, J = 4.8 Hz, 1H), 7.55 (d, J = 7.6 Hz, 1H), 7.17 (dd, J = 7.6, 5.0 Hz, 1H), 5.17 (s, 2H), 5.03 (s, 2H). <sup>13</sup>C NMR (100 MHz, CDCl<sub>3</sub>): δ (ppm) = 161.0, 149.3, 132.3, 129.5, 122.2, 73.2, 72.6. HRMS (EI) m/z calc'd C<sub>7</sub>H<sub>8</sub>NO [M + H]<sup>+</sup>: 122.0600, found: 122.0598.

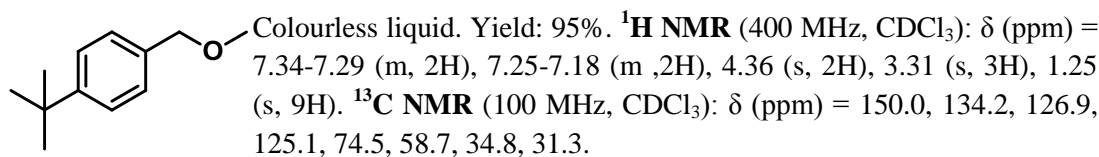
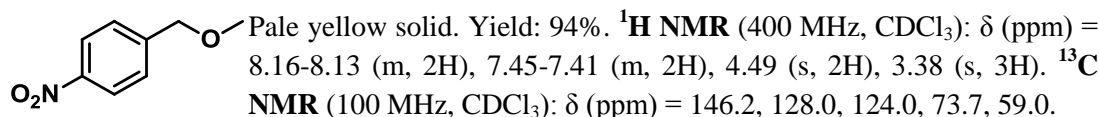
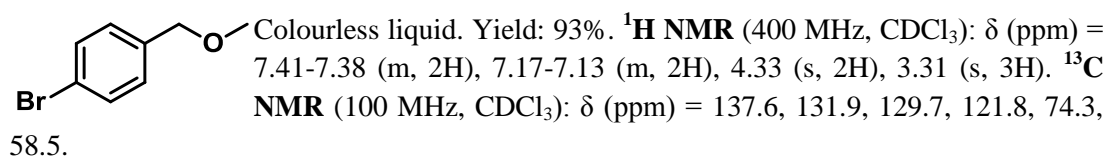
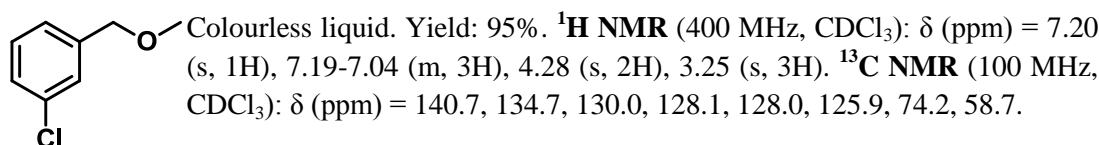
#### 3.5.3.5. Synthesis of alkyl benzyl ethers<sup>58</sup>

Alkyl benzyl ethers were purchased from commercial suppliers or synthesised according to the literature as follows: In a round bottom flask equipped with a stirring bar and a reflux condenser, 4-bromobenzyl bromide (7.0 g, 1.0 equiv) was dissolved in MeOH (60 mL). Sodium methoxyde (1.62 g, 1.2 equiv.) was added slowly to the reaction mixture and then the reaction was refluxed overnight. The reaction was allowed to cool to r.t. and water (100 mL) and DCM (75 mL) were added. The organic layer was extracted and washed with water and brine and dried over MgSO<sub>4</sub>. The solution was filtered and solvents were removed in vacuo. The residue was purified by flash column chromatography (Hexane/DCM 2/1) to afford the desired ether as a colourless light oil (96% yield).

#### (Ethoxymethyl)benzene<sup>59</sup> (98)



Colourless liquid. Yield: 94%. <sup>1</sup>H NMR (400 MHz, CDCl<sub>3</sub>): δ (ppm) = 7.43-7.28 (m, 5H), 4.44 (s, 2H), 3.48 (q, J = 7.2 Hz, 2H), 1.18 (t, J = 7.2 Hz, 3H). <sup>13</sup>C NMR (100 MHz, CDCl<sub>3</sub>): δ (ppm) = 139.0, 128.9, 128.0, 127.9, 73.1, 66.1, 15.6.

**1-(*tert*-Butyl)-4-(methoxymethyl)benzene<sup>60</sup> (102)****1-(Methoxymethyl)-4-nitrobenzene<sup>61</sup> (104)****1-(Bromo)-4-(methoxymethyl)benzene<sup>62</sup> (106)****1-(Chloro)-3-(methoxymethyl)benzene<sup>63</sup> (109)****3.5.4. Representative procedure for the aerobic  $\alpha$ -oxidation of ethers catalysed by Fe(OTf)<sub>2</sub>L1**

In a Radley's tube equipped with a magnetic stir bar ligand **L1** ( $5.6 \times 10^{-3}$  mmol, 5.2mg) and Fe(OTf)<sub>2</sub> ( $5.6 \times 10^{-3}$  mmol, 2.0 mg) were added. The tube was sealed, degassed and left under inert atmosphere (3 times). The corresponding ether (2.0 mL) was added by syringe; the reaction tube was degassed, charged with dioxygen gas (1 atm, 3 times) and keep under oxygen (1 atm) by using a balloon. The reaction mixture was heated to 60 °C and left overnight. The reaction was purified by silica gel column chromatography (Hexane/EtOAc, gradient: 10/1 to 4/1) to afford the unreacted starting material and the reaction products.

## Analytical data

 $\gamma$ -Butyrolactone<sup>64</sup> (43)

Colourless oil (9.5% isol. yield, 200.5 mg, 2.33 mmol). <sup>1</sup>H NMR (400 MHz, CDCl<sub>3</sub>):  $\delta$  (ppm) = 4.37 (t, J = 7.0 Hz, 2H), 2.53 (t, J = 7.0 Hz, 2H), 2.30 (q, J = 7.0 Hz, 2H). <sup>13</sup>C NMR (100 MHz, CDCl<sub>3</sub>):  $\delta$  (ppm) = 178.1, 68.9, 28.2, 22.6. IR (neat)  $\nu$  = 1764, 1375, 1162, 1034, 990 cm<sup>-1</sup>. HRMS (EI) m/z calc'd C<sub>4</sub>H<sub>8</sub>O<sub>2</sub> [M+NH<sub>4</sub>]<sup>+</sup>: 104.0706, found: 104.0707. Anal Calc'd for C<sub>4</sub>H<sub>8</sub>O<sub>2</sub>: C, 55.81, H, 7.02; found: C, 55.87, H, 7.07.

5-Methyldihydrofuran-2(3H)-one<sup>64</sup> (45)

Colourless oil (9% isol. yield, 210.2 mg, 2.10 mmol). <sup>1</sup>H NMR (400 MHz, CDCl<sub>3</sub>):  $\delta$  (ppm) = 4.64 (sextet, J = 6.5 Hz, 1H), 2.57-2.51 (m, 2H), 2.49-2.32 (m, 1H), 1.86-1.83 (m, 1H), 1.45 (d, J = 6.8 Hz, 3H). <sup>13</sup>C NMR (100 MHz, CDCl<sub>3</sub>):  $\delta$  (ppm) = 177.6, 67.2, 30.1, 29.3, 21.4. IR (neat)  $\nu$  = 1774, 1345, 1175, 941 cm<sup>-1</sup>. HRMS (EI) m/z calc'd C<sub>5</sub>H<sub>12</sub>O<sub>2</sub>N [M+NH<sub>4</sub>]<sup>+</sup>: 118.0863, found: 118.0863. Anal Calc'd for C<sub>5</sub>H<sub>8</sub>O<sub>2</sub>: C, 59.98, H, 8.05; found: C, 59.81, H, 8.27.

(5-Oxotetrahydrofuran-2-yl)methyl acetate<sup>65</sup> (47)

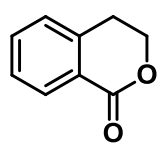
Colourless oil (5.4% isol. yield, 118.6 mg, 0.75 mmol). <sup>1</sup>H NMR (400 MHz, CDCl<sub>3</sub>):  $\delta$  (ppm) = 4.77-4.71 (m, 1H), 4.32 (dd, J = 12.4, 3.2 Hz, 1H), 4.15 (d, J = 12.0, 5.2 Hz, 1H), 2.62-2.51 (m, 2H), 2.39-2.32 (m, 1H), 2.12-2.03 (m, 1H). <sup>13</sup>C NMR (100 MHz, CDCl<sub>3</sub>):  $\delta$  (ppm) = 176.8, 171.0, 65.7, 28.5, 24.3, 21.1. IR (ATR)  $\nu$  = 2952, 1774, 1733, 1461, 1419, 1371, 1232, 1160, 1041, 941, 919, 804, 649. HRMS (EI) m/z calc'd C<sub>7</sub>H<sub>13</sub>O<sub>3</sub> [M+H]<sup>+</sup>: 145.0859, found: 145.0855. Anal Calc'd for C<sub>7</sub>H<sub>12</sub>O<sub>3</sub>: C, 53.16, H, 6.37; found: C, 52.89, H, 6.04.

5-(Chloromethyl)dihydrofuran-2(3H)-one<sup>66</sup> (49)

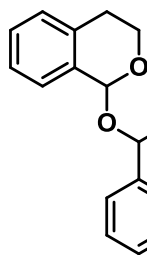
Colourless oil (4.2% isol. yield, 93.5 mg, 0.70 mmol). <sup>1</sup>H NMR (400 MHz, CDCl<sub>3</sub>):  $\delta$  (ppm) = 4.74-4.69 (m, 1H), 3.69-3.60 (m, 2H), 2.64-2.48 (m, 2H), 2.43-2.341 (m, 1H), 2.29-2.17 (m, 1H). <sup>13</sup>C NMR (100 MHz, CDCl<sub>3</sub>):  $\delta$  (ppm) = 176.6, 78.5, 46.4, 28.6, 25.3. IR (neat)  $\nu$  = 2962, 1770, 1421, 1344, 1166, 1141, 1037, 919, 740, 653. HRMS (EI) m/z calc'd C<sub>5</sub>H<sub>11</sub>ClO<sub>2</sub>N [M+NH<sub>4</sub>]<sup>+</sup>: 135.0207, found: 135.0204. Anal Calc'd for C<sub>5</sub>H<sub>8</sub>ClO<sub>2</sub>: C, 44.63, H, 5.24; found: C, 45.04, H, 5.50.

2-(5-Oxotetrahydrofuran-2-yl)acetonitrile<sup>67</sup> (51)

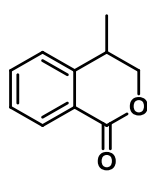
Colourless oil (3% isol. yield, 66.3 mg, 0.53 mmol). <sup>1</sup>H NMR (400 MHz, CDCl<sub>3</sub>):  $\delta$  (ppm) = 4.77-4.70 (m, 1H), 2.82 (d, J = 5.7 Hz, 2H), 2.77-2.49 (m, 3H), 2.13-2.11 (m, 1H). <sup>13</sup>C NMR (100 MHz, CDCl<sub>3</sub>):  $\delta$  (ppm) = 175.5, 115.6, 74.5, 28.5, 27.3, 24.5. IR (neat)  $\nu$  = 2965, 2933, 2254, 1770, 1461, 1421, 1349, 1178, 1149, 1037, 923, 800, 646. HRMS (EI) m/z calc'd for C<sub>6</sub>H<sub>8</sub>NO<sub>2</sub> [M+H]<sup>+</sup>: 126.0550, found: 126.0548. Anal Calc'd for C<sub>6</sub>H<sub>7</sub>NO<sub>2</sub>: C, 57.59, H, 5.64, N, 11.19; found: C, 57.47, H, 5.73, N, 11.05.

**Isochroman-1-one<sup>68</sup> (53)**

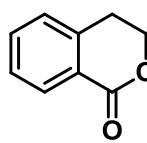
Colourless liquid (30% isol. yield, 706.8 mg, 4.77 mmol). <sup>1</sup>H NMR (400 MHz, CDCl<sub>3</sub>): δ (ppm) = 8.12 (d, J = 7.7 Hz, 1H), 7.57 (t, J = 6.3 Hz, 1H), 7.41 (t, J = 7.6 Hz, 1H), 7.28 (d, J = 7.4 Hz, 1H), 4.56 (t, J = 6.2 Hz, 2H), 3.08 (t, J = 6.0 Hz, 2H). <sup>13</sup>C NMR (100 MHz, CDCl<sub>3</sub>): δ (ppm) = 165.1, 139.5, 133.6, 127.7, 125.3, 124.0, 67.3, 27.8. IR ν (neat) = 1714, 1602, 1459, 1386, 1294, 1240, 1116, 1087, 1024, 954, 744, 693, 636 cm<sup>-1</sup>. HRMS (EI) m/z calc'd C<sub>9</sub>H<sub>9</sub>O<sub>2</sub> [M + H]<sup>+</sup>: 149.0597, found: 149.0597. Anal Calc'd for C<sub>9</sub>H<sub>8</sub>O<sub>2</sub>: C, 72.96, H, 5.44, found: C, 73.37, H, 5.60.

**1,1'-Oxydiisochroman<sup>37-39</sup> (54)**

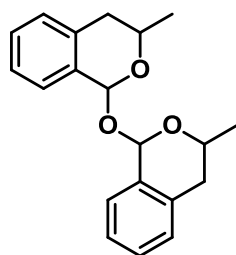
Colourless crystals (10% isol. yield, 448.7 mg, 1.59 mmol). <sup>1</sup>H NMR (400 MHz, CDCl<sub>3</sub>): δ (ppm) = 7.28-7.22 (m, 6H), 7.14 (t, J = 4.9 Hz, 2H), 6.15 (s, 2H), 4.37 (dt, J = 11.7, 3.2 Hz, 2H), 4.10 (dd, J = 11.0, 5.9 Hz, 2H), 3.18-3.10 (m, 2H), 2.68 (dd, J = 16.5, 2.7 Hz, 2H). <sup>13</sup>C NMR (100 MHz, CDCl<sub>3</sub>): δ (ppm) = 132.7, 132.4, 130.3, 126.8, 126.6, 124.8, 91.3, 56.9, 26.4. IR ν (neat) = 1720, 1488, 1455, 1421, 1373, 1321, 1275, 1201, 1088, 1062, 1032, 1002, 950, 868, 779, 745 cm<sup>-1</sup>. HRMS (EI) m/z calc'd C<sub>18</sub>H<sub>18</sub>O<sub>3</sub>Na [M + Na]<sup>+</sup>: 305.1148, found: 305.1151. Anal Calc'd for C<sub>18</sub>H<sub>17</sub>O<sub>3</sub>: C, 76.57, H, 6.43, found: C, 76.34, H, 6.45.

**4-Methylisochroman-1-one<sup>69</sup> (56)**

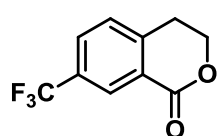
White solid (24% isol. yield, 525.2 mg, 3.24 mmol). <sup>1</sup>H NMR (400 MHz, CDCl<sub>3</sub>): δ (ppm) = 8.04 (d, J = 6.4 Hz, 1H), 7.52 (t, J = 7.6 Hz, 1H), 7.33 (t, J = 7.6 Hz, 1H), 7.23 (d, J = 7.6 Hz, 1H), 4.45 (dd, J = 10.8, 4.0 Hz, 1H), 4.18 (dd, J = 10.8, 6.8 Hz, 1H), 3.12-3.07 (m, 1H), 1.30 (d, J = 7.2 Hz, 3H). <sup>13</sup>C NMR (100 MHz, CDCl<sub>3</sub>): δ (ppm) = 165.5, 144.9, 134.3, 130.9, 127.9, 126.1, 124.8, 72.8, 32.1, 17.1. IR ν (neat) = 2969, 2933, 1720, 1604, 1461, 1396, 1282, 1236, 1124, 1083, 1020, 987, 757, 696. HRMS (EI) m/z calc'd C<sub>10</sub>H<sub>11</sub>O<sub>2</sub> [M + H]<sup>+</sup>: 163.0754, found: 163.0750. Anal Calc'd for C<sub>10</sub>H<sub>10</sub>O<sub>2</sub>: C, 74.06, H, 6.21; found: C, 73.76, H, 6.28.

**3-Methylisochroman-1-one<sup>69</sup> (58)**

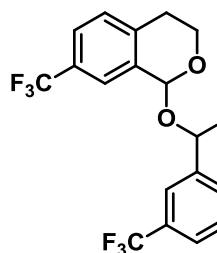
White solid (28% isol. yield, 612.6 mg, 3.78 mmol). <sup>1</sup>H NMR (400 MHz, CDCl<sub>3</sub>): δ (ppm) = 8.10 (d, J = 7.6 Hz, 1H), 7.53 (dt, J = 7.6, 1.6 Hz, 1H), 7.39 (t, J = 7.6 Hz, 1H), 7.26 (t, J = 6.8 Hz, 1H), 4.73-4.64 (m, 1H), 2.99-2.89 (m, 2H), 1.54 (d, J = 6.8 Hz, 3H). <sup>13</sup>C NMR (100 MHz, CDCl<sub>3</sub>): δ (ppm) = 166.0, 139.5, 134.0, 130.7, 128.0, 127.7, 125.4, 75.5, 35.3, 21.3. IR ν (neat) = 1704, 1609, 1455, 1392, 1355, 1282, 1239, 1121, 1088, 1029, 747 cm<sup>-1</sup>. HRMS (EI) m/z calc'd C<sub>10</sub>H<sub>11</sub>O<sub>2</sub> [M + H]<sup>+</sup>: 163.0754, found: 163.0752. Anal Calc'd for C<sub>10</sub>H<sub>10</sub>O<sub>2</sub>: C, 74.06, H, 6.21, found: C, 73.86, H, 6.15.

**1,1'-Oxybis(3-methylisochroman) (59)**

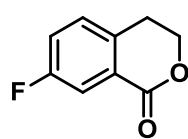
Colourless crystals (10% isol. yield, 418.5 mg, 1.35 mmol).  $^1\text{H NMR}$  (400 MHz,  $\text{CDCl}_3$ ):  $\delta$  (ppm) = 7.25-7.14 (m, 6H), 7.10-7.07 (m, 2H), 6.16 (s, 2H), 4.49-4.41 (m, 2H), 2.78-2.67 (m, 4H), 1.52 (d,  $J = 6.0$  Hz, 3H), 1.48 (d,  $J = 6.0$  Hz, 3H).  $^{13}\text{C NMR}$  (100 MHz,  $\text{CDCl}_3$ ):  $\delta$  (ppm) = 134.9, 134.1, 128.6, 128.3, 127.6, 126.7, 94.2, 64.1, 35.9, 21.7. **IR**  $\nu$  (neat) = 1389, 1363, 1319, 1253, 1202, 1080, 1040, 1007, 948, 934, 802, 751  $\text{cm}^{-1}$ . **HRMS** (EI)  $m/z$  calc'd  $\text{C}_{20}\text{H}_{22}\text{O}_3\text{Na}$  [ $\text{M} + \text{Na}$ ] $^+$ : 333.1461, found: 333.1463. **Anal Calc'd** for  $\text{C}_{20}\text{H}_{22}\text{O}_3$ : C, 77.39, H, 7.14; found: C, 77.37, H, 7.23.

**7-(Trifluoromethyl)isochroman-1-one (61)**

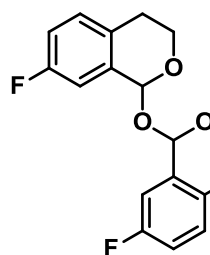
White solid (67% isol. yield, 1.433 g, 6.63 mmol).  $^1\text{H NMR}$  (400 MHz,  $\text{CDCl}_3$ ):  $\delta$  (ppm) = 8.67 (d,  $J = 2.4$  Hz, 1H), 8.11 (dd,  $J = 8.4, 2.4$  Hz, 1H), 7.41 (d,  $J = 8.0$  Hz, 1H), 4.58 (t,  $J = 6.0$  Hz, 2H), 3.14 (t,  $J = 6.0$  Hz, 2H).  $^{13}\text{C NMR}$  (100 MHz,  $\text{CDCl}_3$ ):  $\delta$  (ppm) = 164.1, 143.5, 130.4 (q,  $^3J_{\text{C-F}} = 3.4$  Hz), 128.5 (q,  $^2J_{\text{C-F}} = 32.5$  Hz), 127.9, 126.4, 122.4 (q,  $^1J_{\text{C-F}} = 270.3$  Hz), 67.4, 28.1 (t,  $J_{\text{C-F}} = 2.7$  Hz). **IR**  $\nu$  (neat) = 1724, 1627, 1475, 1432, 1390, 1332, 1274, 1224, 1170, 1024, 1066, 1033, 958, 919, 848, 836, 779, 719, 661. **HRMS** (EI)  $m/z$  calc'd  $\text{C}_{10}\text{H}_8\text{F}_3\text{O}_2$  [ $\text{M} + \text{H}$ ] $^+$ : 217.0471, found: 217.0467.

**1,1'-Oxybis(7-(Trifluoromethyl)isochroman) (62)**

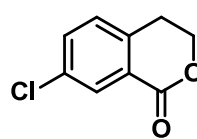
Colourless crystals (15% isol. yield, 620.4 mg, 1.483 mmol).  $^1\text{H NMR}$  (400 MHz,  $\text{CDCl}_3$ ):  $\delta$  (ppm) = 7.68 (s, 2H), 7.57 (d,  $J = 8.0$  Hz, 2H), 7.32 (d,  $J = 8.0$  Hz, 2H), 6.38 (s, 2H), 4.32 (dt,  $J = 11.8, 3.0$  Hz, 2H), 4.13 (dd,  $J = 11.3, 6.0$  Hz, 2H), 3.14 (dt,  $J = 11.7, 6.2$  Hz, 2H), 2.75 (d,  $J = 16.9$  Hz, 2H).  $^{13}\text{C NMR}$  (100 MHz,  $\text{CDCl}_3$ ):  $\delta$  (ppm) = 139.0, 131.2, 130.6, 129.5, 129.2, 126.1, 122.3, 100.8, 58.5, 28.1. **IR**  $\nu$  (neat) = 1627, 1428, 1336, 1311, 1270, 1187, 1162, 1116, 1083, 1002, 944, 912, 848, 819.

**7-Fluoroisochroman-1-one (64)**

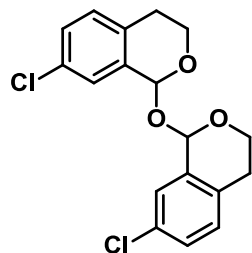
Colourless crystals (54% isol. yield, 1.178 g, 7.09 mmol).  $^1\text{H NMR}$  (400 MHz,  $\text{CDCl}_3$ ):  $\delta$  (ppm) = 7.77 (d,  $J = 8.0$  Hz, 1H), 7.29-7.22 (m, 2H), 4.54 (t,  $J = 6.0$  Hz, 2H), 3.04 (t,  $J = 6.0$  Hz, 2H).  $^{13}\text{C NMR}$  (100 MHz,  $\text{CDCl}_3$ ):  $\delta$  (ppm) = 163.5, 162.2 (d,  $^1J_{\text{C-F}} = 245.9$  Hz), 135.6 (d,  $^3J_{\text{C-F}} = 3.3$  Hz), 129.5 (d,  $^3J_{\text{C-F}} = 7.3$  Hz), 127.4 (d,  $^3J_{\text{C-F}} = 7.5$  Hz), 121.4 (d,  $^2J_{\text{C-F}} = 21.8$  Hz), 117.2 (d,  $^2J_{\text{C-F}} = 23.0$  Hz), 67.8, 27.5. **IR**  $\nu$  (neat) = 1725, 1620, 1594, 1496, 1437, 1390, 1306, 1273, 1240, 1197, 1128, 1083, 923, 887, 828, 781, 715  $\text{cm}^{-1}$ . **HRMS** (EI)  $m/z$  calc'd  $\text{C}_9\text{H}_8\text{FO}_2$  [ $\text{M} + \text{H}$ ] $^+$ : 167.0503, found: 167.0503.

**1,1'-Oxybis(7-fluoroisochroman) (65)**

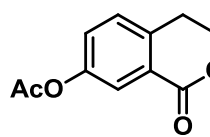
Colourless crystals (16% yield, 669.2 mg, 2.10 mmol).  $^1\text{H NMR}$  (400 MHz,  $\text{CDCl}_3$ ):  $\delta$  (ppm) = 7.11-7.01 (m, 2H), 6.96-6.90 (m, 8H), 6.06 (s, 2H), 4.26 (dt,  $J = 11.6, 3.2$  Hz, 2H), 4.12-4.07 (m, 2H), 3.09-3.00 (m, 2H), 2.66 (dd,  $J = 16.4, 2.8$  Hz, 2H).  $^{13}\text{C NMR}$  (100 MHz,  $\text{CDCl}_3$ ):  $\delta$  (ppm) = 161.5 (d,  $^1J_{\text{C-F}} = 243.0$  Hz), 135.6 (d,  $^3J_{\text{C-F}} = 6.9$  Hz), 130.5 (d,  $^3J_{\text{C-F}} = 7.7$  Hz), 130.2 (d,  $^3J_{\text{C-F}} = 3.1$  Hz), 115.9 (d,  $^2J_{\text{C-F}} = 21.5$  Hz), 114.3 (d,  $^2J_{\text{C-F}} = 21.5$  Hz), 92.8, 58.7, 27.6. **IR**  $\nu$  (neat) = 1752, 1719, 1497, 1426, 1370, 1193, 1092, 1013, 942, 908, 877, 731  $\text{cm}^{-1}$ . **HRMS** (FAB) calc'd  $\text{C}_{18}\text{H}_{16}\text{F}_2\text{O}_3$  [ $\text{M} + \text{H}$ ] $^+$ : 138.1062, found: 138.1058.

**7-Chloroisochroman-1-one<sup>70</sup> (67)**

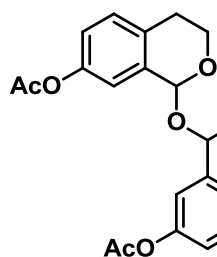
White solid (42% isol. yield, 931.0 mg, 5.10 mmol).  $^1\text{H NMR}$  (400 MHz,  $\text{CDCl}_3$ ):  $\delta$  (ppm) = 8.09 (s, 1H), 7.51 (dd,  $J = 8.4, 2.4$  Hz, 1H), 7.24 (d,  $J = 8.0$  Hz, 1H), 4.54 (t,  $J = 6.0$  Hz, 2H), 3.04 (t,  $J = 6.0$  Hz).  $^{13}\text{C NMR}$  (100 MHz,  $\text{CDCl}_3$ ):  $\delta$  (ppm) = 164.3, 138.1, 134.1, 130.6, 129.1, 127.1, 67.6, 27.7. **IR**  $\nu$  (neat) = 1714, 1598, 1485, 1422, 1298, 1268, 1235, 1194, 1137, 1085, 1033, 954, 831, 782, 700, 651  $\text{cm}^{-1}$ . **HRMS** (EI)  $m/z$  calc'd  $\text{C}_9\text{H}_8\text{ClO}_2$  [ $\text{M} + \text{H}$ ] $^+$ : 183.0207, found: 183.0206. **Anal Calc'd** for  $\text{C}_9\text{H}_7\text{ClO}_2$ : C, 59.20, H, 3.86; found: C, 59.31, H, 3.90.

**1,1'-Oxybis(7-chloroisochroman) (68)**

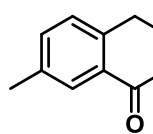
Colourless solid (12% isol. yield, 499.2 mg, 1.42 mmol).  $^1\text{H NMR}$  (400 MHz,  $\text{CDCl}_3$ ):  $\delta$  (ppm) = 7.43 (d,  $J = 2.0$  Hz, 2H), 7.29 (dd,  $J = 8.0, 2.1$  Hz, 2H), 7.12 (d,  $J = 8.2$  Hz, 2H), 6.30 (s, 2H), 4.27 (dt,  $J = 11.6, 8.7$  Hz, 2H), 4.09 (m, 2H), 3.05 (m, 2H), 2.64 (dd,  $J = 16.6, 2.5$  Hz, 2H).  $^{13}\text{C NMR}$  (100 MHz,  $\text{CDCl}_3$ ):  $\delta$  (ppm) = 135.6, 133.1, 132.3, 130.6, 130.3, 129.8, 92.4, 58.5, 27.7. **IR**  $\nu$  (neat) = 2929, 2850, 1602, 1482, 1421, 1378, 1336, 1307, 1261, 1191, 1091, 1012, 983, 948, 883, 844, 811, 682, 665. **Anal Calc'd** for  $\text{C}_{18}\text{H}_{16}\text{Cl}_2\text{O}_3$ : C, 61.55, H, 4.59; found: C, 61.20, H, 4.72.

**1-Oxoisochroman-7-yl acetate (70)**

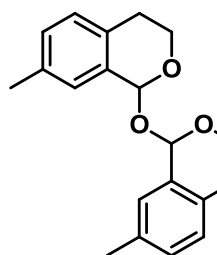
Colourless oil (40% isol. yield, 643.3 mg, 3.12 mmol).  $^1\text{H NMR}$  (400 MHz,  $\text{CDCl}_3$ ):  $\delta$  (ppm) = 7.81 (d,  $J = 1.2$  Hz, 1H), 7.29 (m, 2H), 4.55 (t,  $J = 5.6$  Hz, 2H), 3.06 (t,  $J = 5.6$  Hz, 2H), 2.17 (s, 3H).  $^{13}\text{C NMR}$  (100 MHz,  $\text{CDCl}_3$ ):  $\delta$  (ppm) = 169.7, 164.7, 150.3, 137.4, 128.8, 123.7, 67.7, 27.7, 21.3. **IR**  $\nu$  (neat) = 1755, 1719, 1611, 1496, 1429, 1375, 1300, 1200, 1122, 1093, 1011, 941, 896, 878, 830, 781, 733, 667, 630  $\text{cm}^{-1}$ . **HRMS** (EI)  $m/z$  calc'd  $\text{C}_{11}\text{H}_{11}\text{O}_4$  [ $\text{M} + \text{H}$ ] $^+$ : 207.0652, found: 207.0652. **Anal Calc'd** for  $\text{C}_{11}\text{H}_{10}\text{O}_4$ : C, 64.07, H, 4.89; found: C, 63.69, H, 5.00.

**1,1'-Oxybis(isochroman-7,1-diyl) acetate (71)**

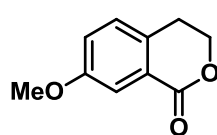
White solid (12% isol. yield, 372.9 mg, 0.956 mmol).  $^1\text{H NMR}$  (400 MHz,  $\text{CDCl}_3$ ):  $\delta$  (ppm) = 7.13 (d,  $J$  = 9.2 Hz, 2H), 6.97-6.95 (m, 4H), 6.07 (s, 2H), 4.30-4.09 (m, 2H), 4.08-4.04 (m, 2H), 3.03 (dd,  $J$  = 11.6, 5.2 Hz, 2H), 2.65 (dd,  $J$  = 16.4, 2.0 Hz, 2H), 2.63 (s, 6H).  $^{13}\text{C NMR}$  (100 MHz,  $\text{CDCl}_3$ ):  $\delta$  (ppm) = 169.9, 149.3, 133.6, 131.1, 130.0, 123.1, 121.9, 99.2, 58.8, 27.7. **IR**  $\nu$  (neat) = 1759, 1500, 1429, 1375, 1311, 1192, 1093, 1011, 941, 904, 856, 815, 729  $\text{cm}^{-1}$ . **HRMS** (EI)  $m/z$  calc'd  $\text{C}_{22}\text{H}_{22}\text{O}_7\text{NH}_4$  [ $\text{M} + \text{NH}_4$ ] $^+$ : 416.1704, found: 416.1703. **Anal Calc'd** for  $\text{C}_{22}\text{H}_{22}\text{O}_7$ : C, 66.32, H, 5.57; found: C, 66.14, H, 5.19.

**7-Methylisochroman-1-one<sup>68</sup> (73)**

Colourless oil (25% isol. yield, 546.9 mg, 3.37 mmol).  $^1\text{H NMR}$  (400 MHz,  $\text{CDCl}_3$ ):  $\delta$  (ppm) = 7.93 (d,  $J$  = 0.8 Hz, 1H), 7.37 (dd,  $J$  = 8.0, 1.6 Hz, 1H), 7.17 (d,  $J$  = 7.6 Hz, 1H), 4.54 (t,  $J$  = 6.0 Hz, 2H), 3.03 (t,  $J$  = 6.0 Hz, 2H), 2.40 (s, 3H).  $^{13}\text{C NMR}$  (100 MHz,  $\text{CDCl}_3$ ):  $\delta$  (ppm) = 165.8, 137.9, 136.9, 134.9, 131.0, 127.5, 125.4, 67.8, 27.8, 21.4. **IR**  $\nu$  (neat) = 1716, 1619, 1504, 1421, 1384, 1301, 1283, 1241, 1175, 1137, 1096, 1058, 1036, 958, 827, 782, 640  $\text{cm}^{-1}$ . **HRMS** (EI)  $m/z$  calc'd  $\text{C}_{10}\text{H}_{11}\text{O}_2$  [ $\text{M} + \text{H}$ ] $^+$ : 163.0754, found: 163.0753. **Anal Calc'd** for  $\text{C}_{10}\text{H}_{10}\text{O}_2$ : C, 74.06, H, 6.21, found: C, 74.51, H, 6.35.

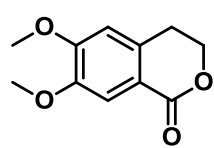
**1,1'-Oxybis(7-methylisochroman) (74)**

Colourless crystals (10% isol. yield, 418.2 mg, 1.35 mmol).  $^1\text{H NMR}$  (400 MHz,  $\text{CDCl}_3$ ):  $\delta$  (ppm) = 7.03-6.98 (6H), 6.07 (2H), 4.36-4.09 (m, 2H), 4.09-4.05 (m, 2H), 3.10-3.02 (m, 2H), 2.61 (dd,  $J$  = 16.4, 2.4 Hz, 2H), 2.29 (s, 6H).  $^{13}\text{C NMR}$  (100 MHz,  $\text{CDCl}_3$ ):  $\delta$  (ppm) = 136.2, 134.0, 131.5, 129.3, 128.6, 128.3, 92.9, 58.7, 28.0, 21.5. **IR**  $\nu$  (neat) = 2927, 1500, 1421, 1378, 1311, 1270, 1232, 1157, 1132, 1091, 1012, 952, 883, 819, 624. **HRMS** (EI)  $m/z$  calc'd  $\text{C}_{20}\text{H}_{22}\text{O}_3\text{Na}$  [ $\text{M} + \text{Na}$ ] $^+$ : 333.1461, found, 333.1462. **Anal Calc'd** for  $\text{C}_{20}\text{H}_{22}\text{O}_3$ : C, 77.39, H, 7.14; found: C, 77.28, H, 7.22.

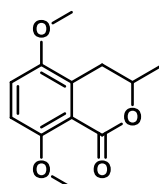
**7-Methoxyisochroman-1-one<sup>71</sup> (76)**

Colourless liquid (18% isol. yield, 390.3 mg, 2.19 mmol).  $^1\text{H NMR}$  (400 MHz,  $\text{CDCl}_3$ ):  $\delta$  (ppm) = 7.59 (d,  $J$  = 2.8 Hz, 1H), 7.17 (d,  $J$  = 8.4 Hz, 1H), 7.10 (dd,  $J$  = 8.0, 2.8 Hz, 1H), 4.52 (t,  $J$  = 5.6 Hz, 2H), 2.99 (t,  $J$  = 5.6 Hz, 2H).  $^{13}\text{C NMR}$  (100 MHz,  $\text{CDCl}_3$ ):  $\delta$  (ppm) = 165.6, 159.4, 132.2, 128.8, 126.5, 122.0, 113.3, 68.0, 56.0, 27.4. **IR**  $\nu$  (neat) = 2950, 2905, 2836, 1710, 1605, 1511, 1451, 1421, 1387, 1276, 1228, 1203, 1161, 1087, 1062, 968. **HRMS** (EI)  $m/z$  calc'd  $\text{C}_{10}\text{H}_{10}\text{O}_3$  [ $\text{M} + \text{H}$ ] $^+$ : 179.0703, found: 179.0709. **Anal Calc'd** for  $\text{C}_{10}\text{H}_9\text{O}_3$ : C, 67.41, H, 5.66; found: C, 67.53, H, 5.74.

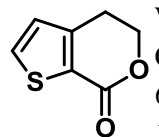


**6,7-Dimethoxyisochroman-1-one<sup>72</sup> (78)**

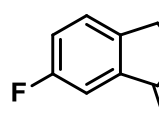
White solid (8% isol. yield, 128.2 mg, 0.616 mmol). <sup>1</sup>H NMR (400 MHz, CDCl<sub>3</sub>): δ (ppm) = 7.54 (s, 1H), 6.69 (s, 1H), 4.51 (t, J = 6.0 Hz, 2H), 3.94 (s, 3H), 3.87 (s, 3H), 2.99 (t, J = 6.0 Hz, 2H). <sup>13</sup>C NMR (100 MHz, CDCl<sub>3</sub>): δ (ppm) = 165.6, 154.0, 148.8, 134.3, 117.8, 112.2, 109.5, 67.7, 56.5, 27.9. IR ν (neat) = 2952, 2911, 2836, 1706, 1602, 1511, 1461, 1421, 1394, 1336, 1270, 1240, 1203, 1157, 1087, 1058, 1027, 962. HRMS (EI) m/z calc'd C<sub>11</sub>H<sub>13</sub>O<sub>4</sub> [M + H]<sup>+</sup>: 209.0808, found: 209.0811. Anal Calc'd for C<sub>11</sub>H<sub>12</sub>O<sub>4</sub>: C, 63.45, H, 5.81, found: C, 63.67, H, 5.98.

**5,8-Dimethoxy-3-methylisochroman-1-one<sup>73</sup> (80)**

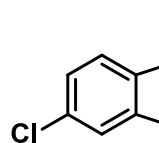
White crystalline solid (5% isol. yield, 79.7 mg, 0.358 mmol). <sup>1</sup>H NMR (400 MHz, CDCl<sub>3</sub>): δ (ppm) = 6.70 (d, J = 8.8 Hz, 1H), 6.59 (d, J = 8.0 Hz, 1H), 4.38 (m, 1H), 3.77 (s, 3H), 3.71 (s, 3H), 2.80 (dd, J = 13.6, 3.6 Hz, 1H), 2.34 (ddd, J = 15.2, 11.6, 0.7 Hz, 1H), 1.42 (d, J = 6.4 Hz, 3H). <sup>13</sup>C NMR (100 MHz, CDCl<sub>3</sub>): δ (ppm) = 169.0, 149.9, 148.7, 131.1, 116.0, 113.2, 112.5, 77.0, 55.8, 56.1, 33.9, 21.1. IR ν (neat) = 1721, 1604, 1485, 1452, 1437, 1311, 1263, 1200, 1122, 1067, 970, 948, 819, 800, 711 cm<sup>-1</sup>. HRMS (EI) m/z calc'd C<sub>12</sub>H<sub>15</sub>O<sub>4</sub> [M + H]<sup>+</sup>: 223.0965, found: 223.0965. Anal Calc'd for C<sub>12</sub>H<sub>14</sub>O<sub>4</sub>: C, 64.85, H, 6.35; found: C, 64.36, H, 6.84.

**4H-Thieno[2,3-c]pyran-7(5H)-one<sup>74</sup> (82)**

White solid (18% isol. yield, 395.4 mg, 2.56 mmol). <sup>1</sup>H NMR (400 MHz, CDCl<sub>3</sub>): δ (ppm) = 7.59 (d, J = 4.8 Hz, 1H), 6.94 (d, J = 4.8 Hz, 1H), 4.52 (t, J = 6.0 Hz, 2H), 2.96 (t, J = 6.0 Hz, 2H). <sup>13</sup>C NMR (100 MHz, CDCl<sub>3</sub>): δ (ppm) = 161.6, 147.8, 134.8, 127.1, 126.9, 68.7, 25.5. IR ν (neat) = 1755, 1492, 1426, 1200, 1163, 1122, 1085 cm<sup>-1</sup>. HRMS (EI) m/z calc'd C<sub>7</sub>H<sub>7</sub>O<sub>2</sub>S [M + H]<sup>+</sup>: 155.0161, found: 155.0159. Anal Calc'd for C<sub>7</sub>H<sub>6</sub>O<sub>2</sub>S: C, 54.53, H, 3.92; found: C, 54.98, H, 41.7.

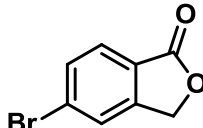
**6-Fluoroisobenzofuran-1(3H)-one<sup>75</sup> (85)**

White solid (60% isol. yield, 1.318 g, 8.66 mmol). <sup>1</sup>H NMR (400 MHz, CDCl<sub>3</sub>): δ (ppm) = 7.75 (d, J = 7.5 Hz, 1H), 7.74-7.52 (m, 1H), 7.38 (t, J = 8.6 Hz, 1H), 5.38 (s, 2H). <sup>13</sup>C NMR (100 MHz, CDCl<sub>3</sub>): δ (ppm) = 170.1, 158.5 (d, <sup>1</sup>J<sub>C-F</sub> = 253.6 Hz), 133.1 (d, <sup>2</sup>J<sub>C-F</sub> = 19.1 Hz), 131.8 (d, <sup>3</sup>J<sub>C-F</sub> = 7.8 Hz), 129.2, 122.1 (d, <sup>3</sup>J<sub>C-F</sub> = 4.1 Hz), 121.0 (d, <sup>2</sup>J<sub>C-F</sub> = 20.3 Hz), 67.2. IR ν (neat) = 1756, 1633, 1602, 1479, 1365, 1307, 1241, 1070, 1049, 1016, 937, 869, 779, 754, 646. HRMS (EI) m/z calc'd for C<sub>8</sub>H<sub>6</sub>O<sub>2</sub>F [M + H]<sup>+</sup>: 153.0346, found: 153.0346.

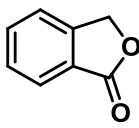
**5-Chloroisobenzofuran-1(3H)-one<sup>68</sup> (87)**

White solid (51% isol. yield, 1.109 g, 6.57 mmol). <sup>1</sup>H NMR (400 MHz, CDCl<sub>3</sub>): δ (ppm) = 7.86 (d, J = 8.0 Hz, 1H), 7.53-7.50 (m, 2H), 5.30 (s, 2H). <sup>13</sup>C NMR (100 MHz, CDCl<sub>3</sub>): δ (ppm) = 170.3, 148.5, 141.2, 130.3, 127.4, 124.7, 122.9, 69.3. IR ν (neat) = 1749, 1612, 1583, 1454, 1428, 1349, 1311, 1265, 1211, 1116, 1049, 995, 887, 833, 757. HRMS (EI) m/z calc'd for C<sub>8</sub>H<sub>6</sub>O<sub>2</sub>Cl [M + H]<sup>+</sup>: 169.0046, found: 169.0051. Anal Calc'd for C<sub>8</sub>H<sub>5</sub>BrO<sub>2</sub>: C, 57.00, H, 2.99; found: C, 57.13, H, 3.02.

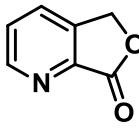
**5-Bromoisobenzofuran-1(3H)-one<sup>68</sup> (89)**

 White solid (40% isol. yield, 856.0 mg, 4.02 mmol). <sup>1</sup>H NMR (400 MHz, CDCl<sub>3</sub>): δ (ppm) = 7.79 (dd, J = 6.7, 1.5 Hz, 1H), 7.69-7.67 (m, 2H), 5.30 (s, 2H). <sup>13</sup>C NMR (100 MHz, CDCl<sub>3</sub>): δ (ppm) = 170.4, 148.6, 133.1, 129.7, 127.5, 126.0, 125.1, 69.3. IR v (neat) = 1745, 1604, 1579, 1454, 1419, 1353, 1307, 1261, 1213, 1116, 1052, 995, 875, 840, 769. HRMS (EI) m/z calc'd for C<sub>8</sub>H<sub>6</sub>O<sub>2</sub>Br [M+ H]<sup>+</sup>: 212.9546, found: 212.9545. Anal Calc'd for C<sub>8</sub>H<sub>5</sub>BrO<sub>2</sub>: C, 45.10, H, 2.37; found: C, 44.88, H, 2.69.

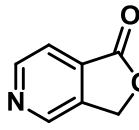
**Phthalide<sup>68</sup> (91)**

 Colourless crystals (17% isol. yield, 379.1 mg, 2.83 mmol). <sup>1</sup>H NMR (400 MHz, CDCl<sub>3</sub>): δ (ppm) = 7.86 (d, J = 7.6 Hz, 1H), 7.62 (t, J = 7.6 Hz, 1H), 7.49-7.42 (m, 2H), 5.26 (s, 2H). <sup>13</sup>C NMR (100 MHz, CDCl<sub>3</sub>): δ (ppm) = 171.5, 146.9, 134.4, 129.4, 126.2, 126.1, 122.5, 70.0. IR v (neat) = 1744, 1050, 998, 736 cm<sup>-1</sup>. HRMS (EI) m/z calc'd C<sub>8</sub>H<sub>7</sub>O<sub>2</sub> [M + H]<sup>+</sup>: 135.0441, found: 135.0441. Anal Calc'd for C<sub>8</sub>H<sub>6</sub>O<sub>2</sub>: C, 71.64, H, 4.51; found: C, 71.54, H, 4.45.

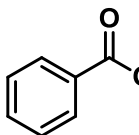
**Furo[3,4-b]pyridine-7(5H)-one<sup>76</sup> (93)**

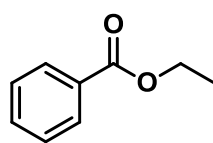
 Colourless crystals (52% isol. yield, 1.158 g, 8.57 mmol). <sup>1</sup>H NMR (400 MHz, CDCl<sub>3</sub>): δ (ppm) = 8.97 (s, 1H), 8.88 (d, J = 5.0 Hz, 1H), 7.82 (dd, J = 5.0, 0.5 Hz, 1H), 5.40 (s, 2H). <sup>13</sup>C NMR (100 MHz, CDCl<sub>3</sub>): δ (ppm) = 169.3, 150.0, 145.1, 140.3, 133.4, 118.9, 68.7. IR v (neat) = 1758, 1587, 1454, 1421, 1357, 1299, 1267, 1240, 1182, 1106, 1056, 1037, 1002, 825, 750, 700. HRMS (EI) m/z calc'd for C<sub>7</sub>H<sub>6</sub>NO<sub>2</sub> [M+H]<sup>+</sup>: 136.0393, found: 136.0390. Anal Calc'd for C<sub>7</sub>H<sub>5</sub>NO<sub>2</sub>: C, 62.22, H, 3.73, N, 10.37; found: C, 62.54, H, 3.80, N, 10.41.

**Furo[3,4-c]pyridine-1(3H)-one<sup>77</sup> (95)**

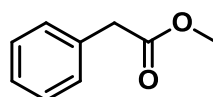
 Pale yellow crystals (19% isol. yield, 423.6 mg, 3.13 mmol). <sup>1</sup>H NMR (400 MHz, CDCl<sub>3</sub>): δ (ppm) = 8.89 (dd, J = 4.8, 1.6 Hz, 1H), 8.23 (dd, J = 7.6, 1.2 Hz, 1H), 7.52-7.49 (m, 1H), 5.36 (s, 3H). <sup>13</sup>C NMR (100 MHz, CDCl<sub>3</sub>): δ (ppm) = 166.9, 155.8, 134.5, 124.4, 120.1, 70.99. IR v (neat) = 1749, 1612, 1587, 1448, 1421, 1346, 1307, 1224, 1187, 1058, 1020, 991, 854, 773, 694. HRMS (EI) m/z calc'd for C<sub>7</sub>H<sub>6</sub>NO<sub>2</sub> [M+H]<sup>+</sup>: 136.0393, found, 136.0392. Anal Calc'd for C<sub>7</sub>H<sub>5</sub>NO<sub>2</sub>: C, 62.22, H, 3.73, N, 10.37; found: C, 62.38, H, 3.79, N, 10.40.

**Methyl benzoate<sup>78</sup> (97)**

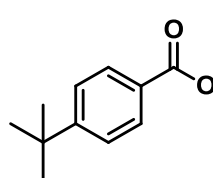
 Colourless liquid (4% isol. yield, 89.3 mg, 0.65 mmol). <sup>1</sup>H NMR (400 MHz, CDCl<sub>3</sub>): δ (ppm) = 8.08-8.05 (m, 2H), 7.60-7.56 (m, 1H), 7.48-7.44 (m, 2H), 3.94 (s, 3H). <sup>13</sup>C NMR (100 MHz, CDCl<sub>3</sub>): δ (ppm) = 167.5, 133.3, 130.5, 129.9, 128.7, 52.5. IR v (neat) = 1720, 1600, 1451, 1436, 1317, 1271, 1189, 1175, 1111, 1066, 1022, 965, 823, 703 cm<sup>-1</sup>. HRMS (EI) m/z calc'd C<sub>8</sub>H<sub>8</sub>O<sub>2</sub> [M + H]<sup>+</sup>: 137.0597, found: 137.0597. Anal Calc'd for C<sub>8</sub>H<sub>8</sub>O<sub>2</sub>: C, 70.57, H, 5.92; found: C, 70.68, H, 5.96.

**Ethyl benzoate**<sup>78</sup> (99)

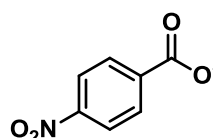
Yellow liquid (2% isol. yield, 44.3 mg, 0.29 mmol). <sup>1</sup>H NMR (400 MHz, CDCl<sub>3</sub>): δ (ppm) = 8.06-8.04 (m, 2H), 7.57-7.52 (m, 1H), 7.45-7.41 (m, 2H), 4.38 (t, J = 7.2 Hz, 2H), 1.39 (t, J = 7.2 Hz, 3H). <sup>13</sup>C NMR (100 MHz, CDCl<sub>3</sub>): δ (ppm) = 167.0, 133.2, 130.9, 129.9, 129.8, 128.7, 61.3, 14.7. IR ν (neat) = 1716, 1608, 1582, 1451, 1369, 1313, 1271, 1182, 1111, 1070, 1028, 703 cm<sup>-1</sup>. HRMS (EI) m/z calc'd C<sub>8</sub>H<sub>9</sub>O<sub>2</sub> [M + H]<sup>+</sup>: 151.0754, found: 151.0761. Anal Calc'd for C<sub>9</sub>H<sub>10</sub>O<sub>2</sub>: C, 71.98, H, 6.71; found: C, 72.32, H, 6.84.

**Methyl 2-phenylacetate**<sup>78</sup> (101)

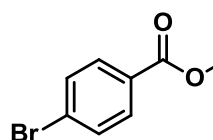
Colourless oil (2% isol. yield, 44.1 mg, 0.29 mmol). <sup>1</sup>H NMR (400 MHz, CDCl<sub>3</sub>): δ (ppm) = 7.35-7.25 (m, 5H), 3.69 (s, 3H), 3.63 (s, 2H). <sup>13</sup>C NMR (100 MHz, CDCl<sub>3</sub>): δ (ppm) = 172.4, 134.4, 129.6, 129.0, 127.5, 52.4, 41.6. IR ν (neat) = 1731, 1500, 1455, 1436, 1347, 1305, 1253, 1223, 1156, 1145, 1010, 726, 693 cm<sup>-1</sup>. HRMS (EI) m/z calc'd C<sub>9</sub>H<sub>11</sub>O<sub>2</sub> [M + H]<sup>+</sup>: 151.0754, found: 151.0750. Anal Calc'd for C<sub>9</sub>H<sub>10</sub>O<sub>2</sub>: C, 71.98, H, 6.71; found: C, 71.80, H, 6.70.

**Methyl 4-(tert-butyl)benzoate**<sup>78</sup> (103)

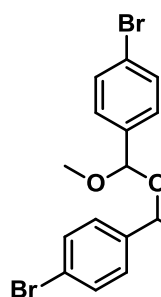
Colourless oil (2% isol. yield, 43.3 mg, 0.22 mmol). <sup>1</sup>H NMR (400 MHz, CDCl<sub>3</sub>): δ (ppm) = 7.96 (dd, J = 6.4, 2.0 Hz, 2H), 7.45 (dd, J = 6.4, 2.0 Hz, 2H), 3.9 (s, 3H), 1.34 (s, 9H). <sup>13</sup>C NMR (100 MHz, CDCl<sub>3</sub>): δ (ppm) = 167.5, 156.9, 129.8, 127.7, 125.7, 52.3, 35.5, 31.5. IR ν (neat) = 1724, 1612, 1436, 1410, 1365, 1279, 1186, 1118, 1022, 969, 857, 779, 711 cm<sup>-1</sup>. HRMS (EI) m/z calc'd for C<sub>12</sub>H<sub>17</sub>O<sub>2</sub> [M+H]<sup>+</sup>: 193.1223, found: 193.1220. Anal Calc'd for C<sub>12</sub>H<sub>16</sub>O<sub>2</sub>: C, 74.97, H, 8.39; found: C, 75.33, H, 8.46.

**Methyl 4-nitrobenzoate**<sup>78</sup> (105)

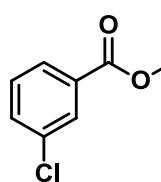
Pale yellow solid (8% isol. yield, 173.8 mg, 0.96 mmol). <sup>1</sup>H NMR (400 MHz, CDCl<sub>3</sub>): δ (ppm) = 8.31-8.28 (m, 2H), 8.26-8.20 (m, 2H), 3.98 (s, 3H). <sup>13</sup>C NMR (100 MHz, CDCl<sub>3</sub>): δ (ppm) = 165.6, 150.9, 135.8, 131.1, 123.9, 53.2. IR ν (neat) = 1715, 1613, 1597, 1521, 1444, 1345, 1267, 1242, 1103, 1011, 960, 879, 853, 820, 783, 722 cm<sup>-1</sup>. HRMS (EI) m/z calc'd C<sub>8</sub>H<sub>8</sub>NO<sub>4</sub> [M + H]<sup>+</sup>: 182.0448, found: 182.0446. Anal Calc'd for C<sub>8</sub>H<sub>7</sub>NO<sub>4</sub>: C, 53.04, H, 3.89, N, 7.73; found: C, 52.83, H, 3.78, N, 7.65.

**Methyl 4-bromobenzoate**<sup>78</sup> (107)

Colourless solid (15% isol. yield, 240.8 mg, 1.12 mmol). <sup>1</sup>H NMR (400 MHz, CDCl<sub>3</sub>): δ (ppm) = 7.89 (dt, J = 9.2, 4.4, 2.4 Hz, 2H), 7.58 (dt, J = 9.0, 4.4, 2.4 Hz, 2H), 3.91 (s, 3H). <sup>13</sup>C NMR (100 MHz, CDCl<sub>3</sub>): δ (ppm) = 166.7, 132.1, 131.5, 129.4, 128.4, 52.6. IR ν (neat) = 1708, 1583, 1436, 1396, 1270, 1195, 1170, 1106, 1066, 1008, 954, 848, 825, 750, 686. HRMS (EI) m/z calc'd C<sub>8</sub>H<sub>8</sub>BrO<sub>2</sub> [M+H]<sup>+</sup>: 214.9700, found: 214.9702. Anal Calc'd for C<sub>8</sub>H<sub>7</sub>BrO<sub>2</sub>: C, 44.68, H, 3.28; found: C, 44.79, H, 3.24.

**4,4'-(Oxybis(methoxymethylene))bis(bromobenzene) (108)**

White solid (1.5% isol. yield, 46.6 mg, 0.11 mmol).  $^1\text{H NMR}$  (400 MHz,  $\text{CDCl}_3$ ):  $\delta$  (ppm) = 7.47 (dd,  $J = 7.4, 2.4$  Hz, 2H), 7.27-7.24 (m, 2H), 5.71 (s, 2H), 3.54 (s, 3H).  $^{13}\text{C NMR}$  (100 MHz,  $\text{CDCl}_3$ ):  $\delta$  (ppm) = 135.2, 131.8, 129.0, 123.6, 107.1, 56.8. **IR**  $\nu$  (neat) = 1590, 1482, 1444, 1396, 1346, 1315, 1191, 1099, 1062, 977, 890, 800. **Anal Calc'd** for  $\text{C}_{16}\text{H}_{16}\text{Br}_2\text{O}_3$ : C, 46.18, H, 3.88; found: C, 46.48, H, 3.71.

**Methyl 3-chlorobenzoate<sup>78</sup> (110)**

Colourless oil (14% isol. yield, 305.4 mg, 1.79 mmol).  $^1\text{H NMR}$  (400 MHz,  $\text{CDCl}_3$ ):  $\delta$  (ppm) = 8.02 (d,  $J = 2.0$  Hz, 1H), 7.93 (dt,  $J = 8.0, 0.8$  Hz, 1H), 7.54-7.51 (m, 1H), 7.38 (t,  $J = 8.0$  Hz, 1H), 3.93 (s, 3H).  $^{13}\text{C NMR}$  (100 MHz,  $\text{CDCl}_3$ ):  $\delta$  (ppm) = 166.3, 134.9, 133.3, 132.2, 130.1, 128.1, 52.8. **IR**  $\nu$  (neat) = 1724, 1573, 1436, 1286, 1253, 1195, 1124, 1078, 977, 902, 840, 808, 740, 674. **HRMS** (EI)  $m/z$  calc'd for  $\text{C}_8\text{H}_7\text{ClO}_2$   $[\text{M}+\text{H}]^+$ : 171.0208, found: 171.0211. **Anal Calc'd** for  $\text{C}_8\text{H}_7\text{ClO}_2$ : C, 56.32, H, 4.14; found: C, 56.79, H, 4.11.

Compounds **43**, **53**, **91**, **97**, **99**, **101**, **103**, **105**, **107** and **110** are commercially available and the analytical data obtained is in agreement with the data reported by the manufacturers.

**3.5.5. Inhibition experiments: general procedures****3.5.5.1. Inhibition by isochromanone**

In a Radley's tube equipped with a magnetic stir bar, isochromanone (706.8 mg, 4.77 mmol),  $[\text{Fe}(\text{OTf})_2\text{L1}(\text{THF})]$  ( $5.67 \times 10^{-3}$  mmol, 8.0 mg) and isochroman (1.4 mL) were added. The reaction tube was degassed (3 times), charged with dioxygen gas (1 atm) and kept under oxygen atmosphere (1 atm) by using a balloon. The reaction mixture was heated to 60 °C and stirred overnight. The reaction was purified by silica gel column chromatography (Hexane/EtOAc, gradient: 10/1 to 4/1) to afford the unreacted starting material, isochromanone (30 + 6% isol. yield, 847.9 mg) and 1,1'-oxydiisochroman (2% isol. yield, 90.3 mg).

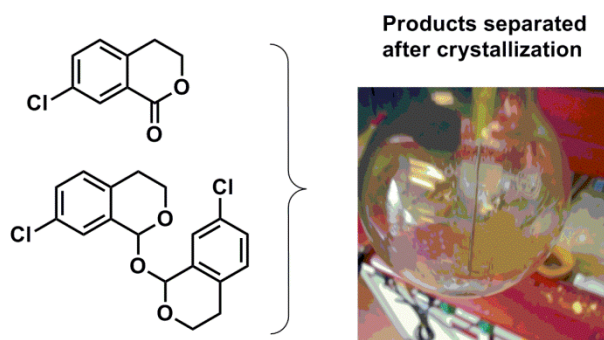
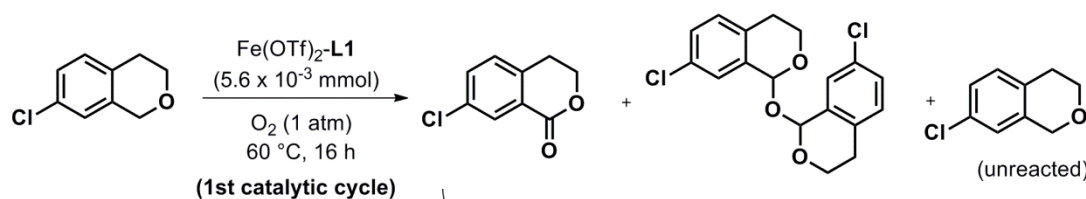
**3.5.5.2. Inhibition by 1,1-oxydiisochroman**

In a Radley's tube equipped with a magnetic stir bar, 1,1-oxydiisochroman (448.7 mg, 1.59 mmol),  $[\text{Fe}(\text{OTf})_2\text{L1}(\text{THF})]$  ( $5.67 \times 10^{-3}$  mmol, 8.0 mg) and isochroman (1.8 mL) were added. The reaction tube was degassed (3 times), charged with dioxygen gas (1 atm) and

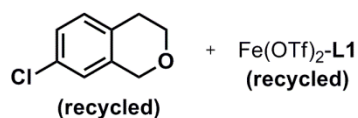
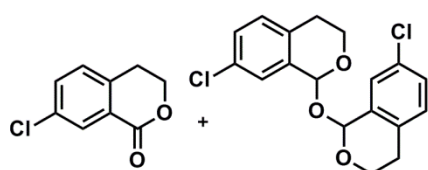
kept under oxygen atmosphere (1 atm) by using a balloon. The reaction mixture was heated to 60 °C and stirred overnight. The reaction was purified by silica gel column chromatography (Hexane/EtOAc, gradient: 10/1 to 4/1) to afford the unreacted starting material, isochromanone (16 % isol. yield, 377.3 mg) and 1,1'-oxydiisochroman (10 + 3% isol. yield, 584.6 mg).

### 3.5.6. Catalyst recycling experiments

In a Radley's tube equipped with a magnetic stir bar ligand **L1** ( $5.67 \times 10^{-3}$  mmol, 5.2 mg) and  $\text{Fe}(\text{OTf})_2$  ( $5.65 \times 10^{-3}$  mmol, 2.0 mg) were added. 4-Chloroisochroman (2.0 mL) was added by syringe; the reaction tube was degassed (3 times), charged with dioxygen gas (1 atm) and kept under oxygen atmosphere (1 atm) by using a balloon. The reaction mixture was heated to 60 °C and stirred overnight. Next morning, the reaction was stopped and cooled down to r.t. and the reaction products were allowed to crystallize **inside** the tube (no solvents were added). The supernadant liquid was extracted by syringe, transferred to a clean Radley's tube and allowed to react overnight at 60 °C under  $\text{O}_2$  (1 atm). All organics were combined together and purified by silica gel column chromatography (Hexane/EtOAc, gradient: 10/1 to 4/1) to afford a small amount of the unreacted starting material, 4-chloroisochromanone (59% isol. yield, 1312.2 mg) and 1,1'-oxybis(7-chloroisochroman) (16% isol. yield, 665.0 mg). The same procedure was repeated using 4-fluoroisochroman affording 4-fluoroisochromanone (65% isol. yield) and 1,1'-oxybis(7-fluoroisochroman) (21% isol. yield).



$\text{O}_2 (1 \text{ atm})$   
 $60 \text{ }^\circ\text{C}, 16 \text{ h}$   
**(2nd catalytic cycle)**



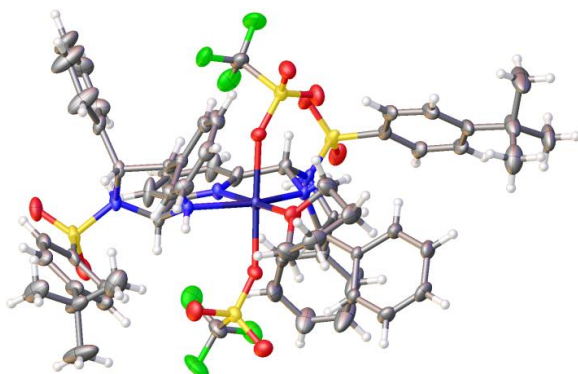
### 3.5.7. Crystallisation of $\text{Fe(OTf)}_2$ L1 (THF)

In a Schlenk tube equipped with a magnetic stirring bar,  $\text{Fe(OTf)}_2$  (70.0 mg, 0.2 mmol) and **L1** (182.0 mg, 0.2 mmol) were added. The tube was degassed (3 times) and placed under  $\text{N}_2$  atmosphere. Freshly distilled THF (2.0 mL) was added by syringe and the mixture was stirred at  $35 \text{ }^\circ\text{C}$  overnight. Next morning, the maroon coloured solution was filtered over Celite under  $\text{N}_2$  atmosphere and concentrated to a final volume of 1.0 mL approximately.

Freshly distilled Et<sub>2</sub>O (1.0 mL) was slowly added by syringe and the biphasic system was left at ambient temperature under a N<sub>2</sub> atmosphere until well shaped white crystals formed.

### 3.5.8. Crystallographic data of Fe(OTf)<sub>2</sub>L1(THF) (CCDC 945601)

The structure determination was performed by the Chemistry Department X-ray Crystallographic Service. Single crystals of each reported compound were mounted on a MiTeGen MicroMount using Fomblin oil. The data were measured at 100 K on a Bruker D8 diffractometer using Mo wavelengths and observed with an Apex II CCD detector. Data collection and processing were completed inside the APEX2 software suite.<sup>79</sup> Data integration and global cell refinement were performed with the program SAINT<sup>80</sup> and data were corrected using SADABS.<sup>81</sup> Structural solutions and least-squares refinements were conducted using the OLEX2 interface<sup>82</sup> to the SHELX suit of packages.<sup>83</sup>



**Crystal Data** for C<sub>61</sub>H<sub>67</sub>F<sub>6</sub>FeN<sub>5</sub>O<sub>11</sub>S<sub>4</sub> (*M* = 1344.29): tetragonal, space group P4<sub>1</sub>2<sub>1</sub>2 (no. 92), *a* = 10.9840(8) Å, *c* = 52.464(4) Å, *V* = 6329.7(8) Å<sup>3</sup>, *Z* = 4, *T* = 100.0 K, μ(MoKα) = 0.450 mm<sup>-1</sup>, *D*<sub>calc</sub> = 1.411 g/mm<sup>3</sup>, 79786 reflections measured (3.78 ≤ 2θ ≤ 52.82), 6501 unique (*R*<sub>int</sub> = 0.0422) which were used in all calculations. The final *R*<sub>1</sub> was 0.0395 (>2σ(I)) and *wR*<sub>2</sub> was 0.0985 (all data).

**Table 1 Crystal data and structure refinement for CCDC 945601**

Identification code	CCDC 945601
Empirical formula	C <sub>61</sub> H <sub>67</sub> F <sub>6</sub> FeN <sub>5</sub> O <sub>11</sub> S <sub>4</sub>
Formula weight	1344.29

Temperature/K	100.0
Crystal system	tetragonal
Space group	P4 <sub>1</sub> 2 <sub>1</sub> 2
a/Å	10.9840(8)
b/Å	10.9840(8)
c/Å	52.464(4)
α/°	90.00
β/°	90.00
γ/°	90.00
Volume/Å <sup>3</sup>	6329.7(8)
Z	4
ρ <sub>calc</sub> /mg/mm <sup>3</sup>	1.411
m/mm <sup>-1</sup>	0.450
F(000)	2800.0
Crystal size/mm <sup>3</sup>	0.32 × 0.26 × 0.16
2θ range for data collection	3.78 to 52.82°
Index ranges	-13 ≤ h ≤ 13, -13 ≤ k ≤ 13, -65 ≤ l ≤ 65
Reflections collected	79786
Independent reflections	6501[R(int) = 0.0422]
Data/restraints/parameters	6501/48/402
Goodness-of-fit on F <sup>2</sup>	1.186
Final R indexes [I ≥ 2σ (I)]	R <sub>1</sub> = 0.0395, wR <sub>2</sub> = 0.0976
Final R indexes [all data]	R <sub>1</sub> = 0.0411, wR <sub>2</sub> = 0.0985
Largest diff. peak/hole / e Å <sup>-3</sup>	0.35/-0.49
Flack parameter	0.013(19)

### 3.6. References:

- [1] Gmelin L., *Handbuch der Chemie, vol. 4: Handbuch der organischen Chemie (vol. 1)* (Heidelberg, Baden (Germany): Karl Winter, **1848**, pg 182).
- [2] Alberts, B.; Bray, D.; Hopkins, K.; Johnson, A. D.; Johnson, A.; Lewis, J.; Raff, M.; Roberts, K.; Walter, P. *Essential cell Biology* (Garland science, 2009, 3<sup>rd</sup> Ed)
- [3] Nelson, D. L.; Cox, M. M. *Lehninger Principles of Biochemistry* (Freeman W. H. And Co, 4<sup>th</sup> Ed., 2004, Chapters 10 and 11).



- [4] Methyl benzoate: (a) Choudhary, M.I.; Naheed, N.; Abbaskhan, A.; Musharraf, S.G.; Siddiqui, H.; Atta-Ur-Ramman, *Phytochemistry* **2008**, *69*, 1018. (b) Schiestl, F.P.; Roubik, D.W. *J. Chem. Ecol.* **2003**, *29*, 253.
- [5] Methyl antranilate: (a) *An Introduction to Perfumery* by Curtis and Williams, 2<sup>nd</sup> Ed., 2009. (b) Fraternali, D.; Ricci, D.; Flamini, G.; Giomaro, G. *Rec. Nat. Prod.* **2011**, *5*, 202.
- [6] Methyl salicylate: (a) James, D. G.; Price, T. S. *J. Chem. Ecol.* **2004**, *30*, 1613. (g) Shulaev, V.; Silverman, P.; Raskin, I. *Nature* **1997**, *385*, 718. (b) Mason, L.; Moore, R. A.; Edwards, J. E.; Mc Quay, H. J.; Derry, S.; Wiffen, P. J. *BMJ* **2004**, *328*, 995.
- [7] (a) Nomura, N.; Ishii, R.; Akakura, M.; Aoi, K. *J. Am. Chem. Soc.* **2002**, *124*, 5938. (b) Takasu, A.; Narukawa, Y.; Hirabayashi, T. *J. Polymer Science: Part A: Polymer Chemistry*, **2006**, *44*, 5247.
- [8] (a) <http://malaysiachemicals.webs.com/documents/GDLLLeaflet.pdf>  
(b) [http://www.hawkinswatts.com/prod\\_acids\\_gdl.htm](http://www.hawkinswatts.com/prod_acids_gdl.htm)
- [9] <http://www.riversidearomatics.com/lactones.htm>
- [10] (a) Huber, G. H.; Iborra, S.; Corma, A. *Chem. Rev.* **2006**, *106*, 4044. (b) Huber, G. W.; Corma, A. *Angew. Chem. Int. Ed.* **2007**, *47*, 7184.
- [11] (a) Van Sassenbroeck, D. K.; De Paepe, P.; Belpaire, F. M.; Buylaert, W. A. *Toxicological Sciences* **2003**, *73*, 270. (b) Van Nieuwenhuijzen, P. S.; McGregor, I. S. *Drug and Alcohol Dependence* **2009**, *103*, 137.
- [12] (a) Crellin, J. K.; Philpott, J.; Tommie Bass A. L. *A Reference Guide to Medicinal Plants: Herbal Medicine Past and Present* (Duke University Press, **1989**, pp 560) (b) Nakawata, M.; Ohno, T., Maruyama, R.; Okubo, M.; Nagatsu, A.; Ionue, M.; Tanabe, H.; Minatoguchi, S.; Fujiwara, H. *Biol. Pharma. Bull.* **2007**, *30*, 1754. (c) Brown, G. "Artemisinin and a new generation of antimalarial drugs" *Educ. Chem.* **2006**. (d) Wesolowska, A.; Nikiforuk, A.; Michalaska, K., Kisiel, W.; Chojnacka-Wojcik, E. *J.*

- Ethnopharmacol.* **2006**, *107*, 254. (e) Bischoff, T. A.; Kelley, C. J.; Karchesy, Y.; Laurantos, M.; Nguyen-Dinh, P.; Arefi, A. G. *J. Ethnopharmacol.* **2004**, *2-3*, 455.
- [13] Atta-Ur-Ramman, *Studies in Natural Product Chemistry*, Vol. 32, Part L. (Elsevier, Amsterdam, 2005, p. 515)
- [14] (a) Mc Inerney, B. V.; Taylor, W. C. *Stud. Nat. Prod. Chem.* **1995**, *15*, 381. (b) Janecki, T. *Natural Lactones and Lactams: Synthesis, Occurrence and Biological Activity* (Wiley-VCH, 2013). Some examples of natural isochromanones: (c) Barbier, J.; Wegner, J.; Benson, S.; Gentsch, J.; Pietschmann, T.; Kirschning, A. *Chem. Eur. J.* **2012**, *18*, 9083. (d) Barbier, J.; Jansen, R.; Irschic, H.; Benson, S.; Gerth, K.; Böhlendorf, B.; Höfle, G.; Reichenbach, H.; Wegner, J.; Zeilinger, C.; Kirschning, A.; Müller, R. *Angew. Chem. Int. Ed.* **2012**, *51*, 1256.
- [15] Lin, G.; Chan, S. S. K.; Chung, H. S.; Li, S. L. *Stud. Nat. Prod. Chem.* **2005**, *32*, 611.
- [16] Peter, K.; Vollhardt, C.; Schore, N. E. *Organic Chemistry: Structure and Function* (4<sup>th</sup> Ed).
- [17] Mitsunobu, O.; Yamada, M. *Bull. Chem. Soc.* **1967**, *40*, 2380.
- [18] Pinner, A.; Klein, Fr. *Chem. Ber.* **1877**, *10*, 1889.
- [19] Testa, E.; Fontanella, L.; Mariant, L. *J. Org. Chem.* **1960**, *25*, 1812.
- [20] Reddy, M. S.; Kumar, Y. K.; Thirupathi, N. *Org. Lett.* **2012**, *14*, 824.
- [21] Tellitu, I.; Serna, S.; Herrero, M. T.; Moreno, I.; Domínguez, E.; SanMartin, R. *J. Org. Chem.* **2007**, *72*, 1526.
- [22] Trend, R. M.; Ramtohul, Y. K.; Ferreira, E. M.; Stoltz, B. *Angew. Chem. Int. Ed.* **2003**, *42*, 2892.
- [23] Huang, L.; Jiang, H.; Qi, C.; Liu, X. *J. Am. Chem. Soc.* **2010**, *132*, 17652.
- [24] Wang, L.; Thai, K.; Gravel, M. *Org. Lett.* **2009**, *11*, 891.
- [25] Fan, Q.; Lin, L.; Liu, J.; Huang, Y.; Feng, X. *Eur. J. Org. Chem.* 2005, 3542.
- [26] (a) Wu, X.; Mahalingam, A. K.; Wan, Y.; Alterman, M. *Tetrahedron Lett.* **2004**, *45*, 4635. (b) Brunet, J. J.; Sidot, C.; Caubere, P. *J. Org. Chem.* **1983**, *48*, 1166.

- [27] Endo, K.; Takahashi, H.; Aihara, M. *Heterocycles* **1996**, *42*, 589.
- [28] Rathore, R.; Bhushan, V.; Chandrasekaran, S. *Chem. Letters* **1984**, 2131.
- [29] Hoover, J.; Stahl, S. S. *J. Am. Chem. Soc.* **2001**, *133*, 16901.
- [30] (a) Hine, J. *Physical Organic Chemistry*, 2<sup>nd</sup> Ed. (Mc Graw-Hill, New York, **1962**, p 269). (b) Stapp, P. R. *J. Org. Chem.* **1973**, *58*, 1433.
- [31] Omura, S.; Fukuyama, T.; Murakami, Y.; Okamoto, H.; Ryu, I. *Chem. Commun.* **2009**, 6741.
- [32] Zhang, Y. H.; Shi, B. F.; Yu, J. Q. *Angew. Chem.* **2009**, *48*, 6097.
- [33] (a) With LiBH<sub>4</sub>: Narasimhan, S. *Heterocycles* **1982**, *18*, 131. (b) with NaBH<sub>4</sub>: Soai, K.; Yokoyama, S.; Mochida, K. *Synthesis* **1987**, *7*, 647. (c) Santaniello, E.; Ferraboschi, P.; Fiecchi, A.; Grisenti, P.; Manzocchi, A. *J. Org. Chem.* **1987**, *52*, 671. (d) with Zn: Graebe, J. *Justus Liebigs Annalen der Chemie* **1887**, *242*, 222.
- [34] See Chapter 1, section 1.3.3
- [35] Thompson, D. W.; Kretzer, R. M.; Lebeau, E. L.; Scaltrito, D. V.; Ghiladi, R. A.; Lam, K.-C.; Rheingold, A. L.; Karlin, K. D.; Meyer, G. J. *Inorg. Chem.* **2003**, *42*, 5211.
- [36] White, M. C. *Science* **2012**, *335*, 807.
- [37] Eikawa, M.; Sakaguchi, S.; Ishii, Y. *J. Org. Chem.* **1999**, *64*, 4676.
- [38] Ritcher, H.; Garcia Mancheno, O. *Eur. J. Org. Chem.* **2010**, 4460.
- [39] Xu, Y. C.; Lebeau, E.; Gillard, W.; Attardo, G. *Tetrahedron Lett.* **1993**, *34*, 3841.
- [40] Myers, A. G.; Fraley, M. E.; Tom, N. J.; Cohen, S. B.; Madar, D. J. *Chemistry and Biology* **1995**, *2*, 33.
- [41] Cho, H.; Kim, M.; Sawamura, M. *Flavour Frag. J.* **2002**, *17*, 49.
- [42] Wilson III. C. W. *J. Food Science* **1970**, *35*, 766.
- [43] Nicoletti, R.; Manzo, E.; Ciavatta, M. L. *Int. J. Mol. Sci.* **2009**, *10*, 1430.
- [44] Devon, T. K.; Scott, A. I. *Handbook of Naturally Occurring Compounds*, **I**, 249 (Academic Press, New York, 1975).
- [45] Bhor, S.; Anilkumar, G.; Tse, M.-K.; Klawonn, M.; Dobler, C.; Bitterlich, B.; Grotevendt, A.; Beller, M. *Org. Lett.* **2005**, *7*, 3393.

- [46] Arai, T.; Mishiro, A.; Yokoyama, N.; Suzuki, K.; Sato, H. *J. Am. Chem. Soc.* **2010**, *132*, 5338.
- [47] Zheng, F.; Yu, Z. *Organometallics* **2009**, *28*, 1855.
- [48] Hoffmann, H.; Martin, R.; Rabe, J. *J. Org. Chem.* **1985**, *50*, 3849.
- [49] Using Y(OTf)<sub>3</sub> (2 mol%) as catalyst following the procedure reported by: Bourgene, B.; Hoffmann, P.; Lherbet, C. *Synthetic Commun.* **2010**, *40*, 915.
- [50] Zhou, M.-Y.; Kong, S.-S.; Zhang, L.-Q.; Zhao, M.; Duan, J.-A.; Ou-Yang, Z.; Wang, M. *Tetrahedron Lett.* **2013**, *54*, 3962.
- [51] Mohler, D. L.; Thompson, D. W. *Tetrahedron Lett.* **1987**, *28*, 2567.
- [52] Shi, T.; Chen, H.; Jing, L.; Sun, X.; Liu, X.; Jiang, R. *Synthetic Commun.* **2011**, *41*, 2594.
- [53] Gerdes, J. M.; Keil, R. N.; Shulgin, A. T.; Mathis, C. A. *J. Fluor. Chem.* **1996**, *78*, 121.
- [54] Favor, D. A.; Johnson, D. S.; Powers, J. J.; Li, T.; Madabattula, R. *Tetrahedron Lett.* **2007**, *48*, 3039.
- [55] Garcia, D.; Foubelo, F.; Yus, M. *Heterocycles* **2009**, *77*, 991
- [56] Eisa RandD Management Co Ltd. Patent: EP2062901 A1 (**2009**)
- [57] Geurtsen, B.; De Bie, D. A.; Van der Plas, H. C. *Tetrahedron* **1989**, *45*, 6519.
- [58] Chen, J.; Dang, L.; Li, Q.; ye, Y.; fu, S.; Zeng, W. *Synlett* **2012**, *4*, 595.
- [59] Sakai, N.; Moriya, T.; Konakahara, T. *J. Org. Chem.* **2007**, *72*, 5920.
- [60] Das, A.; Chaudhur, R.; Liu, R.-S. *Chem. Commun.* **2009**, 4046.
- [61] Girdhar, J.; Subbamayappa, A. *Synthetic Commun.* **2011**, *41*, 720.
- [62] Mayhoub, A. S.; Talukdar, A.; Cushman, M. *J. Org. Chem.* **2010**, *75*, 3507.
- [63] Del Giacco, T.; Rol, C.; Sebastiani, G. *J. Phys. Org. Chem.* **2003**, *16*, 127.
- [64] Sølvhøv, A.; Madsen, R. *Organometallics* **2011**, *30*, 6044.
- [65] Kang, Y. B.; Gade, L. H. *J. Am. Chem. Soc.* **2011**, *133*, 3658.
- [66] Lopez-Lopez, J. A.; Guerra, F. M.; Moreno-Dorado, F. J.; Jorge, Z. D.; Massanet, G. M. *Tetrahedron Lett.* **2007**, *48*, 1749.

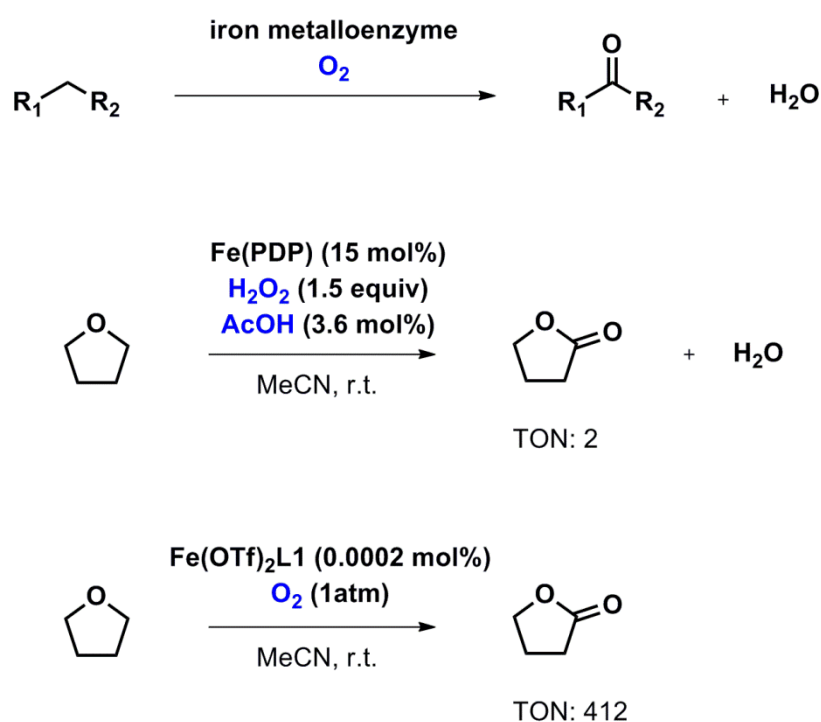
- [67] Movassaghi, M.; Jacobsen, E. N. *J. Am. Chem. Soc.* 2002, **124**, 2456.
- [68] Zhang, Y. H.; Shi, B. F.; Yu, J. Q. *Angew. Chem. Int. Ed.* **2009**, *48*, 6097.
- [69] Rioz-Martinez A.; de Gonzalo, G.; Torres Pazmino, D. E.; Fraaile, M. W.; Gotor, V. J. *Org. Chem.* **2010**, *75*, 2073.
- [70] Odasso, W. *Farmaco, Edizione Scientifica* **1978**, *33*, 148
- [71] Lamarty, G.; Moreau, C.; Mouloungui, Z. *Can. J. Chem.* **1983**, *61*, 2643.
- [72] Song, A.-R.; Yu, J.; Zhang, C. *Synthesis* **2012**, *44*, 2903.
- [73] Harwood, L. M. *J. Chem. Soc. Perkin Trans. 1*, **1984**, *11*, 2577.
- [74] Elli Lilly Co. Patent: WO2007/146758 A2 (2007).
- [75] Irvine, R. W.; Kinloch, S. A.; McCormick, A. S.; Russell, R. A.; Warrener, R. N. *Tetrahedron* **1988**, *44*, 4591.
- [76] He, G.; Chen, G. *Angew. Chem. Int. Ed.* **2011**, *50*, 5192.
- [77] Ashcroft, W. R.; Beal, H. G.; Joule, J. A. *J. Chem. Soc. Perkin Trans. 1* **1981**, 3012.
- [78] Characterisation in agreement with the commercially available materials
- [79] Bruker (2010).APEX2. Version 2010.1-2. Bruker AXS Inc., Madison, Wisconsin, USA.
- [80] Bruker (2001). SAINT. Version 7.68a. Bruker AXS Inc., Madison, Wisconsin, USA
- [81] Sheldrick, G. M. (2003). SADABS. Version 2.10. University ofGöttingen, Germany.
- [82]Dolomanov, O. V.; Bourhis, L. J.; Gildea, R. J.; Howard, J. A. K.; Puschmann, H. J. *Appl. Cryst.* **2009**, *42*, 339.
- [83] XL, Sheldrick, G.M. *Acta Cryst.* **2008**, *A64*, 112.

## *Chapter 4*

# **MECHANISTIC INVESTIGATIONS OF THE Fe(OTf)<sub>2</sub>-PYBISULIDINE CATALYSED AEROBIC $\alpha$ -OXIDATION OF ETHERS**

## 4.1. Introduction

Natural iron metalloenzymes are capable of using molecular oxygen for selective oxidations with water being released as the sole byproduct of the reaction.<sup>1</sup> Because dioxygen activation is still a major challenge in research, biomimetic iron catalysts often employ hydrogen peroxide as oxidant for attempting naturally occurring oxidations.<sup>1</sup> The use of hydrogen peroxide is a shuttle to achieve a relatively clean oxidation reaction as water is once again the only byproduct released from the process; however, additives and specific reaction protocols are often necessary for achieving good reactivity under these conditions.<sup>2</sup> In contrast, the  $\text{Fe}(\text{OTf})_2$ -PyBisulidine complexes have shown high efficiency for activating molecular oxygen under mild and additiveless conditions as presented in Chapter 3 (Scheme 1).



**Scheme 1.** Comparison between the oxidation conditions required by iron metalloenzymes, biomimetic  $\text{Fe}(\text{PDP})$  catalyst<sup>2</sup> and  $\text{Fe}(\text{OTf})_2\text{L1}$  complex

Because of the reaction conditions required, biomimetic iron catalysts can only tolerate a limited variety of functional groups, and electron rich functionalities (for instance:  $\pi$  rich

aromatic rings, olefins and N-based groups) are considered a big remaining challenge.<sup>3</sup> However, the  $\text{Fe}(\text{OTf})_2\text{L1}$  catalyst can tolerate an ample variety of functional groups including several electron rich functionalities with excellent chemoselectivity and mass balance. In addition, no alcohol formation was observed during the  $\text{Fe}(\text{OTf})_2\text{L1}$  catalysed oxidation of ethereal substrates even under conditions of limiting oxidant. In contrast, Gif type catalysts often afford a mixture of ketone and alcohol type products in different ratios (chapter 1) and the biomimetic  $\text{Fe}(\text{PDP})$  complex, which can catalyse the oxidation of THF to  $\gamma$ -butyrolactone, is known to undergo an initial oxidation of the methylene group to an alcohol which is subsequently oxidised to the ketone product.<sup>2</sup>

## 4.2. Aims of this chapter

Previously reported aerobic oxidations of ethers to esters catalysed by a myriad of catalysts suffer from serious limitations in terms of their potential industrial and laboratory applicability.<sup>4</sup> In addition, very little mechanistic investigations have been provided for those reactions, which hamper their improvement. This lack of mechanistic understanding in combination with the aforementioned observations that clearly differ from those made with other catalysts prompted us to perform some mechanistic studies of the  $\text{Fe}(\text{OTf})_2\text{L1}$  catalysed aerobic oxidation of ethers.

This chapter covers all the experimental observations gained from different mechanistic experiments which are discussed and compared with other relevant catalysts. A catalytic cycle is finally hypothesised on the basis of these experimental data.

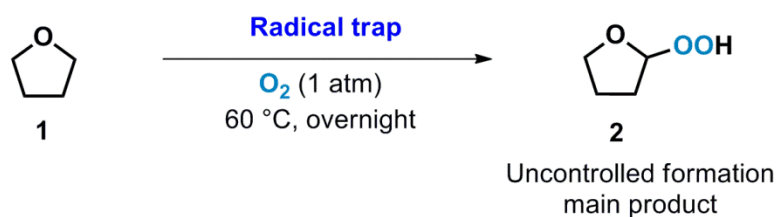
## 4.3. Results and discussion

### 4.3.1. Radical trapping experiments

The excellent chemoselectivity and mass balance observed in the substrate scope of the  $\text{Fe}(\text{OTf})_2\text{L1}$  catalysed aerobic oxidation of ethers initially suggest that no free radical formation takes place during the reaction. In order to elucidate whether radical species are



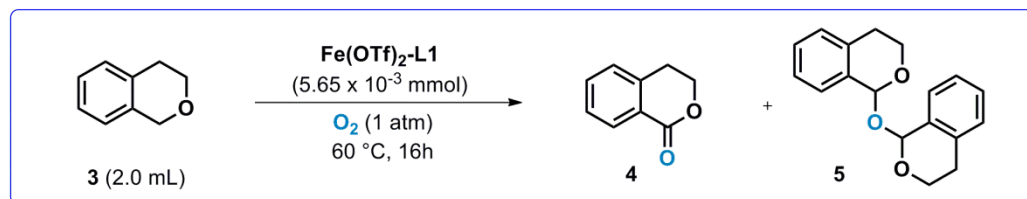
formed and/or involved during this oxidation reaction, we initially conducted the oxidation of THF under optimal conditions in the presence of a radical trapping reagent. Unfortunately, THF had to be discarded as model substrate for this study due to the uncontrolled formation of the autooxidation product **2** in the presence of small amounts of radical traps, even in the absence of catalyst (Scheme 2).

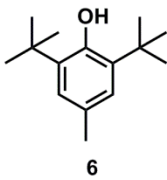
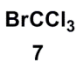
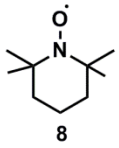
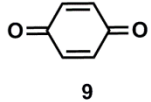
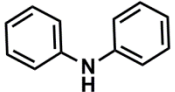
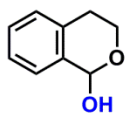
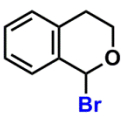


**Scheme 2.** Uncontrolled autooxidation of THF in the presence of radical traps

Isochroman was then selected as a model substrate, as no uncontrolled autooxidation occurs upon addition of C-selective (2,6-di-*tert*-butyl-4-methylphenol, BrCCl<sub>3</sub>, TEMPO, *p*-benzoquinone) and O-selective (Ph<sub>2</sub>NH) radical trapping agents.<sup>5</sup> Addition of equimolecular amounts of catalyst and **6** did not alter the catalyst efficiency or the product distribution; however, a 3- to 5-fold increase in the radical trap concentration strongly inhibited the reaction and affected the product distribution towards the formation of byproduct **5** (Table 1, entries 1-5). At this point, a further increase in the radical trap concentration led to complete reaction inhibition (Table 1, entries 6-8). A similar trend was observed in the presence of the other radical traps that caused strong to complete inhibition of the oxidation reaction (Table 1, entries 9-17). Interestingly, no substrate-trap adducts were observed when the reaction was conducted in the presence of these radical trapping agents. Moreover, the alcohol product **11** was not formed in the presence of any radical trapping reagent and the alkyl bromide byproduct **12**, which can be easily identified in Gif type oxidations performed in the presence of radical trap **7**, was not detected either.<sup>6</sup> These observations in combination with the lack of alcohol product formation suggest that the mechanism of the Fe(OTf)<sub>2</sub>**L1** catalysed aerobic oxidation of ethers to esters differs from that of Gif type oxidations.

However, the absence of substrate-trap adducts may suggest that the inhibition of the reaction might not be due to radical species formation but it might stem from interactions between the catalyst and the radical trap (i.e. coordination of the radical trap to the catalyst).

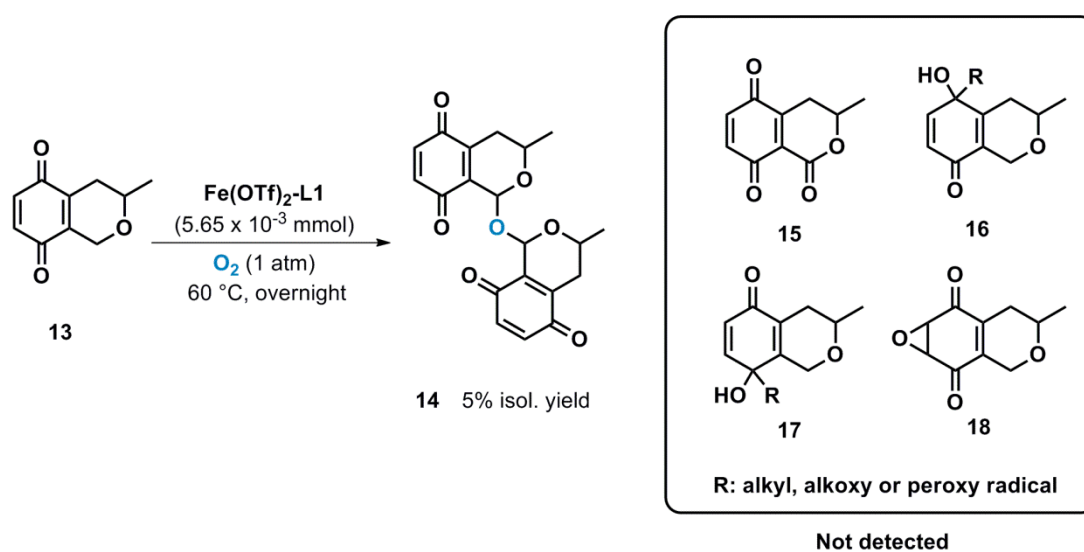


Radical probe	Entry	n (rad probe/catalyst)	chromanone (% yield)	1,1'-oxydiisochroman (% yield)
 6	1	0.5	30	12
	2	1	25	14
	3	2	20	12
	4	3	13	8.5
	5	5	5	6.5
	6	20	0	0
	7	40	0	0
	8	80	0	0
 7	9	9	8	7
	10	45	3	6
 8	11	9	4	1
	12	45	0	0
 9	15	20	0	0
	16	40	0	0
	17	80	0	0
 10	13	5	8	5
	14	10	3.5	9
 11	Not detected			
 12	Not detected in the presence of $\text{BrCCl}_3$			

**Table 1.**  $\text{Fe}(\text{OTf})_2\text{L1}$  catalysed aerobic oxidation of isochroman in the presence of C- and O-selective radical trapping reagents

### 4.3.2. Oxidation of 3-methyl-3,4-dihydro-1*H*-isochromene-5,8-dione

In an attempt to identify whether radical species are formed during the oxidation reaction and to intercept any possible substrate-radical trap adduct, 3-methyl-3,4-dihydro-1*H*-isochromene-5,8-dione **13** bearing a *p*-benzoquinone moiety was subjected to the oxidation reaction (Scheme 3). Surprisingly, the 1,1'-oxydiisochromene-5,8-dione derivative **14** was obtained as the single reaction product with 5% yield, with no substrate decomposition or product **15** formation. When reacted with a radical, quinones can give rise to a variety of products **16-18**; however, no products commonly derived from radicals were detected.<sup>7-9</sup> These results point towards that freely diffusing radical species are not generated during the oxidation reaction and suggest that the formation of the 1,1'-oxydiisochroman byproduct **5** is the result of a different competitive process.



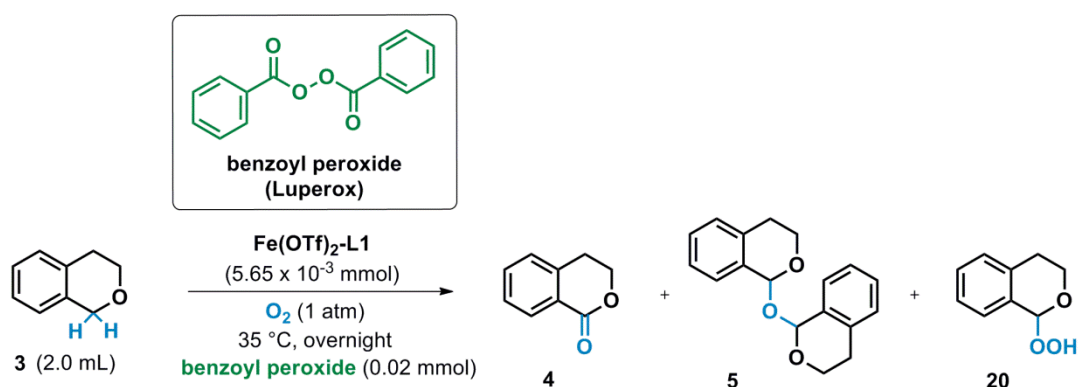
**Scheme 3.** 3-Methyl-3,4-dihydro-1*H*-isochromene-5,8-dione as substrate incorporating a *p*-benzoquinone moiety

### 4.3.3. Effect of a radical initiator

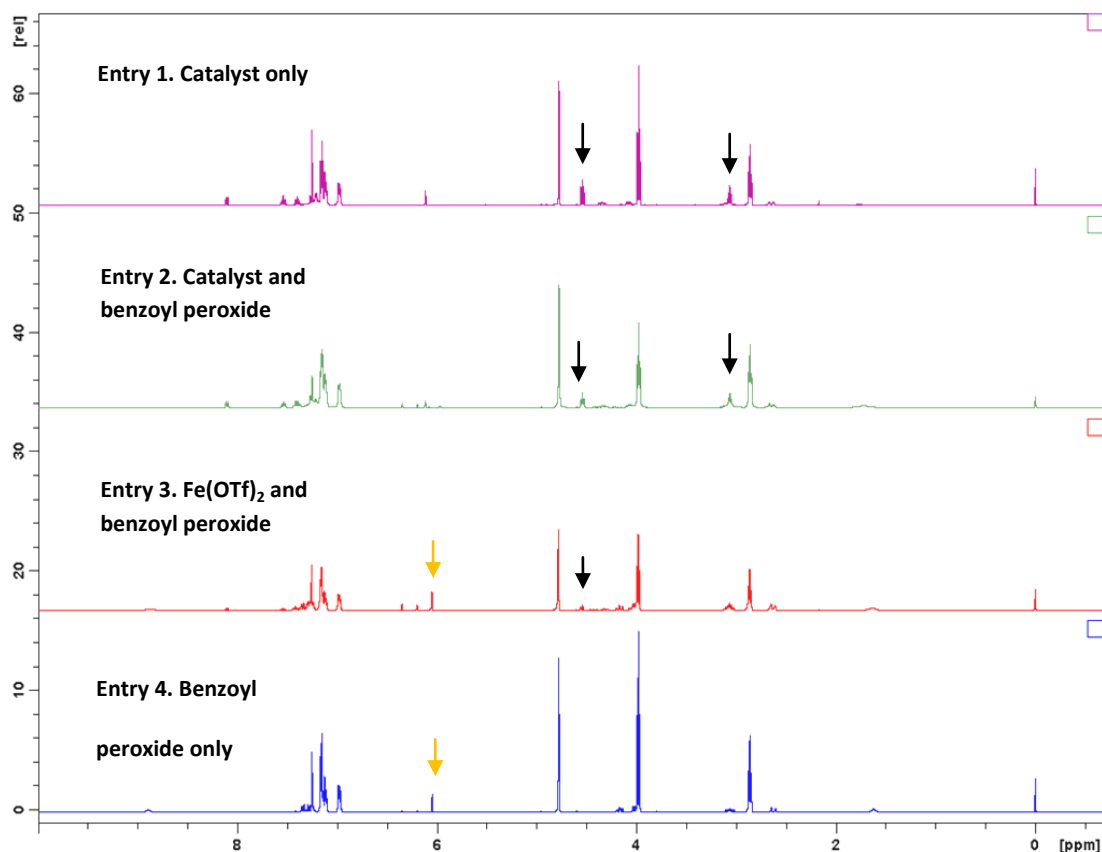
To examine further the possible formation of radicals, the aerobic oxidation of isochroman was conducted in the presence of a radical initiator, benzoyl peroxide,<sup>10</sup> at 35 °C. The presence of the initiator did not affect the oxidation of isochroman to isochromanone (16%

in its presence vs 17% in its absence); however a small amount of radical-derived isochroman hydroperoxide **20** (*ca* 2%) was detected (Scheme 4). Notably, the hydroperoxide product gained significance in the absence of **L1** and became the sole product when the catalyst was omitted. Formation of the oxidation dimer **5** was also observed in the presence of the Fe(OTf)<sub>2</sub>-**L1** catalyst. Although no clear evidence of the mechanism of its formation has been obtained, it is likely that **5** is formed via a competitive, Fe(OTf)<sub>2</sub>-**L1** catalysed process.

From these results it can be concluded that radical intermediate species are generated during the oxidation process; however, its formation is the result of a metal-centre based process in which the iron catalyst does not seem to act as a mere radical initiator.



Entry	Catalyst	Ester product (% conv.)	1,1'-oxydiisochroman (% conv.)	1-hydroperoxy isochroman (% conv.)
1.	Fe(OTf) <sub>2</sub> -L1, no peroxide	16	9	-
2.	Fe(OTf) <sub>2</sub> -L1	17	4	2
3.	Fe(OTf) <sub>2</sub>	4	-	12
4.	-	-	-	8



**Scheme 4.**  $\text{Fe}(\text{OTf})_2\text{L1}$  catalysed aerobic oxidation of isochroman in the presence of a radical initiator. The  $^1\text{H}$  NMR resonances corresponding to the methylene protons of isochromenone are highlighted under the black arrow whereas the  $^1\text{H}$  NMR resonances corresponding to the methyne and hydroperoxy protons corresponding to isochroman hydroperoxide are highlighted under a yellow arrow.

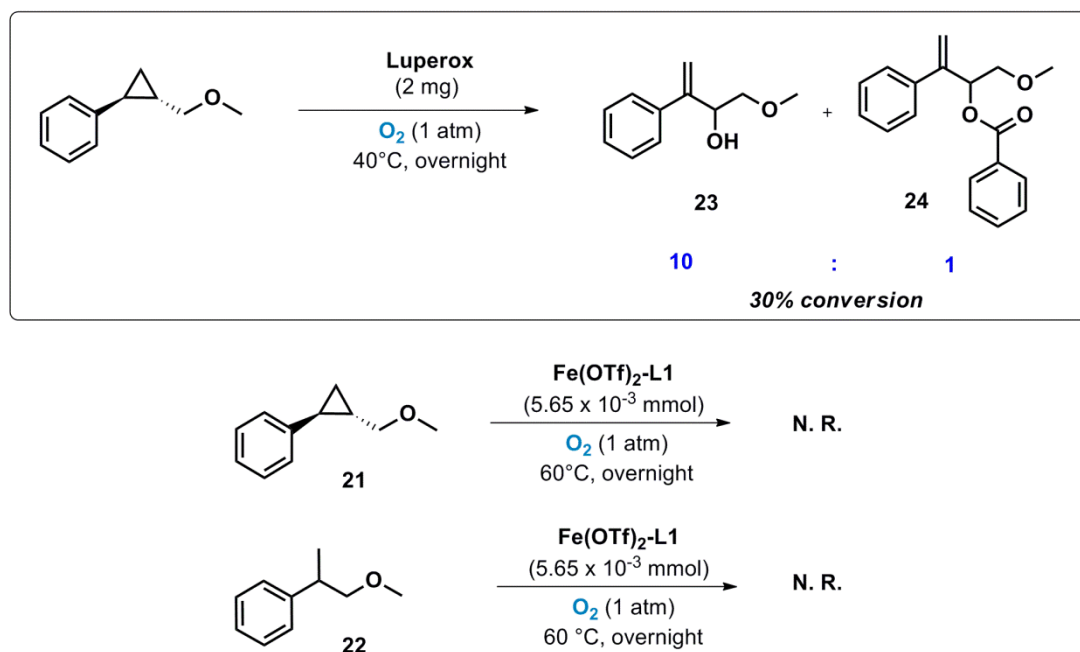
#### 4.3.4. Oxidation of a radical clock

The ability of benzoyl peroxide to initiate radical reactions with such ethereal substrates is also seen in the ultra fast radical clock ( $\pm$ )-*trans*-(2-methoxymethyl)cyclopyl)benzene,<sup>11</sup> which underwent rapid ring opening when exposed to small amounts of benzoyl peroxide under 1 atm of  $\text{O}_2$  (Scheme 5). In contrast, no reaction occurred when the radical initiator was replaced with  $\text{Fe}(\text{OTf})_2\text{L1}$ . Even though the inertness of the catalyst towards the oxidation of **21** is unclear to us, we hypothesise that it can be probably due to the steric

bulkiness of the radical clock, as no reaction was observed either when the less sterically hindered ether **22** was used as substrate.

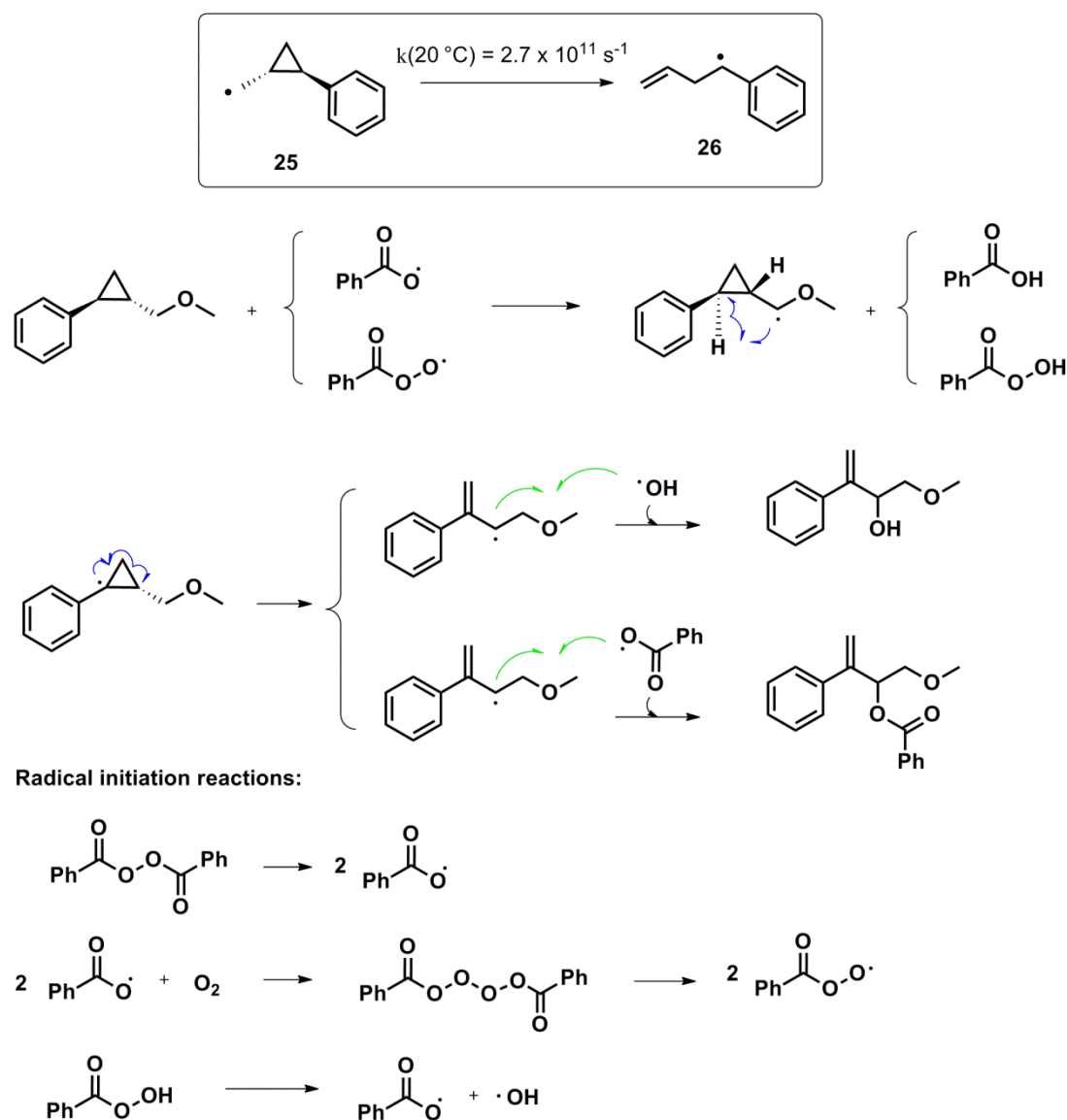
The formation of **23** from the reaction of the radical clock and benzoyl peroxide is also surprising, as the opening of the cyclopropyl ring to furnish benzyl radical **26** followed by its subsequent trapping with other radical species generated during the reaction was expected. Although we have no clear understanding of the mechanism behind the formation of **23** we can hypothesise that it might start with the formation of radical **25**. At higher temperatures (40 °C) the 1,3-radical abstraction of the benzylic hydrogen in *cis*-position would be possible. Ring opening from the resulting benzyl radical can be proposed, leading to the formation of a  $\alpha$ -styrene type radical which can be captured by hydroxyl or benzoyloxy radicals generated *in situ* (Scheme 6).

Taken together these experimental results indicate that whilst radicals may be generated in the Fe(OTf)<sub>2</sub>-L1 catalysed oxidation, freely diffusing carbon or oxygen-based radicals are not involved.



**Scheme 5. Aerobic oxidation using a radical clock.** Ring opening of the radical clock ( $\pm$ )-trans-(2-methoxymethyl)cyclopropylbenzene took place after exposure to the radical initiator

benzoyl peroxide under aerobic conditions. However, no reaction took place after its exposure to  $\text{Fe}(\text{OTf})_2\text{L1}$ .

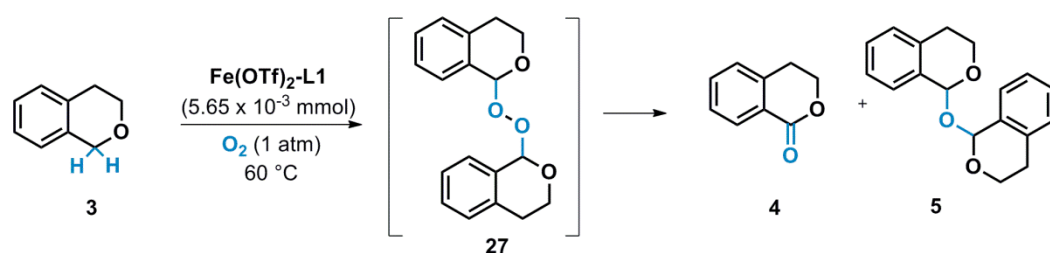


**Scheme 6.** Hypothesised formation of products **23** and **24**

#### 4.3.5. Identification of a peroxide intermediate

The catalytic efficiency of  $\text{Fe}(\text{OTf})_2\text{L1}$  was found dependent on the S/C ratio following an approximate Gaussian distribution with a maximum efficiency found at a S/C of 4315 in the neat reaction. It was also observed that the catalytic efficiency diminishes by increasing the dilution with arene type solvents. In order to understand this concentration effect, some

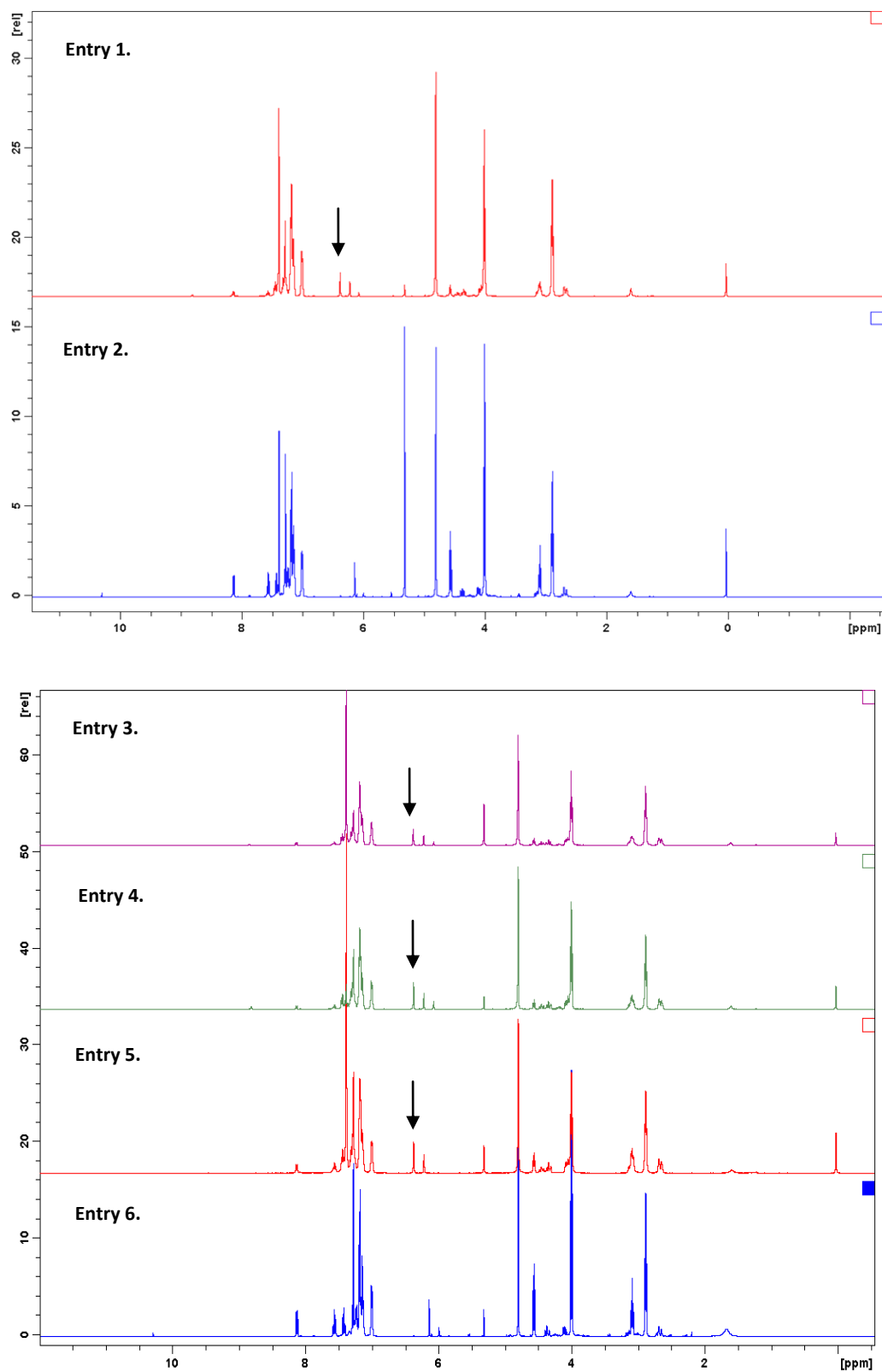
kinetic studies of the  $\text{Fe}(\text{OTf})_2\text{L1}$  catalysed oxidation of isochroman were conducted in a benzene solution of different concentrations (Scheme 7). When the oxidation was stopped after 1 h reaction, 1,1'-peroxydiisochroman<sup>12</sup> was detected, apart from the expected isochromanone and the 1,1'-oxydiisochroman byproduct (Scheme 7, entries 3-5). The peroxy species disappeared, being accompanied with an increase in the yield of isochromanone, following further reacting overnight (Scheme 7, entries 1, 2, 6). Therefore, the peroxy species appears to be an intermediate in the oxidation of isochroman. X-ray crystallographic analysis of the isolated mixture confirmed the structure of 1,1'-oxydiisochroman existing as two conformational isomers and that of 1,1'-oxydiisochroman (Scheme 8). These observations suggests that  $\text{Fe}(\text{OTf})_2\text{L1}$  is capable of catalysing rapid and selective formation of 1,1'-peroxyisochroman, from which the isochromanone results.



Entry	Isochroman: $\text{C}_6\text{H}_6$	1,1'-peroxy isochroman (% conv.)	Ester product (% conv.)	1,1'-oxydiisochroman (% conv.)
1.	1.0: 2.0 <sup>a</sup>	4	15	7
2.	2.0: 1.0 <sup>a</sup>	-	26	10.6
-----				
3.	0.5: 2.0 <sup>b</sup>	9.8	7.5	6.0
4.	1.0: 1.5 <sup>b</sup>	11.5	8.3	7.1
5.	2.0: 0.5 <sup>b</sup>	11.9	14.9	7.3
6.	2.0: 0.5 <sup>a</sup>	-	28	10.6

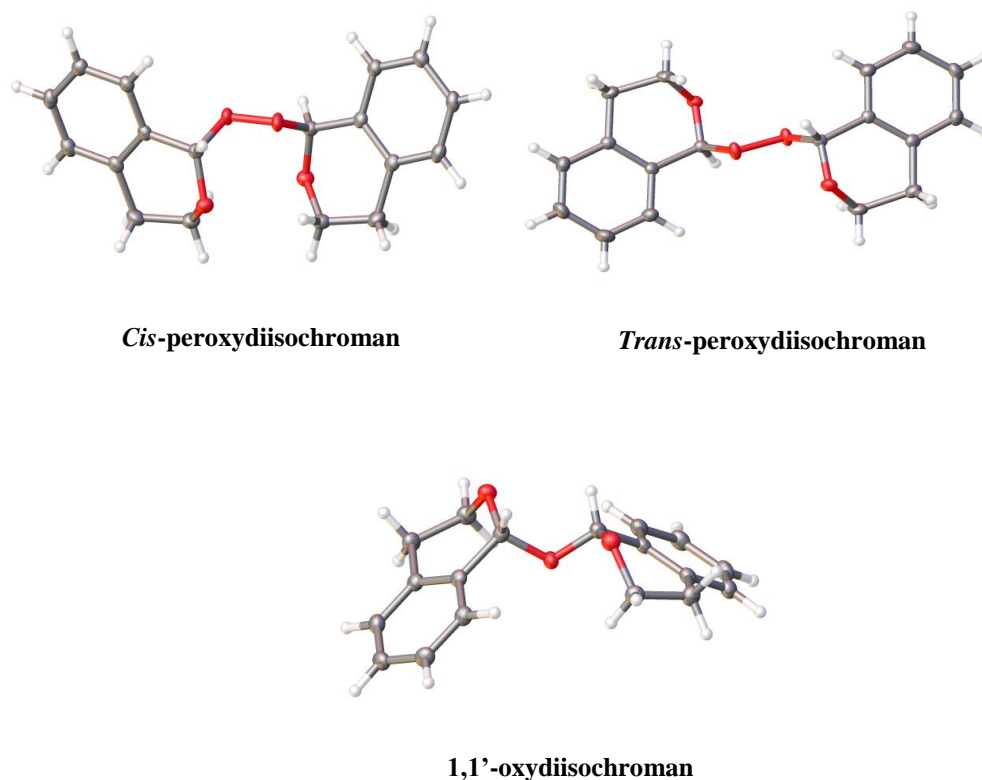
<sup>a</sup> Overnight reaction. <sup>b</sup> Reaction run for 1 h.





**Scheme 7. Kinetic studies of the  $\text{Fe}(\text{OTf})_2\text{L1}$  catalysed oxidation of isochroman.**

Evidence of 1,1'-peroxyisochroman formation in the crude  $^1\text{H}$  NMR is highlighted with a black arrow and it suggest a two step reaction mechanism.

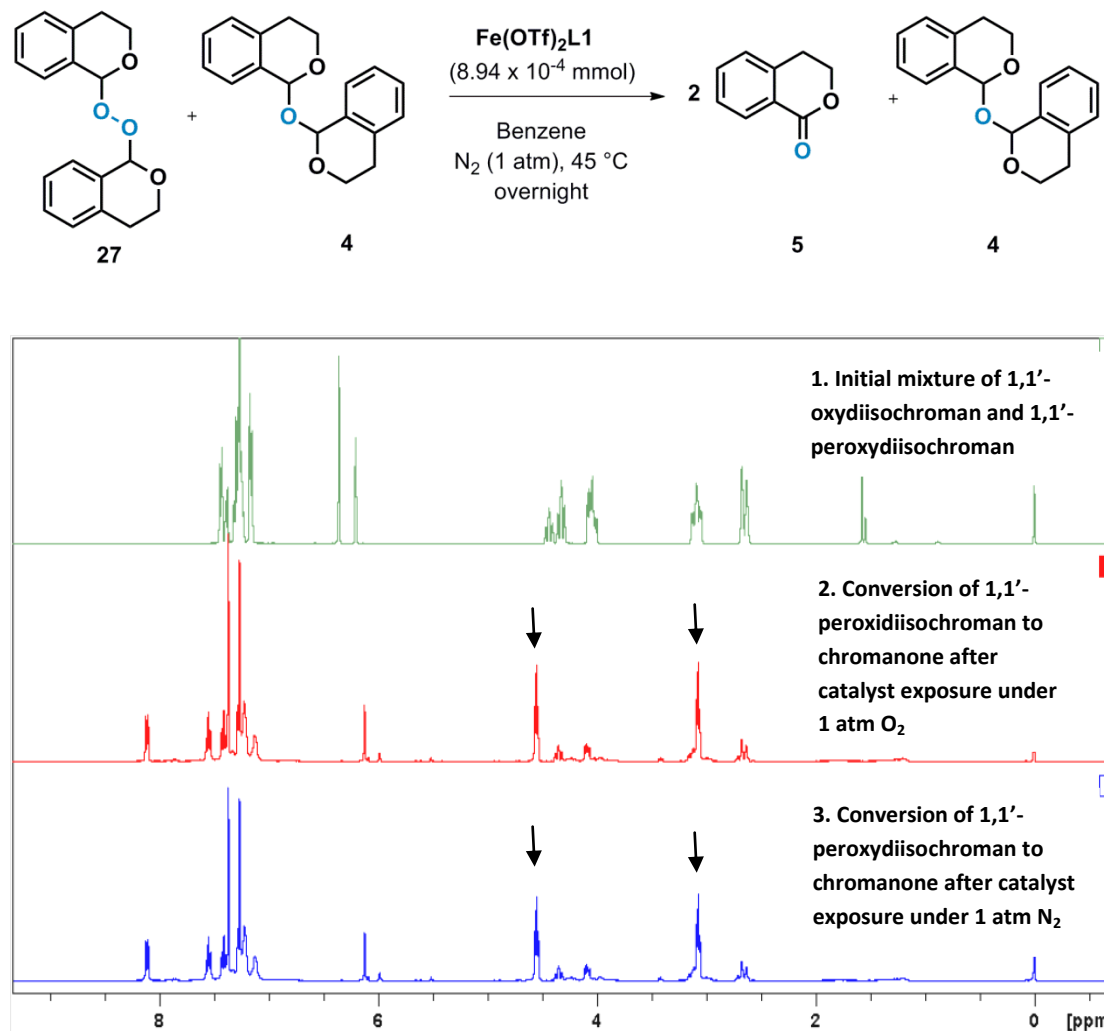


**Scheme 8.** Structures of the *cis* and *trans*-peroxydiisochroman intermediate isomers and the oxydiisochroman byproduct based on X-ray crystallographic analyses

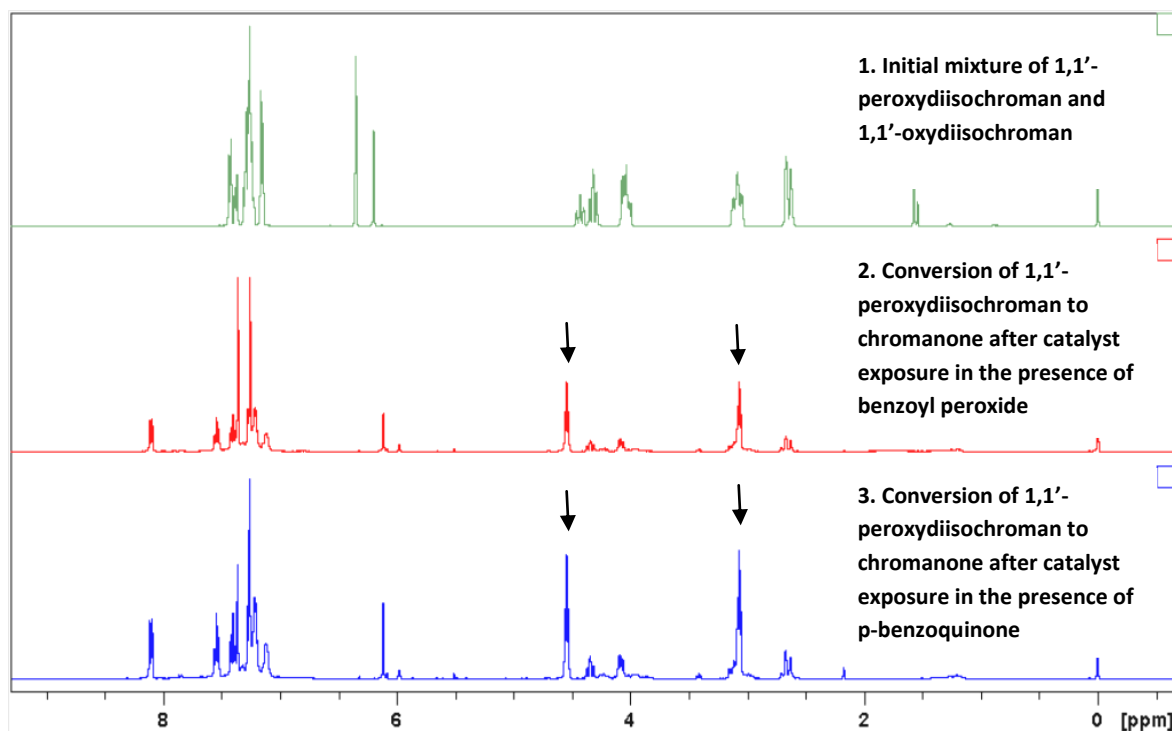
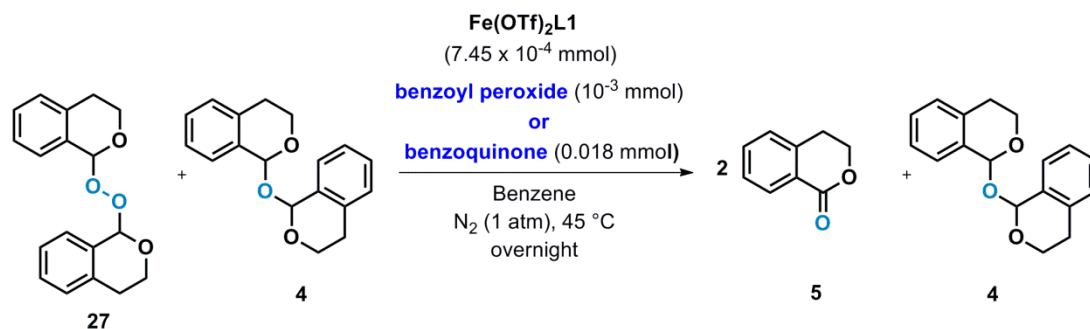
#### 4.3.6. Conversion of 1,1'-peroxyisochroman to chromanone

To gain more evidence of the intermediacy of 1,1'-peroxyisochroman, an isolated mixture of 1,1'-peroxydiisochroman and 1,1'-oxydiisochroman (1.0:0.6 molar ratio, 8.0M in C<sub>6</sub>H<sub>6</sub> solution) was exposed to a catalytic amount of Fe(OTf)<sub>2</sub>-**L1** at 45 °C (Scheme 9). Crude <sup>1</sup>H NMR spectra revealed a clean reaction in which the peroxide was fully converted into two equivalents of isochromanone under an O<sub>2</sub> atmosphere, whereas 1,1'-oxydiisochroman remained intact, establishing the intermediacy of the peroxide to isochromanone. Surprisingly, this clean transformation was also observed under a N<sub>2</sub> atmosphere; however, no reaction occurred in the absence of the iron catalyst. Interestingly, the reaction was not affected by the addition of either an excess of a radical inhibitor *para*-benzoquinone or the radical initiator benzoyl peroxide (Scheme 10), indicating that no radical species are involved at this stage of the isochroman oxidation. The presence of isochroman did not

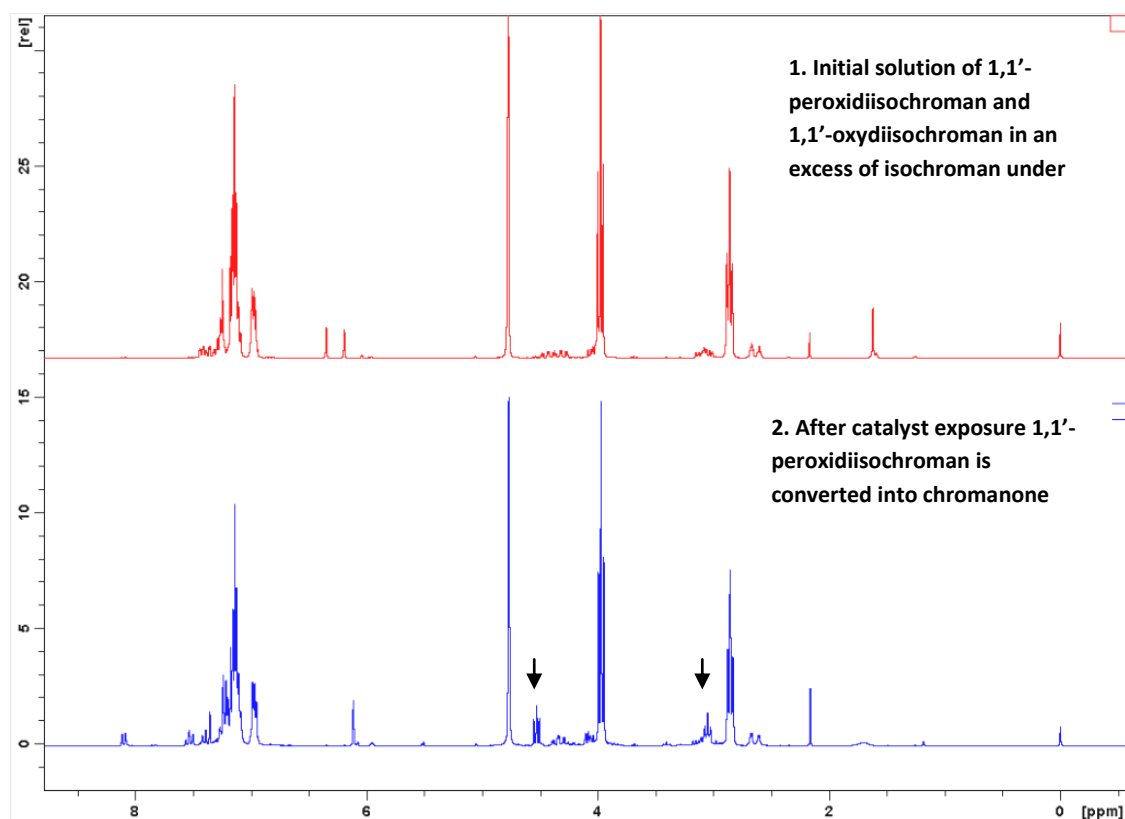
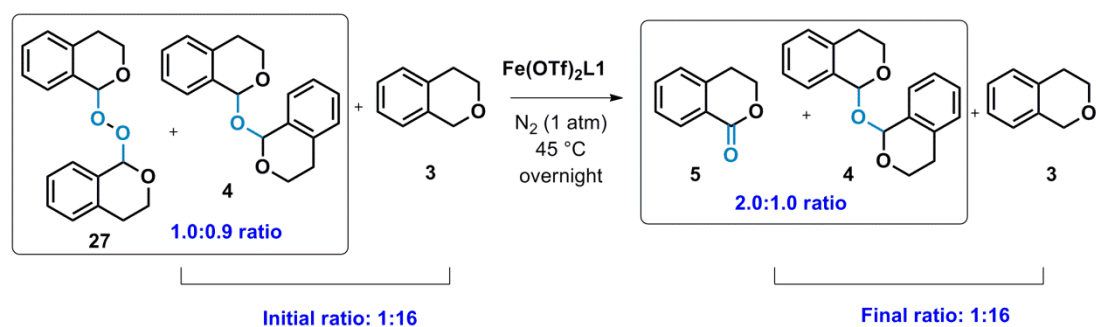
affect this transformation either (Scheme 11), nor was isochroman oxidized under the N<sub>2</sub> atmosphere, reinforcing that the oxidation of isochroman to the peroxide involves O<sub>2</sub> whilst the conversion of the peroxide to the ester does not.



**Scheme 9. 1,1'-Peroxydiisochroman as an intermediate in the Fe(OTf)<sub>2</sub>L1 catalysed conversion of isochroman to isochromanone.** The presence of <sup>1</sup>H NMR resonances corresponding to chromanone in the crude NMRs after catalytic exposure of the initial mixture is highlighted with a black arrow. Note that only the <sup>1</sup>H NMR signal corresponding to the methyne protons of 1,1'-peroxydiisochroman is missing after catalyst exposure.



**Scheme 10. Effect of radical reagents in the catalytic conversion of 1,1'-peroxydiisochroman into chromanone.** No difference in the reactivity was observed when the catalytic reaction was exposed to an excess of a radical inhibitor (*p*-benzoquinone) or a radical initiator (benzoyl peroxide).

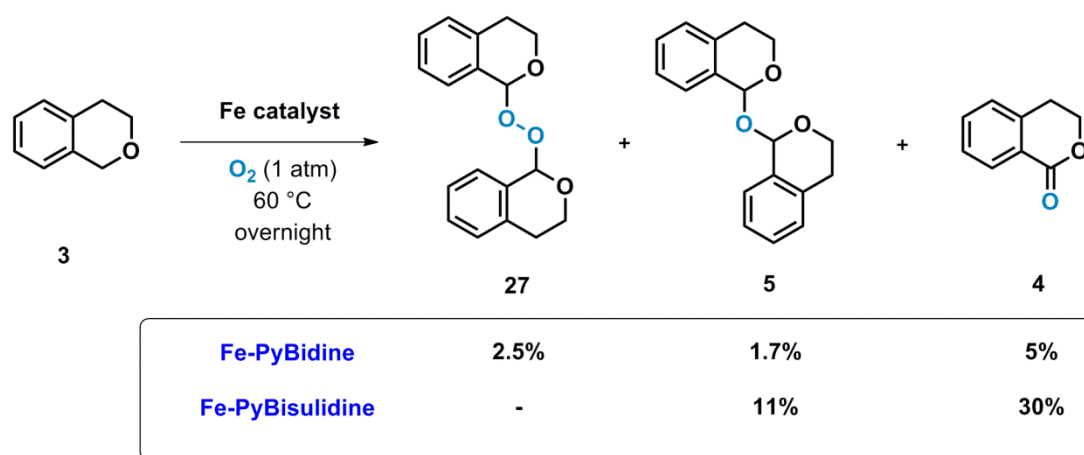


**Scheme 11. Conversion of 1,1'-peroxydiisochroman to chromanone in the presence of an excess of isochroman under  $N_2$  atmosphere.** The  $^1H$  NMR resonances corresponding to chromanone in the crude NMRs after catalytic exposure of the initial mixture are highlighted with a black arrow. No reaction was observed between the isochroman and the peroxide intermediate.

#### 4.3.7. Ligand effect in the conversion of 1,1'-peroxydiisochroman to chromanone

The activity of  $Fe(OTf)_2$ -PyBidine and  $Fe(OTf)_2$ L1 complexes towards the aerobic oxidation of THF was compared, with the latter showing a 7.5 fold increase in the formation of the

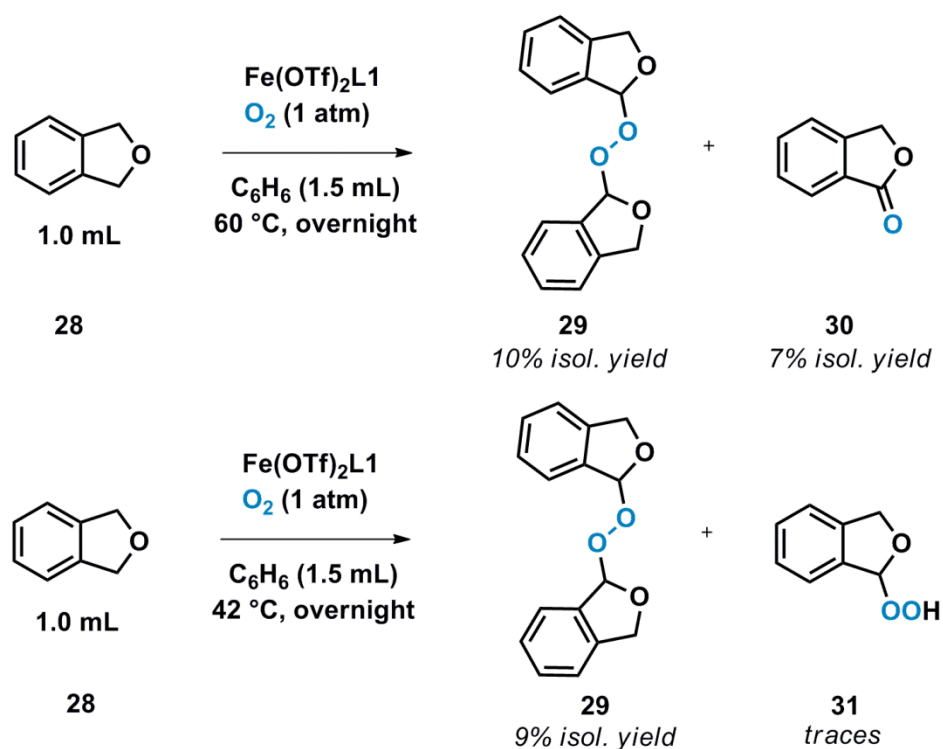
desired  $\gamma$ -butyrolactone product. When the aerobic oxidation of isochroman **3** was performed using  $\text{Fe}(\text{OTf})_2$ -PyBidine as catalyst under optimal reaction conditions, several products were observed with the isochromanone product **4** obtained in poor yields and the peroxide species **27** was isolated in 3% yield. These data suggests that the superior catalytic efficiency of  $\text{Fe}(\text{OTf})_2$ -L1 relies on its capability to easily promote both the formation of the peroxide species **27** and its transformation into two equivalents of lactone product **4**.



**Scheme 12.** Aerobic oxidation of isochroman catalysed by  $\text{Fe}(\text{OTf})_2$ -PyBidine type complex under optimal reaction conditions

#### 4.3.8. Selective formation of the peroxide intermediate

When phthalan type substrates such as **28** were subjected to the  $\text{Fe}(\text{OTf})_2$ -L1 catalysed aerobic oxidation reaction in benzene solution, an analogous peroxide intermediate **29** was formed together with the lactone product **30**. Indeed, upon modifying the reaction conditions to lower temperatures and higher dilution with benzene, the reaction was driven towards the exclusive formation of the peroxide species **29**, with no formation of the lactone product **30**. The autooxidation product **31** was also detected in small amounts (Scheme 13).

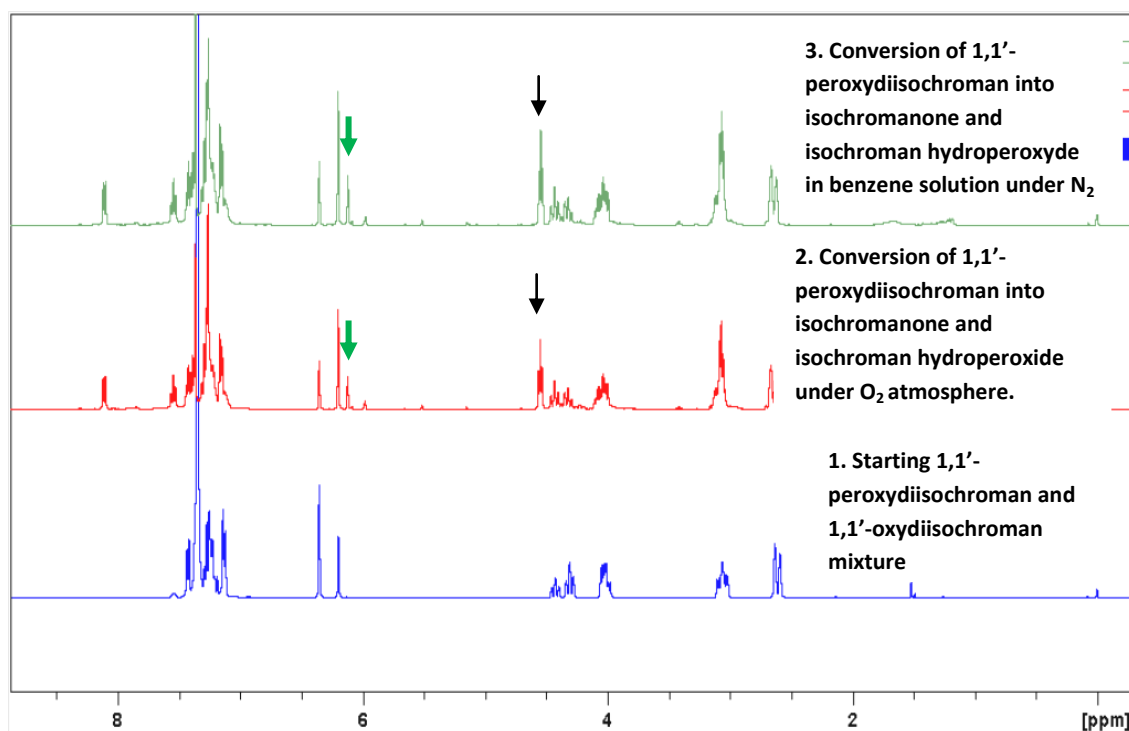
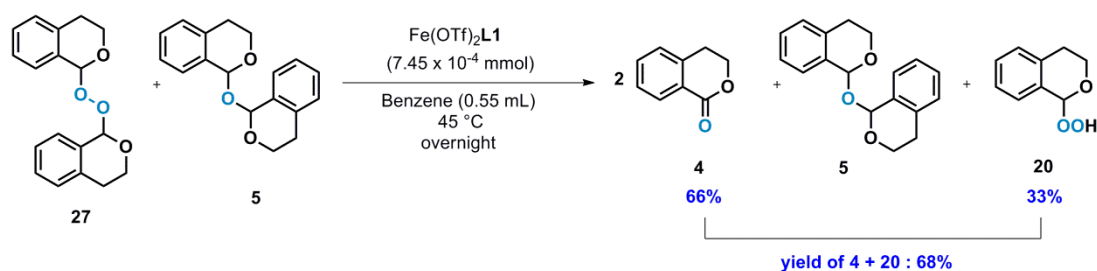


**Scheme 13.** Formation of the peroxide intermediate from phthalan type substrates under kinetically controlled conditions

#### 4.3.9. Formation of hydroperoxides under high dilution conditions

When reacting isochroman **3** or phthalan **28** in lower concentrated benzene solutions, formation of the hydroperoxide byproducts **20** and **31** was observed, respectively. Because these hydroperoxide byproducts were not generated under optimal reaction conditions, further studies were conducted to shed light into their formation in benzene solution. Thus, when a 4.5 M solution of the isolated mixture of 1,1-peroxydiisochroman and 1,1'-oxydiisochroman (1.0 : 0.5 ratio) in benzene was subjected to the catalytic oxidation reaction, formation of both isochromanone and isochroman hydroperoxide was observed with an overall yield of 68% (Scheme 14). The  $^1\text{H}$  NMR showed that the formation of these two products stem from the 1,1-peroxydiisochroman species, whereas the 1,1'-oxydiisochroman **4** remained intact. Analogous results were obtained when the oxidation was performed in the presence of the radical initiator benzoyl peroxide.

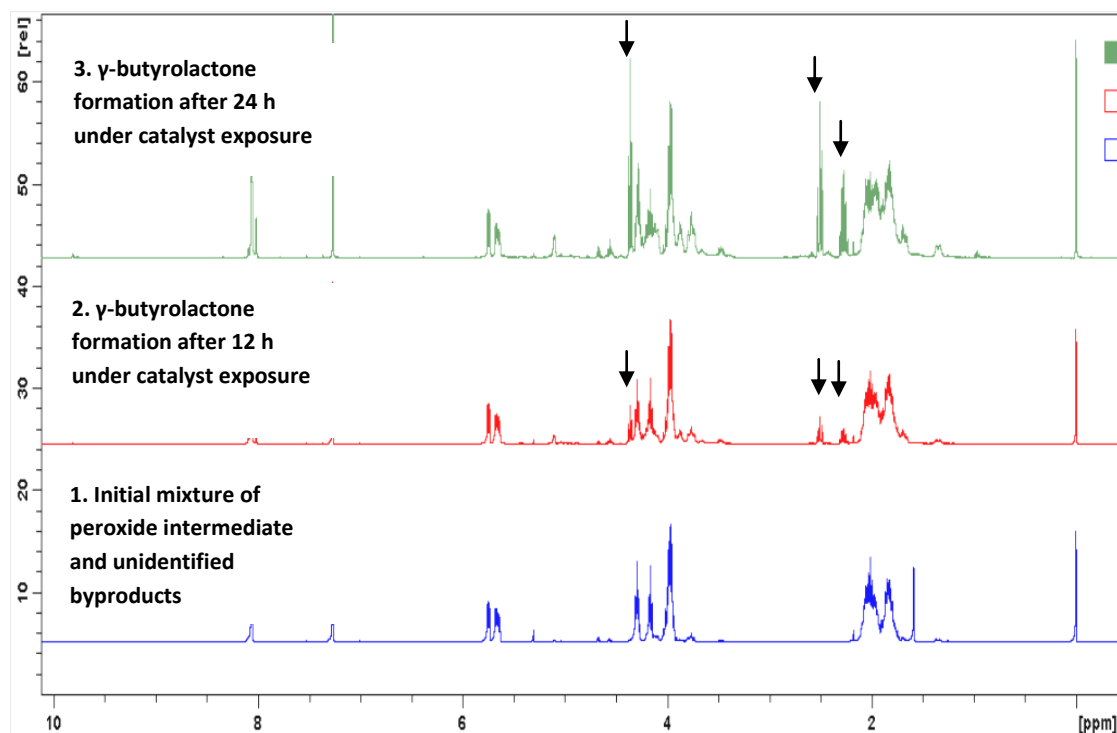
These data suggest that the  $\text{Fe}(\text{OTf})_2\text{L1}$  catalysed conversion of 1,1'-peroxydiisochroman into isochromanone is less efficient when the substrate concentration is low and thus, a higher efficiency was observed under neat substrate conditions. It also indicates that the formation of the hydroperoxides species during the catalytic oxidation under high dilution is not due to free radical reactions of the ether, but the result of different reactivity from the peroxide species.



**Scheme 14. Conversion of 1,1'-peroxydiisochroman into isochromanone and isochroman hydroperoxide in diluted benzene solution.** The  $^1\text{H}$  NMR resonances corresponding to chromanone in the crude NMRs after catalytic exposure of the initial mixture are highlighted with a black arrow, whereas the methyne proton of isochroman hydroperoxide is highlighted with a thick green arrow.



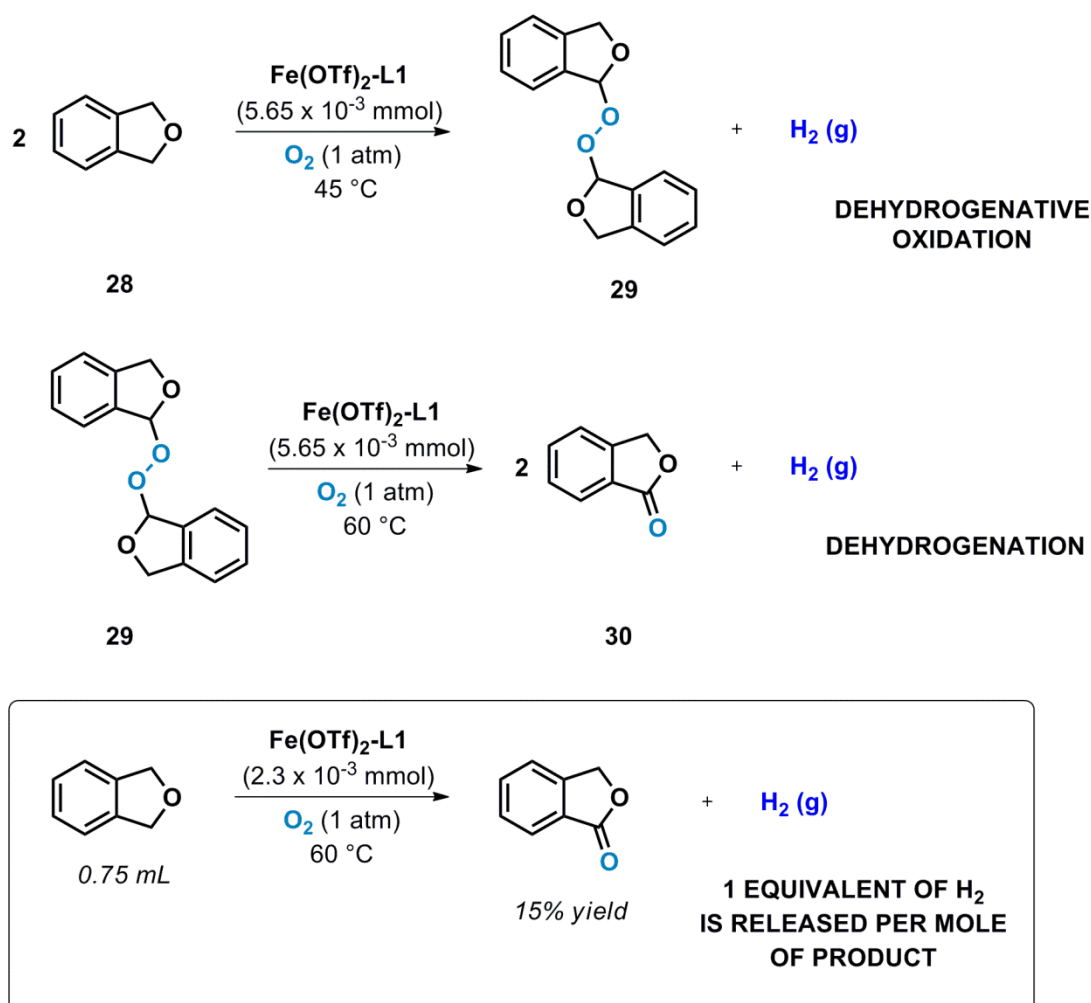




**Scheme 16.** Conversion of the peroxide intermediate **34** into the lactone product **35**

#### 4.3.11. Evidence of $\text{H}_2$ gas release during the oxidation reaction

Further study into how the oxidation proceeds revealed, much to our surprise, that the oxidation is accompanied with release of  $\text{H}_2$ . Quantitative GC analysis indeed established the stoichiometric formation of  $\text{H}_2$  in the  $\text{Fe}(\text{OTf})_2\text{L1}$  catalysed oxidation of phthalan **28** to phthalide **30**, and showed that the  $\text{H}_2$  formation took place in each individual step, i.e. oxidation to afford the peroxide and its subsequent conversion to phthalide (Scheme 17). Therefore, the conversion of **28** to the intermediate peroxide **29** is a dehydrogenative oxidation process whereas the subsequent conversion of the peroxide **29** to the phthalide product **30** is an unusual iron-catalysed dehydrogenation.

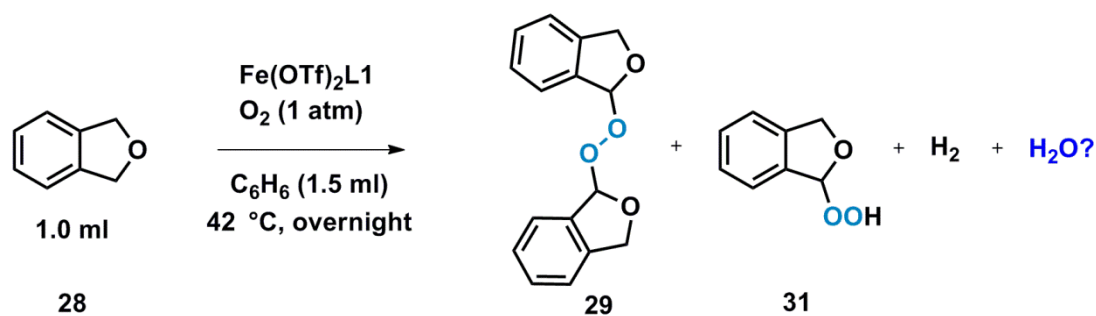


**Scheme 17.** Detection of H<sub>2</sub> gas during the oxidation of phthalan to phthalide

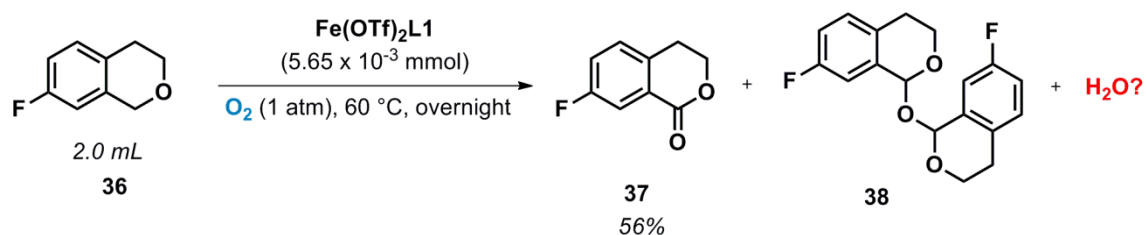
#### 4.3.12. Absence of water formation

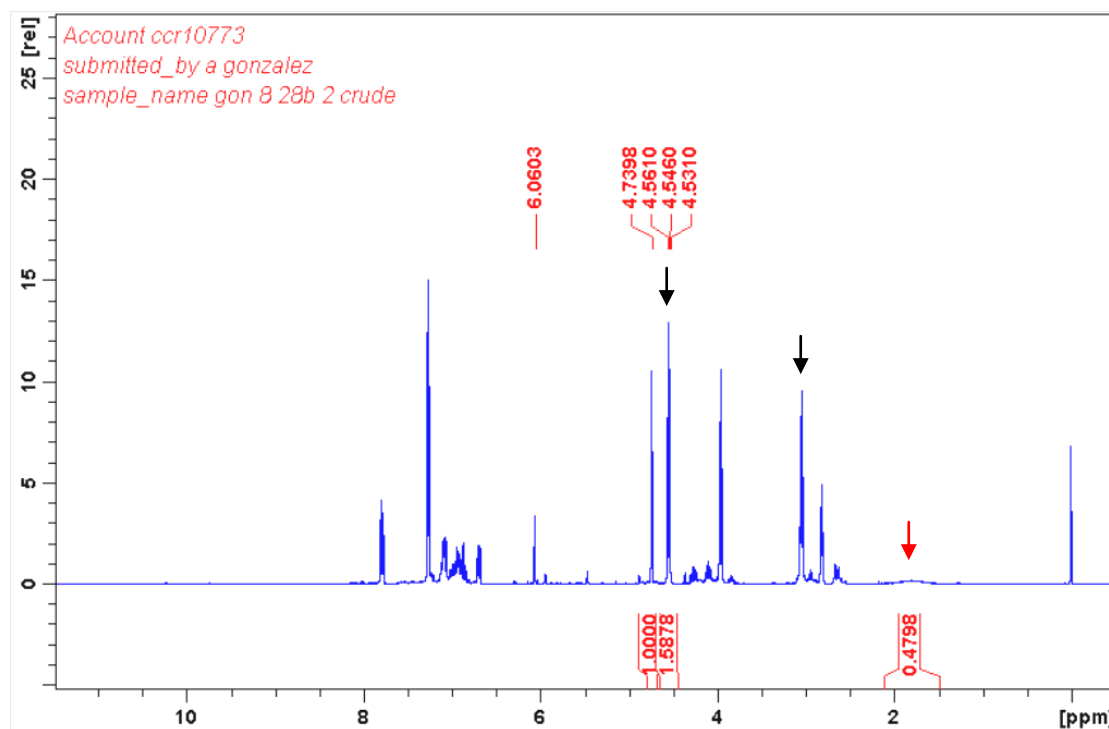
Because iron based catalysts that oxidise organic substrates with H<sub>2</sub>O<sub>2</sub> as oxidant generate H<sub>2</sub>O as sole byproduct, the possibility of water formation during the Fe(OTf)<sub>2</sub>L1 catalysed oxidation reaction was next examined. To determine whether water formation occurs during the initial formation of the peroxide intermediate, phthalan **28** was oxidised under high dilution conditions to a mixture of the peroxide species **29** and traces of the autooxidation byproduct **31**. Remarkably, quantitative analysis with <sup>1</sup>H NMR showed that no water was formed in the oxidation of **28** to **29** (Scheme 18). Similarly, no water formation was revealed in the completed oxidation of 4-fluoroisochroman **36** to 4-fluoroisochromanone **37** (Scheme 19).

These results in combination with the H<sub>2</sub> formation indicate that unlike common enzymatic oxidations, the oxidation in question proceeds via an unusual, sequential dehydrogenative oxygenation process. In fact, to the best of our knowledge, there appears to be no literature report of oxygenation coupled with dehydrogenation in enzymatic or biomimetic catalysis.



**Scheme 18.** No water byproduct formation was detected during the conversion of the ethereal substrate **28** to the peroxide intermediate **29** in the water calibration experiments.





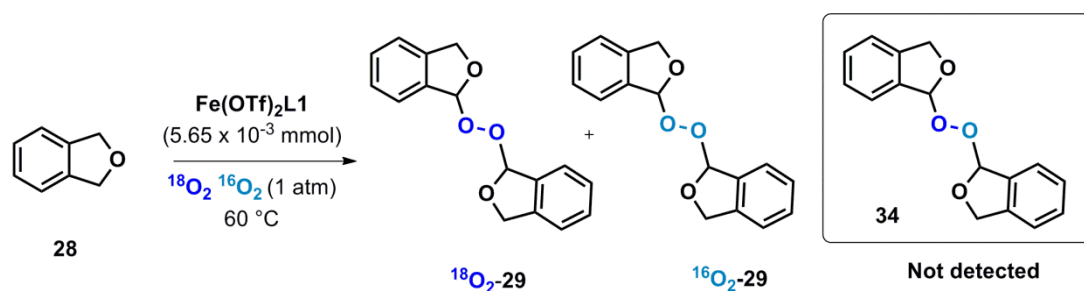
**Scheme 19. Water formation in the conversion of 4-fluoroisochroman to 4-fluoroisochromanone.** On the basis of the calibration, the crude  $^1\text{H}$  NMR above shows no water was formed during the oxidation of 4-fluoroisochroman. The  $^1\text{H}$  NMR resonances corresponding to the methylene protons of chromanone in the crude  $^1\text{H}$  NMR are highlighted with a black arrow whereas the water peak is highlighted under the red arrow.

#### 4.3.13. Isotope labelling experiments

In biomimetic iron complexes capable of undergoing oxidation with  $\text{H}_2\text{O}_2$ , the formation of the active electrophilic iron-oxo oxidant is the result of the peroxide O-O bond cleavage, in which a molecule of water is released as byproduct. Having confirmed that no water formation occurs during the catalytic oxidation and having confirmed that there are radical species involved during the formation of the peroxide intermediate, the origin of the O-O bond of the peroxide intermediate was next investigated by isotopic labelling experiments.

Thus, the oxidation of phthalan **28** to 1,1'-peroxybis(1,3-dihydroisobenzofuran) with a mixture of  $^{18}\text{O}_2$  and  $^{16}\text{O}_2$  afforded  $^{16}\text{O}$ - $^{16}\text{O}$  and  $^{18}\text{O}$ - $^{18}\text{O}$  containing peroxides; however, no cross-over  $^{16}\text{O}$ - $^{18}\text{O}$  peroxy species were detected in the MS analysis (Scheme 20). The

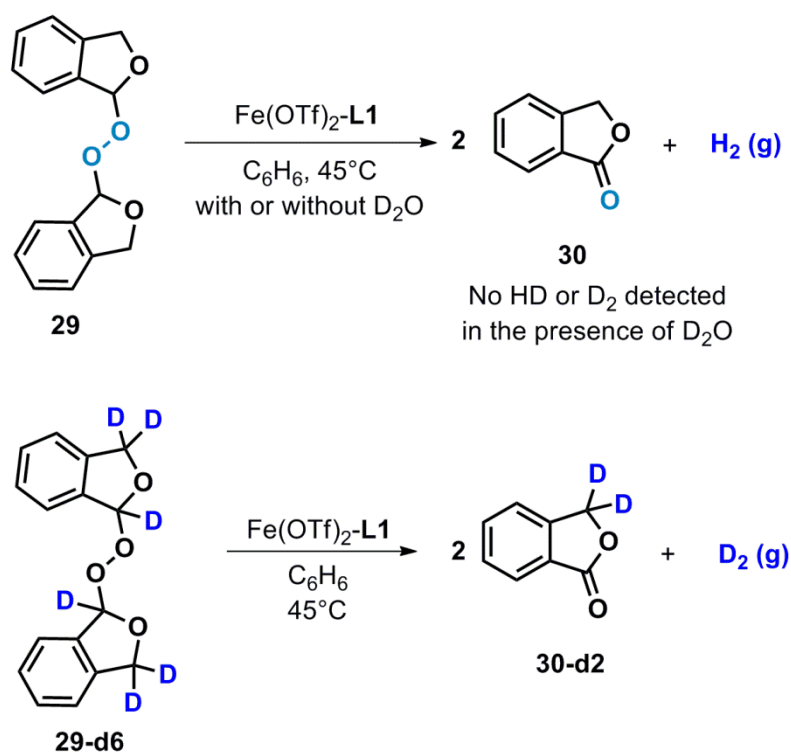
preservation of the O-O bond in the formation of the peroxide suggests that an iron-oxo intermediate is not involved in the oxidation mediated by  $\text{Fe}(\text{OTf})_2\text{L1}$ .



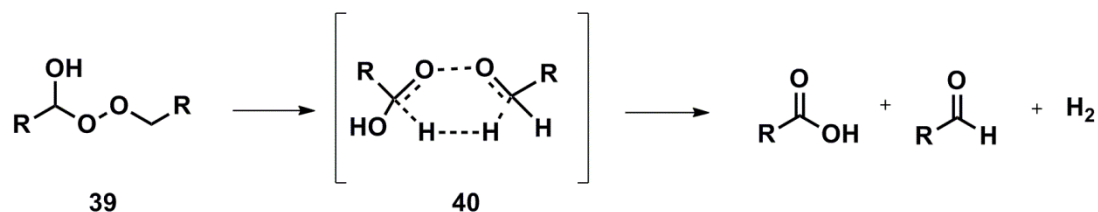
**Scheme 20.** No observation of cross-over peroxide products during the formation of the peroxide intermediate indicates that the O-O bond comes from a single dioxygen molecule

#### 4.3.14. H/D exchange experiments

Having confirmed the formation of hydrogen gas in both steps, obtaining additional data that could shed light on the mechanism of the oxidation reaction was aimed by performing H/D exchange experiments. The cleavage of the peroxide **29** to give off H<sub>2</sub> (Scheme 17) could involve a Fe-H hydride intermediate. Likewise, a Fe-D deuteride may form in the case of the deuterium-labelled peroxide **29-d6**, which afforded D<sub>2</sub>. And if so, it is likely that the iron hydride may undergo H-D exchange with D<sub>2</sub>O. However, no HD or D<sub>2</sub> formation was observed when the oxidation of **29** to **30** was performed in the presence of D<sub>2</sub>O (Scheme 21). We noted that kinetic studies of the pyrolysis of 1-hydroxyalkyl alkyl peroxide **39** are consistent with the formation of H<sub>2</sub> gas as a result of a cyclic concerted mechanism.<sup>13</sup> In this study, a radical-cage mechanism is proposed in which the homolytic O-O cleavage results in the formation of two radical species that can react with each other at a much higher rate than with solvent molecules according to the principles of primary recombination of radicals<sup>14</sup> (Scheme 22). Therefore, no HD or D<sub>2</sub> evolution is observed when undergoing the same reaction in the presence of deuterated species.

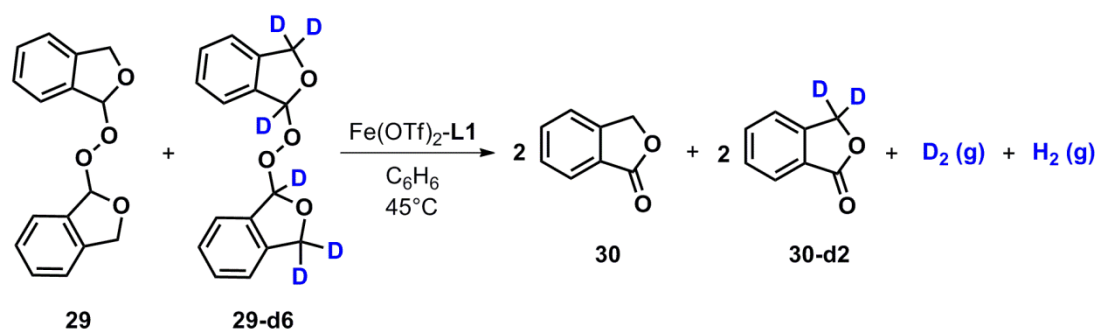


**Scheme 21.** Deuterium labeling experiments revealing no HD or  $D_2$  formation in the dehydrogenation of **29** in the presence of  $D_2O$ .



**Scheme 22.** Radical cage mechanism proposed to explain the  $H_2$  release during the pyrolysis of 1-hydroxyalkyl alkyl peroxides.

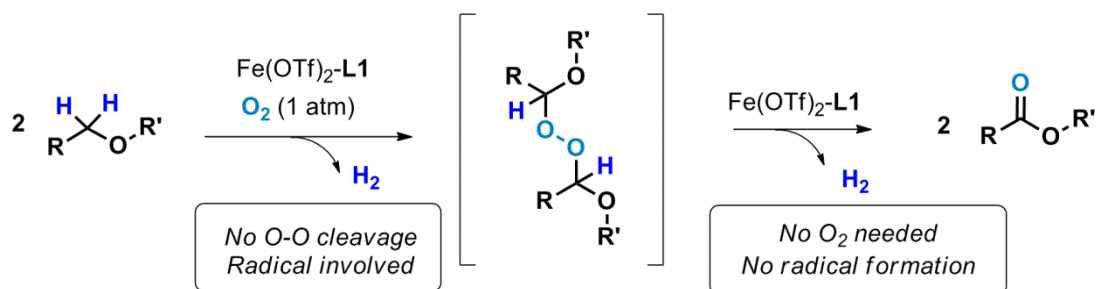
To gain further insight into the conversion of the peroxide intermediate to the ester product, a mixture of peroxides **29** and **29-d6** was exposed to the  $\text{Fe(OTf)}_2\text{-L1}$  catalyst (Scheme 23). GC-MS monitoring of the reaction revealed the exclusive formation of  $H_2$  and  $D_2$ , suggesting that the cleavage of the peroxide is likely to occur within the coordination sphere of the iron center, involving no free alkoxide ion or free alkoxy radical in the solution.



**Scheme 23.** No HD formation was observed in the reaction of a mixture of **29** and **29-d6**.

#### 4.3.15. Postulated mechanism

The experimental evidence collected point to the  $\text{Fe(OTf)}_2\text{-L1}$  catalysed  $\alpha$ -oxidation of ethers follows an unprecedented tandem dehydrogenative-oxygenation process involving the formation of a peroxide intermediate, and the peroxide cleavage appears to be the turnover-limiting step of the catalytic process (Scheme 24).



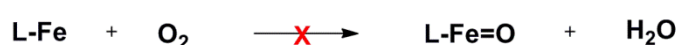
**Scheme 24.**  $\text{Fe(OTf)}_2\text{-L1}$  catalysed  $\alpha$ -oxidation of ethers *via* a tandem dehydrogenative-oxygenation process.

Even though the formation of the peroxide intermediate is unclear mechanistically, the preservation of the O-O bond in the peroxide species  $^{18}\text{O}_2\text{-29}$  and  $^{16}\text{O}_2\text{-29}$  and the absence of water formation during the oxidation point towards an oxidation process that does not involve the formation of a high valent oxo-iron species as in reported biomimetic iron complexes. In addition, radical trapping experiments and the excellent chemoselectivity observed in the substrate scope suggest that no autooxidation or freely diffusing radical processes are involved during the oxidation reaction. Iron-induced CH activation of the

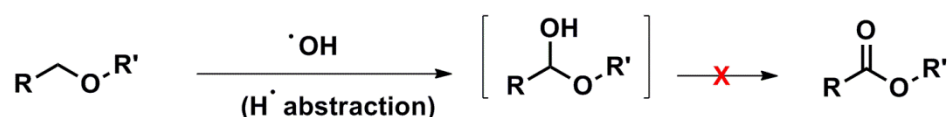


ethereal substrate followed by O<sub>2</sub> attack appears also unlikely<sup>15</sup> due to instability of metalated ethers and the easy formation of cleavage products.<sup>16</sup> This is particularly the case of cyclic ethers like THF as metalation at the  $\alpha$ -position localises a significantly high negative charge on the  $\alpha$ -carbon adjacent to the electron rich oxygen atom causing significant destabilisation that can lead to ring opening (Scheme 25). Thus, such reactivity contradicts with the excellent mass balance observed in the substrate scope.

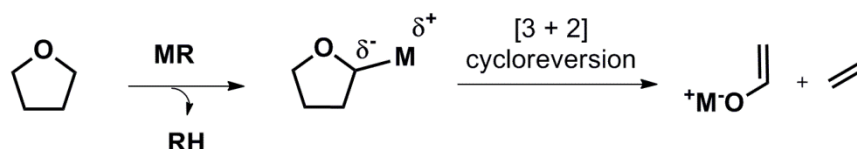
#### Formation of iron-oxo species



#### Radical CH cleavage (Fenton type)



#### Metalation of the ethereal substrate

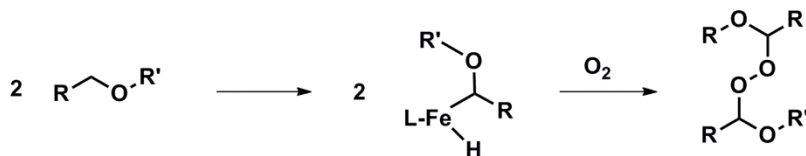


**Scheme 25.** Possible pathways that are in disagreement with experimental observations

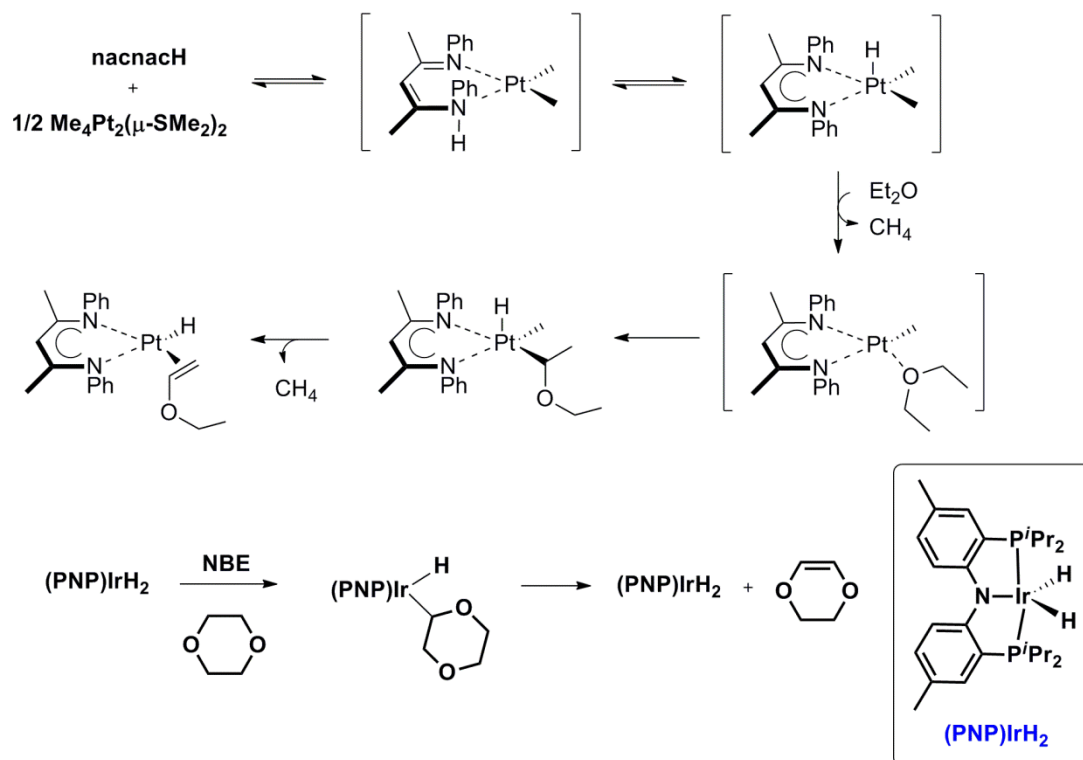
Therefore, a non-classical C-H activation of the ethereal substrate by the Fe(OTf)<sub>2</sub>L1 catalyst was considered as a possible starting point in the formation of the peroxide intermediate (Scheme 26). Support for this hypothetical mechanism is also found in the literature as the CH activation of ethers via the classic  $\beta$ -hydrogen ( $\alpha$ - to the oxygen) elimination following the ether coordination to a metal is known; For instance,  $\beta$ -imidato complexes of Pt were found capable of activating CH bonds of simple ethers such as THF and Et<sub>2</sub>O and induce their subsequent dehydrogenation via  $\beta$ -hydride elimination.<sup>17</sup> Similarly, the amidophosphine pincer (PNP)Ir complexes, where PNP = [N(2-P<sup>i</sup>Pr<sub>2</sub>-4-

$\text{MeC}_6\text{H}_3)_2\text{]}^-$ , was found to dehydrogenate  $\text{Et}_2\text{O}$  and 1,4-dioxane to their vinyl ethers form via an analogue CH activation/ $\beta$ -hydride elimination sequence.<sup>18</sup>

#### Possible non-classical CH activation?



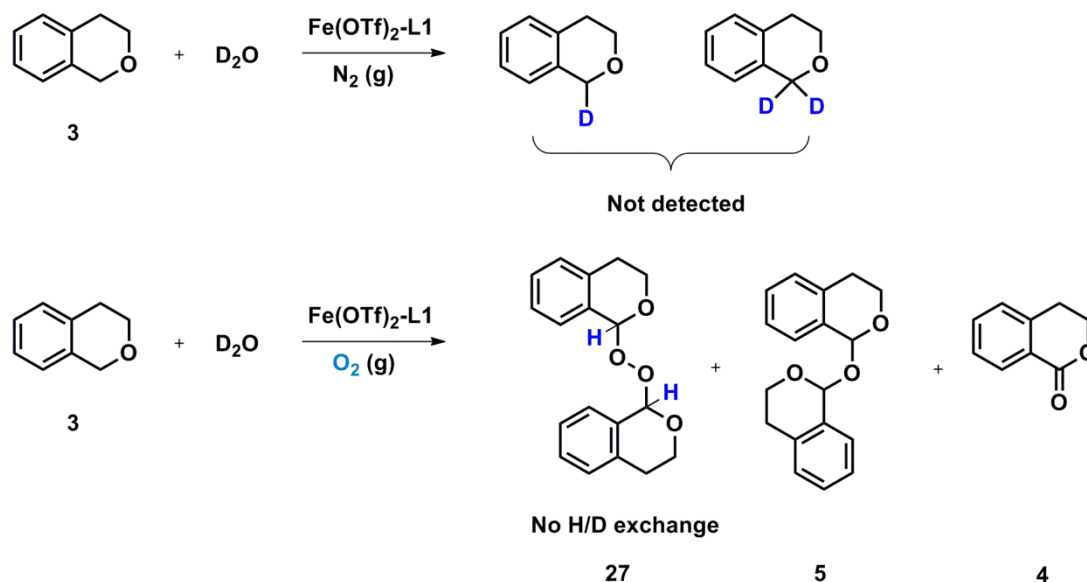
#### Transition metal-mediated CH activation and dehydrogenation of ethers



**Scheme 26.** Possible pathways to explain the formation of the peroxide intermediate

In order to gain evidence of whether the  $\text{Fe}(\text{OTf})_2\mathbf{L1}$  complex is capable of promoting CH activation, some additional H/D exchange experiments were performed. Initially, when isochroman **3** was treated with the  $\text{Fe}(\text{OTf})_2\mathbf{L1}$  complex in the presence of small amounts of  $\text{D}_2\text{O}$  under an inert atmosphere no H/D exchange was observed by  $^1\text{H}$  NMR. This result suggests that the iron complex cannot undergo CH activation of the ethereal substrate conditions when exposed to  $\text{N}_2$ . When the same experiment was performed under aerobic atmosphere, formation of peroxide **27**, lactone **4** and oxidation dimer **5** products was

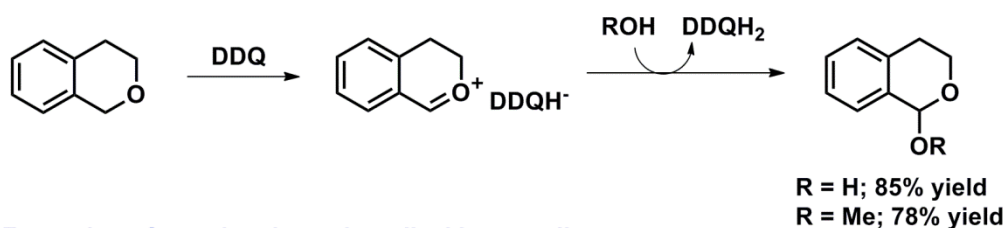
observed in the presence of D<sub>2</sub>O. Nonetheless, <sup>1</sup>H NMR analyses revealed no H/D exchange either in the unreacted isochroman **3** or in the peroxide species **27** (Scheme 27). These results are not consistent with the iron catalyst being capable of forming the peroxide species by inducing an initial anaerobic breakage of the CH bond of the ethereal substrate.



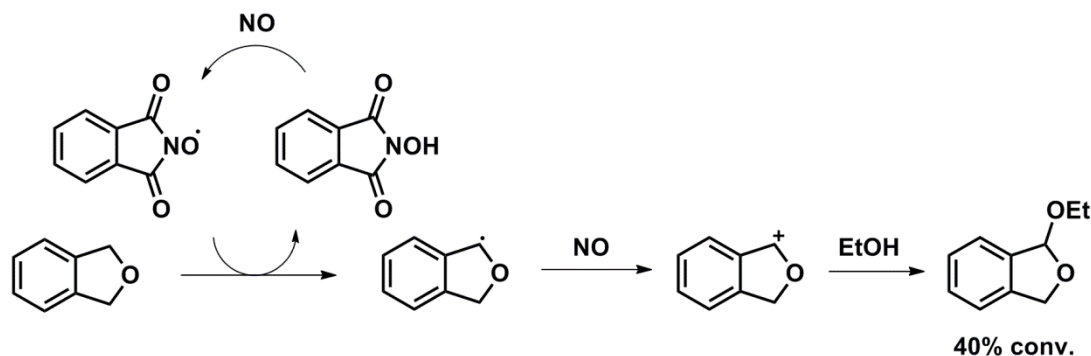
**Scheme 27.** Additional H/D exchange experiments which suggest no C-H activation of the ethereal substrate by the iron complex

The generation of oxonium ions from ethereal substrates under the reaction conditions was also postulated, as some isochroman and phthalan oxidations to esters have been reported to involve the formation of oxonium ions *via* hydride abstraction<sup>19</sup> or *via* a radical formation<sup>20</sup> (Scheme 28). Oxonium ions can be easily trapped by nucleophiles such as water or alcohols;<sup>19,20</sup> however, no lactol formation was observed when the isochroman **3a** was oxidized in the presence of H<sub>2</sub>O or D<sub>2</sub>O (Scheme 27). These results suggest that oxonium ions are not generated during the iron-catalysed oxygenation of ethers.

## Formation of oxonium ions via hydride abstraction



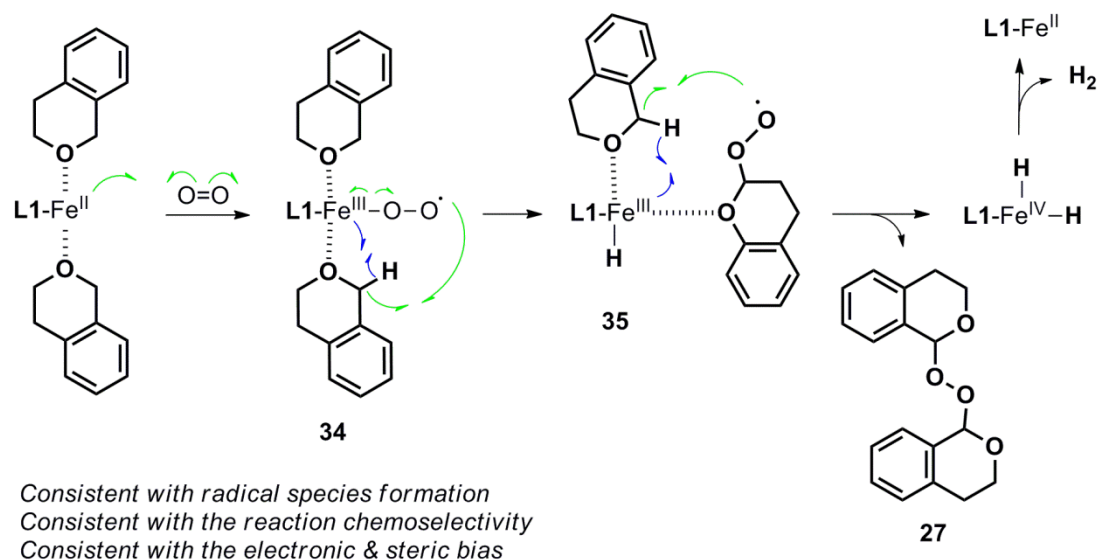
## Formation of oxonium ions via radical intermediates



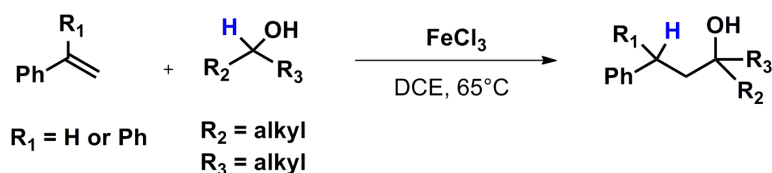
**Scheme 28.** Formation of oxonium ions and their trapping with nucleophiles

Considering the coordination mode of  $[\text{FeL1}(\text{THF})(\text{OTf})_2]$  and particularly the short Fe-O3 (THF) distance (see chapter 3), we hypothesized that under the reaction conditions, the iron complex may coordinate to one or two etheral substrates. Exposure to  $\text{O}_2$  atmosphere would easily result in the formation of a  $\text{Fe}^{\text{III}}$  superoxo species **16** in a similar fashion as with metalloenzymes<sup>3a</sup> and related biomimetics.<sup>21</sup> The  $\text{Fe}^{\text{III}}$  superoxo species could initiate the cleavage of the  $\alpha$ -CH bond of the Fe-bound ether substrate; hydrogen atom transfer to the  $\text{Fe}^{\text{III}}$  center followed by, or concurrent with, the attack of the superoxo radical at the  $\alpha$ -carbon leads to a radical-ligated  $\text{Fe}^{\text{III}}$ -H hydride or a tight hydride-radical pair **17** (Scheme 28). From the species **17**, a second hydrogen atom transfer and radical combination affords **12** and a  $\text{Fe}^{\text{IV}}\text{-(H)}_2$  dihydride, which undergoes reductive elimination to give off  $\text{H}_2$ . This hypothetical mechanism is consistent with the presence of radical species, the high chemoselectivity of the oxidation, and the strong electronic as well as steric bias manifested in the substrate scope. Support for the mechanism is also found in the literature. In particular, hydrogen transfer from a  $\text{sp}^3$  carbon  $\alpha$  to oxygen followed by the formation of  $\text{Fe}^{\text{IV}}\text{-H}$  hydride-radical pair has been suggested for the coupling of alcohols with alkenes<sup>22</sup>

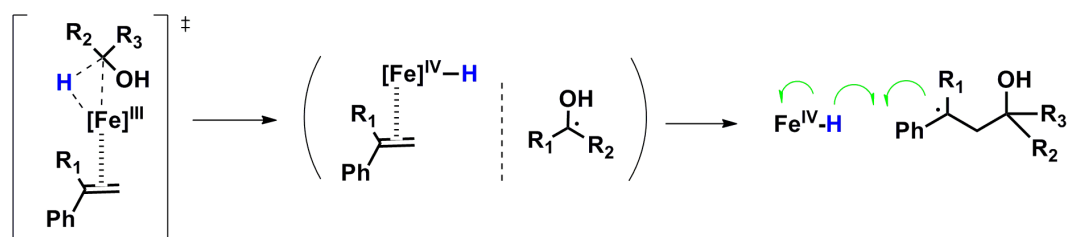
(Scheme 29). Many transition metals, including  $\text{Fe}^{\text{IV}}$ , are known to form metal-dihydride and metal-dihydrogen complexes, from which hydrogen release can occur.<sup>23</sup>



**Scheme 28.** Hypothetic formation of the peroxide intermediate



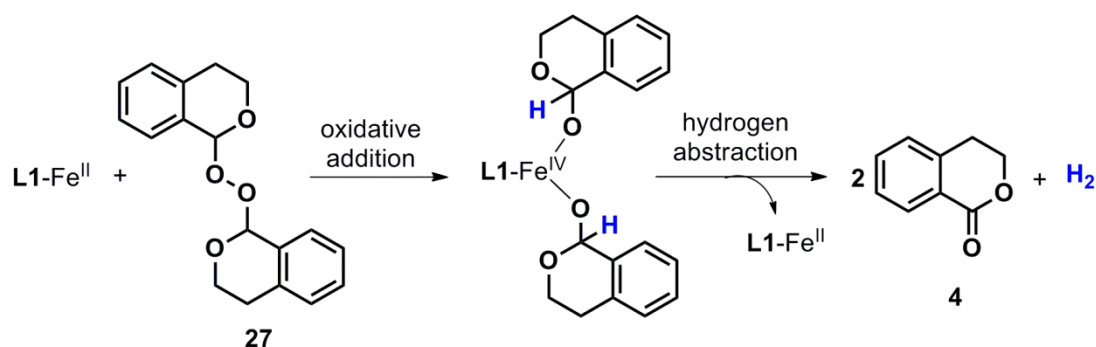
*Proposed mechanism*



**Scheme 29.** Coupling of styrenes with alcohols by the postulated formation of a  $\text{Fe}^{\text{IV}}\text{-H}$  hydride-radical pair

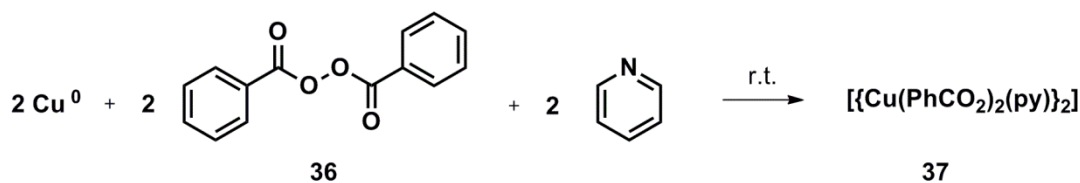
The cleavage of the peroxy bond to form the ester product could proceed via the oxidative addition of the peroxide on the Fe centre followed by  $\beta$ -hydrogen abstraction, giving off  $\text{H}_2$  (Scheme 30). It is known that metal complexes of  $\text{Pt}^{24}$  and  $\text{Cu}^{25}$  can undergo oxidative addition of benzoyl peroxides via O-O bond cleavage (Scheme 31). This cleavage may

involve polar addition of the RO-OR bond to a metal center generating a  $M^+-OR$  cation and a  $RO^-$  anion, or concerted non-polar addition of the peroxide bond to give two M-OR bonds, or a radical mechanism giving rise to a  $M^{\cdot}-OR$  and a  $RO^{\cdot}$  radical.<sup>26</sup> Since the oxidation with  $Fe(OTf)_2$ -**L1** results in no formation of HD (Scheme 23), it readily takes place in non-polar solvents such as benzene, and the catalytic conversion of **12** to **4a** is insensitive to radical inhibitors, the oxidative addition of the peroxide to the iron catalyst is likely to proceed via the concerted pathway.

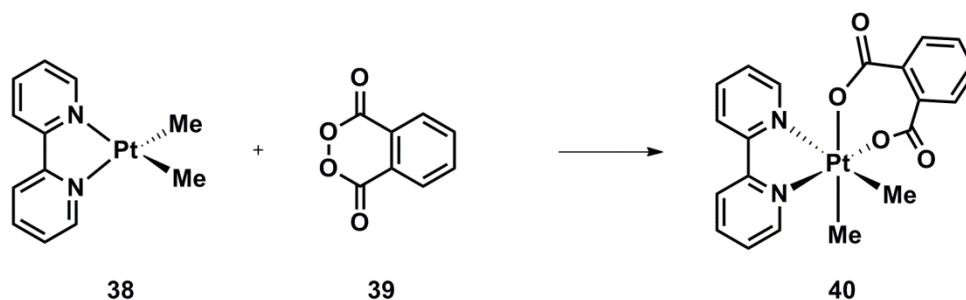


**Scheme 30.** Conversion of **27** to **4** via a hypothetical oxidative addition – hydrogen abstraction sequence

#### Oxidative addition of dibenzoyl peroxide on elemental Cu

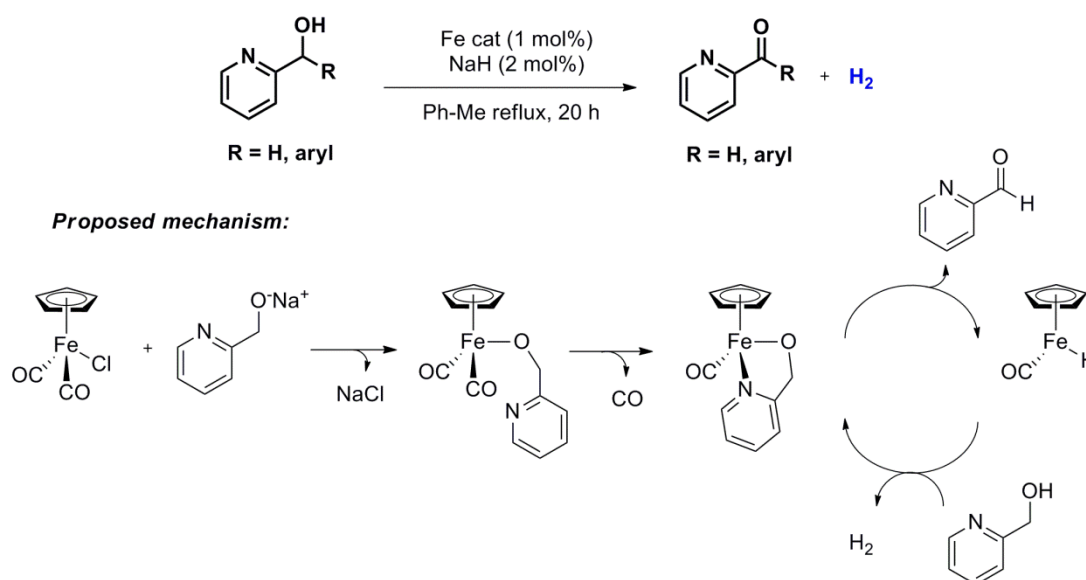


#### Oxidative addition of phthaloyl peroxide on dimethyl Pt complexes



**Scheme 31.** Oxidative addition of peroxides on transition metals

Bearing in mind the observations made with the isotope labeling, the dehydrogenation step shown in Scheme 23 may involve consecutive  $\beta$ -hydrogen migration to the iron followed by fast reductive elimination to release  $\text{H}_2$ . Literature examples are known of hydrogen abstract from iron-alkoxo species, leading to dehydrogenation including release of  $\text{H}_2$ , in catalysis by both metal complexes and enzymes.<sup>27</sup> For instance, an iron piano-stool complex has recently been applied to the dehydrogenation of pyridyl alcohols with concomitant formation of  $\text{H}_2$  gas (Scheme 32). A mechanism involving the  $\beta$ -hydride elimination from an intermediate iron-alkoxo species was postulated. In addition, under pyrolytic conditions, hydroxyl<sup>28</sup> and bis-hydroxyalkyl<sup>29</sup> peroxides can give off hydrogen gas.

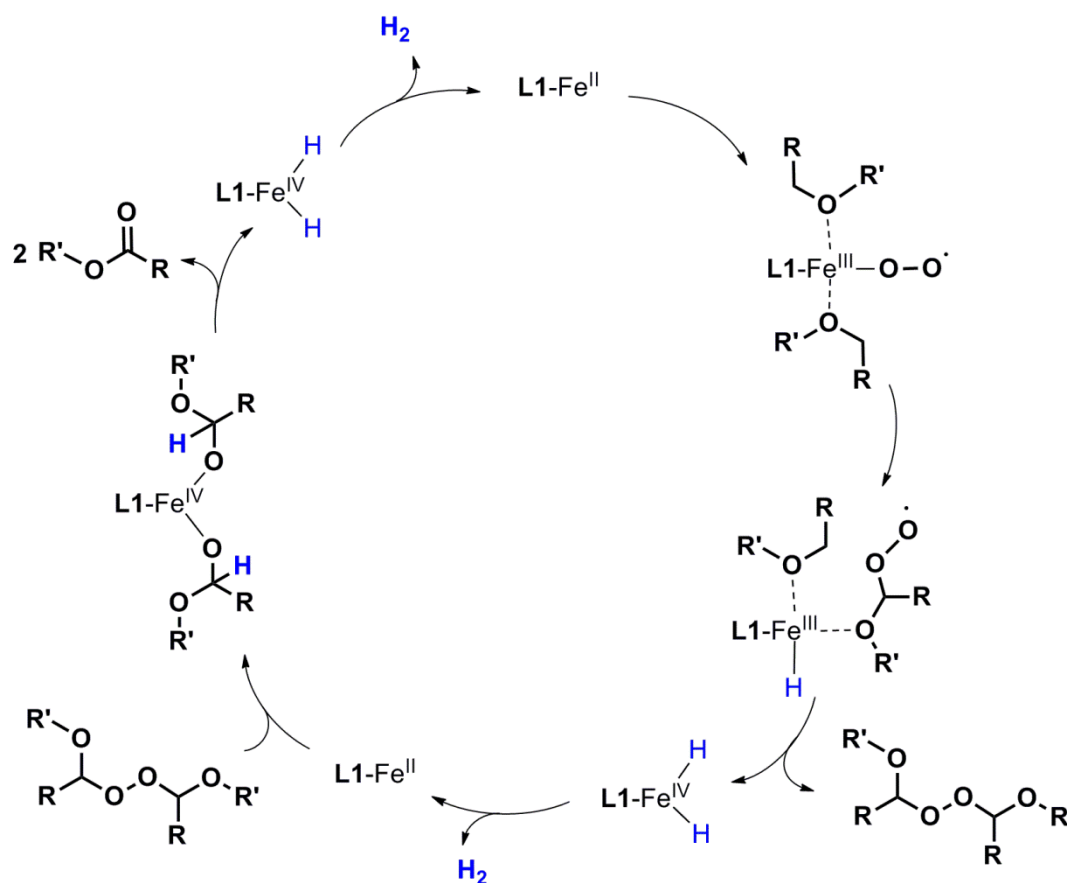


**Scheme 32.** Iron-catalysed dehydrogenation of pyridyl alcohols via hydride elimination from an iron-alkoxo intermediate species

#### 4.3.16. Catalytic cycle

On the basis of these mechanistic investigations, a catalytic cycle involving the inner-sphere formation of a peroxide intermediate via the attack of an iron-superoxo radical at coordinated ethers is postulated (Scheme 33). Subsequent conversion of the isolable peroxide intermediate to the ester product may proceed through a concerted oxidative

addition-hydrogen abstraction sequence. The release of  $\text{H}_2$  is likely to be a result of fast reductive elimination of hydrides at a  $\text{Fe}^{\text{IV}}$  center.



**Scheme 33.** Proposed catalytic cycle for the  $\text{Fe}(\text{OTf})_2\text{-L1}$  catalyzed aerobic oxidation of ethers to esters.

#### 4.4. Conclusions

In conclusion, evidence of an unconventional oxidation mechanism has been found. Molecular oxygen is activated without initial O-O cleavage to form an oxo-iron species and the unprecedented release of  $\text{H}_2$  gas as the sole byproduct of the whole transformation is identified. The mechanistic studies also explain the reasons behind the sharp electronic effect and unprecedented chemoselectivity and functional group tolerance of this family of iron catalysts discussed in Chapter 3. We anticipate that these mechanistic studies may inspire new thinking in understanding and mimicking iron-based mono and di-oxygenases.



## 4.5. Experimental section

### 4.5.1. Radical trapping experiments: General procedure

In a Radley's tube equipped with a magnetic stir bar ligand **L1** ( $5.67 \times 10^{-3}$  mmol, 5.2 mg) and  $\text{Fe}(\text{OTf})_2$  ( $5.65 \times 10^{-3}$  mmol, 2.0 mg) were added. The tube was sealed, degassed (3 times) and left under an inert atmosphere. Isochroman (2.0 mL) was added by syringe and the reaction mixture was stirred under  $\text{N}_2$  atmosphere for 30 min at  $35^\circ\text{C}$ . Next, the corresponding amount of radical trapping agent was added and the tube charged with  $\text{O}_2$  gas and kept under  $\text{O}_2$  (1 atm) by using a balloon. The reaction mixture was then heated up to  $60^\circ\text{C}$  and allowed to react overnight. Product formation was determined by  $^1\text{H}$  NMR conversion and isolated yield after purification by silica gel flash column chromatography. Apart from possible radical reactions, the observed inhibition may also stem from interaction of the radical trap with the iron centre.

### 4.5.2. Intercepting radical trap adducts: oxidation of 3-methyl-3,4-dihydro-1*H*-isochromene-5,8-dione

#### 4.5.2.1 Procedure for the oxidation of 3-methyl-3,4-dihydro-1*H*-isochromene-5,8-dione

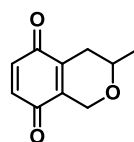
Ligand **L1** ( $5.67 \times 10^{-3}$  mmol, 5.2 mg) and  $\text{Fe}(\text{OTf})_2$  ( $5.65 \times 10^{-3}$  mmol, 2.0 mg) were placed in a Radley's tube equipped with a magnetic stir bar. The tube was degassed (3 times) and placed under  $\text{N}_2$  atmosphere and  $\text{C}_6\text{H}_6$  (0.5 mL) was added by syringe. The catalyst was formed *in situ* after stirring the reaction mixture for 30 min at  $35^\circ\text{C}$ . Then, 3-methyl-3,4-dihydro-1*H*-isochromene-5,8-dione (1.2 g) and  $\text{C}_6\text{H}_6$  (0.2 mL) were added and the Radley's tube heated to  $50^\circ\text{C}$  for a few minutes (until complete solution of the substrate). The tube was degassed and charged with  $\text{O}_2$  and kept under  $\text{O}_2$  (1 atm) with a balloon. The mixture was allowed to react at  $60^\circ\text{C}$  for 24 h with two other additions of  $\text{C}_6\text{H}_6$  (0.2 mL) done after 6 and 18 h. Product formation was determined by  $^1\text{H}$  NMR conversion and isolated yield after silica gel flash column chromatography purification (Hexane/AcOEt, 7/1 to 4/1).

#### 4.5.2.2. Synthesis of 3-methyl-3,4-dihydro-1*H*-isochromene-5,8-dione

3-Methyl-3,4-dihydro-1*H*-isochromene-5,8-dione was synthesised according to the literature by smooth oxidation of 5,8-dimethoxy-3-methylisochroman with CAN.<sup>30</sup>

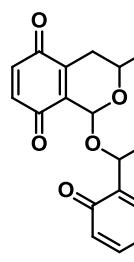
#### Analytical data

##### 3-methyl-3,4-dihydro-1*H*-isochromene-5,8-dione<sup>30</sup> (13)



Tanned solid, 98% isol. yield. <sup>1</sup>H NMR (400 MHz, CDCl<sub>3</sub>): δ (ppm) = 6.65 (dd, J = 10.0, 8.4 Hz, 2H), 4.34 (dd, J = 18.4, 2.4 Hz, 1H), 4.33 (ddd, J = 7.6, 4.4, 3.6 Hz, 1H), 3.61-3.53 (m, 1H), 2.54-2.48 (m, 1H), 2.15-2.12 (m, 1H), 1.28 (d, J = 7.0 Hz, 3H). <sup>13</sup>C NMR (100 MHz, CDCl<sub>3</sub>): δ (ppm) = 186.4, 186.2, 140.7, 140.0, 136.8, 136.5, 69.9, 63.2, 29.3, 21.5.

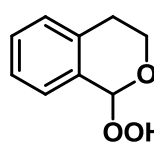
##### 1,1'-oxybis(3-methyl-3,4-dihydro-1*H*-isochromene-5,8-dione) (14)



White solid, 5% isolated yield. <sup>1</sup>H NMR (400 MHz, CDCl<sub>3</sub>): δ (ppm) = 6.68 (d, J = 4.5 Hz, 2H), 6.63 (d, J = 4.8 Hz, 2H), 5.97 (s, 2H), 4.33-4.25 (m, 2H), 2.54 (dd, J = 19.6, 3.6 Hz, 2H), 2.18-2.12 (m, 2H), 1.49 (s, 3H), 1.48 (s, 3H). <sup>13</sup>C NMR (100 MHz, CDCl<sub>3</sub>): δ (ppm) = 186.9, 185.2, 142.8, 137.4, 136.7, 136.5, 87.6, 63.6, 29.1, 21.0. IR (ATR) ν = 1654, 1594, 1450, 1403, 1299, 1261, 1145, 1128, 1062, 1002, 962, 848, 808, 740. HRMS (EI) m/z calc'd C<sub>20</sub>H<sub>19</sub>O<sub>7</sub> [M+H]<sup>+</sup>: 371.1125, found: 371.1120.

#### 4.5.3. Effect of a radical initiator: General procedure

In a Radley's tube equipped with a magnetic stir bar ligand **L1** ( $5.67 \times 10^{-3}$  mmol, 5.2mg) and Fe(OTf)<sub>2</sub> ( $5.65 \times 10^{-3}$  mmol, 2.0 mg) were added. The tube was sealed, degassed (3 times) and left under inert atmosphere. Isochroman (2.0 mL) was added by syringe and the reaction mixture was stirred under N<sub>2</sub> atmosphere for 30 min at r.t. Next, radical initiator benzoyl peroxide (0.02 mmol) was added and the tube was degassed and charged with O<sub>2</sub> and kept under O<sub>2</sub> (1 atm) with a balloon. The reaction mixture was stirred at 35 °C overnight and product formation was determined by <sup>1</sup>H NMR and isolated yield after purification by silica gel flash column chromatography. The same procedure was repeated in the absence of ligand, benzoyl peroxide and catalyst.

**Analytical data of the isolated isochroman hydroperoxide<sup>31</sup>**

Colourless liquid. <sup>1</sup>H NMR (400 MHz, CDCl<sub>3</sub>): δ (ppm) = 9.01 (bs, 1H), 7.43-7.14 (m, 4H), 6.06 (s, 1H), 4.21-4.14 (m, 1H), 4.07-3.99 (m, 1H), 3.11-3.02 (m, 1H), 2.62 (dd, J = 16.6, 2.2 Hz, 1H). <sup>13</sup>C NMR (100 MHz, CDCl<sub>3</sub>): δ (ppm) = 135.6, 129.3, 128.9, 126.9, 101.1, 58.8, 28.2. IR (ATR) ν = 3328, 2940, 2888, 1489, 1453, 1423, 1386, 1312, 1275, 1197, 1083, 1057, 1002, 983, 954, 902, 851, 769, 747, 680, 621, 599. HRMS (EI) m/z calc'd C<sub>9</sub>H<sub>11</sub>O<sub>3</sub> [M+H]<sup>+</sup>: 167.0703, found: 167.0708.

**4.5.4. Oxidation of a radical clock****4.5.4.1. Fe(OTf)<sub>2</sub>L1 catalyzed oxidation of the radical clock**

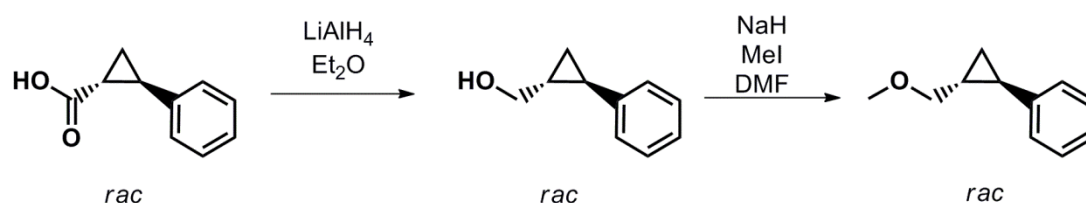
In a Radley's tube equipped with a magnetic stir bar, **L1** ( $5.67 \times 10^{-3}$  mmol, 5.2 mg) and Fe(OTf)<sub>2</sub> ( $5.65 \times 10^{-3}$  mmol, 2.0 mg) were added. The tube was sealed, degassed (3 times) and left under inert atmosphere. The radical clock (±)-*trans*-(2-methoxymethyl)cyclopropylbenzene<sup>11</sup> (2.0 mL) was added by syringe and the tube was degassed and charged with O<sub>2</sub> and kept under O<sub>2</sub> (1 atm) with a balloon. The mixture was allowed to react at 60 °C overnight and the product formation was determined by <sup>1</sup>H NMR and isolated yield after purification by silica gel flash column chromatography. The same procedure was followed using (1-methoxypropan-2-yl)benzene as substrate.

**4.5.4.2. Radical rock reactivity in the presence of radical initiators**

In a small Schlenk tube equipped with a magnetic stir bar, Luperox (2.0 mg) was added. The tube was sealed, degassed (3 times) and left under inert atmosphere. (±)-*trans*-(2-methoxymethyl)cyclopropylbenzene (50 μL) was added by syringe and the tube was degassed and charged with O<sub>2</sub> and kept under O<sub>2</sub> (1 atm) with a balloon. The mixture was allowed to react at 50 °C overnight and the product formation was determined by <sup>1</sup>H NMR and isolated yield after purification by silica gel flash column chromatography.

#### 4.5.4.3. Synthesis of the ((±)-2-(methoxymethyl)cyclopropyl)benzene substrate

(±)-*trans*-(2-Methoxymethyl)cyclopropyl)benzene was synthesised via reduction of (±)-*trans*-2-phenylcyclopropanecarboxylic acid to its alcohol form followed by its subsequent methylation.<sup>32, 33</sup>



#### (±)-*trans*-(2-Methoxymethyl)cyclopropyl)benzene<sup>34</sup>

Colourless liquid, 92% overall yield. <sup>1</sup>H NMR (400 MHz, CDCl<sub>3</sub>): δ (ppm) = 7.27-7.22 (m, 2H), 7.16-7.12 (m, 1H), 7.08-7.06 (m, 2H), 4.42 (dd, J = 10.4, 6.8 Hz, 1H), 3.38 (s, 3H), 3.36 (dd, J = 10.4, 6.8 Hz, 1H, overlapped), 1.80 (quintet, J = 4.8 Hz, 1H), 1.44-1.37 (m, 1H), 0.99-0.91 (m, 2H). <sup>13</sup>C NMR (100 MHz, CDCl<sub>3</sub>): δ (ppm) = 142.9, 128.7, 126.2, 125.9, 58.7, 22.8, 21.8, 14.3. HRMS (EI) m/z calc'd C<sub>11</sub>H<sub>15</sub>O [M+H]<sup>+</sup>: 163.1118, found: 163.1116.

#### 4.5.4.4. Synthesis of (1-methoxypropan-2-yl)benzene

(±)-(1-methoxypropan-2-yl)benzene was synthesized by methylation of (±)-2-phenylpropan-1-ol.<sup>33</sup>

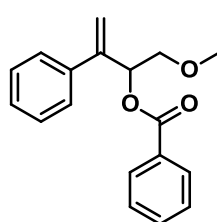
#### (1-Methoxypropan-2-yl)benzene<sup>35</sup>

Colourless liquid, 98% isol. yield. <sup>1</sup>H NMR (400 MHz, CDCl<sub>3</sub>): δ (ppm) = 7.32-7.22 (m, 5H), 3.51 (t, J = 8.8 Hz, 1H), 3.44 (t, J = 8.8 Hz, 1H), 3.33 (s, 3H), 3.03 (q, J = 7.0 Hz, 1H), 1.28 (d, J = 7.0 Hz, 3H). <sup>13</sup>C NMR (100 MHz, CDCl<sub>3</sub>): δ (ppm) = 144.4, 128.4, 127.2, 126.3, 78.7, 58.8, 39.8, 30.9, 18.4. HRMS (EI) m/z calc'd C<sub>9</sub>H<sub>13</sub>O [M+H]<sup>+</sup>: 137.0961, found: 137.0958.

#### 4.5.4.5. Analytical data of the products

##### 1-Methoxy-3-phenylbut-3-en-2-ol

Colorless liquid. <sup>1</sup>H NMR (400 MHz, CDCl<sub>3</sub>): δ (ppm) = 7.44-7.26 (m, 5H), 5.81-5.71 (m, 1H), 5.07 (s, 1H, overlapped), 5.02 (m, 1H, overlapped), 4.16 (t, J = 6.9 Hz, 1H), 3.22 (s, 3H), 2.60-2.53 (m, 1H), 2.44-2.37 (m, 1H). <sup>13</sup>C NMR (100 MHz, CDCl<sub>3</sub>): δ (ppm) = 141.6, 134.3, 128.4, 128.3, 126.7, 116.9, 83.6, 65.6, 42.5. HRMS (EI) m/z calc'd C<sub>10</sub>H<sub>13</sub>O<sub>2</sub> [M+H]<sup>+</sup>: 165.0911, found: 165.0907.

**1-Methoxy-3-phenylbut-3-en-2-yl benzoate**

Colorless liquid.  $^1\text{H NMR}$  (400 MHz,  $\text{CDCl}_3$ ):  $\delta$  (ppm) = 8.12 (d,  $J = 8.0$  Hz, 2H), 7.61-7.58 (m, 1H), 7.5 (m, 2H), 7.44-7.26 (m, 5H, overlapped), 6.09-6.04 (m, 1H), 5.07 (s, 1H, overlapped), 5.03 (t, 1H, overlapped), 3.22 (s, 3H, overlapped), 2.86-2.78 (m, 1H), 2.75-2.63 (m, 1H).

**4.5.5. Isolation of the 1,1'-peroxydiisochroman intermediate**

In a Radley's tube equipped with a magnetic stir bar ligand **L1** ( $5.67 \times 10^{-3}$  mmol, 5.2mg) and  $\text{Fe}(\text{OTf})_2$  ( $5.65 \times 10^{-3}$  mmol, 2.0 mg) were added. The tube was sealed, degassed (3 times) and left under inert atmosphere. Isochroman (1.0 mL) and  $\text{C}_6\text{H}_6$  (2.0 mL) were added by syringe and the tube degassed and charged with  $\text{O}_2$  and kept under  $\text{O}_2$  (1 atm) with a balloon. The reaction mixture was stirred at  $60^\circ\text{C}$  for 1 h or overnight. Then,  $\text{C}_6\text{H}_6$  was removed in vacuo and product formation was determined by  $^1\text{H NMR}$  and isolated yield after purification by silica gel flash column chromatography (Hexane/AcOEt, 12/1 to 4/1). 1,1'-Peroxyisochroman and 1,1'-oxydiisochroman were eluted and crystallized together in  $\text{Et}_2\text{O}$ /Hexane.

**4.5.6. Conversion of 1,1'-peroxyisochroman to chromanone****4.5.6.1. General procedure**

In a small Schlenk tube equipped with a magnetic stirring bar the 1.0:0.56 mixture of 1,1'-peroxyisochroman and 1,1'-oxydiisochroman (250 mg) was dissolved in  $\text{C}_6\text{H}_6$  (300  $\mu\text{L}$ ) under  $\text{N}_2$  atmosphere. An aliquot of the stock solution (100  $\mu\text{L}$ ) was added to a Schlenk tube containing  $[\text{Fe}(\text{OTf})_2\text{L1}]$  (1.2 mg,  $8.94 \times 10^{-4}$  mmol) and the Schlenk tube was degassed and charged with  $\text{O}_2$  (1 atm). The reaction mixture was stirred overnight at  $45^\circ\text{C}$  and the reaction products monitored by  $^1\text{H NMR}$  and isolated yield. The same reaction was performed under air and under  $\text{N}_2$ . The reaction under  $\text{N}_2$  was performed in a glove box with the NMR sample prepared inside the glove box.

#### 4.5.6.2. Reaction in the presence of a radical trapping reagent or a radical initiator

In a small Schlenk tube equipped with a magnetic stirring bar the 1.0:0.56 mixture of 1,1'-peroxyisochroman and 1,1'-oxydiisochroman (250 mg) was dissolved in C<sub>6</sub>H<sub>6</sub> (300 μL) under N<sub>2</sub> atmosphere. An aliquot of this stock solution (100 μL) was added to a Schlenk tube containing [Fe(OTf)<sub>2</sub>L1] (1.0 mg, 7.45 × 10<sup>-4</sup> mmol) and p-benzoquinone (3.5 mg, n(rad trap/cat) : 25/1) or benzoyl peroxide (0.25 mg, 1.03 × 10<sup>-3</sup> mmol). The reaction mixture was degassed (3 times), left under N<sub>2</sub> atmosphere and stirred overnight at 45 °C. The reaction products were monitored by <sup>1</sup>H NMR and isolated yield.

#### 4.5.6.3. Reaction in the presence of an excess of isochroman under inert atmosphere

In a small Schlenk tube equipped with a magnetic stirring bar the 1.0:0.56 mixture of 1,1'-peroxyisochroman and 1,1'-oxydiisochroman (75 mg) was dissolved in isochroman (200 μL) under N<sub>2</sub> atmosphere. An aliquot of this stock solution (110 μL) was added to a Schlenk tube containing [Fe(OTf)<sub>2</sub>L1] (1.0 mg, 7.45 × 10<sup>-4</sup> mmol) under N<sub>2</sub> atmosphere. The reaction mixture was stirred overnight at 45 °C. The reaction products were monitored by <sup>1</sup>H NMR and isolated yield. A second experiment was run by the same procedure in the absence of catalyst.

#### 4.5.7. Effect of the sulfonamide: Comparison between Fe(OTf)<sub>2</sub>PyBisulidine and Fe(OTf)<sub>2</sub>PyBidine in isochroman oxidation

In a Radley's tube equipped with a magnetic stir bar PyBidine ligand L9 (5.67 × 10<sup>-3</sup> mmol, 5.0 mg) and Fe(OTf)<sub>2</sub> (5.65 × 10<sup>-3</sup> mmol, 2.0 mg) were added. The tube was sealed, degassed and left under inert atmosphere (3 times). Isochroman (2.0 mL) was added by syringe and the reaction tube was degassed, charged with dioxygen gas (1 atm, 3 times) and kept under oxygen (1 atm) by using a balloon. The reaction mixture was heated to 60 °C and left overnight. The reaction was purified by silica gel column chromatography

(Hexane/EtOAc, gradient: 10/1 to 4/1) to afford the unreacted starting material and the reaction products.

#### 4.5.8. Selective formation of the peroxide intermediate

In a Radley's tube equipped with a magnetic stir bar ligand **L1** ( $5.67 \times 10^{-3}$  mmol, 5.2mg) and  $\text{Fe}(\text{OTf})_2$  ( $5.65 \times 10^{-3}$  mmol, 2.0 mg) were added. The tube was sealed, degassed (3 times) and left under inert atmosphere. Phthalan (1.0 mL) and  $\text{C}_6\text{H}_6$  (1.5 mL) were added by syringe and the tube degassed and charged with  $\text{O}_2$  and kept under  $\text{O}_2$  (1 atm) with a balloon. The reaction mixture was stirred at  $42^\circ\text{C}$  overnight. Then,  $\text{C}_6\text{H}_6$  was removed in vacuo and product formation was determined by  $^1\text{H}$  NMR and isolated yield after purification by silica gel flash column chromatography (Hexane/AcOEt, 12/1).

#### 4.5.9. Formation of hydroperoxides under high dilution

The reactions were performed according to the procedure specified in section 4.5.6. using 100 mg of the starting 1,1'-oxydiisochroman and 1,1'-peroxydiisochroman mixture in  $\text{C}_6\text{H}_6$  solution (4.5 M).

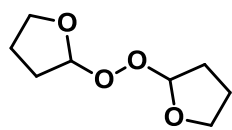
#### 4.5.10. Oxidation of THF to $\gamma$ -butyrolactone: identifying the rate-limiting step

##### 4.5.10.1. General procedure for the isolation of the peroxide intermediate and a byproduct

In a Radley's tube equipped with a magnetic stirring bar,  $\text{Fe}(\text{OTf})_2$  (2.0 mg,  $5.67 \times 10^{-3}$  mmol) and **L1** (5.2 mg,  $5.65 \times 10^{-3}$  mmol) were added. Freshly distilled THF (2.0 mL) was added to the sealed tube by syringe. Next, the tube was degassed and charged with  $\text{O}_2$  (1 atm, 3 times) and kept under excess of  $\text{O}_2$  (1 atm) by using a balloon. The reaction mixture was heated to  $60^\circ\text{C}$  for 24h and the products isolated by flash column chromatography (Hexane/AcOEt, 6/1 to 4/1 to 2/1).

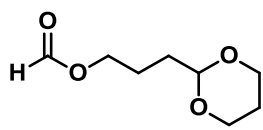
## Analytical data and characterisation of compounds

### 2,2'-peroxybis(tetrahydrofuran)



Colourless liquid, (96% purity).  $^1\text{H NMR}$  (400 MHz,  $\text{CDCl}_3$ ):  $\delta$  (ppm) = 5.68 (dd,  $J = 6.1, 2.0$  Hz, 2H), 3.91-3.88 (m, 4H), 2.03-1.77 (m, 8H).  $^{13}\text{C NMR}$  (100 MHz,  $\text{CDCl}_3$ ):  $\delta$  (ppm) = 108.0, 67.8, 29.9, 24.2. **HRMS** (EI)  $m/z$  calc'd  $\text{C}_8\text{H}_{15}\text{O}_4$   $[\text{M} + \text{H}]^+$ : 175.0965, found: 175.0962.

### 3-(1,3-dioxan-2-yl)propyl formate



Colourless liquid (aprox. 95% purity).  $^1\text{H NMR}$  (400 MHz,  $\text{CDCl}_3$ ):  $\delta$  (ppm) = 8.05 (s, 1H), 4.55 (t,  $J = 6.0$  Hz, 1H), 4.18 (dt,  $J = 6.5, 1.0$  Hz, 2H), 4.12-4.08 (m, 2H), 3.78 (t,  $J = 12$  Hz, 2H), 2.08-2.05 (m, 1H), 1.80-1.75 (m, 2H), 1.70-1.65 (m, 2H), 1.37-1.32 (m, 1H).  $^{13}\text{C NMR}$  (100 MHz,  $\text{CDCl}_3$ ):  $\delta$  (ppm) = 161.5, 101.9, 67.2, 64.1, 31.7, 26.1, 23.4. **IR (ATR)**  $\nu = 2965, 2854, 1720, 1468, 1382, 1174, 1137, 1091, 991, 919, 858$ . **HRMS** (EI)  $m/z$  calc'd  $\text{C}_8\text{H}_{15}\text{O}_4$   $[\text{M} + \text{H}]^+$ : 175.0965, found: 175.0967. **Anal Calc'd** for  $\text{C}_8\text{H}_{14}\text{O}_4$ : C, 55.16, H, 8.10; found: C, 54.99, H, 8.01.

#### 4.5.10.2. Conversion of the peroxide intermediate to $\gamma$ -butyrolactone

In a Schlenk tube equipped with a magnetic stirring bar,  $\text{Fe}(\text{OTf})_2$  (1.0 mg,  $2.85 \times 10^{-3}$  mmol) and L1 (2.6 mg,  $2.85 \times 10^{-3}$  mmol) were added. The tube was degassed (3 times) and placed under  $\text{N}_2$  atmosphere. Next, an isolated mixture of 2,2'-peroxybis(tetrahydrofuran) and other unidentified byproducts (150  $\mu\text{L}$ ) was added and the reaction mixture heated to 60  $^\circ\text{C}$  for 24h. Aliquots of the sample were extracted after 12 and 24 h of reaction and submitted to  $^1\text{H NMR}$  analysis.

#### 4.5.11. Identification and quantification of hydrogen gas in the aerobic oxidation of ethers

##### 4.5.11.1. General procedures for hydrogen identification

##### A. Complete reaction: from phthalan to phthalide

In a Radley's tube equipped with a magnetic stirring bar and a new rubber septum,  $\text{Fe}(\text{OTf})_2$  (0.8 mg,  $2.3 \times 10^{-3}$  mmol), L1 (2.0 mg,  $2.3 \times 10^{-3}$  mmol) and phthalan (0.75 mL) were added. The tube was sealed, degassed and charged with dioxygen gas (1 atm, 3 times) and kept under excess of oxygen (1 atm) by using a balloon. The



reaction mixture was heated to 60 °C and stirred overnight. Next morning the reaction was stopped and cooled to r.t. (23°C). For the GC analysis, a gas syringe was degassed with pure N<sub>2</sub> gas (5 times) and then a sample (300 µL volume) of the gas phase contained inside the sealed Radley's tube was taken and injected in the GC.

**B. First step: from phthalan to 1,1'-peroxybis(1,3-dihydrobenzofuran)**

In a Radley's tube equipped with a magnetic stirring bar and a new rubber septum, Fe(OTf)<sub>2</sub> (2.0 mg, 5.65 x 10<sup>-3</sup> mmol), **L1** (5.2 mg, 5.67 x 10<sup>-3</sup> mmol), phthalan (1.0 mL) and benzene (1.5 mL) were added. The tube was sealed, degassed and charged with dioxygen gas (1 atm, 3 times) and kept under excess of oxygen (1 atm) by using a balloon. The reaction mixture was heated to 42 °C and stirred overnight. Next morning the reaction was stopped and cooled to r.t. (23 °C). For the GC analysis, a gas syringe was degassed with pure N<sub>2</sub> gas (5 times) and then a sample (400 µL volume) of the gas phase contained inside the sealed Radley's tube was taken and injected in the GC.

**C. Second step: from 1,1'-peroxybis(1,3-dihydrobenzofuran) to phthalide**

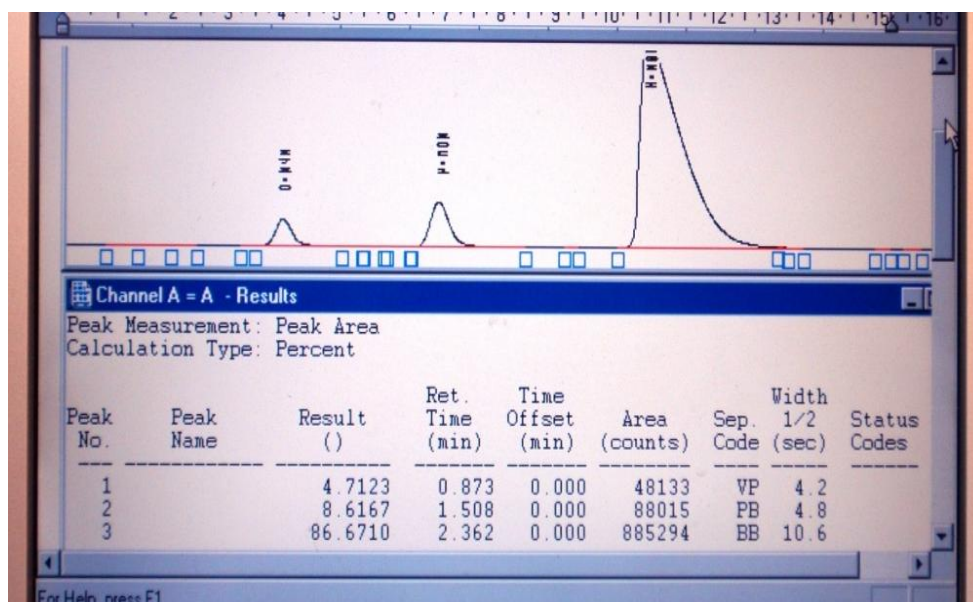
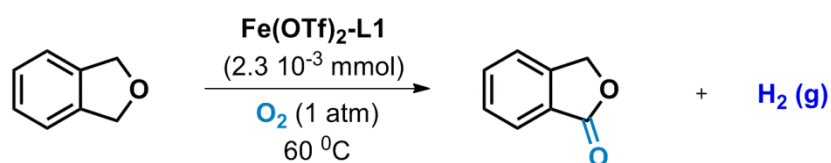
In a Radley's tube equipped with a magnetic stirring bar and a new rubber septum, [Fe(OTf)<sub>2</sub>L1] (1.0 mg, 5.65 x 10<sup>-3</sup> mmol) and 1,1'-peroxybis(1,3-dihydrobenzofuran) (50 mg) and benzene (50 µL) were added. The tube was sealed, degassed and charged with dioxygen gas (1 atm, 3 times) and kept under excess of oxygen (1 atm) by using a balloon. The reaction mixture was heated to 60 °C and stirred overnight. Next morning the reaction was stopped and cooled to r.t. (23 °C). For the GC analysis, a gas syringe was degassed with pure N<sub>2</sub> gas (5 times) and then a sample (400 µL volume) of the gas phase contained inside the sealed Radley's tube was taken and injected into the GC.

#### D. Blank reaction for GC analysis

A Radley's tube equipped with a magnetic stirring bar and a new rubber septum was degassed and charged with dioxygen gas (1 atm, 3 times). A gas syringe was degassed with pure N<sub>2</sub> gas (5 times) and then a sample (300  $\mu$ L volume) of the gas phase contained inside the sealed Radley's tube was taken and injected into the GC.

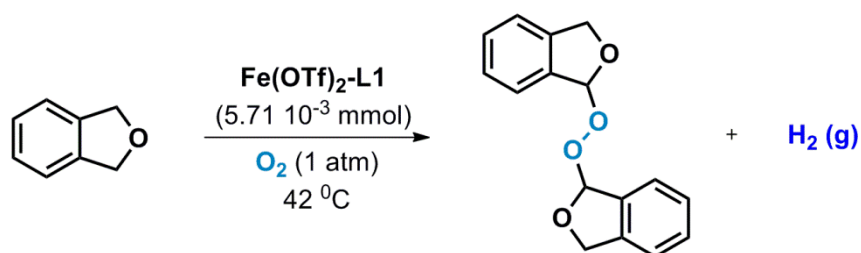
#### 4.5.11.2. Chromatograms collected in the hydrogen identification

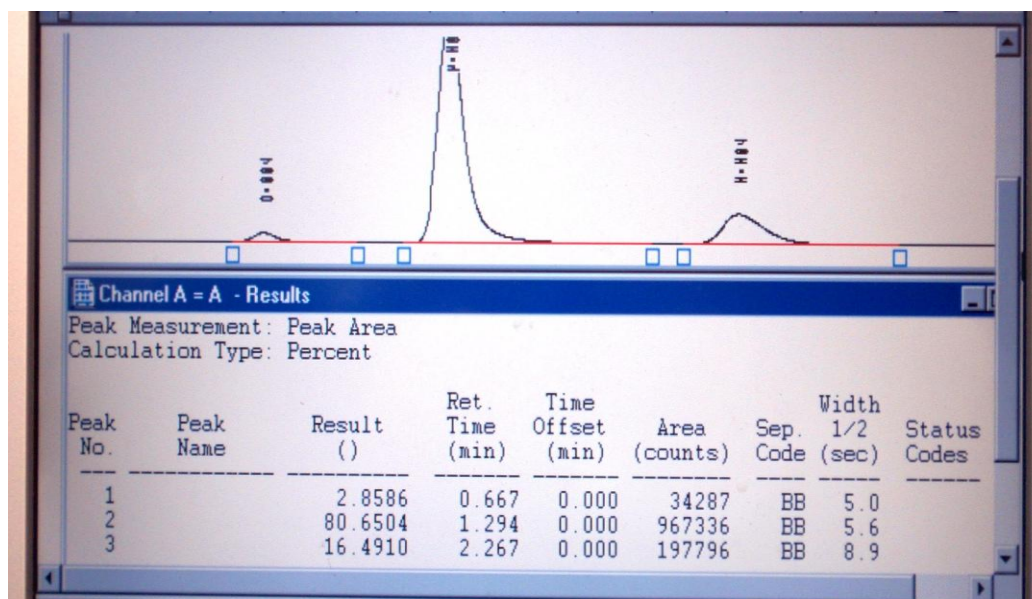
##### A. Complete reaction: from phthalan to phthalide



**Retention times:** rt (H<sub>2</sub>): 0.873, rt (N<sub>2</sub>): 1.508, rt (O<sub>2</sub>): 2.362

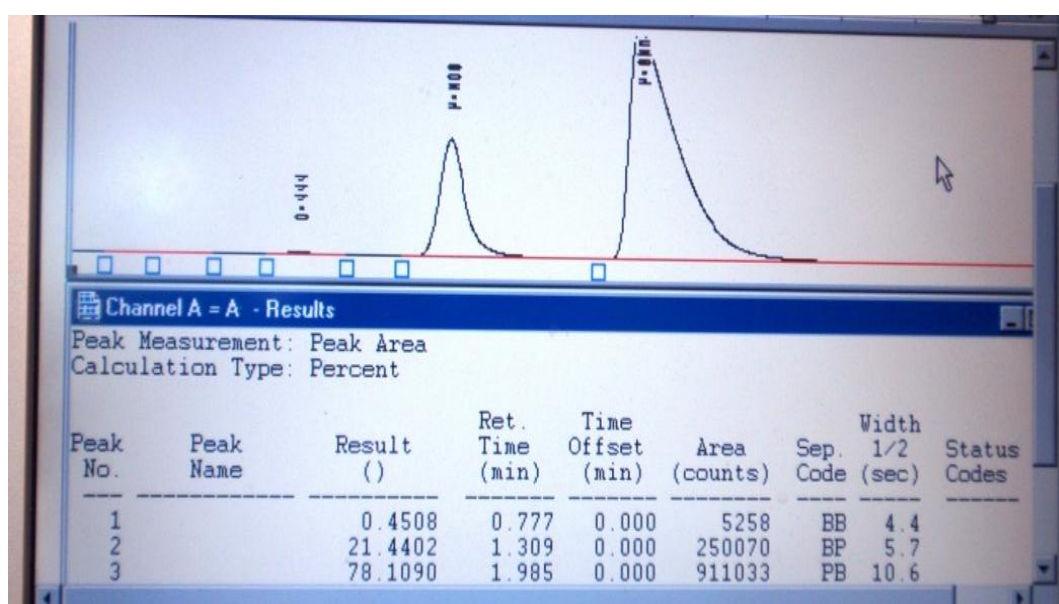
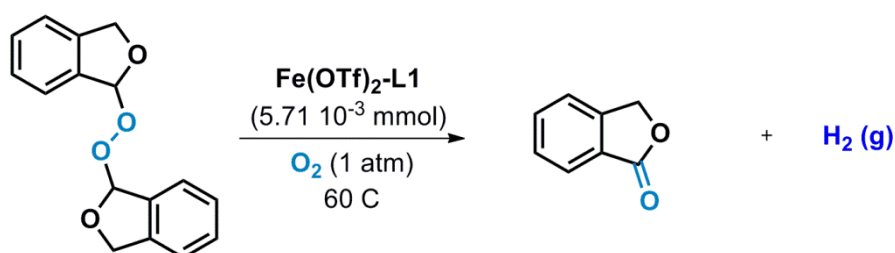
##### B. First step: from phthalan to 1,1'-peroxybis(1,3-dihydrobenzofuran)





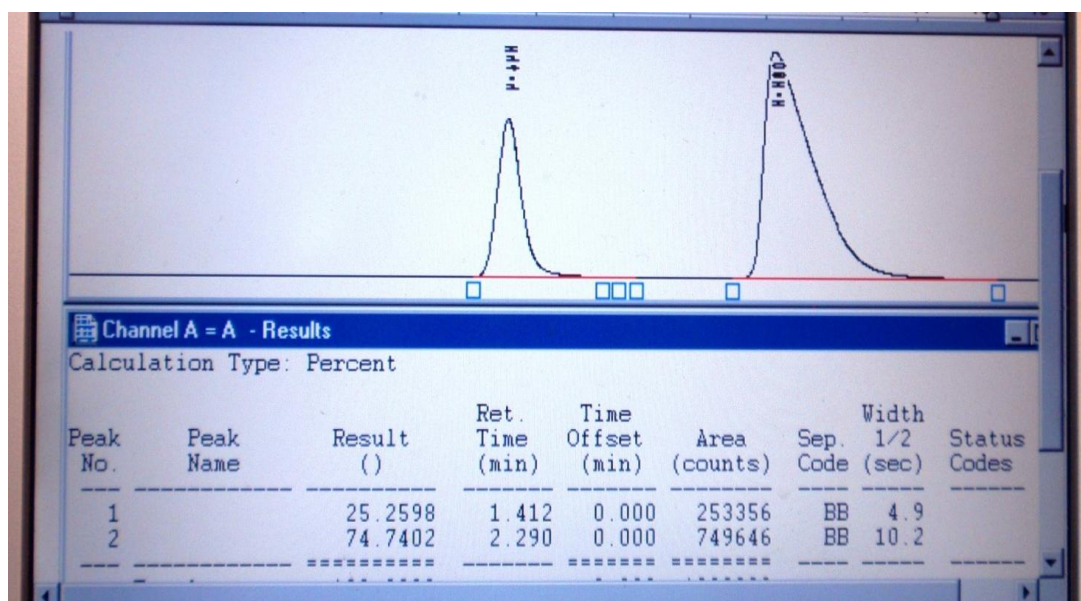
Retention times:  $rt(\text{H}_2)$ : 0.667,  $rt(\text{N}_2)$ : 1.294,  $rt(\text{O}_2)$ : 2.267

C. Second step: from 1,1'-peroxybis(1,3-dihydrobenzofuran) to phthalide



Retention times:  $rt(\text{H}_2)$ : 0.777,  $rt(\text{N}_2)$ : 1.309,  $rt(\text{O}_2)$ : 1.985

#### D. Blank reaction



**Retention times: rt (N<sub>2</sub>): 1.412, rt (O<sub>2</sub>): 2.290. No H<sub>2</sub> peak is observed.**

#### 4.5.11.3. General procedures for hydrogen quantification

##### 4.5.11.3.1. General procedure for calibration

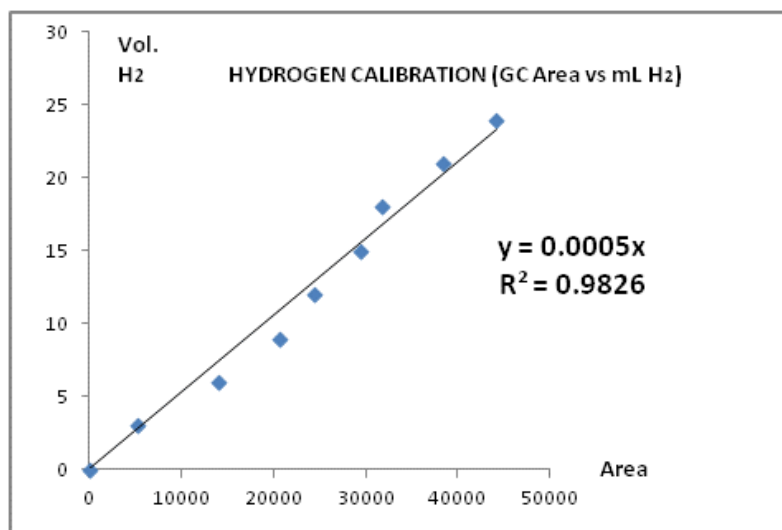
A Radley's tube (same used in 7.9) equipped with a magnetic stirring bar and a new rubber septum was sealed, degassed and charged with dioxygen gas (1 atm, 3 times) and kept under excess of oxygen (1 atm) by using a new balloon. A Schlenk tube was sealed, degassed and charged with hydrogen gas (1 atm, 3 times) and kept under excess of hydrogen (1 atm) by using a balloon. For the GC analyses, hydrogen gas (3.0 mL) was added into the Radley's tube with a gas syringe previously degassed with pure N<sub>2</sub>. A sample (300 μL) of the gas phase from that Radley's tube at r.t. (23°C) was taken with a previously degassed gas syringe and injected into the GC spectrometer. The same procedure was repeated for the complete calibration by doing subsequent hydrogen additions (3.0 ml each) on the same Radley's tube.

##### 4.5.11.3.2. Calibration curve

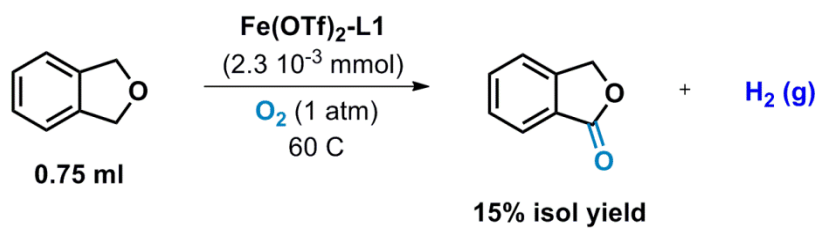
The following calibration curve was constructed from the data obtained by following the aforementioned calibration procedure.

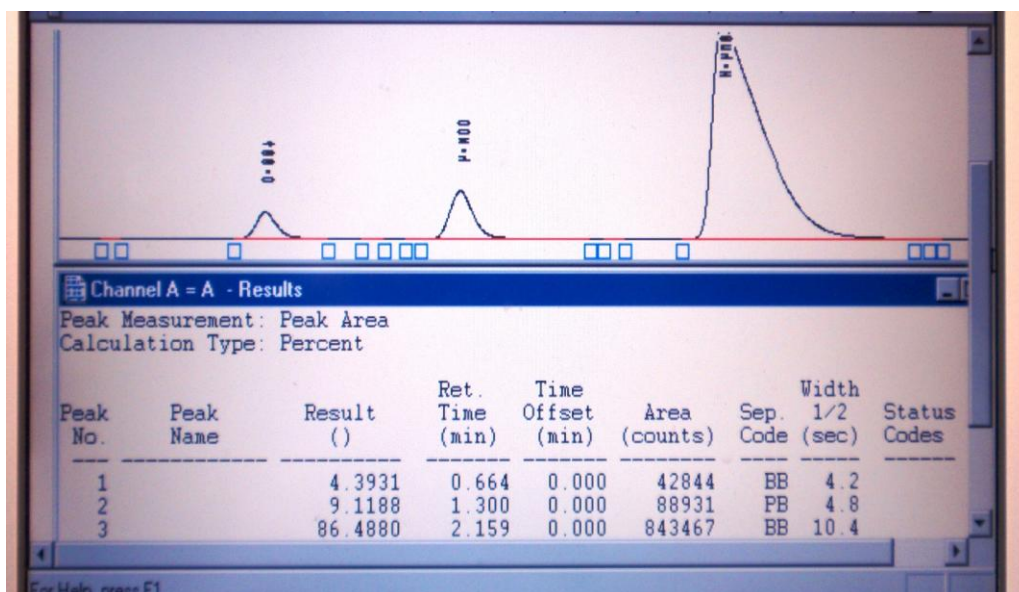
Area	H <sub>2</sub> injection <sup>a</sup> (ml)
0	0
5319	3
14061	6
20725	9
24382	12
29457	15
31760	18
38439	21
44152	24

<sup>a</sup> The volume of H<sub>2</sub> added into the Radley's tube at 23 °C.



#### 4.5.11.3.3. Sample analysis: chromatogram and calculations





**Retention times:** rt (H<sub>2</sub>): 0.664, rt (N<sub>2</sub>): 1.300, rt (O<sub>2</sub>): 2.159

**Area:** 42844, V (H<sub>2</sub>, 23 °C, 1 atm): 21.44 ml

**Calculated V (H<sub>2</sub>, 23 °C, 1 atm):** 23.16 ml: 15% conversion of phthalan to phthalide and 1 equivalent of H<sub>2</sub> gas being released per equivalent of phthalide.

MW: 120.15 g mol<sup>-1</sup>, ρ: 1.098 g ml<sup>-1</sup> for phthalan.

Therefore the quantification of H<sub>2</sub> by GC indicates that 1 equivalent of H<sub>2</sub> is released in the complete reaction of phthalan to phthalide, which is consistent with H<sub>2</sub> gas being released in the two reaction steps of phthalan oxidation.

The calculation of the volume occupied by 1 mol of H<sub>2</sub> at 23 °C was carried out according to Van der Waals equation shown below:

$$\left(p + \frac{n^2 a}{V^2}\right) (V - nb) = nRT$$

Where:

**R:** 8.3145 m<sup>3</sup> Pa mol<sup>-1</sup> K<sup>-1</sup>

**T:** 296.15 K

**p:** 101,325 Pa

**a** (H<sub>2</sub>): 0.002476 m<sup>6</sup> Pa mol<sup>-2</sup>

**b** (H<sub>2</sub>): 0.02661 10<sup>-3</sup> m<sup>3</sup> mol<sup>-1</sup>

Hence, V (H<sub>2</sub>, 23 °C, 1 atm): 22.53 L mol<sup>-1</sup>

#### 4.5.12. Water quantification

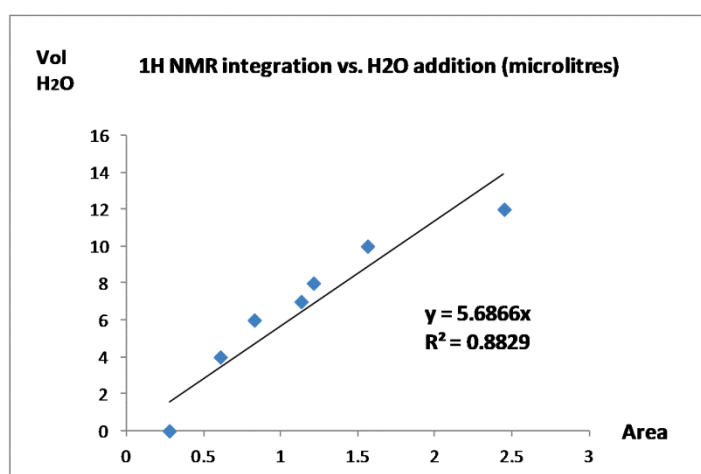
##### 4.5.12.1. General procedure

This experiment was attempted to show that no water is formed in the oxidation catalysed by  $\text{Fe}(\text{OTf})_2\text{-L1}$ . In a Radley's tube equipped with a magnetic stirring bar and a new rubber septum,  $\text{Fe}(\text{OTf})_2$  (2.0 mg,  $5.65 \times 10^{-3}$  mmol), **L1** (5.2 mg,  $5.67 \times 10^{-3}$  mmol), phthalan (1.0 mL) and  $\text{C}_6\text{H}_6$  (1.5 mL) were added. The tube was sealed, degassed and charged with dioxygen gas (1 atm, 3 times) and kept under excess of oxygen (1 atm) by using a balloon. The reaction mixture was heated to  $42^\circ\text{C}$  and stirred overnight. The reaction was cooled at r.t. and the solvent removed under reduced pressure. The crude reaction mixture was analyzed by  $^1\text{H}$  NMR, showing formation of 1,1'-peroxybis(1,3-dihydrobenzofuran) without any phthalide formation. Distilled water (4  $\mu\text{L}$ ) was added and the mixture stirred for 10 min before  $^1\text{H}$  NMR submission. Subsequent water additions were done under the same procedure. The calibration shows that no water is formed in the oxidation of phthalan.

##### 4.5.12.2. Calibration curve

The following calibration curve was constructed by following the aforementioned procedure

Area (MNR)	$\mu\text{l H}_2\text{O}$
0.276	0
0.6074	4
0.8278	6
1.1311	7
1.2110	8
1.5622	10
2.4482	20



### 4.5.13. Isotope labelling experiments

#### 4.5.13.1. General procedures

##### A. Reaction under $^{16}\text{O}_2$

In a Radley's tube equipped with a magnetic stirring bar and a new rubber septum,  $\text{Fe}(\text{OTf})_2$  (2.0 mg,  $5.65 \times 10^{-3}$  mmol), **L1** (5.2 mg,  $5.67 \times 10^{-3}$  mmol), phthalan (1.0 mL) and benzene (1.5 mL) were added. The tube was sealed, degassed and charged with  $^{16}\text{O}_2$  (1 atm, 3 times) and stirred under excess of  $^{16}\text{O}_2$  (1 atm) by using a balloon. The reaction mixture was heated to  $60^\circ\text{C}$  overnight and the products isolated by flash column chromatography (Hexane/EtOAc, 12/1 to 8/1 to 4/1) and fully characterized.

##### B. Reaction under $^{18}\text{O}_2$ (98%)

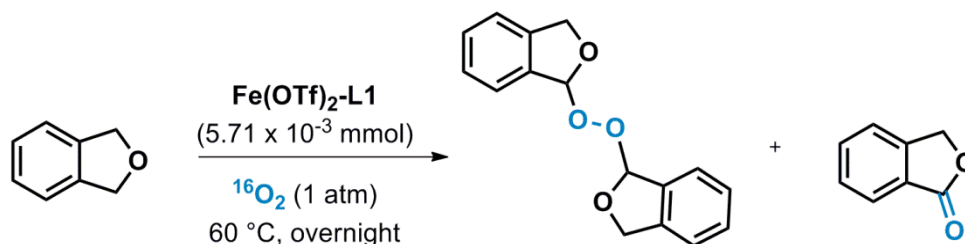
In a Radley's tube equipped with a magnetic stirring bar and a new rubber septum,  $\text{Fe}(\text{OTf})_2$  (2.0 mg,  $5.65 \times 10^{-3}$  mmol), **L1** (5.2 mg,  $5.67 \times 10^{-3}$  mmol), phthalan (1.0 mL) and benzene (1.5 mL) were added. The tube was sealed, degassed and charged with  $^{18}\text{O}_2$  (1 atm, 2 times) and kept under excess of  $^{18}\text{O}_2$  (1 atm) by using a balloon. The reaction mixture was heated up to  $60^\circ\text{C}$  overnight and the products isolated by flash column chromatography (Hexane/EtOAc, 12/1 to 8/1 to 4/1) and fully characterized.

##### C. Reaction under $^{16}\text{O}_2$ and $^{18}\text{O}_2$ (98%):

In a Radley's tube equipped with a magnetic stirring bar and a new rubber septum,  $\text{Fe}(\text{OTf})_2$  (2.0 mg,  $5.65 \times 10^{-3}$  mmol), **L1** (5.2 mg,  $5.67 \times 10^{-3}$  mmol), phthalan (1.0 ml) and benzene (1.5 ml) were added. The tube was sealed, degassed (1 atm, 2 times) and charged with a balloon containing similar amounts of  $^{16}\text{O}_2$  and  $^{18}\text{O}_2$  and kept under excess of the same gas mixture by using a balloon. The reaction mixture was heated to  $60^\circ\text{C}$  overnight and the products isolated by flash column chromatography (Hexane/EtOAc, 12/1 to 8/1 to 4/1) and fully characterized.

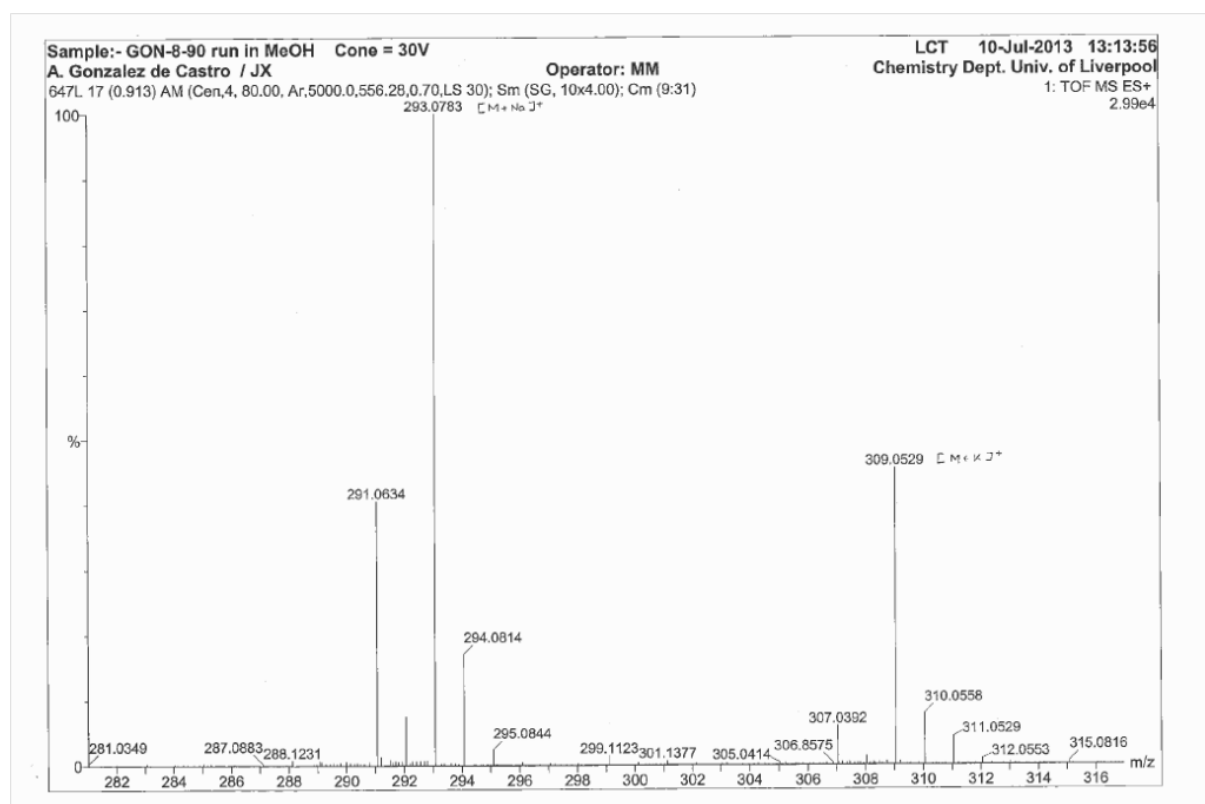


## 4.5.13.2. Characterisation and spectra of the peroxide products

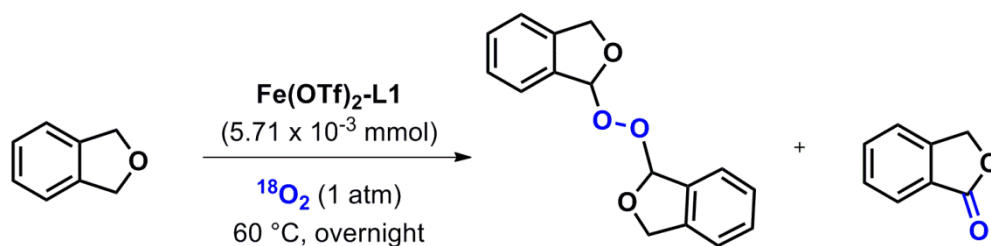
A. Synthesis of 1,1-peroxydiisochroman under  $^{16}\text{O}_2$  atmosphere

**1,1-Peroxydiisochroman:** White solid, 9% isolated yield.  $^1\text{H}$  NMR (400 MHz,  $\text{CDCl}_3$ ):  $\delta$  (ppm) = 7.44-7.23 (m, 8H), 6.74 (d,  $J = 2.0$  Hz, 2H), 5.30 (d,  $J = 12.8$  Hz, 2H), 5.09 (d,  $J = 12.8$  Hz, 2H).  $^{13}\text{C}$  NMR (100 MHz,  $\text{CDCl}_3$ ):  $\delta$  (ppm) = 141.4, 134.3, 130.3, 128.0, 124.2, 121.4, 110.8, 73.1. **IR (ATR)**  $\nu = 2865, 1752, 1461, 1365, 1340, 1315, 1257, 1211, 1041, 958, 923, 754$ . **IR**  $\nu$  (neat) = 2937, 2919, 2865, 1752, 1461, 1365, 1340, 1315, 1257, 1211, 1041, 958, 923, 754. **Anal Calc'd** for  $\text{C}_{16}\text{H}_{14}\text{O}_4$ : C, 71.10, H, 5.22, found: C, 70.85, H, 5.06.

HRMS (EI)  $m/z$  calc'd  $\text{C}_{16}\text{H}_{14}\text{O}^{16}_4\text{K} [\text{M}+\text{K}]^+$ : 309.0529, found: 309.0529. HRMS(EI)  $m/z$  calc'd  $\text{C}_{16}\text{H}_{14}\text{O}^{16}_4\text{Na} [\text{M}+\text{Na}]^+$ : 293.0790, found: 293.0783.

**HRMS spectra:**

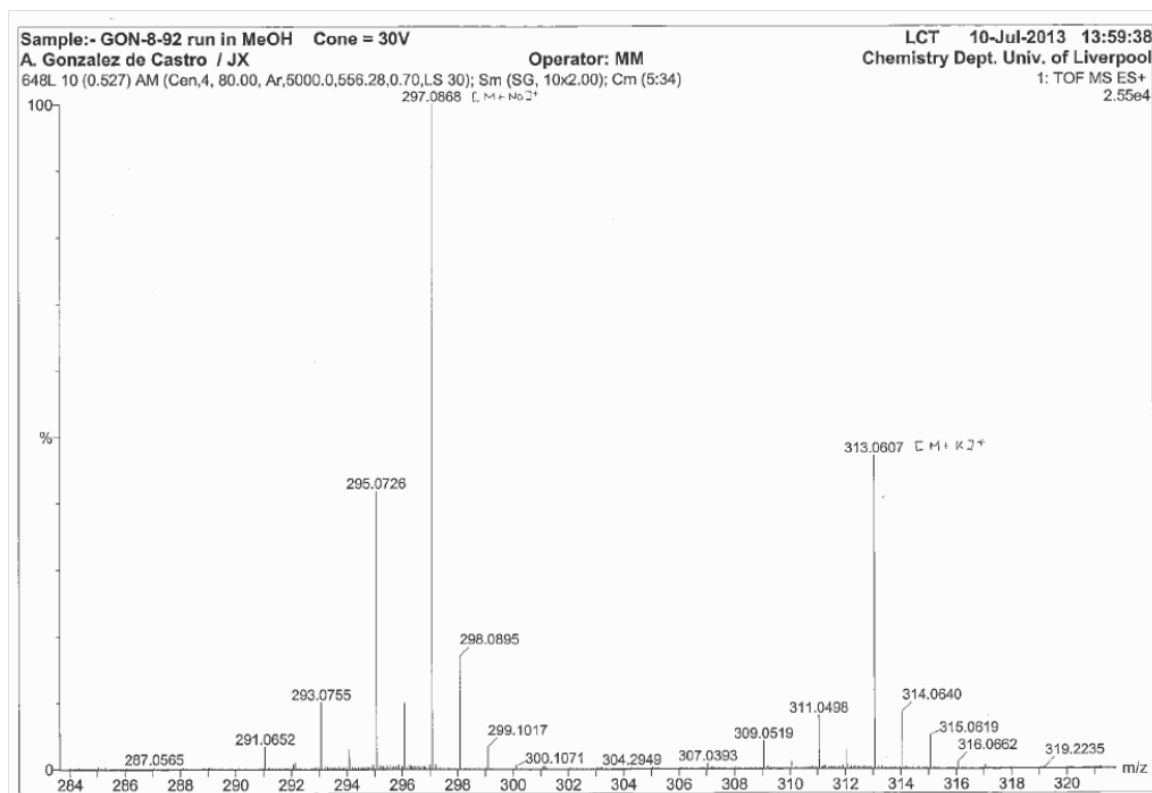
## B. Synthesis of 1,1-peroxydiisochroman under $^{18}\text{O}_2$ atmosphere



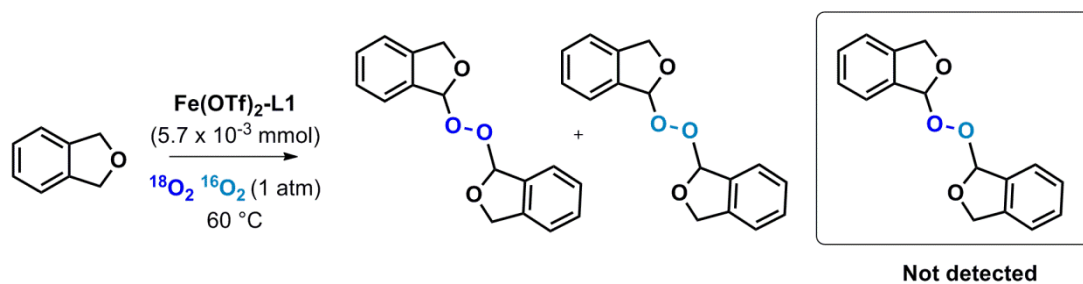
**1,1-Peroxydiisochroman:** White solid, 9% isolated yield.  $^1\text{H}$  NMR (400 MHz,  $\text{CDCl}_3$ ):  $\delta$  (ppm) = 7.43-7.23 (m, 8H), 6.74 (d,  $J = 2.0$  Hz, 2H), 5.31 (d,  $J = 12.8$  Hz, 2H), 5.09 (d,  $J = 12.8$  Hz, 2H).  $^{13}\text{C}$  NMR (100 MHz,  $\text{CDCl}_3$ ):  $\delta$  (ppm) = 141.4, 134.3, 130.3, 128.0, 124.2, 121.4, 110.8, 73.1. IR (ATR)  $\nu = 1461, 1367, 1340, 1315, 1253, 1039, 956, 919, 752, 715$ . IR  $\nu$  (neat) = 2937, 2919, 2865, 1461, 1367, 1340, 1315, 1253, 1039, 956, 919, 752, 715. Anal Calc'd for  $\text{C}_{16}\text{H}_{14}\text{O}^{16}_2\text{O}^{18}_2$ : C, 70.07, H, 5.14, found: C, 70.29, H, 5.09.

HRMS (EI)  $m/z$  calc'd  $\text{C}_{16}\text{H}_{14}\text{O}^{16}_2\text{O}^{18}_2\text{K} [\text{M}+\text{K}]^+$ : 313.0614, found: 313.0607. HRMS (EI)  $m/z$  calc'd  $\text{C}_{16}\text{H}_{14}\text{O}^{16}_2\text{O}^{18}_2\text{Na} [\text{M}+\text{Na}]^+$ : 297.0875, found: 297.0868.

### HRMS spectra:



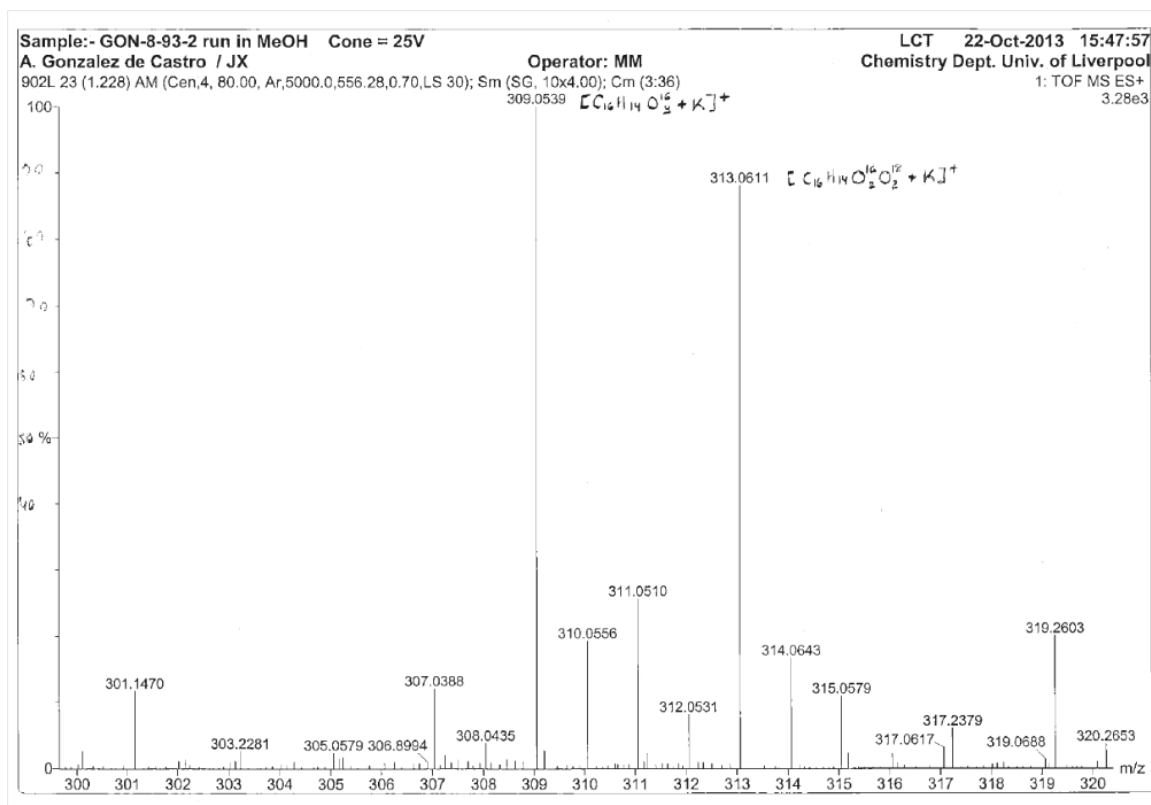
### C. Synthesis of 1,1-peroxydiisochroman under $^{16}\text{O}_2$ and $^{18}\text{O}_2$ atmosphere.

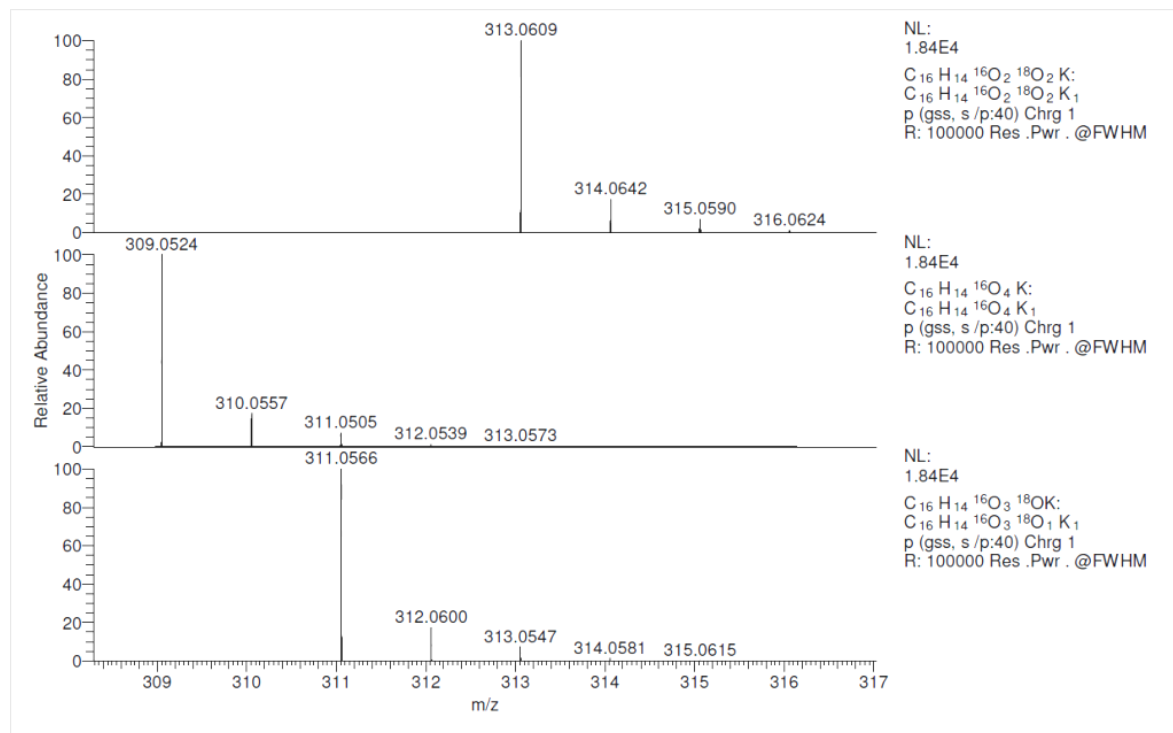


**C1. MS analysis of 1,1-peroxydiisochroman, made under  $^{16}\text{O}_2$  and  $^{18}\text{O}_2$  :** White solid, 9% isolated yield.

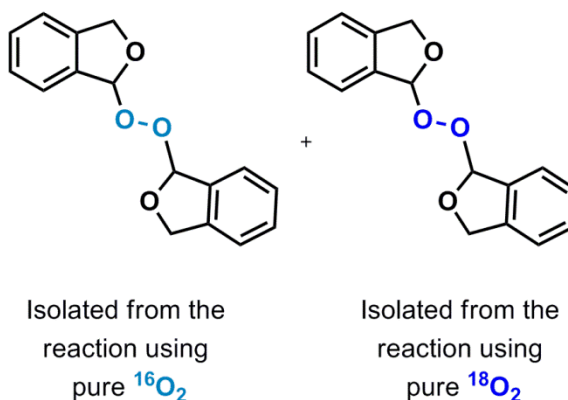
HRMS (EI)  $m/z$  calc'd  $\text{C}_{16}\text{H}_{14}\text{O}^{16}_4\text{K} [\text{M}+\text{K}]^+$  : 309.0524, found: 309.0539. HRMS (EI)  $m/z$  calc'd  $\text{C}_{16}\text{H}_{14}\text{O}^{16}_2\text{O}^{18}_2\text{K} [\text{M}+\text{K}]^+$ : 313.0614, found: 313.0611

**HRMS spectra:**

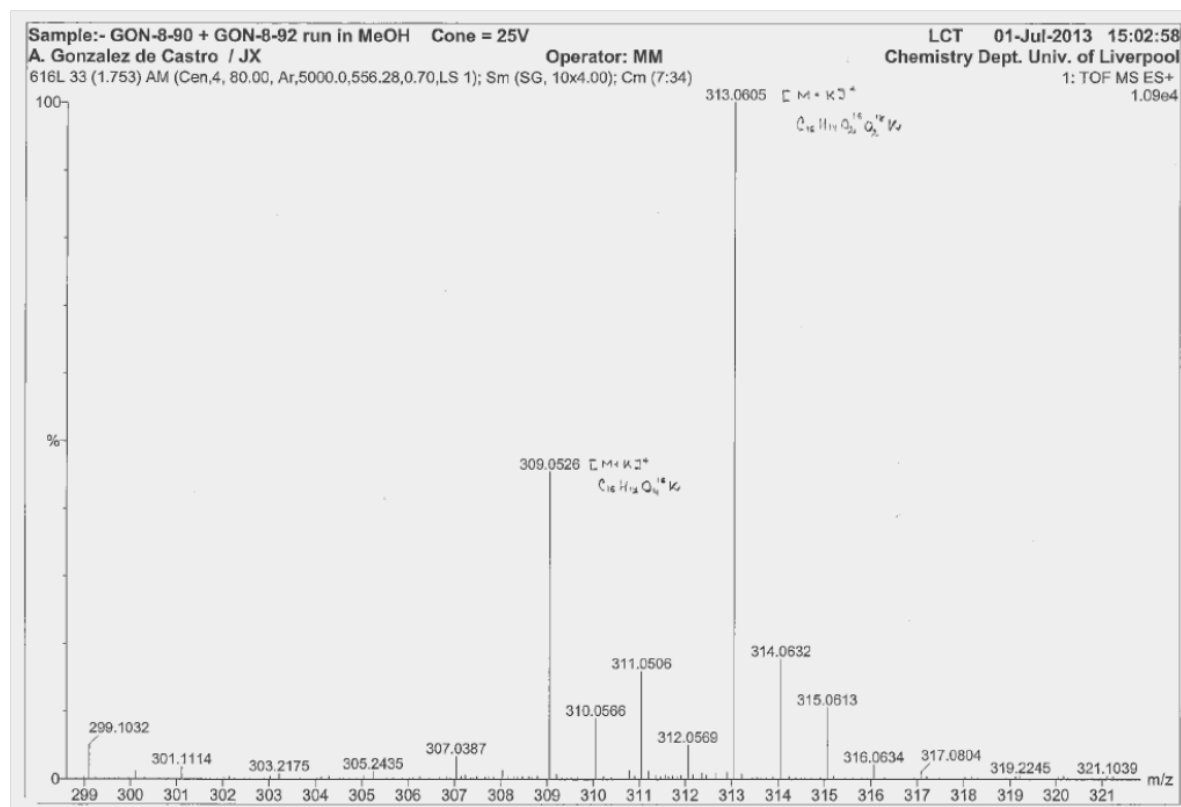


Theoretical fragmentations for the three peroxide species as  $[M + K]^+$  ions

**D. Control experiments: MS analysis of 1,1-peroxydiisochroman, mixing similar amounts of  $^{16}O_2$  peroxide (A) and  $^{18}O_2$  peroxide (B)**



HRMS (EI) m/z calc'd  $C_{16}H_{14}O^{16}_4K [M+K]^+$ : 309.0524, found: 309.0526. HRMS (EI) m/z calc'd  $C_{16}H_{14}O^{16}_2O^{18}_2K [M+K]^+$ : 313.0614, found: 313.0605.



#### 4.5.14. H/D exchange experiments

##### A. Reaction under N<sub>2</sub> atmosphere

In a Radley's tube equipped with a magnetic stir bar ligand L1 ( $5.67 \times 10^{-3}$  mmol, 5.2 mg) and Fe(OTf)<sub>2</sub> ( $5.65 \times 10^{-3}$  mmol, 2.0 mg) were added. The tube was sealed, degassed and left under inert atmosphere (3 times). Isochroman (2.0 mL) was added by syringe and the reaction mixture was stirred under N<sub>2</sub> atmosphere overnight at 60 °C. Product formation was determined by <sup>1</sup>H NMR conversion and isolated yield after silica gel flash column chromatography purification. The same procedure was repeated in the presence of D<sub>2</sub>O (300 μL).

##### B. Reaction under O<sub>2</sub> atmosphere

In a Radley's tube equipped with a magnetic stir bar ligand L1 ( $5.67 \times 10^{-3}$  mmol, 5.2 mg) and Fe(OTf)<sub>2</sub> ( $5.65 \times 10^{-3}$  mmol, 2.0 mg) were added. The tube was sealed, degassed and left

under inert atmosphere (3 times). Isochroman (2.0 mL) was added by syringe and the reaction mixture was stirred under N<sub>2</sub> atmosphere for 30 min at 35 °C. Next, D<sub>2</sub>O (300 μL) was added and the tube charged with O<sub>2</sub> gas and kept under O<sub>2</sub> (1 atm) by using a balloon. The reaction mixture was then heated to 60 °C and allowed to react overnight. Product formation was determined by <sup>1</sup>H NMR conversion and isolated yield after silica gel flash column chromatography purification.

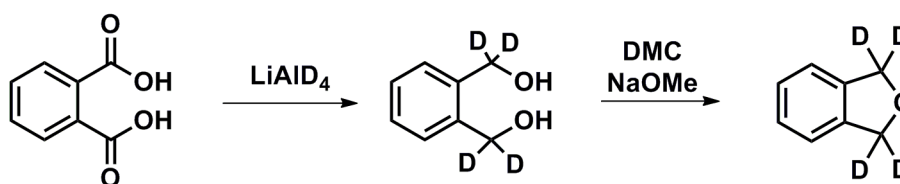
### B. Conversion of 1,1'-peroxybis(1,3-dihydroisobenzofuran) to phthalide

In a Young's tube equipped with a GC-MS connector and a magnetic stir bar [Fe(OTf)<sub>2</sub>L1(THF)] (7.45 x 10<sup>-4</sup> mmol, 1.0 mg), C<sub>6</sub>H<sub>6</sub> (100 μL) and peroxide **13** (80 mg) were added. The tube was sealed and the reaction mixture was stirred overnight at 45 °C. The Young's tube was connected to the GC-MS equipment and cooled to -78 °C to solidify the liquid phase. Gases released during the reaction were monitored in the MS spectrum by slowly opening the detector valve. The same procedure was repeated in the presence of D<sub>2</sub>O (30 μL). Although H<sub>2</sub> gas formation was clearly observed in both cases, HD or D<sub>2</sub> formation was not detected in the presence of D<sub>2</sub>O.

### 4.5.15. Experiments with <sup>2</sup>H-labelled peroxides

#### Synthesis of Phthalan-d4

Phthalan-d4 was synthesized from the deuterated-diol as reported in the literature.<sup>28</sup>



Deuterated 1,1'-peroxybis(1,3-dihydroisobenzofuran) was synthesized from phthalan-d4 according to the procedure described in section 7.13.

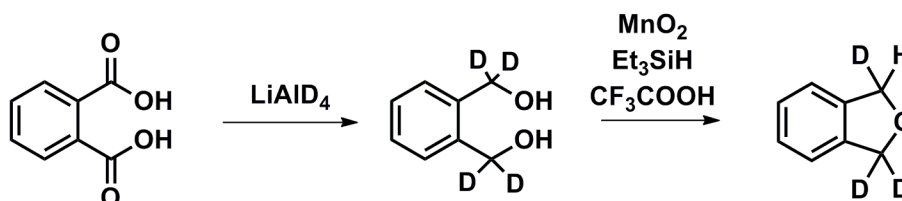
1,1'-Peroxybis(1,3-dihydroisobenzofuran)-d6: White solid, 7% isol. yield. <sup>1</sup>H NMR (400 MHz, CDCl<sub>3</sub>): δ (ppm) = 7.43-7.24 (m, 8H). <sup>13</sup>C NMR (100 MHz, CDCl<sub>3</sub>): δ (ppm) = 139.0, 132.2, 130.9, 130.1, 127.2, 120.9 (d, <sup>3</sup>J<sub>C-D</sub> = 2.4 Hz). HRMS (EI) m/z calc'd C<sub>16</sub>H<sub>9</sub>D<sub>6</sub>O<sub>4</sub> [M+H]<sup>+</sup>: 277.1342, found: 277.1345.

### Procedure for the GC-MS analysis

In a Young's tube equipped with a GC-MS connector and a magnetic stir bar  $[\text{Fe}(\text{OTf})_2\text{L1}(\text{THF})]$  ( $7.45 \times 10^{-4}$  mmol, 1.0 mg),  $\text{C}_6\text{H}_6$  (60  $\mu\text{L}$ ) and peroxide **13** (25 mg) and **14** (35 mg) were added. The tube was sealed and the reaction mixture was stirred overnight at 45 °C. The Young's tube was connected to the GC-MS equipment and cooled to -78 °C to solidify the liquid phase. Gases released during the reaction were monitored in the MS spectrum by slowly opening the detector valve. The same procedure was repeated for each peroxide.

### Synthesis of Phthalan-d3

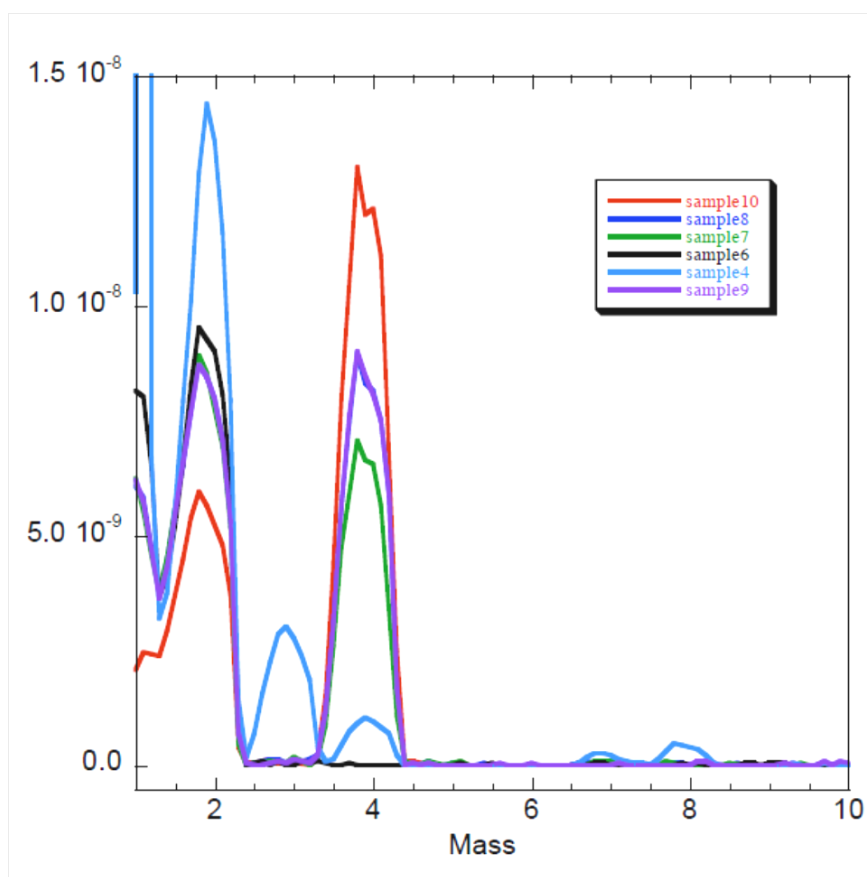
Phthalan-d3 was synthesized from the deuterated-diol as reported in the literature.<sup>29</sup>



Phthalan-d3: Pale yellow liquid.  $^1\text{H}$  NMR (400 MHz,  $\text{CDCl}_3$ ):  $\delta$  (ppm) = 7.26-7.23 (m, 4H, overlapped), 5.10 (s, 1H). HRMS (EI)  $m/z$  calc'd  $\text{C}_8\text{H}_6\text{D}_3\text{O}$   $[\text{M}+\text{H}]^+$ : 124.0836, found: 124.0832.

### Procedure for the GC-MS analysis

In a Young's tube equipped with a GC-MS connector and a magnetic stir bar  $[\text{Fe}(\text{OTf})_2\text{L1}(\text{THF})]$  ( $7.45 \times 10^{-4}$  mmol, 1.0 mg),  $\text{C}_6\text{H}_6$  (15  $\mu\text{L}$ ) and phthalan-d1 (40  $\mu\text{L}$ ) were added. The tube was charged with  $\text{O}_2$  (1 atm) and sealed and the reaction mixture was stirred 8h at 60 °C. The Young's tube was connected to the GC-MS equipment and cooled to -78 °C to solidify the liquid phase. Gases released during the reaction were monitored in the MS spectrum by slowly opening the detector valve.

*Gas evolution monitored from the catalytic reactions (Pressure/mbar vs mass)*

**Sample 10:** D<sub>2</sub> evolution from the deuterated 1,1'-peroxybis(1,3-dihydroisobenzofuran)

**Samples 9, 8, 7:** H<sub>2</sub> and D<sub>2</sub> evolution from the mixture of 1,1'-peroxybis(1,3-dihydroisobenzofuran) and deuterated 1,1'-peroxybis(1,3-dihydroisobenzofuran)

**Sample 6:** H<sub>2</sub> evolution from 1,1'-peroxybis(1,3-dihydroisobenzofuran)

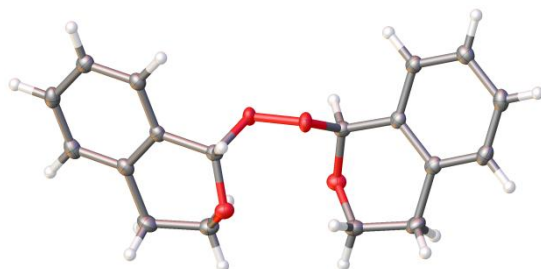
**Sample 4:** H<sub>2</sub>, HD and D<sub>2</sub> evolution from the oxidation of phthalan-d<sub>3</sub> to phthalides

#### 4.5.16. Crystallisation of 1,1'-peroxydiisochroman and 1,1'-oxydiisochroman

In a test tube a mixture of 1,1'-peroxydiisochroman and 1,1'-oxydiisochroman (200 mg) was dissolved in Et<sub>2</sub>O (0.5 ml). Hexane (0.75 ml) was slowly added and the closed tube was left at ambient temperature until well shaped transparent crystals formed.



## 4.5.17. Crystallographic data of compounds

*Cis* 1,1'-peroxydiisochroman

CCDC 945602 contains the supplementary crystallographic data for this compound. This data can be obtained free of charge from The Cambridge Crystallographic Data Centre via [www.ccdc.cam.ac.uk/data\\_request/cif](http://www.ccdc.cam.ac.uk/data_request/cif).

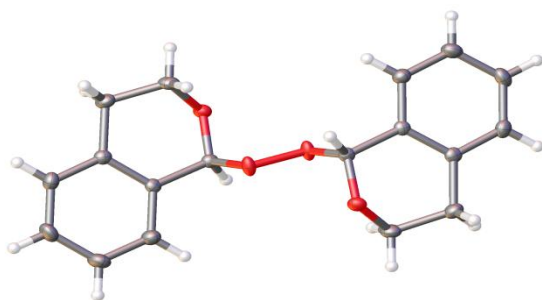
**Crystal Data** for  $C_{36}H_{36}O_8$  ( $M=596.65$ ): monoclinic, space group  $C2/c$  (no. 15),  $a = 14.926(3)$  Å,  $b = 12.592(3)$  Å,  $c = 7.6268(16)$  Å,  $\beta = 90.730(6)^\circ$ ,  $V = 1433.3(5)$  Å<sup>3</sup>,  $Z = 2$ ,  $T = 100.0$  K,  $\mu(\text{MoK}\alpha) = 0.097$  mm<sup>-1</sup>,  $D_{\text{calc}} = 1.383$  g/mm<sup>3</sup>, 5377 reflections measured ( $4.24 \leq 2\theta \leq 52.84$ ), 1473 unique ( $R_{\text{int}} = 0.0271$ ) which were used in all calculations. The final  $R_1$  was 0.0373 ( $>2\sigma(I)$ ) and  $wR_2$  was 0.0950 (all data).

**Table 1 Crystal data and structure refinement for CCDC 945602**

Identification code	CCDC 945602
Empirical formula	$C_{36}H_{36}O_8$
Formula weight	596.65
Temperature/K	100.0
Crystal system	monoclinic
Space group	$C2/c$
$a/\text{Å}$	14.926(3)
$b/\text{Å}$	12.592(3)
$c/\text{Å}$	7.6268(16)
$\alpha/^\circ$	90.00
$\beta/^\circ$	90.730(6)
$\gamma/^\circ$	90.00
Volume/Å <sup>3</sup>	1433.3(5)
$Z$	2
$\rho_{\text{calc}}/\text{mg/mm}^3$	1.383

$m/mm^{-1}$	0.097
F(000)	632.0
Crystal size/ $mm^3$	$0.5 \times 0.12 \times 0.1$
$2\theta$ range for data collection	4.24 to $52.84^\circ$
Index ranges	$-18 \leq h \leq 18, -15 \leq k \leq 15, -8 \leq l \leq 9$
Reflections collected	5377
Independent reflections	1473[R(int) = 0.0271]
Data/restraints/parameters	1473/0/136
Goodness-of-fit on $F^2$	1.033
Final R indexes [ $I \geq 2\sigma(I)$ ]	$R_1 = 0.0373, wR_2 = 0.0890$
Final R indexes [all data]	$R_1 = 0.0446, wR_2 = 0.0950$
Largest diff. peak/hole / $e \text{ \AA}^{-3}$	0.21/-0.26

### Trans 1,1'-peroxydiisochroman



CCDC 945603 contains the supplementary crystallographic data for this compound. This data can be obtained free of charge from The Cambridge Crystallographic Data Centre via [www.ccdc.cam.ac.uk/data\\_request/cif](http://www.ccdc.cam.ac.uk/data_request/cif).

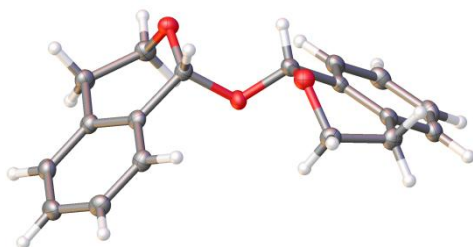
**Crystal Data** for  $C_{36}H_{36}O_8$  ( $M = 596.65$ ): monoclinic, space group  $P2_1/c$  (no. 14),  $a = 7.2839(14) \text{ \AA}$ ,  $b = 7.6923(15) \text{ \AA}$ ,  $c = 26.517(5) \text{ \AA}$ ,  $\beta = 90.255(3)^\circ$ ,  $V = 1485.7(5) \text{ \AA}^3$ ,  $Z = 2$ ,  $T = 100.0 \text{ K}$ ,  $\mu(\text{MoK}\alpha) = 0.094 \text{ mm}^{-1}$ ,  $D_{\text{calc}} = 1.334 \text{ g/mm}^3$ , 18112 reflections measured ( $5.52 \leq 2\theta \leq 52.96$ ), 3058 unique ( $R_{\text{int}} = 0.0370$ ) which were used in all calculations. The final  $R_1$  was 0.0458 ( $>2\sigma(I)$ ) and  $wR_2$  was 0.1153 (all data).

### Table 1 Crystal data and structure refinement for CCDC 945603

Identification code	CCDC 945603
---------------------	-------------

Empirical formula	C <sub>36</sub> H <sub>36</sub> O <sub>8</sub>
Formula weight	596.65
Temperature/K	100.0
Crystal system	monoclinic
Space group	P2 <sub>1</sub> /c
a/Å	7.2839(14)
b/Å	7.6923(15)
c/Å	26.517(5)
α/°	90.00
β/°	90.255(3)
γ/°	90.00
Volume/Å <sup>3</sup>	1485.7(5)
Z	2
ρ <sub>calc</sub> /mg/mm <sup>3</sup>	1.334
m/mm <sup>-1</sup>	0.094
F(000)	632.0
Crystal size/mm <sup>3</sup>	0.5 × 0.49 × 0.1
2θ range for data collection	5.52 to 52.96°
Index ranges	-9 ≤ h ≤ 9, -9 ≤ k ≤ 9, -33 ≤ l ≤ 33
Reflections collected	18112
Independent reflections	3058[R(int) = 0.0370]
Data/restraints/parameters	3058/0/199
Goodness-of-fit on F <sup>2</sup>	1.022
Final R indexes [I >= 2σ (I)]	R <sub>1</sub> = 0.0458, wR <sub>2</sub> = 0.1082
Final R indexes [all data]	R <sub>1</sub> = 0.0573, wR <sub>2</sub> = 0.1153
Largest diff. peak/hole / e Å <sup>-3</sup>	0.32/-0.29

### 1,1'-oxydiisochroman



CCDC 945604 contains the supplementary crystallographic data for this compound. This data can be obtained free of charge from The Cambridge Crystallographic Data Centre via

[www.ccdc.cam.ac.uk/data\\_request/cif](http://www.ccdc.cam.ac.uk/data_request/cif). The X-ray structure of this compound (with a different space group) was reported before.<sup>20</sup>

**Crystal Data** for C<sub>18</sub>H<sub>18</sub>O<sub>3</sub> (*M*=282.32): monoclinic, space group I2/a (no. 15), *a* = 15.852(3) Å, *b* = 4.2770(8) Å, *c* = 21.043(4) Å,  $\beta$  = 103.334(5)°, *V* = 1388.2(5) Å<sup>3</sup>, *Z* = 4, *T* = 100.0 K,  $\mu(\text{MoK}\alpha)$  = 0.091 mm<sup>-1</sup>, *D*<sub>calc</sub> = 1.351 g/mm<sup>3</sup>, 7386 reflections measured (3.98 ≤ 2 $\theta$  ≤ 52.68), 1421 unique (*R*<sub>int</sub> = 0.0342) which were used in all calculations. The final *R*<sub>1</sub> was 0.0359 (>2 $\sigma$ (*I*)) and *wR*<sub>2</sub> was 0.0937 (all data).

**Table 1 Crystal data and structure refinement for CCDC 945604**

Identification code	CCDC 945604
Empirical formula	C <sub>18</sub> H <sub>18</sub> O <sub>3</sub>
Formula weight	282.32
Temperature/K	100.0
Crystal system	monoclinic
Space group	I2/a
<i>a</i> /Å	15.852(3)
<i>b</i> /Å	4.2770(8)
<i>c</i> /Å	21.043(4)
$\alpha$ /°	90.00
$\beta$ /°	103.334(5)
$\gamma$ /°	90.00
Volume/Å <sup>3</sup>	1388.2(5)
<i>Z</i>	4
$\rho_{\text{calc}}$ /mg/mm <sup>3</sup>	1.351
$\mu$ /mm <sup>-1</sup>	0.091
<i>F</i> (000)	600.0
Crystal size/mm <sup>3</sup>	0.44 × 0.4 × 0.12
2 $\theta$ range for data collection	3.98 to 52.68°
Index ranges	-19 ≤ <i>h</i> ≤ 19, -5 ≤ <i>k</i> ≤ 5, -26 ≤ <i>l</i> ≤ 26
Reflections collected	7386
Independent reflections	1421 [ <i>R</i> (int) = 0.0342]
Data/restraints/parameters	1421/0/132
Goodness-of-fit on <i>F</i> <sup>2</sup>	1.059
Final <i>R</i> indexes [ <i>I</i> ≥ 2 $\sigma$ ( <i>I</i> )]	<i>R</i> <sub>1</sub> = 0.0359, <i>wR</i> <sub>2</sub> = 0.0911
Final <i>R</i> indexes [all data]	<i>R</i> <sub>1</sub> = 0.0389, <i>wR</i> <sub>2</sub> = 0.0937
Largest diff. peak/hole / e Å <sup>-3</sup>	0.18/-0.30

**4.6. References**

- [1] Que Jr., L.; Tolman, W. B. *Nature* **2008**, *455*, 333.
- [2] Chen, M.; White, M. C. *Science* **2010**, *327*, 566.
- [3] White M. C. *Science* **2012**, *335*, 807.
- [4] See Chapter 1, section 1.3.3
- [5] Kirillov A. M.; Kopylovich, M. N.; Kirillova, M. V.; Karabach, E. Y.; Haukka, M.; Guedes da Silva, M. F. C.; Pombeiro, A. J. L. *Adv. Synth. Catal.* **2006**, *348*, 159.
- [6] Shilov, A. E.; Shul'pin, G. B. *Activation and Catalytic Reactions of Saturated Hydrocarbons in the Presence of Metal Complexes* (Kluwer Academic Publishers, Dordrecht/Boston/London, 2000).
- [7] Denisov, E. T. *Kinetics and Catalysis* **2006**, *47*, 662.
- [8] Denisov, E. T.; Azatyan, V. V. *Inhibition of Chain Reactions* (London: Gordon and Breach, 2000)
- [9] Selke, M.; Valentine, J. S. *J. Am. Chem. Soc.* **1998**, *120*, 2652.
- [10] Scianamea, V.; Jerome, R.; Detrembleur, C. *Chem. Rev.* **2008**, *108*, 1104.
- [11] Newcomb, M. in *Encyclopedia of Radicals in Chemistry, Biology and Materials* (C. Chatgililoglu, A. Studer, Eds; Wiley and Sons Ltd., 2012).
- [12] Pint, A.; Klussmann, M. *Adv. Synth. Catal.* **2012**, *354*, 701.
- [13] Durham, L. J.; Mosher, H. S. *J. Am. Chem. Soc.* **1962**, *84*, 2811.
- [14] (a) Franck, J. E.; Rabinowitch, E. *Trans. Faraday Soc.* **1934**, *30*, 120. (b) Matheson, M. *J. J. Chem. Phys.* **1945**, *13*, 584.
- [15] Sen, A.; Lin, M.; Kao, L. C.; Hutson, A. C. *J. Am. Chem. Soc.* **1992**, *114*, 6385.
- [16] Kennedy, A. R.; Klett, J.; Mulvey, R. E.; Wright, D. S.; *Science* **2009**, *326*, 706.
- [17] West, N. M.; White, P. S.; Templeton, J. L. *J. Am. Chem. Soc.* **2007**, *129*, 12372.
- [18] Whited, M. T.; Zhu, Y.; Timpa, S. D.; Chen, C.-H.; Foxman, B. M.; Ozerov, O. V.; Grubbs, R. H. *Organometallics* **2009**, *28*, 4560.
- [19] Xu, Y. C.; Lebeau, E.; Gillard, W.; Attardo, G. *Tetrahedron Lett.* **1993**, *34*, 3841.

- [20] Eikawa, M.; Sakaguchi, S.; Ishii, Y. *J. Org. Chem.* **1999**, *64*, 4676.
- [21] Siewert, I.; Limberg, C.; Demeshko, S.; Hoppe, E. *Chem. Eur. J.* **2008**, *14*, 9377.
- [22] Zhang, S.-Y.; Tu, Y.-Q.; Fan, C.-A.; Zhang, F.-M.; Shi, L. *Angew. Chem. Int. Ed.* **2009**, *48*, 8761.
- [23] (a) Kaesz, H. D.; Saillant, R. B. *Chem. Rev.* **1972**, *72*, 231. (b) Heinekey, D. M.; Oldham, W. J. Jr. *Chem. Rev.* **1993**, *93*, 913. (c) Nakazawa, H.; Itazaki, M. *Top. Organomet. Chem.* **2011**, *33*, 27. (d) Chen, T. Y.; Bullock, M. R. *Organometallics* **2002**, *21*, 2325. (e) Gilberstone, J. D.; Szymczak, N. K.; Crossland, J. L.; Miller, W. K.; Lyon, D. K.; Foxman, B. M.; Davis, J.; Tyler, D. R. *Inorg. Chem.* **2007**, *46*, 1205.
- [24] Pellarin, K. R., McCready, M. S., Sutherland, T. I., Puddephatt, R. J. *Organometallics* **31**, 8291-8300 (2012).
- [25] Speier, G., Fullop, V. *J. Chem. Soc. Dalton Trans.* 2331-2333 (1989).
- [26] Pellarin, K. R.; McCready, M. S.; Sutherland, T. I.; Puddephatt, R. J. *Organometallics* **2012**, *31*, 8291.
- [27] (a) Srimani, D.; Ben-David, Y.; Milstein, D. *Angew. Chem. Int. Ed.* **2013**, *52*, 4012. (b) Srimani, D.; Ben-David, Y.; Milstein, D. *Chem. Commun.* **2013**, *49*, 6632. (c) Yang, X. *ACS Catal.* **2013**, *3*, 2684. (d) Kamitani, M.; Ito, M.; Itazaki, M.; Nakazawa, H. *Chem. Commun.* **2014**, *50*, 7941. (e) Grove, T. L.; Ahlum, J. H.; Sharma, P.; Krebs, C.; Booker, S. J. *Biochemistry* **2010**, *49*, 3783.
- [28] Durham, L. J.; Mosher, H. S. *J. Am. Chem. Soc.* **1962**, *84*, 2811.
- [29] Jenkins, A. D.; Style, D. W. G. *J. Chem. Soc.* **1953**, 2337.
- [30] Hugo, V. I.; Oosthuizen, F. J.; Green, I. R. *Synthetic Commun.* **2003**, *33*, 1425.
- [31] The compound is described in the literature but full analytical description is not provided. See: Rieche, A.; Schmitz, E. *Chemische Berichte* **1957**, *90*, 1094.
- [32] Baldwin, J. E.; Patapoff, T. W.; Barden, T. C. *J. Am. Chem. Soc.* **1984**, *106*, 1421.

- [33] Using DMF as solvent according to: Blagg J.; Davies, S. G.; Holman, N. J.; Laughton, C. A.; Mobbs, B. E. *J. Chem. Soc., Perkin Trans 1: Organic and Bio-Organic Chemistry* **1986**, 1581.
- [34] Elphinoff-Felkin, I.; Sarda, P. *Tetrahedron* **1975**, 31, 2785.
- [35] Li, G.; Leow, D.; Wan, L.; Yu, J.-Q. *Angew. Chem. Int. Ed.* **2013**, 125, 1283.

## *Chapter 5*

# **Fe(OTf)<sub>2</sub>-PYBISULIDINE CATALYSED SELECTIVE AEROBIC CLEAVAGE OF ALIPHATIC C-O AND C-C BONDS**

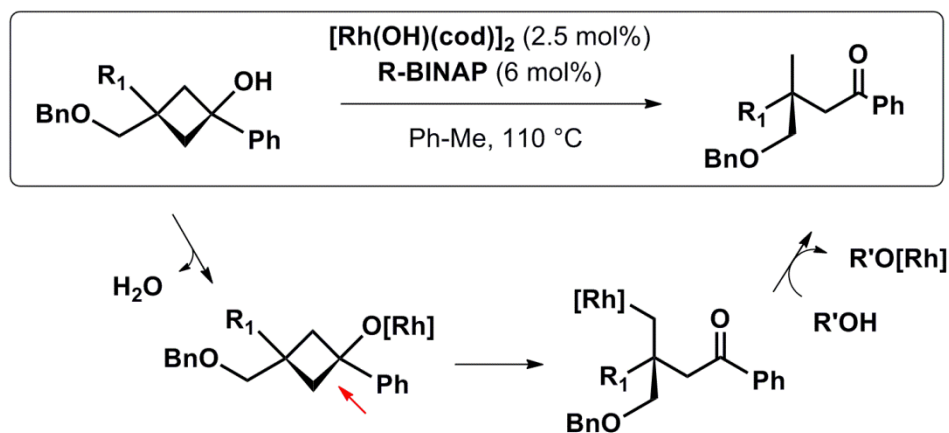


## 5.1. Introduction

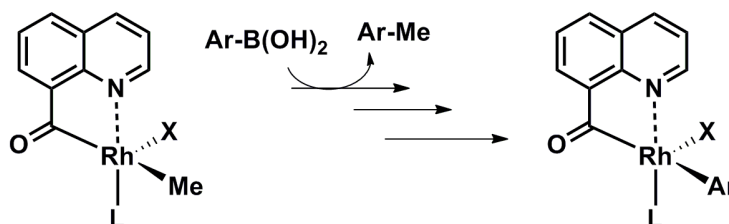
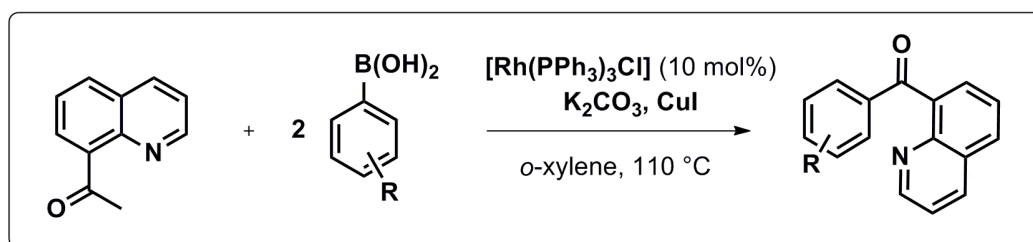
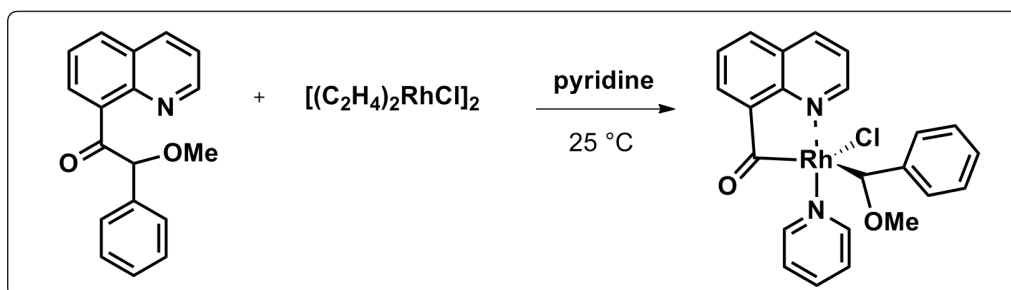
### 5.1.1. Selective cleavage of aliphatic C-C bonds

The cleavage and subsequent functionalisation of C-C bonds with transition metals is an extensive area of research due to the natural inertness of these bonds and the attractiveness of developing more efficient methodologies for the synthesis of complex molecular skeletons.<sup>1</sup> The development of catalytic methods for cleaving strained C-C bonds has been particularly explored and efficient methodologies that even allow the construction of stereocentres have been reported<sup>2</sup> (Scheme 1 a). The cleavage of unstrained C-C bonds is more challenging as a strong thermodynamic driving force is needed to break the stable C-C bond.<sup>1a</sup> However, other alternatives to selectively cleave unstrained C-C bonds such as metal chelation<sup>3</sup> (Scheme 1b) or the use of carbonyl groups<sup>4</sup> to direct the cleavage to the weaker  $\alpha$ -C-C bond (Scheme 1c) have been reported.

#### a) Strained C-C bonds:



## b) Chelation strategies:

c) C-C bonds  $\alpha$ -to a carbonyl:

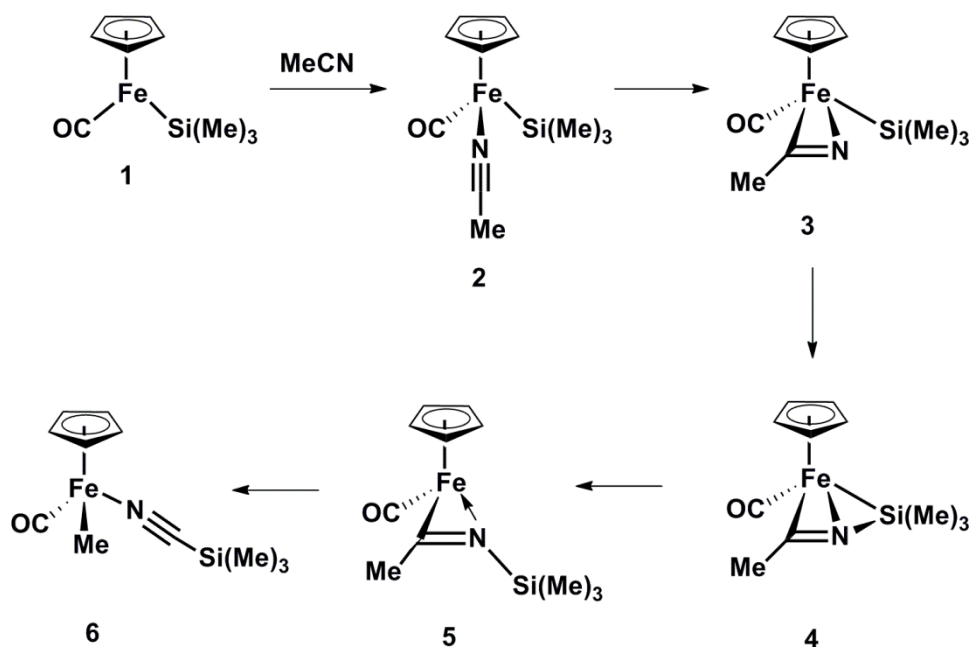
Scheme 1. Examples of transition metal-mediated selective C-C cleavages

## 5.1.2. Iron-catalysed selective cleavage of aliphatic C-C bonds

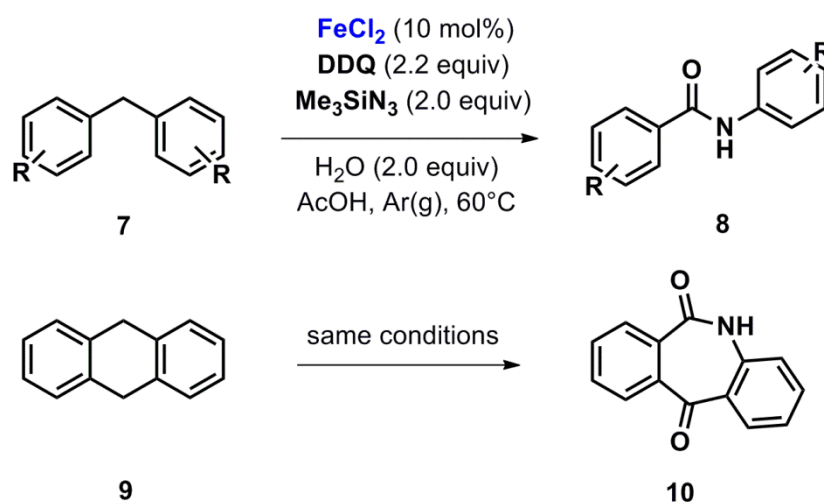
In 2004 the group of Nakazawa reported the activation of the C-C bond in acetonitrile by the iron complex **1** bearing a trimethylsilyl ligand.<sup>5</sup> On the basis of DFT calculations, the C-C cleavage is proposed to occur via the insertion of the CN bond of acetonitrile into the Fe-Si bond followed by the migration of the methyl group to the iron centre (Scheme 2). The presence of the silyl ligand was found essential to lower the energy barriers of the CN insertion and methyl migration.

More recent investigations from Jiao and co-workers demonstrated the use of FeCl<sub>2</sub> for promoting the conversion of hydrocarbons to amides via selective C-H and C-C cleavage.<sup>6</sup> The reactions proceeded with good yields but required more than stoichiometric amounts of

DDQ as an oxidant to activate the benzylic C-H bond and an excess of azide as a nitrogen source. When cyclic substrates such as **9** were investigated, ring expansions with concomitant C-C bond cleavage were successfully achieved (Scheme 3).



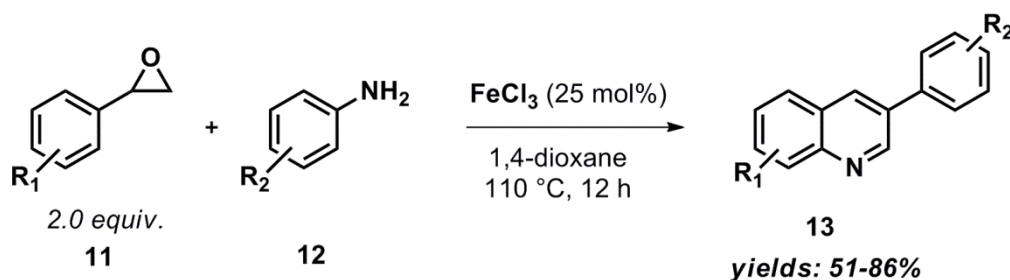
**Scheme 2.** Iron-based activation of the C-C bond of acetonitrile



**Scheme 3.** Iron promoted C-H and C-C cleavage of hydrocarbons

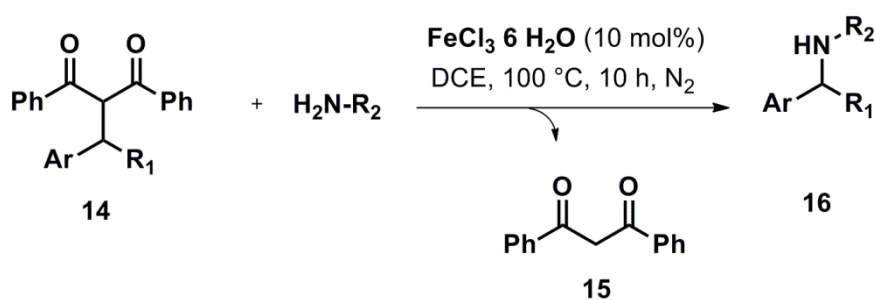
A combined C-C cleavage and C-H activation strategy has been reported by the group of Wang to convert styrene epoxides and anilines into 3-arylquinolines using  $\text{FeCl}_3$  as a

promoter<sup>7</sup> (Scheme 4). A broad substrate scope was demonstrated affording quinolines with good to moderate yields, although a high iron loading (25 mol%) and high temperatures were used. However, mechanistic investigations for this transformation have not been reported so far.



**Scheme 4.** Iron-promoted tandem reaction of styrene epoxides and anilines to afford quinolines

The  $\text{FeCl}_3$  catalysed cleavage of an aliphatic C-C bond in 1,3-dicarbonyl compounds combined with a subsequent C-N bond formation with anilines and sulfonamides to afford amines has been investigated by Li and co-workers.<sup>8</sup> The reactions proceed at 100 °C, with the 1,3-dicarbonyl moiety **15** acting as a leaving group to thermodynamically favour the C-C cleavage (Scheme 5).

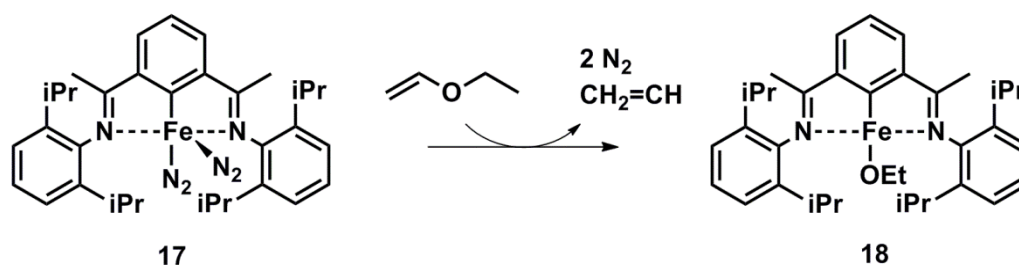


**Scheme 5.**  $\text{FeCl}_3$ -catalysed C-C cleavage and C-N bond formation

### 5.1.3. Iron-catalysed selective cleavage of aliphatic C-O bonds

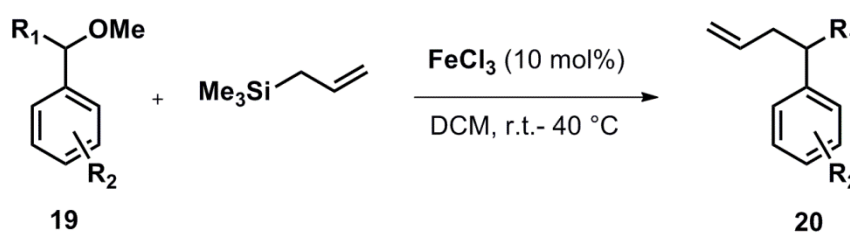
When investigating the (bis)iminopyridine iron-catalysed hydrogenation of ester-containing olefins, the group of Chirik identified that the iron-promoted C-O cleavage of the ester

functionality was the main factor in deactivating the catalyst.<sup>9</sup> For ethyl vinyl ether, clean stoichiometric formation of the iron-ethoxyde complex **18** was detected with loss of the vinyl fragment (Scheme 6).



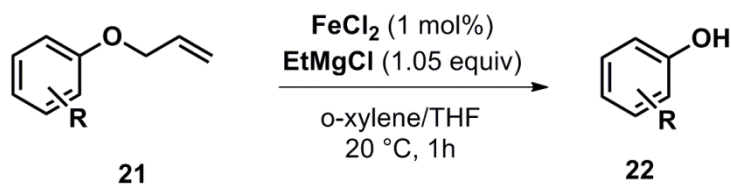
**Scheme 6.** Iron-promoted C-O cleavage of vinyl ether

More recently, the group of Fan demonstrated the cross coupling of benzylic and allylic ethers with allyl silanes via  $\text{FeCl}_3$  catalysed selective C-O bond cleavage.<sup>10</sup> An ample variety of benzyl and allyl ethers were transformed into allylic hydrocarbons with good yields and mild conditions (Scheme 7). However, the reaction can only be applied to secondary benzyl ethers, and a high catalyst loading (10 mol%) was needed to achieve good yields. No mechanistic investigations have been reported.



**Scheme 7.** Iron-catalysed C-O cleavage of benzyl ethers

The use of  $\text{FeCl}_2$  as catalyst for the selective C-O cleavage of allyl benzyl ethers to afford phenols in the presence of ethyl magnesium chloride has been recently reported.<sup>11</sup> The reactions proceeded with good yields under mild conditions in the presence of several functional groups with the allyl fragment being degraded to volatile hydrocarbons; however, stoichiometric amounts of the ethylmagnesium chloride were required (Scheme 8).



**Scheme 8.** Iron-catalysed cleavage of allylic C-O bonds

## 5.2. Aims of the chapter

Natural metalloenzymes such as dioxygenases are capable of selectively cleaving C-C bonds of organic substrates with incorporation of two oxygen atoms into the final product<sup>12</sup>. High complexity and/or significant structural modifications are introduced in organic substrates by such elegant enzymatic cleavages. Thus, such reactions often take place in bacteria or metabolism and, in contrast with transition metal mediated C-C cleavages, they occur under very mild conditions. Even though few iron complexes capable of mimicking some of these cleavages have been developed, they are often seen as tools to investigate and understand enzymatic processes. Their application as potential catalysts in chemical processes is mostly limited to bioremediation processes or biomass degradation.

Our efforts to highlight the potential application of selective iron-catalysed aerobic cleavage of C-O bonds and unstrained aliphatic C-C bonds in general organic syntheses are presented in this chapter, with the main goals being:

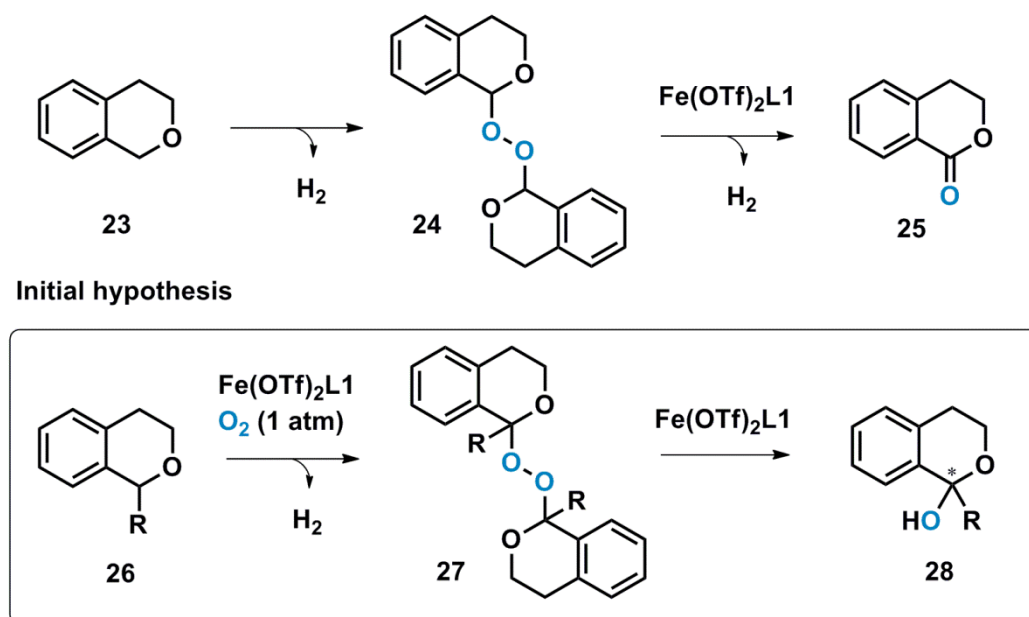
1. To provide alternative synthetic pathways for synthesising complex oxygenated compounds that cannot be obtained by iron-catalysed selective oxidation methods.
2. To show that classical synthetic methodologies can be replaced by greener and economical selective aerobic C-C and C-O cleavages.
3. To develop novel synthetic methodologies in the area of selective C-C and C-O cleavage.

### 5.3. Results and discussion

#### 5.3.1. Selective cleavage of Csp<sup>3</sup>-O bonds

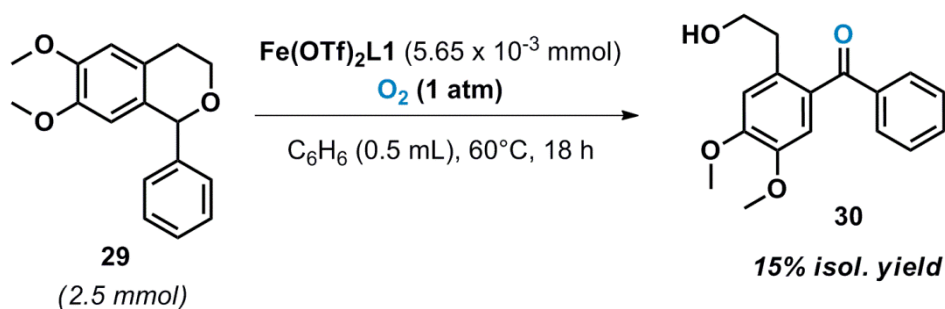
##### 5.3.1.1. Discovery and scope of the Fe(OTf)<sub>2</sub>L1 catalysed aerobic cleavage of Csp<sup>3</sup>-O bonds

Chen and White demonstrated that the Fe(PDP) complex can oxidise unactivated CH bonds in non functionalised compounds. The catalyst preferentially oxidises tertiary CH bonds to alcohols; however, secondary electron rich CH bonds could be oxidised to their keto form in compounds containing sterically hindered, tertiary CH bonds.<sup>13</sup> On the contrary, Fe(OTf)<sub>2</sub>-PyBisulidine complexes were found to selectively oxidise secondary CH bonds, even in substrates containing tertiary CH bonds in benzylic position or in  $\alpha$ -position to the ether functionality (Chapter 3). As this methylene oxidation involves the initial formation of a peroxybisether intermediate followed by its dehydrogenative cleavage (Chapter 4), we next wondered whether the Fe(OTf)<sub>2</sub>-PyBisulidine promoted cleavage of peroxide **27** would lead to the formation of the enantioenriched hemiacetal product **28** if the 1-substituted isochroman **26** was used as substrate (Scheme 9).



**Scheme 9.** Hypothesised reactivity of 1-substituted isochroman substrates under  $\text{Fe}(\text{OTf})_2\text{L1}$  catalysed aerobic conditions

In order to investigate whether the  $\text{Fe}(\text{OTf})_2\text{-PyBisulidone}$  complexes could catalyse the oxidation of tertiary CH bonds to alcohols, the 1-arylisochroman **29** was subjected to the  $\text{Fe}(\text{OTf})_2\text{L1}$  catalysed aerobic oxidation reaction (Scheme 10). Unexpectedly, reaction of **29** afforded the aryl ketone **30** in a 15% yield as the sole reaction product, with the starting material being easily recovered and no formation of the expected hemiacetal.



**Scheme 10.**  $\text{Fe}(\text{OTf})_2\text{L1}$  catalysed aerobic  $\text{Csp}^3\text{-O}$  bond cleavage of **29**

This result indicates that the  $\text{Fe}(\text{OTf})_2\text{L1}$  complex is capable of selectively cleaving the  $\text{Csp}^3\text{-O}$  bond in  $\alpha$ -position to the ether functionality under very mild reaction conditions and in a catalytic fashion. Like dioxygenases capable of cleaving aliphatic C-C bonds, the



Fe(OTf)<sub>2</sub>**L1** promotes a significant structural modification of an organic substrate with the incorporation of an oxygen-based functionality into the final product.

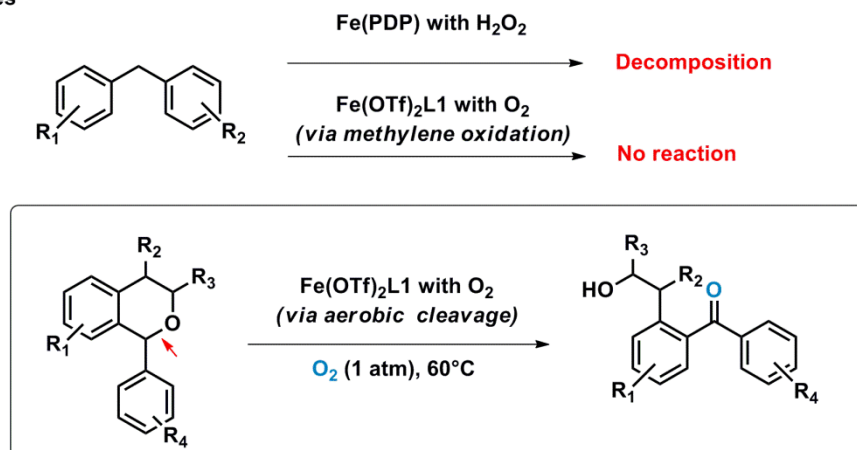
From a synthetic perspective, this transformation allows the formation of bulky and functionalised, open chain aromatic ketones whose preparation via iron-catalysed selective oxidation methods has been challenging. For instance, Chen and White's Fe(PDP) complex was found to degrade compounds bearing aromatic rings,<sup>13b</sup> whereas the Fe(OTf)<sub>2</sub>**L1** complex was not found capable of directly oxidising non-etheral aromatics (Scheme 11). In addition, a facile one-step synthesis of highly functionalised hydrocarbons can be problematic without introducing protection and deprotection steps (such as Friedel-Crafts reactions); however, 1-arylisochromans can be facilely synthesised from commercially available phenethyl alcohols and benzaldehydes in a simple one-step, Lewis acid-catalysed reaction.

As the Fe(OTf)<sub>2</sub>**L1** catalysed aerobic cleavage of 1-arylisochromans appears to be a good alternative for synthesising valuable 2-(hydroxyethyl)benzophenone derivatives, the scope of this reaction was further investigated (Scheme 11). The catalyst was found capable of selectively cleaving a variety of 1-arylisochromans containing either electron rich or electron deficient aryl groups with moderate yields (entries 1,2). Other heterocyclic groups (entries 3-5) were also tolerated, providing an ample and versatile substrate scope for this transformation.

Even though aryl ketones can be synthesised by different methods, methodologies for obtaining 2-(hydroxyethyl)benzophenone derivatives are scarce and often involve SnCl<sub>4</sub> mediated Friedel-Crafts reactions. However, this type of compounds are key intermediates for the synthesis of benzodiazepine-4-ones,<sup>14</sup> which are potent antagonist for AMPA receptors, and often used as photochemically removable protecting groups,<sup>15</sup> which can be used in the fabrication of DNA microarrays. Therefore, the Fe(OTf)<sub>2</sub>**L1** catalysed aerobic

cleavage of 1-arylisochromans appears to be an efficient and selective method for obtaining this class of compounds.

Synthetic application: Conversion of arylistochromans into 2-(hydroxyethyl)benzophenone derivatives



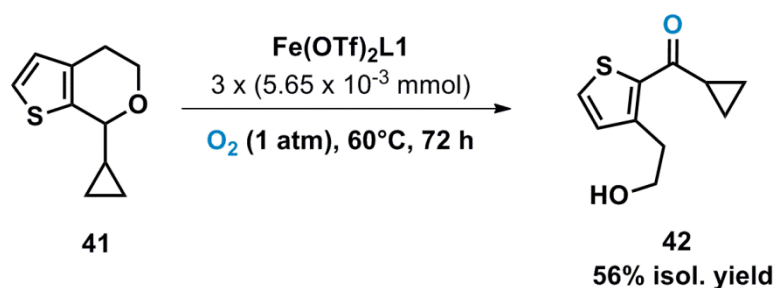
Entry	Starting material (rsm % <sup>a</sup> )	Product (isol. yield%)
1	 31. R = F (32% <sup>b</sup> )	 32. 68% <sup>b</sup> ; (40%) <sup>c</sup>
2	 33. R = OMe (40% <sup>b</sup> )	 34. 60% <sup>b</sup> ; (20%) <sup>c</sup>
3	 35. R = F <sup>d</sup> (40% <sup>b</sup> )	 36. 60% <sup>b</sup> ; (18%) <sup>c</sup>
4	 37. R = CF <sub>3</sub> <sup>d</sup> (41% <sup>b</sup> )	 38. 59% <sup>b</sup> ; (21%) <sup>c</sup>
5	 39. (22% <sup>e</sup> )	 40. 78% <sup>e</sup> ; (50%) <sup>c</sup>

Reaction conditions: Substrate (0.3 mmol) neat or in C<sub>6</sub>H<sub>6</sub> (0.5 mL) at 60 °C. <sup>a</sup> rms = % recovered starting material (unoxidised). <sup>b</sup> Three additions of catalyst (5.65 × 10<sup>-3</sup> mmol each), 72 h reaction. <sup>c</sup> One addition of catalyst (5.65 × 10<sup>-3</sup> mmol), 16 h reaction. <sup>d</sup> 2mL of substrate were added. <sup>e</sup> Two additions of catalyst (5.65 × 10<sup>-3</sup> mmol each)

**Scheme 11.** Selective aerobic cleavage of 1-arylistochromans as an alternative to the iron-catalysed oxidation of benzyl ethers

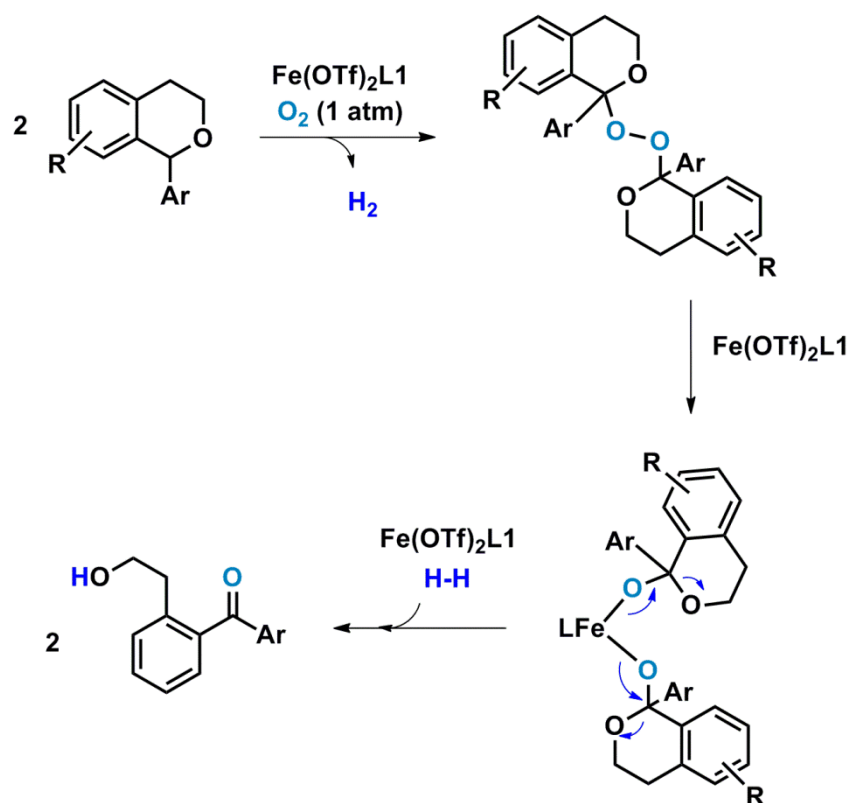
### 5.3.1.2. Mechanistic investigations of the Fe(OTf)<sub>2</sub>L1 catalysed aerobic cleavage of Csp<sup>3</sup>-O bonds

In order to determine whether radical species are generated during the catalytic reaction, the 1-cyclopropyl substituted compound **41** was subjected to the Fe(OTf)<sub>2</sub>L1 catalysed aerobic cleavage. Compound **42** was generated in 56% yield as the sole reaction product with no decomposition of the starting material being observed (Scheme 12). This result indicates that the catalytic reaction does not involve the formation of C-based radical species.



**Scheme 12.** The aerobic cleavage of a radical trap showing no side reactivity

On the basis of these results and the mechanistic observations presented in Chapter 4, the initial dehydrogenative formation of a peroxybisether species was postulated. Subsequent oxidative addition of the peroxide to the iron centre, followed by the cleavage of the Csp<sup>3</sup>-O bond with the concomitant formation of the conjugated ketone as the thermodynamic driving force of the process seems plausible (Scheme 13). In agreement with this hypothesis, no lactol formation was manifested during the aerobic cleavages even in conditions of limiting oxidant or shorter reaction times. Attempts to identify and isolate the hypothesised peroxide intermediate and isotopic labelling experiments with a O<sub>2</sub>/D<sub>2</sub> gas mixture and with deuterated substrates are in current progress to shed some light into this reaction mechanism. Such mechanistic experiments are very relevant for ascertaining whether the Fe(OTf)<sub>2</sub>L1 catalyst is actually activating both O<sub>2</sub> and H<sub>2</sub> gases during the reaction. To the best of our knowledge, there are no examples in the literature of an iron catalyst capable of activating both O<sub>2</sub> and H<sub>2</sub> during the same catalytic process.



**Scheme 13.** Proposed pathway for the  $\text{Fe}(\text{OTf})_2\text{L1}$  catalysed selective  $\text{Csp}^3\text{-O}$  cleavage of 1-arylisochromans

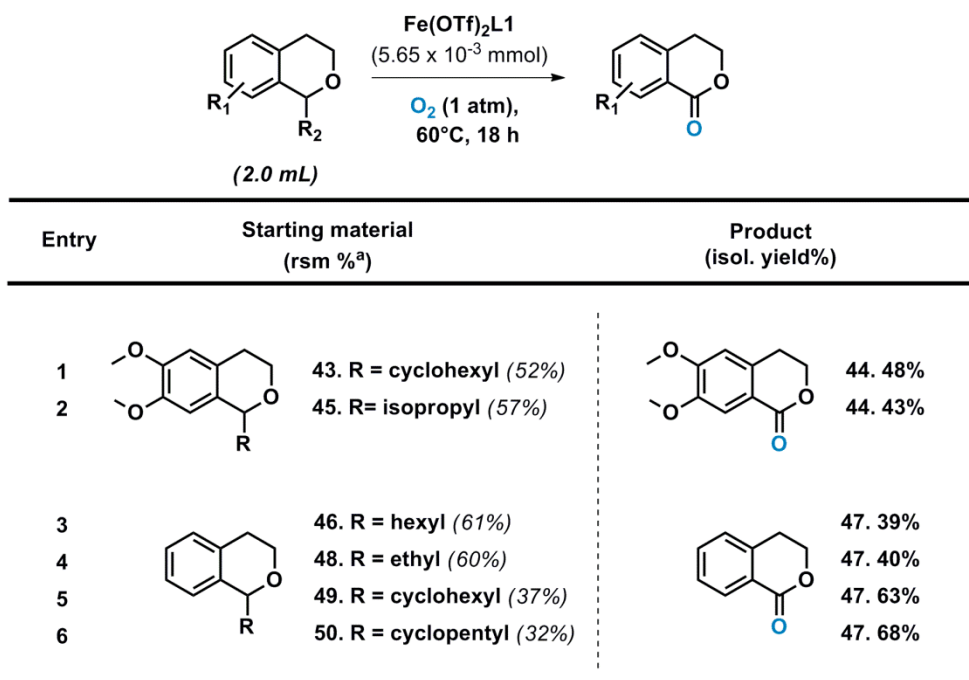
### 5.3.2. Selective cleavage of $\text{Csp}^3\text{-Csp}^3$ bonds

#### 5.3.2.1. Conversion of isochromans into isochromanones *via* selective aerobic cleavage of exocyclic $\text{Csp}^3\text{-Csp}^3$ bonds

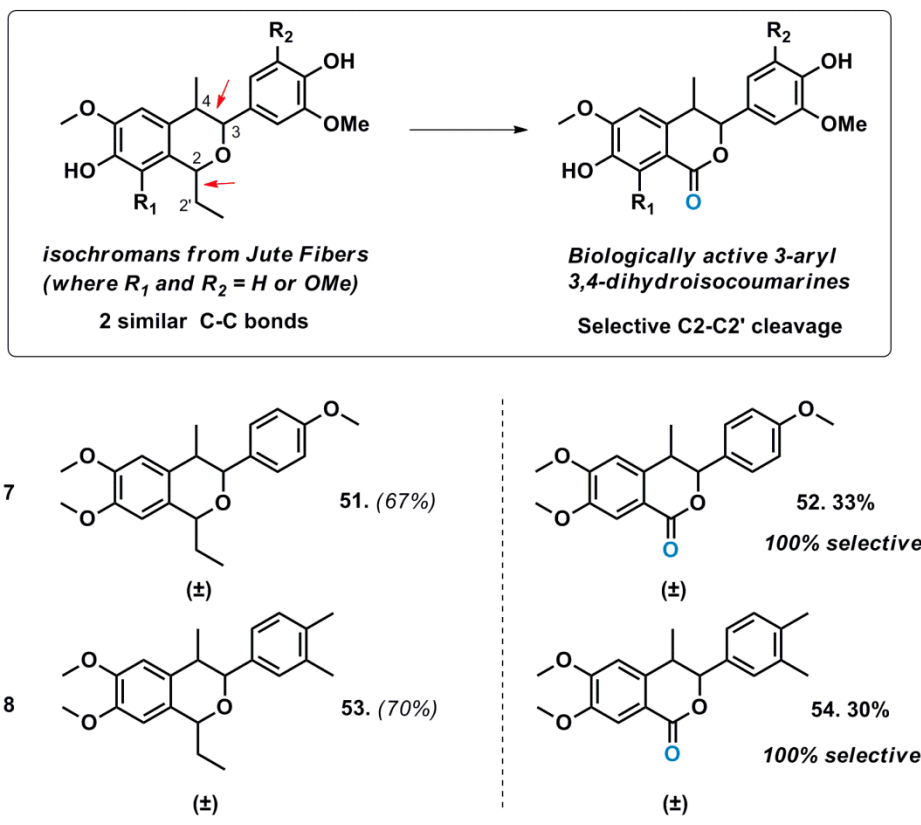
In an attempt to expand the aerobic  $\text{Csp}^3\text{-O}$  cleavage to the synthesis of aliphatic ketones, 1-alkyl substituted isochromans were next subjected to the  $\text{Fe}(\text{OTf})_2\text{L1}$  catalysed aerobic reaction (Scheme 14). Surprisingly, isochromanone **44** was generated in moderate yields from isochromans **43** and **45** with no formation of the corresponding aliphatic ketones being detected by  $^1\text{H}$  NMR (entries 1,2). In fact, isochromanone **47** was generated as the reaction product from a variety of isochromans bearing different aliphatic substituents (entries 3-6). Therefore, the  $\text{Fe}(\text{OTf})_2\text{L1}$  complex is also capable of selectively catalysing the aerobic cleavage of the unstrained exocyclic  $\text{Csp}^3\text{-Csp}^3$  bonds when 1-alkylsubstituted isochromans

are used as substrates and under surprisingly mild conditions. This preferential cleavage of the exocyclic Csp<sup>3</sup>-Csp<sup>3</sup> bond in 1-alkyl isochromans allows the formation of a conjugated cyclic benzoate which can act as the thermodynamic driving force of the process, and thus it can be seen as the main factor in defining the selectivity of this cleavage.

From a synthetic perspective, the selective cleavage of unstrained Csp<sup>3</sup>-Csp<sup>3</sup> bonds under mild conditions can be of utmost interest. As an example of the potential of such type of reactions, electron rich, highly functionalised isochromans **51** and **53** with a molecular skeleton analogous to those found in isochromans isolated from softwood lignings were subjected to the Fe(OTf)<sub>2</sub>**L1** catalysed aerobic cleavage. These molecules are particularly challenging because the cleavage of the exocyclic C2-C2' bond or the endocyclic C3-C4 bond would result in the formation of a conjugated benzoate that could potentially act as the thermodynamic force of the process. However, only the selective C2-C2' bond cleavage would allow the direct synthesis of biologically active 3-aryl-3,4-dihydroisocoumarines, which have shown a variety of pharmacological activities including cytotoxic activity against human gastric cancer cell line and human nasopharyngeal carcinoma cell lines,<sup>16</sup> antifungal,<sup>17</sup> antiallergic<sup>18</sup> and differentiation-inducing<sup>19</sup> activities. Delightfully, the Fe(OTf)<sub>2</sub>**L1** complex afforded exclusively the desired dihydroisocoumarine products **52** and **54** with moderate yields, excellent selectivity, and excellent mass balance and functional group tolerance (entries 7,8). Therefore, the Fe(OTf)<sub>2</sub>**L1** catalysed aerobic cleavage of unstrained Csp<sup>3</sup>-Csp<sup>3</sup> bonds can be potentially applied to the conversion of naturally occurring isochromans into biologically important 3-aryl-3,4-dihydroisocoumarines.



Synthetic application: Conversion of softwood ligning type isochromans into biologically active 3-aryl-1,3-dihydrocoumarines



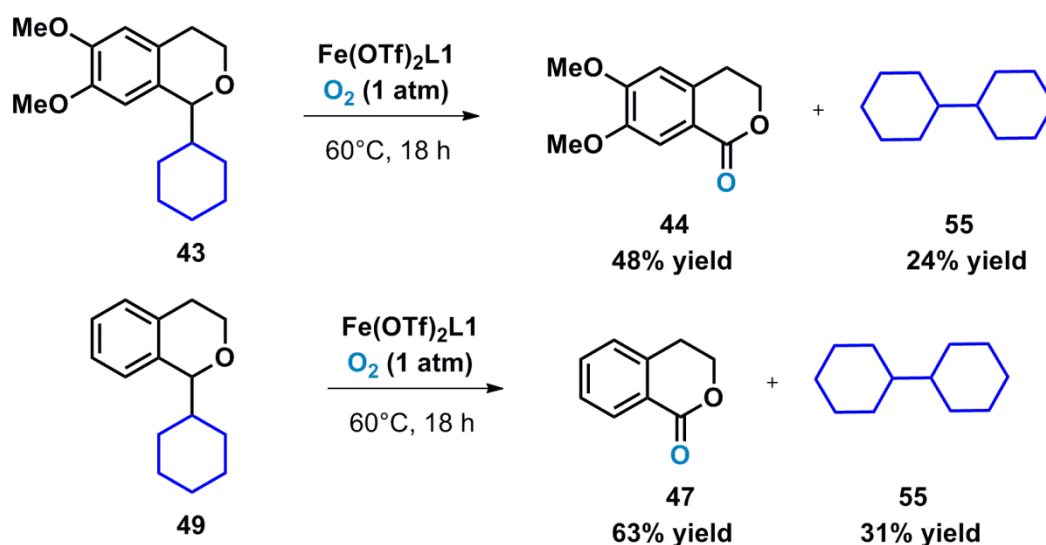
<sup>a</sup> rms: % recovered starting material (unoxidised)

**Scheme 14.** Selective aerobic cleavage of Csp<sup>3</sup>-Csp<sup>3</sup> bonds in isochroman type substrates

### 5.3.2.2. Mechanistic investigations of the selective exocyclic Csp<sup>3</sup>-Csp<sup>3</sup> cleavage

#### 5.3.2.2.1. Merging selective oxidation with selective alkyl coupling

When investigating the substrate scope of the Fe(OTf)<sub>2</sub>L1 catalysed aerobic cleavage of 1-alkylisochromans, we wondered whether the alkyl fragment was also being oxidised during the catalytic reaction. To our surprise, linear 1-alkylisochromans **46** and **48** were cleanly oxidised to isochromanone **47** and no other reaction products were isolated during the purification. Similarly, the oxidation of highly functionalised isochromans **51** and **53** afforded the dihydroisocoumarin products exclusively. However, when 1-cyclohexyl substituted isochromanones **43** and **49** were subjected to the aerobic reaction, the alkyl coupling product 1,1'-bi(cyclohexane) was also isolated in 24% and 31% yields, respectively (Scheme 15).

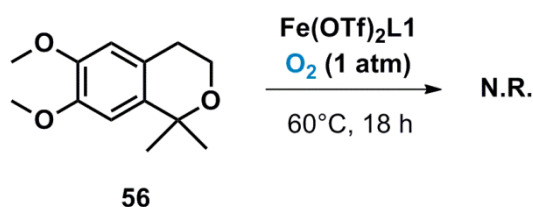


**Scheme 15.** Formation of the alkyl coupling product **55** from 1-cyclohexylisochromans

These results indicate that the iron catalyst is capable of undergoing both the selective oxidation of the isochroman substrate and the selective alkyl coupling during the catalytic process. These results align with the oxidations of linear 1-alkylisochromans being so clean, as the corresponding alkyl coupling products which would generate from them are very volatile species. In line with these results, the Fe(OTf)<sub>3</sub>L1 complex has also been found

capable of generating volatile hydrocarbon products during the aerobic cleavage of olefinic substrates (chapter 6). Additional GC analyses for confirming the structure of the alkyl coupling products generated in those reactions are in current progress.

In order to investigate whether the cleavage of the Csp<sup>3</sup>-Csp<sup>3</sup> bonds occurs after or before the oxygenation step, the 1,1-dimethyl substituted isochroman **56** was subjected to the Fe(OTf)<sub>2</sub>L1 catalysed aerobic cleavage (Scheme 16). As no reaction was observed on the <sup>1</sup>H NMR spectrum of the crude reaction, the oxidation of the CH bond in α-position to the ether functionality should take place prior the Csp<sup>3</sup>-Csp<sup>3</sup> cleavage.

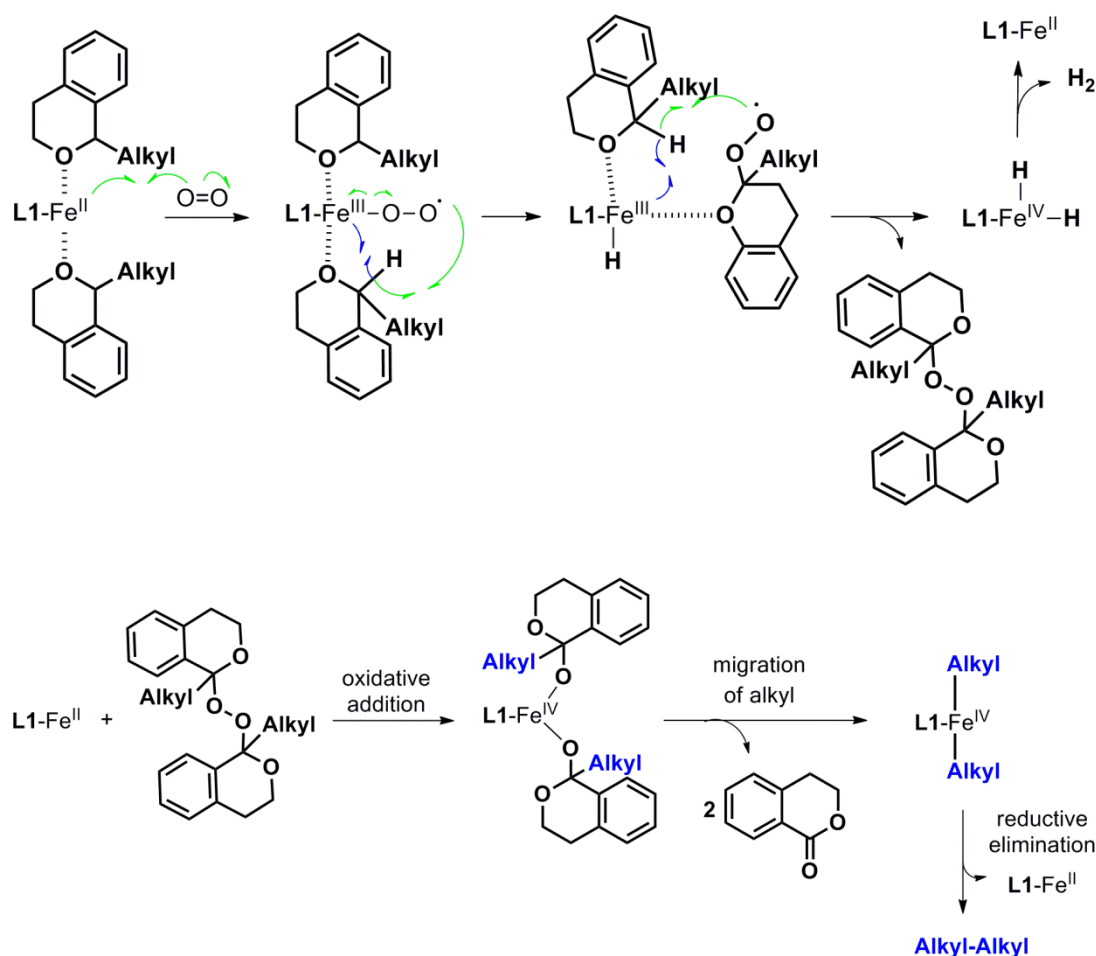


**Scheme 16.** Reaction indicating that the oxidation of the CH bond is prior to the C-C cleavage

#### 5.3.2.2.2. Postulated catalytic cycle

On the basis of these results, the mechanism for the Fe(OTf)<sub>2</sub>L1 catalysed aerobic oxidation of the 1-alkylisochromans could initially involve the coordination of two ethereal molecules to the iron centre (Chapter 10). Exposure to O<sub>2</sub> atmosphere would again allow the formation of a Fe<sup>III</sup> superoxo species from which a peroxide intermediate can be generated with concomitant formation of H<sub>2</sub> gas (Scheme 17). Subsequent cleavage of the peroxide intermediate by oxidative addition of the peroxide O-O bond to the iron centre would result in the formation of a Fe<sup>IV</sup> alkoxo compound (Chapter 10). Migration of the alkyl fragment to the iron centre either by a concerted radical process or by the less common β-alkyl elimination<sup>20</sup> would result in the formation of the isochromanone product and a Fe<sup>IV</sup> dialkyl species. Reductive elimination from the Fe<sup>IV</sup> dialkyl intermediate would generate the observed 1,1'-bi(alkyl) byproducts.



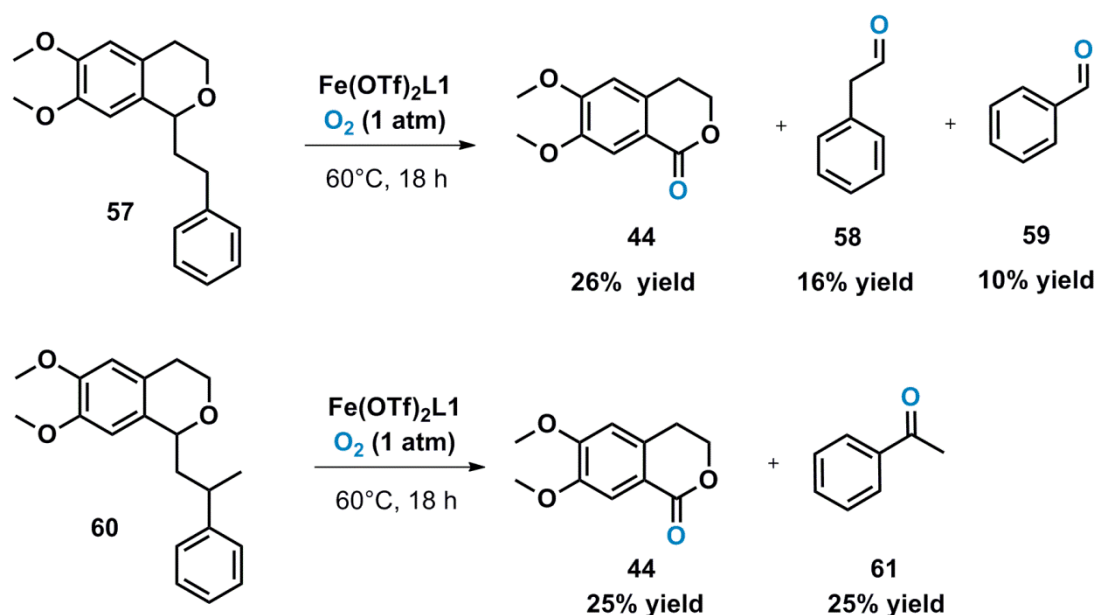


**Scheme 17.** Proposed reaction pathway for the  $\text{Fe}(\text{OTf})_2\text{L1}$  catalysed aerobic cleavage of  $\text{Csp}^3\text{-Csp}^3$  bonds in 1-alkylisochromans

Attempts to isolate and characterise the hypothesised peroxide intermediate are in current progress for gaining more experimental evidence to support the proposed mechanism. Such mechanistic studies are very relevant as the selective alkane-alkane coupling mediated by homogeneous catalysts is very rare.<sup>21</sup> However, the development of catalyst capable of performing a selective alkyl coupling is highly desirable due to the importance of such reaction for producing higher hydrocarbons in an industrial scale.<sup>22</sup> In addition, there are no reports in the literature of any iron catalysts capable of promoting the selective cleavage of unstrained  $\text{Csp}^3\text{-Csp}^3$  bonds by combining a selective CH oxidation and a selective alkyl coupling under mild conditions.

### 5.3.2.2.3. Overriding alkyl coupling: oxidation of the alkyl fragment

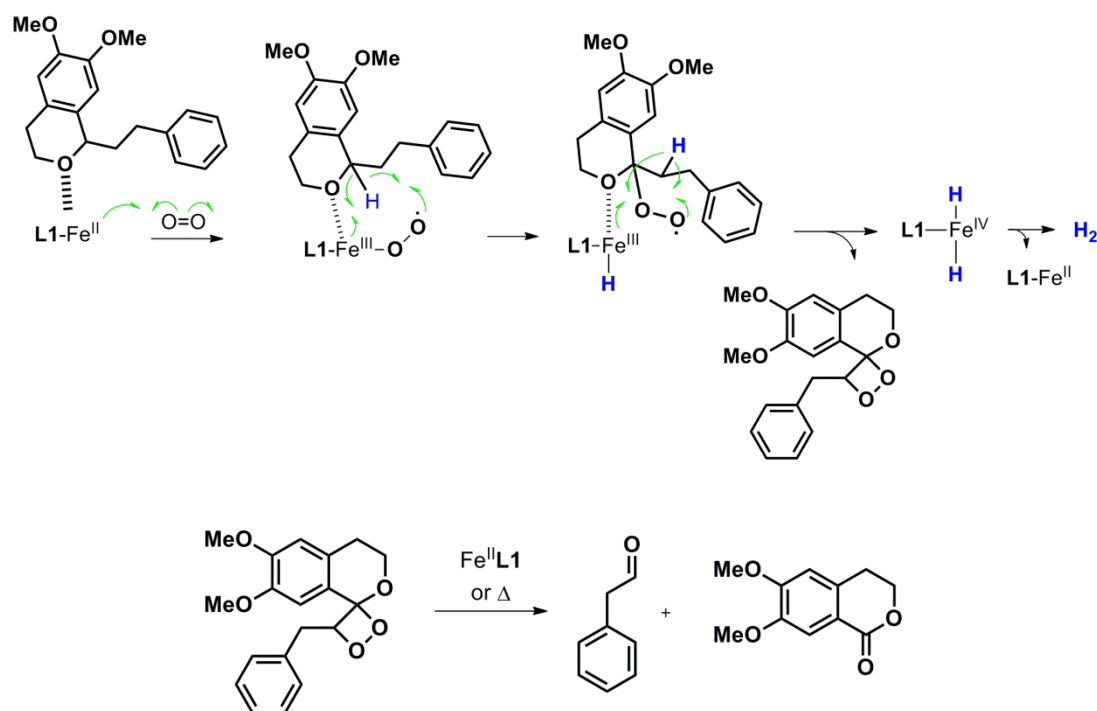
When 1-alkylisochromans incorporating a phenethyl group were subjected to the  $\text{Fe}(\text{OTf})_2\text{L1}$  catalysed aerobic cleavage, different oxygenated products were generated; aldehydes **58** and **59** were obtained in a 1.6 : 1.0 ratio from the cleavage of isochroman **57**, whereas acetophenone **61** was exclusively formed during the aerobic cleavage of isochroman **60**. These results indicate that modifications in the nature of the alkyl fragment can induce different reaction pathways and thus, the alkyl coupling can be overrode by introducing weaker CH bonds which are susceptible to be easily oxidised. In addition, the oxygenation of the alkyl fragments in the phenethyl derived isochromans suggest that an intramolecular  $\text{Csp}^3\text{-Csp}^3$  cleavage may be taking place instead of an intermolecular reaction involving two ethereal molecules.



**Scheme 18.** Different oxidation products are obtained depending on the nature of the alkyl group

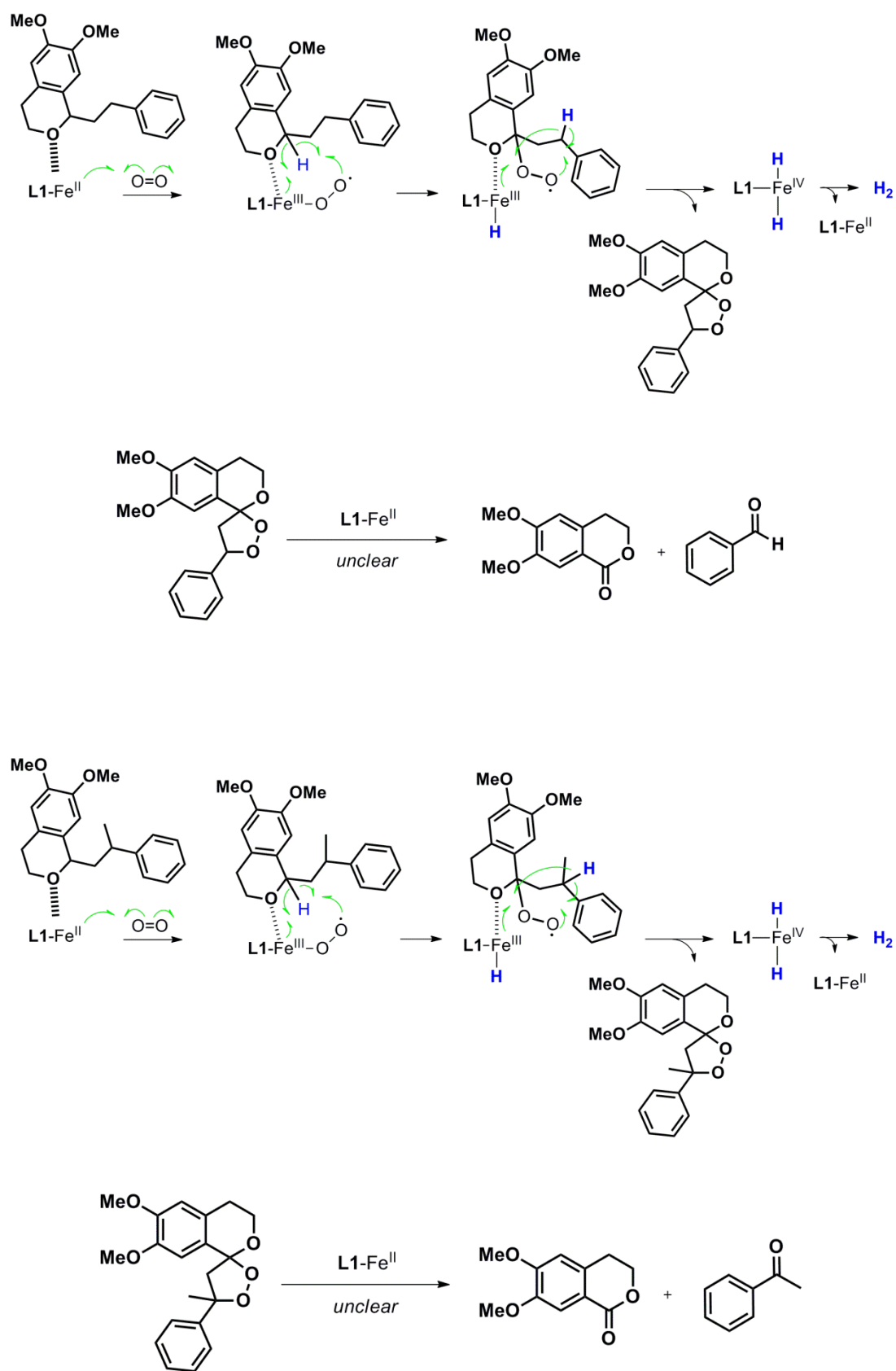
From a mechanistic perspective, the cleavage of isochroman **56** to afford the aldehyde byproduct **57** can be seen as the attack of the superoxo radical to the methylene in  $\beta$ -position, from which a dioxetane species and a  $\text{Fe}^{\text{IV}}$ -dihydride intermediate result (Scheme

19). The subsequent thermal or iron-mediated cleavage of the dioxetane (chapter 12) would furnish the detected isochromanone and aldehyde **58**.



**Scheme 19.** Proposed reaction pathway for the Fe(OTf)<sub>2</sub>L1 catalysed aerobic cleavage of Csp<sup>3</sup>-Csp<sup>3</sup> bonds in 1-phenethylisochroman **57** to afford isochromanone **44** and aldehyde **58**

However, the mechanism behind the formation of carbonyl products **59** and **61** is unclear to us. By analogy to the aforementioned mechanism, the attack of the superoxo radical to the methylene in γ-position would initially allow the formation of a 1,2-dioxolane intermediate and a Fe<sup>IV</sup>-dihydride (Schemes 20). The cleavage of the proposed dioxolane into the oxygenated products is however unknown to us. We suspect that volatile hydrocarbons are also generated during such cleavage due to the strong gas smell emanating from the crude reactions. GC analyses to identify the formation of volatile products from these cleavages are in current progress.



**Scheme 20.** Proposed reaction pathway for the Fe(OTf)<sub>2</sub>L1 catalyzed aerobic cleavage of

C<sup>sp3</sup>-C<sup>sp3</sup> bonds in 1-phenethylisochroman **56** and **60**

### 5.3.2.2.4. Factors determining the selectivity of the Csp<sup>3</sup>-Csp<sup>3</sup> vs Csp<sup>3</sup>-O bond cleavage

The Fe(OTf)<sub>2</sub>L1 complex exhibited excellent selectivity in promoting the C-O cleavage of 1-aryl isochromans and the exocyclic C-C cleavage of 1-alkyl substrates. However, when 1-alkyl substituted 5,7-dihydro-4*H*-thieno[2,3*c*]pyranes were subjected to the Fe(OTf)<sub>2</sub>L1 catalysed aerobic reaction both products derived from both C-O and C-C cleavage were obtained (Scheme 21). Independently of the alkyl substituent, both 4-*H*-thieno[2,3-*c*]pyran-7(5*H*)-one **64** and the aliphatic ketone products were obtained in almost identical yields. Increasing the steric bulkiness of the alkyl fragment did not alter the product distribution; however, the reaction yields for both products were slightly reduced.

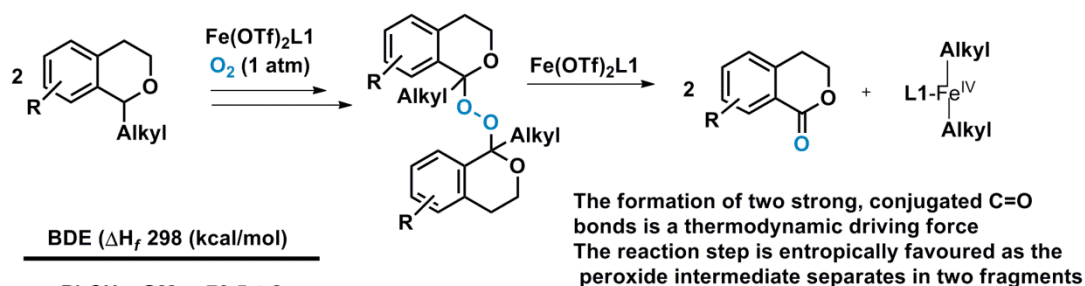
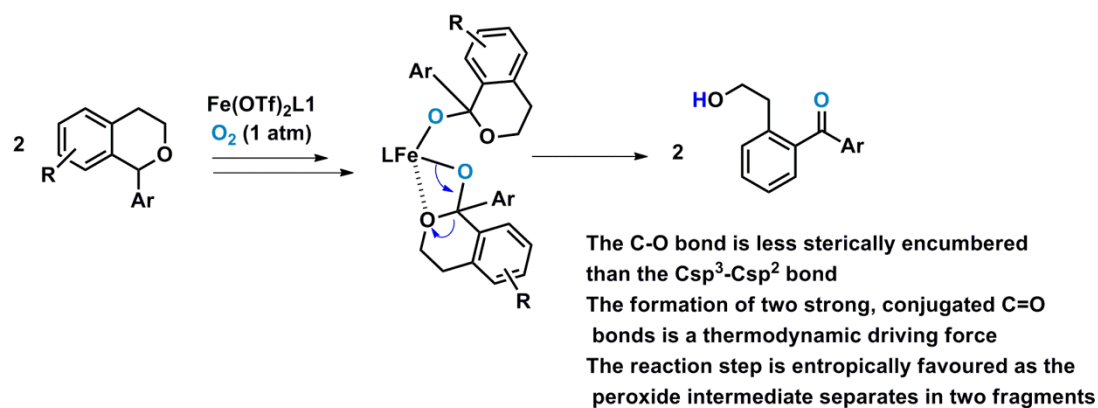
Entry	Starting material (rsm % <sup>a</sup> )	Product (isol. yield%)
1	 <b>62.</b> (59%)	 <b>63.</b> 20% + <b>64.</b> 21%
2	 <b>65.</b> (71%)	 <b>66.</b> 13% + <b>64.</b> 16%
3	 <b>67.</b> (76%)	 <b>68.</b> 12% + <b>64.</b> 12%

Reaction conditions: Substrate (2.0 mL), Fe(OTf)<sub>2</sub> (2.0 mg), L1 (5.2 mg) at 60 °C, 18 h.

<sup>a</sup> rms = % recovered starting material (unoxidised)

**Scheme 21.** Fe(OTf)<sub>2</sub>L1 catalysed cleavage of alkyl substituted 5,7-dihydro-4*H*-thieno[2,3*c*]pyranes

The selectivity showed by the  $\text{Fe}(\text{OTf})_2\mathbf{L1}$  complex in cleaving the  $\text{Csp}^3\text{-O}$  bond of 1-arylisochromans and the  $\text{Csp}^3\text{-Csp}^3$  bond in 1-alkylisochromans can be interpreted in terms of the free energy changes associated to these reactions. In both types of cleavages, the formation of very stable conjugated carbonyl bonds can serve as a thermodynamic driving force to promote bond cleavage. In addition, as the bond cleavage makes the peroxide intermediates separate in two fragments, its cleavage is entropically favoured (Scheme 22). In 1-aryl isochromans, the cleavage of the C-O bond would be easier than the cleavage of the more stable and sterically encumbered  $\text{Csp}^3\text{-Csp}^2$  bond (BDE of 70.5 vs 71.8 kcal/mol respectively). In 1-alkyl isochromans, the cleavage of the  $\text{Csp}^3\text{-Csp}^3$  would be thermodynamically easier than cleaving the C-O bond (BDE of 69.2 (average) vs 70.5 kcal/mol respectively). Thus, the selectivity observed in the reactions stems from the  $\text{Fe}(\text{OTf})_2\mathbf{L1}$  complex being prone to cleavage the weakest (and accessible) bond of the 1-substituted isochroman. In addition, the higher yields observed in 1-cycloalkylisochromans are consistent with the progressive energy decrease of the  $\text{Csp}^3\text{-Csp}^3$  bond.



BDE ( $\Delta H_f$  298 (kcal/mol))

PhCH<sub>2</sub>--OMe : 70.5 ± 2

PhCH<sub>2</sub>--R:

R = Et : 70.3 ± 1

R = Propyl : 70.0 ± 1

R = <sup>i</sup>Pr : 69.6 ± 2

R = <sup>t</sup>Butyl : 67.2 ± 1

Ph--R:

R = Et : 71.8 ± 1

R = Propyl : 72.1 ± 1

C=O : 179.0

**Scheme 22.** Enthalpic and entropic factors in the C-O and C-C cleavage of 1-substituted isochromans. Bond dissociation energies are provided in terms of formation enthalpies as reported in the literature.<sup>23</sup>

In the case of 1-alkyl substituted 5,7-dihydro-4H-thieno[2,3c]pyranes, the formation of products resulting from both Csp<sup>3</sup>-O and Csp<sup>3</sup>-Csp<sup>3</sup> bond cleavages may stem from the energies of these two bonds being much more similar than in the case of 1-alkyl isochromans. However, contributions from other factors, such as the ring size or the reduced aromaticity in comparison with benzene type rings may also affect the selectivity of the cleavage.

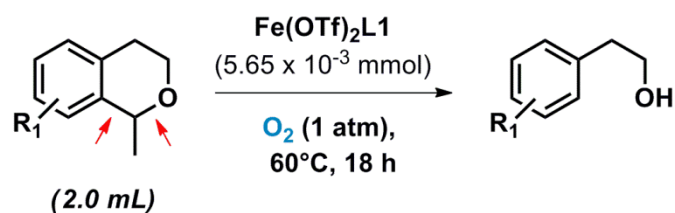
### 5.3.3. Combined Fe(OTf)<sub>2</sub>L1 catalysed selective Csp<sup>2</sup>-Csp<sup>3</sup> and Csp<sup>3</sup>-O cleavage

The Fe(OTf)<sub>2</sub>L1 catalysed Csp<sup>3</sup>-Csp<sup>3</sup> cleavage of 1-alkyl isochromans was also studied in 1-methylisochromans substrates (Scheme 23). Surprisingly, when isochroman **71** was subjected to the aerobic reaction, the phenethyl alcohol **72** was obtained in very good yield as the sole reaction product (entry 2). In fact, phenethyl alcohols were obtained exclusively from a variety of 1-methylisochromans with good to moderate yields. A sharp electronic bias was manifested, with reaction yields highly increasing in isochromans bearing electron withdrawing substituent (entries 1,2) and gradually decreasing in more electron rich substrates (entries 3-5). These data indicates that the Fe(OTf)<sub>2</sub>L1 complex is also capable of catalysing a sequential Csp<sup>2</sup>-Csp<sup>3</sup> and Csp<sup>3</sup>-O cleavage under aerobic conditions.

The reaction mechanism is unclear; however, the strong electronic bias is in agreement with the initial oxidation of the C2 bond of the 1-methylisochroman to form a peroxybisether species. Small amounts of acetaldehyde were also detected in <sup>1</sup>H NMR spectra of the crude reactions; however, the yields were clearly lower than those found for the phenethyl alcohols, which may be an indication of the observed acetaldehyde being a byproduct originated from an unknown intermediate.

From a synthetic perspective, the conversion of 1-methylisochromans to phenethyl alcohols can be seen as a greener alternative to oxidative ether deprotection reactions, which often require stoichiometric amounts of strong oxidants<sup>24</sup> and/or exhibit limited selectivity and functional group tolerance<sup>25</sup> (Scheme 23).





Entry	Starting material (rsm % <sup>a</sup> )	Product (isol. yield%)
1	69. (9%)	70. 91%
2	71. (13%)	72. 87%
3	73. (53%)	74. 47%
4	75. (66%)	76. 34%
5	77. (90%)	78. 10%

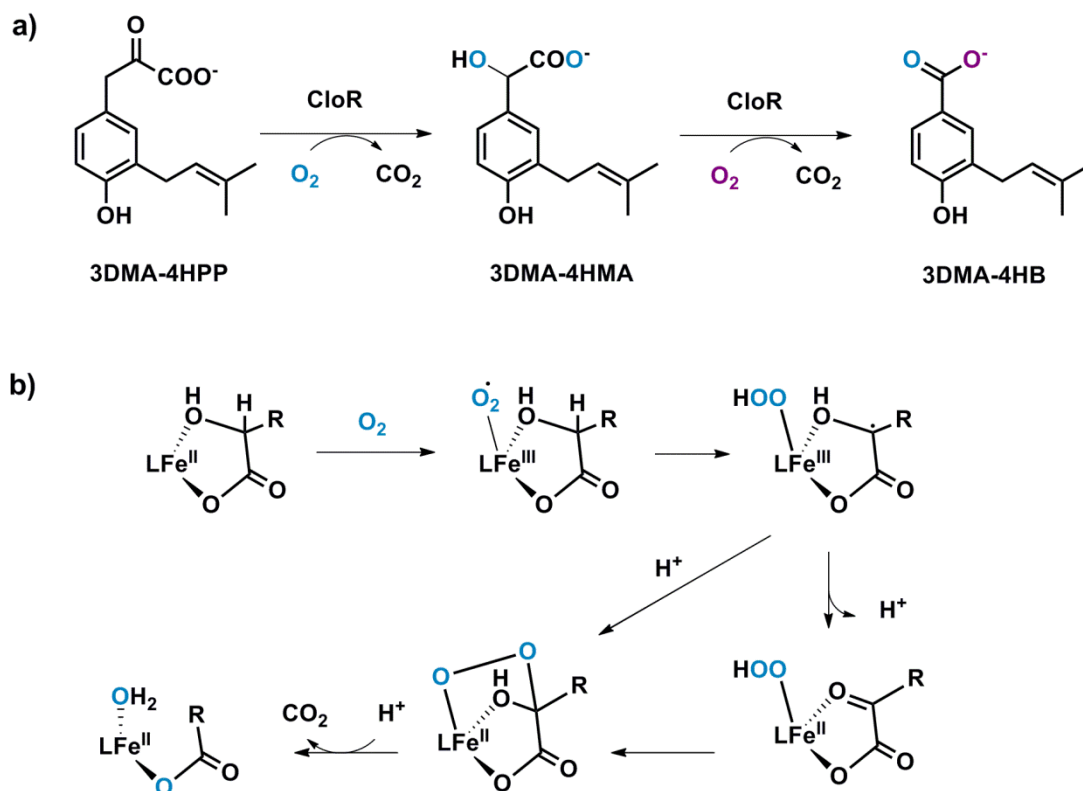
<sup>a</sup> rsm = % recovered starting material (unoxidised)

**Scheme 23.** Combined  $\text{Fe}(\text{OTf})_2\text{L1}$  catalysed selective  $\text{Csp}^2\text{-Csp}^3$  and  $\text{Csp}^3\text{-O}$  cleavage in 1-methylisochromans

### 5.3.4. Combined $\text{Fe}(\text{OTf})_2\text{L1}$ catalysed selective $\text{Csp}^3\text{-Csp}^2$ and $\text{Csp}^2\text{-X}$ ( $\text{X} = \text{O}, \text{N}$ ) cleavage via decarboxylation

CloR enzymes participating in the biosynthesis of clorobiocin and aminocoumarine are known to undergo the decarboxylation of aliphatic C-C bonds of the mandelic acid fragment of 3DMA-4HPP affording the benzoic acid derivative 3DMA-4HB<sup>26</sup> (Scheme 24 a).

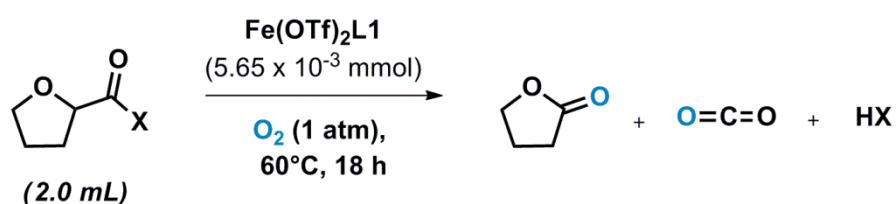
Inspired by this biological system, the groups of Paine and Que Jr. reported a biomimetic  $\text{Fe}^{\text{II}}$   $\alpha$ -hydroxy acid complex capable of undergoing the aerobic decarboxylation of the  $\alpha$ -hydroxy acid moiety to generate benzoate, mimicking the activity of the natural system<sup>27</sup> (Scheme 24 b).

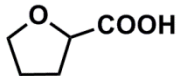
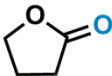
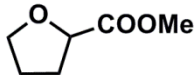
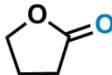
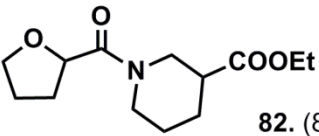
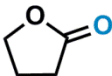
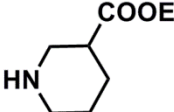


**Scheme 24.** CloR oxidative decarboxylation of 3DMA-4HPP and a related  $\text{Fe}^{\text{II}}$   $\alpha$ -hydroxy acid mimicking the natural activity

Inspired by these natural decarboxylations, we envisioned that the selective  $\text{Fe}(\text{OTf})_2\mathbf{L1}$  catalysed C-C cleavage could be combined with the decarboxylation of acid-derived functionalities. The  $\text{CO}_2$  release could be used as the thermodynamic driving force for cleaving the strong C-O or C-N bonds of esters and amides. In order to evaluate whether the  $\text{Fe}(\text{OTf})_2\mathbf{L1}$  complex could promote a tandem C-C and C-X cleavage via decarboxylation, tetrahydrofuran-2-carboxylic acid **79** was subjected to the  $\text{Fe}(\text{OTf})_2\mathbf{L1}$  catalysed aerobic reaction (Scheme 25). Delightfully,  $\gamma$ -butyrolactone **80** was obtained with a 10% yield in a clean reaction, with the starting material being easily recovered (entry 1). Indeed, the methyl

ester derivative **81** was also oxidatively decarboxylated with similar yields (entry 2). When the amide **82** was subjected to the reaction,  $\gamma$ -butyrolactone and ethyl piperidin-3-carboxylate **83** were isolated as reaction products (entry 3). These data is in agreement with the proposed oxidative decarboxylation and highlight the excellent selectivity of the catalyst as no decarboxylation of the ester functionality was observed. The scope of this reaction and GC analysis to determine the possible CO<sub>2</sub> release are under current investigation.



Entry	Starting material (rsm % <sup>a</sup> )	Product (isol. yield%)
1	 <b>79.</b> (90%)	 <b>80.</b> 10%
2	 <b>81.</b> (87%)	 <b>80.</b> 13%
3	 <b>82.</b> (84%)	 <b>80.</b> 16% +  <b>83.</b> 16%

<sup>a</sup> rms = % recovered starting material (unoxidised)

**Scheme 25.** Fe(OTf)<sub>2</sub>L1 catalysed oxidative decarboxylation of THFs substrates

#### 5.4. Conclusions

The Fe(OTf)<sub>2</sub>-PyBisulidine complexes were found capable of catalysing a wide variety of selective aerobic C-C and C-O cleavages under mild reaction conditions. Some of these oxidative cleavages represent a good synthetic alternative for obtaining complex and/or

valuable oxygenated compounds, such as the conversion of 1-arylisochromans into aromatic ketones. Others, such as the conversion of natural isochromans into 3-aryl-3,4-dihydrocoumarines, constitute an example of new and green synthetic transformations of potential commercial interest. The  $\text{Fe}(\text{OTf})_2$ -PyBisulidine was also found to promote tandem C-C and C-O cleavages, allowing the conversion of 1-methylisochromans into phenethyl alcohols, and active in the oxidative decarboxylation of THF's. Therefore, many different cleavages can be accomplished on a selective manner using the same family of iron catalysts.

Even though the selective oxidation of organic compounds has been identified as the most important area to impact future industrial transformations, we anticipate that selective iron-catalysed aerobic C-C and C-X cleavages would potentially become an equally important area of research in future organic syntheses.

## **5.5. Experimental section**

### **5.5.1. General techniques**

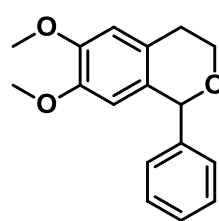
Chemicals used in the synthesis of non-commercially available substrates were purchased from commercial suppliers and used without further purification.

### **5.5.2. Substrate synthesis**

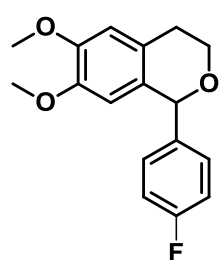
#### **5.5.2.1. Synthesis of 1-arylisochromans**

1-Aryl isochromans were synthesised according to the acid-catalysed oxa-Pictet-Spengler reaction procedure described in Chapter 3.

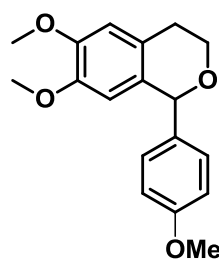
#### **Analytical data**

**6,7-Dimethoxy-1-phenylisochroman**<sup>28</sup>

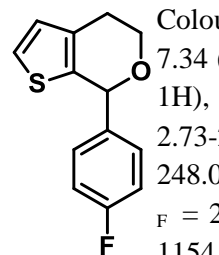
White solid, 97% isol. yield. <sup>1</sup>H NMR (400 MHz, CDCl<sub>3</sub>): δ (ppm) = 7.35-7.27 (m, 5H), 6.64 (s, 1H), 6.22 (s, 1H), 5.67 (s, 1H), 4.14-4.09 (m, 1H), 4.08-4.02 (m, 1H), 3.96 (s, 3H), 3.82 (s, 3H), 3.05-2.98 (m, 1H), 2.74-2.68 (m, 1H). <sup>13</sup>C NMR (100 MHz, CDCl<sub>3</sub>): δ (ppm) = 147.9, 147.6, 142.2, 129.2, 128.7, 128.5, 128.2, 126.1, 111.5, 109.7, 79.1, 63.5, 56.2, 55.8, 28.3. **IR** (neat): ν = 2965, 2922, 2859, 2830, 1607, 1510, 1480, 1455, 1383, 1359, 1342, 1331, 1275, 1254, 1243, 1219, 1204, 1175, 1110, 1088, 1036, 1027, 1012, 948, 837, 822, 774, 691, 608, 566, 532 cm<sup>-1</sup>. **HRMS** (CI) m/z calc'd C<sub>17</sub>H<sub>19</sub>O<sub>3</sub> [M + H]<sup>+</sup>: 271.1329, found: 271.1335.

**1-(4-Fluorophenyl)-6,7-dimethoxyisochroman**<sup>29</sup>

White solid, 98% isol. yield. <sup>1</sup>H NMR (400 MHz, CDCl<sub>3</sub>): δ (ppm) = 7.27 (t, J = 5.9 Hz, 2H), 7.02 (t, J = 5.9 Hz, 2H), 6.65 (s, 1H), 6.18 (s, 1H), 5.66 (s, 1H), 4.15-4.10 (m, 1H), 3.87 (s, 3H, overlapped), 3.85 (m, 1H, overlapped), 3.65 (s, 3H), 3.07-2.99 (m, 1H), 2.74-2.70 (m, 1H). <sup>13</sup>C NMR (100 MHz, CDCl<sub>3</sub>): δ (ppm) = 163.7 (<sup>1</sup>J<sub>C-F</sub> = 245.0 Hz), 147.9, 147.3, 138.1 (<sup>4</sup>J<sub>C-F</sub> = 3.1 Hz), 130.6 (<sup>3</sup>J<sub>C-F</sub> = 8.2 Hz), 128.7, 126.1, 115.3 (<sup>2</sup>J<sub>C-F</sub> = 21.3 Hz), 111.2, 109.6, 78.4, 63.6, 55.8, 28.3. **IR** (neat): ν = 2967, 2923, 2862, 2832, 1603, 1511, 1469, 1358, 1331, 1308, 1294, 1256, 1230, 1218, 1155, 1111, 1085, 1064, 1035, 1013, 948, 910, 858, 833, 817, 796, 767, 562, 535 cm<sup>-1</sup>. **HRMS** (CI) m/z calc'd C<sub>17</sub>H<sub>18</sub>FO<sub>3</sub> [M + H]<sup>+</sup>: 289.1234, found: 289.1238.

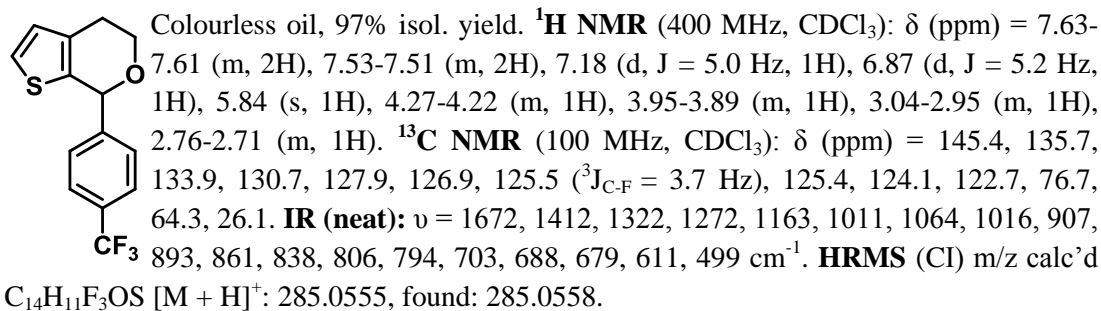
**1-(4-Methoxyphenyl)-6,7-dimethoxyisochroman**<sup>30</sup>

White solid, 94% isol. yield. <sup>1</sup>H NMR (400 MHz, CDCl<sub>3</sub>): δ (ppm) = 7.26 (d, J = 8.8 Hz, 2H), 6.89 (d, J = 8.4 Hz, 2H), 6.64 (s, 1H), 6.23 (s, 1H), 5.64 (s, 1H), 4.16-4.07 (m, 1H), 3.92-3.88 (m, 1H), 3.84 (s, 3H), 3.80 (s, 3H), 3.66 (s, 3H), 3.08-2.96 (m, 1H), 2.77-2.67 (m, 1H). <sup>13</sup>C NMR (100 MHz, CDCl<sub>3</sub>): δ (ppm) = 159.4, 147.8, 147.2, 134.4, 130.1, 129.2, 126.1, 113.7, 111.1, 109.8, 78.6, 63.4, 55.9, 55.8, 55.2, 28.3. **IR** (neat): ν = 2965, 2924, 2857, 2839, 1607, 1586, 1513, 1466, 1442, 1383, 1357, 1329, 1305, 1252, 1206, 1186, 1170, 1112, 1088, 1064, 1031, 1014, 855, 827, 818, 768, 578, 563, 541 cm<sup>-1</sup>. **HRMS** (CI) m/z calc'd C<sub>18</sub>H<sub>21</sub>O<sub>4</sub> [M + H]<sup>+</sup>: 301.1434, found: 301.1430.

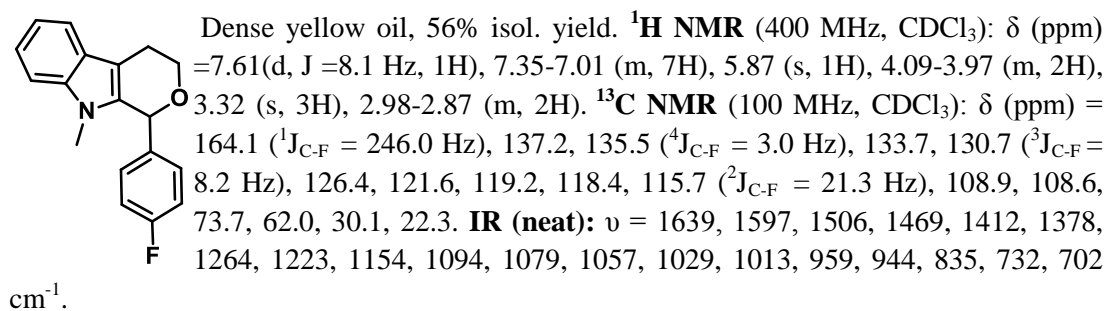
**7-(4-Fluorophenyl)-5,7-dihydro-4H-thieno[2,3c]pyran**

Colourless oil, 97% isol. yield. <sup>1</sup>H NMR (400 MHz, CDCl<sub>3</sub>): δ (ppm) = 7.38-7.34 (m, 2H), 7.17 (d, J = 5.6 Hz, 1H), 7.06-7.02 (m, 2H), 6.86 (d, J = 5.0 Hz, 1H), 5.77 (s, 1H), 4.26-4.21 (m, 1H), 3.94-3.87 (m, 1H), 3.02-2.94 (m, 1H), 2.73-2.69 (m, 1H). <sup>13</sup>C NMR (100 MHz, CDCl<sub>3</sub>): δ (ppm) = 163.1 (<sup>1</sup>J<sub>C-F</sub> = 248.0 Hz), 137.4, 136.6, 133.8, 129.6 (<sup>3</sup>J<sub>C-F</sub> = 8.2 Hz), 126.8, 123.9, 115.5 (<sup>2</sup>J<sub>C-F</sub> = 21.4 Hz), 76.6, 64.3, 26.1. **IR** (neat): ν = 1674, 1601, 1507, 1270, 1221, 1154, 1114, 1078, 1055, 1014, 979, 893, 856, 834, 780, 767, 706, 688, 670, 611, 537 cm<sup>-1</sup>. **HRMS** (CI) m/z calc'd C<sub>13</sub>H<sub>12</sub>FOS [M + H]<sup>+</sup>: 235.0587, found: 235.0593.

## 7-(4-(Trifluoromethyl)phenyl)-5,7-dihydro-4H-thieno[2,3c]pyran



## 1-(4-Fluorophenyl)-9-methyl-1,3,4,9-tetrahydropyrano[3,4-c]indole



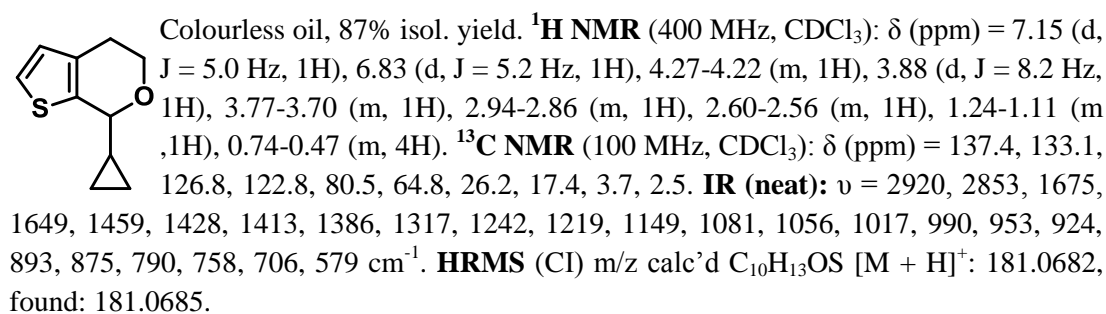
## 5.5.2.2. Synthesis of 1-alkyl substituted isochromans

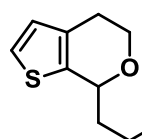
## 5.5.2.2.1. Electron rich isochromans

Electron rich 1-alkyl isochromans were synthesised according to the acid-catalysed oxapictet-Spengler reaction procedure described in Chapter 3.

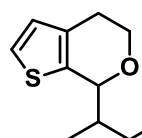
## Analytical data

## 7-Cyclopropyl-5,7-dihydro-4H-thieno[2,3-c]pyran

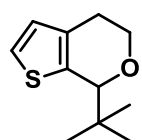


**7-Pentyl-5,7-dihydro-4H-thieno[2,3-c]pyran**<sup>30</sup>

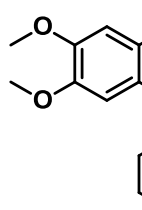
Colourless oil, 89% isol. yield. <sup>1</sup>H NMR (400 MHz, CDCl<sub>3</sub>): δ (ppm) = 7.13 (d, J = 5.0 Hz, 1H), 6.81 (d, J = 5.1 Hz, 1H), 4.74 (s, 1H), 4.22-4.18 (m, 1H), 3.77-3.71 (m, 1H), 2.90-2.82 (m, 1H), 2.60-2.56 (m, 1H), 1.82-1.75 (m, 2H), 1.53-1.32 (m, 7H), 0.89 (t, J = 7.0 Hz, 3H). <sup>13</sup>C NMR (100 MHz, CDCl<sub>3</sub>): δ (ppm) = 137.8, 133.2, 127.1, 122.4, 75.2, 64.4, 37.4, 31.8, 26.3, 24.9, 22.6, 14.0. HRMS (CI) m/z calc'd C<sub>12</sub>H<sub>19</sub>OS [M + H]<sup>+</sup>: 211.1151, found: 211.1154.

**7-(sec-Butyl)-5,7-dihydro-4H-thieno[2,3-c]pyran**

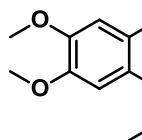
Colourless oil, 80% isol. yield. <sup>1</sup>H NMR (400 MHz, CDCl<sub>3</sub>): δ (ppm) = 7.15 (d, J = 5.0 Hz, 1H), 6.81 (d, J = 5.0 Hz, 1H), 4.75 (d, J = 16.7 Hz, 1H), 4.23-4.19 (m, 1H), 3.71-3.65 (m, 1H), 1.87-1.84 (m, 1H), 1.45-1.20 (m, 2H), 0.95-0.81 (m, 6H). <sup>13</sup>C NMR (100 MHz, CDCl<sub>3</sub>): δ (ppm) = 137.1, 134.4, 127.1, 122.5, 80.0, 64.8, 39.6, 25.5, 20.7, 14.3, 13.4. HRMS (CI) m/z calc'd C<sub>11</sub>H<sub>17</sub>OS [M + H]<sup>+</sup>: 197.0995, found: 197.0992.

**7-(tert-Butyl)-5,7-dihydro-4H-thieno[2,3-c]pyran**

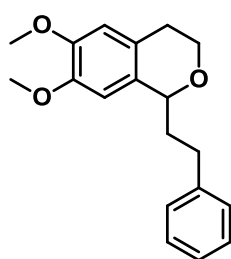
Colourless oil, 80% isol. yield. <sup>1</sup>H NMR (400 MHz, CDCl<sub>3</sub>): δ (ppm) = 7.13 (d, J = 5.1 Hz, 1H), 6.83 (d, J = 5.2 Hz, 1H), 4.40 (s, 1H), 4.22-4.18 (m, 1H), 3.64-3.58 (m, 1H), 2.88-2.80 (m, 1H), 2.56 (m, 1H), 1.05 (s, 9H). <sup>13</sup>C NMR (100 MHz, CDCl<sub>3</sub>): δ (ppm) = 135.6, 134.5, 126.8, 122.6, 83.8, 64.8, 35.7, 26.9, 26.0. HRMS (CI) m/z calc'd C<sub>11</sub>H<sub>17</sub>OS [M + H]<sup>+</sup>: 197.0995, found: 197.0996.

**1-Cyclohexyl-6,7-dimethoxyisochroman**<sup>31</sup>

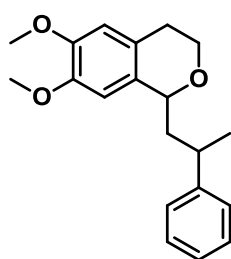
Colourless wax, 79% isol. yield. <sup>1</sup>H NMR (400 MHz, CDCl<sub>3</sub>): δ (ppm) = 6.58 (s, 1H), 6.57 (s, 1H), 4.57 (s, 1H), 4.16-4.12 (m, 1H), 3.85 (s, 6H), 3.67-3.61 (m, 1H), 2.96-2.88 (m, 1H), 2.49-2.45 (m, 1H), 1.84-1.72 (m, 5H), 1.32-1.11 (m, 5H). <sup>13</sup>C NMR (100 MHz, CDCl<sub>3</sub>): δ (ppm) = 147.4, 147.2, 129.3, 127.1, 111.2, 107.8, 79.7, 64.1, 56.0, 55.8, 43.8, 30.2, 28.9, 26.9, 26.5, 26.4, 25.3. IR (neat): ν = 2919, 2848, 1515, 1466, 1377, 1353, 1251, 1234, 1218, 1203, 1106, 1093, 1034, 1007, 858, 819, 764 cm<sup>-1</sup>. HRMS (CI) m/z calc'd C<sub>17</sub>H<sub>25</sub>O<sub>3</sub> [M + H]<sup>+</sup>: 277.1798, found: 277.1809.

**1-Isopropyl-6,7-dimethoxyisochroman**<sup>31</sup>

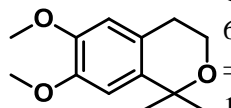
White solid, 81% isol. yield. <sup>1</sup>H NMR (400 MHz, CDCl<sub>3</sub>): δ (ppm) = 6.59 (s, 1H), 6.56 (s, 1H), 4.60 (s, 1H), 4.18-4.14 (m, 1H), 3.86 (s, 3H), 3.84 (s, 3H), 3.68-3.63 (m, 1H), 2.99-2.90 (m, 1H), 2.49-2.45 (m, 1H), 2.22-2.16 (m, 1H), 1.16 (d, J = 6.8 Hz, 3H), 0.71 (d, J = 6.9 Hz, 3H). <sup>13</sup>C NMR (100 MHz, CDCl<sub>3</sub>): δ (ppm) = 147.4, 147.1, 129.7, 127.0, 111.2, 107.6, 79.9, 64.2, 55.9, 55.8, 33.4, 28.9, 19.8, 15.0. IR (neat): ν = 2966, 2928, 2860, 1607, 1509, 1470, 1458, 1449, 1377, 1318, 1246, 1224, 1202, 1116, 1102, 1085, 1063, 1008, 950, 928, 895, 856, 810, 769 cm<sup>-1</sup>. HRMS (CI) m/z calc'd C<sub>14</sub>H<sub>21</sub>O<sub>3</sub> [M + H]<sup>+</sup>: 237.1485, found: 237.1492.

**6,7-Dimethoxy-1-phenethylisochroman**

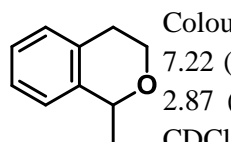
Dense colourless oil, 84% isol. yield.  $^1\text{H NMR}$  (400 MHz,  $\text{CDCl}_3$ ):  $\delta$  (ppm) = 7.39-7.12 (m, 5H), 6.62 (s, 1H), 6.54 (s, 1H), 4.73 (m, 1H), 4.20-4.12 (m, 1H), 3.89 (s, 3H), 3.84 (s, 3H), 3.82 (m, 1H), 2.98-2.87 (m, 1H), 2.78 (t,  $J = 6.8$  Hz, 2H), 2.50-2.46 (m, 1H), 2.24-1.87 (m, 2H).  $^{13}\text{C NMR}$  (100 MHz,  $\text{CDCl}_3$ ):  $\delta$  (ppm) = 147.5, 142.7, 130.0, 128.5, 128.3, 128.1, 126.4, 125.7, 111.7, 107.8, 74.8, 63.2, 56.0, 55.8, 37.8, 30.9, 28.7. **IR** (neat):  $\nu = 2931, 2855, 2833, 1609, 1511, 1463, 1452, 1408, 1331, 1314, 1253, 1226, 1204, 1107, 1029, 999, 858, 771, 749, 734, 699$   $\text{cm}^{-1}$ . **HRMS** (CI)  $m/z$  calc'd  $\text{C}_{19}\text{H}_{23}\text{O}_3$   $[\text{M} + \text{H}]^+$ : 299.1642, found: 299.1644.

**6,7-Dimethoxy-1-(2-phenylpropyl)isochroman**

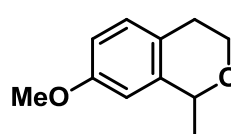
Dense colourless oil, 84% isol. yield. Data for the predominant diastereoisomer:  $^1\text{H NMR}$  (400 MHz,  $\text{CDCl}_3$ ):  $\delta$  (ppm) = 7.33-7.24 (m, 5H), 6.47 (s, 1H), 6.36 (s, 1H), 4.81 (bs, 1H), 4.09 (m, 1H), 3.83 (s, 3H), 3.81 (s, 3H), 3.16-3.15 (m, 1H), 2.67-2.62 (m, 1H), 2.62 (t,  $J = 6.9$  Hz, 1H), 2.08-1.96 (m, 2H), 1.38 (d,  $J = 6.9$  Hz, 3H).  $^{13}\text{C NMR}$  (100 MHz,  $\text{CDCl}_3$ ):  $\delta$  (ppm) = 148.2, 147.4, 146.6, 130.7, 130.3, 128.4, 127.3, 125.8, 111.5, 108.0, 73.3, 62.6, 56.0, 55.8, 45.1, 36.3, 28.6, 23.1. **IR** (neat):  $\nu = 2955, 2930, 2832, 1610, 1509, 1494, 1374, 1330, 1253, 1227, 1204, 1130, 1098, 1015, 1006, 853, 803, 781, 761, 699, 543$   $\text{cm}^{-1}$ . **HRMS** (CI)  $m/z$  calc'd  $\text{C}_{20}\text{H}_{25}\text{O}_3$   $[\text{M} + \text{H}]^+$ : 313.1798, found: 313.1808.

**6,7-Dimethoxy-1,1-dimethylisochroman**<sup>30</sup>

Colourless oil, 96% isol. yield.  $^1\text{H NMR}$  (400 MHz,  $\text{CDCl}_3$ ):  $\delta$  (ppm) = 6.56 (s, 2H), 3.93 (t,  $J = 5.6$  Hz, 2H), 3.86 (s, 3H), 3.85 (s, 3H), 2.74 (t,  $J = 5.8$  Hz, 2H), 1.51 (s, 6H).  $^{13}\text{C NMR}$  (100 MHz,  $\text{CDCl}_3$ ):  $\delta$  (ppm) = 147.4, 147.3, 134.8, 125.1, 111.2, 108.5, 74.1, 59.6, 56.0, 55.8, 29.7, 29.1. **IR** (neat):  $\nu = 2970, 2932, 1611, 1511, 1463, 1450, 1402, 1359, 1350, 1327, 1259, 1245, 1210, 1182, 1155, 1091, 1072, 1057, 1028, 997, 954, 856, 786, 555, 504$   $\text{cm}^{-1}$ . **HRMS** (CI)  $m/z$  calc'd  $\text{C}_{13}\text{H}_{19}\text{O}_3$   $[\text{M} + \text{H}]^+$ : 223.1329, found: 223.1327.

**1-Methylisochroman**<sup>28</sup>

Colourless oil, 48% isol. yield.  $^1\text{H NMR}$  (400 MHz,  $\text{CDCl}_3$ ):  $\delta$  (ppm) = 7.34-7.22 (m, 4H), 4.71 (q,  $J = 5.6$  Hz, 1H), 3.77-3.71 (m, 1H), 3.63-3.57 (m, 1H), 2.87 (t,  $J = 7.0$  Hz, 2H), 1.31 (d,  $J = 7.0$  Hz, 3H).  $^{13}\text{C NMR}$  (100 MHz,  $\text{CDCl}_3$ ):  $\delta$  (ppm) = 139.4, 129.3, 128.7, 126.5, 100.1, 66.4, 36.8, 20.0. **HRMS** (CI)  $m/z$  calc'd  $\text{C}_{10}\text{H}_{13}\text{O}$   $[\text{M} + \text{H}]^+$ : 149.0958, found: 149.0961.

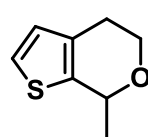
**7-Methoxy-1-methylisochroman**

Colourless oil, 68% isol. yield.  $^1\text{H NMR}$  (400 MHz,  $\text{CDCl}_3$ ):  $\delta$  (ppm) = 7.10 (d,  $J = 7.7$  Hz, 2H), 6.82 (m, 1H), 4.66 (q,  $J = 5.3$  Hz, 1H), 3.77 (s, 3H), 3.68-3.62 (m, 1H), 3.55-3.49 (m, 1H), 2.76 (t,  $J = 7.2$  Hz, 2H), 1.28 (d,  $J = 5.3$  Hz, 3H).  $^{13}\text{C NMR}$  (100 MHz,  $\text{CDCl}_3$ ):  $\delta$  (ppm) = 158.3, 129.8, 114.0, 113.7, 99.6, 66.2, 55.3, 55.2, 38.2, 21.3. **IR** (neat):  $\nu = 2936, 2909, 2867,$



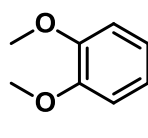
1612, 1583, 1511, 1464, 1442, 1319, 1300, 1242, 1177, 1128, 1096, 1060, 1030, 990, 921, 823, 750, 557, 516  $\text{cm}^{-1}$ . **HRMS** (CI)  $m/z$  calc'd  $\text{C}_{11}\text{H}_{15}\text{O}_2$   $[\text{M} + \text{H}]^+$ : 179.1067, found: 179.1070.

### 7-Methyl-5,7-dihydro-4H-thieno[2,3-c]pyran



Colourless oil, 96% isol. yield.  **$^1\text{H}$  NMR** (400 MHz,  $\text{CDCl}_3$ ):  $\delta$  (ppm) = 7.14 (d,  $J = 5.0\text{ Hz}$ , 1H), 6.82 (d,  $J = 5.1\text{ Hz}$ , 1H), 4.89 (q,  $J = 5.7\text{ Hz}$ , 1H), 4.23-4.18 (m, 1H), 3.81-3.74 (m, 1H), 2.93-2.84 (m, 1H), 2.61-2.55 (m, 1H), 1.52 (d,  $J = 6.4\text{ Hz}$ , 3H).  **$^{13}\text{C}$  NMR** (100 MHz,  $\text{CDCl}_3$ ):  $\delta$  (ppm) = 138.5, 132.8, 127.1, 122.4, 71.3, 64.6, 26.2, 22.9. **IR** (neat):  $\nu = 2973, 2924, 2849, 1443, 1372, 1316, 1264, 1166, 1119, 1089, 1049, 1011, 997, 868, 843, 822, 723, 705, 659, 612, 578, 533\text{ cm}^{-1}$ . **HRMS** (CI)  $m/z$  calc'd  $\text{C}_8\text{H}_{11}\text{OS}$   $[\text{M} + \text{H}]^+$ : 155.0525, found: 155.0529.

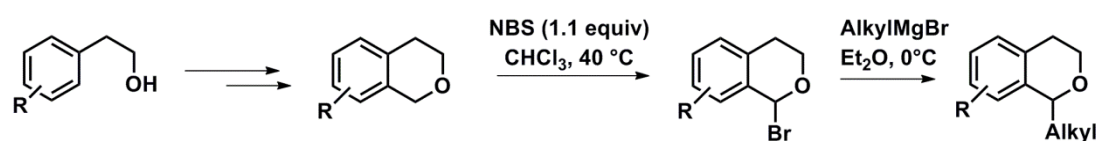
### 6,7-Dimethoxy-1-methylisochroman



Colourless oil, 97% isol. yield.  **$^1\text{H}$  NMR** (400 MHz,  $\text{CDCl}_3$ ):  $\delta$  (ppm) = 6.52 (s, 1H), 6.48 (s, 1H), 4.72 (q,  $J = 6.3\text{ Hz}$ , 1H), 4.08-4.04 (m, 1H), 3.78 (s, 6H), 3.73-3.66 (m, 1H), 2.91-2.83 (m, 1H), 2.54-2.50 (m, 1H), 1.43 (d,  $J = 6.2\text{ Hz}$ , 3H).  **$^{13}\text{C}$  NMR** (100 MHz,  $\text{CDCl}_3$ ):  $\delta$  (ppm) = 147.5, 147.4, 131.4, 125.4, 111.4, 107.8, 72.0, 63.6, 56.0, 55.8, 28.6, 21.9. **IR** (neat):  $\nu = 2932, 2833, 1610, 1509, 1463, 1451, 1372, 1355, 1331, 1313, 1248, 1226, 1205, 1161, 1137, 1029, 1010, 853, 796, 738, 708, 494\text{ cm}^{-1}$ . **HRMS** (CI)  $m/z$  calc'd  $\text{C}_{12}\text{H}_{17}\text{O}_3$   $[\text{M} + \text{H}]^+$ : 209.1172, found: 209.1180.

#### 5.5.2.2.2. Neutral and electron deficient 1-alkyl isochromans

The following multistep route was used to synthesise 1-alkyl isochromans which could not be obtained by oxa-Pictet-Spengler reactions:



#### General procedure for the bromination of isochromans

In a two-necked round bottom flask equipped with a magnetic bar, the corresponding isochroman (1.0 equiv, 3.0 mL) and NBS (1.1 equiv, 4.77 g) were added. The flask was degassed and placed under a  $\text{N}_2$  atmosphere. Freshly distilled  $\text{CHCl}_3$  (40 mL) was added by syringe and the reaction was heated gradually to  $40\text{ }^\circ\text{C}$ . The reaction was stirred at  $40\text{ }^\circ\text{C}$  for 24 h and then allowed to cool at r.t. The solvent was eliminated under reduced pressure and  $\text{Et}_2\text{O}$  (20 mL) were added to the residue. The solution was filtered to remove the white solid

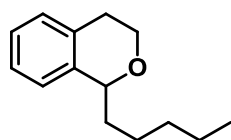
and then the solvent was evaporated in vacuo to afford the desired 1-bromoisochroman (4.57g, 90% yield) as a dense oil.

### General procedure for the alkylation of 1-bromoisochromans

In a two-necked round bottom flask equipped with a magnetic bar, the crude 1-bromoisochroman (1.0 equiv., 4.57 g) was added. The flask was degassed and placed under a N<sub>2</sub> atmosphere. Freshly distilled Et<sub>2</sub>O (40 mL) was added by syringe and the reaction was cooled down to 0 °C or -78°C. The corresponding alkylmagnesium bromide (1.4 equiv, 3.0 M in hexanes sol.) was added dropwise to the reaction mixture. Once the addition was completed, the reaction mixture was stirred at 0 °C for an additional hour and at r.t. overnight. The reaction was slowly quenched with NH<sub>4</sub>Cl (aq.) and the two phases were separated. The organic phase was washed with water and brine, dried over MgSO<sub>4</sub> and filtered. The solvent was removed in vacuo and the residue was purified by silica gel column chromatography (Hexane/EtOAc, 18/1) to afford the desired product as a clear oil.

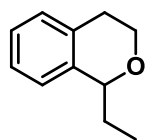
### Analytical data

#### 1-Pentylisochroman



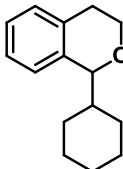
Colourless oil, 74% isol. yield. <sup>1</sup>H NMR (400 MHz, CDCl<sub>3</sub>): δ (ppm) = 7.16-7.08 (m, 4H), 4.75 (d, J = 7.8 Hz, 1H), 4.16-4.11 (m, 1H), 3.79-3.73 (m, 1H), 3.02-2.94 (m, 1H), 2.71-2.67 (m, 1H), 1.92-1.77 (m, 2H), 1.45-1.25 (m, 5H), 0.87 (t, J = 6.6 Hz, 3H). <sup>13</sup>C NMR (100 MHz, CDCl<sub>3</sub>): δ (ppm) = 138.6, 133.9, 128.8, 127.4, 126.0, 124.7, 75.9, 63.1, 36.0, 31.8, 29.4, 25.2, 22.6, 14.1. IR (neat): ν = 2955, 2926, 2856, 1491, 1454, 1425, 1376, 1311, 1286, 1158, 1104, 1077, 1049, 934, 758, 642 cm<sup>-1</sup>. HRMS (CI) m/z calc'd C<sub>14</sub>H<sub>21</sub>O [M + H]<sup>+</sup>: 205.1587, found: 205.1590.

#### 1-Ethylisochroman<sup>28</sup>

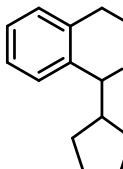


Colourless oil, 65% isol. yield. <sup>1</sup>H NMR (400 MHz, CDCl<sub>3</sub>): δ (ppm) = 7.19-7.06 (m, 4H), 4.71(d, J = 7.3 Hz, 1H), 4.16-4.11 (m, 1H), 3.80-3.74 (m, 1H), 3.02-2.94 (m, 1H), 2.70-2.66 (m, 1H), 2.01-1.93 (m, 1H), 1.85-1.78 (m, 2H), 0.98 (t, J = 7.3 Hz, 3H). <sup>13</sup>C NMR (100 MHz, CDCl<sub>3</sub>): δ (ppm) = 138.3, 134.1, 128.8, 126.1, 126.0, 124.8, 76.2, 63.1, 29.2, 28.7, 9.5. HRMS (CI) m/z calc'd C<sub>11</sub>H<sub>15</sub>O [M + H]<sup>+</sup>: 163.1118, found: 163.1115.

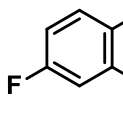
### 1-Cyclohexylisochroman


 Colourless oil, 40% isol. yield.  $^1\text{H NMR}$  (400 MHz,  $\text{CDCl}_3$ ):  $\delta$  (ppm) = 7.17-7.02 (m, 4H), 4.74 (d,  $J = 7.0$  Hz, 1H), 4.21-4.12 (m, 1H), 3.85-3.76 (m, 1H), 3.14-2.97 (m, 1H), 2.68-2.59 (m, 1H), 1.74-1.42 (m, 4H), 134-1.10 (m, 6H).  $^{13}\text{C NMR}$  (100 MHz,  $\text{CDCl}_3$ ):  $\delta$  (ppm) = 137.5, 134.2, 128.6, 126.3, 126.0, 80.1, 64.1, 43.4, 29.5, 27.0, 26.9, 26.5, 26.4. **IR** (neat):  $\nu = 2922, 2850, 1490, 1450, 1425, 1255, 1231, 1156, 1112, 1082, 1054, 1035, 1014, 1002, 890, 756, 743$   $\text{cm}^{-1}$ . **HRMS** (CI)  $m/z$  calc'd  $\text{C}_{15}\text{H}_{21}\text{O}$   $[\text{M} + \text{H}]^+$ : 217.1587, found: 217.1586.

### 1-Cyclopentylisochroman

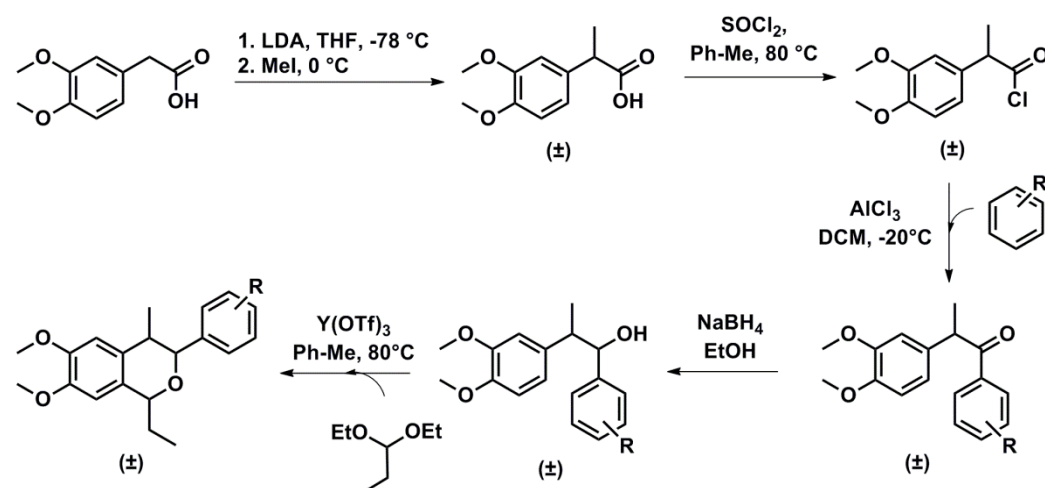

 Colourless oil, 55% isol. yield.  $^1\text{H NMR}$  (400 MHz,  $\text{CDCl}_3$ ):  $\delta$  (ppm) = 7.14-7.09 (m, 4H), 4.74 (d,  $J = 6.9$  Hz, 1H), 4.19-4.14 (m, 1H), 3.76-3.70 (m, 1H), 3.04-2.96 (m, 1H), 2.66-2.60 (m, 1H), 2.53-2.47 (m, 1H), 1.79-1.26 (m, 10H).  $^{13}\text{C NMR}$  (100 MHz,  $\text{CDCl}_3$ ):  $\delta$  (ppm) = 138.6, 134.3, 128.7, 125.9, 125.8, 125.0, 77.8, 63.6, 44.8, 29.3, 29.1. **IR** (neat):  $\nu = 2952, 1606, 1459, 1393, 1293, 1242, 1192, 1158, 1060, 1028, 1001, 950, 744, 694, 639$   $\text{cm}^{-1}$ . **HRMS** (CI)  $m/z$  calc'd  $\text{C}_{14}\text{H}_{19}\text{O}$   $[\text{M} + \text{H}]^+$ : 220.1696, found: 220.1699.

### 7-Fluoro-1-methylisochroman


 Colourless oil, 57% isol. yield.  $^1\text{H NMR}$  (400 MHz,  $\text{CDCl}_3$ ):  $\delta$  (ppm) = 7.09-7.03 (m, 1H), 6.93-6.75 (m, 3H), 4.84 (d,  $J = 7.0$  Hz, 1H), 4.19-4.11 (m, 1H), 3.81-3.73 (m, 1H), 3.03-2.91 (m, 1H), 2.68-2.61 (m, 1H), 1.50 (d,  $J = 6.9$  Hz, 3H).  $^{13}\text{C NMR}$  (100 MHz,  $\text{CDCl}_3$ ):  $\delta$  (ppm) = 162.3 ( $^1J_{\text{C-F}} = 242.1$  Hz), 141.3 ( $^3J_{\text{C-F}} = 6.4$  Hz), 130.2 ( $^3J_{\text{C-F}} = 7.6$  Hz), 113.4 ( $^2J_{\text{C-F}} = 21.3$  Hz), 111.5 ( $^2J_{\text{C-F}} = 21.6$  Hz), 72.2, 63.7, 28.3, 21.6. **HRMS** (CI)  $m/z$  calc'd  $\text{C}_{10}\text{H}_{12}\text{FO}$   $[\text{M} + \text{H}]^+$ : 167.0867, found: 167.0870.

#### 5.5.2.3. Synthesis of natural isochromans

Isochromans with a similar molecular skeleton to those found in softwood lignings were prepared according to the following synthetic route:



**Procedure for the preparation of 2-(3,4-dimethoxy)propanoic acid<sup>32</sup>**

In a two-necked round bottom flask equipped with a magnetic bar, diisopropylamine (5.64 g, 7.81 mL) was added. The flask was degassed (3 times) and placed under a N<sub>2</sub> atmosphere. Freshly distilled THF (40 mL) was added by syringe and the flask was cooled to -78 °C. n-BuLi (22 mL, 2.5 M sol.) was added dropwise and once the addition was completed, the mixture was stirred for an additional 30 min. In a separated two-necked round bottom flask, 3,4-dimethoxy phenylacetic acid (26.55 mmol, 5.2 g) was added, the flask was degassed (3 times) and placed under a N<sub>2</sub> atmosphere. Freshly distilled THF (10 mL) was added by syringe and the flask was cooled to -78 °C and the LDA solution was added dropwise. Once the addition was completed, the reaction was stirred for an additional hour. Then, the flask was warmed to 0 °C and MeI (7.54g, 3.31 mL) was added dropwise. The reaction was stirred overnight at r.t. Next morning, the reaction was slowly quenched with NH<sub>4</sub>Cl (aq). The organic phase was extracted with Et<sub>2</sub>O and separated. The aqueous phase was acidified with HCl (aq) to pH = 2.00 and extracted with Et<sub>2</sub>O. The latter organic phase was washed with water and brine and dried over MgSO<sub>4</sub>. The solution was filtered and the solvent removed in vacuo to afford the desired 2-(3,4-dimethoxy)propanoic acid as a dense yellow oil (5.12 g, 92% yield).

**Procedure for the preparation of 2-(3,4-dimethoxyphenyl)propanoyl chloride<sup>32</sup>**

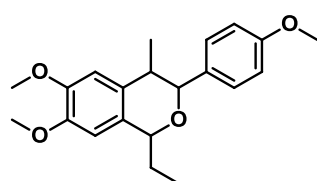
In a round bottom flask equipped with a magnetic bar, 2-(3,4-dimethoxy)propanoic acid (5.12 g) was added. The oil was dissolved in toluene (40 mL) and cooled to 0 °C. Thionyl chloride (2.3 equiv., 6.0 mL) was added dropwise and once the addition was completed, the reaction was stirred for an additional 15 min. The reaction mixture was gradually heated to 80 °C and stirred for an additional 5 h. The flask was cooled down to r.t. and the solvent eliminated in vacuo to afford the 2-(3,4-dimethoxyphenyl)propanoyl chloride (5.15 g, 92% yield) as a dark oil.

### Procedure for the Friedel Crafts reactions<sup>32</sup>

In a two-necked round bottom flask equipped with a magnetic bar, AlCl<sub>3</sub> (2.4 equiv., 7.2g) was added. The flask was degassed (3 times) and placed under a N<sub>2</sub> atmosphere. Freshly distilled DCM (40 mL) was added and the flask was cooled to -20 °C. Anisole (1.1 equiv, 2.7 mL) was added slowly and once the addition was completed, 2-(3,4-dimethoxyphenyl) propanoyl chloride (1.0 equiv, 5.15 g in 10 mL of DCM) was added over a period of 40 min. Once the addition was completed, the reaction mixture was stirred for an additional 3 h at -20 °C. The reaction was warmed up to r.t. and slowly quenched with HCl (3.0M). The organic phase was extracted with DCM and washed with water and brine. The solution was dried over MgSO<sub>4</sub>, filtered and the solvent eliminated in vacuo. The crude was purified by silica gel column chromatography (Hexane/EtOAc, gradient: 7/2 to 3/2) to afford the desired product (2.03 g, 30% yield) as a pale yellow oil.

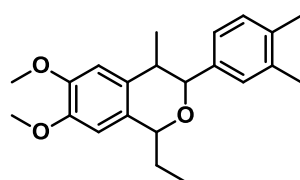
### Analytical data

#### (±)-1-Ethyl-6,7-dimethoxy-3-(4-methoxyphenyl)-4-methylisochroman



Dense colourless oil, 39% yield. <sup>1</sup>H NMR (400 MHz, CDCl<sub>3</sub>): δ (ppm) = 7.41-7.38 (m, 2H), 6.97-6.78 (m, 4H), 4.95 (bs, 1H), 4.18 (d, J = 9.4 Hz, 1H), 3.86 (s, 3H), 3.85 (s, 3H), 3.83 (s, 3H), 3.50-3.42 (m, 1H), 1.62-1.54 (m, 2H), 1.15 (d, J = 6.9 Hz, 3H), 0.98 (t, J = 7.0 Hz, 3H). <sup>13</sup>C NMR (100 MHz, CDCl<sub>3</sub>): δ (ppm) = 157.4, 147.5, 147.3, 139.1, 130.9, 128.4, 128.3, 114.9, 109.7, 108.1, 83.4, 55.9, 55.8, 55.7, 38.9, 29.4, 18.7, 8.9. IR (neat): ν = 2961, 2933, 2834, 1607, 1586, 1508, 1462, 1417, 1300, 1245, 1171, 1141, 1108, 1027, 852, 825, 807, 764, 569, 543 cm<sup>-1</sup>. HRMS (CI) m/z calc'd C<sub>21</sub>H<sub>27</sub>O<sub>4</sub> [M + H]<sup>+</sup>: 343.1904, found: 343.1913.

#### (±)-3-(3,4-Dimethylphenyl)-1-ethyl-6,7-dimethoxy-4-methylisochroman



Dense colourless oil, 39% yield. <sup>1</sup>H NMR (400 MHz, CDCl<sub>3</sub>): δ (ppm) = 7.18 (s, 1H), 7.13 (s, 2H), 6.81 (s, 1H), 6.61 (s, 1H), 4.89 (bs, 1H), 4.14 (d, J = 9.8 Hz, 1H), 3.87 (s, 6H), 3.09-2.99 (m, 1H), 2.28 (s, 3H), 2.26 (s, 3H), 2.09-2.01 (m, 1H), 1.83-1.75 (m, 1H), 1.07 (d, J = 6.8 Hz, 3H), 0.91 (t, J = 7.3 Hz, 3H). <sup>13</sup>C NMR (100 MHz, CDCl<sub>3</sub>): δ (ppm) = 147.5, 147.2, 141.7, 139.1, 136.4, 136.1, 132.2, 129.9, 129.5, 128.7, 128.3, 125.0, 109.5, 107.2, 83.2, 55.9, 55.6, 37.7, 28.8, 19.8, 19.4, 16.2, 8.6. HRMS (CI) m/z calc'd C<sub>22</sub>H<sub>28</sub>O<sub>3</sub> [M + H]<sup>+</sup>: 341.2111, found: 341.2119.

### 5.5.3. General procedure for the Fe(OTf)<sub>2</sub>L1 catalysed aerobic cleavage of Csp<sup>3</sup>-O bonds

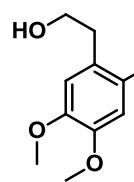
#### Liquid samples:

In a Radley's tube equipped with a magnetic stir bar, ligand **L1** ( $5.67 \times 10^{-3}$  mmol, 5.2 mg) and Fe(OTf)<sub>2</sub> ( $5.65 \times 10^{-3}$  mmol, 2.0 mg) were added. The corresponding ether (2.0 mL) was added and the reaction tube was degassed, charged with dioxygen gas (1 atm, 3 times) and kept under oxygen (1 atm) by using a balloon. The reaction mixture was heated to 60 °C and left overnight. Next morning, a second addition of catalyst was made ( $5.67 \times 10^{-3}$  mmol) and the reaction mixture was reacted at 60 °C overnight. If needed, a third addition of catalyst was made the following morning following the same procedure. The reaction was purified by silica gel column chromatography (Hexane/EtOAc, gradient: 10/1 to 4/1 or 2/1) to afford the unreacted starting material and the reaction products.

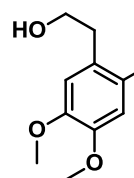
#### Solid samples:

In a Radley's tube equipped with a magnetic stir bar ligand **L1** ( $5.67 \times 10^{-3}$  mmol, 5.2 mg) and Fe(OTf)<sub>2</sub> ( $5.65 \times 10^{-3}$  mmol, 2.0 mg) were added. The tube was sealed, degassed (3 times) and left under an inert atmosphere. C<sub>6</sub>H<sub>6</sub> (0.5 mL) was added by syringe and the reaction mixture was stirred at 40 °C for 1 h. The corresponding ether (2.5 mmol) was added and the reaction tube was degassed, charged with dioxygen gas (1 atm, 3 times) and kept under oxygen (1 atm) by using a balloon. The reaction mixture was heated to 60 °C and left overnight. One or two more additions of catalyst were done according to the same procedure. The reaction was purified by silica gel column chromatography (Hexane/EtOAc, gradient: 6/1 to 3/2) to afford the unreacted starting material and the reaction products.

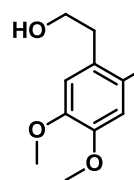
## Analytical data

**(2-(2-Hydroxyethyl)-4,5-dimethoxyphenyl)(phenyl)methanone**

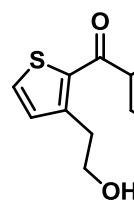
White solid, 15% isol. yield.  $^1\text{H NMR}$  (400 MHz,  $\text{CDCl}_3$ ):  $\delta$  (ppm) = 7.82 (d,  $J = 7.2$  Hz, 2H), 7.63 (t,  $J = 7.4$  Hz, 1H), 7.49 (m, 2H), 6.88 (m, 2H, overlapped), 3.96 (s, 3H), 3.92 (t,  $J = 6.8$  Hz, 2H), 3.77 (s, 3H), 2.94 (t,  $J = 6.4$  Hz, 2H), 2.17 (bs, 1H).  $^{13}\text{C NMR}$  (100 MHz,  $\text{CDCl}_3$ ):  $\delta$  (ppm) = 198.0, 151.4, 146.2, 138.0, 133.9, 133.6, 133.2, 130.6, 130.3, 130.1, 129.3, 128.4, 128.2, 128.0, 126.8, 113.4, 64.1, 56.1, 55.8, 36.0. **HRMS** (EI)  $m/z$  calc'd  $\text{C}_{17}\text{H}_{19}\text{O}_4$   $[\text{M} + \text{H}]^+$ : 287.1278, found: 287.1274.

**(4-Fluorophenyl)(2-(2-hydroxyethyl)-4,5-dimethoxyphenyl)methanone**

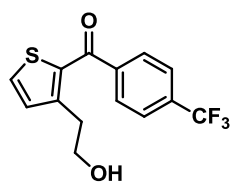
Pale yellow oil, 68% isol. yield.  $^1\text{H NMR}$  (400 MHz,  $\text{CDCl}_3$ ):  $\delta$  (ppm) = 7.85 (m, 2H), 7.15 (t,  $J = 8.6$  Hz, 2H), 6.88 (s, 1H), 6.82 (s, 2H), 3.96 (s, 3H), 3.89 (t,  $J = 6.3$  Hz, 2H), 3.78 (s, 3H), 2.91 (t,  $J = 6.0$  Hz, 2H), 1.78 (bs, 1H).  $^{13}\text{C NMR}$  (100 MHz,  $\text{CDCl}_3$ ):  $\delta$  (ppm) = 196.4, 151.5, 146.4, 134.4, 133.7, 133.2 ( $^3J_{\text{C-F}} = 9.3$  Hz), 130.1, 115.7 ( $^2J_{\text{C-F}} = 21.6$  Hz), 113.5, 113.1, 64.0, 56.1, 56.0, 36.0. **IR** (neat):  $\nu = 3365, 2934, 2847, 1728, 1655, 1596, 1509, 1464, 1408, 1257, 1209, 1174, 1153, 1094, 1064, 948, 909, 855, 792, 544, 506$   $\text{cm}^{-1}$ . **HRMS** (EI)  $m/z$  calc'd  $\text{C}_{17}\text{H}_{19}\text{O}_4\text{F}$   $[\text{M} + \text{H}]^+$ : 305.1184, found: 305.1182.

**(2-(2-Hydroxyethyl)-4,5-dimethoxyphenyl)(4-methoxyphenyl)methanone**

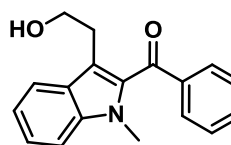
Pale oil, 60% isol. yield.  $^1\text{H NMR}$  (400 MHz,  $\text{CDCl}_3$ ):  $\delta$  (ppm) = 7.82 (d,  $J = 8.7$  Hz, 2H), 6.94 (m, 4H), 3.95 (s, 3H), 3.87 (s, 3H), 3.85 (m, 2H, overlapped), 3.79 (s, 3H), 2.89 (t,  $J = 5.96$  Hz, 2H), 2.05 (bs, 1H).  $^{13}\text{C NMR}$  (100 MHz,  $\text{CDCl}_3$ ):  $\delta$  (ppm) = 196.7, 163.7, 151.1, 146.2, 133.2, 133.0, 130.8, 130.6, 113.6, 113.3, 112.8, 63.9, 56.1, 56.0, 55.5, 35.9. **IR** (neat):  $\nu = 3378, 2971, 2931, 2841, 1729, 1639, 1595, 1510, 1454, 1392, 1288, 1256, 1218, 1181, 1163, 1102, 1070, 1050, 1021, 999, 953, 845, 820, 708$   $\text{cm}^{-1}$ . **HRMS** (EI)  $m/z$  calc'd  $\text{C}_{18}\text{H}_{21}\text{O}_5$   $[\text{M} + \text{H}]^+$ : 317.1384, found: 317.1387.

**(4-Fluorophenethyl)(3-(2-hydroxyethyl)thiophen-2-yl)methanone**

Pale yellow oil, 60% isol. yield.  $^1\text{H NMR}$  (400 MHz,  $\text{CDCl}_3$ ):  $\delta$  (ppm) = 7.92 (m, 2H), 7.59 (d,  $J = 4.9$  Hz, 1H), 7.16 (m, 3H), 3.95 (t,  $J = 6.0$  Hz, 2H), 3.22 (t,  $J = 6.0$  Hz, 2H), 2.05 (bs, 1H).  $^{13}\text{C NMR}$  (100 MHz,  $\text{CDCl}_3$ ):  $\delta$  (ppm) = 188.4, 166.7 ( $^1J_{\text{C-F}} = 252.9$  Hz), 148.2, 135.6 ( $^4J_{\text{C-F}} = 3.0$  Hz), 135.3, 132.3 ( $^3J_{\text{C-F}} = 9.2$  Hz), 131.6, 131.4, 115.5 ( $^2J_{\text{C-F}} = 21.7$  Hz), 63.3, 33.1. **IR** (neat):  $\nu = 3245, 3128, 1622, 1596, 1519, 1503, 1410, 1381, 1343, 1293, 1281, 1265, 1234, 1154, 1067, 1048, 1034, 1012, 974, 961, 907, 843, 833, 809, 771, 745, 655, 630, 592, 524$   $\text{cm}^{-1}$ . **HRMS** (EI)  $m/z$  calc'd  $\text{C}_{13}\text{H}_{12}\text{FO}_2\text{S}$   $[\text{M} + \text{H}]^+$ : 251.0537, found: 251.0539.

**(3-(2-Hydroxyethyl)thiophen-2-yl)(4-(trifluoromethyl)phenyl)methanone**

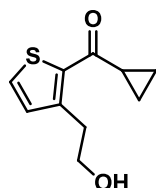
Pale yellow oil, 59% isol. yield.  $^1\text{H NMR}$  (400 MHz,  $\text{CDCl}_3$ ):  $\delta$  (ppm) = 7.96 (d,  $J = 8.0$  Hz, 2H), 7.76 (d,  $J = 8.1$  Hz, 2H), 7.63 (d,  $J = 4.9$  Hz, 2H), 7.19 (s, 1H), 7.17 (s, 1H), 3.97 (t,  $J = 6.0$  Hz, 2H), 3.28 (t,  $J = 6.1$  Hz, 2H), 2.11 (bs, 1H).  $^{13}\text{C NMR}$  (100 MHz,  $\text{CDCl}_3$ ):  $\delta$  (ppm) = 188.6, 149.0, 142.6, 134.9, 133.9, 133.6, 132.4, 131.8, 129.8, 125.3 ( $^3J_{\text{C-F}} = 3.6$  Hz), 63.2, 33.3. **IR** (neat):  $\nu = 3404, 2948, 2898, 1640, 1579, 1515, 1409, 1381, 1320, 1275, 1243, 1164, 1122, 1108, 1063, 1037, 1015, 997, 980, 879, 851, 833, 773, 745, 713, 696, 677, 669, 654, 630$   $\text{cm}^{-1}$ . **HRMS** (EI)  $m/z$  calc'd  $\text{C}_{14}\text{H}_{12}\text{F}_3\text{O}_2\text{S}$   $[\text{M} + \text{H}]^+$ : 301.0505, found: 301.0508.

**(4-Fluorophenyl)(3-(2-hydroxyethyl)-1-methyl-1H-indol-2-yl)methanone**

Bright yellow liquid, 78% isol. yield.  $^1\text{H NMR}$  (250 MHz,  $\text{CDCl}_3$ ):  $\delta$  (ppm) = 7.99-7.87 (m, 2H), 7.61 (d,  $J = 7.9$  Hz, 1H), 7.31-7.19 (m, 5H), 3.84 (t,  $J = 6.1$  Hz, 2H), 3.72 (s, 3H), 3.02 (t,  $J = 6.0$  Hz, 2H), 2.36 (bs, 1H).  $^{13}\text{C NMR}$  (62.5 MHz,  $\text{CDCl}_3$ ):  $\delta$  (ppm) = 188.6, 167.9 ( $^1J_{\text{C-F}} = 349.0$  Hz), 138.9, 135.2, 132.5 ( $^3J_{\text{C-F}} = 9.3$  Hz), 126.8, 125.4, 120.7, 120.4., 119.6, 116.1 ( $^2J_{\text{C-F}} = 21.8$  Hz), 110.2, 63.0, 32.3, 28.3. **IR** (neat):  $\nu = 3411, 3057, 2941, 2875, 1713, 1634, 1595, 1528, 1503, 1463, 1428, 1410, 1360, 1341, 1295, 1225, 1197, 1093, 1045, 1012, 980, 944, 841, 813, 779, 616, 543$   $\text{cm}^{-1}$ . **HRMS** (EI)  $m/z$  calc'd  $\text{C}_{18}\text{H}_{16}\text{FO}_2\text{NNa}$   $[\text{M} + \text{Na}]^+$ : 320.1063, found: 320.1063.

**5.5.4. Reaction with a 1-cyclopropyl substituted substrate**

The reaction was performed according to the procedure in section 5.2.

**Analytical data****Cyclopropyl(3-(2-hydroxyethyl)thiophen-2-yl)methanone**

Pale oil, 56% isol. yield.  $^1\text{H NMR}$  (400 MHz,  $\text{CDCl}_3$ ):  $\delta$  (ppm) = 7.50 (d,  $J = 4.9$  Hz, 2H), 7.07 (d,  $J = 4.9$  Hz, 1H), 3.89 (t,  $J = 5.5$  Hz, 2H), 3.24 (t,  $J = 6.0$  Hz, 2H), 2.74 (bs, 1H), 2.44 (m, 1H), 1.24 (m, 2H), 1.04 (m, 2H).  $^{13}\text{C NMR}$  (100 MHz,  $\text{CDCl}_3$ ):  $\delta$  (ppm) = 194.7, 146.0, 137.2, 132.0, 130.2, 63.4, 33.3, 30.9, 20.6, 11.9. **IR** (neat):  $\nu = 3421, 2930, 2874, 1713, 1644, 1520, 1410, 1387, 1325, 1216, 1180, 1099, 1030, 988, 955, 919, 865, 840, 759, 712, 677, 590$   $\text{cm}^{-1}$ . **HRMS** (EI)  $m/z$  calc'd  $\text{C}_{10}\text{H}_{13}\text{O}_2\text{S}$   $[\text{M} + \text{H}]^+$ : 197.0631, found: 197.0628.

**5.5.5. General procedure for the  $\text{Fe}(\text{OTf})_2\text{L1}$  catalysed aerobic cleavage of  $\text{Csp}^3\text{-Csp}^3$** 

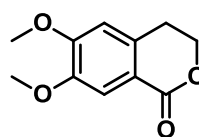
In a Radley's tube equipped with a magnetic stir bar ligand **L1** ( $5.67 \times 10^{-3}$  mmol, 5.2 mg) and  $\text{Fe}(\text{OTf})_2$  ( $5.65 \times 10^{-3}$  mmol, 2.0 mg) were added. The tube was sealed, degassed (3 times) and left under an inert atmosphere. The corresponding ether (2.0 mL) was added and the reaction tube was degassed, charged with dioxygen gas (1 atm, 3 times) and kept under oxygen (1 atm) by using a balloon. The reaction mixture was heated to  $60^\circ\text{C}$  and left



overnight. The reaction was purified by silica gel column chromatography (Hexane/EtOAc, gradient: 10/1 to 4/1 or 2/1) to afford the unreacted starting material and the reaction products.

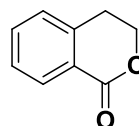
### Analytical data

#### 6,7-Dimethoxyisochroman-1-one<sup>33</sup>



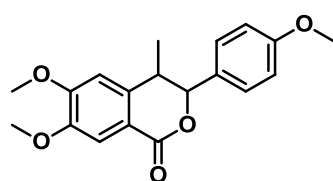
White solid. <sup>1</sup>H NMR (400 MHz, CDCl<sub>3</sub>): δ (ppm) = 7.54 (s, 1H), 6.69 (s, 1H), 4.51 (t, J = 6.0 Hz, 2H), 3.94 (s, 3H), 3.87 (s, 3H), 2.99 (t, J = 6.0 Hz, 2H). <sup>13</sup>C NMR (100 MHz, CDCl<sub>3</sub>): δ (ppm) = 165.6, 154.0, 148.8, 134.3, 117.8, 112.2, 109.5, 67.7, 56.5, 27.9. IR (neat): ν = 2952, 2911, 2836, 1706, 1602, 1511, 1461, 1421, 1394, 1336, 1270, 1240, 1203, 1157, 1087, 1058, 1027, 962. HRMS (EI) m/z calc'd C<sub>11</sub>H<sub>13</sub>O<sub>4</sub> [M + H]<sup>+</sup>: 209.0808, found, 209.0811.

#### Isochroman-1-one<sup>34</sup>



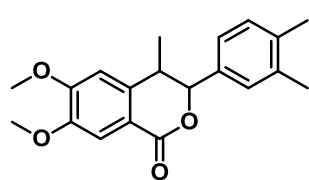
Colourless liquid. <sup>1</sup>H NMR (400 MHz, CDCl<sub>3</sub>): δ (ppm) = 8.12 (d, J = 7.7 Hz, 1H), 7.57 (t, J = 6.3 Hz, 1H), 7.41 (t, J = 7.6 Hz, 1H), 7.28 (d, J = 7.4 Hz, 1H), 4.56 (t, J = 6.2 Hz, 2H), 3.08 (t, J = 6.0 Hz, 2H). <sup>13</sup>C NMR (100 MHz, CDCl<sub>3</sub>): δ (ppm) = 165.1, 139.5, 133.6, 127.7, 125.3, 124.0, 67.3, 27.8. IR (neat): ν = 1714, 1602, 1459, 1386, 1294, 1240, 1116, 1087, 1024, 954, 744, 693, 636 cm<sup>-1</sup>. HRMS (EI) m/z calc'd C<sub>9</sub>H<sub>9</sub>O<sub>2</sub> [M + H]<sup>+</sup>: 149.0597, found, 149.0597.

#### (±)-6,7-Dimethoxy-3-(4-methoxyphenyl)-4-methylisochroman-1-one



White solid, 30% isol. yield. <sup>1</sup>H NMR (400 MHz, CDCl<sub>3</sub>): δ (ppm) = 7.60 (s, 1H), 7.29 (m, 2H), 6.91 (d, J = 8.7 Hz, 2H), 6.77 (s, 1H), 5.14 (d, J = 9.0 Hz, 1H), 3.96 (s, 3H), 3.93 (s, 3H), 3.81 (s, 3H), 3.31 (m, 1H), 1.25 (d, J = 6.96 Hz, 3H). <sup>13</sup>C NMR (100 MHz, CDCl<sub>3</sub>): δ (ppm) = 165.1, 159.8, 153.9, 148.2, 137.9, 130.1, 128.5, 117.1, 113.9, 111.9, 107.5, 85.5, 56.2, 56.1, 55.3, 36.8, 15.9. IR (neat): ν = 2968, 2932, 2836, 1709, 1604, 1511, 1457, 1411, 1379, 1282, 1248, 1213, 1178, 1165, 1134, 1084, 1073, 1025, 876, 834, 559, 528 cm<sup>-1</sup>. HRMS (EI) m/z calc'd C<sub>19</sub>H<sub>21</sub>O<sub>5</sub> [M + H]<sup>+</sup>: 329.1384, found, 329.1390. Anal Calc'd for C<sub>19</sub>H<sub>20</sub>O<sub>5</sub>: C, 60.50, H, 6.14, found: C, 60.14, H, 6.05.

#### (±)-3-(3,4-Dimethylphenyl)-6,7-dimethoxy-4-methylisochroman-1-one



White solid, 27% isol. yield. <sup>1</sup>H NMR (400 MHz, CDCl<sub>3</sub>): δ (ppm) = 7.60 (s, 1H), 7.08 (m, 3H), 6.76 (s, 1H), 5.13 (d, J = 8.9 Hz, 1H), 3.95 (s, 3H), 3.93 (s, 3H), 3.31 (m, 1H), 2.26 (s, 3H), 2.25 (s, 3H), 1.26 (d, J = 7.0 Hz, 3H). <sup>13</sup>C NMR (100 MHz, CDCl<sub>3</sub>): δ (ppm) = 165.1, 153.9, 148.2, 137.9, 137.1, 136.8, 135.4, 129.6, 128.3, 124.6, 117.1, 111.8, 107.5, 85.7, 56.2, 56.1, 36.7, 19.8, 19.5, 16.1. IR (neat): ν = 1698, 1604, 1507, 1454, 1413, 1356, 1290, 1252, 1213, 1196, 1169, 1157, 1087, 1072, 1037, 950, 875, 875, 820, 802, 774, 752 cm<sup>-1</sup>. HRMS (EI) m/z calc'd C<sub>20</sub>H<sub>23</sub>O<sub>4</sub> [M +

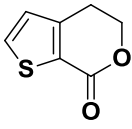
$H]^+$ : 327.1591, found, 327.1598. **Anal Calc'd** for  $C_{20}H_{22}O_4$ : C, 73.60, H, 6.79, found: C, 73.28, H, 6.75.

### 5.5.6. Factors determining the selectivity of the $Csp^3-Csp^3$ vs $Csp^3-O$ bond cleavage

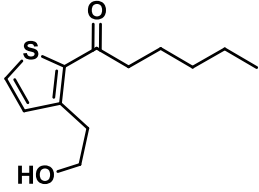
The reactions were performed according to the procedure described in section 5.4.

#### Analytical data

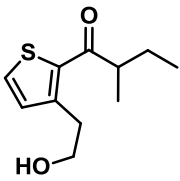
#### 4*H*-Thieno[2,3-*c*]pyran-7(5*H*)-one<sup>35</sup>

 White solid, 18% isol. yield.  $^1H$  NMR (400 MHz,  $CDCl_3$ ):  $\delta$  (ppm) = 7.59 (d,  $J$  = 4.8 Hz, 1H), 6.94 (d,  $J$  = 4.8 Hz, 1H), 4.52 (t,  $J$  = 6.0 Hz, 2H), 2.96 (t,  $J$  = 6.0 Hz, 2H).  $^{13}C$  NMR (100 MHz,  $CDCl_3$ ):  $\delta$  (ppm) = 161.6, 147.8, 134.8, 127.1, 126.9, 68.7, 25.5. **IR (neat)**:  $\nu$  = 1755, 1492, 1426, 1200, 1163, 1122, 1085  $cm^{-1}$ . **HRMS** (EI)  $m/z$  calc'd  $C_7H_7O_2S$  [ $M + H$ ] $^+$ : 155.0161, found, 155.0159.

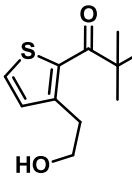
#### 1-(3-(2-Hydroxyethyl)thiophene-2-yl)hexan-1-one

 Colourless oil, 20% isol. yield.  $^1H$  NMR (400 MHz,  $CDCl_3$ ):  $\delta$  (ppm) = 7.49 (d,  $J$  = 4.8 Hz, 1H), 7.05 (d,  $J$  = 4.7 Hz, 1H), 3.87 (t,  $J$  = 6.1 Hz, 2H), 3.28 (t,  $J$  = 6.0 Hz, 2H), 2.87 (t,  $J$  = 7.0 Hz, 2H), 25.25 (bs, 1H), 1.72 (m, 2H), 1.34 (m, 4H), 0.87 (m, 3H).  $^{13}C$  NMR (100 MHz,  $CDCl_3$ ):  $\delta$  (ppm) = 195.2, 146.7, 132.1, 129.8, 126.5, 63.3, 42.0, 33.3, 31.4, 24.4, 22.4, 13.9. **HRMS** (CI)  $m/z$  calc'd  $C_{12}H_{17}OS$  [ $(M - H_2O) + H$ ] $^+$ : 209.0995, found, 209.1000.

#### 1-(3-(2-Hydroxyethyl)thiophene-2-yl)-2-methylbutan-1-one

 Colourless oil, 13% isol. yield.  $^1H$  NMR (400 MHz,  $CDCl_3$ ):  $\delta$  (ppm) = 7.49 (d,  $J$  = 4.8 Hz, 1H), 7.05 (d,  $J$  = 4.8 Hz, 1H), 3.90 (t,  $J$  = 5.9 Hz, 2H), 3.27 (t,  $J$  = 6.0 Hz, 2H), 2.30 (bs, 1H), 1.80 (m, 1H), 1.44 (m, 2H), 1.20 (d,  $J$  = 7.0 Hz, 3H), 0.90 (t,  $J$  = 7.0 Hz, 3H).  $^{13}C$  NMR (100 MHz,  $CDCl_3$ ):  $\delta$  (ppm) = 195.6, 146.5, 133.0, 128.9, 122.5, 68.1, 41.1, 35.9, 25.1, 22.7, 13.9. **HRMS** (CI)  $m/z$  calc'd  $C_{11}H_{17}O_2S$  [ $M + H$ ] $^+$ : 213.0944, found, 213.0949.

#### 1-(3-(2-Hydroxyethyl)thiophene-2-yl)-2,2-dimethylpropan-1-one

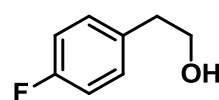
 Colourless oil, 12% isol. yield.  $^1H$  NMR (400 MHz,  $CDCl_3$ ):  $\delta$  (ppm) = 7.43 (d,  $J$  = 4.9 Hz, 1H), 7.02 (d,  $J$  = 4.9 Hz, 1H), 3.89 (t,  $J$  = 5.8 Hz, 2H), 3.08 (t,  $J$  = 6.0 Hz, 2H), 1.60 (bs, 1H), 1.37 (s, 9H).  $^{13}C$  NMR (100 MHz,  $CDCl_3$ ):  $\delta$  (ppm) = 202.5, 147.4, 133.2, 130.4, 128.3, 63.3, 44.6, 33.4, 27.7. **HRMS** (CI)  $m/z$  calc'd  $C_{11}H_{17}O_2S$  [ $M + H$ ] $^+$ : 213.0944, found, 213.0950.

### 5.5.7. General procedure for the Fe(OTf)<sub>2</sub>L1 catalysed aerobic cleavage of Csp<sup>2</sup>-Csp<sup>3</sup> and Csp<sup>3</sup>-O bonds

In a Radley's tube equipped with a magnetic stir bar ligand **L1** ( $5.67 \times 10^{-3}$  mmol, 5.2 mg) and Fe(OTf)<sub>2</sub> ( $5.65 \times 10^{-3}$  mmol, 2.0 mg) were added. The tube was sealed, degassed (3 times) and left under an inert atmosphere. The corresponding ether (2.0 mL) was added and the reaction tube was degassed, charged with dioxygen gas (1 atm, 3 times) and kept under oxygen (1 atm) by using a balloon. The reaction mixture was heated to 60 °C and left overnight. The reaction was purified by silica gel column chromatography (Hexane/EtOAc, gradient: 10/1 to 2/1) to afford the unreacted starting material and the phenethyl alcohol.

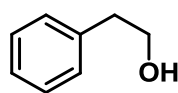
#### Analytical data

##### 2-(4-Fluorophenyl)ethanol <sup>36</sup>



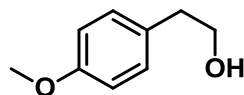
Colourless oil, 91% isol. yield. <sup>1</sup>H NMR (400 MHz, CDCl<sub>3</sub>): δ (ppm) = 7.18 (m, 2H), 7.00 (m, 2H), 3.84 (t, J = 6.0 Hz, 2H), 2.84 (t, J = 6.4 Hz, 2H), 1.42 (bs, 1H). <sup>13</sup>C NMR (100 MHz, CDCl<sub>3</sub>): δ (ppm) = 162.8 (<sup>1</sup>J<sub>C-F</sub> = 242.7 Hz), 134.1 (<sup>4</sup>J<sub>C-F</sub> = 3.1 Hz), 130.4 (<sup>3</sup>J<sub>C-F</sub> = 7.7 Hz), 115.4 (<sup>2</sup>J<sub>C-F</sub> = 20.8 Hz), 63.6, 38.3. **IR (neat):** ν = 3322, 2939, 2877, 1601, 1508, 1219, 1158, 1097, 1043, 1016, 934, 851, 820, 767, 722, 544, 502 cm<sup>-1</sup>. **HRMS (CI)** m/z calc'd C<sub>8</sub>H<sub>13</sub>FON [M + NH<sub>4</sub>]<sup>+</sup>: 158.0976, found, 158.0976.

##### 2-Phenylethanol <sup>37</sup>

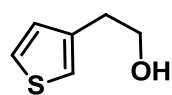


Colourless oil, 87 % isol. yield. <sup>1</sup>H NMR (400 MHz, CDCl<sub>3</sub>): δ (ppm) = 7.36 (m, 2H), 7.28 (m, 3H), 3.88 (t, J = 6.3 Hz, 2H), 2.89 (t, J = 6.4 Hz, 2H), 1.58 (bs, 1H). <sup>13</sup>C NMR (100 MHz, CDCl<sub>3</sub>): δ (ppm) = 138.7, 129.3, 128.8, 126.7, 63.9, 39.5, 31.2. **HRMS (CI)** m/z calc'd C<sub>8</sub>H<sub>14</sub>NO [M + NH<sub>4</sub>]<sup>+</sup>: 140.1070, found, 140.1071.

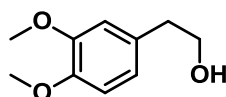
##### 2-(4-Methoxyphenyl)ethanol <sup>37</sup>



Dense colourless oil, 47 % isol. yield. <sup>1</sup>H NMR (400 MHz, CDCl<sub>3</sub>): δ (ppm) = 7.15 (m, 2H), 6.86 (m, 2H), 3.81 (t, J = 6.0 Hz, 2H), 3.79 (s, 3H, overlapped), 2.81 (t, J = 6.5 Hz, 2H), 1.53 (bs, 1H). <sup>13</sup>C NMR (100 MHz, CDCl<sub>3</sub>): δ (ppm) = 158.2, 130.4, 129.9, 114.0, 63.8, 55.2, 38.2. **IR (neat):** ν = 3342, 2935, 2835, 1611, 1510, 1464, 1441, 1300, 1241, 1177, 1110, 1033, 819, 809, 560, 518 cm<sup>-1</sup>. **HRMS (CI)** m/z calc'd C<sub>9</sub>H<sub>12</sub>O<sub>2</sub> [M + H]<sup>+</sup>: 153.091, found, 153.0909.

**2-(Thiophen-3-yl)ethanol**<sup>38</sup>

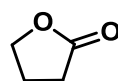
Colourless oil, 34 % isol. yield. **<sup>1</sup>H NMR** (400 MHz, CDCl<sub>3</sub>): δ (ppm) = 7.34 (d, J = 4.91 Hz, 1H), 7.14 (s, 1H), 7.04 (d, J = 4.8 Hz, 1H), 3.98 (t, J = 5.9 Hz, 2H), 2.97 (t, J = 6.0 Hz, 2H), 1.6 (bs, 1H). **<sup>13</sup>C NMR** (100 MHz, CDCl<sub>3</sub>): δ (ppm) = 138.7, 128.3, 125.9, 121.7, 62.9, 33.6. **IR** (neat): ν = 3321, 2933, 2876, 1409, 1389, 1331, 1153, 1044, 1018, 860, 834, 768, 689, 662, 630, 582 cm<sup>-1</sup>. **HRMS** (CI) m/z calc'd C<sub>6</sub>H<sub>6</sub>S [M + H]<sup>+</sup>: 111.0263, found, 111.0261.

**2-(3,4-Dimethoxyphenyl)ethanol**<sup>39</sup>

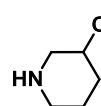
White solid, 10 % isol. yield. **<sup>1</sup>H NMR** (400 MHz, CDCl<sub>3</sub>): δ (ppm) = 6.82 (m, 3H), 3.88 (s, 3H), 3.85 (s, 3H, overlapped), 3.83 (t, 2H, overlapped), 2.82 (t, J = 6.0 Hz, 2H), 1.50 (bs, 1H). **<sup>13</sup>C NMR** (100 MHz, CDCl<sub>3</sub>): δ (ppm) = 149.0, 147.7, 130.9, 120.9, 112.1, 111.3, 63.7, 55.9, 55.8, 38.7. **IR** (neat): ν = 3234, 2981, 2884, 2837, 1588, 1514, 1470, 1481, 1444, 1417, 1332, 1255, 1235, 1189, 1154, 1136, 1073, 1042, 1024, 859, 849, 807, 763, 631 cm<sup>-1</sup>. **HRMS** (CI) m/z calc'd C<sub>10</sub>H<sub>14</sub>O<sub>3</sub> [M + H]<sup>+</sup>: 183.1016, found, 183.1020.

### 5.5.8. General procedure for the Fe(OTf)<sub>2</sub>L1 catalysed aerobic cleavage of Csp<sup>3</sup>-Csp<sup>3</sup> with decarboxylative cleavage of Csp<sup>2</sup>-O or Csp<sup>2</sup>-N bonds

In a Radley's tube equipped with a magnetic stir bar ligand **L1** (5.67 x 10<sup>-3</sup> mmol, 5.2 mg) and Fe(OTf)<sub>2</sub> (5.65 x 10<sup>-3</sup> mmol, 2.0 mg) were added. The tube was sealed, degassed (3 times) and left under an inert atmosphere. The corresponding ether (2.0 mL) was added and the reaction tube was degassed, charged with dioxygen gas (1 atm, 3 times) and kept under oxygen (1 atm) by using a balloon. The reaction mixture was heated to 60 °C and left overnight. The reaction was purified by silica gel column chromatography (Hexane/EtOAc, gradient: 4/1 to 1/1) to afford the unreacted starting material and the products.

**Analytical data****γ-Butyrolactone**<sup>40</sup>

Colourless oil. **<sup>1</sup>H NMR** (400 MHz, CDCl<sub>3</sub>): δ (ppm) = 4.37 (t, J = 7.0 Hz, 2H), 2.53 (t, J = 7.0 Hz, 2H), 2.30 (q, J = 7.0 Hz, 2H). **<sup>13</sup>C NMR** (100 MHz, CDCl<sub>3</sub>): δ (ppm) = 178.1, 68.9, 28.2, 22.6. **IR** ν (neat) = 1764, 1375, 1162, 1034, 990 cm<sup>-1</sup>. **HRMS** (ESI) m/z calc'd C<sub>4</sub>H<sub>8</sub>O<sub>2</sub>N [M+NH<sub>4</sub>]<sup>+</sup>: 104.0706, found, 104.0707.

**Ethyl piperidine-3-carboxylate**<sup>41</sup>

Colourless oil, 16% isol. yield. <sup>1</sup>H NMR (400 MHz, CDCl<sub>3</sub>): δ (ppm) = 4.12 (q, J = 6.8 Hz, 2H), 3.20 (d, J = 12.3, 3.8 Hz, 1H), 2.99-2.94 (m, 1H), 2.85 (dt, J = 12.3, 9.3 Hz, 1H), 2.65 (dt, J = 12.4, 10.3 Hz, 1H), 2.45-2.41 (m, 2H), 2.09-1.97 (m, 1H), 1.67 (bs, 1H), 1.66 (m, 1H, overlapped), 1.48 (m, 1H), 1.28 (t, J = 6.8 Hz, 3H). <sup>13</sup>C NMR (100 MHz, CDCl<sub>3</sub>): δ (ppm) = 174.4, 60.2, 48.5, 46.3, 42.5, 27.3, 25.5, 14.2. HRMS (CI) m/z calc'd C<sub>8</sub>H<sub>16</sub>O<sub>2</sub>N [M+H]<sup>+</sup>: 158.1176, found, 158.1176.

**5.6. References**

- [1] (a) Murakami, M.; Ito, Y. in *Cleavage of Carbon-Carbon Single Bonds by Transition Metals*, Topics in Organomet. Chem. Vol. 3 (Springer-Verlag Berlin 1999) (b) Dreis, A. M.; Douglas, C. J. *J. Am. Chem. Soc.* **2009**, *131*, 412.
- [2] In Scheme 1: Seiser, T.; Cramer, N. *J. Am. Chem. Soc.* **2010**, *132*, 5340. Additional examples: (a) Winter, C.; Krause, N. *Angew. Chem. Int. Ed.* **2009**, *48*, 2460. (b) Matsuda, T.; Shigeno, M.; Murakami, M. *J. Am. Chem. Soc.* **2007**, *129*, 12086. (c) Murakami, M.; Ashida, S.; Matsuda, T. *J. Am. Chem. Soc.* **2005**, *127*, 6932.
- [3] In Scheme 1: Wang, J.; Chen, W.; Zuo, S.; Liu, L.; Zhang, X.; Wang, J. *Angew. Chem. Int. Ed.* **2012**, *51*, 12334. Additional examples: (a) Li, H.; Li, Y.; Zhang, X. S.; Chen, K.; Wang, X.; Shi, Z.-J. *J. Am. Chem. Soc.* **2011**, *113*, 15244.
- [4] In Scheme 1: Suggs, J. W.; Jun, C.-H. *J. Am. Chem. Soc.* **1986**, *108*, 4679. Additional examples: Suggs, J. W.; Jun, C.-H. *J. Am. Chem. Soc.* **1984**, *106*, 3054.
- [5] Nakazawa, H.; Kawasaki, T.; Miyoshi, K.; Suresh, C. H.; Koga, N. *Organometallics* **2004**, *23*, 117.
- [6] Qin, C.; Zhou, W.; Chen, F.; Ou, Y.; Jiao, N. *Angew. Chem. Int. Ed.* **2011**, *50*, 12595.
- [7] Zhang, Y.; Wang, M.; Li, P.; Wang, L. *Org. Lett.* **2012**, *14*, 2206.
- [8] Li, W.; Zheng, X.; Li, Z. *Adv. Synth. Catal.* **2013**, *355*, 181.
- [9] Trovitch, J. R.; Lobkovski, E.; Bouwkamp, M. W.; Chirik, P. J. *Organometallics* **2008**, *27*, 6264.

- [10] Fan, X.; Cui, X.-M.; Guan, Y.-H.; Fu, L.-A.; Lv, H.; Guo, K.; Zhu, H.-B. *Eur. J. Org. Chem.* **2014**, 3, 498.
- [11] Gartner, D.; Konnert, H.; von Wangelin, A. J. *Catal. Sci. Technol.* **2013**, 3, 2541.
- [12] Lange, S. J.; Que Jr., L. *Curr. Opin. Chem. Biol.* **1998**, 2, 159.
- [13] (a) Chen, M.S.; White, M. C. *Science* **2007**, 318, 783. (b) Chen, M.S.; White, M. C. *Science* **2010**, 327, 566.
- [14] Wang, Y.; Konkoy, C. S.; Ilyn, V. I.; Vanover, K. E.; Carter, R. B.; Weber, E.; Keana, J. F. W.; Woodward, R. M.; Cai, S. X. *J. Med. Chem.* **1998**, 41, 2621.
- [15] Pirrung, M. C.; Roy, B. G.; Gadamssetti, S. *Tetrahedron* **2010**, 66, 3147.
- [16] Patman, R.; Chang, F. R.; Chen, C. Y.; Kuo, R. Y.; Lee, H. Y.; Wu, Y. C. *J. Nat. Prod.* **2001**, 64, 948.
- [17] Nozawa, K.; Yamada, M.; Tsuda, Y.; Kawai, K.; Nakajima, S. *Chem. Pharm. Bull.* **1981**, 29, 2689.
- [18] Yoshikawa, M.; Uchida, E.; Chatan, N.; Kobayashi, H.; Naitoh, Y.; Okuno, Y.; Matsuda, H.; Yamahara, J.; Murakami, N. *Chem. Pharm. Bull.* **1992**, 40, 3352.
- [19] Umehara, K.; Matsumoto, M.; Nakamura, M.; Miyase, T.; Kuroyanagi, M.; Noguchi, H. *Chem. Pharm. Bull.* **2000**, 48, 566.
- [20] Examples of  $\beta$ -alkyl eliminations with Fe: (a) Eibracht, P.; Dahler, P. *Chem. Ber.* **1980**, 113, 542. (b) with Pt: Thomson, S. K.; Young, G. B. *Organometallics* **1984**, 3, 1795. (c) with Ni: Miller, R. G.; Pinke, P. A.; Stauffer, R. D.; Golden, H. J.; Baker, D. J. *J. Am. Chem. Soc.* **1974**, 96, 4211.
- [21] Lotz, M. D.; Remy, M. S.; Lao, D. B.; Ariafard, A.; Yates, B. F.; Canty, A. J.; Mayer, J. M.; Sandford, M. S. *J. Am. Chem. Soc.* **2014**, 136, 8237.
- [22] (a) Koerts, T.; vanSanten, R. A. *J. Chem. Soc. Chem. Commun.* **1991**, 1281. (b) Belgued, M.; Pareja, P.; Amariglio, A.; Amariglio, H. *Nature* **1991**, 352, 789.
- [23] Mc Millen, D. F.; Golden, D. M. *Ann. Rev. Phys. Chem.* **1982**, 33, 493 and <http://www.q1.fcen.uba.ar/materias/qi1/Tablas/disocia.pdf> (C=O bond) .

- [24] (a) He, L.; Wang, Q.; Zhou, G.-C.; Guo, L.; Yu, X.-Q. *Arkivoc* **2008**, 103. (b) Alonso, E.; Ramon, D. J.; Yus, M. *Tetrahedron* **1997**, *53*, 14355. (c) Okano, K.; Okuyama, K.; Fukuyama, T.; Tokuyama, H. *Synlett* **2008**, *13*, 1977. (d) Congreve, M.S. *Synlett* 1993, 663. (e) Rahim, M. A.; Matsumura, S.; Toshima, K. *Tetrahedron Lett.* **2005**, *46*, 7307.
- [25] (a) Boovanahalli, K.; Kim, D. W.; Chi, D. Y. *J. Org. Chem.* **2004**, *69*, 3340. (b) Guindon, Y.; Morton, H. E.; Yoakim, C. *Tetrahedron Lett.* **1983**, *24*, 3969.
- [26] (a) Pojer, F.; Kahlich, R.; Kammerer, B.; Li S.-M.; Heide L. *J. Biol.Chem.* **2003**, *278*, 30661. (b) Kampranis, S. C.; Gormley, N. A.; Tranter, R.; Orphanides, G.; Maxwell, A. *Biochemistry* **1999**, *38*, 1967.
- [27] Paine, T. K.; Paria, S.; Que Jr., L. *Chem. Commun.* **2010**, *46*, 1830.
- [28] Muramatsu, W.; Nakano, K. *Org. Lett.* **2014**, *16*, 2042.
- [29] Reported in the literature with incomplete characterisation: Saeed, A. *Chinese Chem. Lett.* **2010**, *21*, 261.
- [30] Bourguerne, B.; Hoffmann, P.; Lherbert, C. *Synthetic Commun.* **2010**, *40*, 915.
- [31] Saito, A.; Takayama, M.; Yamazaki, A.; Numaguchi, J.; Hanzawa, Y. *Tetrahedron* **2007**, *63*, 4039.
- [32] Majetich, G., Liu, S., Fang, J., Siesel, D., Zhang, Y. *J. Org. Chem.* **62**, 6928-6951 (1997)
- [33] Song, A.-R.; Yu, J.; Zhang, C. *Synthesis* **2012**, *44*, 2903
- [34] Zhang, Y. H.; Shi, B. F.; Yu, J. Q. *Angew. Chem. Int. Ed.* **2009**, *48*, 6097
- [35] Elli Lilly Co. Patent: WO2007/146758 A2 (2007).
- [36] Junge, K.; Wendt, B.; Zhou, S.; Beller, M. *Eur. J. Org. Chem.* **2013**, *11*, 2061.
- [37] Szostak, M.; Spain, M.; Procter, D. J. *Chem. Eur. J.* **2014**, *20*, 4222.
- [38] Pearson, D. L.; Tour, J. M. *J. Org. Chem.* **1997**, *62*, 1376.
- [39] Handy, S. T.; Zhang, Y.; Bregman, H. *J. Org. Chem.* **2004**, *69*, 2362.
- [40] Sølvhøv, A.; Madsen, R. *Organometallics* **2011**, *30*, 6044.
- [41] Mishra, S. K.; Chaudhari, S. R.; Suryaprakash, N. *Org. Biomol. Chem.* **2014**, *12*, 495.

## *Chapter 6*

# **Fe(OTf)<sub>3</sub>-PYBISULIDINE CATALYSED AEROBIC C-C CLEAVAGE OF OLEFINS TO CARBONYL COMPOUNDS**



## 6.1. Introduction

### 6.1.1. Oxidative cleavage of olefins

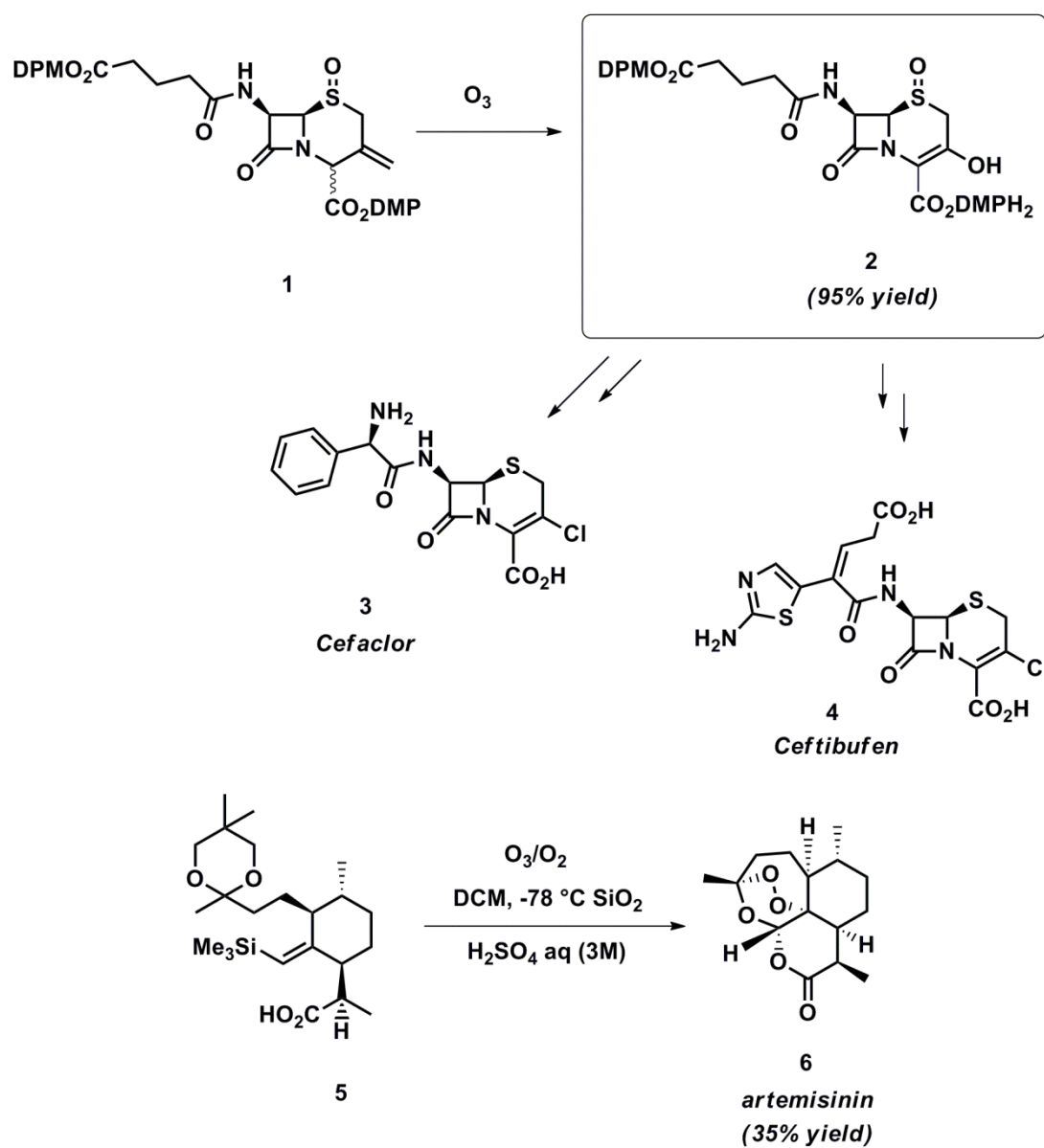
#### 6.1.1.1. Ozonolysis

In synthetic chemistry, the oxidative cleavage of alkenes is a widely employed methodology as it allows the introduction of oxygen functionalities in molecules, functional group deprotection or degradation of large molecules.<sup>1</sup> Additionally, it is a frequent transformation in the synthesis of pharmaceutical and biologically active compounds or in total synthesis of complex molecules.<sup>2</sup> For instance, the oxidative cleavage of the olefin functionality in precursor **1** allows a facile preparation of intermediate **2** which is used in the synthesis of cephalosporin antibiotics cefaclor and ceftibuten<sup>3</sup> (Scheme 1). In addition, the oxidative olefin cleavage in species **5** is a crucial final step in Avery's ten step total synthesis of the antimalarial drug (+)-artemisinin<sup>4</sup> (Scheme 1).

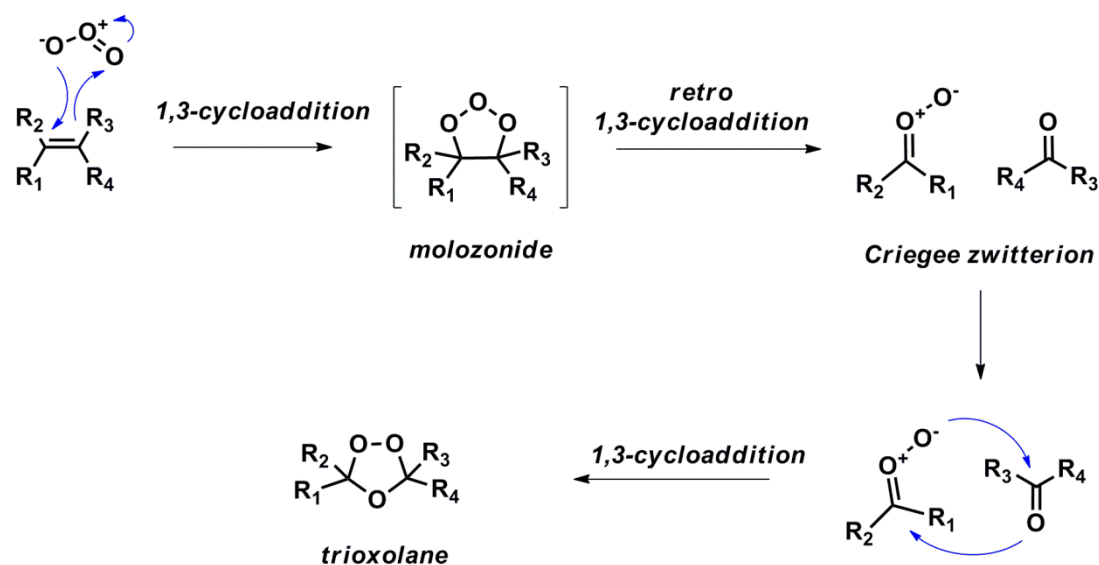
Since its discovery by C. Friedrich Schönbein in 1840, ozonolysis has initially been employed as an important method for structural elucidation of unknown molecules and with the development of modern spectroscopic techniques, it has evolved to a widely applied methodology in synthetic chemistry for the selective oxidation of organic compounds.<sup>5</sup> Harries ozonolysis, i.e. the oxidative cleavage of olefins to carbonyl groups mediated by ozone, has gained particular attention as a useful synthetic method for obtaining carbonyl compounds from olefins with good efficiency and cleanness.<sup>6</sup>

The accepted reaction mechanism was proposed by Criegee in 1953 and involves the 1,3-cycloaddition of ozone to the olefin affording a molozonide intermediate that rapidly decomposes into the Criegee zwitterion via 1,3-retrocycloaddition. A subsequent 1,3-cycloaddition of the zwitterion generates a more stable trioxolane intermediate<sup>7</sup> (Scheme 2). Experimental evidence in agreement with this mechanism has been provided by Berger et al. using <sup>17</sup>O-NMR techniques and other isotopic labeling experiments.<sup>8</sup> Further exposure of the resulting trioxolane to reducing or oxidizing conditions as well as the addition of different

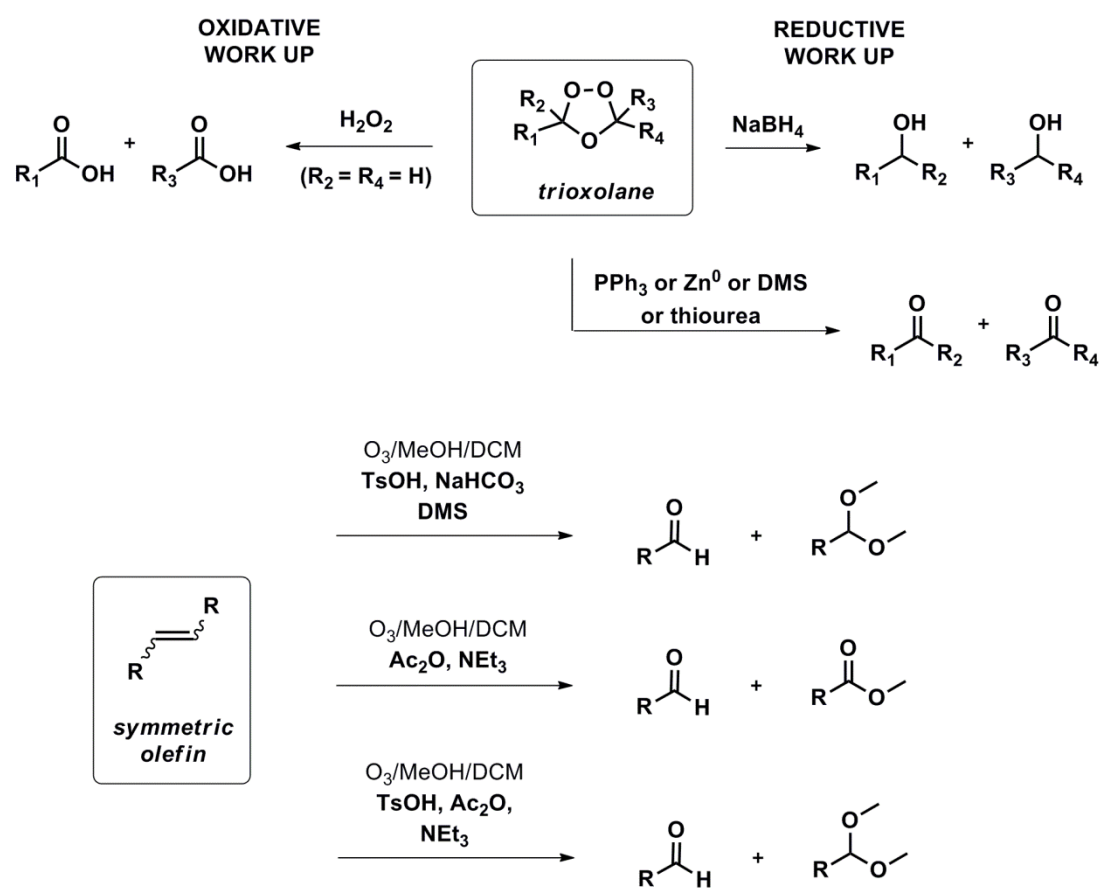
additives allow strict control of the degree of oxidation in the final reaction product expanding the versatility of this method<sup>9</sup> (Scheme 3).



**Scheme 1.** Examples of oxidative cleavage of olefins in the synthesis of pharmaceutical compounds



**Scheme 2.** Generally accepted mechanism of the ozonolysis of olefins

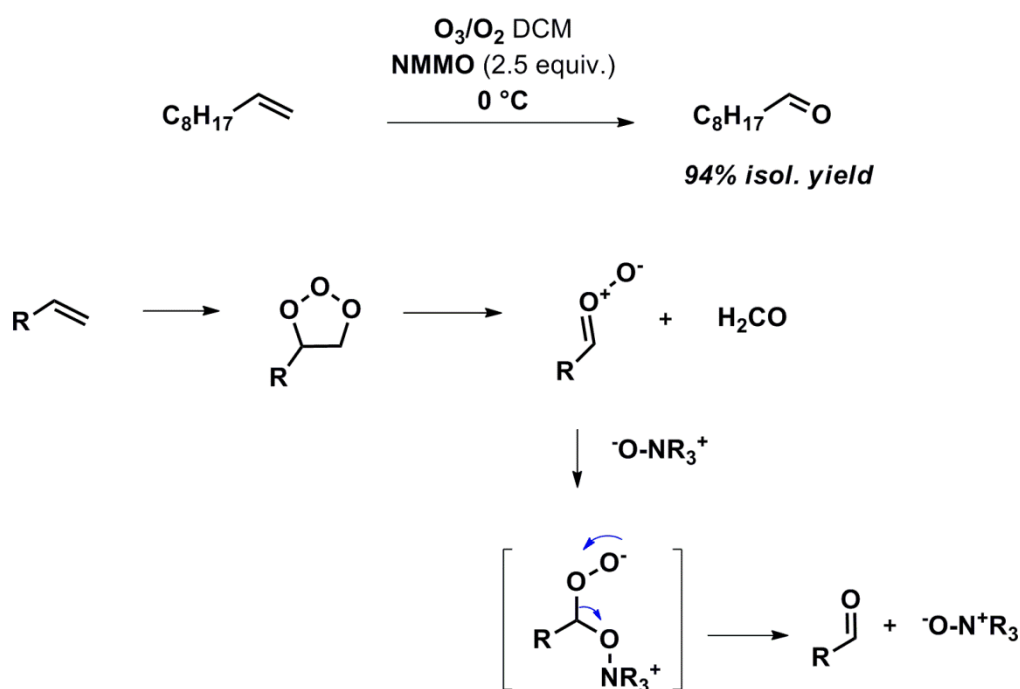


**Scheme 3.** Control of the product distribution by reductive or oxidant conditions and additives

In spite of the versatility and cleanness of the Harries ozonolysis, safety issues related to the use of ozone and the *in situ* formation of explosive peroxide intermediates tend to make difficult its large scale applications.<sup>10</sup> Additionally, the stoichiometric amounts of reducing or oxidizing agents needed during the work up and low reaction temperatures required (-78 °C) do not fit in the context of sustainable chemistry.

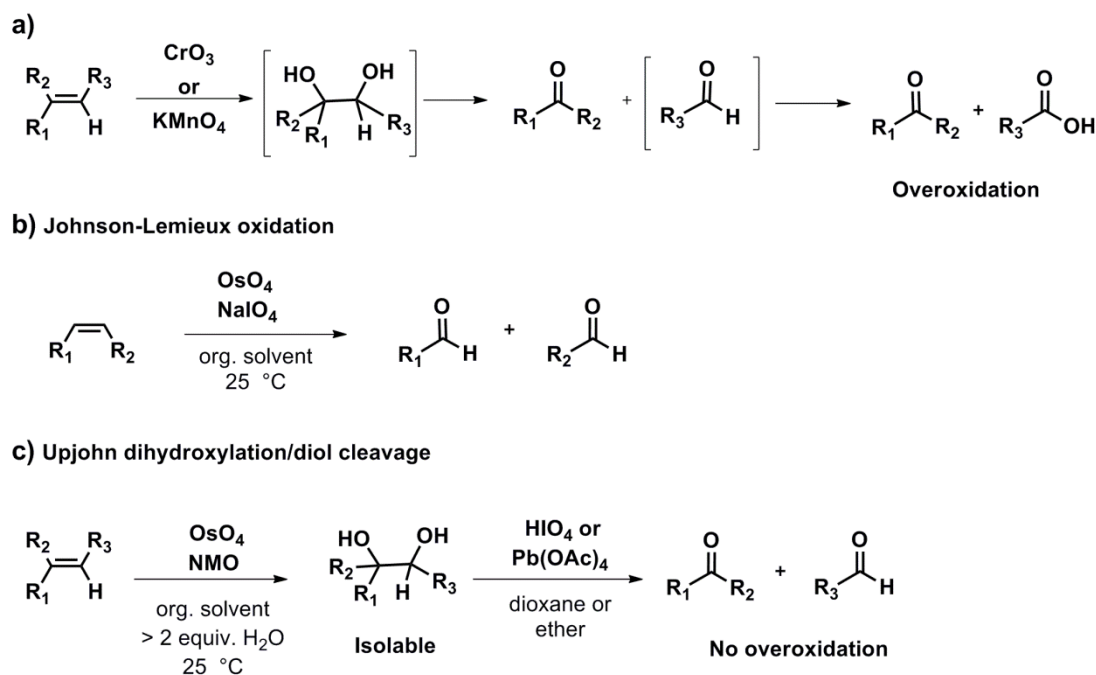
#### 6.1.1.2. Alternatives to ozonolysis

In an attempt to overcome the operational issues related to the ozonolysis reaction, Dussault *et al.* demonstrated a safer reductive ozonolysis in the presence of amine N-Oxides.<sup>11</sup> Aldehydes were selectively obtained upon reaction of monosubstituted olefins with an excess of NMMO under ozone at significantly higher temperatures (*circa* 0 °C) than a conventional ozonolysis. From a mechanistic perspective, an initial molozonide formation followed by its decomposition into the zwitterion species is proposed. However, the resulting carbonyl oxide fragment is attacked by the nucleophilic amine *N*-oxide generating an unstable zwitterion that rapidly decomposes releasing oxygen, amine and the aldehyde product (Scheme 4).



**Scheme 4.** Ozonolysis in the presence of amine *N*-oxides

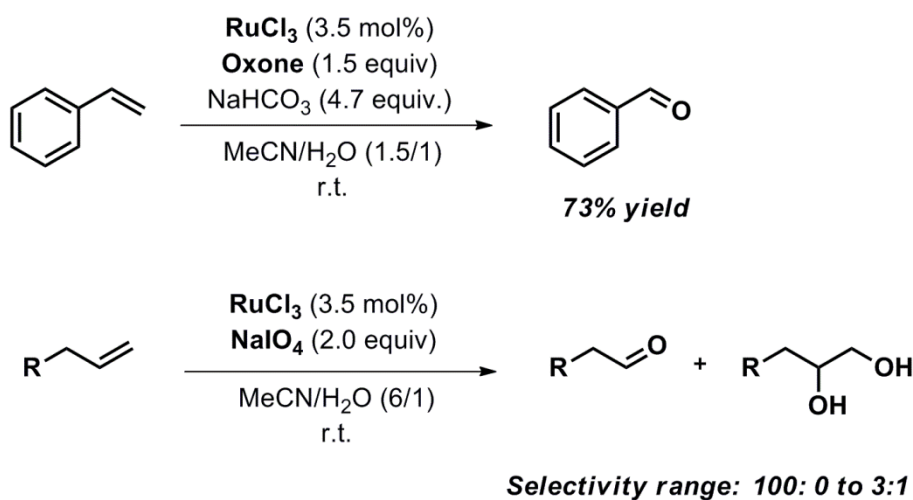
Other operationally safer methodologies based on the use of metal oxidants have been widely explored. However, they normally exhibit lower efficiencies and poorer selectivity and involve the use of toxic metals. Toxic and strong oxidizing agents such as  $\text{CrO}_3$  and neutral or acidic solutions of  $\text{KMnO}_4$  can undergo the oxidation of olefins to carbonyl compounds on its highest oxidation state.<sup>12</sup> The reaction mechanism involves the oxidation of the olefin substrate to a diol intermediate and its subsequent cleavage to carbonyl compounds. Under the aqueous reaction conditions, the aldehyde products can undergo facile overoxidation to carboxylic acids. In the case of  $\text{KMnO}_4$ , the selectivity towards the formation of the carbonyl product can be improved by using a benzene solution with crown ether to trap the  $\text{K}^+$  cations (Scheme 5a)).



**Scheme 5.** Additional methods for olefin oxidation to carbonyls using toxic metals have limitations such as overoxidation or multistep syntheses

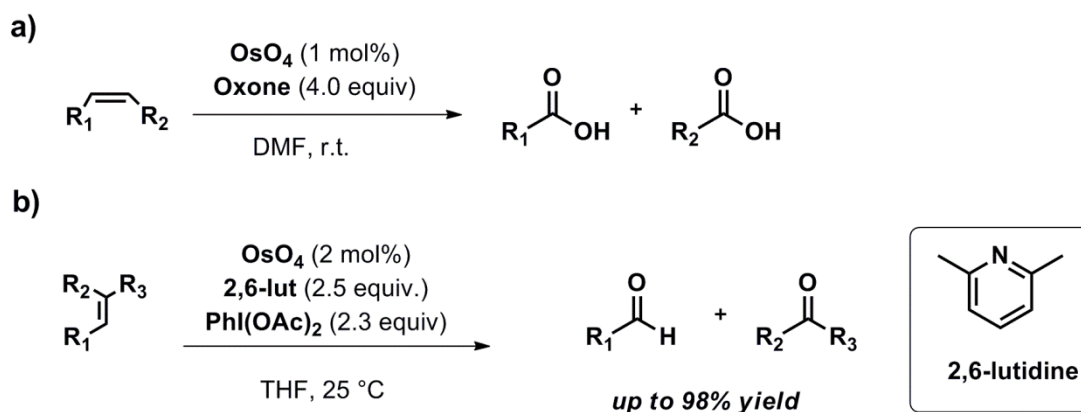
The overoxidation problem can be overcome with the Johnson-Lemieux oxidation<sup>13</sup> that uses a combination of  $\text{OsO}_4$  and  $\text{NaIO}_4$  in an organic solvent to prevent the overoxidation of aldehydes to carboxylic acids (Scheme 5 b)), or by using  $\text{OsO}_4$  as oxidizing agent to afford a *cis*-diol intermediate that can be further cleaved to carbonyl groups by subsequent treatment

with periodic acid or  $\text{Pb}(\text{OAc})_4$  (Upjohn dihydroxylation/ diol cleavage)<sup>14</sup> (Scheme 5 c)). In order to avoid the use of toxic  $\text{OsO}_4$ , combinations of  $\text{RuCl}_3$  with oxidants such as Oxone or  $\text{HIO}_4$  under buffered conditions have been applied to the selective oxidation of olefins to aldehydes.<sup>15</sup> Even though the scope of this method covered an ample variety of olefins, high catalyst loadings and more than stoichiometric amounts of oxidants were required to afford the carbonyl products in good yields. Additionally, undesired diol formation was also observed when monosubstituted olefins were used as substrates (Scheme 6).



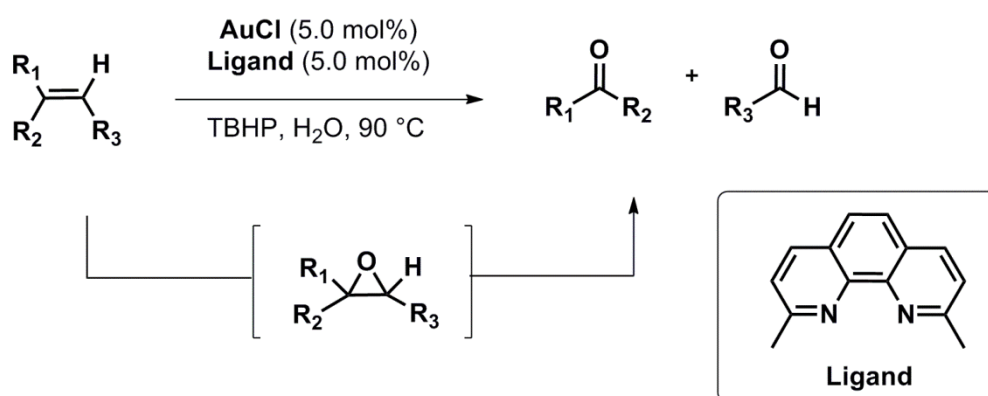
**Scheme 6.** Ru catalysed oxidative cleavage of olefins

Similarly, combinations of  $\text{OsO}_4$  with Oxone as the oxidizing reagent have been reported by Borhan et al. as an alternative to ozonolysis.<sup>16</sup> Aromatic and aliphatic olefins were converted to carboxylic acids with good yields by this method without the formation of an intermediate diol species (Scheme 7 a)). However, a large excess of oxidant was required and the use of toxic  $\text{OsO}_4$  even in catalytic amounts question the environmental friendliness of this method. On the contrary, the combination of  $\text{OsO}_4$  with 2,6-lutidine and  $\text{PhI}(\text{OAc})_2$  as oxidant was successfully applied to the selective cleavage of olefins to aldehydes with moderate to good yields.<sup>17</sup> Although good selectivity towards the formation of the aldehyde was achieved, some undesired  $\alpha$ -ketoalcohol formation was also observed in specific substrates and a large amount of waste was generated due to the large amounts of additives needed (Scheme 7 b)).



**Scheme 7.** Oxidative cleavage of olefins to carboxylic acids catalysed by  $\text{OsO}_4$

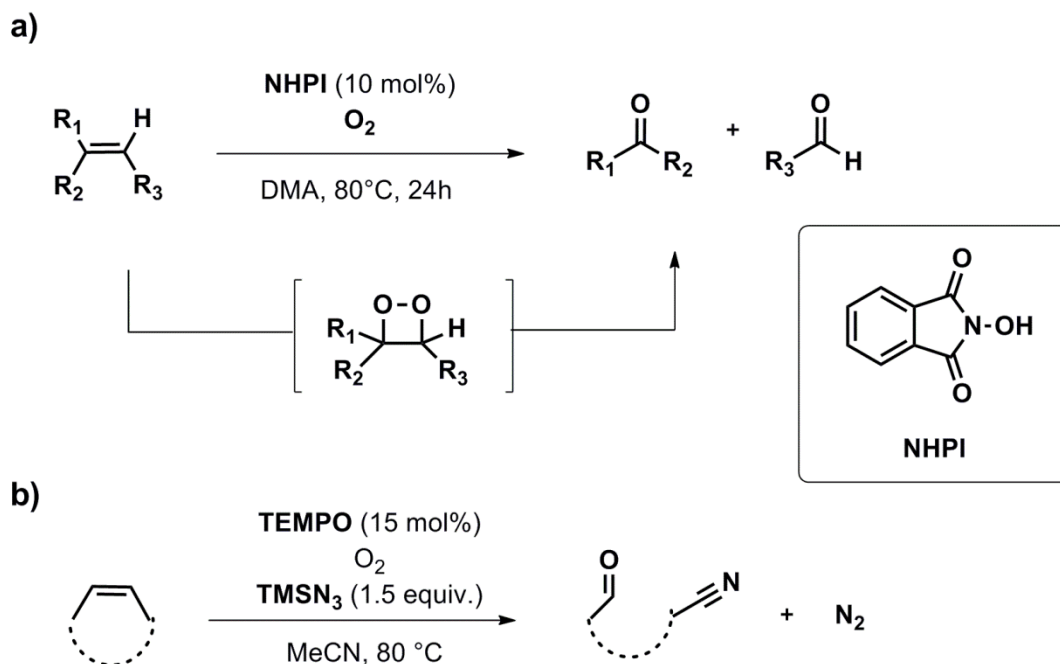
More recently, greener approaches to the oxidative cleavage of olefins have merged. Aromatic olefins can be selectively cleaved to aldehydes and ketones with moderate yields upon exposure to catalytic amounts of  $\text{AuCl}$ -neocuprine.<sup>18</sup> The reaction is proposed to proceed *via* initial epoxidation of the olefin followed by its oxidation to the carbonyl functionalities. Even though the reaction proceeds in water and gold salts are less toxic than osmium ones, high catalyst loadings and a large excess of a peroxide oxidant are required to accomplish the reaction (Scheme 8).



**Scheme 8.** Au-catalysed oxidative cleavage of olefins

Additionally, an organocatalytic oxidative cleavage of styrenes to carbonyls has been reported recently.<sup>19</sup> This method provides access to ketones with moderate yields under

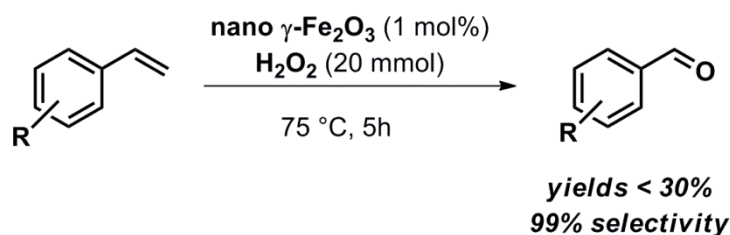
aerobic exposure and the reaction is believed to occur *via* the formation of a dioxetane intermediate. Nonetheless, a high catalyst loading is needed and low efficiency is achieved in the case of monosubstituted styrenes (Scheme 9 a)). Wang and Jiao have also reported the use of TEMPO as an organocatalyst for the oxidative nitrogenation of olefins by C-C cleavage allowing the formation of synthetically useful and versatile oxo nitrile scaffolds<sup>20</sup> (Scheme 9 b)).



**Scheme 9.** Organocatalytic cleavage of olefins

Due to the potential usefulness of iron in oxidation chemistry and due to its environmental friendliness, Beller and co-workers reported the use of  $\text{Fe}_2\text{O}_3$  nanoparticles as heterogeneous catalysts for the selective oxidation of styrenes to aldehydes using  $\text{H}_2\text{O}_2$  as oxidant.<sup>21</sup> Although excellent selectivity was achieved, this method still suffers from limited efficiency and poor scope which hampers its applicability in conventional organic synthesis (Scheme 10).





**Scheme 10.** Oxidative cleavage of styrenes catalysed by  $\text{Fe}_2\text{O}_3$  nanoparticles

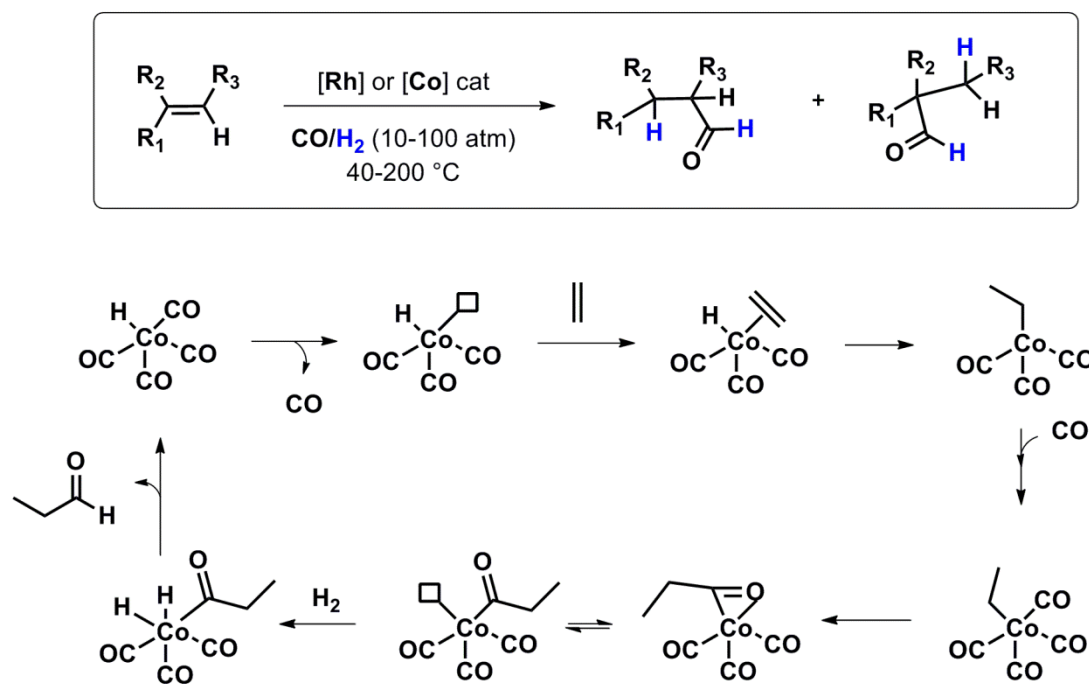
Finally, the direct oxidative cleavage of olefins to carbonyl compounds has also been attempted in the absence of catalytic species by using singlet oxygen ( $^1\text{O}_2$ ) that can be generated from the chemical reaction of  $\text{H}_2\text{O}_2$  and  $\text{NaOCl}$  or by irradiating  $\text{O}_2$  with light. For instance, the photooxidation of monosubstituted olefins has been achieved in biphasic media under UV light irradiation using molecular oxygen as the sole oxidant.<sup>22</sup> However, in the absence of a molecular catalyst selectivity becomes problematic with an ample distribution of products being obtained and a very limited substrate scope being achieved.

## 6.1.2. Additional strategies for transforming olefins into carbonyls

### 6.1.2.1. Hydroformylation

Aldehydes can be obtained from alkenes under high pressures of  $\text{CO}/\text{H}_2$  (10-100 atm) and high temperatures (40 to 200 °C) in the presence of catalytic amounts of a Rh complex (Scheme 11). The process is known as hydroformylation, oxo synthesis or oxo process and since its introduction in 1938 it has become probably one of the most relevant industrial processes of the 20<sup>th</sup> century, reaching a production of  $6,6 \times 10^6$  tons in 1995.<sup>23</sup> Otto Roelen demonstrated the use of  $\text{HCo}(\text{CO})_3$  as the first catalyst for hydroformylation; however, Co based catalysts have been replaced since 1970 with more selective and highly active rhodium-based catalysts.<sup>24</sup> Many improvements have been successfully introduced to the initial reaction including asymmetric versions<sup>25</sup> and water soluble catalysts that simplify product separation from the catalyst.<sup>26</sup> The  $\text{HCo}(\text{CO})_4$  catalysed conversion of ethene into propanal (Scheme 11) involves the coordination of ethene to the Co catalyst and its insertion into the Co-H bond, followed by a fast migratory insertion of a carbonyl into the resulting

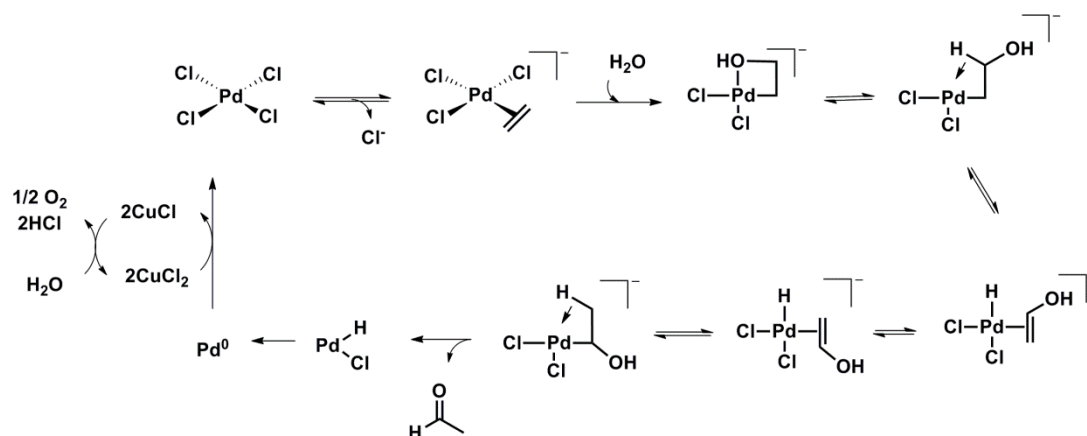
Co-C bond. Oxidative addition of  $H_2$  followed by reductive elimination affords the aldehyde product and regenerates the initial catalytic species  $HCo(CO)_4$ . Due to the incorporation of the carbonyl moiety during the catalytic cycle, the hydroformylation reaction promotes the aldehyde chain extension with one additional carbon.



**Scheme 11.** General scheme of the hydroformylation reaction and the catalytic cycle proposed for the conversion of ethene to propanal

### 6.1.2.2. Wacker oxidation

The Wacker-Tsuji oxidation is a widely applied methodology for the production of ketone type compounds from olefinic substrates under aerobic conditions on a laboratory scale.<sup>27</sup> This transformation originally stems from the Wacker process that allows the conversion of ethene into acetaldehyde on an industrial scale.<sup>28</sup> Wacker processes rely on the use of  $PdCl_2$  as catalyst, water as the oxygen source and  $CuCl$  as additive to regenerate the active catalytic species (Scheme 12). Important industrial applications have originated from Wacker chemistry. Thus it is considered one of the most relevant processes of the century.



**Scheme 12.** Proposed catalytic cycle for the Wacker oxidation of ethane to acetaldehyde

### 6.1.3. Additional alternatives for synthesizing carbonyl compounds

Apart from oxidation reactions and hydroformylation, other relevant methodologies for the preparation of carbonyl compounds from precursors different from olefins include hydration of alkynes, oxidation of alcohols and Friedel Crafts acylation of aromatics.

## 6.2. Aims of this chapter

Research conducted in the area of iron-catalysed oxidation of olefins is mainly focused on undergoing epoxidation reactions or *cis*-diol synthesis.<sup>29</sup> Olefins have indeed proven challenging substrates for biomimetic iron catalysts as they are prone to decompose  $\pi$ -rich substrates under oxidative reaction conditions.<sup>30</sup> However, iron-based metalloenzymes are capable of selectively cleaving olefinic substrates under aerobic atmosphere with excellent efficiency.<sup>31</sup> Beller and co-workers have shown that iron nanoparticles can undergo olefin cleavage in the presence of  $\text{H}_2\text{O}_2$  (*vide supra*); but to the best of our knowledge, there are no reports in the literature of an iron catalyst that specifically attempts the oxidative cleavage of olefins with  $\text{O}_2$ . The synthetic relevance of this transformation in conjunction with the environmental and safety issues of the currently available methodologies suggests that a mild, selective and environmentally friendly iron-catalysed oxidative cleavage of olefinic substrates under aerobic conditions would be highly desirable for synthetic chemists. In this chapter, two main targets are attempted:

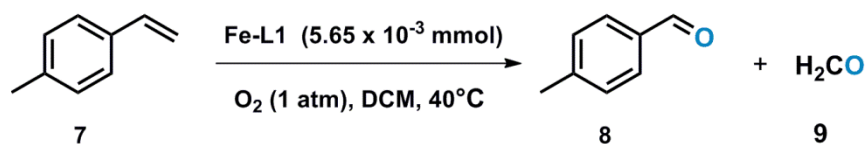
1. To expand the scope of the catalytic applications of Fe(OTf)<sub>2</sub>L1 in oxidation chemistry, evolving from the selective aerobic oxidations and C-C cleavages of ethereal substrates to alkene type substrates which represent a current challenge for oxidation chemistry.
2. To develop an efficient and highly selective iron-catalysed methodology for the aerobic cleavage of olefins to carbonyl compounds that can overcome the limitations of the already available methods.

### 6.3. Results and discussion

#### 6.3.1. Optimisation of the Fe-catalysed aerobic cleavage of olefins

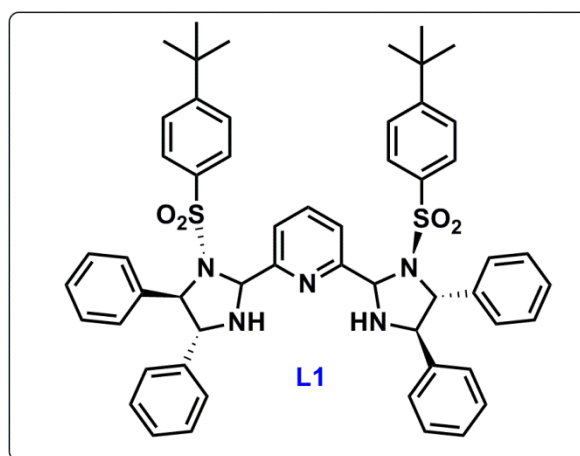
##### 6.3.1.1. Model reaction for optimization studies

To start our investigations, the non-sterically encumbered and slightly electron rich 4-methylstyrene **7** was chosen as model substrate. Due to their superior performance in the selective oxidation and cleavage of ethereal substrates, iron triflates were initially chosen as preferred metals salts. Almost no oxidative cleavage was observed when **7** was exposed to catalytic amounts of Fe(OTf)<sub>2</sub>-L1 under aerobic atmosphere, however, replacement of the iron salt with the stronger Lewis acid Fe(OTf)<sub>3</sub><sup>32</sup> cleanly furnished the aldehyde product **8** in low yields (Scheme 13). Among the PyBisulidine ligands, L1 was selected as the starting ligand as it showed the highest efficiency in the aerobic oxidation of ethers. Due to our interest in developing oxidation reactions under aerobic atmosphere, oxygen was targeted as the desired oxidant for accomplishing this transformation.



Entry	Fe salt	Conversion (%) <sup>a</sup>
1	Fe(OTf) <sub>2</sub>	2
2	Fe(OTf) <sub>3</sub>	14

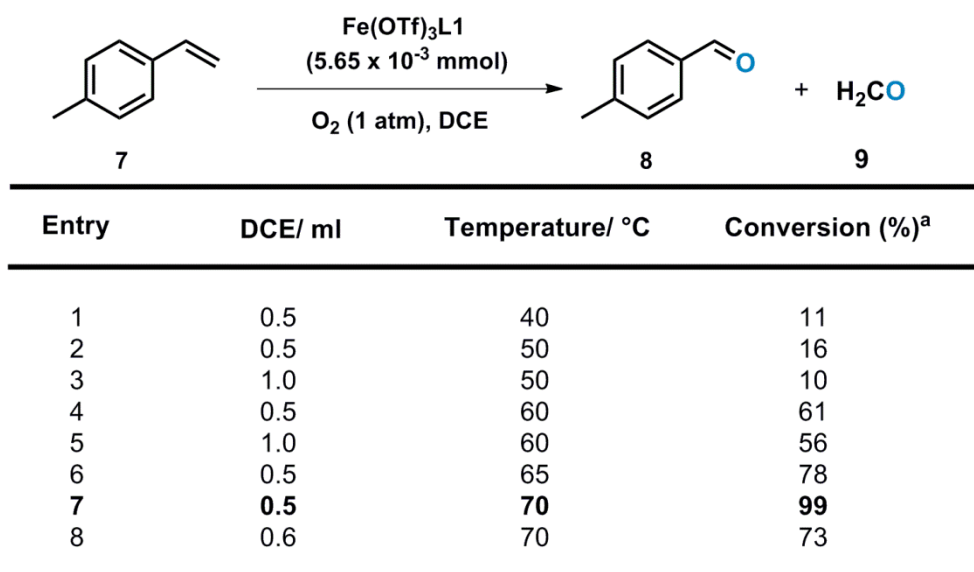
Reaction conditions: Fe salt ( $5.65 \times 10^{-3}$  mmol), **L1** ( $5.67 \times 10^{-3}$  mmol), **7** (0.75 mmol), DCM (0.5 mL), 5 h, 40 °C, O<sub>2</sub> (1 atm). [a] Determined by <sup>1</sup>H NMR.



**Scheme 13.** Reaction conditions for screening

### 6.3.1.2. Effect of temperature and concentration

Under the conditions in Scheme 13, the oxidative cleavage of **7** to afford aldehyde **8** was observed and further investigated in a range of temperatures and concentrations. Formation of **8** was found to increase gradually with temperature until full conversion was achieved at 70 °C (Scheme 14, entry 7). Additionally, more concentrated solutions of **7** resulted in higher conversions under identical reaction conditions in agreement with the significant concentration effect observed during the oxidation of ethereal substrates. Formation of formaldehyde **9** was also observed by <sup>1</sup>H NMR.

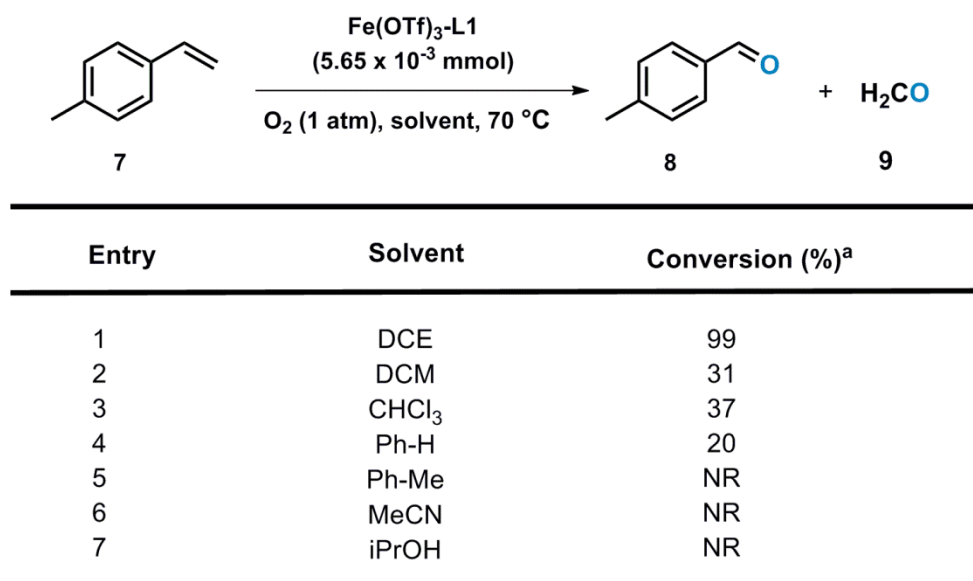


Reaction conditions:  $\text{Fe(OTf)}_3$  ( $5.65 \times 10^{-3}$  mmol), **L1** ( $5.67 \times 10^{-3}$  mmol), **7** (0.75 mmol), 5 h,  $\text{O}_2$  (1 atm). [a] Determined by  $^1\text{H}$  NMR.

**Scheme 14.** Effect of temperature and concentration in the oxidative cleavage of **7**

### 6.3.1.3. Solvent effect

The  $\text{Fe(OTf)}_3$ -**L1** catalysed aerobic oxidation of **7** showed strong dependency on the reaction solvent (Scheme 15). Chlorinated solvents afforded the oxidised product **8** with moderate to very good yields, whereas poor activity was found in aryl solvents. This trend is opposite to the solvent effect observed during the oxidation of ethers where chlorinated solvents were found detrimental for the reactivity of the complex. The catalytic activity of the  $\text{Fe(OTf)}_3$ -**L1** complex was also inhibited in coordinating solvents such as alcohols or MeCN.

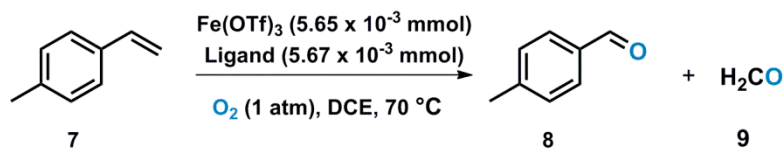


Reaction conditions: Fe(OTf)<sub>3</sub>L1 made *in situ* (5.65 × 10<sup>-3</sup> mmol), **7** (0.75 mmol), solvent (0.5 mL), 5 h, 70 °C, O<sub>2</sub> (1 atm). [a] Determined by <sup>1</sup>H NMR.

**Scheme 15.** Solvent studies

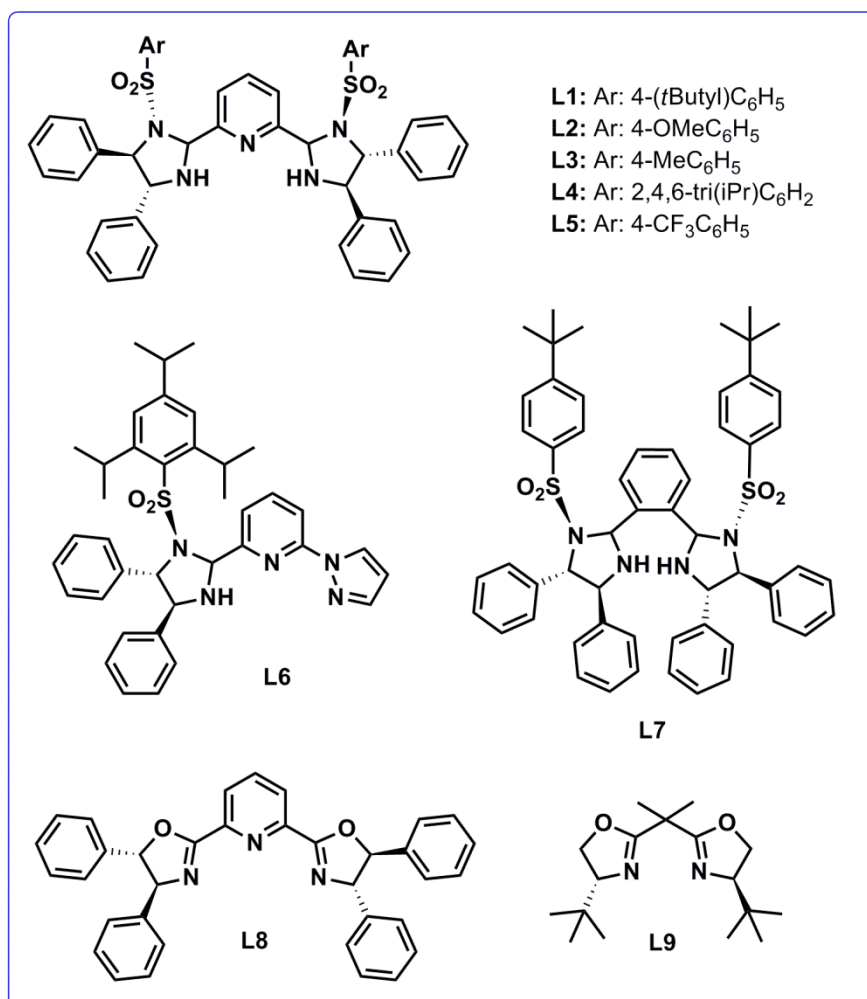
#### 6.3.1.4. Ligand effect

Among all the reaction parameters investigated, the ligand selection was found crucial for achieving good catalytic activity in the oxidation of **7** (Scheme 16). Iron-PyBisulidine complexes afforded the best conversions, with **L1** showing the highest efficiency. Combinations of Fe(OTf)<sub>3</sub> with the slightly electron rich PyBisulidines **L2** and **L3** also afforded **8** in good conversions whereas moderate conversions were obtained with the more sterically demanding **L4** and the more electron deficient **L5**. However, replacement of PyBisulidine skeletons with asymmetric or bidentate derivatives was found very detrimental for the aerobic cleavage of **7**. Saturated tridentate and bidentate Box type ligands also showed poor efficiency. In the absence of ligand, catalytic amounts of Fe(OTf)<sub>3</sub> caused total decomposition of the initial substrate, highlighting again the importance of the ligand in tuning the metal properties and achieving good selectivity.



Entry	Ligand	Conversion (%) <sup>a</sup>
1	L1	99
2	L2	84
3	L3	82
4	L4	60
5	L5	51
6	L6	NR
7	L7	NR
8	L8	32
9	L9	4
10	-	- <sup>b</sup>

Reaction conditions:  $\text{Fe}(\text{OTf})_3$  ( $5.65 \times 10^{-3}$  mmol), **L** ( $5.67 \times 10^{-3}$  mmol), **7** (0.75 mmol), DCM (0.5 mL), 5 h, 70 °C,  $\text{O}_2$  (1 atm). [a] Determined by  $^1\text{H}$  NMR. [b] Substrate decomposition



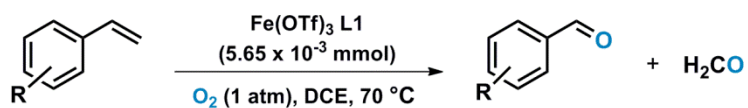
**Scheme 16.** Ligand effect in the aerobic cleavage of **7**



### 6.3.2. Substrate scope

#### 6.3.2.1. Aerobic cleavage of monosubstituted styrenes

Under optimised conditions an ample variety of styrenes were subjected to the  $\text{Fe}(\text{OTf})_3\mathbf{L1}$  catalysed aerobic cleavage (Scheme 17). Good to excellent yields were obtained for styrene substrates with very low catalyst loadings (0.7 mol%). The catalyst tolerated the presence of electron-withdrawing groups in both *meta*- and *para*-positions and similar efficiency was observed with more electron rich substrates. Nonetheless, medium conversions were achieved with more sterically demanding substrates probably because their interaction with the iron centre is hampered by the steric hindrance of the bulky  $\mathbf{L1}$  ligand. In fact, *ortho*-methylstyrene was oxidatively cleaved in lower yield (*circa* 12%), probably because of such steric effects. Interestingly, the reactions proceeded cleanly and selectively to afford the aldehyde product without any further oxidation to their carboxylic acid form as no aqueous media is needed to accomplish the reaction. Diol byproduct formation was not observed either under these reaction conditions with the formaldehyde resulting from the olefin cleavage being the only additional species detected by  $^1\text{H}$  NMR spectroscopy. In addition, the use of a previously formed  $\text{Fe}(\text{OTf})_3\mathbf{L1}$  complex did not improve the reaction conversion; thus a facile methodology involving an *in situ* prepared complex can be used.



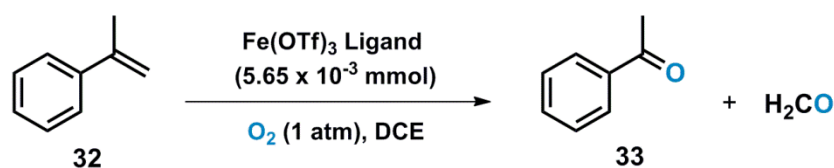
Entry	Substrate	Product	Conversion (%) <sup>a</sup>	Yield (%) <sup>b</sup>
1			95	90
2			83	78
3			92	87
4			83	79
5			96	93
6			78	75
7			82	77
8			99	95
9			83	78
10			47	30
11			63	57

Reaction conditions:  $\text{Fe(OTf)}_3$  ( $5.65 \times 10^{-3}$  mmol), L ( $5.67 \times 10^{-3}$  mmol), styrene (0.75 mmol), DCE (0.5 mL), 5 h, 70 °C,  $\text{O}_2$  (1 atm). [a] Determined by  $^1\text{H}$  NMR. [b] Isolated yield.

**Scheme 17.** Aerobic cleavage of monosubstituted styrenes

### 6.3.2.2. Aerobic cleavage of 1,1,-substituted styrenes

Generating ketone products from 1,1-disubstituted styrenes via aerobic cleavage was next targeted. The conjugated alkene  $\alpha$ -methylstyrene was selected as model substrate and under optimised conditions it was successfully converted to acetophenone **11** with moderate yield. A slight increase in the reaction temperature and a decrease in the S/C ratio contributed to an increase in the conversion (Scheme 18). Nonetheless, replacement of PyBisulidine ligand **L1** with the bulkier **L4** provided very good conversion too.

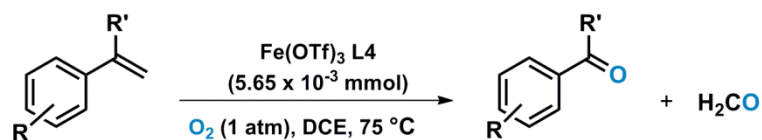


Entry	Ligand	Temperature /°C	Conversion (%) <sup>a</sup>
1	L1	70	42 <sup>b</sup>
2	L1	70	68
3	L1	75	72
4	L2	75	68
5	L3	75	54
6	L4	75	89
7	L4	70	79

Reaction conditions: Fe(OTf)<sub>3</sub> (5.65 x 10<sup>-3</sup> mmol), Ligand (5.67 x 10<sup>-3</sup> mmol), styrene (0.50 mmol), DCE (0.5 mL), 5h, O<sub>2</sub> (1 atm). [a] Determined by <sup>1</sup>H NMR. [b] styrene (0.75 mmol)

**Scheme 18.** Optimisation of the aerobic cleavage of **32**

With the optimal conditions in hands, the scope of the Fe(OTf)<sub>3</sub>L4 catalysed aerobic cleavage of  $\alpha$ -methylstyrenes was next investigated (Scheme 19).  $\alpha$ -Methylstyrenes bearing electron withdrawing functionalities were efficiently oxidised to ketones in very good yields with low catalyst loadings (1 mol%). To our delight, the very challenging 4-(prop-1-en-2-yl)pyridine (entry 5) was also partially oxidized to its ketone form in moderate yields. Remarkably, the catalytic aerobic cleavage proceeded with very good yields even after replacement of the  $\alpha$ -methyl group with bulkier pi-, *pseudo*-pi, or alkyl cycles (entries 6-9).



Entry	Substrate	Product	Conversion (%) <sup>a</sup>	Yield (%) <sup>b</sup>
1			89	87
2			47	42
3			86	83
4			88	85
5			22	20
6			98	95
7			99	87
8			58	54
9			76	73

Reaction conditions:  $\text{Fe(OTf)}_3$  ( $5.65 \times 10^{-3}$  mmol), **L4** ( $5.67 \times 10^{-3}$  mmol), styrene (0.50 mmol), DCE (0.5 mL), 5 h, 75 °C,  $\text{O}_2$  (1 atm). [a] Determined by  $^1\text{H}$  NMR. [b] Isolated yield.

**Scheme 19.** Aerobic cleavage of 1,1-disubstituted styrenes

### 6.3.3. Mechanistic investigations

#### 6.3.3.1. Involvement of radical species

In order to elucidate whether radical species are generated in the oxidative cleavage of olefins, styrene **22** was subjected to the Fe(OTf)<sub>3</sub>**L1** catalysed aerobic cleavage under optimal conditions in the presence of a radical trapping reagent (Table 1). Whereas 2,6-di-*t*-butyl-4-methylphenol caused complete inhibition of the reaction even in equimolecular amounts of catalyst (entries 1-3), other C-selective radical traps hardly affected the oxidative cleavage (BrCCl<sub>3</sub>) or caused significant inhibition when added in large excess (*p*-benzoquinone). O-selective trapping reagents (Ph<sub>2</sub>NH) also caused total inhibition of the reaction in small amounts.

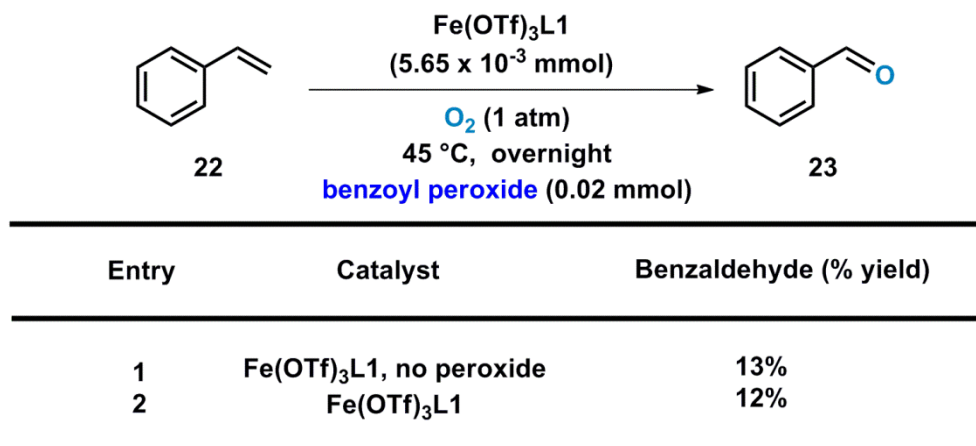
These results suggest that radical species may be generated during the aerobic cleavage. However, it cannot be discarded that the reduced reactivity observed may stem from the catalysts being deactivated by interacting with some of the trapping reagents rather than from proper radical formation.

C=Cc1ccccc1 (22)  $\xrightarrow[\text{O}_2 (1 \text{ atm}), 70 \text{ }^\circ\text{C}, 5 \text{ h}]{\text{Fe(OTf)}_3\text{L1} (5.65 \times 10^{-3} \text{ mmol})}$  O=Cc1ccccc1 (23)

Radical probe	Entry	n(rad probe/catalyst)	Benzaldehyde (% yield)
	1	1	-
	2	5	-
	3	10	-
BrCCl <sub>3</sub>	4	5	72
	5	10	65
	6	5	54
	7	10	8
	8	5	-
	9	10	-

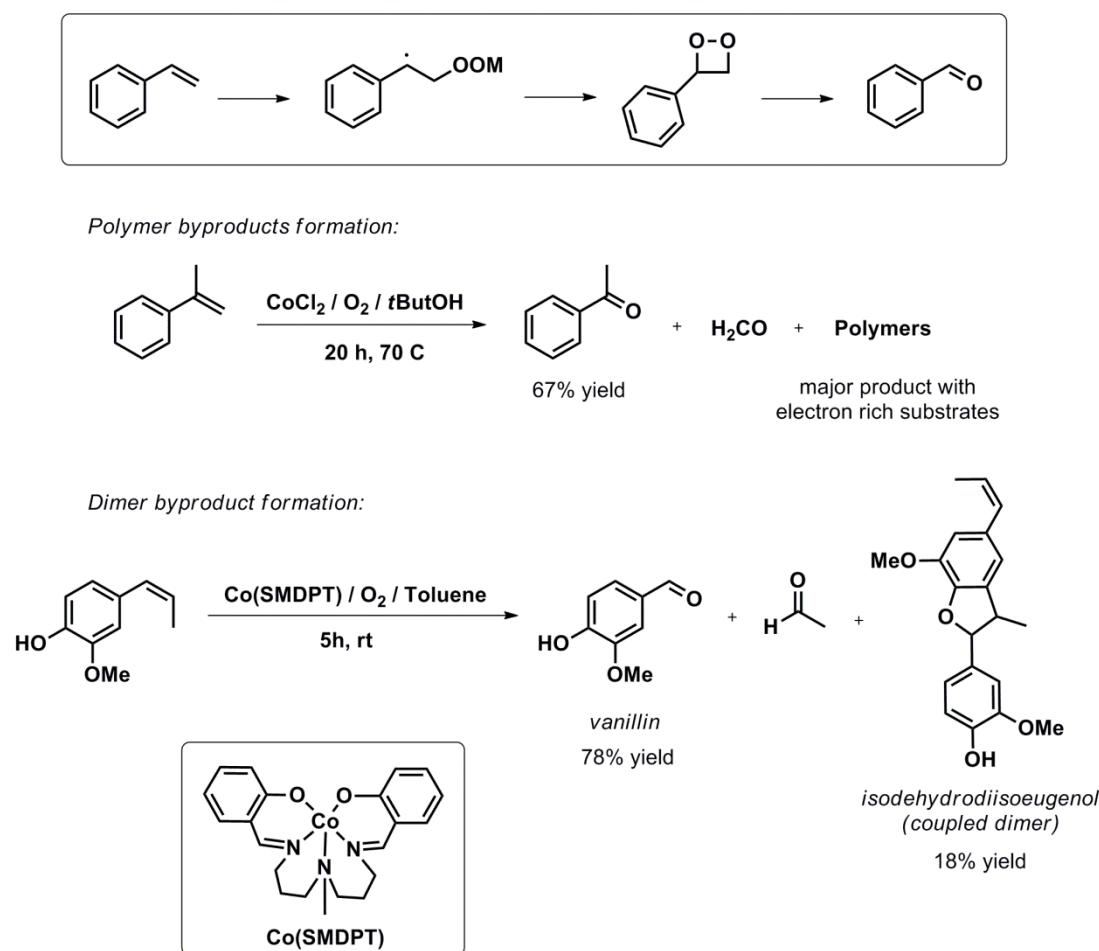
**Table 1.** Fe(OTf)<sub>3</sub>L1 catalysed aerobic cleavage of **22** in the presence of C- and O-selective radical trapping reagents.

To shed some light into the possible radical formation, the aerobic cleavage of styrene **22** was next conducted in the presence of the radical initiator benzoyl peroxide at 45 °C (Scheme 24). The presence of the radical initiator did not affect the aerobic cleavage of **22** (13% vs 12%), nor did it result in other products formation. These results suggest that a freely diffusing carbon-based radical species are not involved in the iron-catalysed aerobic cleavage.



**Scheme 24.** Fe(OTf)<sub>3</sub>L1 catalysed aerobic cleavage of **22** in the presence of a radical initiator

Interestingly, catalytic oxidative cleavages of styrene type substrates normally involve the formation of benzyl radical intermediates<sup>33</sup> from which polymerization or dimer byproducts are also generated (Scheme 25). In contrast, formation of radical-derived byproducts was not detected during the Fe(OTf)<sub>3</sub>-L1 catalysed oxidative cleavages. Moreover, catalysts following radical pathways are inactive towards the oxidation of electron deficient styrenes probably because of the lower stability of the radical intermediates. In contrast, the Fe(OTf)<sub>3</sub>-L1 catalyst can oxidise electron deficient styrenes with good yields (Scheme 17 and 19).

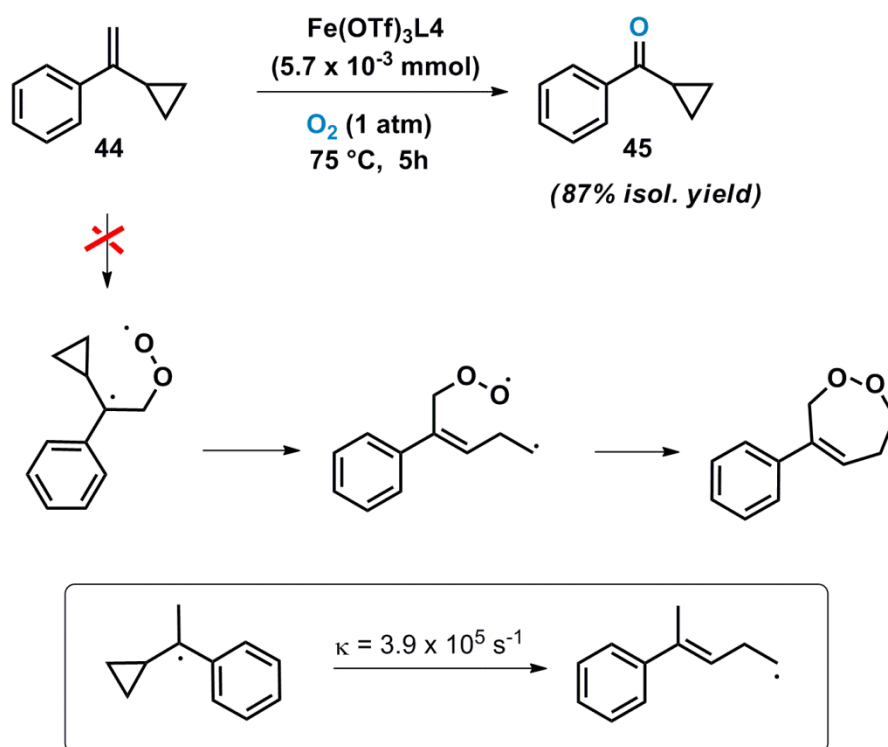


**Scheme 25.** Catalytic aerobic cleavage of styrene type substrates involving benzyl radical intermediates

Further evidence of the absence of free radical species formation was manifested during the chemoselective aerobic cleavage of **44** to **45** and formaldehyde (Scheme 19, entries 7,8). Formation of radical species during the oxidation of this *pseudo-pi* compound would generate cyclopropylbenzyl radical clocks which are known to undergo fast ring-opening rearrangements<sup>34</sup> ( $k = 3.9 \times 10^5 \text{ s}^{-1}$ ) and thus, the formation of different oxidised products would be expected (Scheme 26). Indeed, ring opening products have been characterised during the photooxidation of some cyclopropyl substituted-alkenes<sup>35</sup> (Scheme 27). However, singlet oxygen mediated cleavages of cyclopropyl substituted olefins are highly substrate dependent. For instance, allylic hydroperoxides have been observed as major products during the cleavage of electron rich cyclopropyl olefins probably *via* a mechanism involving H-abstraction from zwitterionic intermediates<sup>36</sup> (Scheme 27). On the other hand, the

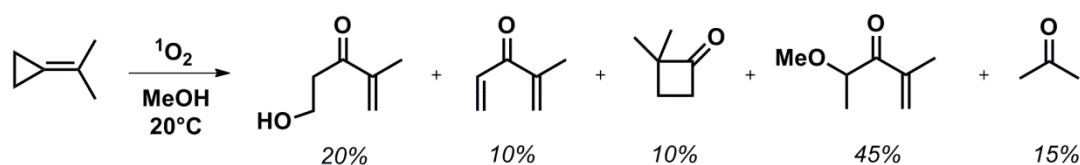


photooxidation of **44** is known to furnish a distribution of products with the carbonyl product **45** being generated as a minor byproduct<sup>37</sup> (Scheme 27).

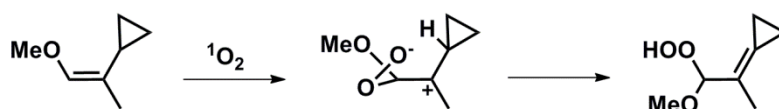


**Scheme 26.** Iron-catalysed aerobic cleavage of **44** to afford **45** does not involve the formation of byproducts resulting from ring opening processes.

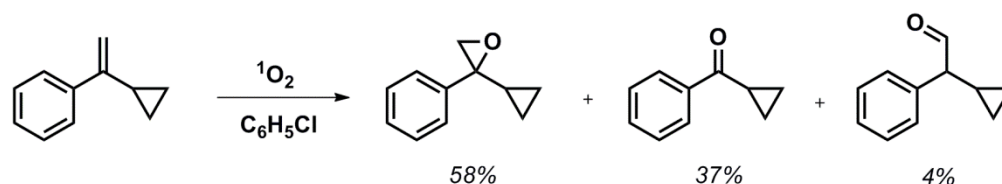
Photooxidation of cyclopropyl substituted olefins with ring opening products formation:



Photooxidation of cyclopropyl substituted olefins with allylic hydroperoxide formation:



Photooxidation of **44** affording a distribution of products:



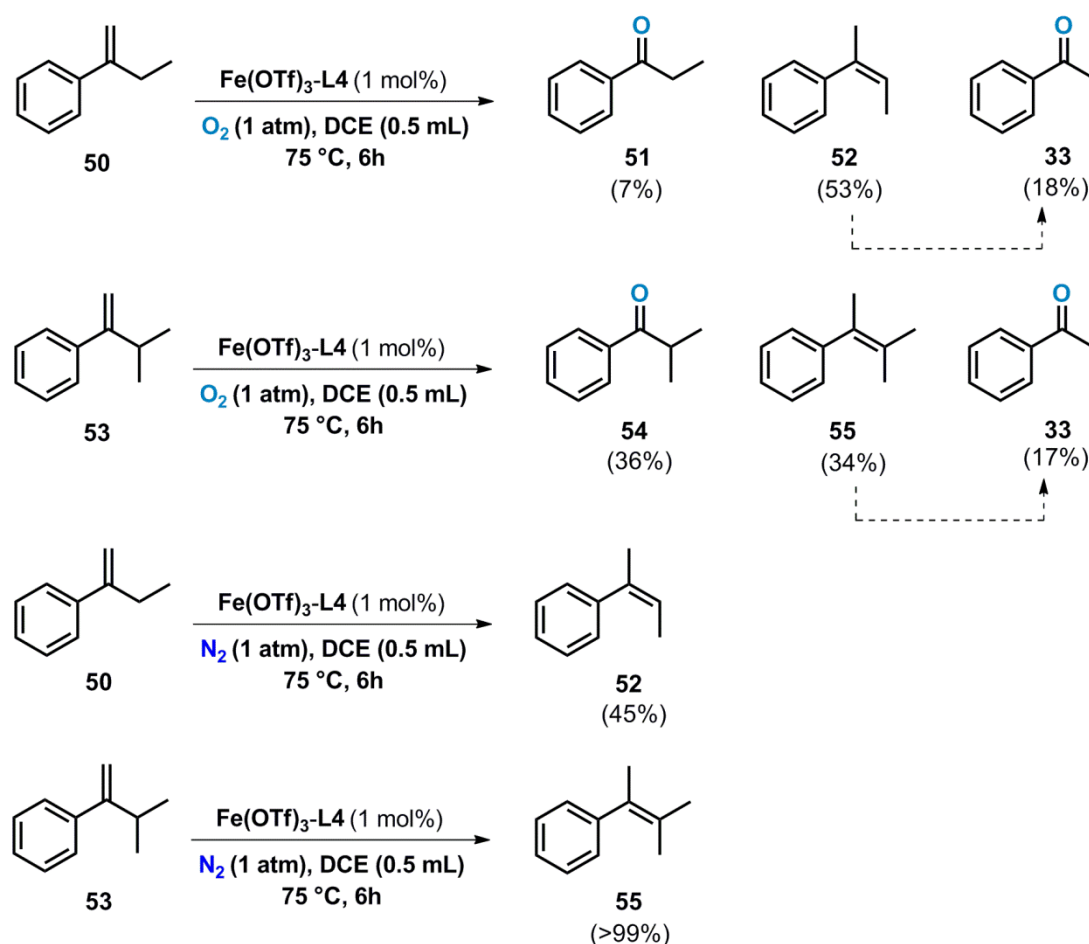
**Scheme 27.** Photooxidation of cyclopropyl substituted olefins.

Even though the formation of radical intermediates cannot be discarded, from these observations it can be concluded that freely diffusing C-based radicals are not being generated during the iron catalysed aerobic cleavage. In addition, the oxidative cleavage of radical-sensitive substrate to selectively afford ketone products seems to suggest that formation of singlet oxygen is not involved during the iron-catalysed oxidation reaction.

### 6.3.3.2. Coordination of the olefin to the catalyst

As the reactions between olefins and singlet oxygen are well known and oxidative cleavages to carbonyls have been widely observed from  $^1\text{O}_2$  reactions,<sup>38</sup> we next investigated the differences between the  $^1\text{O}_2$  promoted and the  $\text{Fe}(\text{OTf})_3$ -**L4** catalyzed aerobic cleavages of olefins. The 1,3-addition of singlet oxygen to olefins possessing at least one allylic hydrogen is known to afford mainly allylic hydroperoxides.<sup>39</sup> However, when  $\alpha$ -alkyl styrenes **50** and **53** possessing allylic hydrogens were subjected to the  $\text{Fe}(\text{OTf})_3$ -**L4** catalytic reaction, the carbonyl compounds **51** and **54** were obtained as oxidised products respectively, with no

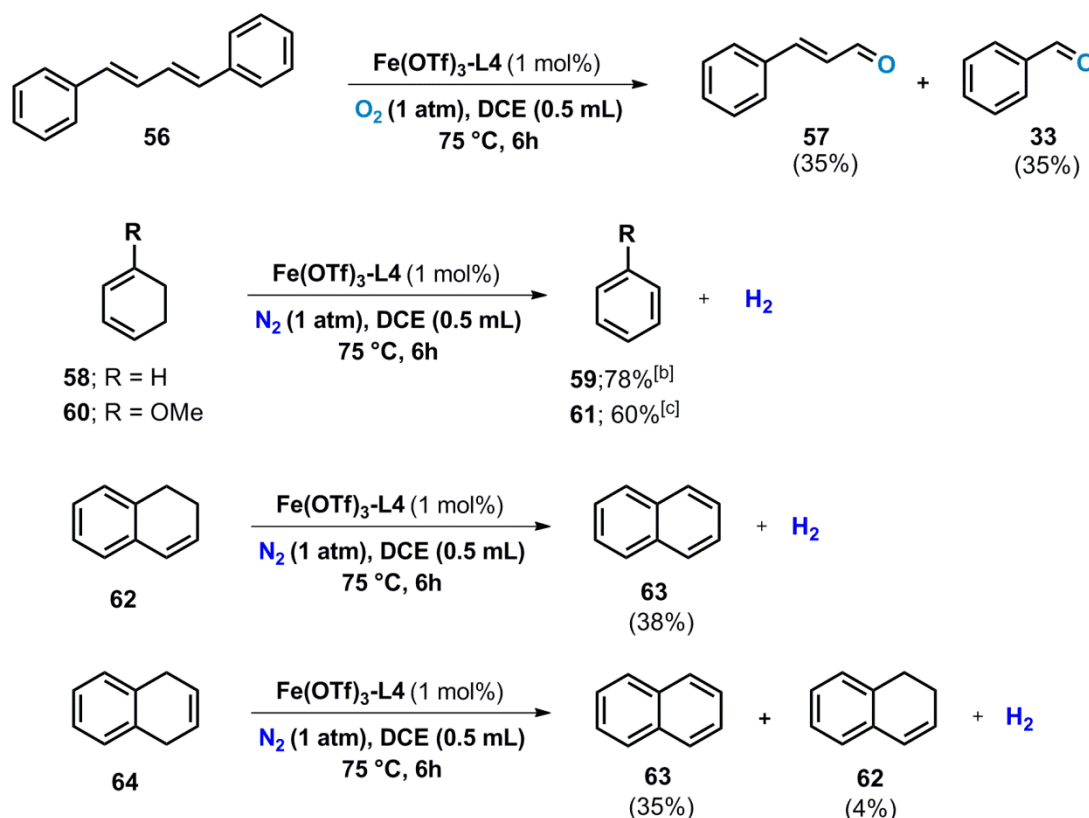
formation of allylic hydroperoxides being observed (Scheme 28). Interestingly, the competing isomerization of the *Z*-olefin to its *E*-isomer was observed under the reaction conditions (products **52** and **55** respectively). Moreover, under inert atmosphere the iron catalyst furnished such isomerization products exclusively<sup>40</sup> (Scheme 28), whereas under O<sub>2</sub> atmosphere oxidation products generated from the *E*-isomer were also observed albeit in low yields (product **33**). Similarly, previously reported iron-catalysed isomerizations of olefins involve the initial coordination of the olefin to the iron centre.<sup>41</sup> Thus, the observed isomerization points towards an initial coordination of the olefinic substrate to the iron catalyst during the aerobic cleavage.



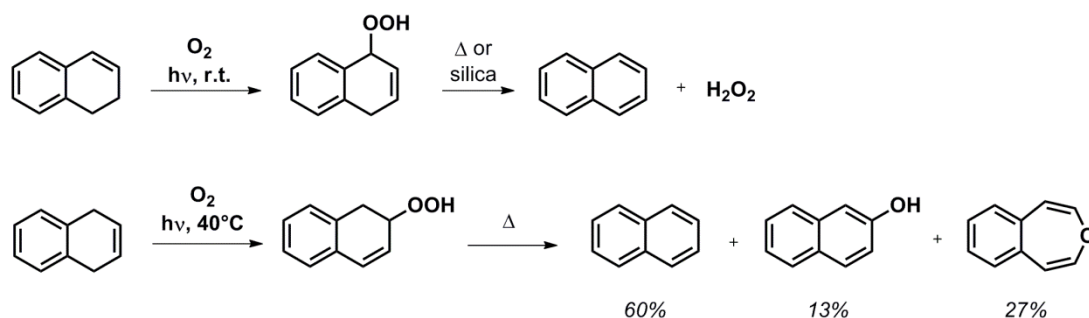
**Scheme 28.** Fe(OTf)<sub>3</sub>L4 catalysed aerobic cleavage of styrenes possessing allylic hydrogens

### 6.3.3.3. Competitive direct dehydrogenation of dienes

Next we focus our attention in the oxidative cleavage of diene substrates. The 1,4-addition of singlet oxygen to these substrates is prone to yield endoperoxides, although depending on the substrate and/or reaction conditions subsequent rearrangements to afford different products have been reported.<sup>42</sup> Delightfully, the *trans*-diene **56** was oxidatively cleaved into cinnamaldehyde and benzaldehyde when exposed to the catalytic reaction (Scheme 29). In stark contrast, *cis*-dienes **58** and **60** were dehydrogenated to arene products either under inert or aerobic atmosphere (Scheme 29). As discussed before the Fe(OTf)<sub>2</sub>**L1** catalyst can undergo oxygenative dehydrogenation of ethereal substrates under aerobic conditions (chapter 4), however, the Fe(OTf)<sub>3</sub>**L1** complex is capable of promoting the direct dehydrogenation of partially oxidised substrates under inert conditions. Similarly, exposure of dihydronaphthalenes **62** and **64** to the iron catalyst under inert atmosphere afforded naphthalene in low yields (Scheme 29). Interestingly, traces of **62** were detected during the dehydrogenation of **64** suggesting a reaction mechanism that involves the initial isomerization of the substrate followed by the direct dehydrogenation<sup>43</sup> of the relatively weak allylic CH bond in **62** (~85 kcal/mol).<sup>44</sup> In contrast, the reaction of **62** with singlet oxygen initially affords the allylic hydroperoxide, which easily loses H<sub>2</sub>O<sub>2</sub> yielding naphthalene<sup>45</sup> (Scheme 30). In addition, exposure of **64** to singlet oxygen yields a distribution of products including naphthalene and a hydroperoxide<sup>46</sup> (Scheme 30).



**Scheme 29.** Competitive dehydrogenation of *cis*-dienes was observed in the presence of the iron catalyst under inert conditions

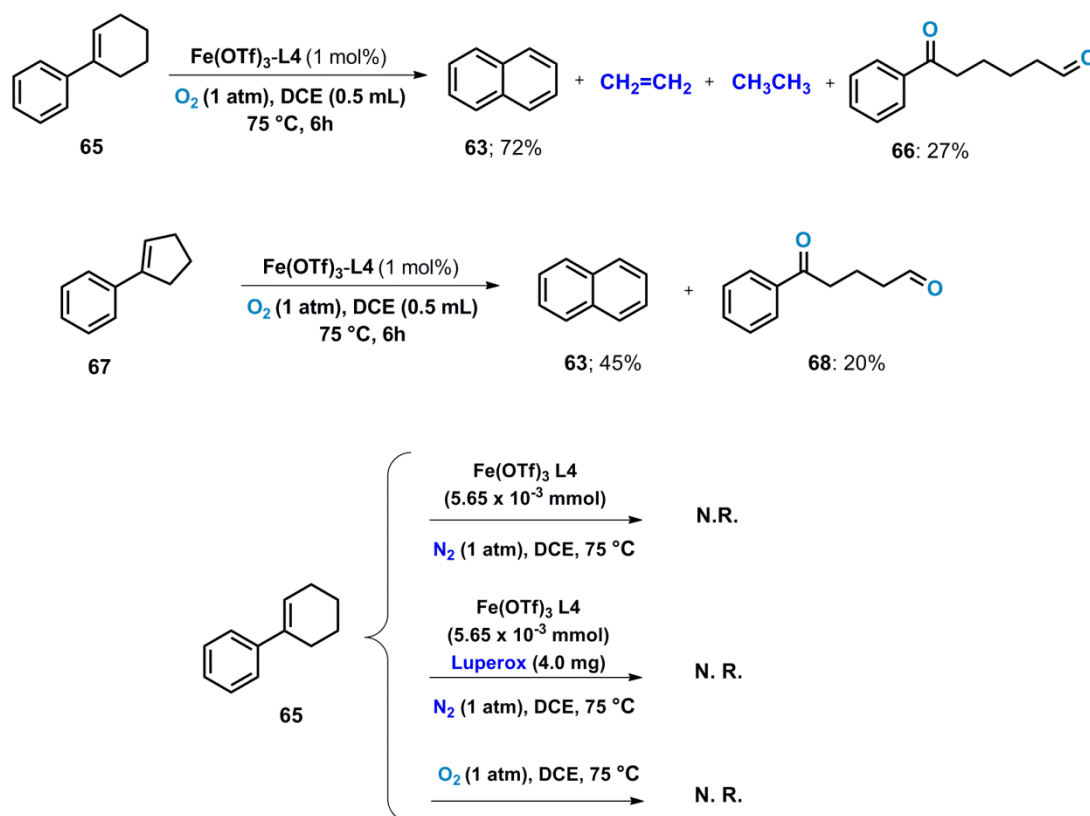


**Scheme 30.** Reaction of **62** and **64** with singlet oxygen

The photooxygenation of 1-phenyl-1-cycloalkenes **65** and **67** is known to afford hydroperoxides,<sup>47</sup> however, exposure of these phenyl-1-cycloalkenes to the Fe(OTf)<sub>3</sub>-L4 catalyzed oxidation reaction furnished, much to our surprise, naphthalene as major product (Scheme 31). The acyclic dialdehydes **66** and **68** were also obtained albeit in lower yields. Interestingly, ethene and small amounts of ethane were also identified as reaction byproducts

by GC, highlighting again the potential of the iron catalyst to promote C-C bond cleavages under aerobic conditions. Although the mechanism by which naphthalene is generated from **65** and **67** is unclear, it might involve the iron-promoted rearrangement of the olefinic substrate under aerobic conditions, as no reaction takes place in the absence of O<sub>2</sub> or the iron catalyst or in the presence of the radical initiator benzoyl peroxide. In fact, rearrangements of olefinic substrates in the presence of singlet oxygen have been widely reported and often led to unexpected products.<sup>48</sup>

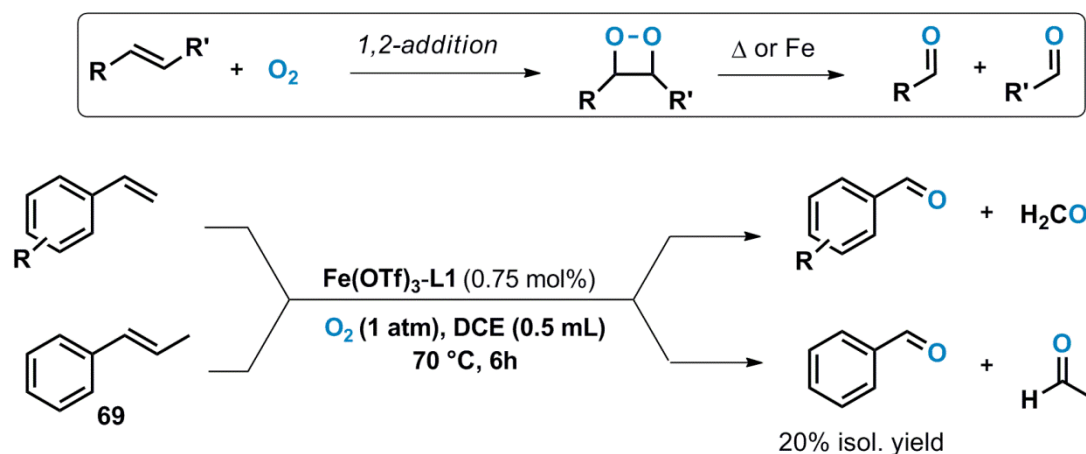
These results indicate that the iron catalyst can promote the aerobic cleavage of *trans*-dienes, however, *cis*-dienes are either selectively dehydrogenated or cleaved to afford unexpected products.



**Scheme 31.** Fe(OTf)<sub>3</sub>-L4 catalysed aerobic cleavage of phenyl-1-cycloalkanes

### 6.3.3.4. Dioxetane intermediate formation

Products resulting from the 1,3-addition of  $O_2$  to substrates possessing allylic hydrogens (Scheme 28) or from the 1,4-addition of  $O_2$  to dienes (Scheme 29) were not observed when investigating the substrate scope of the iron catalyzed aerobic oxidation. Nonetheless, the 1,2-addition of  $^1O_2$  to very electron rich olefins is known to furnish dioxetane species that can easily cleave, affording carbonyl compounds.<sup>49</sup> In contrast, the  $Fe(OTf)_3$ -**L1** catalyst was found capable of promoting the aerobic cleavage of electron deficient styrenes with high yields (Schemes 17 and 19). The iron-mediated 1,2-addition of  $O_2$  to the olefinic substrates to form a dioxetane species followed by its subsequent thermal or iron-mediated cleavage appears to be a plausible mechanism to explain the experimental observations. Indeed, formaldehyde and acetaldehyde were detected by NMR during the aerobic cleavages of monosubstituted styrenes and the 1,2-disubstituted styrene **12** respectively (Scheme 32). Significantly, the oxidation of **12** took place with lower yields than the cleavage of styrenes.

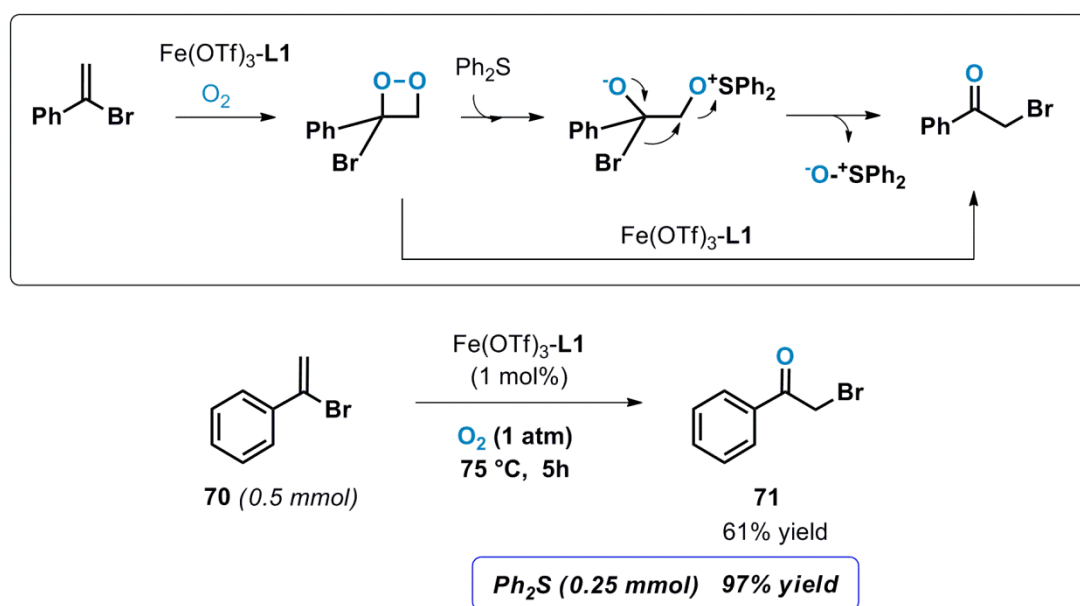


**Scheme 32.** Postulated 1,2-addition of oxygen to olefins catalysed by  $Fe(OTf)_3$ -**L1**

Attempts to isolate any possible intermediate from the aerobic cleavage of **22** were unsuccessful probably because dioxetanes are thermally sensitive and can be cleaved even in the presence of metal traces<sup>50</sup> and silica.<sup>51</sup> Nonetheless, dioxetanes resulting from the 1,2-addition of  $^1O_2$  to electron rich olefins can further react with diphenyl sulfide furnishing ketone type products. This is due to the diphenyl sulfide being capable of rapidly react with

dioxetanes whilst being inert towards endoperoxides, hydroperoxides and singlet oxygen.<sup>52</sup> Bearing this in mind and considering that the iron catalysts can oxidize electron deficient olefins, we envisioned that exposure of vinyl bromide **70** to the iron-catalyzed aerobic oxidation reaction would afford a dioxetane intermediate, which could be further cleaved with the assistance of diphenyl sulfide affording phenacyl bromide **71** via halogen migration (Scheme 33). To our delight, **71** was obtained in 61% yield as the sole reaction product after exposure to the iron catalyst under aerobic atmosphere. Moreover, addition of diphenyl sulfide to the catalytic reaction furnished **71** in 96% yield, suggesting that dioxetane intermediates are involved in the oxidation reaction and that diphenyl sulfide can assist the iron catalyst in promoting their subsequent cleavage (Scheme 33).

Some substrate scope in the oxygenation of vinyl halides with halogen migration has also been performed.



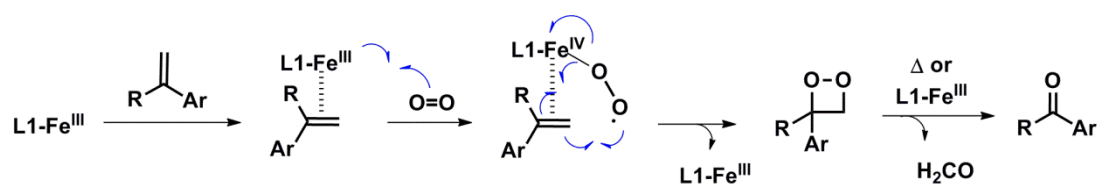
**Scheme 33.** Iron catalysed conversion of vinyl bromide into phenacyl bromide is consistent with dioxetane intermediates



### 6.3.3.5. Postulated catalytic cycle

The results above point to the  $\text{Fe}(\text{OTf})_3\text{-L1}$  catalyzed oxygenation of olefins to afford a labile dioxetane intermediate followed by its iron or thermal-mediated cleavage to furnish carbonyl compounds. The formation of the peroxide intermediate is unclear mechanistically, however, its formation *via* 1,2-addition of singlet oxygen is not in agreement with experimental observations. Formation of the dioxetane *via* a radical pathway also seems unlikely as no byproducts derived from benzyl radicals were observed and no ring-opening of *pseudo-pi* substituted styrenes was observed.

Having in mind the observed isomerization of olefins displaying allylic hydrogens, a mechanism involving the coordination of the substrate and the oxygen to the iron centre with concomitant formation of the dioxetane intermediate seems to be in operation. Such mechanism resembles the aerobic cleavages performed by some natural dioxygenases, such as tryptophan pyrrolase,<sup>53</sup> which is known to cleave the C=C bond of the pyrrole ring in tryptophan probably *via* the formation of a ternary complex in which both molecular oxygen and substrate coordinate to the metalloenzyme.<sup>54</sup> Due to the lack of free radicals formation, we suspect that the  $\text{Fe}(\text{OTf})_3\text{-L1}$  mediated formation of the dioxetane species is likely to occur in a concerted fashion, with the both C-O bonds being formed almost simultaneously (Scheme 34).



**Scheme 34.** Proposed catalytic cycle for the  $\text{Fe}(\text{OTf})_3\text{-L1}$  catalyzed oxidative cleavage of olefins to carbonyls

## 6.4. Conclusions

In conclusion, an operationally simple and environmentally friendly method for the oxidative cleavage of olefins is presented. An ample variety of olefins can be transformed to aldehydes or ketones with excellent chemoselectivity, good yields and high functional group tolerance. A catalytic cycle involving the formation of dioxetane intermediates is postulated on the basis of mechanistic studies.

## 6.5. Experimental section

### 6.5.1. General techniques

Olefins were purchased from commercial suppliers and used without further purification unless otherwise specified. DCE was refluxed over  $\text{CaH}_2$  and distilled under  $\text{N}_2$  atmosphere.

### 6.5.2. Synthesis of 1-substituted styrenes

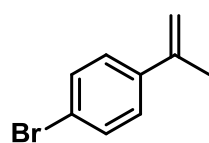
1-Substituted styrenes were synthesized *via* methylenation of the corresponding ketones as reported in the literature.<sup>55</sup> A representative synthetic procedure is described below:

#### Synthesis of 4-bromo- $\alpha$ -methylstyrene

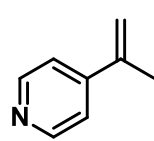
In a round bottom flask equipped with a magnetic bar, methyltriphenylphosphonium bromide (1.4 equiv., 7.0 mmol, 2.5 g), potassium tert-butoxide (1.4 equiv., 7.0 mmol, 785 mg) and 4-bromoacetophenone (1.0 equiv., 5.00 mmol, 1.0 g) were added and dissolved in THF (20 mL). The reaction was stirred for 24h at r.t. and monitored by t.l.c. Upon completion, the solvent was eliminated in vacuo and the residue was purified by flash column chromatography (Hex/AcOEt 40/1) to afford the desired product as a colorless liquid (98% yield, 965 mg).

#### Substrate characterization

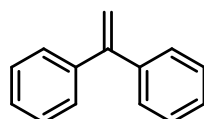
##### 4-Bromo- $\alpha$ -methylstyrene<sup>56</sup> (38)



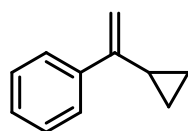
Colourless liquid, 95% isol. yield. Purification by flash chromatography (Hexane/ AcOEt, 40/1).  $^1\text{H NMR}$  (400 MHz,  $\text{CDCl}_3$ ):  $\delta$  (ppm) = 7.46-7.42 (m, 2H), 7.34-7.31 (m, 2H), 5.35 (d,  $J = 0.4$  Hz, 1H), 5.10 (q,  $J = 1.2$  Hz, 1H), 2.12 (d,  $J = 0.8$  Hz, 3H).  $^{13}\text{C NMR}$  (100 MHz,  $\text{CDCl}_3$ ):  $\delta$  (ppm) = 142.6, 140.5, 131.6, 127.5, 121.7, 113.4, 22.1. **HRMS** (EI)  $m/z$  calc'd  $\text{C}_9\text{H}_9\text{Br}$   $[\text{M} + \text{H}]^+$ : 196.9961, found: 196.9957.

**(Pyridin-4-yl)- $\alpha$ -methylstyrene<sup>57</sup> (40)**

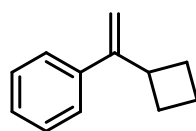
Yellowish liquid, 87% isol. yield. Purification by flash chromatography (AcOEt/ Hexane, 3/2).  $^1\text{H NMR}$  (400 MHz,  $\text{CDCl}_3$ ):  $\delta$  (ppm) = 8.55 (dd,  $J$  = 1.6, 4.8 Hz, 2H), 7.33 (dd,  $J$  = 1.6, 4.8 Hz, 2H), 5.57 (s, 1H), 5.26 (q,  $J$  = 1.6 Hz, 1H), 2.14 (d,  $J$  = 1.6 Hz, 3H).  $^{13}\text{C NMR}$  (100 MHz,  $\text{CDCl}_3$ ):  $\delta$  (ppm) = 150.2, 133.4, 132.5, 132.4, 128.8, 120.5, 116.3, 21.2. **HRMS** (EI)  $m/z$  calc'd  $\text{C}_8\text{H}_{10}\text{N}[\text{M} + \text{H}]^+$ : 120.0808, found: 120.0810.

**Ethene, 11-diylidibenzene<sup>58</sup> (42)**

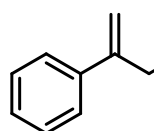
Colourless liquid, 96% isol. yield. Purification by flash chromatography (Hexane/ AcOEt, 40/1).  $^1\text{H NMR}$  (400 MHz,  $\text{CDCl}_3$ ):  $\delta$  (ppm) = 7.34-7.24 (m, 10H), 5.46 (s, 2H).  $^{13}\text{C NMR}$  (100 MHz,  $\text{CDCl}_3$ ):  $\delta$  (ppm) = 150.0, 141.6, 128.2, 128.1, 127.7, 114.3. **HRMS** (EI)  $m/z$  calc'd  $\text{C}_{14}\text{H}_{13}[\text{M} + \text{H}]^+$ : 181.1012, found: 181.1013.

**(1-Cyclopropylvinyl)benzene<sup>59</sup> (44)**

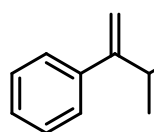
Colourless liquid, 97% isol. yield. Purification by flash chromatography (Hexane/ AcOEt, 40/1).  $^1\text{H NMR}$  (400 MHz,  $\text{CDCl}_3$ ):  $\delta$  (ppm) = 7.36-7.24 (m, 5H), 5.14 (d,  $J$  = 0.2 Hz, 1H), 5.03 (t,  $J$  = 1.6 Hz, 1H), 1.71 (m, 1H), 1.10 (m, 4H).  $^{13}\text{C NMR}$  (100 MHz,  $\text{CDCl}_3$ ):  $\delta$  (ppm) = 156.1, 143.2, 128.5, 127.4, 127.0, 110.3, 19.8, 11.0. **HRMS** (EI)  $m/z$  calc'd  $\text{C}_{14}\text{H}_{13}[\text{M} + \text{H}]^+$ : 145.1012, found: 145.1012.

**(1-Cyclobutylvinyl)benzene<sup>60</sup> (46)**

Colourless liquid, 87% isol. Yield. Purification by flash chromatography (Hexane/AcOEt, 30/1).  $^1\text{H NMR}$  (400 MHz,  $\text{CDCl}_3$ ):  $\delta$  (ppm) = 7.46-7.13 (m, 5H), 5.38 (s, 1H), 5.02 (s, 1H), 3.56-3.34 (m, 1H), 2.31-2.15 (m, 2H), 2.08-1.92 (m, 3H), 1.87-1.74 (m, 1H).  $^{13}\text{C NMR}$  (100 MHz,  $\text{CDCl}_3$ ):  $\delta$  (ppm) = 152.0, 140.7, 128.1, 127.2, 126.1, 109.7, 39.5, 28.4, 17.7. **HRMS** (EI)  $m/z$  calc'd  $\text{C}_{12}\text{H}_{15}[\text{M} + \text{H}]^+$ : 159.1168, found: 159.1169.

**But-1-en-2-ylbenzene<sup>56</sup> (50)**

Colourless liquid, 97% isol. yield. Purification by flash chromatography (Hexane/ AcOEt, 40/1).  $^1\text{H NMR}$  (400 MHz,  $\text{CDCl}_3$ ):  $\delta$  (ppm) = 7.42-7.39 (m, 2H), 7.34-7.30 (m, 2H), 7.28-7.23 (m, 1H), 5.27 (s, 1H), 5.06 (q,  $J$  = 1.6 Hz, 1H), 2.54-2.49 (m, 2H), 1.11 (t,  $J$  = 6.8 Hz, 3H).  $^{13}\text{C NMR}$  (100 MHz,  $\text{CDCl}_3$ ):  $\delta$  (ppm) = 150.4, 141.9, 128.6, 127.6, 126.4, 111.3, 28.4, 13.3. **HRMS** (EI)  $m/z$  calc'd  $\text{C}_{10}\text{H}_{13}[\text{M} + \text{H}]^+$ : 133.1012, found: 133.1011.

**(3-Methylbut-1-en-2-yl)benzene<sup>61</sup> (53)**

Colourless liquid, 96% isol. yield. Purification by flash chromatography (Hexane/ AcOEt 40/1).  $^1\text{H NMR}$  (400 MHz,  $\text{CDCl}_3$ ):  $\delta$  (ppm) = 7.61-7.58 (m, 2H), 7.36-7.25 (m, 3H), 5.27 (d,  $J$  = 0.8 Hz, 1H), 4.93 (t,  $J$  = 1.2 Hz, 1H), 1.68-1.65 (m, 1H), 0.87-0.81 (m, 3H), 0.60-0.57 (m, 3H).  $^{13}\text{C NMR}$  (100

MHz, CDCl<sub>3</sub>):  $\delta$  (ppm) = 149.7, 142.0, 128.5, 127.8, 126.5, 109.4, 16.0, 7.0. **HRMS** (EI)  $m/z$  calc'd C<sub>11</sub>H<sub>14</sub> [M + H]<sup>+</sup>: 147.1168, found: 147.11741.

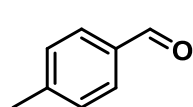
Analytical data for compounds 44-53 is in agreement with the commercially available materials.

### 6.5.3. General procedure for the Fe(OTf)<sub>3</sub>L1 catalysed aerobic cleavage of styrenes

In a Radley's tube equipped with a magnetic stirring bar, Fe(OTf)<sub>3</sub> (5.65 x 10<sup>-3</sup> mmol, 2.9 mg) and **L1** (5.67 x 10<sup>-3</sup> mmol, 5.2 mg) were added. The tube was sealed, degassed and left under inert atmosphere (3 times). Freshly distilled DCE (0.5 mL) was injected by syringe and the reaction mixture was allowed stirring for 1 hour at 40 °C. 4-Methylstyrene (0.75 mmol, 90  $\mu$ L) was added by syringe and the reaction tube was degassed with dioxygen gas (1 atm, 3 times) and keep under oxygen (1 atm) by using a balloon. The tube was gradually heated to 70 °C and allowed to react for 5 hours. The reaction was purified by silica gel column chromatography (Hexane/EtOAc, 20/1) to afford the unreacted starting material and the aldehyde product.

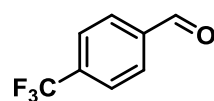
#### Product characterisation

##### 4-Methylbenzaldehyde<sup>62</sup> (**8**)

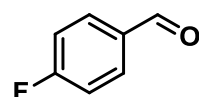


Colourless liquid (92% isol. yield, 0.69 mmol, 82.8 mg). Purification by flash chromatography (Hexane/AcOEt, 20/1). **<sup>1</sup>H NMR** (400 MHz, CDCl<sub>3</sub>):  $\delta$  (ppm) = 9.96 (s, 1H), 7.80 (d, J = 8.0 Hz, 2H), 7.33 (d, J = 8.0 Hz, 2H), 2.44 (s, 3H). **<sup>13</sup>C NMR** (100 MHz, CDCl<sub>3</sub>):  $\delta$  (ppm) = 192.0, 145.5, 134.2, 129.8, 129.7, 21.9. **IR** (neat)  $\nu$  = 3084, 2917, 1705, 1670, 1608, 1514, 1281, 1179, 1117, 807, 806, 751, 540, 467 cm<sup>-1</sup>. **HRMS** (EI)  $m/z$  calc'd C<sub>8</sub>H<sub>9</sub>O [M + H]<sup>+</sup>: 121.0648, found: 121.0645.

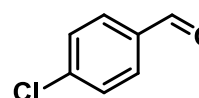
##### 4-(Trifluoromethyl)benzaldehyde<sup>62</sup> (**11**)



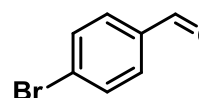
Colourless liquid (90% isol. yield, 0.67 mmol, 116.4 mg). Purification by flash chromatography (Hexane/AcOEt, 20/1). **<sup>1</sup>H NMR** (400 MHz, DMSO-d<sub>6</sub>):  $\delta$  (ppm) = 10.12 (s, 1H), 8.12 (d, J = 8.0 Hz, 2H), 7.88 (d, J = 8.4 Hz, 2H). **<sup>13</sup>C NMR** (100 MHz, DMSO-d<sub>6</sub>):  $\delta$  (ppm) = 193.0, 166.5, 134.9, 130.5, 126.4, 122.8. **IR** (neat)  $\nu$  = 2670, 2549, 1691, 1583, 1515, 1425, 1315, 1286, 1162, 1135, 1106, 1058, 1016, 937, 858, 775, 754, 700. **HRMS** (EI)  $m/z$  calc'd C<sub>8</sub>H<sub>6</sub>F<sub>3</sub>O [M + H]<sup>+</sup>: 175.0366, found: 175.0364.

**4-Fluorobenzaldehyde<sup>63</sup> (13)**

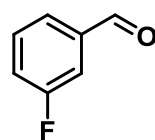
Colourless oil (78% isol. yield, 0.58 mmol, 71.8 mg). Purification by flash chromatography (Hexane/AcOEt, 20/1). **<sup>1</sup>H NMR** (400 MHz, CDCl<sub>3</sub>): δ (ppm) = 9.97 (s, 1H), 7.99-7.90 (m, 2H), 7.32-7.21 (m, 3H). **<sup>13</sup>C NMR** (100 MHz, CDCl<sub>3</sub>): δ (ppm) = 190.4, 167.8 (<sup>1</sup>J<sub>C-F</sub> = 255 Hz), 133.0 (<sup>4</sup>J<sub>C-F</sub> = 3 Hz), 132.2 (<sup>3</sup>J<sub>C-F</sub> = 10 Hz), 116.4 (<sup>2</sup>J<sub>C-F</sub> = 22 Hz). **IR (neat)** ν = 3098, 1701, 1601, 1508, 1424, 1312, 1291, 1225, 1156, 1129, 853, 845, 767, 609, 495 cm<sup>-1</sup>. **HRMS** (EI) m/z calc'd C<sub>7</sub>H<sub>6</sub>OF [M + H]<sup>+</sup>: 121.0397, found: 125.0398.

**4-Chlorobenzaldehyde<sup>64</sup> (15)**

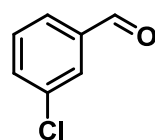
White solid (87% isol. yield, 0.65 mmol, 91.1 mg). Purification by flash chromatography (Hexane/AcOEt, 20/1). **<sup>1</sup>H NMR** (400 MHz, CDCl<sub>3</sub>): δ (ppm) = 9.98 (s, 1H), 7.84 (d, J = 8.6 Hz, 2H), 7.59 (d, J = 8.4 Hz, 2H). **<sup>13</sup>C NMR** (100 MHz, CDCl<sub>3</sub>): δ (ppm) = 190.8, 140.9, 134.7, 130.9, 129.4. **IR (neat)** ν = 2840, 2654, 2588, 1702, 1590, 1573, 1486, 1400, 1286, 1257, 1207, 1166, 1087, 1012, 966, 937, 823, 761. **HRMS** (EI) m/z calc'd C<sub>7</sub>H<sub>6</sub>ClO [M + H]<sup>+</sup>: 141.0102, found: 141.0100.

**4-Bromobenzaldehyde<sup>62</sup> (17)**

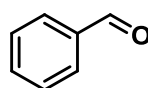
White solid (79% isol. yield, 0.59 mmol, 146.0 mg). Purification by flash chromatography (Hexane/AcOEt, 20/1). **<sup>1</sup>H NMR** (400 MHz, CDCl<sub>3</sub>): δ (ppm) = 9.98, 7.76 (dd, J = 8.4, 2.0 Hz, 2H), 7.68 (dd, J = 8.3, 2.0 Hz, 2H). **<sup>13</sup>C NMR** (100 MHz, CDCl<sub>3</sub>): δ (ppm) = 191.4, 137.2, 132.8, 131.3, 130.2. **IR (neat)** ν = 2857, 2761, 1683, 1583, 1569, 1475, 1386, 1290, 1199, 1149, 1062, 1006, 829, 808, 678. **HRMS** (EI) m/z calc'd C<sub>7</sub>H<sub>6</sub>BrO [M + H]<sup>+</sup>: 184.9597, found: 184.9595.

**3-Fluorobenzaldehyde<sup>65</sup> (19)**

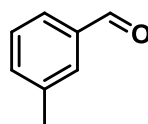
Colourless liquid (93% isol. yield, 0.70 mmol, 86.9 mg). Purification by flash chromatography (Hexane/AcOEt, 20/1). **<sup>1</sup>H NMR** (400 MHz, CDCl<sub>3</sub>): δ (ppm) = 9.99 (s, 1H), 7.81 (d, J = 2.1 Hz, 1H), 7.68-7.54 (m, 2H), 7.34-7.24 (m, 1H). **<sup>13</sup>C NMR** (100 MHz, CDCl<sub>3</sub>): δ (ppm) = 190.9, 164.3 (<sup>1</sup>J<sub>C-F</sub> = 248 Hz), 138.4 (<sup>3</sup>J<sub>C-F</sub> = 6 Hz), 130.8 (<sup>3</sup>J<sub>C-F</sub> = 8 Hz), 126.0 (<sup>3</sup>J<sub>C-F</sub> = 3 Hz), 121.7 (<sup>2</sup>J<sub>C-F</sub> = 22 Hz), 115.4 (<sup>2</sup>J<sub>C-F</sub> = 22 Hz). **IR (neat)** ν = 3067, 3021, 1712, 1698, 1608, 1413, 1287, 1154, 769, 748, 640, 485 cm<sup>-1</sup>. **HRMS** (EI) m/z calc'd C<sub>7</sub>H<sub>6</sub>FO [M + H]<sup>+</sup>: 125.0398, found: 125.0395.

**3-Chlorobenzaldehyde<sup>65</sup> (21)**

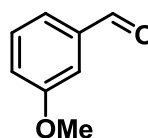
Colourless liquid (75% isol. yield, 0.56 mmol, 78.5 mg). Purification by flash chromatography (Hexane/AcOEt, 20/1). **<sup>1</sup>H NMR** (400 MHz, CDCl<sub>3</sub>): δ (ppm) = 9.98 (s, 1H), 7.95 (s, 1H), 7.84 (d, J = 7.5 Hz, 1H), 7.62 (d, J = 7.8 Hz, 1H), 7.58-7.74 (m, 1H). **<sup>13</sup>C NMR** (100 MHz, CDCl<sub>3</sub>): δ (ppm) = 190.8, 137.8, 135.4, 134.4, 130.4, 127.9, 126.5. **IR (neat)** ν = 2937, 2836, 1714, 1678, 1588, 1573, 1488, 1420, 1400, 1253, 1169, 1127, 1013, 712, 681 cm<sup>-1</sup>. **HRMS** (EI) m/z calc'd C<sub>7</sub>H<sub>6</sub>ClO [M + H]<sup>+</sup>: 141.0102, found: 141.0106.

**Benzaldehyde<sup>62</sup> (23)**

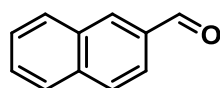
Colourless liquid (77% isol. yield, 0.58 mmol, 61.4 mg). Purification by flash chromatography (Hexane/AcOEt, 20/1). **<sup>1</sup>H NMR** (400 MHz, CDCl<sub>3</sub>): δ (ppm) = 10.02 (s, 1H), 8.13-8.10 (m, 2H), 7.89-7.87 (m, 1H), 7.65-7.62 (m, 2H). **<sup>13</sup>C NMR** (100 MHz, CDCl<sub>3</sub>): δ (ppm) = 192.8, 136.8, 134.8, 129.9, 129.4. **IR (neat)** ν = 3062, 2819, 2736, 1698, 1652, 1598, 1583, 1454, 1390, 1311, 1207, 1162, 1070, 1020, 1002, 825, 744, 682, 642. **HRMS** (EI) m/z calc'd C<sub>7</sub>H<sub>6</sub>O [M + H]<sup>+</sup>: 107.0492, found: 107.0488.

**3-Methylbenzaldehyde<sup>63</sup> (25)**

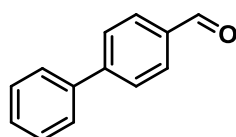
Colourless liquid (95% isol. yield, 0.71 mmol, 85.2 mg). Purification by flash chromatography (Hexane/AcOEt, 20/1). **<sup>1</sup>H NMR** (400 MHz, CDCl<sub>3</sub>): δ (ppm) = 10.00 (s, 1H), 7.69-7.67 (m, 2H), 7.46-7.40 (m, 2H), 2.44 (s, 3H). **<sup>13</sup>C NMR** (100 MHz, CDCl<sub>3</sub>): δ (ppm) = 192.6, 138.9, 136.4, 135.3, 130.0, 128.8, 127.2, 21.2. **IR (neat)** ν = 3078, 2921, 1701, 1606, 1588, 1488, 1433, 1278, 1246, 1158, 1142, 778, 745, 684, 653 cm<sup>-1</sup>. **HRMS** (EI) m/z calc'd C<sub>8</sub>H<sub>8</sub>O [M + H]<sup>+</sup>: 121.0648, found: 121.0646.

**3-Methoxybenzaldehyde<sup>66</sup> (27)**

Colourless liquid (78% isol. yield, 0.58 mmol, 78.8 mg). Purification by flash chromatography (Hexane/AcOEt, 20/1). **<sup>1</sup>H NMR** (400 MHz, CDCl<sub>3</sub>): δ (ppm) = 9.98 (s, 1H), 7.47-7.42 (m, 2H), 7.40 (d, J = 2.0 Hz, 1H), 7.26-7.16 (m, 1H), 3.87 (s, 3H). **<sup>13</sup>C NMR** (100 MHz, CDCl<sub>3</sub>): δ (ppm) = 192.5, 160.5, 138.2, 130.4, 123.9, 121.9, 112.4, 55.8. **IR (neat)** ν = 2840, 2732, 1698, 1587, 1482, 1457, 1436, 1382, 1321, 1286, 1261, 1203, 1145, 1066, 1037, 1006, 927, 869, 833, 815, 786, 744, 678, 628. **HRMS** (EI) m/z calc'd C<sub>8</sub>H<sub>8</sub>O<sub>2</sub> [M + H]<sup>+</sup>: 137.0597, found: 137.0596.

**2-Naphthaldehyde<sup>63</sup> (29)**

White solid (30% isol. yield, 0.22 mmol, 34.4 mg). Purification by flash chromatography (Hexane/AcOEt, 30/1). **<sup>1</sup>H NMR** (400 MHz, CDCl<sub>3</sub>): δ (ppm) = 10.17 (s, 1H), 8.35 (s, 1H), 8.02-7.85 (m, 4H), 7.64-7.57 (m, 2H). **<sup>13</sup>C NMR** (100 MHz, CDCl<sub>3</sub>): δ (ppm) = 192.6, 136.8, 134.9, 134.5, 133.0, 129.9, 129.5, 128.5, 127.5, 123.1. **IR (neat)** ν = 3062, 2846, 2829, 1689, 1661, 1598, 1402, 1365, 1165, 1142, 909, 800, 746, 699, 501 cm<sup>-1</sup>. **HRMS** (EI) m/z calc'd C<sub>11</sub>H<sub>8</sub>O [M + H]<sup>+</sup>: 157.0648, found: 157.0646.

**Biphenyl-4-carboxaldehyde<sup>64</sup> (31)**

White solid (57% isol. yield, 0.43 mmol, 78.2 mg). Purification by flash chromatography (Hexane/ AcOEt 20/1). **<sup>1</sup>H NMR** (400 MHz, CDCl<sub>3</sub>): δ (ppm) = 10.06 (s, 1H), 7.95 (dd, J = 1.6, 8.4 Hz, 2H), 7.75 (dd, J = 1.5, 8.4 Hz, 2H), 7.64 (dd, J = 1.8, 8.4 Hz, 2H), 7.62-7.50 (m, 3H). **<sup>13</sup>C NMR** (100 MHz, CDCl<sub>3</sub>): δ (ppm) = 192.3, 140.1, 135.6, 130.6, 129.4, 128.8, 128.1, 127.7. **IR (neat)** ν = 3058, 3033, 2829, 2736, 1695, 1602, 1562, 1482, 1450, 1411, 1386, 1307, 1213, 1166, 1078, 1008, 833, 761, 725, 694. **HRMS** (EI) m/z calc'd C<sub>13</sub>H<sub>10</sub>O [M + H]<sup>+</sup>: 183.0805, found: 183.0805.

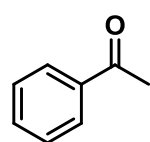
The aldehyde products are commercially available and the analytical data obtained is in agreement with the data reported by the manufacturers.

#### 6.5.4. General procedure for the Fe(OTf)<sub>3</sub>L4 catalysed aerobic cleavage of styrenes

In a Radley's tube equipped with a magnetic stirring bar, Fe(OTf)<sub>3</sub> (5.65 x 10<sup>-3</sup> mmol, 2.9 mg) and **L4** (5.67 x 10<sup>-3</sup> mmol, 7.1 mg) were added. The tube was sealed, degassed and left under inert atmosphere (3 times). Freshly distilled DCE (0.5 mL) was injected by syringe and the reaction mixture was allowed stirring for 1 hour at 40 °C.  $\alpha$ -Methylstyrene (0.50 mmol, 40  $\mu$ L) was added by syringe and the reaction tube was degassed, charged with dioxygen gas (1 atm, 3 times) and kept under oxygen (1 atm) by using a balloon. The tube was gradually heated to 75 °C and allowed to react for 5 hours. The reaction was purified by silica gel column chromatography (Hexane/EtOAc: 20:1) to afford the unreacted starting material and the ketone product.

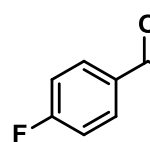
#### Product characterisation

##### Acetophenone<sup>63</sup> (33)



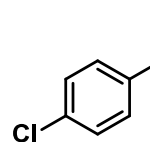
Colourless liquid (87% isol. yield, 0.43 mmol, 51.6 mg). Purification by flash chromatography (Hexane/AcOEt, 20/1). <sup>1</sup>H NMR (400 MHz, CDCl<sub>3</sub>):  $\delta$  (ppm) = 7.97-7.95 (m, 2H), 7.59-7.54 (m, 1H), 7.48-7.45 (m, 2H), 2.61 (s, 3H). <sup>13</sup>C NMR (100 MHz, CDCl<sub>3</sub>):  $\delta$  (ppm) = 198.5, 137.5, 133.5, 129.1, 128.9, 128.7, 27.0. IR (neat)  $\nu$  = 1681, 1598, 1583, 1448, 1357, 1303, 1265, 1178, 1078, 1024, 952, 761, 686. HRMS (EI)  $m/z$  calc'd C<sub>8</sub>H<sub>8</sub>O [M + H]<sup>+</sup>: 121.0648, found: 121.0647.

##### 4-Fluoroacetophenone<sup>63</sup> (35)



Colourless liquid (40% isol. yield, 0.20 mmol, 27.5 mmol). Purification by flash chromatography (Hexane/AcOEt, 20/1). <sup>1</sup>H NMR (400 MHz, CDCl<sub>3</sub>):  $\delta$  (ppm) = 8.00-7.97 (m, 2H), 7.16-7.11 (m, 2H), 2.59 (s, 3H). <sup>13</sup>C NMR (100 MHz, CDCl<sub>3</sub>):  $\delta$  (ppm) = 196.8, 167.4 (d, <sup>1</sup>J<sub>C-F</sub> = 253.1 Hz), 134.0, 133.9 (d, <sup>4</sup>J<sub>C-F</sub> = 3 Hz), 131.3 (d, <sup>3</sup>J<sub>C-F</sub> = 9.3 Hz), 116.1 (d, <sup>2</sup>J<sub>C-F</sub> = 21.8 Hz), 26.9. IR (neat)  $\nu$  = 1681, 1594, 1500, 1407, 1361, 1261, 1224, 1153, 1103, 1012, 958, 833. HRMS (EI)  $m/z$  calc'd C<sub>8</sub>H<sub>7</sub>FO [M + H]<sup>+</sup>: 139.0554, found: 139.0551.

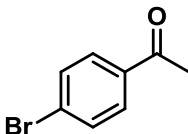
##### 4-Chloroacetophenone<sup>67</sup> (37)



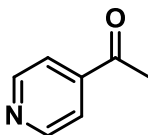
Colourless liquid (83% isol. yield, 0.41 mmol, 63.4 mg). Purification by flash chromatography (Hexane/AcOEt, 20/1). <sup>1</sup>H NMR (400 MHz, CDCl<sub>3</sub>):  $\delta$  (ppm) = 7.91-7.88 (m, 2H), 7.45-7.42 (m, 2H), 2.59 (s, 3H). <sup>13</sup>C NMR (100 MHz, CDCl<sub>3</sub>):  $\delta$  (ppm) = 197.2, 139.9, 135.8, 130.1, 129.2, 26.9. IR

(neat)  $\nu = 1683, 1587, 1486, 1428, 1394, 1357, 1261, 1174, 1087, 1016, 954, 823, 757, 620$ .  
**HRMS** (EI)  $m/z$  calc'd  $C_8H_8ClO$   $[M + H]^+$ : 155.0259, found: 155.0264.

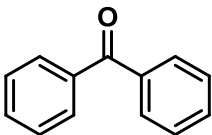
#### 4-Bromoacetophenone<sup>67</sup> (39)

 White solid (85% isol. yield, 0.42 mmol, 83.7 mg). Purification by flash chromatography (Hexane/AcOEt, 20/1). **<sup>1</sup>H NMR** (400 MHz,  $CDCl_3$ ):  $\delta$  (ppm) = 7.84-7.80 (m, 2H), 7.62-7.59 (m, 2H), 2.59 (s, 3H). **<sup>13</sup>C NMR** (100 MHz,  $CDCl_3$ ):  $\delta$  (ppm) = 197.4, 136.2, 132.3, 130.2, 128.7, 26.9. **IR** (neat)  $\nu = 1670, 1583, 1482, 1425, 1396, 1353, 1267, 1178, 1074, 1008, 954, 819, 750, 711$ .  
**HRMS** (EI)  $m/z$  calc'd  $C_8H_8BrO$   $[M + H]^+$ : 198.9754, found: 198.9750.

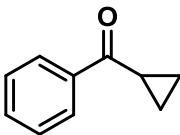
#### 4-Acetylpyridine<sup>67</sup> (41)

 Yellow liquid (20% isol. yield, 0.10 mmol, 12.2 mg). Purification by flash chromatography (Hexane/AcOEt, 2/3). **<sup>1</sup>H NMR** (400 MHz,  $CDCl_3$ ):  $\delta$  (ppm) = 8.82 (dd,  $J = 1.6, 4.4$  Hz, 2H), 7.74 (dd,  $J = 1.6, 5.6$  Hz, 2H), 2.64 (s, 3H). **<sup>13</sup>C NMR** (100 MHz,  $CDCl_3$ ):  $\delta$  (ppm) = 197.7, 151.3, 143.1, 121.6, 27.0. **IR** (neat)  $\nu = 1691, 1598, 1554, 1407, 1361, 1265, 1216, 1062, 995, 962, 815$ .  
**HRMS** (EI)  $m/z$  calc'd  $C_7H_8NO$   $[M + H]^+$ : 122.0601, found: 122.0606.

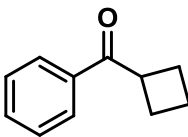
#### Benzophenone<sup>64</sup> (43)

 White solid (98% isol. yield, 0.49 mmol, 89.3 mg). Purification by flash chromatography (Hexane/AcOEt, 20/1). **<sup>1</sup>H NMR** (400 MHz,  $CDCl_3$ ):  $\delta$  (ppm) = 7.81-7.79 (m, 4H), 7.60-7.56 (m, 2H), 7.49-7.45 (m, 4H). **<sup>13</sup>C NMR** (100 MHz,  $CDCl_3$ ):  $\delta$  (ppm) = 197.1, 138.0, 132.5, 130.4, 128.6. **IR** (neat)  $\nu = 1650, 1593, 1575, 1447, 1320, 1275, 1175, 1160, 1150, 1075, 998, 944, 935, 918, 813, 764, 702, 692, 636$   $cm^{-1}$ .  
**HRMS** (EI)  $m/z$  calc'd  $C_{13}H_{10}O$   $[M + H]^+$ : 183.0804, found: 183.0808.

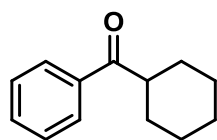
#### Cyclopropyl phenyl ketone<sup>68</sup> (45)

 Colourless liquid (87% isol. yield, 0.43 mmol, 62.9 mg). Purification by flash chromatography (Hexane/AcOEt, 25/1). **<sup>1</sup>H NMR** (400 MHz,  $CDCl_3$ ):  $\delta$  (ppm) = 8.03-8.01 (m, 2H), 7.59-7.54 (m, 1H), 7.49-7.45 (m, 2H), 2.71-2.65 (m, 1H), 1.26-1.19 (m, 2H), 1.08-1.03 (m, 2H). **<sup>13</sup>C NMR** (100 MHz,  $CDCl_3$ ):  $\delta$  (ppm) = 201.0, 138.4, 133.1, 128.9, 128.4, 17.5, 12.0. **IR** (neat)  $\nu = 3062, 3008, 1666, 1598, 1577, 1448, 1382, 1224, 1178, 1033, 987, 869, 815, 782, 703, 646$ .  
**HRMS** (EI)  $m/z$  calc'd  $C_{10}H_{11}O$   $[M + H]^+$ : 147.0805, found: 147.0804.

#### Cyclobutyl phenyl ketone<sup>69</sup> (47)

 Colourless liquid (54% isol. yield, 0.27 mmol, 43.2 mg). Purification by flash chromatography (Hexane/AcOEt, 30/1). **<sup>1</sup>H NMR** (400 MHz,  $CDCl_3$ ):  $\delta$  (ppm) = 7.98-7.87 (m, 2H), 7.71-7.62 (m, 1H), 7.58-7.50 (m, 2H), 4.05 (q,  $J = 6.7$  Hz, 1H), 2.54-2.38 (m, 3H), 2.21-2.02 (m, 2H), 1.97-1.84 (m, 1H). **IR** (neat)  $\nu = 2983, 2942, 1674, 1597, 1579, 1448, 1346, 1248, 1221, 1177, 966, 771, 737, 692, 659$   $cm^{-1}$ . **<sup>13</sup>C NMR** (100 MHz,  $CDCl_3$ ):  $\delta$  (ppm) = 201.0, 135.6, 132.8, 128.5, 128.3, 42.2, 25.1, 18.1. **HRMS** (EI)  $m/z$  calc'd  $C_{11}H_{13}O$   $[M + H]^+$ : 161.0961, found: 161.0960.



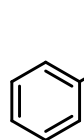
**Cyclohexyl phenyl ketone<sup>65</sup> (49)**

Colourless liquid (73% isol. yield, 0.36 mmol, 67.8 mg). Purification by flash chromatography (Hexane/AcOEt, 30/1). **<sup>1</sup>H NMR** (400 MHz, CDCl<sub>3</sub>): δ (ppm) = 7.98 (d, J = 7.8 Hz, 2H), 7.74-7.68 (m, 1H), 7.64-7.58 (m, 2H), 3.37 (q, J = 7.0 Hz, 1H), 1.97-1.35 (m, 10H). **<sup>13</sup>C NMR** (100 MHz, CDCl<sub>3</sub>): δ (ppm) = 203.9, 136.3, 132.7, 128.5, 128.2, 45.6, 29.4, 26.2, 25.8. **IR (neat)** ν = 2928, 2853, 1679, 1597, 1580, 1447, 1288, 1250, 1206, 1172, 973, 763, 696, 660 cm<sup>-1</sup>. **HRMS** (EI) m/z calc'd C<sub>13</sub>H<sub>17</sub>O [M + H]<sup>+</sup>: 189.1274, found: 189.1267.

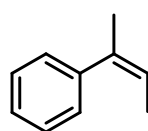
The carbonyl products are commercially available and the analytical data obtained is in agreement with the data reported by the manufacturers.

**6.5.5. Coordination of the olefin to the catalyst**

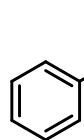
Reactions were performed as described in section 6.5.4.

**Product characterisation****Propiophenone<sup>64</sup> (51)**

Colourless liquid (7% isol. yield, 0.04 mmol, 5.4 mg). Purification by flash chromatography (Hexane/AcOEt, 40/1 to 20/1). **<sup>1</sup>H NMR** (400 MHz, CDCl<sub>3</sub>): δ (ppm) = 7.98-7.95 (m, 2H), 7.57-7.53 (m, 1H), 7.49-7.44 (m, 2H), 3.02 (q, J = 6.8 Hz, 2H), 1.24 (t, J = 6.8 Hz, 3H). **<sup>13</sup>C NMR** (100 MHz, CDCl<sub>3</sub>): δ (ppm) = 201.2, 137.3, 133.2, 128.9, 128.3, 32.1, 8.6. **IR (neat)** ν = 2977, 2940, 2904, 1683, 1598, 1450, 1411, 1349, 1213, 1178, 1081, 1012, 954, 744, 690, 642. **HRMS** (EI) m/z calc'd C<sub>9</sub>H<sub>10</sub>O [M + H]<sup>+</sup>: 135.0805, found: 135.0811.

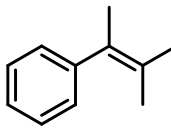
**(Z)- 2-Buten-2-ylbenzene<sup>70</sup> (52)**

Colourless liquid (53% isol. yield, 0.26 mmol, 34.3 mg). Purification by flash chromatography (Hexane/AcOEt, 40/1). **<sup>1</sup>H NMR** (400 MHz, CDCl<sub>3</sub>): δ (ppm) = 7.40-7.15 (m, 5H), 5.89-5.83 (m, 1H), 2.03 (s, 3H), 1.80 (dd, J = 1.2, 5.6 Hz, 3H). **<sup>13</sup>C NMR** (100 MHz, CDCl<sub>3</sub>): δ (ppm) = 144.4, 135.9, 128.5, 126.7, 125.9, 122.8, 15.8, 14.7. **HRMS** (EI) m/z calc'd C<sub>10</sub>H<sub>13</sub> [M + H]<sup>+</sup>: 133.1012, found: 133.1008.

**Isobutyrophenone<sup>72</sup> (54)**

Colourless liquid (36% isol. yield, 0.18 mmol, 26.7 mg). Purification by flash chromatography (Hexane/AcOEt, 40/1 to 20/1). **<sup>1</sup>H NMR** (400 MHz, CDCl<sub>3</sub>): δ (ppm) = 7.97-7.94 (m, 2H), 7.57-7.53 (m, 1H), 7.48-7.44 (m, 2H), 3.56 (quintet, J = 7.2 Hz, 1H), 1.22 (d, J = 7.2 Hz, 6H). **<sup>13</sup>C NMR** (100 MHz, CDCl<sub>3</sub>): δ (ppm) = 204.9, 136.6, 133.1, 129.0, 128.7, 35.7, 19.5. **IR (neat)** ν = 2973, 2933, 2875, 1681, 1598, 1577, 1469, 1448, 1382, 1353, 1216, 1162, 1087, 979, 794, 696, 646. **HRMS** (EI) m/z calc'd C<sub>10</sub>H<sub>13</sub>O [M + H]<sup>+</sup>: 149.0961, found: 149.0960.

**(3-Methylbut-2-en-2-yl)benzene<sup>71</sup>(55)**

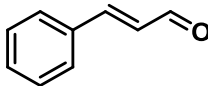
 Colourless liquid (34% isol. yield, 0.17 mmol, 24.8 mg). Purification by flash chromatography (Hexane/AcOEt, 40/1). **<sup>1</sup>H NMR** (400 MHz, CDCl<sub>3</sub>): δ (ppm) = 7.36-7.12 (m, 5H), 2.01 (s, 3H), 1.87 (s, 3H), 1.68 (s, 3H). **<sup>13</sup>C NMR** (100 MHz, CDCl<sub>3</sub>): δ (ppm) = 144.3, 139.6, 130.2, 128.7, 127.8, 126.9, 21.4, 21.1, 13.1. **HRMS** (EI) m/z calc'd C<sub>11</sub>H<sub>15</sub> [M + H]<sup>+</sup>: 147.1169, found: 147.1162.

These products are commercially available and the analytical data obtained is in agreement with the data reported by the manufacturers.

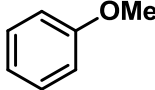
**6.5.6. Competitive direct dehydrogenation**

Reactions were performed as described in section 6.5.4.

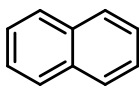
**Product characterisation****Cinnamaldehyde<sup>64</sup> (57)**

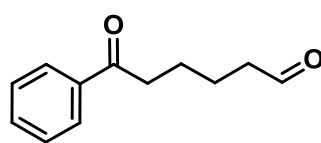
 Colourless liquid (35% isol yield, 0.17 mmol, 23.1 mg). Purification by flash chromatography (Hexane/AcOEt, 20/1). **<sup>1</sup>H NMR** (400 MHz, CDCl<sub>3</sub>): δ (ppm) = 9.91 (d, J = 7.2 Hz, 1H), 7.81-7.42 (m, 6H), 6.72 (dd, J = 15.8, 7.2 Hz, 1H). **<sup>13</sup>C NMR** (100 MHz, CDCl<sub>3</sub>): δ (ppm) = 193.8, 152.9, 134.0, 131.3, 129.1, 128.5. **IR (neat)** ν = 3066, 3027, 2827, 1672, 1626, 1495, 1449, 1418, 1282, 1225, 1176, 1159, 1134, 976, 943, 911, 766, 697, 682, 589, 541, 480 cm<sup>-1</sup>. **HRMS** (CI) m/z calc'd C<sub>9</sub>H<sub>9</sub>O [M + H]<sup>+</sup>: 133.0648, found: 133.0649.

**Anisole<sup>73</sup> (61)**

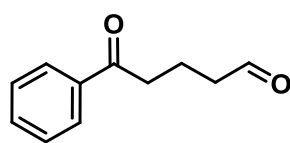
 Colourless liquid (60% isol. yield, 0.30 mmol, 32.4 mg). Purification by flash chromatography (Hexane/AcOEt, 30/1). **<sup>1</sup>H NMR** (400 MHz, CDCl<sub>3</sub>): δ (ppm) = 7.42-7.36 (m, 2H), 6.99-6.87 (m, 3H), 3.87 (s, 3H). **<sup>13</sup>C NMR** (100 MHz, CDCl<sub>3</sub>): δ (ppm) = 159.5, 129.7, 120.6, 113.8, 55.1. **IR (neat)** ν = 2957, 2836, 1599, 1587, 1495, 1467, 1454, 1302, 1243, 1172, 1153, 1077, 1153, 1077, 1038, 1020, 883, 783, 700, 689, 552, 509 cm<sup>-1</sup>.

**Naphthalene<sup>74</sup> (63)**

 White solid. Purification by flash chromatography (Hexane/AcOEt, 50/1). **<sup>1</sup>H NMR** (400 MHz, CDCl<sub>3</sub>): δ (ppm) = 7.84-7.78 (m, 4H), 7.47-7.44 (m, 4H). **<sup>13</sup>C NMR** (100 MHz, CDCl<sub>3</sub>): δ (ppm) = 133.8, 128.3, 126.2. **IR (neat)** ν = 2923, 2854, 1702, 1590, 1504, 1457, 1386, 1267, 1207, 1120, 1006, 958, 775. **HRMS** (EI) m/z calc'd C<sub>10</sub>H<sub>8</sub> [M + H]<sup>+</sup>: 129.0699, found: 129.0696.

**6-Oxo-6-phenylhexanal<sup>75</sup> (66)**

Yellowish liquid (27% isol. yield, 0.13 mmol, 25.7 mg). Purification by flash chromatography (Hexane/AcOEt, 50/1 to 20/1). **<sup>1</sup>H NMR** (400 MHz, CDCl<sub>3</sub>): δ (ppm) = 9.45 (s, 1H), 8.09-7.98 (m, 2H), 7.74-7.34 (m, 3H), 3.02 (t, J = 7.0Hz, 2H), 2.51 (t, J = 7.0 Hz, 2H), 1.98-1.76 (m, 4H). **<sup>13</sup>C NMR** (100 MHz, CDCl<sub>3</sub>): δ (ppm) = 202.3, 199.8, 136.7, 132.7, 128.0, 128.4, 43.2, 37.8, 23.5, 21.4. **HRMS** (CI) m/z calc'd C<sub>12</sub>H<sub>15</sub>O<sub>2</sub> [M + H]<sup>+</sup>: 191.1067, found: 191.1062.

**5-Oxo-5-phenylpentanal<sup>75</sup> (68)**

Yellowish liquid (20% isol. yield, 0.10 mmol, 17.6 mg). Purification by flash chromatography (Hexane/AcOEt, 50/1 to 20/1). **<sup>1</sup>H NMR** (400 MHz, CDCl<sub>3</sub>): δ (ppm) = 9.80 (s, 1H), 7.96 (d, J = 7.8 Hz, 2H), 7.52-7.45 (m, 3H), 3.05 (t, J = 7.0 Hz, 2H), 2.57 (t, J = 6.9 Hz, 2H), 2.09-2.03 (m, 2H). **<sup>13</sup>C NMR** (100 MHz, CDCl<sub>3</sub>): δ (ppm) = 202.0, 199.9, 137.1, 134.0, 128.7, 127.9, 43.3, 37.5, 16.8. **HRMS** (CI) m/z calc'd C<sub>11</sub>H<sub>13</sub>O<sub>2</sub> [M + H]<sup>+</sup>: 177.0911, found: 177.0919.

Analytical data of the isolated products is in agreement with that of the commercially available compounds.

**6.5.6. Detection of volatile hydrocarbon byproducts**

In a Radley's tube equipped with a magnetic stirring bar, Fe(OTf)<sub>3</sub> (5.65 x 10<sup>-3</sup> mmol, 2.9 mg) and **L4** (5.67 x 10<sup>-3</sup> mmol, 7.1 mg) were added. The tube was sealed, degassed and left under inert atmosphere (3 times). Freshly distilled DCE (0.5 mL) was injected by syringe and the reaction mixture was allowed stirring for 1 hour at 40 °C. 1-Phenyl-1-cyclohexene (0.50 mmol) was added by syringe and the reaction tube was degassed, charged with dioxygen gas (1 atm, 3 times) and keep under oxygen (1 atm) by using a balloon. The tube was gradually heated to 75 °C and allowed to react for 4 hours. For the GC analysis, a sample of gas phase (100 μL) contained on the sealed Radley's tube was taken and injected on a Varian star GC spectrometer for hydrocarbon detection. The retention times obtained were 4.637 (CH<sub>3</sub>CH<sub>3</sub>) and 4.756 (CH<sub>2</sub>=CH<sub>2</sub>).

## Sample 1: Chromatogram data

Print Date: Tue Jun 17 19:31:38 2014 Page 1 of 1

Title :  
 Run File : C:\STAR\MODULE16\HOSSEIN\MODULE16\MODULE16\STAR185.RUN  
 Method File : C:\STAR\MODULE16\ABDULLAH\ABD1.MTH  
 Sample ID : Manual Sample

Injection Date: 17-JUN-14 7:21 PM Calculation Date: 17-JUN-14 7:28 PM

Operator : Ekaterina Detector Type: ADCB (1 Volt)  
 Workstation: HARD DISK Bus Address : 16  
 Instrument : Varian Star #1 Sample Rate : 10.00 Hz  
 Channel : A = A Run Time : 7.675 min

\*\*\*\*\* Star Chromatography workstation \*\*\*\*\* Version 4.51 \*\*\*\*\*

Run Mode : Analysis  
 Peak Measurement: Peak Area  
 Calculation Type: Percent

Peak No.	Peak Name	Result ( )	Ret. Time (min)	Time Offset (min)	Area (counts)	Sep. Code	width 1/2 (sec)	Status Codes
1		11.1941	4.367	0.000	73	BB	0.0	
2		88.8059	4.756	0.000	578	BB	1.1	
Totals:		100.0000		0.000	651			

Total Unidentified Counts : 651 counts

Detected Peaks: 4 Rejected Peaks: 2 Identified Peaks: 0

Multiplier: 1 Divisor: 1

Baseline Offset: 1792 microVolts

Noise (used): 17 microVolts - monitored before this run

Manual injection

## Sample 2 (duplicate): Chromatogram data

Print Date: Tue Jun 17 19:40:26 2014 Page 1 of 1

Title :  
 Run File : C:\STAR\MODULE16\HOSSEIN\MODULE16\MODULE16\STAR186.RUN  
 Method File : C:\STAR\MODULE16\ABDULLAH\ABD1.MTH  
 Sample ID : Manual Sample

Injection Date: 17-JUN-14 7:32 PM Calculation Date: 17-JUN-14 7:38 PM

Operator : Ekaterina Detector Type: ADCB (1 Volt)  
 Workstation: HARD DISK Bus Address : 16  
 Instrument : Varian Star #1 Sample Rate : 10.00 Hz  
 Channel : A = A Run Time : 6.535 min

\*\*\*\*\* Star Chromatography workstation \*\*\*\*\* Version 4.51 \*\*\*\*\*

Run Mode : Analysis  
 Peak Measurement: Peak Area  
 Calculation Type: Percent

Peak No.	Peak Name	Result ( )	Ret. Time (min)	Time Offset (min)	Area (counts)	Sep. Code	width 1/2 (sec)	Status Codes
1		19.2748	4.376	0.000	51	BB	0.0	
2		80.7252	4.757	0.000	212	BB	1.1	
Totals:		100.0000		0.000	263			

Total Unidentified Counts : 262 counts

Detected Peaks: 2 Rejected Peaks: 0 Identified Peaks: 0

Multiplier: 1 Divisor: 1

Baseline Offset: 1795 microVolts

Noise (used): 16 microVolts - monitored before this run

### 6.5.5. Radical trapping experiments: General procedure

In a Radley's tube equipped with a magnetic stirring bar,  $\text{Fe}(\text{OTf})_3$  ( $5.65 \times 10^{-3}$  mmol, 2.9 mg) and **L1** ( $6.67 \times 10^{-3}$  mmol, 5.2 mg) were added. The tube was sealed, degassed and left under an inert atmosphere (3 times). Freshly distilled DCE (0.5 mL) was injected by syringe and the reaction mixture was allowed stirring for 1 hour at  $40^\circ\text{C}$ . Next, styrene (0.75 mmol, 90  $\mu\text{L}$ ) and a certain amount of radical trapping reagent were added. The reaction tube was degassed with dioxygen gas (1 atm, 3 times) and kept under oxygen (1 atm) by using a balloon. The tube was gradually heated to  $70^\circ\text{C}$  and allowed to react for 5 hours. The reaction was purified by silica gel flash column chromatography (Hexane/EtOAc, 20/1) to afford the unreacted starting material and the aldehyde product.

### 6.5.6. Effect of a radical initiator: General procedure

In a Radley's tube equipped with a magnetic stirring bar,  $\text{Fe}(\text{OTf})_3$  ( $5.65 \times 10^{-3}$  mmol, 2.9 mg) and **L1** ( $5.67 \times 10^{-3}$  mmol, 5.2 mg) were added. The tube was sealed, degassed and left under an inert atmosphere (3 times). Freshly distilled DCE (0.5 mL) was injected by syringe and the reaction mixture was allowed stirring for 1 hour at  $40^\circ\text{C}$ . Next, styrene (0.75 mmol, 90  $\mu\text{L}$ ) and the radical initiator benzoyl peroxide (0.02 mmol) were added. The reaction tube was degassed with dioxygen gas (1 atm, 3 times) and kept under oxygen (1 atm) by using a balloon. The tube was gradually heated to  $45^\circ\text{C}$  and allowed to react overnight. The reaction was purified by silica gel flash column chromatography (Hexane/EtOAc, 20/1) to afford the unreacted starting material and the aldehyde product. The same procedure was repeated in the absence of the radical initiator.

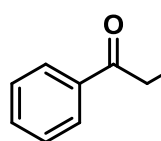
### 6.5.7. Oxidation of vinyl halides

In a Radley's tube equipped with a magnetic stirring bar,  $\text{Fe}(\text{OTf})_3$  ( $5.65 \times 10^{-3}$  mmol, 2.9 mg) and **L1** ( $5.67 \times 10^{-3}$  mmol, 5.7 mg) were added. The tube was sealed, degassed and left under an inert atmosphere (3 times). Freshly distilled DCE (0.5 mL) was injected by syringe and the reaction mixture was allowed stirring for 1 hour at  $40^\circ\text{C}$ . Next,  $\alpha$ -bromostyrene (0.50 mmol, 60  $\mu\text{L}$ ) and diphenyl sulphide (0.25 mmol, 40  $\mu\text{L}$ ) were added by syringe. The

reaction tube was degassed with dioxygen gas (1 atm, 3 times) and kept under oxygen (1 atm) by using a balloon. The tube was gradually heated to 75 °C and allowed to react overnight. The reaction was purified by silica gel flash column chromatography (Hexane/EtOAc, 30/1) to afford the unreacted starting material and the ketone product. The same procedure was repeated in the absence of diphenyl sulfide.

### Product characterisation

#### Phenacyl bromide<sup>76</sup> (71)



White solid (61% isol. yield, 0.30 mmol, 59.8 mg). Purification by flash chromatography (Hexane/AcOEt, 30/1). <sup>1</sup>H NMR (400 MHz, CDCl<sub>3</sub>): δ (ppm) = 8.00 (d, J = 7.8 Hz, 2H), 7.64-7.60 (m, 1H), 7.58-7.50 (m, 2H), 4.52 (s, 2H). <sup>13</sup>C NMR (100 MHz, CDCl<sub>3</sub>): δ (ppm) = 193.2, 133.9, 133.7, 128.9, 128.8, 30.9. IR (neat) ν = 1702, 1677, 1595, 1580, 1448, 1427, 1320, 1307, 1277, 1193, 1012, 989, 749, 709, 685, 622, 608, 590, 527 cm<sup>-1</sup>. HRMS (EI) m/z calc'd C<sub>8</sub>H<sub>7</sub>BrO [M + H]<sup>+</sup>: 198.9753, found: 198.9753.

### 6.6. References

- [1] Mutti, F. G., *Bioinorganic Chemistry and Applications* (2012) doi:10.1155/2012/626909
- [2] Van Ornum, S. C.; Champeau, R. M.; Pariza, R. *Chem. Rev.* **2006**, *106*, 2990.
- [3] (a) Bernasconi, E.; Lee, J.; Roletto, J.; Sogli, L.; Walker, D. *Org. Process Res. DeV.* **2006**, *6*, 152. (b) Bernasconi, E.; Genders, D.; Lee, J.; Longoni, D.; Martin, C. R.; Menon, V.; Roletto, J.; Sogli, L.; Walker, D.; Zappi, G.; Zelenay, P.; Zhang, H. *Org. Process. Res. DeV.* **2002**, *6*, 158. (c) Bernasconi, E.; Lee, J.; Roletto, J.; Sogli, L.; Walker, D. *Org. Process. Res. DeV.* **2002**, *6*, 169.
- [4] Avery, M. A.; Chong, W. K. M.; Jennings-White, C. *J. Am. Chem. Soc.* **1992**, *114*, 974.
- [5] Rubin, M. B. "The History of Ozone", *Helvetica Chimica Acta* **2003**, *86*, 930.
- [6] Since 1903 Harries has published *circa* 80 papers on ozonolysis, two of the most detailed summaries are: (a) Harries, C. *Liebigs Ann. Chem.* **1905**, *343*, 31. (b) Harries, C. "Untersuchungen über das Ozon und seine Einwirkung auf organische Verbindungen", Julius Springer, Berlin, **1916**. A later review on the work (c) Willstatter R. *Ber. Dtsch. Chem. Ges.* **1926**, *59*, 123.

- [7] Criegee, R. *Angew. Chem. Int. Ed.* **1975**, *14*, 745.
- [8] Geletneky, C.; Berger, S. *Eur. J. Org. Chem.* **1998**, 1625.
- [9] Claus, R. E.; Schreiber, S. L. *Org. Synth.* **1986**, *64*, 150.
- [10] Koike, K.; Inoue, G.; Fukuda, T. "Explosion hazard of gaseous ozone," *Journal of Chemical Engineering of Japan* **1999**, *32*, 295.
- [11] Schwartz, C.; Raible, J.; Mott, K.; Dussault, P. H. *Org. Lett.* **2006**, *8*, 3199.
- [12] Lee, D. in *Oxidation in Organic Chemistry* (Trahanovsky W. S. Ed., Academic, NY, 1982)
- [13] Pappo, R.; Allen Jr., D. S.; Lemieux, R. U.; Johnson, W. S. *J. Org. Chem.* **1956**, *21*, 478.
- [14] VanRheenen, V.; Kelly, R. C.; Cha, D. Y. *Tetrahedron Lett.* **1976**, *23*, 1973.
- [15] Yang, D.; Zhang, C. *J. Org. Chem.* **2001**, *66*, 4814.
- [16] Travis, B. R.; Narayan, R. S.; Borhan, B. *J. Am. Chem. Soc.* **2002**, *124*, 3824.
- [17] Nicolaou, K. C.; Adsool, V. A.; Hale, C. R. H. *Org. Lett.* **2010**, *12*, 1552.
- [18] Xing, D.; Guan, B.; Cai, G.; Fang, Z.; Yang, L.; Shi, Z. *Org. Lett.* **2006**, *8*, 693.
- [19] Lin, R.; Chen, F.; Jiao, N. *Org. Lett.* **2012**, *14*, 4158.
- [20] Wang, T.; Jiao, N. *J. Am. Chem. Soc.* **2013**, *135*, 11692.
- [21] Shi, F.; Tse, M. K.; Pohl, M. M.; Bruckner, A.; Zhang, S.; Beller, M. *Angew. Chem. Int. Ed.* **2007**, *46*, 8866.
- [22] Ren, Y.; Che, Y.; Ma, W.; Zhang, X.; Shen, T.; Zhao, J. *New J. Chem.* **2004**, *28*, 1464.
- [23] Cornils, B.; Herrmann, W. A.; Rasch, M. *Angew. Chem. Int. Ed.* **1994**, *33*, 2144.
- [24] (a) Evans, D.; Osborn, J. A.; Wilkinson, G. *J. Chem. Soc. A* **1968**, 3133. (b) Hartwig, J. F. *Organotransition Metal Chemistry: from Bonding to Catalysis*. (University Science Books, 2009, 753, 757-578).
- [25] Watkins, A. L.; Hasahiguchi, B. G.; Landis, C. R. *Org. Lett.* **2008**, *10*, 4553.
- [26] Cornils, B.; Herrmann, W. A. in *Aqueous-Phase Organometallic Catalysis* (VCH, Weinheim: 1998).

- [27] (a) Tsuji, J.; Nagashima, H.; Nemoto, H. *Org. Synth.* **1984**, *62*, 9. (b) McDonald, R.I.; Liu, G.; Stahl, S.S. *Chem. Rev.* **2011**, *111*, 2981.
- [28] Jira, R. *Angew. Chem. Int. Ed.* **2007**, *48*, 9034.
- [29] See Chapter I, section 1.2.2.
- [30] White, M. C. *Science* **2012**, *335*, 807.
- [31] See Chapter 1, section 1.3.4.3.
- [32] Ionisation potentials for Fe<sup>II</sup> and Fe<sup>III</sup> in eV: 30.6 and 54.8 respectively. Rodriguez, M.; Rubin, R. H. in *Recycling intergalactic and interstellar matter. IAU Symposium Series* Vol. 217, **2014**.
- [33] (a) Lin, Y. H.; Williams, I. D.; Li, P. *Appl. Cat. A: Gen.* **1997**, *150*, 221. (b) Ganeshpure, P. A.; Satish, S. *Tetrahedron Lett.* **1988**, *29*, 6629.
- [34] Masnovi, J.; Samsel, E. G.; Morris Bullock, R. *J. Chem. Soc. Chem. Commun.* **1989**, 1044.
- [35] (a) Frimer, A. A.; Farkash, T.; Sprecher, M. *J. Org. Chem.* **1979**, *44*, 989. (b) Anderson, G. H.; Smith, J. G. *Can. J. Chem.* **1968**, *46*, 1561. (c) Rousseau, G.; le Perchec, P.; Conia, J. M. *Tetrahedron* **1976**, *32*, 2533.
- [36] (a) Rousseau, G.; le Perchec, P.; Conia, J. M. *Tetrahedron Lett.* **1977**, *18*, 45. (b) Rousseau, G.; Lechevallier, A.; Huet, F.; Conia, J. M. *Tetrahedron Lett.* **1978**, *19*, 3287.
- [37] Suprun, W. Ya *J. Prakt. Chem.* **1999**, *341*, 52.
- [38] Frimer, A. A. *Chem. Rev.* **1979**, *79*, 359.
- [39] (a) Foote, C. S.; Denny, R. W. *J. Am. Chem. Soc.* **1971**, *93*, 5162. (b) Foote, C. S.; Denny, R. W. *J. Am. Chem. Soc.* **1971**, *93*, 5168. (c) with a biological enzyme: Chan, H. W.-S. *J. Am. Chem. Soc.* **1971**, *93*, 4632.
- [40] The isomerization of **53** to **55** can be achieved quantitatively using Fe(OTf)<sub>3</sub> as catalyst, whereas the isomerization of **50** to **52** only occurred in the presence of the Fe(OTf)<sub>3</sub>-**L4** complex, suggesting coordination of the complex to the olefinic substrate. The



- isomerization of **53** to **55** can also be achieved in the presence of a Lewis acid at high temperature: Grimbaud, J.; Laurent, A. *Bull. Soc. Chim. Fr.* **1967**, 3599.
- [41] (a) Stille, J. K.; Becker, Y. *J. Org. Chem.* **1980**, *45*, 2139. (b) Jennerjahn, R.; Jackstell, R.; Piras, I.; Franke, R.; Jiao, H.; Bauer, M.; Beller, M. *ChemSusChem* **2012**, *5*, 734.
- [42] (a) Gollnick, K. ; Schenck G. O. in *1,4-Cycloaddition Reactions* (J. Hamer Ed. Academic Press, New York, 1967, p 255). Selected examples of 1,4-additions of singlet oxygen to vinyl aromatics: (b) Foote, C. S.; Mazur, S.; Burns, P. A.; Lerdal, D. *J. Am. Chem. Soc.* **1973**, *95*, 586. (c) Burns, P. A.; Foote, C. S. *J. Am. Chem. Soc.* **1974**, *96*, 3945. (d) Burns, P. A.; Foote, C. S.; Mazur, S. *J. Org. Chem.* **1976**, *41*, 899. (e) Matsumoto, M.; Kondo, K. *Tetrahedron Lett.* **1975**, 3935.
- [43] Cho, J.; MacArthur, A. H. R.; Brookhart, M.; Goldman, A. S. *Chem. Rev.* **2011**, *111*, 1761.
- [44] Kerr, J. A. *Chem. Rev.* **1966**, *66*, 465.
- [45] Burns, P. A.; Foote, C. S. *J. Org. Chem.* **1976**, *41*, 908.
- [46] Jeffrey, A. M.; Jerina, D. M. *J. Am. Chem. Soc.* **1972**, *94*, 4048.
- [47] Jefford, C. W.; Rimbault, C. G. *Tetrahedron Lett.* **1976**, *28*, 2479.
- [48] Selected examples of rearrangements: (a) Fox, J. E.; Scott, A. I.; Young, D. W. *Chem. Commun. (London)* **1967**, 1105. (b) Wasserman, H. H.; Scheffer, J. R. *J. Am. Chem. Soc.* **1967**, *89*, 3073. (c) Schulte-Elte, K. H.; Willhalm, B.; Ohloff, G. *Angew. Chem. Int. Ed.* **1969**, *8*, 985. (d) Le Roux, J. P.; Goasdove, C. *Tetrahedron* **1975**, *31*, 2761. (e) Schaap, A. P.; Burns, P. A.; Zaklika, K. A. *J. Am. Chem. Soc.* **1977**, *99*, 1270.
- [49] Selected examples: (a) Bartlett, P. D.; Schaap, A. P. *J. Am. Chem. Soc.* **1970**, *92*, 3223. (b) Wieringa, J. H.; Strating, J.; Wynberg, H. *Tetrahedron Lett.* **1972**, *13*, 169. (c) Takeshita, H.; Hatsui, T.; Jinnai, O. *Chem. Lett.* **1976**, 1059. (d) Foote, C. S. *Pure Appl. Chem.* **1971**, *27*, 639.
- [50] (a) Wilson, T.; Landis, M. E.; Baumstark, A. L.; Bartlett, P. D. *J. Am. Chem. Soc.* **1973**, *95*, 4765. (b) Bartlett, P. D.; Baumstark, A. L.; Landis, M. E. *J. Am. Chem. Soc.* **1974**, *96*,

5557. (c) Bartlett, P. D.; McKennis, J. S. *J. Am. Chem. Soc.* **1977**, *99*, 5334. (d) Richardson, W. H.; Montgomery, F. C.; Slusser, P.; Yelvington, M. B. *J. Am. Chem. Soc.* **1975**, *97*, 2819.
- [51] Kaklika, K. A.; Burns, P. A.; Schaap, A. P. *J. Am. Chem. Soc.* **1978**, *100*, 318.
- [52] Nickon, A.; Covey, D. F.; Huang, F. C.; Kuo, Y.-N. *J. Am. Chem. Soc.* **1975**, *97*, 905.
- [53] Ishimura, Y.; Nozaki, M.; Hayaishi, O.; Tamura, M.; Yamazaki, I. *J. Biol. Chem.* **1967**, *242*, 2574.
- [54] Hayaishi, O.; Nozaki, M. *Science* **1969**, *164*, 389.
- [55] Hikeda, H.; Hoshi, Y.; Namai, H.; Tanaka, F.; Goodman, J. L.; Mizuno, K. *Chem. Eur. J.* **2007**, *13*, 9207.
- [56] Ohsugi, S.-I.; Nishide, K.; Node, M. *Tetrahedron* **2003**, *59*, 1859.
- [57] Feuer, H.; Doty, J.; Lawrence, J. P. *J. Org. Chem.* **1973**, *38*, 417.
- [58] Modak, A.; Deb, A.; Patra, T.; Rana, S.; Maity, S.; Maity, D. *Chem. Commun.* **2012**, *48*, 4253.
- [59] Liwosz, T. W.; Chemler, S. R. *Chem. Eur. J.* **2013**, *19*, 12771.
- [60] Hansen, A. I.; Ebran, J.-P.; Gogsig, T. M.; Skrydstrup, T. *J. Org. Chem.* **2007**, *17*, 6464.
- [61] Bert, K.; Noel, T.; Kimpe, W.; Goeman, J. L.; Van Der Eycken, J. *Org. Biomol. Chem.* **2012**, *10*, 8539.
- [62] Li, H.; Misal Castro, L. C.; Zheng, J.; Roisnel, T.; Dorcet, V.; Sortais, J.-B.; Darcel, C. *Angew. Chem. Int. Ed.* **2013**, *125*, 8203.
- [63] Wang, A.; Jiang, H. *J. Org. Chem.* **2010**, *75*, 2321.
- [64] Iinuma, M.; Moriyama, K.; Togo, H. *Tetrahedron* **2013**, *69*, 2961.
- [65] Feng, Q.; Song, Q. *J. Org. Chem.* **2014**, *79*, 1867.
- [66] Xie, A.; Zhou, X.; Feng, L.; Hu, X.; Dong, W. *Tetrahedron* **2014**, *70*, 3514.
- [67] Chen, Z.-W.; Ye, D.-N.; Quian, Y.-P.; Ye, M.; Liu, L.-X. *Tetrahedron* **2013**, *69*, 6116.
- [68] Hanson, S. K.; Wu, R.; Silks, L. A. *Org. Lett.* **2011**, *13*, 1908.

- 
- [69] Somers, J. B. M.; Couture, A.; Lablanche-Combier, A.; Laarhoven, W. H. *J. Am. Chem. Soc.* **1985**, *107*, 1387.
- [70] Kawai, Y.; Inaba, Y.; Tokitoh, N. *Tetrahedron: Asymmetry* **2001**, *12*, 309.
- [71] Waser, J.; Carreira, E. M. *Angew. Chem. Int. Ed.* **2004**, *43*, 4099.
- [72] Yin, L.; Wu, J.; Xiao, J.; Cao, S. *Tetrahedron Lett.* **2012**, *53*, 4418.
- [73] Sawamura, Y.; Yabe, Y.; Shigetsura, M.; Yamada, T.; Nagata, S.; Fujiwara, Y.; Maegawa, T.; Manguchi, Y.; Sajiki, H. *Adv. Synth. Catal.* **2012**, *354*, 777.
- [74] Barbero, N.; Martin, R. *Org. Lett.* **2012**, *14*, 796.
- [75] Atmaca, U.; Usanmaz, H. K.; Celik, M. *Tetrahedron Lett.* **2014**, *56*, 2230.
- [76] Jiang, Q.; Sheng, W.; Guo, C. *Green Chem.* **2013**, *15*, 2175.

## *Chapter 7*

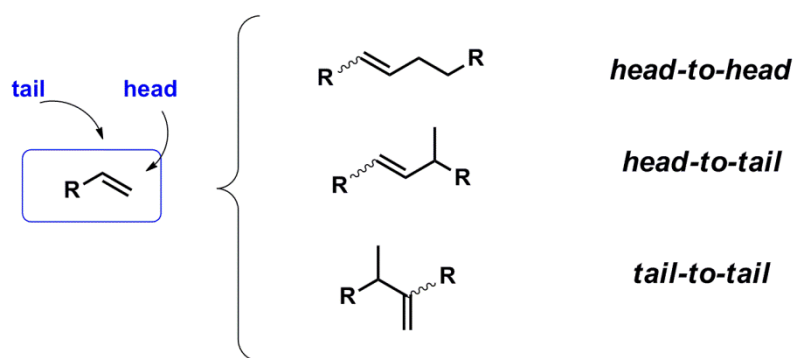
# **Fe(OTf)<sub>3</sub>-PYBISULIDINE CATALYSED REGIOSELECTIVE OLEFIN DIMERISATION**

## 7.1. Introduction

### 7.1.1. Dimerisation of styrenes: importance and challenges

The dimerisation of olefins is a C-C bond forming reaction that has attracted industrial interest because it allows the synthesis of useful intermediates<sup>1</sup> with excellent atom economy.<sup>2</sup> For instance, styrene dimers can be used as intermediates in lubricants or fluids, co-monomers in polymers and plastics, and chain transfer reagents for acrylics.<sup>3</sup>

Despite its industrial relevance, olefin dimerisation processes often provide a distribution of products that varies depending on the reaction conditions and/or catalysts employed<sup>2</sup> (Scheme 1). Thus, the development of chemo- and regioselective methods for olefin dimerisation is still in demand. Traditionally, catalysts based on Ni or Pd have been investigated for olefin dimerisation processes; however, a mixture of oligomers and polymers is normally obtained due to low catalyst selectivity.<sup>4</sup> In addition to uncontrolled polymerisation, competing side reactivity<sup>5</sup> (i.e. Friedel Crafts reactions) is often observed, limiting the reaction efficiency.



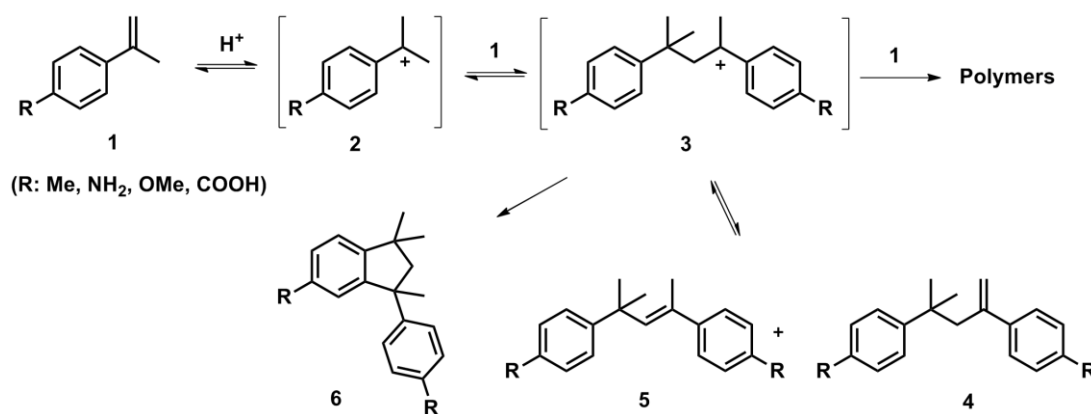
**Scheme 1.** Reaction pathways for the dimerisation of olefins

### 7.1.2. Catalytic methods for the dimerisation of $\alpha$ -methylstyrenes

#### 7.1.2.1. Acid catalysts

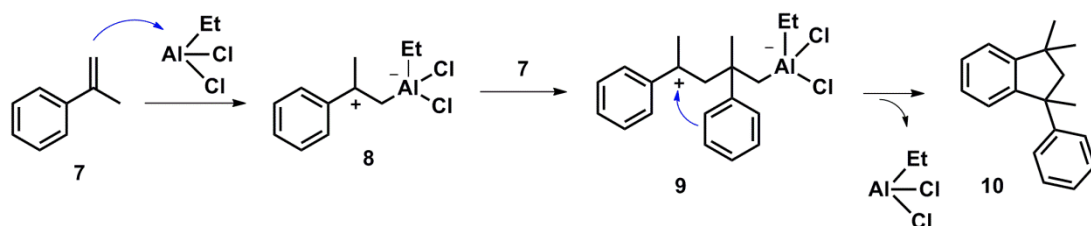
In 1958, Petropoulos and Fischer demonstrated that strong mineral acids such as  $\text{H}_2\text{SO}_4$ ,  $\text{HCl}$  or *p*-toluenesulfonic acid catalysed the dimerisation of  $\alpha$ -methylstyrene to afford a mixture

of dimers and indene products.<sup>6</sup> The proposed reaction mechanism involved the protonation of the olefin to give a benzylic carbocation intermediate **2**. Attack by another olefin molecule results in the formation of the intermediate **3** from which polymerisation (*via* attack of a second monomer) or dimerisation (*via* deprotonation of **3**) could occur (Scheme 2). The scope of the reaction was expanded to another three *p*-substituted  $\alpha$ -methylstyrenes; however, indene products were obtained predominantly and exhaustive control of the temperature and acid concentration was essential to reproduce the reactions and reduce the yield of polymerisation products.



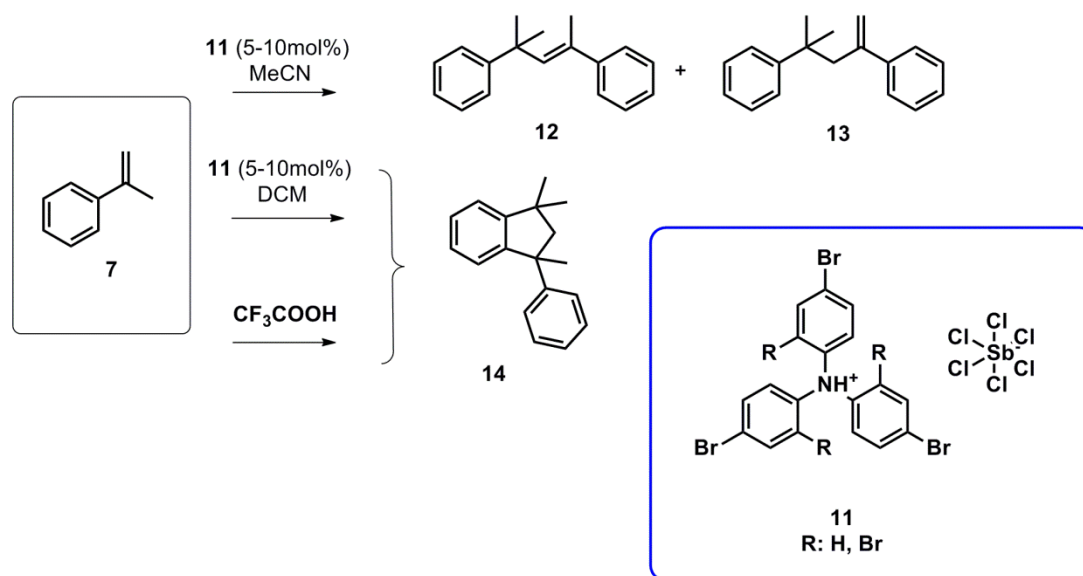
**Scheme 2.** Acid-catalysed dimerisation of  $\alpha$ -methylstyrenes

Wolovsky and co-workers reported the use of ethylaluminium chloride (EADC) as catalyst for the conversion of  $\alpha$ -methylstyrene to indene-type dimers and trimers in benzene solution<sup>7</sup> (Scheme 3). The product distribution varied with the temperature, with the percentage of the dimer product increasing with temperature and reaching a maximum 73% yield at 80 °C. However, the substrate scope of the reaction was not further explored.



**Scheme 3.** EADC-catalysed dimerisation of  $\alpha$ -methylstyrene

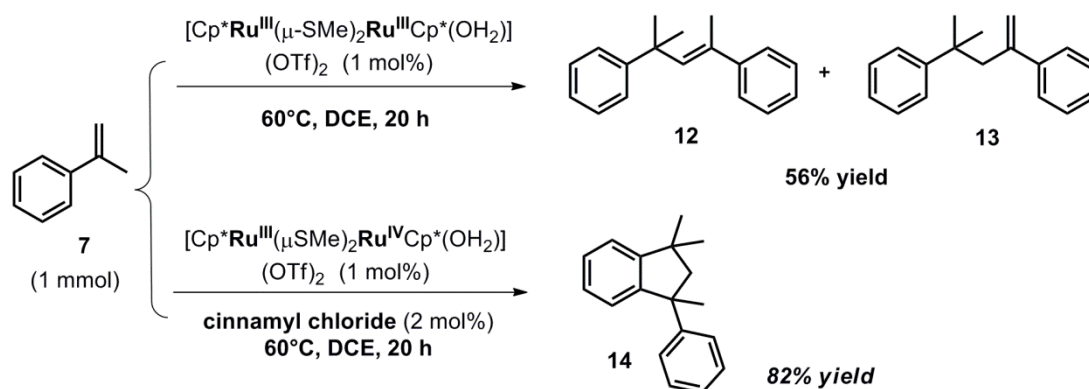
Aminium salts such as *tris*-(2,4-dibromophenyl) aminium hexachloroantimonate and *tris*-(4-dibromophenyl) aminium hexachloroantimonate were also investigated as potential catalysts for the dimerisation of  $\alpha$ -methylstyrene.<sup>8</sup> In MeCN solution, a mixture of the linear dimers was detected whereas in  $\text{CH}_2\text{Cl}_2$  the indene dimer and small amount of indene trimers were obtained. Similarly, the indene dimer was formed predominantly when trifluoroacetic acid was used as catalyst (Scheme 4).



**Scheme 4.** Aminium salts-catalysed dimerisation of  $\alpha$ -methylstyrene

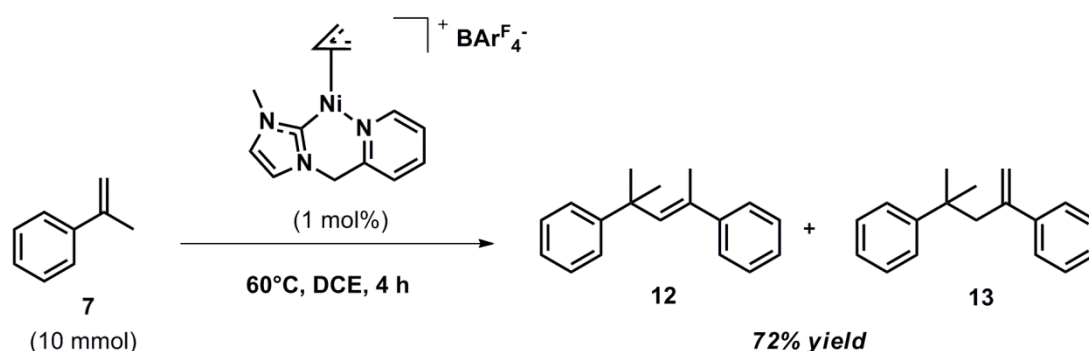
#### 7.1.2.2. Transition metal-based catalysts

The group of Nishibayashi demonstrated that the dicationic diruthenium complex  $[\text{Cp}^*\text{Ru}(\mu\text{-SMe})_2\text{RuCp}^*(\text{OH}_2)](\text{OTf})_2$  could be used as catalysts for the dimerisation of  $\alpha$ -methylstyrene.<sup>9</sup> Interestingly, the  $\text{Ru}^{\text{III}}\text{-Ru}^{\text{III}}$  complex afforded the acyclic dimers **12** and **13** in a 3:1 ratio whereas the mixed valence complex  $\text{Ru}^{\text{III}}\text{-Ru}^{\text{IV}}$  generated the indene dimer in the presence of cinnamyl alcohol as additive (Scheme 5). The scope was extended to four substrates with the indene products obtained with good yields. However, more moderate yields were achieved for the linear dimers.



**Scheme 5.** Dimerisation of  $\alpha$ -methylstyrene catalysed by dinuclear Ru complexes.

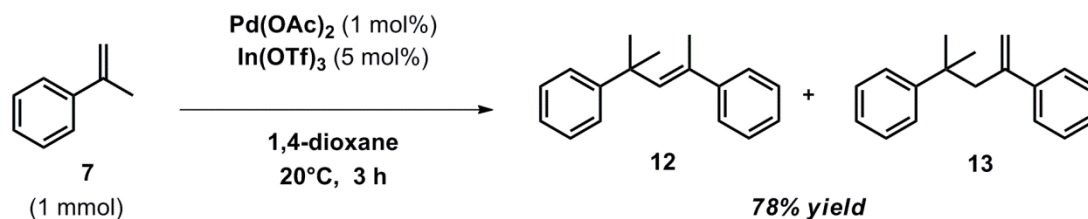
The group of Valerga reported a family of Ni-based complexes bearing *N*-carbene ligands of the formula  $[(\text{L})\text{Ni}(\text{NHC})][\text{BAr}^{\text{F}}_4]$  and its catalytic application for the dimerisation of  $\alpha$ -methylstyrene and 4-methylstyrene<sup>10</sup> (Scheme 6). Most of the catalysts showed high activity under mild conditions without any need for a co-catalyst. However, no additional substrate scope was reported.



**Scheme 6.** Nickel-catalysed dimerisation of  $\alpha$ -methylstyrene

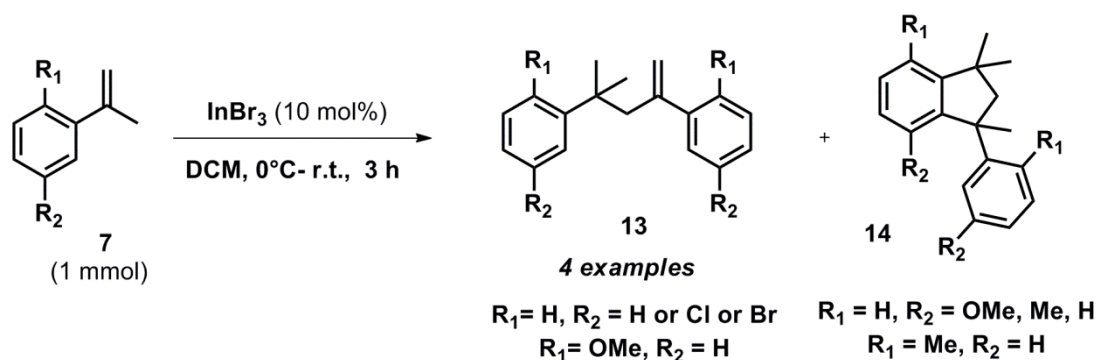
$\text{Pd}(\text{OAc})_2$  has also been explored as catalyst for  $\alpha$ -methylstyrene and styrene dimerisation by Shirakawa and co-workers.<sup>11</sup> In combination with  $\text{In}(\text{OTf})_3$  as an activator of the alkene, a mixture of the linear dimers **12** and **13** was obtained in 78% yield under mild conditions (Scheme 7). However, the substrate scope was not further expanded to substituted analogues.





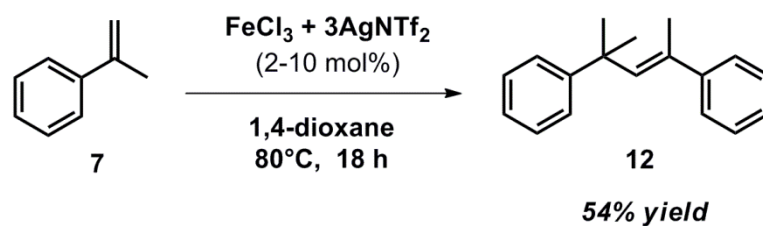
**Scheme 7.**  $\text{Pd(OAc)}_2/\text{In(OTf)}_3$  catalysed dimerisation of  $\alpha$ -methylstyrene

Inspired by this study, the group ofeppe reported the use of  $\text{InBr}_3$  as a Lewis acid catalyst for the dimerisation of substituted  $\alpha$ -methylstyrenes<sup>12</sup> (Scheme 8). The reaction proceeded under mild conditions but high catalysts loading (10 mol%) were needed to afford the linear dimer **13**. However, in many cases the indene product **14** was formed exclusively, limiting the scope to only 4 linear dimers.



**Scheme 8.** Indium-catalysed dimerisation of  $\alpha$ -methylstyrenes

The use of iron-based catalysts for the dimerisation of styrenes was explored by the group of Corma, who demonstrated that the *in situ* prepared  $\text{Fe(NTf}_2)_3$  was an effective catalyst for the regioselective head-to-tail dimerisation of styrenes and  $\alpha$ -methylstyrene.<sup>2</sup> Indeed, the linear dimer **12** was obtained exclusively with 51% yield and no side products formation (Scheme 9). However, the scope is limited to a few styrene substrates and normally high loadings of the expensive  $\text{AgNTf}_2$  were required to achieve good yields.



**Scheme 9.** Iron-catalysed dimerisation of  $\alpha$ -methylstyrene

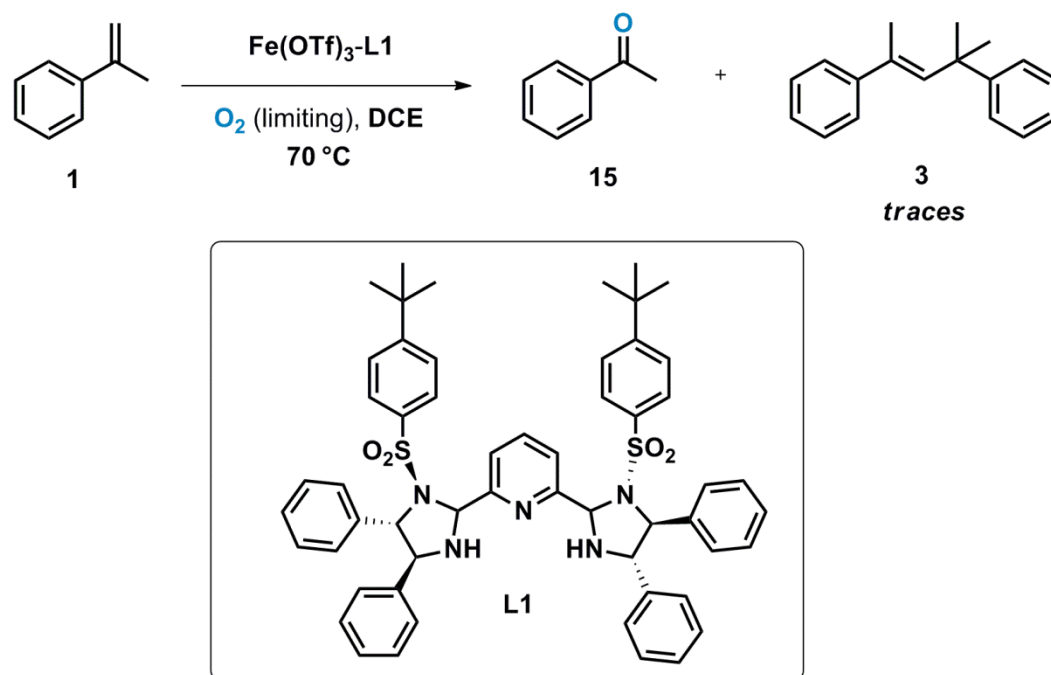
## 7.2. Aims of this chapter

Even though many different catalysts have been tested for the dimerisation of  $\alpha$ -methylstyrene, the development of new catalyst capable of selectively convert  $\alpha$ -methylstyrene to its linear dimers is still challenging. This chapter presents our efforts in the development of a greener iron-catalysed methodology for the selective dimerisation of  $\alpha$ -methylstyrenes to its linear dimers without generating a complex mixture of oligomers. Considering the limitations of the current methods, a wider substrate scope and a catalyst design that allows controlling the regioselectivity of the double bond of the dimer are the main targets.

## 7.3. Results and discussion

### 7.3.1. Discovery and optimisation of the iron-catalysed olefin dimerisation

$\text{Fe}(\text{OTf})_3$ -PyBisulidine complexes were found to catalyse the aerobic cleavage of olefins to its corresponding carbonyl form under aerobic atmosphere. Surprisingly, under conditions of limiting oxidant unexpected head-to-tail dimerisation of the starting  $\alpha$ -methylstyrene was observed in low yields (Scheme 10). The industrial relevance of olefin dimerisation prompted us to investigate whether this family of iron-PyBisulidine complexes could be used as potential catalysts for the selective dimerisation of  $\alpha$ -methylstyrenes under inert atmosphere.

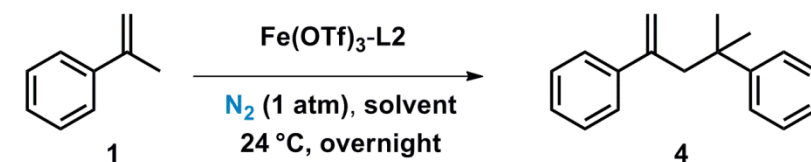


**Scheme 10.** Formation of the styrene dimer **3** under conditions of limiting oxidant

On the basis of this preliminary data,  $\alpha$ -methylstyrene **1** was selected as a model substrate for investigating the  $\text{Fe}(\text{OTf})_3$ -PyBisulidone catalysed olefin dimerisation.

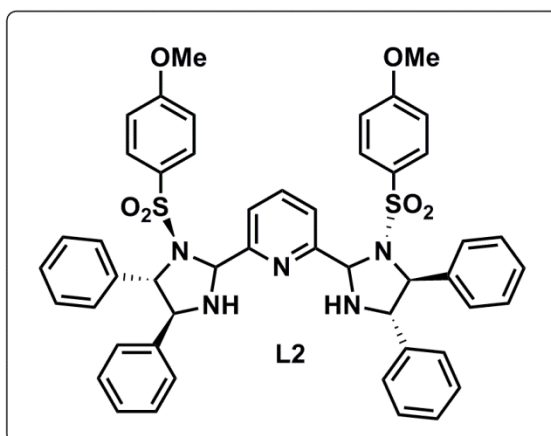
#### 7.3.1.1. Solvent effect

Chlorinated solvents were found ideal for the regioselective formation of the terminal dimer **4** with DCM showing the best efficiency (Scheme 11). Interestingly, arene and coordinating solvents were all found detrimental for the dimerisation reaction (entries 4-9), probably due to either poor catalyst solubility or competing coordination of solvent molecules to the iron centre.



Entry	Solvent	Conversion (%) <sup>a</sup>
1	DCE	20
2	DCM	41
3	CHCl <sub>3</sub>	11
4	Ph-H	-
5	Ph-Me	-
6	Dioxane	-
7	MeCN	-
8	THF	-
9	Et <sub>2</sub> O	-

Conditions: in situ prepared  $\text{Fe(OTf)}_3\text{L2}$  (3 mol%),  $\alpha$ -methylstyrene (0.3 mmol), solvent (2.0 mL), 24 °C, overnight. [a] Determined by <sup>1</sup>H NMR.

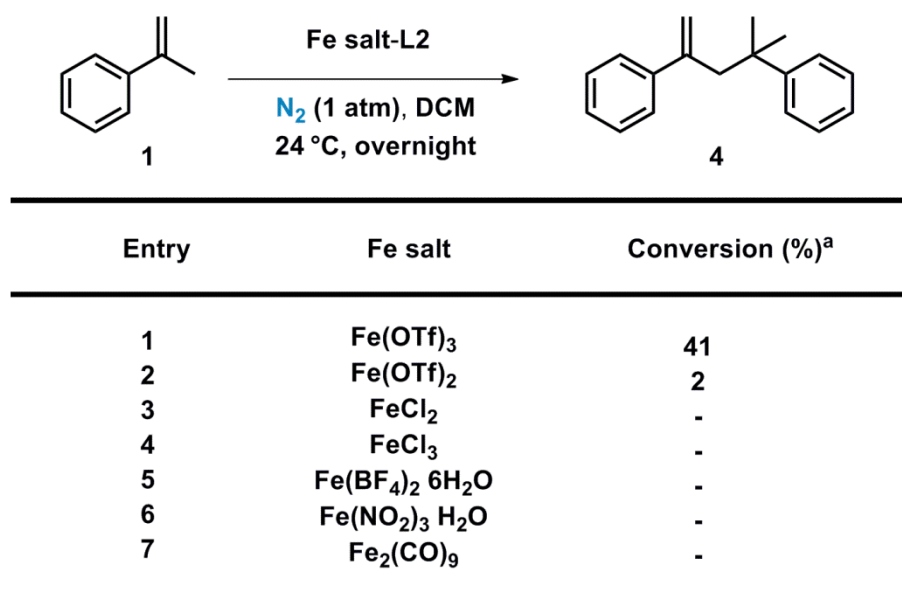


**Scheme 11.** Effect of solvent in the  $\text{Fe(OTf)}_3\text{-PyBisulidone}$  catalysed dimerization of **1**

### 7.3.1.2. Effect of the iron salt

The iron salt was also found to play a crucial role in the dimerisation reaction (Scheme 12). Significantly,  $\text{Fe(OTf)}_3$  was found to be the only efficient iron salt due to its better solubility in DCM and its superior Lewis acidity than its  $\text{Fe(OTf)}_2$  analogue. Other iron salts, covering oxidation states ranging from 0 to 3 were found completely inactive (entries 3-7), revealing that both high Lewis acidity and good leaving groups as counterions are required for

achieving good catalytic activity in the dimerisation of **1**. In the absence of ligand **L2**, both  $\text{Fe}(\text{OTf})_3$  and  $\text{Fe}(\text{OTf})_2$  were found inactive for dimerisation.

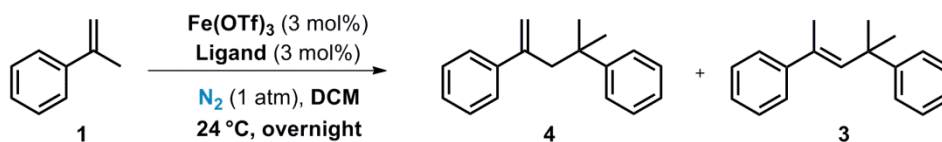


Conditions: in situ prepared Fe salt (3 mol%), **L2** (3 mol%),  $\alpha$ -methylstyrene (0.3 mmol), solvent (2.0 mL), 24 °C, overnight. [a] Determined by  $^1\text{H}$  NMR.

**Scheme 12.** Effect of the iron salt in the  $\text{Fe}(\text{OTf})_3$ -PyBisulidine catalysed dimerization of **1**

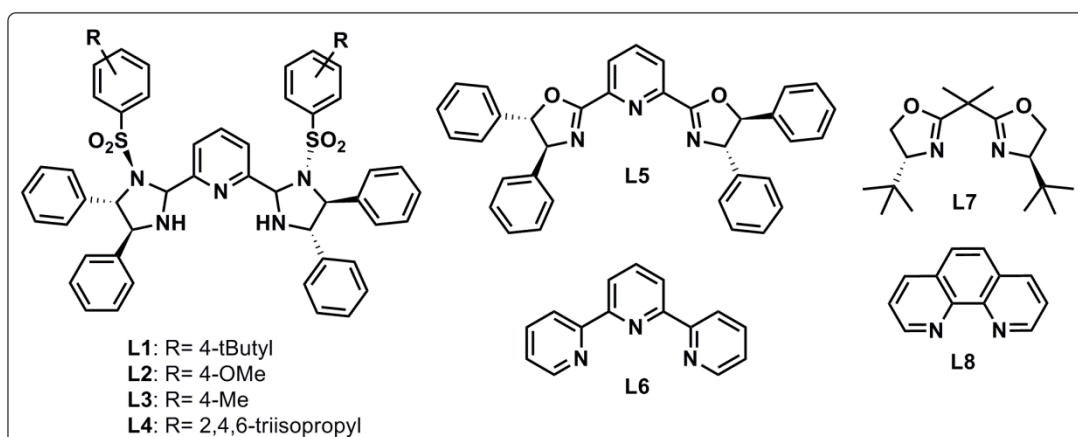
### 7.3.1.3. Ligand effect

The effect of the ligand in the iron-catalysed dimerisation of **1** was next investigated (Scheme 13). Tridentate PyBisulidine ligands in combination with equimolecular amounts of  $\text{Fe}(\text{OTf})_3$  showed certain efficiency in catalysing the dimerisation of **1** to the terminal dimer **4**, with **L2** showing the best results (entries 1-4). On the contrary, conjugated tridentate ligands such as PyBox or terpy were found inactive for the dimerisation of **1** (entries 5-6). Nonetheless, conjugated bidentate ligands showed certain efficiency for this transformation with phenantroline affording a mixture of both regioisomers **3** and **4**. The superior efficiency of conjugated bidentate ligands in comparison with the conjugated tridentate ones prompted us to investigate whether the bidentate Bisulidines or the asymmetric PyBisulidines could indeed show superior performance to their analogue tridentate PyBisulidines.



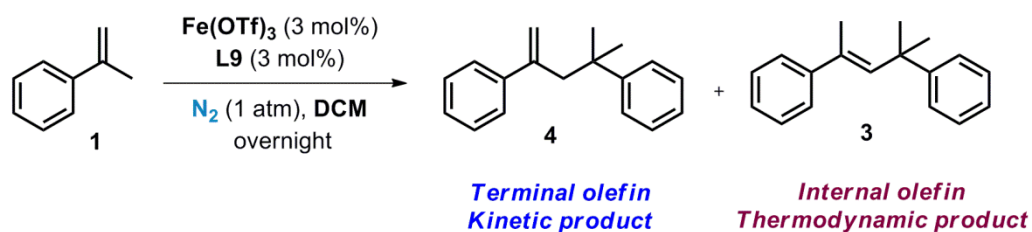
Entry	Ligand	Conversion (%) <sup>a</sup>
1	L1	17 (4)
2	L2	45 (4)
3	L3	5 (4)
4	L4	-
5	L5	-
6	L6	-
7	L7	21 (4)
8	L8	50 (4) + 20 (3) + 30 (oligomerization)

Conditions: in situ prepared Fe(OTf)<sub>3</sub> (3 mol%)-Ligand (3 mol%),  $\alpha$ -methylstyrene (0.3 mmol), solvent (2.0 mL), 24 °C, overnight. [a] Determined by <sup>1</sup>H NMR.



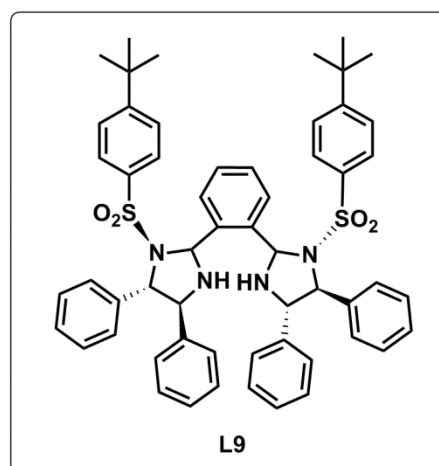
**Scheme 13.** Ligand effect in the Fe(OTf)<sub>3</sub>-PyBisulidine catalysed dimerization of **1**

Indeed, the combination of Fe(OTf)<sub>3</sub> with equimolar amounts of the bidentate Bisulidine **L9** afforded a mixture of dimers **3** and **4** with 70% <sup>1</sup>H NMR conversion at 24 °C (Scheme 14), showing improved activity in comparison with the tridentate **L2** under identical reaction conditions. In addition, small modifications in the reaction temperature significantly affected the product distribution with the terminal olefin being formed predominantly at lower temperatures and the proportion of the internal isomer increasing progressively at higher temperatures. Therefore, at ambient temperature (*circa* 19 °C) the Fe(OTf)<sub>3</sub>**L9** complex can be used to generate the kinetic product **4** predominantly (ratio > 3:1).



Entry	Temperature/ °C	Product 4 Conversion (%) <sup>a</sup>	Product 3 Conversion (%) <sup>a</sup>
1	0	47	10
2	r.t.	<b>55</b>	<b>21</b>
3	24	45	25
4	35	27	54

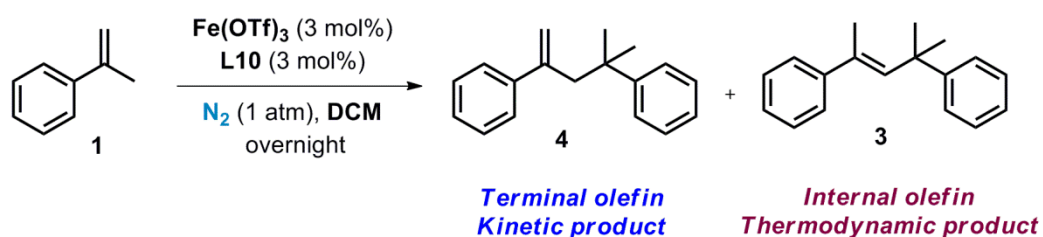
Conditions: in situ prepared  $\text{Fe(OTf)}_3$  (3 mol%), **L9** (3 mol%),  $\alpha$ -methylstyrene (0.3 mmol), DCM (2.0 mL), overnight. [a] Determined by  $^1\text{H}$  NMR.



**Scheme 14.**  $\text{Fe(OTf)}_3$ **L9** catalysed regioselective formation of the terminal dimer **4**

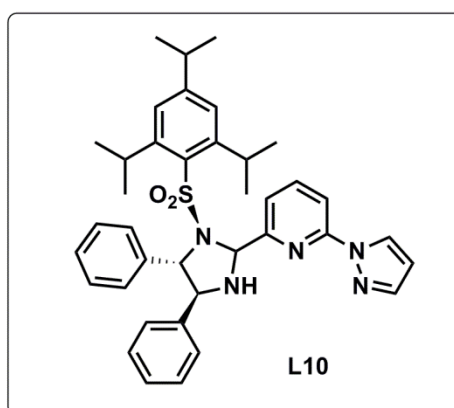
Similarly, complexation of  $\text{Fe(OTf)}_3$  with the asymmetric ligand **L10** contributed to increase the efficiency in the catalytic dimerisation of **1** (Scheme 15). However, the internal dimer was obtained preferably even at ambient temperatures and its proportion increased smoothly with temperature until reaching a maximal 65%  $^1\text{H}$  NMR conversion (89% total conversion) at 40 °C (entry 5). Thus, the  $\text{Fe(OTf)}_3$ **L10** complex can be applied for the predominant formation of the thermodynamic product **3** (ratio > 3:1). This opposite selectivity towards the internal olefin **3** can be attributed to the minimised steric bulkiness of **L10** in comparison with the Bisulidone **L9**. Therefore and for the first time, the regioselectivity of the double bond in the head-to-tail dimerisation of **1** can be controlled by simple replacement of the

ligand in the  $\text{Fe}(\text{OTf})_3$  complex and by controlling the reaction temperature with no oligomerisation derived byproducts formation.



Entry	Temperature/ °C	Product 4 Conversion (%) <sup>a</sup>	Product 3 Conversion (%) <sup>a</sup>
1	0	37	-
2	a.t.	40	50
3	24	18	53
4	35	32	55
5	<b>40</b>	<b>24</b>	<b>65</b>
6	45	25	63

Conditions: in situ prepared  $\text{Fe}(\text{OTf})_3$  (3 mol%)- $\text{L10}$  (3 mol%),  $\alpha$ -methylstyrene (0.3 mmol),  $\text{DCM}$  (2.0 mL), overnight. [a] Determined by  $^1\text{H}$  NMR.



**Scheme 15.**  $\text{Fe}(\text{OTf})_3\text{L10}$  catalysed regioselective formation of the terminal dimer **3** under thermodynamic conditions

### 7.3.2. Substrate scope

#### 7.3.2.1. Electron rich substrates

With the optimised conditions in hand, the substrate scope of the regioselective head-to-tail dimerisation of electron rich  $\alpha$ -methylstyrenes was next investigated (Scheme 16). These

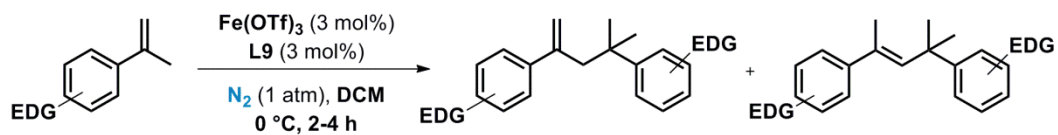


---

substrates are particularly challenging due to the frequent uncontrolled byproduct and oligomer formation.

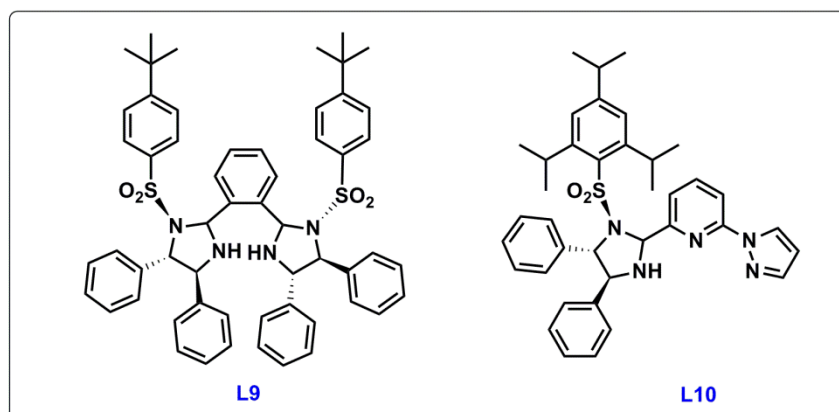
The Fe(OTf)<sub>3</sub>**L9** catalysts afforded a mixture of the kinetic and thermodynamic dimers with good overall yields (*circa* 80%) and no undesired byproduct formation. Nonetheless, lower temperatures (0 °C) and shorter reaction times (maximum 4 hours) were required to achieve good catalytic performance without uncontrolled oligomer formation. Unfortunately, even under such reaction conditions the internal olefin was obtained as the major product preventing the control of the C=C bond regioselectivity in the dimer products (entries 1,2). Regiocontrolled dimerisation in favour of the terminal olefin was finally achieved with the less electron rich substrate **22** under identical low temperatures and shorter reaction times (entry 3). On the other hand, when **L10** was used, the selectivity was reversed to favour **24**.

Additionally, olefins bearing several electron donating functionalities such as **25** can be facily dimerised with the Fe(OTf)<sub>3</sub>**L9** catalyst, however; the resulting dimer product undergoes a rapid Friedel-Crafts cyclisation and thus, the indane product **27** is obtained exclusively (Scheme 17).

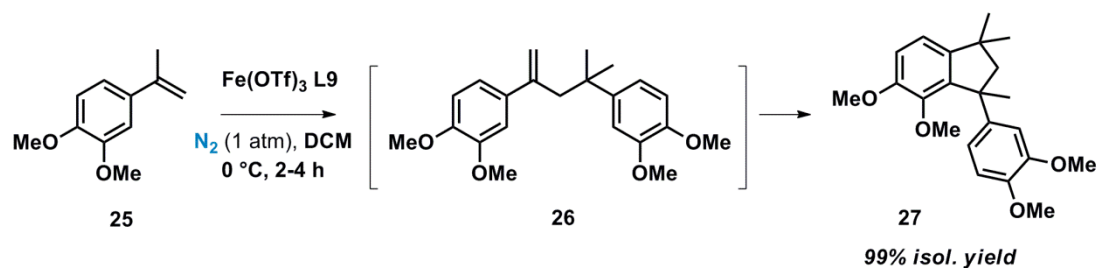


Entry	Starting material	Kinetic Product (conv%) <sup>a</sup>	Thermodynamic Product (conv%) <sup>a</sup>
ELECTRON RICH SUBSTRATES			
1		 22%	 65%
2		 21%	 61%
3		 50% 23% <sup>b</sup>	 26% 51% <sup>b</sup>

Conditions: in situ prepared  $\text{Fe}(\text{OTf})_3$  (3 mol%), **L9** (3 mol%),  $\alpha$ -methylstyrene (0.3 mmol), solvent (2.0 mL), 0 °C, 2-4 h. [a] Determined by  $^1\text{H}$  NMR. [b]  $\text{Fe}(\text{OTf})_3$  (3 mol%), **L10** (3 mol%) was used as catalysts.



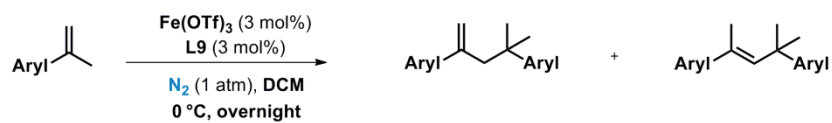
**Scheme 16.** Dimerisation of electron rich styrenes catalysed by  $\text{Fe}(\text{OTf})_3$ -**L9** and/or  $\text{Fe}(\text{OTf})_3$ -**L10**



**Scheme 17.** Friedel-Crafts side reaction with electron rich olefins

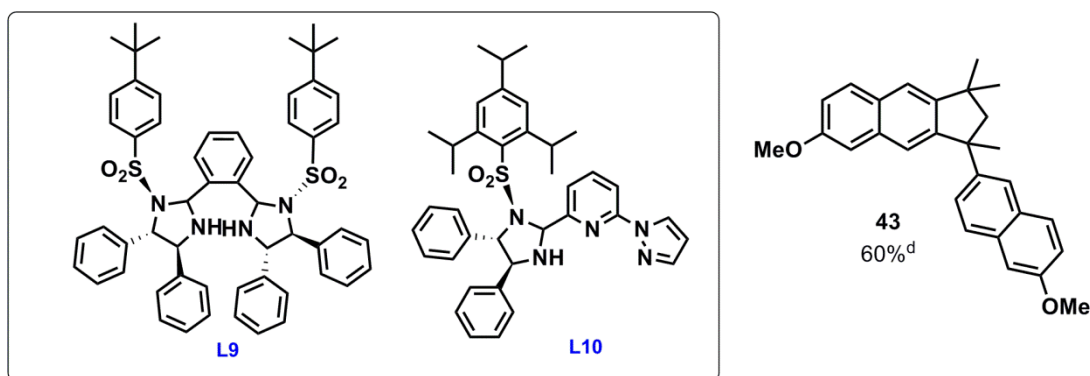
Next, the effect of fused aryl and heterocyclic substitution in the regioselective dimerisation of  $\alpha$ -methylstyrenes was studied (Scheme 18). Regioselective dimerisation of bulky substrates such as **28** and **31** was achieved with very good yields under smooth conditions by simple ligand replacement (entries 1, 2). To our surprise, the resulting dimers **29-33** exhibited luminescence properties (glow in darkness) and thus, these products could be applied as potential monomers in luminescent materials syntheses. Sulphur-based heterocycles were well tolerated by both catalysts affording regioselectively the kinetic and thermodynamic products with good yields (entry 3). Dimers **35** and **36** showed a strong citric aroma and thus, they could potentially be used in fragrance industries as replacements or complements of the commonly used dimers **3** and **4**.

However, some limitations were observed in this type of substrates. For instance, the Friedel-Crafts byproduct **43** was obtained predominantly with the more electron rich substrate **37** even at lower reaction temperatures and shorter reaction times. In addition, very sterically demanding substrates such as **40** can only be subjected to dimerisation with the less sterically hindered  $\text{Fe}(\text{OTf})_3\text{L10}$  catalyst which affords the internal olefin predominantly.



Entry	Starting material	Kinetic Product (conv %) <sup>a</sup>	Thermodynamic Product (conv %) <sup>a</sup>
HETEROCYCLIC SUBSTITUTION			
1		 29 76% 14% <sup>b</sup>	 30 - 86% <sup>b</sup>
2		 32 60% <sup>c</sup> 43% <sup>b</sup>	 33 - 52% <sup>b</sup>
3		 35 87% 38% <sup>b</sup>	 36 13% 61% <sup>b</sup>
4		 38 20% <sup>d</sup>	 39 20% <sup>d</sup>
5		 41 28% <sup>e</sup>	 42 68% <sup>e</sup>

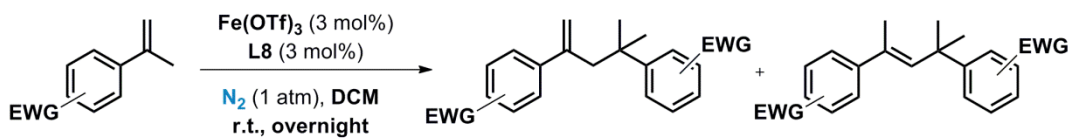
Conditions: in situ prepared Fe(OTf)<sub>3</sub>-L9 (3 mol%),  $\alpha$ -methylstyrene (0.3 mmol), DCM (2.0 mL), 0 °C, overnight. [a] Determined by <sup>1</sup>H NMR. [b] Fe(OTf)<sub>3</sub>-L10 (3 mol%) as catalyst at 35 °C. [c] Reaction run at 24 °C. [d] Reaction using Fe(OTf)<sub>3</sub>-L10 (3 mol%) as catalyst at 0 °C. The Friedel-Crafts byproduct was obtained with 60% conversion. [e] Fe(OTf)<sub>3</sub>-L10 (3 mol%) as catalyst at 0 °C.



**Scheme 18.** Dimerisation of aryl and heterocyclic-substituted styrenes catalysed by  $\text{Fe}(\text{OTf})_3\mathbf{L9}$  and/or  $\text{Fe}(\text{OTf})_3\mathbf{L10}$

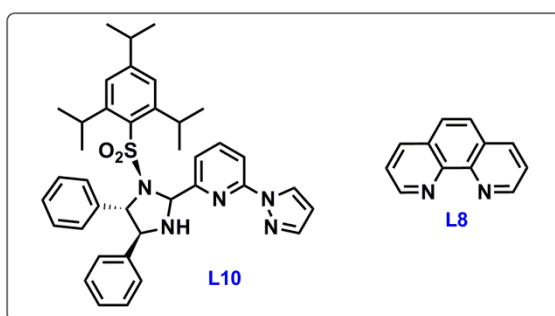
### 7.3.2.2. Electron deficient substrates

Electron deficient  $\alpha$ -methylstyrenes were next targeted as substrates (Scheme 19). Unfortunately, the  $\text{Fe}(\text{OTf})_3\mathbf{L10}$  complex showed limited efficiency in the dimerisation of electron deficient substrates whereas the  $\text{Fe}(\text{OTf})_3\mathbf{L9}$  complex was found completely inactive. Surprised by this lack of activity, the bidentate ligand **L7** and the conjugated bidentate **L8**, which showed some efficiency in the dimerisation of **1**, were also tested for this reaction. Indeed, the phenenatroline skeleton **L8** afforded the dimer products with moderate to good yields and no oligomerisation (Scheme 19). Some regiocontrol was also achieved with this catalytic system particularly in the selective formation of the internal olefin. However, application of this  $\text{Fe}(\text{OTf})_3\mathbf{L8}$  complex in the dimerisation of more electron rich substrates afforded predominantly undesired oligomerisation products.



Entry	Starting material	Kinetic Product (conv %) <sup>a</sup>	Thermodynamic Product (conv %) <sup>a</sup>
ELECTRON DEFICIENT SUBSTRATES			
1		 30% <sup>b</sup> 45% 31% <sup>c</sup>	 - 47% 65% <sup>c</sup>
2		 25% <sup>b</sup> 48% 28% <sup>c</sup>	 - 13% 63% <sup>c</sup>
3		 49% 19% <sup>c</sup>	 19% 68% <sup>c</sup>

Conditions: in situ prepared  $\text{Fe}(\text{OTf})_3$ -L8 (3 mol%),  $\alpha$ -methylstyrene (0.3 mmol), DCM (2.0 mL), r.t., overnight.  
[a] Determined by  $^1\text{H}$  NMR. [b]  $\text{Fe}(\text{OTf})_3$ -L10 (3 mol%) was used as catalysts. [c] Reaction run at 40 °C overnight.



**Scheme 19.** Dimerisation of electron deficient  $\alpha$ -methylstyrenes catalysed by  $\text{Fe}(\text{OTf})_3$ -L8.

### 7.3.3. Mechanistic considerations

#### 7.3.3.1. Coordination of the substrate to the catalyst

Throughout the substrate scope of the iron-catalysed olefin dimerisation, the head-to-tail dimers were obtained exclusively. In addition, no oligomerisation products or uncontrolled polymerisation were observed under the reaction conditions, suggesting that free radical species are not involved in the dimerisation reaction.

As discussed in chapter 6, coordination of the substrate to the iron catalyst can be initially postulated due to the higher efficiency exhibited by the Fe<sup>III</sup> complexes in comparison with the weaker Lewis acidic Fe<sup>II</sup> complexes (Scheme 12).

#### 7.3.3.2. Carbocation intermediate formation

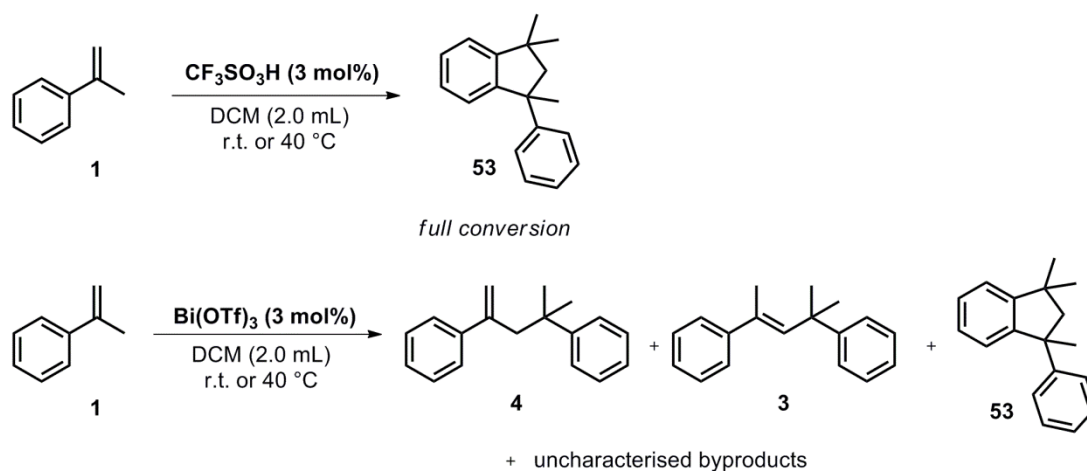
Although the Fe(OTf)<sub>3</sub>-L1 catalyst was capable of undergoing the aerobic cleavage of electron rich and electron deficient styrenes with comparable high efficiency, the iron catalysed dimerisation of styrenes proceeded easily for electron rich styrenes but much harsher conditions were needed for accomplishing the dimerisation of electron deficient substrates (scheme 19). This different reactivity may result from the involvement of cationic species during the dimerisation reaction.

#### 7.3.3.2. Comparison with protic and Lewis acidic catalysts

In order to further understand the role of the iron complex in controlling the selectivity of the dimerisation reaction, the dimerisation of **1** was investigated using trifluoromethanesulfonic acid and Bi(OTf)<sub>3</sub> as catalysts (Scheme 20). Interestingly, the use of trifluoromethanesulfonic acid as a protic acid catalyst resulted in the selective formation of the indane product. Moreover, temperature modifications did not alter the reaction selectivity and conversion, nor yielded the desired linear dimers. In contrast, when Bi(OTf)<sub>3</sub> was used as a Lewis acid catalyst at 25 °C, a complex distribution of products was observed including linear and cyclic dimers (3.3 : 2.6 : 1.0 approximated ratio for **53** : **3** : **4**) and other

uncharacterised products. Again, the reaction temperature did not modify the reaction conversion or the product distribution.

These results clearly indicate that the iron complex is acting as the catalyst of the regioselective dimerisation reaction and that the observed selectivity is controlled by the ligand and reaction temperature.



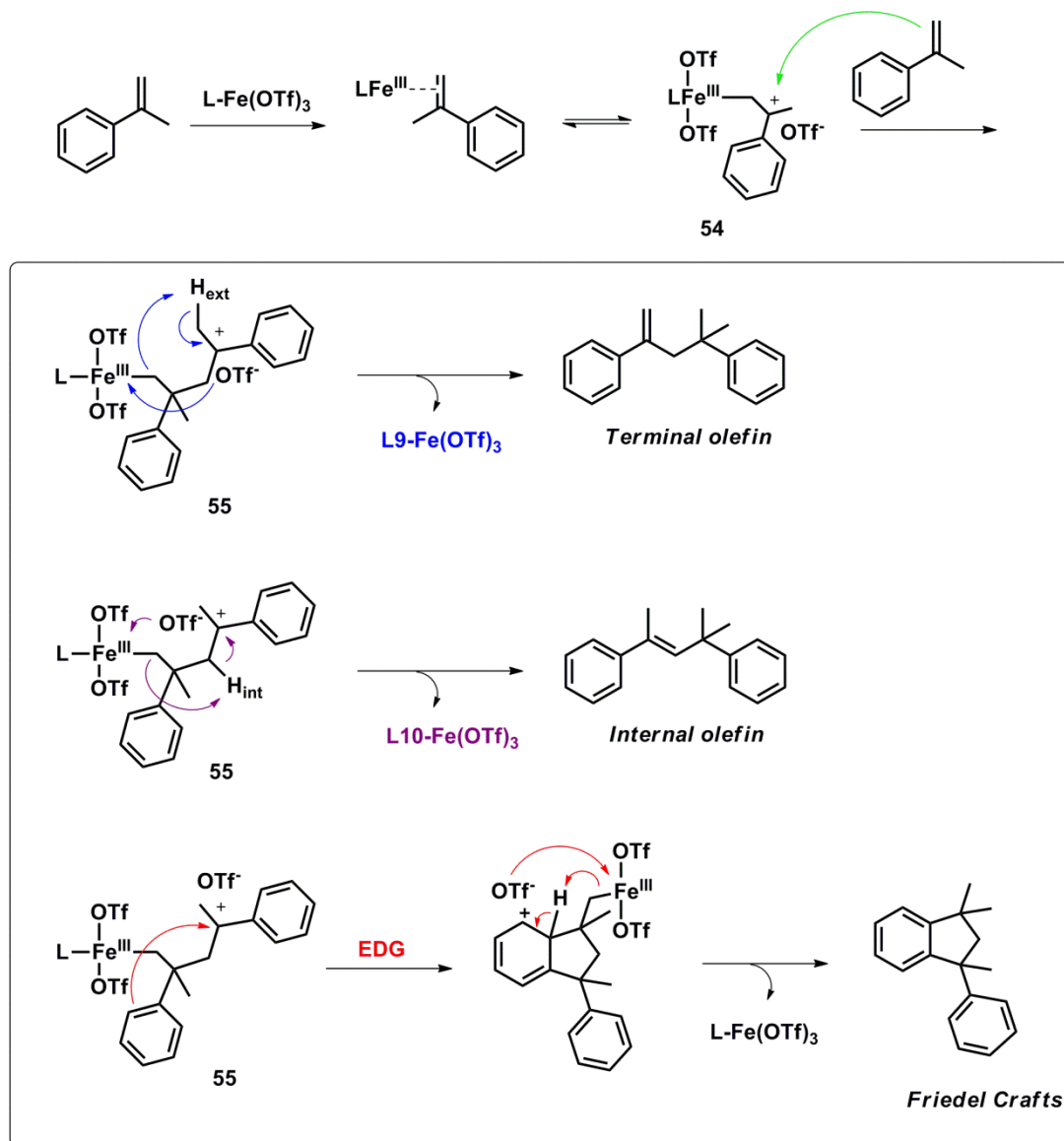
**Scheme 20.** The use of protic and Lewis acids as catalysts for the dimerisation of **1** afforded a different product distribution highlighting the essential role of the iron catalyst in defining the reaction selectivity.

#### 7.3.3.4. Postulated catalytic cycle

To explain the reaction selectivity, we propose that the highly Lewis acidic  $\text{Fe}^{\text{III}}$  catalyst can activate  $\alpha$ -methylstyrenes, forming the intermediate species **54** where the benzylic cation is stabilised by both the methyl group and the phenyl ring (Scheme 20). This electrophilic species **54** can be attacked by a weak nucleophile such as another  $\alpha$ -methylstyrene molecule, generating the key intermediate **55**. From intermediate **55**, elimination of the  $\text{H}_{\text{ext}}$  proton can occur in the presence of the bulkier  $\text{Fe}(\text{OTf})_3\text{L9}$  catalyst at low temperatures, affording the terminal olefin as product. The formation of the internal olefin can be achieved *via*  $\text{H}_{\text{int}}$  elimination with the less sterically hindered  $\text{Fe}(\text{OTf})_3\text{L10}$  complex at higher reaction temperatures. The unexpected formation of indane byproducts when using some electron



rich  $\alpha$ -methylstyrenes can be attributed to a rapid intramolecular Friedel Crafts reaction from intermediate **55**. However, this Friedel-Crafts reactivity is substrate dependent and thus, it was not observed with more electron deficient substrates.



**Scheme 20.** Proposed reaction mechanism for the iron catalyzed olefin dimerisation.

#### 7.4. Conclusions

A facile and regioselective method for the linear dimerisation of  $\alpha$ -methylstyrenes is presented. For the first time, a variety of substrates were covered with the dimers being generated with good to excellent yields. Moreover, by modifying the bulkiness of the *N*-

donor ligand, good to moderate regiocontrol of the double bond position of the resulting dimers was also achieved.

## 7.5. Experimental section

### 7.5.1 General techniques

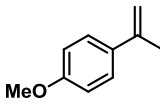
Unless otherwise specified, alkene substrates and the chemicals used in the synthesis of non commercially available substrates were purchased from commercial suppliers and used without further purification. Solvents used in these experiments were reagent grade or better. MeCN, DCM, DCE and CHCl<sub>3</sub> were refluxed over CaH<sub>2</sub> and THF and Et<sub>2</sub>O were refluxed over Na/benzophenone and distilled under purified N<sub>2</sub> atmosphere. Anhydrous benzene 99.9% was purchased from Aldrich and stored over CaH<sub>2</sub> under N<sub>2</sub> atmosphere. Experiments involving air or moisture sensitive reagents were performed under an atmosphere of purified N<sub>2</sub> using standard Schlenk techniques.

### 7.5.2. Substrate syntheses

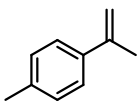
Non commercially available styrenes were synthesised via ketone methylenation according to the experimental procedure described in Chapter 6.

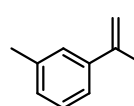
#### Analytical data

##### 1-Methoxy-4-(prop-1-en-2-yl)benzene<sup>13</sup>

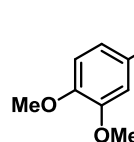
 Colourless liquid. Yield: 77%. <sup>1</sup>H NMR (400 MHz, CDCl<sub>3</sub>): δ (ppm) = 7.43 (d, J= 7.6 Hz, 2H), 6.87 (d, J= 7.6 Hz, 2H), 5.28 (t, J= 0.8 Hz, 1H), 4.99 (q, J= 1.2 Hz, 1H), 3.81 (s, 3H), 2.12 (s, 3H). <sup>13</sup>C NMR (100 MHz, CDCl<sub>3</sub>): δ (ppm) = 159.8, 142.6, 133.7, 126.9, 113.9, 111.0, 55.6, 22.3.

##### 1-Methyl-4-(prop-1-en-2-yl)benzene<sup>13</sup>

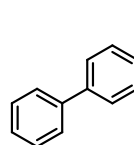
 Colourless liquid. Yield: 97%. <sup>1</sup>H NMR (400 MHz, CDCl<sub>3</sub>): δ (ppm) = 7.38-7.35 (m, 2H), 7.14-7.12 (m, 2H), 5.33 (t, J= 0.8 Hz, 1H), 5.03 (q, J= 1.0 Hz, 1H), 2.34 (s, 3H), 2.13 (s, 3H). <sup>13</sup>C NMR (100 MHz, CDCl<sub>3</sub>): δ (ppm) = 143.5, 138.7, 137.5, 129.3, 125.7, 111.9, 22.2, 21.4.

**1-Methyl-3-(prop-1-en-2-yl)benzene<sup>14</sup>**

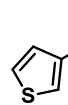
Colourless liquid. Yield: 89%. <sup>1</sup>H NMR (400 MHz, CDCl<sub>3</sub>): δ (ppm) = 7.28-7.20 (m, 3H), 7.09-7.07 (m, 1H), 5.34 (q, J= 0.8 Hz, 1H), 5.06 (q, J= 1.2 Hz, 1H), 2.36 (s, 3H), 2.14 (s, 3H). <sup>13</sup>C NMR (100 MHz, CDCl<sub>3</sub>): δ (ppm) = 143.8, 141.6, 138.1, 128.6, 128.5, 126.6, 123.0, 112.6, 23.0, 22.2.

**1,2-Dimethoxy-4-(prop-1-en-2-yl)benzene<sup>15</sup>**

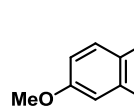
Colourless liquid. Yield: 98%. <sup>1</sup>H NMR (400 MHz, CDCl<sub>3</sub>): δ (ppm) = 7.26-7.01 (m, 2H), 6.83 (t, J= 4.4 Hz, 1H), 5.29 (d, J= 0.4 Hz, 1H), 5.01 (t, J= 1.2 Hz, 1H), 3.91 (s, 3H), 3.89 (s, 3H), 2.14 (s, 3H). <sup>13</sup>C NMR (100 MHz, CDCl<sub>3</sub>): δ (ppm) = 157.9, 158.7, 142.5, 133.8, 126.8, 113.7, 110.9, 55.8, 55.6, 22.3.

**4-(Prop-1-en-2-yl)-1,1'-biphenyl<sup>16</sup>**

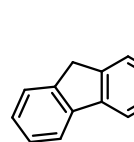
White solid. Yield: 92%. <sup>1</sup>H NMR (400 MHz, CDCl<sub>3</sub>): δ (ppm) = 7.62-7.46 (m, 6H), 7.46-7.41 (m, 2H), 7.36-7.32 (m, 1H), 5.43 (q, J= 0.8 Hz, 1H), 5.11 (q, J= 1.6 Hz, 1H), 2.19 (s, 3H). <sup>13</sup>C NMR (100 MHz, CDCl<sub>3</sub>): δ (ppm) = 143.1, 140.8, 140.2, 129.1, 127.6, 127.4, 127.3, 126.3, 112.8, 22.2.

**3-(Prop-1-en-2-yl)thiophene<sup>17</sup>**

Colourless liquid. Yield: 97%. <sup>1</sup>H NMR (400 MHz, CDCl<sub>3</sub>): δ (ppm) = 7.17 (dd, J= 5.2, 1.2 Hz, 1H), 7.03 (dd, J= 3.6, 1.2 Hz, 1H), 6.97 (dd, J= 5.2, 3.6 Hz, 1H), 5.37 (s, 1H), 4.95 (t, J= 1.2 Hz, 1H), 2.15 (s, 3H). <sup>13</sup>C NMR (100 MHz, CDCl<sub>3</sub>): δ (ppm) = 145.8, 137.2, 127.3, 124.2, 123.5, 111.2, 21.8.

**2-Methoxy-6-(prop-1-en-2-yl)naphthalene<sup>18</sup>**

White solid. Yield: 96%. <sup>1</sup>H NMR (400 MHz, CDCl<sub>3</sub>): δ (ppm) = 7.79 (s, 1H), 7.74-7.63 (m, 3H), 7.26-7.12 (m, 2H), 5.49 (s, 1H), 5.14 (d, J= 1.2 Hz, 1H), 3.92 (s, 3H), 2.25 (s, 3H). <sup>13</sup>C NMR (100 MHz, CDCl<sub>3</sub>): δ (ppm) = 157.0, 142.6, 139.4, 138.9, 130.1, 129.1, 126.9, 124.7, 124.5, 119.2, 112.5, 106.0, 55.7, 22.2.

**2-(Prop-1-en-2-yl)-9H-fluorene<sup>19</sup>**

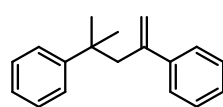
White solid. Yield: 76%. <sup>1</sup>H NMR (400 MHz, CDCl<sub>3</sub>): δ (ppm) = 7.78-7.72 (m, 2H), 7.66 (s, 1H), 7.55-7.49 (m, 2H), 7.39-7.31 (m, 1H), 7.29-7.26 (m, 1H), 5.43 (d, J= 0.8 Hz, 1H), 5.10 (t, J= 1.6 Hz, 1H), 3.91 (s, 2H), 2.22 (s, 3H). <sup>13</sup>C NMR (100 MHz, CDCl<sub>3</sub>): δ (ppm) = 143.1, 143.0, 142.7, 141.0, 140.6, 140.2, 127.1, 127.0, 126.3, 125.4, 122.5, 120.2, 119.9, 112.5, 37.3, 22.5.

### 7.5.3. Representative procedure for the iron-catalysed regioselective dimerisation of $\alpha$ -methylstyrenes

In a Radley's tube equipped with a stirring bar, ligand **L9** (9.1 mg, 0.01 mmol) and  $\text{Fe}(\text{OTf})_3$  (5.0 mg, 0.01 mmol) were added. The tube was sealed, degassed and left under  $\text{N}_2$  atmosphere (3 times). Freshly distilled DCM (2.0 mL) was added by syringe and the catalyst was allowed to form in situ upon stirring at  $40^\circ\text{C}$  for 1 h. Then, the tube was cooled to r.t. and  $\alpha$ -methylstyrene (40  $\mu\text{L}$ , 0.3 mmol) was added by syringe. The tube was stirred overnight at r.t. and conversion was calculated from  $^1\text{H}$  NMR analysis. The reaction products were purified by silica gel column chromatography (Hexane/EtOAc, gradient: 20/1) to afford the unreacted starting material and the desired products.

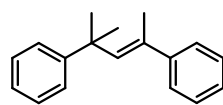
#### Analytical data

##### (4-Methylpent-1-ene-2,4-diyl)dibenzene<sup>20</sup>



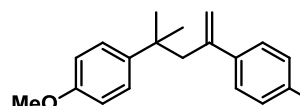
Colourless oil, 55% yield (**L9**).  $^1\text{H}$  NMR (400 MHz,  $\text{CDCl}_3$ ):  $\delta$  (ppm) = 7.42-7.09 (m, 10H), 5.13 (d,  $J=2.0$  Hz, 1H), 4.78 (d,  $J=2.0$  Hz, 1H), 2.83 (s, 2H), 1.21 (s, 3H).  $^{13}\text{C}$  NMR (100 MHz,  $\text{CDCl}_3$ ):  $\delta$  (ppm) = 150.5, 149.2, 145.4, 127.2, 127.1, 127.0, 125.8, 125.7, 125.5, 125.1, 124.9, 124.8, 124.4, 115.9, 56.1, 40.0, 29.5, 28.7. MS (ESI)  $m/z$  calc'd  $\text{C}_{18}\text{H}_{21}$   $[\text{M} + \text{H}]^+$ : 237.3, found: 237.3.

##### (4-Methylpent-2-ene-2,4-diyl)benzene<sup>21</sup>

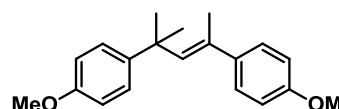


Colourless oil, 65% yield (**L10**).  $^1\text{H}$  NMR (400 MHz,  $\text{CDCl}_3$ ):  $\delta$  (ppm) = 7.51-7.21 (m, 10H), 6.12 (s, 1H), 2.78 (s, 3H), 1.68 (s, 6H).  $^{13}\text{C}$  NMR (100 MHz,  $\text{CDCl}_3$ ):  $\delta$  (ppm) = 150.7, 144.8, 138.7, 128.0, 127.7, 126.2, 125.9, 125.0, 49.6, 31.6, 31.4, 17.2. MS (ESI)  $m/z$  calc'd  $\text{C}_{18}\text{H}_{21}$   $[\text{M} + \text{H}]^+$ : 237.3, found: 237.3.

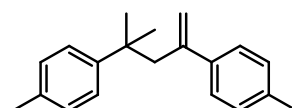
##### 4,4'-(4-Methylpent-1-ene-2,4-diyl)bis(methoxybenzene)<sup>22</sup>



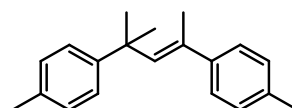
Colourless oil, 22% yield (**L9**).  $^1\text{H}$  NMR (400 MHz,  $\text{CDCl}_3$ ):  $\delta$  (ppm) = 7.2-7.16 (m, 4H), 6.77-6.75 (m, 4H), 5.08 (d,  $J=2.0$  Hz, 1H), 4.70 (d,  $J=2.0$  Hz, 1H), 3.78 (s, 3H), 3.77 (s, 3H), 2.16 (s, 2H), 1.55 (s, 6H).  $^{13}\text{C}$  NMR (100 MHz,  $\text{CDCl}_3$ ):  $\delta$  (ppm) = 157.6, 142.1, 135.8, 127.9, 127.1, 115.8, 113.5, 55.7, 50.2, 38.4, 32.1. MS (ESI)  $m/z$  calc'd  $\text{C}_{20}\text{H}_{25}\text{O}_2$   $[\text{M} + \text{H}]^+$ : 297.1, found: 297.1.

**4,4'-(4-Methylpent-2-ene-2,4-diyl)bis(methoxybenzene)**

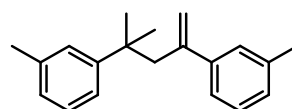
Colourless oil, 65% yield (**L9**).  $^1\text{H NMR}$  (400 MHz,  $\text{CDCl}_3$ ):  $\delta$  (ppm) = 7.33-7.29 (m, 4H), 6.86-6.75 (m, 4H), 6.03 (d,  $J=2.0$  Hz, 1H), 3.80 (s, 3H), 3.79 (s, 3H), 1.47 (s, 6H), 1.19 (s, 3H).  $^{13}\text{C NMR}$  (100 MHz,  $\text{CDCl}_3$ ):  $\delta$  (ppm) = 159.0, 143.2, 137.8, 127.5, 127.3, 113.9, 113.8, 55.6, 39.7, 32.0, 17.5. **MS** (ESI)  $m/z$  calc'd  $\text{C}_{20}\text{H}_{25}\text{O}_2$   $[\text{M} + \text{H}]^+$ : 297.2, found: 297.2.

**4,4'-(4-Methylpent-1-ene-2,4-diyl)bis(methylbenzene)<sup>23</sup>**

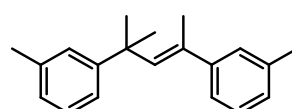
Colourless liquid, 21% yield (**L9**).  $^1\text{H NMR}$  (400 MHz,  $\text{CDCl}_3$ ):  $\delta$  (ppm) = 7.24-7.16 (m, 4H), 7.06-7.04 (m, 4H), 5.12 (d,  $J=2.0$  Hz, 1H), 4.80 (d,  $J=2.0$  Hz, 1H), 2.78 (s, 2H), 2.33 (s, 3H), 2.32 (s, 3H), 1.53 (s, 6H).  $^{13}\text{C NMR}$  (100 MHz,  $\text{CDCl}_3$ ):  $\delta$  (ppm) = 145.6, 139.8, 137.2, 135.4, 130.1, 129.2, 129.1, 126.7, 126.1, 40.0, 29.1, 21.4, 21.3, 17.6. **MS** (ESI)  $m/z$  calc'd  $\text{C}_{20}\text{H}_{25}$   $[\text{M} + \text{H}]^+$ : 265.2, found: 265.2.

**4,4'-(4-Methylpent-2-ene-2,4-diyl)bis(methylbenzene)**

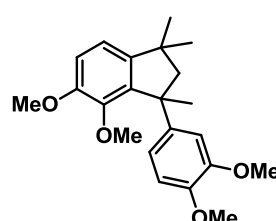
Colourless liquid, 61% yield (**L9**).  $^1\text{H NMR}$  (400 MHz,  $\text{CDCl}_3$ ):  $\delta$  (ppm) = 7.30-7.27 (m, 4H), 7.12-7.08 (m, 4H), 6.08 (d,  $J=2.0$  Hz, 1H), 2.30 (s, 3H), 2.29 (s, 3H), 1.55 (s, 3H), 1.48 (s, 6H).  $^{13}\text{C NMR}$  (100 MHz,  $\text{CDCl}_3$ ):  $\delta$  (ppm) = 147.9, 142.4, 138.4, 136.6, 136.3, 135.0, 129.2, 126.4, 126.0, 40.0, 29.1, 23.0, 14.5. **MS** (ESI)  $m/z$  calc'd  $\text{C}_{20}\text{H}_{25}$   $[\text{M} + \text{H}]^+$ : 265.2, found: 265.2.

**3,3'-(4-Methylpent-1-ene-2,4-diyl)bis(methylbenzene)**

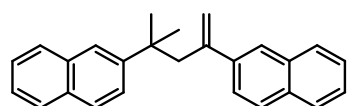
White solid, 50% yield (**L9**).  $^1\text{H NMR}$  (400 MHz,  $\text{CDCl}_3$ ):  $\delta$  (ppm) = 7.20-6.86 (m, 8H), 5.13 (d,  $J=2.0$  Hz, 1H), 4.80 (d,  $J=2.0$  Hz, 1H), 2.80 (s, 2H), 2.32 (s, 6H), 1.21 (s, 6H).  $^{13}\text{C NMR}$  (100 MHz,  $\text{CDCl}_3$ ):  $\delta$  (ppm) = 147.6, 137.7, 137.4, 128.4, 128.1, 127.9, 127.7, 127.6, 127.2, 126.9, 126.5, 124.0, 123.3, 116.9, 50.0, 38.8, 29.1, 22.1. **MS** (ESI)  $m/z$  calc'd  $\text{C}_{20}\text{H}_{25}$   $[\text{M} + \text{H}]^+$ : 265.2, found: 265.2.

**3,3'-(4-Methylpent-2-ene-2,4-diyl)bis(methylbenzene)**

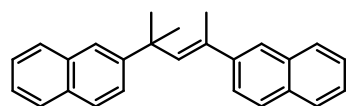
White solid, 26% yield (**L9**).  $^1\text{H NMR}$  (400 MHz,  $\text{CDCl}_3$ ):  $\delta$  (ppm) = 7.25-6.87 (m, 8H), 6.09 (s, 1H), 2.34 (s, 3H), 2.32 (s, 3H), 1.56 (s, 3H), 1.53 (s, 6H).  $^{13}\text{C NMR}$  (100 MHz,  $\text{CDCl}_3$ ):  $\delta$  (ppm) = 149.1, 138.6, 137.8, 129.88, 128.0, 127.8, 126.8, 126.3, 123.6, 123.3, 40.0, 28.7, 21.4, 21.2, 17.2. **MS** (ESI)  $m/z$  calc'd  $\text{C}_{20}\text{H}_{25}$   $[\text{M} + \text{H}]^+$ : 265.2, found: 265.2.

**3-(3,4-Dimethoxyphenyl)-4,5-dimethoxy-1,1,3-trimethyl-2,3-dihydro-1H-indene**

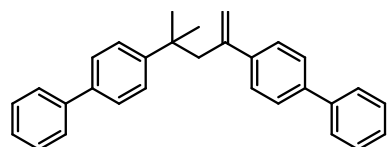
Colourless oil, 99% yield (**L9**).  $^1\text{H NMR}$  (400 MHz,  $\text{CDCl}_3$ ):  $\delta$  (ppm) = 6.76-6.6 (m, 5H), 3.9 (s, 3H), 3.85 (s, 3H), 3.83 (s, 3H), 3.76 (s, 3H), 2.34 (d,  $J=12.8$  Hz, 1H), 2.17 (d,  $J=12.7$  Hz, 1H), 1.66 (s, 3H), 1.32 (s, 3H), 1.05 (s, 3H).  $^{13}\text{C NMR}$  (100 MHz,  $\text{CDCl}_3$ ):  $\delta$  (ppm) = 149.2, 148.8, 148.7, 147.2, 144.4, 144.3, 140.6, 119.0, 110.9, 107.8, 105.6, 60.2, 56.5, 56.3, 56.2, 50.7, 43.1, 31.2, 30.9. **MS** (ESI)  $m/z$  calc'd  $\text{C}_{22}\text{H}_{29}\text{O}_4$   $[\text{M} + \text{H}]^+$ : 357.2, found: 357.2.

**2,2'-(4-Methylpent-1-ene-2,4-diyl)dinaphthalene**

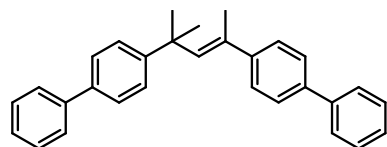
White solid, 70% yield (**L9**).  $^1\text{H NMR}$  (400 MHz,  $\text{CDCl}_3$ ):  $\delta$  (ppm) = 7.84-7.63 (m, 7H), 7.53-7.37 (m, 7H), 5.24 (d,  $J$ = 2.0 Hz, 1H), 4.88 (d,  $J$ = 2.0 Hz, 1H), 3.03 (s, 2H), 1.54 (s, 6H).  $^{13}\text{C NMR}$  (100 MHz,  $\text{CDCl}_3$ ):  $\delta$  (ppm) = 149.3, 148.7, 142.3, 134.6, 132.4, 128.3, 128.2, 127.9, 127.8, 127.7, 127.6, 126.3, 126.0, 125.9, 125.5, 125.4, 124.4, 117.8, 49.7, 39.4, 29.2. **MS** (ESI)  $m/z$  calc'd  $\text{C}_{26}\text{H}_{25}$   $[\text{M} + \text{H}]^+$ : 337.5, found: 337.5.

**2,2'-(4-Methylpent-2-ene-2,4-diyl)dinaphthalene**

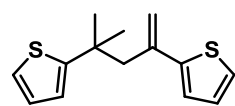
White solid, 86% yield (**L10**).  $^1\text{H NMR}$  (400 MHz,  $\text{CDCl}_3$ ):  $\delta$  (ppm) = 7.87-7.62 (m, 7H), 7.59-7.07 (m, 7H), 6.35 (d,  $J$ = 2.0 Hz, 1H), 2.07 (s, 3H), 1.65 (s, 6H).  $^{13}\text{C NMR}$  (100 MHz,  $\text{CDCl}_3$ ):  $\delta$  (ppm) = 149.0, 143.1, 133.4, 132.6, 130.1, 129.2, 129.1, 128.5, 128.4, 127.8, 126.7, 126.2, 125.9, 125.7, 125.4, 124.9, 123.9, 121.7, 41.7, 31.8, 21.3. **MS** (ESI)  $m/z$  calc'd  $\text{C}_{26}\text{H}_{25}$   $[\text{M} + \text{H}]^+$ : 337.5, found: 337.5.

**4,4'-(4-Methylpent-1-ene-2,4-diyl)di-1,1'-biphenyl<sup>24</sup>**

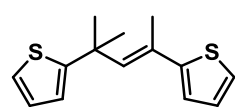
White solid, 60% yield (**L10, r.t.**).  $^1\text{H NMR}$  (400 MHz,  $\text{CDCl}_3$ ):  $\delta$  (ppm) = 7.65-7.12 (m, 18H), 5.21 (s, 1H), 4.89 (s, 1H), 2.89 (s, 2H), 1.31 (s, 6H).  $^{13}\text{C NMR}$  (100 MHz,  $\text{CDCl}_3$ ):  $\delta$  (ppm) = 150.0, 148.6, 141.3, 141.2, 139.1, 138.6, 129.1, 129.0, 127.5, 127.4, 127.3, 127.2, 126.9, 126.8, 126.5, 117.2, 50.3, 40.3, 29.1. **MS** (ESI)  $m/z$  calc'd  $\text{C}_{30}\text{H}_{29}$   $[\text{M} + \text{H}]^+$ : 389.2, found: 389.2.

**4,4'-(4-Methylpent-2-ene-2,4-diyl)di-1,1'-biphenyl<sup>24</sup>**

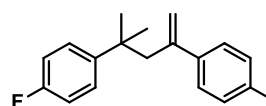
White solid, 52% yield (**L10, 35 °C**).  $^1\text{H NMR}$  (400 MHz,  $\text{CDCl}_3$ ):  $\delta$  (ppm) = 7.63-7.23 (m, 18H), 6.23 (d,  $J$ = 2.0 Hz, 1H), 1.65 (s, 3H), 1.32 (s, 6H).  $^{13}\text{C NMR}$  (100 MHz,  $\text{CDCl}_3$ ):  $\delta$  (ppm) = 148.6, 146.8, 142.5, 141.3, 139.8, 139.1, 129.1, 129.0, 127.5, 127.4, 127.3, 127.2, 126.9, 126.8, 126.5, 38.7, 32.0, 17.6. **MS** (ESI)  $m/z$  calc'd  $\text{C}_{30}\text{H}_{29}$   $[\text{M} + \text{H}]^+$ : 389.2, found: 389.2.

**2,2'-(4-Methylpent-1-ene-2,4-diyl)dithiophene**

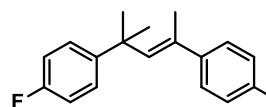
Pale yellow liquid, 87% yield (**L9**).  $^1\text{H NMR}$  (400 MHz,  $\text{CDCl}_3$ ):  $\delta$  (ppm) = 7.14-7.10 (m, 2H), 6.90-6.84 (m, 2H), 6.80 (d,  $J$ = 3.6 Hz, 2H), 5.41 (s, 1H), 4.70 (s, 1H), 2.80 (s, 2H), 1.33 (s, 6H).  $^{13}\text{C NMR}$  (100 MHz,  $\text{CDCl}_3$ ):  $\delta$  (ppm) = 156.5, 148.8, 136.6, 127.6, 126.6, 124.3, 124.0, 123.6, 123.4, 122.9, 115.7, 51.0, 38.7, 30.3. **MS** (ESI)  $m/z$  calc'd  $\text{C}_{14}\text{H}_{17}\text{S}_2$   $[\text{M} + \text{H}]^+$ : 249.1, found: 249.1.

**2,2'-(4-Methylpent-2-ene-2,4-diyl)dithiophene**

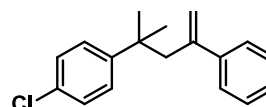
Pale yellow liquid, 61% yield (**L10, 35 °C**).  $^1\text{H NMR}$  (400 MHz,  $\text{CDCl}_3$ ):  $\delta$  (ppm) = 7.21-7.12 (m, 2H), 6.97-6.93 (m, 2H), 6.79-6.78 (m, 2H), 6.29 (s, 1H), 1.77 (s, 3H), 1.58 (s, 6H).  $^{13}\text{C NMR}$  (100 MHz,  $\text{CDCl}_3$ ):  $\delta$  (ppm) = 147.2, 136.6, 131.2, 126.7, 126.6, 124.0, 123.4, 123.0, 122.9, 122.7, 39.0, 33.2, 17.2. **MS** (ESI)  $m/z$  calc'd  $\text{C}_{14}\text{H}_{17}\text{S}_2$   $[\text{M} + \text{H}]^+$ : 249.1, found: 249.1.

**4,4'-(4-Methylpent-1-ene-2,4-diyl)bis(fluorobenzene)**

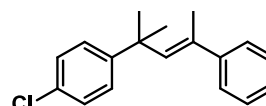
Colourless liquid, 45% yield.  $^1\text{H NMR}$  (400 MHz,  $\text{CDCl}_3$ ):  $\delta$  (ppm) = 7.19-7.09 (m, 4H), 6.90-6.83 (m, 4H), 5.08 (s, 1H), 4.77 (s, 1H), 2.77 (s, 2H), 1.22 (s, 6H).  $^{13}\text{C NMR}$  (100 MHz,  $\text{CDCl}_3$ ):  $\delta$  (ppm) = 160.0, 149.7, 143.8, 138.8, 128.4 ( $^3J_{\text{C-F}} = 7.8$  Hz), 127.6 ( $^3J_{\text{C-F}} = 7.8$  Hz), 115.2 ( $^2J_{\text{C-F}} = 11.4$  Hz), 115.0, 114.8 ( $^2J_{\text{C-F}} = 21.0$  Hz), 51.4, 38.6, 32.0. **MS** (ESI)  $m/z$  calc'd  $\text{C}_{18}\text{H}_{19}\text{F}_2$  [ $\text{M} + \text{H}$ ] $^+$ : 273.1, found: 273.1.

**4,4'-(4-Methylpent-2-ene-2,4-diyl)bis(fluorobenzene)**

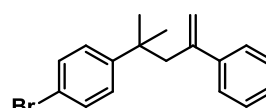
Colourless liquid, 65% yield.  $^1\text{H NMR}$  (400 MHz,  $\text{CDCl}_3$ ):  $\delta$  (ppm) = 7.37-7.30 (m, 4H), 7.01-6.99 (m, 2H), 6.98-6.83 (m, 2H), 6.04 (s, 1H), 1.58 (s, 3H), 1.53 (s, 6H).  $^{13}\text{C NMR}$  (100 MHz,  $\text{CDCl}_3$ ):  $\delta$  (ppm) = 161.0 ( $^1J_{\text{C-F}} = 253.0$  Hz), 143.0, 138.8, 136.0, 127.9 ( $^3J_{\text{C-F}} = 7.6$  Hz), 127.6 ( $^3J_{\text{C-F}} = 8.2$  Hz), 115.3 ( $^2J_{\text{C-F}} = 21.0$  Hz), 40.0, 29.4, 17.7. **MS** (ESI)  $m/z$  calc'd  $\text{C}_{18}\text{H}_{19}\text{F}_2$  [ $\text{M} + \text{H}$ ] $^+$ : 273.1, found: 273.1.

**4,4'-(4-Methylpent-1-ene-2,4-diyl)bis(chlorobenzene)**<sup>12</sup>

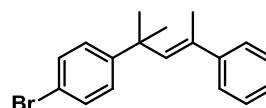
Colourless liquid, 48% yield.  $^1\text{H NMR}$  (400 MHz,  $\text{CDCl}_3$ ):  $\delta$  (ppm) = 7.18-7.07 (m, 8H), 5.11 (d,  $J = 2.0$  Hz, 1H), 4.79 (d,  $J = 2.0$  Hz, 1H), 2.76 (s, 2H), 1.20 (s, 6H).  $^{13}\text{C NMR}$  (100 MHz,  $\text{CDCl}_3$ ):  $\delta$  (ppm) = 147.7, 145.8, 141.9, 133.0, 131.7, 128.5, 128.2, 128.2, 128.1, 127.8, 117.9, 50.1, 38.8, 29.1. **MS** (ESI)  $m/z$  calc'd  $\text{C}_{18}\text{H}_{19}\text{Cl}_2$  [ $\text{M} + \text{H}$ ] $^+$ : 305.1, found: 305.1.

**4,4'-(4-Methylpent-2-ene-2,4-diyl)bis(chlorobenzene)**

Colourless liquid, 63% yield.  $^1\text{H NMR}$  (400 MHz,  $\text{CDCl}_3$ ):  $\delta$  (ppm) = 7.33-7.24 (m, 8H), 6.07 (s, 1H), 1.48 (s, 6H), 1.20 (s, 3H).  $^{13}\text{C NMR}$  (100 MHz,  $\text{CDCl}_3$ ):  $\delta$  (ppm) = 149.2, 143.3, 139.0, 136.0, 132.9, 131.6, 129.5, 128.5, 128.1, 127.4, 40.2, 31.7, 17.6. **MS** (ESI)  $m/z$  calc'd  $\text{C}_{18}\text{H}_{19}\text{Cl}_2$  [ $\text{M} + \text{H}$ ] $^+$ : 305.1, found: 305.1.

**4,4'-(4-Methylpent-1-ene-2,4-diyl)bis(bromobenzene)**<sup>12</sup>

Colourless liquid, 49% yield.  $^1\text{H NMR}$  (100 MHz,  $\text{CDCl}_3$ ):  $\delta$  (ppm) = 7.33-7.27 (m, 4H), 7.10-06 (m, 2H), 7.04-7.00 (m, 2H), 5.11 (d,  $J = 2.0$  Hz, 1H), 4.80 (d,  $J = 2.0$  Hz, 1H), 2.75 (s, 2H), 2.17 (s, 6H).  $^{13}\text{C NMR}$  (62.5 MHz,  $\text{CDCl}_3$ ):  $\delta$  (ppm) = 149.4, 145.8, 140.8, 132.5, 131.2, 128.7, 128.5, 128.0, 127.3, 116.5, 50.1, 38.5, 28.9. **MS** (ESI)  $m/z$  calc'd  $\text{C}_{18}\text{H}_{19}\text{Br}_2$  [ $\text{M} + \text{H}$ ] $^+$ : 395.0, found: 395.0.

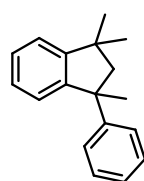
**4,4'-(4-Methylpent-2-ene-2,4-diyl)bis(bromobenzene)**

Colourless liquid, 68% yield.  $^1\text{H NMR}$  (100 MHz,  $\text{CDCl}_3$ ):  $\delta$  (ppm) = 7.43-7.39 (m, 4H), 7.28-7.21 (m, 4H), 6.07 (d,  $J = 2.0$  Hz, 1H), 1.53 (s, 6H), 1.20 (s, 3H).  $^{13}\text{C NMR}$  (62.5 MHz,  $\text{CDCl}_3$ ):  $\delta$  (ppm) = 148.9, 142.2, 132.5, 132.1, 130.7, 128.5, 127.4, 123.8, 122.8, 121.2, 40.2, 31.5, 17.4. **MS** (ESI)  $m/z$  calc'd  $\text{C}_{18}\text{H}_{19}\text{Br}_2$  [ $\text{M} + \text{H}$ ] $^+$ : 395.0, found: 395.0.

#### 7.5.4. Procedure for the protic and Lewis acid catalysed dimerisation of $\alpha$ -methylstyrene

In a vial equipped with a stirring bar, freshly distilled DCM (2.0 mL) and  $\alpha$ -methylstyrene (0.3 mmol, 40  $\mu$ L) were added. Bi(OTf)<sub>3</sub> (3 mol%, 6.8 mg) was added and the reaction was stirred at r.t. for 24h. The same procedure was repeated using triflic acid (3 mol%, 2  $\mu$ L) as catalyst and running both reactions at 40 °C. The reaction products were characterised by <sup>1</sup>H NMR.

#### 1,1,3-Trimethyl-3-phenyl-2,3-dihydro-1H-indene<sup>25</sup>



Colourless liquid, 100% yield. <sup>1</sup>H NMR (400 MHz, CDCl<sub>3</sub>):  $\delta$  (ppm) = 7.41-7.12 (m, 9H), 2.45 (d, J = 13.0 Hz, 1H), 2.24 (d, J = 13.0 Hz, 1H), 1.76 (s, 3H), 1.42 (s, 3H), 1.12 (s, 3H). <sup>13</sup>C NMR (100 MHz, CDCl<sub>3</sub>):  $\delta$  (ppm) = 152.2, 151.0, 148.7, 127.9, 127.1, 126.8, 126.6, 125.4, 125.0, 122.5, 59.2, 50.8, 42.8, 30.8, 30.6, 30.3. HRMS (EI) m/z calc'd C<sub>18</sub>H<sub>21</sub> [M + H]<sup>+</sup>: 237.1638, found: 237.1630.

#### 7.6. References

- [1] Skupinska, J. *Chem. Rev.* **1991**, *91*, 613.
- [2] Cabrero-Antonino, J. R., Leyva-Perez, A., Corma, A. *Adv. Synth. Catal.* **2010**, *352*, 1571.
- [3] <http://www.omgi.com/product-adv-poly.html> ,  
<http://www.siigroup.com/productinfo.asp?ID=353>
- [4] Selected examples: (a) Jimenez-Tenorio, M.; Puerta, M. C.; Salcedo, I.; Valerga, P.; de los Rios, I.; Mereiter, K. *Dalton Trans.* **2009**, 1842. (b) Campora, J.; Ortiz de la Tabla, L.; Palma, P.; Alvarez, E.; Lahoz, F.; Mereiter, K. *Organometallics* **2006**, *25*, 3314. (c) Li, W.; Sun, H.; Chen, M.; Wang, Z.; Hu, D.; Shen, Q.; Zhang, Y. *Organometallics* **2005**, *24*, 5925. (d) Buchowicz, W.; Koziol, A.; Jerzykiewicz, L. B.; Lis, T.; Pasynekiewicz, S.; Pecherzewska, A.; Pietrzykowski, A. *J. Mol. Catal. A: Chem.* **2006**, *257*, 118.



- [5] Himashigura, M., Imamura, K., Yokogawa, Y., Sakakibara, T. *Chem. Lett.* **33**, 728-729 (2004).
- [6] Petropoulos, J. C., Fischer, J.J. *J. Am. Chem. Soc.* **1958**, *80*, 1938.
- [7] Wolovsky, R., Maoz, N. *J. Org. Chem.* **1973**, *38*, 4040.
- [8] Ciminale, F., Lopez, L., Paradiso, V., Nacci, A. *Tetrahedron* **1996**, *52*, 13971.
- [9] Miyake, Y., Moriyama, T., Tanabe, Y., Onodera, G., Nishibayashi, Y. *Organometallics* **2011**, *30*, 5972.
- [10] Benitez Junquera, L., Puerta, M. C., Valerga, P. *Organometallics* **2012**, *31*, 2175.
- [11] Tsuchimoto, T., Kamiyama, S., Negoro, R., Shirakawa, E., Kawakami, Y. *Chem. Commun.* **2003**, 852.
- [12] Peppe, C., Schulz Lang, E., Molinos de Andrade, F., Borges de Castro, L., *Synlett* **2004**, *10*, 1723.
- [13] Bastug, G.; Nolan, S. P. *Organometallics* **2014**, *33*, 1253.
- [14] Hornback, J. M.; Barrows, R. D. *J. Org. Chem.* **1982**, *47*, 4285.
- [15] Flores-Gaspar, A.; Martin, R. *Adv. Synth. Catal.* **2011**, *353*, 1223.
- [16] Jiang, M.; Wei, Y.; Shin, M. *Eur. J. Org. Chem.* **2010**, *17*, 3307.
- [17] Gronowitz, E. *Chemica Scripta* **1874**, *5*, 217.
- [18] Lin, M.-Y.; Das, A.; Li, R.-S. *J. Am. Chem. Soc.* **2006**, *128*, 9340.
- [19] Hsieh, Y.-T.; Luh, T.-Y. *Heterocycles* **2000**, *52*, 1125.
- [20] Howard, F.; Sawadjoon, S.; Samec, J. S. M. *Tetrahedron Lett.* **2010**, *51*, 4208.
- [21] Kawakami, Y.; Toyashima, N.; Yamashita, Y. *Chem. Lett.* **1980**, 13.
- [22] Del Giacco, T.; Faltoni, A.; Elisei, F. *Phys. Chem. Chem. Phys.* **2008**, *10*, 200.
- [23] Morimoto, K.; Hirano, K.; Satoh, T.; Miura, M. *J. Org. Chem.* **2011**, *76*, 9548.
- [24] Miyake, Y.; Moriyama, T.; Tanabe, Y.; Onodera, G.; Nishibayashi, Y. *Organometallics* **2011**, *30*, 5972.
- [25] Lopez-Carrillo, V.; Echavarren, A. M. *J. Am. Chem. Soc.* **2010**, *132*, 9292.

## *Chapter 8*

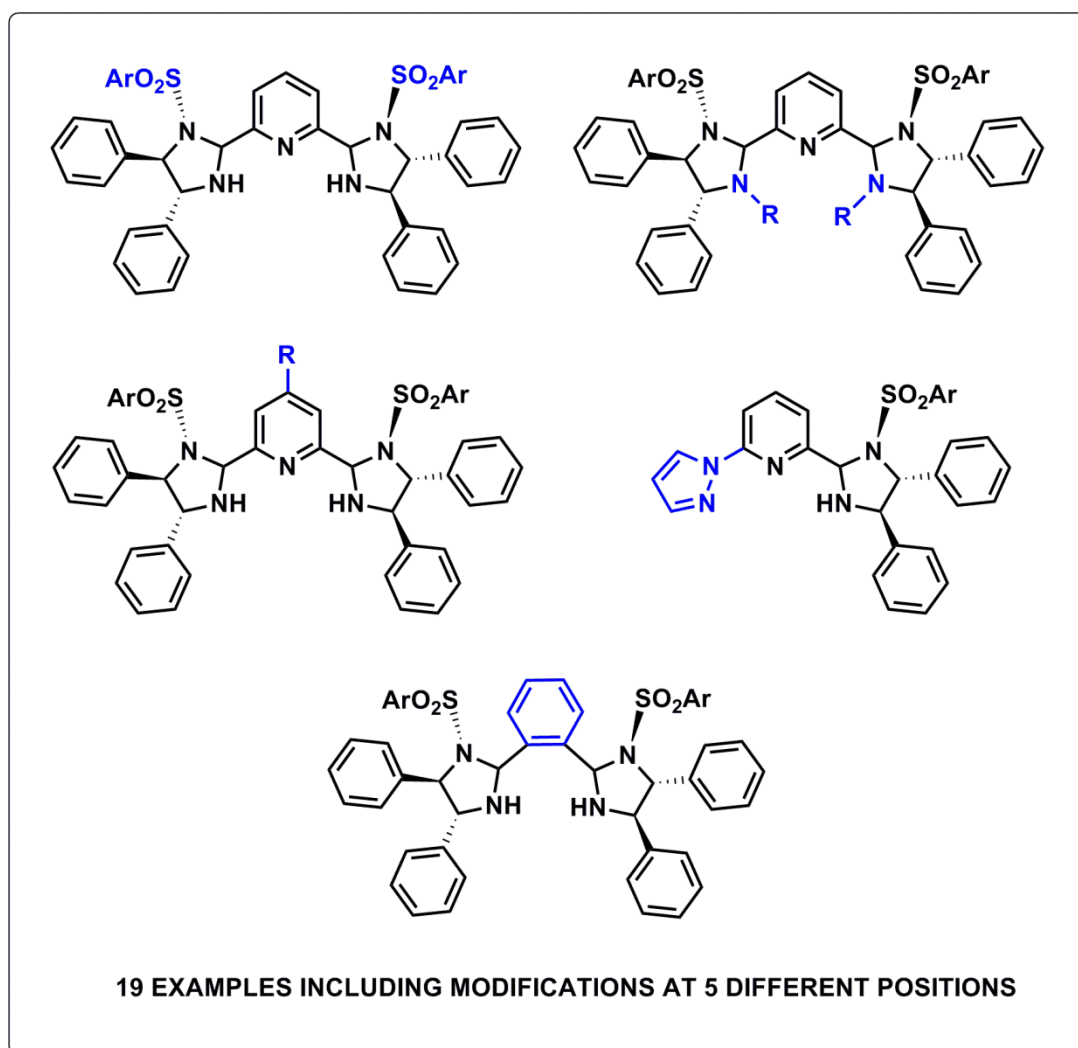
### **PERSPECTIVE AND FUTURE WORK**

### 8.1. General perspective of the Thesis

Selective oxidation has been highlighted as one of the most important areas of research in catalysis for future industrial applications in the “Technology Vision 2020: The Chemical Industry” report. Some of the most important goals of the report include methods for the selective oxidation and dehydrogenative oxidation of alkanes, methods for the selective oxidation of olefins and aromatics and for activating molecular oxygen.

This thesis covers our efforts in tackling some of the major issues affecting current oxidation methods in the field of iron catalysis. Most of the iron catalysts rely on the use of tetradentate *N*-donor ligands and require strong hydrogen peroxide as the oxidising agent in order to generate an iron-oxo species that ultimately acts as the real oxidant in the reaction. Thus, selectivity issues, poor functional group tolerance to electron rich functionalities (mainly ethers, aromatics, olefins, alcohols and amines) and poor mass balances are major limitations.

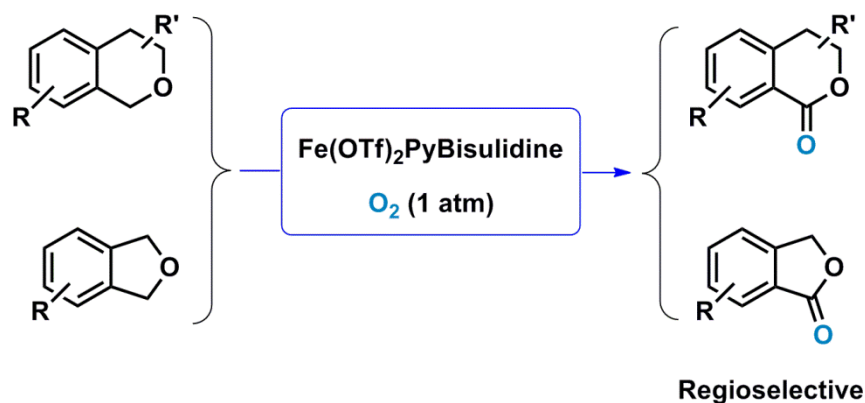
In this thesis, we have demonstrated that novel tridentate *N*-donor ligands incorporating electron-withdrawing sulfonamide groups can coordinate to commercial iron salts and facily tune its electrophilic properties, enhancing the ability of the iron centre for O<sub>2</sub> activation. An ample ligand library was created by selectively modifying the initial ligand skeleton, allowing control of the steric hindrance around the metal centre (Scheme 1).



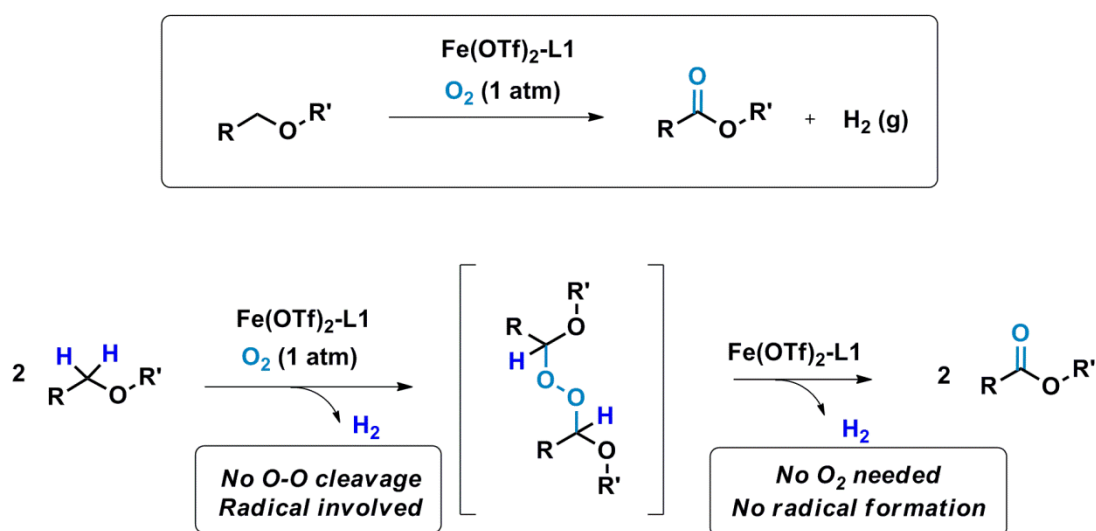
**Scheme 1.** Library of Pybisulidone type ligands presented in this thesis

Complexes of iron triflates bearing Pybisulidone ligands were found active for the selective  $\alpha$ -aerobic oxidation of ethereal substrates under very mild conditions. In particular, the oxidation of isochromans and phthalans was achieved with high efficiency, allowing the construction of synthetically useful isochromanones and phthalides (Scheme 2). To the best of our knowledge these iron complexes represent the first type of iron catalysts capable of highly selectively oxidising CH bonds in the presence of electron rich functionalities and one of the most efficient types of catalysts in activating dioxygen for oxidation reactions.

From a mechanistic perspective, evidence of an unprecedented two step mechanism involving the dehydrogenative oxygenation of two ethereal molecules to form a peroxybisether intermediate, followed by its dehydrogenative cleavage to afford two ester molecules was presented (Scheme 3). These mechanistic studies may have important implications in understanding biological oxygenases and in inspiring new biomimetic iron complex designs.



**Scheme 2.** Selective oxidation of isochromans and phthalans

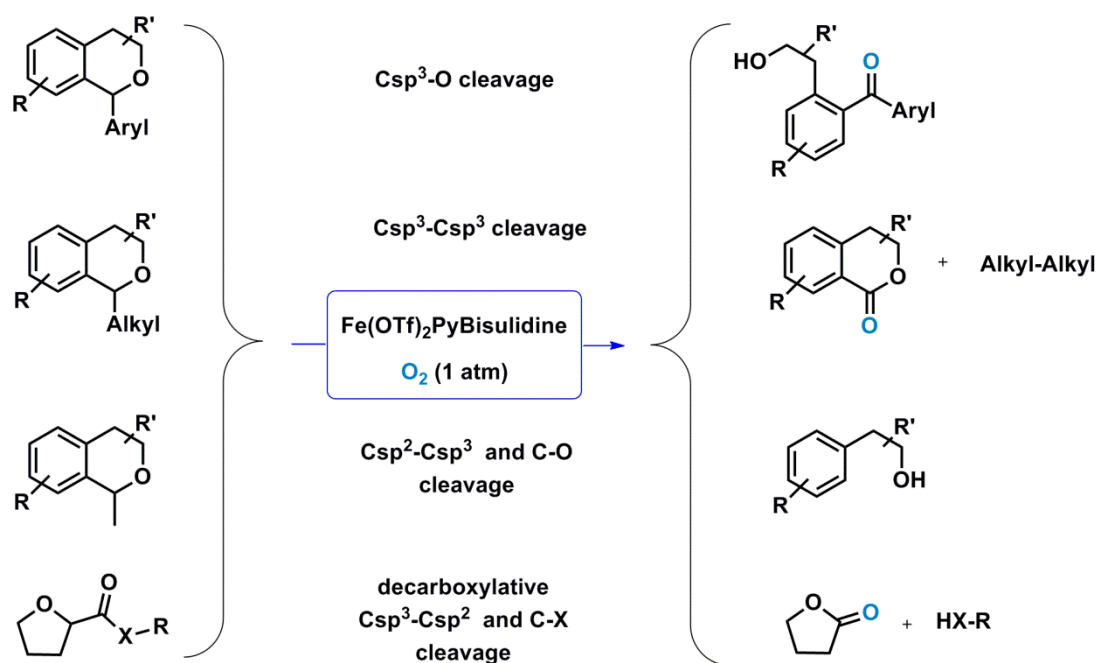


**Scheme 3.** Selective dehydrogenative oxygenation of ethers

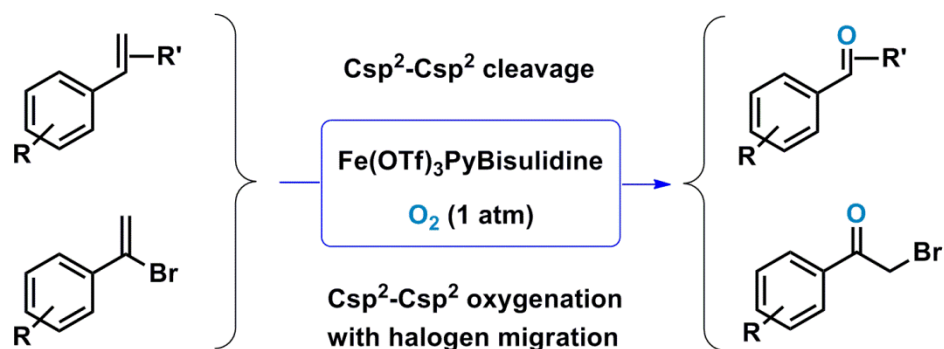
Natural oxygenases capable of selectively oxidise organic substrates are also capable of selectively cleaving C-C bonds under mild aerobic conditions. However, biomimetic iron complexes have been mainly used for selective oxidation reactions. In this thesis we have

demonstrated that the same family of iron-Pybisulidine complexes can selectively cleavage aliphatic C-O and C-C bonds of ethereal substrates under aerobic conditions (Scheme 4). Moreover, some of these reactions allow the formation of complex and/or valuable oxygenated compounds, highlighting the potential applicability of selective aerobic cleavages in organic synthesis.

The cleavage of olefinic C-C bonds to afford carbonyl compounds was also demonstrated, providing a greener and safer alternative to traditional ozonolysis (Scheme 5). To the best of our knowledge, this is the first iron catalysts capable of efficiently promoting the aerobic cleavage of olefinic bonds.



**Scheme 4.** Selective aerobic cleavage of aliphatic bonds



**Scheme 5.** Selective aerobic cleavage of olefinic bonds

## 8.2. Future work

An ample variety of iron-Pybisulidine aerobic transformations have been presented in this thesis. However, other challenging reactions, such as oxidation of unactivated CH bonds to alcohols and oxidation of aromatic rings to phenols are attractive transformations to investigate by other members of this group. Additionally, the modification of the ligand structure to improve its efficiency can be further explored for instance, by introducing tetradentate or asymmetric multidentate designs.

Additional investigations and computational studies on the reaction mechanisms of the oxidations presented in this thesis can be further continued in order to shed more light into the catalytic performance of iron-PyBisulidine complexes.

The discovery of the iron-Pybisulidine catalysed head-to-tail dimerisation of  $\alpha$ -methylstyrenes under inert atmosphere also indicates that this family of complexes may be capable of promoting other catalytic reactions in fields different from selective oxidation. Further investigations in the fields of enantioselective C-C bond forming reactions or reduction chemistry are other alternatives to explore in the future.

# **APPENDIX**



## 1. Additional X-ray diffraction data

### 1.1. Complex (S,S)-[Fe(BF<sub>4</sub>)(NNN)(MeCN)<sub>2</sub>](BF<sub>4</sub>) (20)

**Table 2. Fractional Atomic Coordinates ( $\times 10^4$ ) and Equivalent Isotropic Displacement Parameters ( $\text{\AA}^2 \times 10^3$ ) for (S,S)-20.  $U_{\text{eq}}$  is defined as 1/3 of the trace of the orthogonalised  $U_{\text{IJ}}$  tensor.**

Atom	<i>x</i>	<i>y</i>	<i>z</i>	$U(\text{eq})$
Fe1	3616.8(3)	5510.0(3)	8955.3(1)	15.6(1)
S1	2876.1(6)	9095.1(5)	8458.3(2)	22.8(2)
S2	4858.4(6)	2825.7(5)	7919.4(2)	17.9(2)
F1	1587.8(14)	5756.8(11)	8928.3(4)	27.5(5)
F2	33.8(17)	6846.1(13)	8941.6(5)	41.5(7)
F3	134.8(17)	5809.9(13)	9389.9(5)	35.2(6)
F4	1654.7(15)	6897.5(11)	9340.5(4)	25.5(5)
O1	3644.9(19)	9805.4(13)	8314.4(6)	26.2(6)
O2	1731.4(18)	8811.6(14)	8283.9(6)	33.2(7)
O3	4188.9(18)	2092.2(14)	7755.9(5)	25.0(6)
O4	5502.9(17)	3489.7(14)	7705.8(5)	22.7(6)
N1	3656.8(19)	5776.2(14)	8397.3(6)	15.4(6)
N2	3853.5(18)	7014.5(14)	8899.8(6)	15.5(7)
N3	3803.6(19)	8190.5(14)	8470.1(6)	16.4(6)
N4	3662(2)	4129.1(15)	8704.9(6)	15.9(6)
N5	3769(2)	3400.2(15)	8146.7(6)	16.4(7)
N6	5596(2)	5294.6(15)	9016.3(6)	20.8(8)
N7	3288(2)	5095.0(18)	9481.0(7)	27.1(8)
C1	3413(2)	6610.4(17)	8277.4(7)	15.4(8)
C2	3209(2)	7311.9(18)	8570.3(7)	17.6(8)
C3	5177(2)	7375.1(18)	8865.2(7)	15.6(8)
C4	5036(2)	8289.3(18)	8664.9(7)	16.4(8)
C5	2536(3)	9383(2)	8908.2(9)	31.9(10)
C6	1575(3)	8934(2)	9087.1(10)	41.2(11)
C7	1412(4)	9104(3)	9451.3(11)	52.7(14)
C8	2218(4)	9691(3)	9631.7(11)	52.0(14)
C9	3163(4)	10139(3)	9447.1(11)	45.7(12)
C10	3323(3)	9986(2)	9086.9(9)	35.4(11)
C11	2055(6)	9848(3)	10030.3(12)	74.3(19)
C12	6170(2)	8507.6(17)	8432.1(7)	17.3(8)
C13	6203(3)	8313.3(19)	8073.0(7)	21.1(8)
C14	7282(3)	8501(2)	7872.8(8)	25.2(9)
C15	8339(3)	8887(2)	8030.3(8)	27.6(9)
C16	8325(3)	9073(2)	8391.6(9)	27.2(9)

---

C17	7242(3)	8880.6(19)	8593.2(8)	23.5(9)
C18	5856(2)	7492.1(18)	9217.2(7)	17.5(8)
C19	7127(3)	7264(2)	9244.3(8)	22.3(9)
C20	7811(3)	7439(2)	9553.3(8)	28.3(10)
C21	7216(3)	7846(2)	9838.2(8)	32.1(10)
C22	5933(3)	8095(2)	9814.7(9)	32.9(10)
C23	5261(3)	7914(2)	9504.5(8)	25.6(9)
C24	3303(2)	6798.6(19)	7919.9(7)	19.5(8)
C25	3446(2)	6085.6(18)	7681.6(7)	19.3(8)
C26	3703(2)	5220.3(19)	7805.4(7)	19.1(8)
C27	3811(2)	5084.1(18)	8169.3(7)	14.5(8)
C28	4219(2)	4210.7(18)	8346.2(7)	15.7(8)
C29	2462(2)	3608.2(18)	8644.7(7)	15.5(8)
C30	2869(2)	2881.2(18)	8375.1(7)	17.0(8)
C31	5976(2)	2377.5(19)	8219.3(7)	19.4(8)
C32	5729(3)	1550(2)	8381.0(8)	25.3(9)
C33	6606(3)	1213(2)	8622.7(8)	30.9(10)
C34	7728(3)	1667(2)	8696.2(8)	28(1)
C35	7969(3)	2479(2)	8523.7(8)	25.1(9)
C36	7101(2)	2845(2)	8288.4(8)	22.0(9)
C37	8678(3)	1298(2)	8961.5(9)	40.5(11)
C38	1762(2)	2460.1(19)	8177.3(7)	18.6(8)
C39	1463(3)	1558(2)	8239.1(8)	27.2(9)
C40	428(3)	1162(2)	8065.9(9)	35.6(11)
C41	-296(3)	1665(3)	7835.6(9)	39.7(11)
C42	-16(3)	2564(2)	7774.2(8)	32.6(10)
C43	1018(3)	2972(2)	7948.0(8)	25.0(9)
C44	1890(2)	3261.6(18)	8984.3(7)	17.7(8)
C45	2485(3)	2629(2)	9196.8(8)	28.0(9)
C46	1937(3)	2362(2)	9517.6(9)	35.0(11)
C47	781(3)	2705(2)	9620.4(9)	34.7(11)
C48	182(3)	3340(3)	9409.4(9)	40.8(13)
C49	721(3)	3622(2)	9094.0(8)	28.6(10)
C50	6618(3)	5044.4(19)	9000.3(8)	22.0(9)
C51	7912(3)	4713(2)	8972.1(9)	30.5(10)
C52	3124(3)	4747(2)	9745.5(9)	36.4(11)
C53	2926(5)	4312(3)	10087(1)	61.3(16)
B1	833(3)	6333(2)	9156.3(9)	22.8(10)
N8	10401(4)	5206(3)	8167.3(13)	75.7(16)
C54	10017(3)	5927(3)	8152.5(10)	39.4(11)
C55	9538(3)	6832(2)	8134.4(9)	35.9(11)

N9	6816(3)	5588(3)	8187.6(9)	55.9(13)
C56	6974(3)	5440(3)	7894.7(10)	36.8(11)
C57	7177(3)	5259(2)	7520.9(9)	40.3(11)
F5	5622.6(16)	3072.5(12)	9057.0(5)	31.8(6)
F6	7107.3(18)	2890.0(16)	9490.9(6)	50.4(8)
F7	5108(2)	3339.5(14)	9632.9(5)	44.4(7)
F8	5478(2)	1895.4(13)	9448.0(6)	46.0(7)
B2	5841(3)	2796(3)	9409.6(10)	30.2(11)

**Table 3 Anisotropic Displacement Parameters ( $\text{\AA}^2 \times 10^3$ ) for (S,S)-20. The Anisotropic displacement factor exponent takes the form:  $2\pi^2[h^2a^{*2}U_{11}+2hka^*b^*U_{12}+\dots]$ .**

Atom	$U_{11}$	$U_{22}$	$U_{33}$	$U_{23}$	$U_{13}$	$U_{12}$
Fe1	17.7(2)	14.8(2)	14.1(2)	1.3(2)	0.5(2)	0.4(1)
S1	19.5(3)	17.0(4)	31.9(4)	5.7(3)	0.6(3)	4.4(3)
S2	17.9(3)	18.9(4)	16.9(3)	-2.9(3)	4.0(2)	1.3(2)
F1	20.9(8)	35(1)	26.5(9)	-5.6(8)	3.3(7)	0.2(7)
F2	35.1(10)	57.0(13)	32.5(11)	-2.5(10)	-5.5(9)	21.8(9)
F3	33.2(10)	43.0(12)	29.4(10)	-6.6(9)	13.8(8)	-14.5(8)
F4	24.2(9)	26.6(9)	25.8(9)	-7.9(7)	4.9(7)	-4.0(7)
O1	27(1)	18.8(11)	32.9(12)	7.0(9)	0.2(9)	4.0(8)
O2	21.5(10)	25.8(12)	52.4(15)	9.3(11)	-6.0(9)	3.7(8)
O3	23.8(10)	24.0(11)	27.3(12)	-10.2(9)	1.1(8)	1.4(8)
O4	22.6(10)	29.5(12)	16.1(10)	2.1(9)	4.7(8)	1.1(8)
N1	12.5(10)	17.6(12)	16.2(11)	1.9(9)	-0.1(9)	0.3(8)
N2	12.1(10)	17.4(12)	16.9(12)	0.5(9)	1.6(8)	0.8(8)
N3	15.1(10)	12.9(11)	21.3(12)	1.1(9)	0.6(9)	1.5(8)
N4	16.2(10)	18.1(11)	13.4(11)	3.7(9)	1.3(9)	-0.3(9)
N5	16.9(11)	15.0(12)	17.2(12)	-1.6(9)	3.4(9)	-1.0(9)
N6	19.7(12)	18.7(13)	24.0(14)	0.5(10)	-3.6(9)	-0.6(9)
N7	32.1(14)	29.4(14)	19.8(14)	4.9(12)	3.4(10)	2.3(11)
C1	12.4(12)	14.9(14)	19.0(14)	2.8(11)	0.1(10)	-2(1)
C2	17.6(13)	14.6(14)	20.7(14)	5.9(11)	0.7(10)	2.1(10)
C3	14.2(12)	15.9(14)	16.6(14)	0.9(11)	2.9(10)	1.7(10)
C4	17.0(12)	14.1(14)	18.2(14)	-0.6(11)	-0.6(10)	2.2(10)
C5	31.3(15)	27.6(18)	36.7(19)	7.6(15)	9.3(14)	13.1(13)
C6	47(2)	25.6(19)	51(2)	-2.0(16)	18.5(17)	10.3(15)
C7	68(3)	39(2)	51(2)	5.2(19)	31(2)	7(2)
C8	83(3)	27(2)	46(2)	-11.7(18)	13(2)	14.3(19)
C9	63(2)	29(2)	45(2)	-5.4(17)	2.6(19)	9.4(17)

C10	44.4(19)	23.7(18)	38(2)	-2.5(15)	5.7(15)	9.9(14)
C11	123(4)	48(3)	52(3)	-2(2)	29(3)	17(3)
C12	18.5(13)	11.1(13)	22.2(15)	3.1(11)	1.0(11)	1.4(9)
C13	18.2(13)	24.2(16)	20.9(15)	1.5(12)	-2.9(11)	-1.2(11)
C14	26.5(15)	28.6(17)	20.4(16)	5.1(13)	3.6(12)	1.7(12)
C15	22.8(14)	26.4(17)	33.5(18)	4.8(13)	8.1(12)	-2.6(12)
C16	22.2(14)	24.2(16)	35.1(18)	-1.1(14)	0.1(12)	-7.8(12)
C17	24.9(14)	20.9(16)	24.8(16)	1.0(12)	1.4(11)	-2.2(11)
C18	19.9(13)	14.9(15)	17.7(14)	3.7(11)	0.5(10)	0.2(10)
C19	22.1(14)	21.1(16)	23.6(16)	-3.6(12)	2.5(11)	-1.0(11)
C20	19.8(14)	36.9(19)	28.3(17)	0.2(14)	-4.6(12)	2.9(12)
C21	32.3(16)	44(2)	20.1(16)	-0.9(15)	-7.0(12)	1.0(14)
C22	31.0(17)	48(2)	19.8(16)	-2.8(15)	1.0(12)	0.8(14)
C23	19.3(14)	35.2(18)	22.2(16)	-0.9(13)	-0.3(11)	3.9(12)
C24	18.6(13)	16.3(14)	23.6(15)	5.9(12)	-1.4(11)	-1.4(10)
C25	19.1(13)	25.0(16)	13.7(13)	2.0(11)	0.2(10)	-3.6(11)
C26	17.1(12)	25.5(15)	14.6(13)	-2.3(11)	1.6(10)	-2.9(11)
C27	9.8(11)	16.2(14)	17.6(14)	-0.4(11)	1.2(10)	-3.0(9)
C28	16.6(12)	16.8(14)	13.8(14)	-1.2(11)	2.9(10)	-2.1(10)
C29	15.6(12)	13.5(14)	17.5(14)	0.2(11)	0.6(10)	1.1(9)
C30	18.2(12)	16.5(14)	16.4(14)	-0.3(11)	2.2(10)	-0.2(10)
C31	20.0(13)	22.1(16)	16.0(14)	-2.2(12)	3.9(10)	7.1(10)
C32	27.1(15)	18.2(16)	30.7(17)	-2.8(13)	4.4(13)	3.9(12)
C33	38.2(18)	21.1(17)	33.5(18)	5.8(14)	8.9(14)	10.2(13)
C34	31.6(16)	29.6(18)	22.9(16)	-3.0(14)	1.7(13)	12.9(13)
C35	23.3(14)	30.6(17)	21.3(16)	-6.4(13)	2.9(11)	2.5(12)
C36	22.1(14)	21.7(16)	22.2(15)	-2.8(12)	5.2(11)	3.7(11)
C37	42.1(18)	44(2)	35.4(19)	6.4(17)	-5.6(17)	14.0(16)
C38	16.1(12)	21.0(15)	18.8(14)	-5.9(12)	5.8(10)	-3.8(10)
C39	24.8(14)	26.7(17)	30.1(17)	-5.1(13)	8.1(13)	-2.2(13)
C40	30.1(16)	30.6(19)	46(2)	-16.2(16)	12.8(15)	-14.4(14)
C41	24.2(16)	57(2)	38(2)	-23.2(18)	7.9(14)	-15.7(15)
C42	20.3(14)	55(2)	22.6(16)	-8.1(15)	0.4(12)	-1.1(14)
C43	22.6(14)	32.3(18)	20.2(16)	-4.7(13)	4.7(11)	-1.7(12)
C44	19.0(12)	16.6(14)	17.5(14)	-0.3(12)	0.6(10)	-3.8(10)
C45	31.5(15)	26.3(17)	26.1(17)	5.1(13)	7.7(12)	7.6(13)
C46	52(2)	27.4(19)	25.6(18)	9.4(14)	1.6(14)	4.0(15)
C47	38.6(17)	41(2)	24.4(18)	10.0(16)	9.0(14)	-8.4(15)
C48	25.0(16)	65(3)	32.4(19)	12.1(18)	8.1(14)	2.3(16)
C49	20.2(14)	42(2)	23.7(16)	9.0(14)	2.5(12)	5.0(13)
C50	24.6(15)	18.1(15)	23.2(16)	-1.0(12)	-5.7(12)	0.0(11)

C51	20.9(14)	33.8(18)	36.9(18)	-2.1(15)	-3.8(13)	4.8(12)
C52	45.4(19)	33(2)	30.7(19)	0.3(15)	3.2(15)	6.1(14)
C53	95(3)	60(3)	29(2)	8(2)	13(2)	5(2)
B1	20.5(15)	29(2)	19.0(18)	-1.5(15)	2.5(12)	2.1(13)
N8	60(2)	46(2)	121(4)	15(2)	-20(2)	15.5(18)
C54	31.1(17)	43(2)	44(2)	6.3(18)	-10.7(15)	-3.6(16)
C55	46(2)	29.7(19)	31.9(19)	4.0(15)	-1.6(15)	-3.3(14)
N9	35.8(16)	97(3)	34.9(19)	10(2)	-2.0(13)	-24.1(17)
C56	21.5(14)	49(2)	40(2)	17.4(18)	-3.3(14)	-12.4(14)
C57	42.9(19)	42(2)	36(2)	8.4(16)	10.8(16)	-0.6(16)
F5	35.8(9)	35.9(11)	23.8(10)	9.0(8)	5.2(7)	13.6(8)
F6	32.1(11)	73.5(16)	45.6(13)	10.3(12)	-4.6(9)	-1.1(10)
F7	55.0(12)	51.7(13)	26.5(11)	2.8(10)	6.2(9)	19.6(10)
F8	57.9(13)	31.9(12)	48.2(13)	15.7(10)	-1.8(10)	-0.4(9)
B2	28.6(18)	36(2)	26(2)	9.7(17)	3.2(14)	8.0(15)

**Table 4 Bond Lengths for (S,S)-20.**

Atom	Atom	Length/Å	Atom	Atom	Length/Å
Fe1	F1	2.1632(15)	C14	C15	1.381(4)
Fe1	N1	2.136(2)	C15	C16	1.387(5)
Fe1	N2	2.242(2)	C16	C17	1.396(4)
Fe1	N4	2.244(2)	C18	C19	1.380(4)
Fe1	N6	2.114(2)	C18	C23	1.395(4)
Fe1	N7	2.099(3)	C19	C20	1.390(4)
S1	O1	1.429(2)	C20	C21	1.378(4)
S1	O2	1.432(2)	C21	C22	1.399(4)
S1	N3	1.652(2)	C22	C23	1.389(4)
S1	C5	1.781(3)	C24	C25	1.390(4)
S2	O3	1.429(2)	C25	C26	1.385(4)
S2	O4	1.436(2)	C26	C27	1.388(4)
S2	N5	1.660(2)	C27	C28	1.512(4)
S2	C31	1.757(3)	C29	C30	1.536(4)
F1	B1	1.444(4)	C29	C44	1.501(4)
F2	B1	1.389(4)	C30	C38	1.513(3)
F3	B1	1.380(4)	C31	C32	1.388(4)
F4	B1	1.385(4)	C31	C36	1.392(3)
N1	C1	1.335(3)	C32	C33	1.386(4)
N1	C27	1.343(3)	C33	C34	1.383(4)
N2	C2	1.479(3)	C34	C35	1.385(4)

N2	C3	1.493(3)	C34	C37	1.512(4)
N3	C2	1.487(3)	C35	C36	1.380(4)
N3	C4	1.494(3)	C38	C39	1.386(4)
N4	C28	1.476(3)	C38	C43	1.387(4)
N4	C29	1.493(3)	C39	C40	1.395(4)
N5	C28	1.488(3)	C40	C41	1.371(5)
N5	C30	1.489(3)	C41	C42	1.377(5)
N6	C50	1.136(4)	C42	C43	1.403(4)
N7	C52	1.133(4)	C44	C45	1.378(4)
C1	C2	1.526(4)	C44	C49	1.400(4)
C1	C24	1.378(4)	C45	C46	1.394(4)
C3	C4	1.552(4)	C46	C47	1.370(4)
C3	C18	1.514(4)	C47	C48	1.379(5)
C4	C12	1.513(3)	C48	C49	1.379(5)
C5	C6	1.382(5)	C50	C51	1.448(4)
C5	C10	1.388(4)	C52	C53	1.451(5)
C6	C7	1.403(6)	N8	C54	1.138(6)
C7	C8	1.388(6)	C54	C55	1.428(5)
C8	C9	1.379(6)	N9	C56	1.135(5)
C8	C11	1.527(6)	C56	C57	1.447(5)
C9	C10	1.384(5)	F5	B2	1.407(4)
C12	C13	1.381(4)	F6	B2	1.371(4)
C12	C17	1.392(4)	F7	B2	1.393(4)
C13	C14	1.388(4)	F8	B2	1.389(5)

Table 5. Bond Angles for (*S,S*-20).

Atom	Atom	Atom	Angle/°	Atom	Atom	Atom	Angle/°
F1	Fe1	N1	86.69(7)	C12	C13	C14	120.6(3)
F1	Fe1	N2	86.46(7)	C13	C14	C15	120.3(3)
F1	Fe1	N4	98.85(7)	C14	C15	C16	119.6(3)
F1	Fe1	N6	176.32(8)	C15	C16	C17	120.1(3)
F1	Fe1	N7	86.06(7)	C12	C17	C16	120.2(3)
N1	Fe1	N2	74.01(8)	C3	C18	C19	119.5(2)
N1	Fe1	N4	75.75(8)	C3	C18	C23	121.2(2)
N1	Fe1	N6	96.60(8)	C19	C18	C23	119.0(3)
N1	Fe1	N7	169.39(9)	C18	C19	C20	121.1(3)
N2	Fe1	N4	148.92(8)	C19	C20	C21	119.8(3)
N2	Fe1	N6	92.86(8)	C20	C21	C22	120.1(3)
N2	Fe1	N7	113.23(9)	C21	C22	C23	119.4(3)

---

N4	Fe1	N6	83.60(8)	C18	C23	C22	120.6(3)
N4	Fe1	N7	97.72(9)	C1	C24	C25	117.9(2)
N6	Fe1	N7	90.89(9)	C24	C25	C26	120.1(2)
O1	S1	O2	120.97(13)	C25	C26	C27	118.7(2)
O1	S1	N3	105.62(11)	N1	C27	C26	120.7(2)
O1	S1	C5	107.37(14)	N1	C27	C28	113.6(2)
O2	S1	N3	105.74(12)	C26	C27	C28	125.5(2)
O2	S1	C5	109.69(14)	N4	C28	N5	105.66(19)
N3	S1	C5	106.56(13)	N4	C28	C27	111.1(2)
O3	S2	O4	120.46(12)	N5	C28	C27	111.9(2)
O3	S2	N5	105.61(11)	N4	C29	C30	102.98(18)
O3	S2	C31	108.67(13)	N4	C29	C44	112.6(2)
O4	S2	N5	105.35(12)	C30	C29	C44	115.8(2)
O4	S2	C31	107.53(11)	N5	C30	C29	101.5(2)
N5	S2	C31	108.74(12)	N5	C30	C38	114.5(2)
Fe1	F1	B1	127.69(16)	C29	C30	C38	113.42(18)
Fe1	N1	C1	119.84(17)	S2	C31	C32	119.2(2)
Fe1	N1	C27	119.36(17)	S2	C31	C36	120.0(2)
C1	N1	C27	120.5(2)	C32	C31	C36	120.8(2)
Fe1	N2	C2	108.71(15)	C31	C32	C33	118.6(3)
Fe1	N2	C3	117.62(15)	C32	C33	C34	121.6(3)
C2	N2	C3	104.30(19)	C33	C34	C35	118.7(3)
S1	N3	C2	117.58(15)	C33	C34	C37	121.3(3)
S1	N3	C4	116.41(17)	C35	C34	C37	120.0(3)
C2	N3	C4	108.92(19)	C34	C35	C36	121.2(3)
Fe1	N4	C28	108.56(16)	C31	C36	C35	119.1(3)
Fe1	N4	C29	120.85(15)	C30	C38	C39	119.0(2)
C28	N4	C29	103.75(19)	C30	C38	C43	121.0(2)
S2	N5	C28	116.80(16)	C39	C38	C43	119.9(2)
S2	N5	C30	118.16(17)	C38	C39	C40	120.0(3)
C28	N5	C30	108.9(2)	C39	C40	C41	120.0(3)
Fe1	N6	C50	166.2(2)	C40	C41	C42	120.6(3)
Fe1	N7	C52	170.0(3)	C41	C42	C43	120.0(3)
N1	C1	C2	114.1(2)	C38	C43	C42	119.5(3)
N1	C1	C24	122.1(2)	C29	C44	C45	122.9(2)
C2	C1	C24	123.8(2)	C29	C44	C49	118.2(2)
N2	C2	N3	106.20(19)	C45	C44	C49	118.9(3)
N2	C2	C1	109.9(2)	C44	C45	C46	120.4(3)
N3	C2	C1	110.4(2)	C45	C46	C47	120.4(3)
N2	C3	C4	105.25(18)	C46	C47	C48	119.5(3)
N2	C3	C18	113.7(2)	C47	C48	C49	120.9(3)

C4	C3	C18	111.8(2)	C44	C49	C48	119.9(3)
N3	C4	C3	103.66(19)	N6	C50	C51	178.6(3)
N3	C4	C12	114.7(2)	N7	C52	C53	179.1(3)
C3	C4	C12	113.02(19)	F1	B1	F2	107.9(2)
S1	C5	C6	119.7(2)	F1	B1	F3	109.9(2)
S1	C5	C10	119.6(2)	F1	B1	F4	108.0(2)
C6	C5	C10	120.4(3)	F2	B1	F3	110.7(2)
C5	C6	C7	118.6(3)	F2	B1	F4	109.9(2)
C6	C7	C8	121.0(4)	F3	B1	F4	110.4(3)
C7	C8	C9	119.4(4)	N8	C54	C55	179.9(6)
C7	C8	C11	120.4(4)	N9	C56	C57	179.5(5)
C9	C8	C11	120.2(4)	F5	B2	F6	109.8(3)
C8	C9	C10	120.1(4)	F5	B2	F7	108.2(3)
C5	C10	C9	120.4(3)	F5	B2	F8	109.3(3)
C4	C12	C13	122.8(2)	F6	B2	F7	110.1(3)
C4	C12	C17	117.9(2)	F6	B2	F8	109.8(3)
C13	C12	C17	119.2(2)	F7	B2	F8	109.6(3)

Table 6. Hydrogen Bonds for (S,S-20).

D	H	A	d(D-H)/Å	d(H-A)/Å	d(D-A)/Å	D-H-A/°
N2	H2	F4	0.9800	2.1500	2.847(3)	127.00
N4	H4	F5	0.9300	2.0100	2.901(3)	159.00
C10	H10	O1	0.9500	2.5600	2.938(4)	104.00
C13	H13	N3	0.9500	2.6100	2.934(4)	101.00
C21	H21	F4 <sup>1</sup>	0.9500	2.5400	3.168(3)	124.00
C26	H26	O4	0.9500	2.5600	3.197(3)	124.00
C32	H32	O1 <sup>2</sup>	0.9500	2.5100	3.386(4)	153.00
C36	H36	O4	0.9500	2.5600	2.919(3)	102.00
C47	H47	F7 <sup>3</sup>	0.9500	2.3800	3.281(4)	159.00
C51	H51A	F3 <sup>4</sup>	0.9800	2.3000	3.245(4)	162.00
C57	H57B	O3 <sup>5</sup>	0.9800	2.5000	3.232(4)	132.00
C57	H57C	O4	0.9800	2.5900	3.222(4)	122.00

<sup>1</sup>1/2+X,3/2-Y,2-Z; <sup>2</sup>+X,-1+Y,+Z; <sup>3</sup>-1/2+X,1/2-Y,2-Z; <sup>4</sup>1+X,+Y,+Z; <sup>5</sup>1-X,1/2+Y,3/2-Z



Table 7. Torsion Angles for (S,S-20).

A	B	C	D	Angle/°	A	B	C	D	Angle/°
Fe1	F1	B1	F2	134.33(18)	N7	Fe1	N4	C29	75.38(19)
Fe1	F1	B1	F3	-104.9(2)	C1	N1	C27	C26	-0.9(3)
Fe1	F1	B1	F4	15.6(3)	C1	N1	C27	C28	173.80(19)
Fe1	N1	C1	C2	3.8(2)	C1	C24	C25	C26	-0.6(3)
Fe1	N1	C1	C24	-173.48(16)	C2	N2	C3	C4	34.2(2)
Fe1	N1	C27	C26	172.96(16)	C2	N2	C3	C18	156.8(2)
Fe1	N1	C27	C28	-12.4(2)	C2	N3	C4	C3	4.1(2)
Fe1	N2	C2	N3	-157.94(14)	C2	N3	C4	C12	127.8(2)
Fe1	N2	C2	C1	-38.5(2)	C2	C1	C24	C25	-176.6(2)
Fe1	N2	C3	C4	154.64(16)	C3	N2	C2	N3	-31.7(2)
Fe1	N2	C3	C18	-82.7(2)	C3	N2	C2	C1	87.7(2)
Fe1	N4	C28	N5	-158.24(14)	C3	C4	C12	C13	96.0(3)
Fe1	N4	C28	C27	-36.7(2)	C3	C4	C12	C17	-80.9(3)
Fe1	N4	C29	C30	163.22(16)	C3	C18	C19	C20	174.1(3)
Fe1	N4	C29	C44	-71.4(2)	C3	C18	C23	C22	-173.8(3)
S1	N3	C2	N2	-118.22(18)	C4	N3	C2	N2	17.0(2)
S1	N3	C2	C1	122.72(18)	C4	N3	C2	C1	-102.1(2)
S1	N3	C4	C3	139.91(17)	C4	C3	C18	C19	-101.2(3)
S1	N3	C4	C12	-96.4(2)	C4	C3	C18	C23	72.0(3)
S1	C5	C6	C7	173.4(3)	C4	C12	C13	C14	-178.0(3)
S1	C5	C10	C9	-172.6(3)	C4	C12	C17	C16	178.4(2)
S2	N5	C28	N4	-132.50(17)	C5	S1	N3	C2	72.9(2)
S2	N5	C28	C27	106.5(2)	C5	S1	N3	C4	-59.0(2)
S2	N5	C30	C29	156.73(16)	C5	C6	C7	C8	-1.8(6)
S2	N5	C30	C38	-80.7(2)	C6	C5	C10	C9	0.6(5)
S2	C31	C32	C33	-178.7(2)	C6	C7	C8	C9	2.4(6)
S2	C31	C36	C35	-179.7(2)	C6	C7	C8	C11	-178.2(4)
F1	Fe1	N1	C1	67.53(17)	C7	C8	C9	C10	-1.6(6)
F1	Fe1	N1	C27	-106.35(17)	C8	C9	C10	C5	0.1(6)
F1	Fe1	N2	C2	-56.63(14)	C10	C5	C6	C7	0.2(5)
F1	Fe1	N2	C3	-174.77(18)	C11	C8	C9	C10	179.0(4)
F1	Fe1	N4	C28	107.69(14)	C12	C13	C14	C15	-0.1(4)
F1	Fe1	N4	C29	-11.82(19)	C13	C12	C17	C16	1.4(4)
O1	S1	N3	C2	-173.08(19)	C13	C14	C15	C16	1.1(4)
O1	S1	N3	C4	55.0(2)	C14	C15	C16	C17	-0.8(4)
O1	S1	C5	C6	164.9(2)	C15	C16	C17	C12	-0.5(4)
O1	S1	C5	C10	-21.9(3)	C17	C12	C13	C14	-1.1(4)
O2	S1	N3	C2	-43.7(2)	C18	C3	C4	N3	-147.42(19)
O2	S1	N3	C4	-175.64(18)	C18	C3	C4	C12	87.8(2)

O2	S1	C5	C6	31.7(3)	C18	C19	C20	C21	0.1(4)
O2	S1	C5	C10	-155.1(2)	C19	C18	C23	C22	-0.6(4)
O3	S2	N5	C28	179.87(18)	C19	C20	C21	C22	-1.0(4)
O3	S2	N5	C30	46.9(2)	C20	C21	C22	C23	1.1(4)
O3	S2	C31	C32	-28.8(3)	C21	C22	C23	C18	-0.3(4)
O3	S2	C31	C36	150.3(2)	C23	C18	C19	C20	0.7(4)
O4	S2	N5	C28	-51.6(2)	C24	C1	C2	N2	-158.5(2)
O4	S2	N5	C30	175.44(18)	C24	C1	C2	N3	-41.7(3)
O4	S2	C31	C32	-160.7(2)	C24	C25	C26	C27	0.1(3)
O4	S2	C31	C36	18.4(3)	C25	C26	C27	N1	0.7(3)
N1	Fe1	F1	B1	-131.3(2)	C25	C26	C27	C28	-173.4(2)
N1	Fe1	N2	C2	30.94(14)	C26	C27	C28	N4	-152.3(2)
N1	Fe1	N2	C3	-87.20(18)	C26	C27	C28	N5	-34.5(3)
N1	Fe1	N4	C28	23.41(14)	C27	N1	C1	C2	177.60(19)
N1	Fe1	N4	C29	-96.09(19)	C27	N1	C1	C24	0.3(3)
N1	C1	C2	N2	24.3(3)	C28	N4	C29	C30	41.4(2)
N1	C1	C2	N3	141.1(2)	C28	N4	C29	C44	166.8(2)
N1	C1	C24	C25	0.4(3)	C28	N5	C30	C29	20.4(2)
N1	C27	C28	N4	33.4(3)	C28	N5	C30	C38	143.0(2)
N1	C27	C28	N5	151.2(2)	C29	N4	C28	N5	-28.5(2)
N2	Fe1	F1	B1	-57.2(2)	C29	N4	C28	C27	93.0(2)
N2	Fe1	N1	C1	-19.73(16)	C29	C30	C38	C39	-112.2(3)
N2	Fe1	N1	C27	166.39(18)	C29	C30	C38	C43	65.2(3)
N2	Fe1	N4	C28	9.8(2)	C29	C44	C45	C46	177.1(3)
N2	Fe1	N4	C29	-109.7(2)	C29	C44	C49	C48	-178.2(3)
N2	C3	C4	N3	-23.5(2)	C30	N5	C28	N4	4.5(2)
N2	C3	C4	C12	-148.3(2)	C30	N5	C28	C27	-116.5(2)
N2	C3	C18	C19	139.8(2)	C30	C29	C44	C45	53.3(3)
N2	C3	C18	C23	-47.0(3)	C30	C29	C44	C49	-128.9(2)
N3	S1	C5	C6	-82.4(3)	C30	C38	C39	C40	178.5(3)
N3	S1	C5	C10	90.9(3)	C30	C38	C43	C42	-178.8(3)
N3	C4	C12	C13	-22.6(4)	C31	S2	N5	C28	63.4(2)
N3	C4	C12	C17	160.5(2)	C31	S2	N5	C30	-69.5(2)
N4	Fe1	F1	B1	153.7(2)	C31	C32	C33	C34	-2.1(5)
N4	Fe1	N1	C1	167.53(19)	C32	C31	C36	C35	-0.6(4)
N4	Fe1	N1	C27	-6.35(16)	C32	C33	C34	C35	0.3(5)
N4	Fe1	N2	C2	44.7(2)	C32	C33	C34	C37	179.7(3)
N4	Fe1	N2	C3	-73.5(2)	C33	C34	C35	C36	1.4(5)
N4	C29	C30	N5	-37.6(2)	C34	C35	C36	C31	-1.2(4)
N4	C29	C30	C38	-160.8(2)	C36	C31	C32	C33	2.3(4)
N4	C29	C44	C45	-64.8(3)	C37	C34	C35	C36	-178.0(3)

N4	C29	C44	C49	113.0(3)	C38	C39	C40	C41	-0.2(5)
N5	S2	C31	C32	85.7(2)	C39	C38	C43	C42	-1.4(4)
N5	S2	C31	C36	-95.2(2)	C39	C40	C41	C42	-0.4(5)
N5	C30	C38	C39	132.0(3)	C40	C41	C42	C43	0.0(5)
N5	C30	C38	C43	-50.6(3)	C41	C42	C43	C38	0.9(5)
N6	Fe1	N1	C1	-110.82(18)	C43	C38	C39	C40	1.1(4)
N6	Fe1	N1	C27	75.30(18)	C44	C29	C30	N5	-160.84(19)
N6	Fe1	N2	C2	126.99(15)	C44	C29	C30	C38	75.9(3)
N6	Fe1	N2	C3	8.86(18)	C44	C45	C46	C47	2.0(5)
N6	Fe1	N4	C28	-75.09(15)	C45	C44	C49	C48	-0.3(4)
N6	Fe1	N4	C29	165.41(19)	C45	C46	C47	C48	-2.1(5)
N7	Fe1	F1	B1	56.5(2)	C46	C47	C48	C49	1.1(5)
N7	Fe1	N2	C2	-140.81(14)	C47	C48	C49	C44	0.1(5)
N7	Fe1	N2	C3	101.05(18)	C49	C44	C45	C46	-0.8(4)
N7	Fe1	N4	C28	-165.12(15)					

**Table 8. Hydrogen Atom Coordinates ( $\text{\AA}\times 10^4$ ) and Isotropic Displacement Parameters ( $\text{\AA}^2\times 10^3$ ) for (S,S-20).**

Atom	x	y	z	U(eq)
H2	3412	7315	9097	41.6(14)
H2A	2272	7377	8641	41.3(15)
H3	5581	6957	8722	41.5(14)
H4	4122	3728	8847	41.6(14)
H4A	4942	8782	8841	41.5(14)
H6	1036	8519	8966	41.6(16)
H7	739	8814	9576	42.0(16)
H9	3705	10553	9568	42.1(16)
H10	3976	10296	8961	41.9(15)
H11A	1862	10488	10074	42.6(17)
H11B	2845	9685	10154	42.3(16)
H11C	1355	9471	10119	42.4(17)
H13	5480	8049	7962	41.5(14)
H14	7293	8364	7626	41.5(15)
H15	9072	9023	7892	41.5(16)
H16	9053	9333	8502	41.7(15)
H17	7237	9004	8841	41.5(15)
H19	7541	6982	9049	41.5(14)
H20	8686	7279	9568	41.6(15)
H21	7678	7957	10051	41.6(16)
H22	5524	8386	10009	41.8(15)

---

H23	4389	8079	9488	41.8(15)
H24	3136	7397	7839	41.4(15)
H25	3367	6192	7433	41.3(15)
H26	3803	4729	7644	41.3(15)
H28	5112	4257	8368	41.4(14)
H29	1838	3990	8536	41.3(14)
H30	3331	2390	8488	41.3(15)
H32	4974	1222	8327	41.4(15)
H33	6432	656	8741	41.5(15)
H35	8746	2790	8568	41.6(15)
H36	7269	3408	8175	41.7(14)
H37A	8558	1599	9191	41.8(16)
H37B	9545	1411	8875	41.9(16)
H37C	8547	643	8990	41.8(17)
H39	1963	1210	8399	41.3(15)
H40	225	543	8108	41.4(17)
H41	-997	1392	7717	41.3(18)
H42	-523	2908	7614	41.2(17)
H43	1208	3594	7909	41.3(15)
H45	3274	2373	9124	41.5(15)
H46	2367	1940	9666	41.6(15)
H47	396	2506	9835	41.6(16)
H48	-613	3587	9482	41.9(16)
H49	300	4060	8951	41.6(15)
H51A	8453	5034	9143	41.6(15)
H51B	8230	4820	8731	41.7(15)
H51C	7929	4062	9023	41.7(15)
H53A	3366	4657	10273	42.2(16)
H53B	3267	3693	10079	42.3(17)
H53C	2013	4290	10140	42.5(17)
H55A	8888	6918	8318	41.8(14)
H55B	9161	6937	7900	41.8(15)
H55C	10237	7261	8173	41.8(15)
H57A	7931	4875	7492	41.8(15)
H57B	7307	5833	7394	41.8(15)
H57C	6430	4948	7423	41.9(15)

## Experimental

Single crystals of  $C_{57}H_{57}B_2F_8FeN_9O_4S_2$  were grown in MeCN/Et<sub>2</sub>O. A suitable crystal was selected and placed on a diffractometer. The crystal was kept at 110(2) K during data collection. Using Olex2 [1], the structure was solved with the [2] structure solution program using and refined with the [3] refinement package using minimisation.

1. Dolomanov, O.V., Bourhis, L.J., Gildea, R.J, Howard, J.A.K. & Puschmann, H. (2009), *J. Appl. Cryst.* 42, 339-341.

### 1.2. Complex (*R,R*)-[Fe(BF<sub>4</sub>)(NNN)(MeCN)<sub>2</sub>](BF<sub>4</sub>) (20)

**Table 2 Fractional Atomic Coordinates ( $\times 10^4$ ) and Equivalent Isotropic Displacement Parameters ( $\text{\AA}^2 \times 10^3$ ) for (*R,R*)-20.  $U_{eq}$  is defined as 1/3 of the trace of the orthogonalised  $U_{ij}$  tensor.**

Atom	x	y	z	U(eq)
Fe1	6386.1(2)	4480.0(2)	1043.5(1)	13.3(1)
S1	7122.8(4)	887.0(3)	1538.4(1)	19.2(1)
S2	5142.2(4)	7164.7(3)	2080.4(1)	16.0(1)
F1	8417.3(11)	4230.1(7)	1071.6(3)	23.6(3)
F2	9970.9(12)	3138.2(9)	1058.4(3)	36.8(4)
F3	9873.6(12)	4179.7(8)	610.6(3)	30.2(4)
F4	8349.0(11)	3091.2(7)	658.7(3)	22.8(3)
O1	6351.9(14)	176.8(8)	1683.5(3)	23.2(4)
O2	8273.4(13)	1168.5(9)	1711.7(4)	28.0(4)
O3	5810.1(13)	7899.5(9)	2244.4(3)	22.4(4)
O4	4500.5(13)	6498.5(9)	2294.6(3)	20.2(4)
N1	6351.1(14)	4214.1(9)	1600.4(3)	13.4(4)
N2	6152.4(13)	2970.5(9)	1098.3(4)	14.2(4)
N3	6195.5(14)	1796.6(9)	1528.9(4)	14.6(4)
N4	6341.1(14)	5856.8(9)	1294.7(3)	13.5(4)
N5	6231.8(14)	6593.2(9)	1852.7(4)	14.1(4)
N6	4408.3(15)	4695.6(10)	981.4(4)	18.4(4)
N7	6721.0(17)	4896.7(11)	517.3(4)	23.7(5)
C1	6595.4(17)	3374.9(11)	1719.8(4)	13.9(5)
C2	6792.9(17)	2673.3(11)	1427.9(4)	14.8(5)
C3	4827.1(17)	2618.8(11)	1133.4(4)	13.7(4)
C4	4965.6(17)	1694.4(11)	1333.8(4)	14.5(5)
C5	7460(2)	603.0(13)	1089.7(5)	25.4(6)
C6	8424(2)	1053.0(14)	909.4(6)	32.6(7)
C7	8582(3)	890.3(16)	545.7(6)	43.1(8)

---

C8	7772(3)	304.0(15)	361.9(6)	41.8(8)
C9	6832(3)	-147.5(15)	548.7(6)	39.1(7)
C10	6669(2)	-2.8(14)	910.3(5)	30.0(6)
C11	7937(4)	149(2)	-34.3(7)	62.1(12)
C12	3826.2(17)	1479.5(11)	1566.1(5)	15.5(5)
C13	3800.6(19)	1675.4(12)	1928.1(5)	19.3(5)
C14	2716(2)	1486.7(13)	2127.8(5)	23.1(6)
C15	1654(2)	1105.2(13)	1970.0(5)	24.1(6)
C16	1663.5(19)	922.7(13)	1606.7(5)	24.1(6)
C17	2750.7(19)	1110.2(12)	1407.0(5)	20.8(5)
C18	4141.8(18)	2498.7(12)	782.7(4)	16.2(5)
C19	2866.1(18)	2733.5(12)	755.2(5)	18.9(5)
C20	2186(2)	2551.6(14)	445.4(5)	25.0(6)
C21	2784(2)	2135.0(15)	160.9(5)	28.1(6)
C22	4060(2)	1891.0(15)	184.4(5)	27.4(6)
C23	4738.4(19)	2070.1(14)	494.5(5)	22.2(5)
C24	6701.9(17)	3187.5(12)	2080.5(4)	17.0(5)
C25	6559.6(17)	3899.3(12)	2318.4(4)	17.5(5)
C26	6303.6(18)	4769.3(12)	2194.4(4)	16.5(5)
C27	6195.0(16)	4901.2(11)	1829.7(4)	13.7(5)
C28	5779.2(17)	5781.8(11)	1654.0(4)	13.8(5)
C29	7539.8(17)	6380.6(11)	1356.0(4)	13.9(5)
C30	7135.2(17)	7116.2(11)	1623.5(4)	14.5(5)
C31	4018.4(17)	7610.5(12)	1781.2(4)	17.1(5)
C32	4265(2)	8442.8(12)	1617.6(5)	21.8(5)
C33	3379(2)	8774.8(13)	1377.4(5)	26.7(6)
C34	2257(2)	8320.2(14)	1303.1(5)	26.0(6)
C35	2018(2)	7499.7(14)	1477.6(5)	23.1(6)
C36	2898.9(18)	7137.9(13)	1713.1(5)	19.2(5)
C37	1302(2)	8688.6(16)	1039.1(6)	36.2(7)
C38	8239.9(17)	7533.5(12)	1822.3(4)	16.9(5)
C39	8542(2)	8440.0(13)	1759.7(5)	23.5(5)
C40	9578(2)	8837.6(15)	1932.9(6)	32.4(7)
C41	10296(2)	8334.5(17)	2166.0(6)	34.5(7)
C42	10013(2)	7431.5(16)	2227.9(5)	29.5(6)
C43	8983.4(18)	7026.9(14)	2053.9(5)	21.8(5)
C44	8124.5(17)	6727.3(11)	1014.0(4)	15.5(5)
C45	7523(2)	7368.7(13)	803.9(5)	23.8(5)
C46	8073(2)	7635.8(14)	481.8(5)	29.4(6)
C47	9223(2)	7273.8(15)	375.5(5)	29.9(6)
C48	9821(2)	6628.7(17)	583.7(5)	32.6(7)

C49	9274.3(19)	6357.5(14)	903.1(5)	24.1(6)
C50	3387.3(19)	4952.9(12)	1000.4(4)	19.0(5)
C51	2089.2(19)	5285.5(13)	1029.6(6)	26.2(6)
C52	6876(2)	5246.7(14)	252.3(5)	30.0(6)
C53	7071(3)	5698(2)	-90.4(6)	52.9(10)
B1	9179(2)	3655.0(15)	843.8(5)	20.2(6)
N8	-390(3)	4796.1(17)	1835.9(8)	67(1)
C54	-15(2)	4073.9(17)	1848.4(6)	35.1(7)
C55	459(2)	3159.5(15)	1864.6(6)	32.0(7)
N9	3200(2)	4386.4(18)	1812.5(5)	48.5(8)
C56	3035(2)	4537.8(17)	2103.9(6)	33.1(7)
C57	2816(2)	4730.1(15)	2478.9(5)	36.7(7)
F5	4384.5(12)	6924.8(8)	945.7(3)	27.8(3)
F6	2890.8(13)	7107.2(10)	511.7(3)	41.2(4)
F7	4898.9(14)	6661.7(9)	368.1(3)	37.5(4)
F8	4525.8(14)	8108.9(8)	555.3(3)	38.1(4)
B2	4170(2)	7204.7(16)	592.4(6)	25.1(6)

**Table 3 Anisotropic Displacement Parameters ( $\text{\AA}^2 \times 10^3$ ) for (R,R)-20. The Anisotropic displacement factor exponent takes the form:  $-2\pi^2[\text{h}^2\text{a}^{*2}\text{U}_{11} + \dots + 2\text{hka} \times \text{b} \times \text{U}_{12}]$**

Atom	$U_{11}$	$U_{22}$	$U_{33}$	$U_{23}$	$U_{13}$	$U_{12}$
Fe1	15.4(1)	12.8(1)	11.6(1)	0.9(1)	0.5(1)	0.2(1)
S1	17.5(2)	14.3(2)	25.7(2)	4.3(2)	-0.4(2)	3.6(2)
S2	16.4(2)	16.7(2)	14.8(2)	-3.0(2)	3.1(2)	0.9(2)
F1	19.9(6)	28.7(6)	22.3(5)	-5.0(4)	2.1(5)	-0.4(5)
F2	31.2(7)	49.2(8)	30.1(6)	-1.9(6)	-4.9(6)	20.1(6)
F3	28.6(7)	35.8(7)	26.2(5)	-6.2(5)	10.8(5)	-11.7(6)
F4	22.4(6)	23.2(5)	22.7(5)	-6.0(4)	4.7(4)	-4.0(5)
O1	25.3(7)	16.5(6)	27.9(6)	5.7(5)	-0.3(6)	0.8(6)
O2	20.0(8)	23.0(7)	41.0(8)	6.4(6)	-5.6(6)	3.0(6)
O3	22.0(7)	22.6(7)	22.7(6)	-8.0(5)	1.3(5)	0.7(6)
O4	19.8(7)	25.3(7)	15.4(6)	0.5(5)	4.4(5)	1.0(6)
N1	10.6(7)	13.9(6)	15.7(6)	0.4(5)	0.3(6)	-2.4(6)
N2	11.4(7)	16.0(7)	15.2(7)	-0.1(5)	1.3(5)	0.8(6)
N3	12.7(8)	11.8(6)	19.4(7)	0.5(5)	-0.1(6)	2.0(6)
N4	13.8(7)	14.8(6)	11.8(6)	1.5(5)	1.9(6)	0.3(6)
N5	15.0(8)	12.6(7)	14.8(6)	-1.5(5)	4.2(6)	-0.5(6)
N6	18.6(8)	16.8(7)	19.7(7)	0.0(6)	-3.2(6)	-0.2(6)
N7	27.0(9)	25.2(8)	18.9(7)	1.3(6)	2.5(6)	4.8(7)

C1	10.8(9)	13.4(8)	17.6(8)	0.6(6)	0.4(6)	-0.7(7)
C2	14.3(9)	13.3(8)	16.7(7)	3.4(6)	0.7(6)	0.7(7)
C3	13.0(8)	13.1(8)	14.9(7)	-0.1(6)	1.0(6)	0.6(7)
C4	15.8(9)	12.6(8)	15.1(7)	-0.7(6)	0.2(7)	1.0(7)
C5	28.6(11)	19.3(9)	28.2(9)	3.0(8)	6.3(8)	9.6(8)
C6	36.6(13)	20.2(10)	41.1(11)	-3.4(8)	12.1(10)	4.8(9)
C7	57.4(17)	29.8(11)	42.1(12)	2.6(10)	24.1(13)	6.3(12)
C8	64.9(18)	27.5(12)	33.1(11)	-5.0(9)	10.8(12)	14.2(12)
C9	55.8(16)	24.5(11)	36.9(11)	-8.4(9)	0.1(11)	9.6(11)
C10	36.8(13)	20.4(10)	32.8(10)	-3.7(8)	3.5(9)	8.4(9)
C11	105(3)	45.9(16)	35.4(13)	-5.2(12)	20.9(17)	12.4(18)
C12	16.5(9)	10.5(7)	19.6(8)	3.3(6)	0.8(7)	1.5(6)
C13	18.4(10)	20.1(9)	19.5(8)	1.9(7)	0.1(7)	-0.1(8)
C14	25.1(11)	25.2(10)	18.9(8)	2.0(7)	3.9(8)	1.9(8)
C15	21.5(11)	21.9(9)	28.9(9)	3.6(7)	8.6(8)	-2.4(8)
C16	19.8(10)	21.8(9)	30.8(10)	0.3(8)	0.0(8)	-4.4(8)
C17	23(1)	17.0(9)	22.3(8)	0.0(7)	1.1(7)	-2.4(8)
C18	18.0(9)	14.5(8)	16.1(8)	2.4(6)	-0.1(7)	-0.7(7)
C19	17.8(10)	18.2(9)	20.6(8)	-3.1(7)	0.1(7)	1.4(8)
C20	17(1)	31(1)	27.0(9)	-1.4(8)	-4.9(8)	1.8(8)
C21	27.3(11)	38.1(12)	19.0(9)	-1.3(8)	-6.5(8)	-0.5(10)
C22	27.6(11)	37.8(12)	16.8(8)	-4.7(8)	1.0(8)	0.7(9)
C23	17.4(10)	30.1(10)	19.0(8)	-0.2(7)	0.8(7)	4.1(8)
C24	16.0(9)	16.2(8)	18.7(8)	4.4(7)	-1.5(7)	-0.9(7)
C25	15.9(9)	23.4(9)	13.1(7)	2.5(6)	-0.1(7)	-3.5(8)
C26	16.2(9)	19.1(8)	14.1(7)	-1.3(6)	0.4(7)	-2.6(7)
C27	7.7(8)	15.3(8)	18.1(8)	-0.2(6)	2.1(6)	-2.4(7)
C28	14.0(9)	14.0(8)	13.5(7)	-1.9(6)	2.3(6)	-1.3(7)
C29	14.7(9)	11.9(8)	15.2(7)	0.0(6)	0.9(6)	1.0(6)
C30	16.8(9)	12.3(8)	14.5(7)	0.8(6)	3.3(6)	0.4(7)
C31	18.0(9)	16.9(8)	16.4(8)	-2.6(6)	2.7(7)	4.2(7)
C32	22.6(10)	16.2(9)	26.6(9)	-1.4(7)	3.3(8)	0.5(8)
C33	32.4(12)	18.3(9)	29.3(10)	4.4(8)	6.9(8)	7.0(9)
C34	30.7(12)	27.8(10)	19.6(8)	-1.1(8)	2.4(8)	11.8(9)
C35	20.1(10)	27.8(10)	21.3(9)	-4.4(7)	1.7(7)	2.0(8)
C36	18.9(10)	18.5(9)	20.2(8)	-1.8(7)	4.5(7)	0.5(8)
C37	40.7(14)	39.9(12)	28.1(10)	4.3(9)	-5.1(10)	13.3(11)
C38	15.3(9)	18.7(8)	16.8(8)	-5.0(7)	6.6(6)	-3.5(7)
C39	21.5(10)	19.7(9)	29.2(9)	-4.7(7)	7.2(8)	-2.1(8)
C40	28.5(12)	27.8(11)	40.8(12)	-16.1(9)	11.0(9)	-13.2(9)
C41	21.5(11)	49.1(13)	33.0(11)	-21(1)	6.2(9)	-14.6(10)



C42	18.2(10)	49.9(13)	20.4(9)	-6.2(9)	0.8(8)	0.6(10)
C43	18.9(10)	27.9(10)	18.6(8)	-2.7(7)	3.6(7)	-1.4(8)
C44	18.1(9)	14.7(8)	13.8(7)	-0.8(6)	0.6(7)	-4.1(7)
C45	28.1(11)	21.5(9)	21.7(8)	4.4(7)	6.4(8)	4.8(8)
C46	44.3(14)	22.6(10)	21.3(9)	7.5(8)	3.8(9)	3.3(9)
C47	31.1(12)	36.7(12)	21.9(9)	7.6(9)	7.8(8)	-6.5(10)
C48	20.5(11)	49.9(14)	27.3(10)	6.9(9)	7.8(8)	3.1(10)
C49	17.1(10)	34.0(11)	21.3(9)	6.7(8)	2.1(7)	1.3(8)
C50	23.3(10)	15.4(8)	18.2(8)	-0.9(7)	-2.4(7)	-0.8(7)
C51	18.7(10)	28.1(10)	31.9(10)	-2.7(8)	-1.9(8)	4.1(8)
C52	39.6(13)	28.5(11)	21.9(9)	-0.2(8)	4.5(9)	4.9(9)
C53	83(2)	53.5(18)	22.2(11)	9.5(11)	10.6(12)	2.3(16)
B1	17.9(11)	25.3(11)	17.4(9)	-2.1(8)	1.3(8)	1.4(9)
N8	56.2(17)	44.8(14)	100(2)	8.5(14)	-19.9(15)	17.1(12)
C54	25.7(12)	40.0(13)	39.6(11)	1.1(10)	-11.2(9)	-0.8(10)
C55	40.3(14)	28.1(11)	27.7(10)	2.0(8)	-1.4(9)	-1(1)
N9	31.1(11)	82.5(17)	32(1)	8.6(11)	-3.2(8)	-21.8(12)
C56	19.8(11)	45.0(13)	34.6(11)	15.6(10)	-1.8(9)	-10.3(10)
C57	42.9(15)	33.2(12)	34.1(11)	8.6(9)	11.2(10)	0.5(11)
F5	32.6(7)	30.2(6)	20.6(5)	6.7(5)	3.2(5)	10.1(5)
F6	28.1(7)	56.8(9)	38.7(7)	5.8(7)	-4.6(6)	-0.7(7)
F7	47.1(8)	41.3(7)	24.2(6)	2.5(5)	6.2(6)	16.2(7)
F8	48.7(9)	26.9(6)	38.8(7)	11.1(5)	-1.9(6)	-1.2(6)
B2	27.0(12)	26.0(11)	22.4(10)	9.0(9)	1.6(9)	5.1(10)

**Table 4 Bond Lengths for (R,R)-20.**

Atom	Atom	Length/Å	Atom	Atom	Length/Å
Fe1	F1	2.1646(12)	C14	C15	1.382(3)
Fe1	N1	2.1303(12)	C15	C16	1.392(3)
Fe1	N2	2.2461(14)	C16	C17	1.393(3)
Fe1	N4	2.2374(13)	C18	C19	1.386(3)
Fe1	N6	2.1116(16)	C18	C23	1.401(3)
Fe1	N7	2.1009(15)	C19	C20	1.392(3)
S1	O1	1.4303(13)	C20	C21	1.383(3)
S1	O2	1.4328(15)	C21	C22	1.389(3)
S1	N3	1.6559(14)	C22	C23	1.391(3)
S1	C5	1.7735(19)	C24	C25	1.386(2)
S2	O3	1.4291(14)	C25	C26	1.390(2)
S2	O4	1.4368(13)	C26	C27	1.390(2)

S2	N5	1.6574(15)	C27	C28	1.519(2)
S2	C31	1.7565(17)	C29	C30	1.538(2)
F1	B1	1.445(2)	C29	C44	1.513(2)
F2	B1	1.386(2)	C30	C38	1.510(2)
F3	B1	1.377(2)	C31	C32	1.396(2)
F4	B1	1.390(2)	C31	C36	1.389(3)
N1	C1	1.340(2)	C32	C33	1.385(3)
N1	C27	1.339(2)	C33	C34	1.383(3)
N2	C2	1.476(2)	C34	C35	1.398(3)
N2	C3	1.489(2)	C34	C37	1.511(3)
N3	C2	1.485(2)	C35	C36	1.386(3)
N3	C4	1.492(2)	C38	C39	1.392(3)
N4	C28	1.478(2)	C38	C43	1.387(3)
N4	C29	1.493(2)	C39	C40	1.396(3)
N5	C28	1.487(2)	C40	C41	1.373(3)
N5	C30	1.495(2)	C41	C42	1.382(3)
N6	C50	1.138(3)	C42	C43	1.396(3)
N7	C52	1.133(2)	C44	C45	1.384(3)
C1	C2	1.522(2)	C44	C49	1.387(3)
C1	C24	1.388(2)	C45	C46	1.398(3)
C3	C4	1.563(2)	C46	C47	1.378(3)
C3	C18	1.512(2)	C47	C48	1.382(3)
C4	C12	1.514(2)	C48	C49	1.389(3)
C5	C6	1.386(3)	C50	C51	1.451(3)
C5	C10	1.393(3)	C52	C53	1.464(3)
C6	C7	1.398(3)	N8	C54	1.135(4)
C7	C8	1.395(4)	C54	C55	1.437(3)
C8	C9	1.381(4)	N9	C56	1.131(3)
C8	C11	1.517(4)	C56	C57	1.456(3)
C9	C10	1.387(3)	F5	B2	1.409(3)
C12	C13	1.391(3)	F6	B2	1.383(3)
C12	C17	1.388(3)	F7	B2	1.391(3)
C13	C14	1.391(3)	F8	B2	1.390(3)

**Table 5. Bond Angles for (R,R)-20**

Atom	Atom	Atom	Angle/°	Atom	Atom	Atom	Angle/°
F1	Fe1	N1	86.43(5)	C12	C13	C14	120.15(18)
F1	Fe1	N2	86.26(5)	C13	C14	C15	120.59(18)
F1	Fe1	N4	98.87(5)	C14	C15	C16	119.61(18)

---

F1	Fe1	N6	176.28(5)	C15	C16	C17	119.76(18)
F1	Fe1	N7	86.05(6)	C12	C17	C16	120.72(17)
N1	Fe1	N2	74.10(5)	C3	C18	C19	119.66(15)
N1	Fe1	N4	75.61(5)	C3	C18	C23	120.97(16)
N1	Fe1	N6	96.86(6)	C19	C18	C23	119.07(16)
N1	Fe1	N7	169.12(6)	C18	C19	C20	120.61(17)
N2	Fe1	N4	148.88(5)	C19	C20	C21	120.00(19)
N2	Fe1	N6	92.97(5)	C20	C21	C22	120.17(18)
N2	Fe1	N7	113.19(6)	C21	C22	C23	119.82(18)
N4	Fe1	N6	83.66(6)	C18	C23	C22	120.33(18)
N4	Fe1	N7	97.83(5)	C1	C24	C25	118.11(16)
N6	Fe1	N7	90.93(6)	C24	C25	C26	120.11(14)
O1	S1	O2	120.95(8)	C25	C26	C27	118.41(15)
O1	S1	N3	105.53(8)	N1	C27	C26	121.30(15)
O1	S1	C5	107.65(8)	N1	C27	C28	113.59(13)
O2	S1	N3	105.69(8)	C26	C27	C28	124.88(14)
O2	S1	C5	109.44(9)	N4	C28	N5	105.77(13)
N3	S1	C5	106.71(9)	N4	C28	C27	110.28(13)
O3	S2	O4	120.32(7)	N5	C28	C27	112.08(13)
O3	S2	N5	105.63(8)	N4	C29	C30	103.45(13)
O3	S2	C31	108.80(8)	N4	C29	C44	112.61(13)
O4	S2	N5	105.41(8)	C30	C29	C44	115.45(13)
O4	S2	C31	107.45(8)	N5	C30	C29	100.89(13)
N5	S2	C31	108.78(8)	N5	C30	C38	114.27(13)
Fe1	F1	B1	127.93(11)	C29	C30	C38	113.50(14)
Fe1	N1	C1	119.71(10)	S2	C31	C32	119.09(14)
Fe1	N1	C27	119.72(10)	S2	C31	C36	119.87(14)
C1	N1	C27	120.32(13)	C32	C31	C36	121.04(17)
Fe1	N2	C2	108.72(10)	C31	C32	C33	118.23(18)
Fe1	N2	C3	117.02(10)	C32	C33	C34	122.14(18)
C2	N2	C3	104.32(13)	C33	C34	C35	118.46(18)
S1	N3	C2	117.47(12)	C33	C34	C37	121.55(18)
S1	N3	C4	115.91(11)	C35	C34	C37	119.99(19)
C2	N3	C4	109.09(13)	C34	C35	C36	120.84(19)
Fe1	N4	C28	109.05(9)	C31	C36	C35	119.25(17)
Fe1	N4	C29	121.04(10)	C30	C38	C39	118.78(15)
C28	N4	C29	103.50(11)	C30	C38	C43	121.56(16)
S2	N5	C28	116.58(11)	C39	C38	C43	119.61(17)
S2	N5	C30	118.24(11)	C38	C39	C40	120.05(18)
C28	N5	C30	109.08(13)	C39	C40	C41	119.9(2)
Fe1	N6	C50	165.34(14)	C40	C41	C42	120.6(2)

Fe1	N7	C52	169.91(16)	C41	C42	C43	119.86(19)
N1	C1	C2	114.26(13)	C38	C43	C42	119.97(19)
N1	C1	C24	121.74(14)	C29	C44	C45	122.05(16)
C2	C1	C24	123.95(15)	C29	C44	C49	118.37(15)
N2	C2	N3	106.29(13)	C45	C44	C49	119.53(16)
N2	C2	C1	110.01(13)	C44	C45	C46	119.90(18)
N3	C2	C1	110.41(13)	C45	C46	C47	120.24(19)
N2	C3	C4	105.01(13)	C46	C47	C48	119.94(18)
N2	C3	C18	114.03(13)	C47	C48	C49	120.00(19)
C4	C3	C18	111.26(13)	C44	C49	C48	120.37(18)
N3	C4	C3	103.27(13)	N6	C50	C51	179.20(18)
N3	C4	C12	114.85(13)	N7	C52	C53	179.8(3)
C3	C4	C12	112.76(14)	F1	B1	F2	107.95(14)
S1	C5	C6	119.86(15)	F1	B1	F3	109.93(16)
S1	C5	C10	119.53(15)	F1	B1	F4	107.49(15)
C6	C5	C10	120.27(18)	F2	B1	F3	111.21(16)
C5	C6	C7	118.9(2)	F2	B1	F4	109.80(16)
C6	C7	C8	121.2(2)	F3	B1	F4	110.36(14)
C7	C8	C9	118.8(2)	N8	C54	C55	179.9(4)
C7	C8	C11	120.7(3)	N9	C56	C57	179.7(3)
C9	C8	C11	120.6(2)	F5	B2	F6	109.35(16)
C8	C9	C10	120.8(2)	F5	B2	F7	108.39(17)
C5	C10	C9	120.0(2)	F5	B2	F8	109.39(17)
C4	C12	C13	122.43(16)	F6	B2	F7	109.91(17)
C4	C12	C17	118.36(16)	F6	B2	F8	109.75(17)
C13	C12	C17	119.15(17)	F7	B2	F8	110.02(17)

**Table 6. Hydrogen Bonds for (R,R)-20**

D	H	A	d(D-H)/Å	d(H-A)/Å	d(D-A)/Å	D-H-A/°
N2	H2	F4	0.9600	2.1600	2.8410(18)	127.00
N4	H4	F5	0.9400	1.9900	2.8996(18)	160.00
C10	H10	O1	0.9500	2.5600	2.938(2)	104.00
C13	H13	N3	0.9500	2.6100	2.932(2)	101.00
C21	H21	F4 <sup>1</sup>	0.9500	2.5300	3.155(2)	123.00
C26	H26	O4	0.9500	2.5600	3.195(2)	124.00
C32	H32	O1 <sup>2</sup>	0.9500	2.5000	3.373(2)	153.00
C36	H36	O4	0.9500	2.5500	2.913(2)	103.00
C47	H47	F7 <sup>3</sup>	0.9500	2.3800	3.283(2)	158.00
C51	H51A	F3 <sup>4</sup>	0.9800	2.3000	3.246(2)	162.00

C57 H57B O4	0.9800	2.5800	3.223(3)	123.00
C57 H57C O3 <sup>5</sup>	0.9800	2.5000	3.229(3)	131.00

<sup>1</sup>-1/2+X,1/2-Y,-Z; <sup>2</sup>+X,1+Y,+Z; <sup>3</sup>1/2+X,3/2-Y,-Z; <sup>4</sup>-1+X,+Y,+Z; <sup>5</sup>1-X,-1/2+Y,1/2-Z

**Table 7 Torsion Angles for (R,R)-20**

A	B	C	D	Angle/°	A	B	C	D	Angle/°
Fe1	F1	B1	F2	-134.11(12)	N7	Fe1	N4	C29	-75.21(11)
Fe1	F1	B1	F3	104.43(15)	C1	N1	C27	C26	1.2(3)
Fe1	F1	B1	F4	-15.7(2)	C1	N1	C27	C28	-173.52(15)
Fe1	N1	C1	C2	-3.9(2)	C1	C24	C25	C26	0.7(3)
Fe1	N1	C1	C24	173.83(13)	C2	N2	C3	C4	-34.70(15)
Fe1	N1	C27	C26	-173.01(13)	C2	N2	C3	C18	-156.74(14)
Fe1	N1	C27	C28	12.29(19)	C2	N3	C4	C3	-4.59(16)
Fe1	N2	C2	N3	157.58(10)	C2	N3	C4	C12	-127.77(14)
Fe1	N2	C2	C1	38.03(15)	C2	C1	C24	C25	176.88(16)
Fe1	N2	C3	C4	-154.82(10)	C3	N2	C2	N3	32.03(16)
Fe1	N2	C3	C18	83.14(15)	C3	N2	C2	C1	-87.52(15)
Fe1	N4	C28	N5	158.25(10)	C3	C4	C12	C13	-96.02(19)
Fe1	N4	C28	C27	36.86(15)	C3	C4	C12	C17	81.09(19)
Fe1	N4	C29	C30	-163.84(9)	C3	C18	C19	C20	-174.06(17)
Fe1	N4	C29	C44	70.84(15)	C3	C18	C23	C22	174.19(18)
S1	N3	C2	N2	117.70(13)	C4	N3	C2	N2	-16.80(17)
S1	N3	C2	C1	-123.01(13)	C4	N3	C2	C1	102.48(15)
S1	N3	C4	C3	-139.88(11)	C4	C3	C18	C19	101.66(19)
S1	N3	C4	C12	96.94(15)	C4	C3	C18	C23	-71.9(2)
S1	C5	C6	C7	-173.06(18)	C4	C12	C13	C14	178.23(16)
S1	C5	C10	C9	172.37(18)	C4	C12	C17	C16	-178.24(16)
S2	N5	C28	N4	133.04(12)	C5	S1	N3	C2	-72.54(14)
S2	N5	C28	C27	-106.74(14)	C5	S1	N3	C4	58.93(14)
S2	N5	C30	C29	-156.99(11)	C5	C6	C7	C8	1.5(4)
S2	N5	C30	C38	80.86(17)	C6	C5	C10	C9	-1.0(3)
S2	C31	C32	C33	178.78(14)	C6	C7	C8	C9	-2.6(4)
S2	C31	C36	C35	179.72(14)	C6	C7	C8	C11	178.7(3)
F1	Fe1	N1	C1	-67.58(13)	C7	C8	C9	C10	1.9(4)
F1	Fe1	N1	C27	106.64(13)	C8	C9	C10	C5	-0.1(4)
F1	Fe1	N2	C2	56.73(10)	C10	C5	C6	C7	0.3(3)
F1	Fe1	N2	C3	174.50(11)	C11	C8	C9	C10	-179.4(3)
F1	Fe1	N4	C28	-107.76(10)	C12	C13	C14	C15	-0.1(3)
F1	Fe1	N4	C29	11.98(11)	C13	C12	C17	C16	-1.0(3)

---

O1	S1	N3	C2	173.13(11)	C13 C14 C15 C16	-1.1(3)
O1	S1	N3	C4	-55.40(13)	C14 C15 C16 C17	1.2(3)
O1	S1	C5	C6	-164.86(16)	C15 C16 C17 C12	-0.1(3)
O1	S1	C5	C10	21.77(19)	C17 C12 C13 C14	1.2(3)
O2	S1	N3	C2	43.90(14)	C18 C3 C4 N3	147.91(14)
O2	S1	N3	C4	175.37(12)	C18 C3 C4 C12	-87.53(17)
O2	S1	C5	C6	-31.66(19)	C18 C19 C20 C21	-0.2(3)
O2	S1	C5	C10	154.97(16)	C19 C18 C23 C22	0.6(3)
O3	S2	N5	C28	179.97(13)	C19 C20 C21 C22	0.5(3)
O3	S2	N5	C30	-46.90(14)	C20 C21 C22 C23	-0.3(3)
O3	S2	C31	C32	29.16(16)	C21 C22 C23 C18	-0.3(3)
O3	S2	C31	C36	-150.30(14)	C23 C18 C19 C20	-0.3(3)
O4	S2	N5	C28	51.60(13)	C24 C1 C2 N2	158.36(16)
O4	S2	N5	C30	-175.27(12)	C24 C1 C2 N3	41.4(2)
O4	S2	C31	C32	160.92(14)	C24 C25 C26 C27	0.1(3)
O4	S2	C31	C36	-18.55(16)	C25 C26 C27 N1	-1.0(3)
N1	Fe1	F1	B1	131.58(14)	C25 C26 C27 C28	173.05(16)
N1	Fe1	N2	C2	-30.62(10)	C26 C27 C28 N4	152.32(16)
N1	Fe1	N2	C3	87.15(11)	C26 C27 C28 N5	34.8(2)
N1	Fe1	N4	C28	-23.79(10)	C27 N1 C1 C2	-178.05(15)
N1	Fe1	N4	C29	95.95(11)	C27 N1 C1 C24	-0.4(3)
N1	C1	C2	N2	-24.0(2)	C28 N4 C29 C30	-41.41(15)
N1	C1	C2	N3	-141.01(15)	C28 N4 C29 C44	-166.73(13)
N1	C1	C24	C25	-0.6(3)	C28 N5 C30 C29	-20.68(16)
N1	C27	C28	N4	-33.2(2)	C28 N5 C30 C38	-142.83(14)
N1	C27	C28	N5	-150.76(14)	C29 N4 C28 N5	28.16(16)
N2	Fe1	F1	B1	57.30(13)	C29 N4 C28 C27	-93.23(15)
N2	Fe1	N1	C1	19.54(13)	C29 C30 C38 C39	112.70(18)
N2	Fe1	N1	C27	-166.24(14)	C29 C30 C38 C43	-64.8(2)
N2	Fe1	N4	C28	-10.25(17)	C29 C44 C45 C46	-176.96(17)
N2	Fe1	N4	C29	109.49(13)	C29 C44 C49 C48	177.42(18)
N2	C3	C4	N3	24.09(15)	C30 N5 C28 N4	-4.09(17)
N2	C3	C4	C12	148.65(14)	C30 N5 C28 C27	116.13(15)
N2	C3	C18	C19	-139.81(16)	C30 C29 C44 C45	-52.9(2)
N2	C3	C18	C23	46.6(2)	C30 C29 C44 C49	129.81(17)
N3	S1	C5	C6	82.25(18)	C30 C38 C39 C40	-178.39(17)
N3	S1	C5	C10	-91.12(17)	C30 C38 C43 C42	178.75(17)
N3	C4	C12	C13	21.9(2)	C31 S2 N5 C28	-63.37(13)
N3	C4	C12	C17	-160.97(15)	C31 S2 N5 C30	69.75(14)
N4	Fe1	F1	B1	-153.60(13)	C31 C32 C33 C34	1.6(3)
N4	Fe1	N1	C1	-167.69(14)	C32 C31 C36 C35	0.3(3)

N4 Fe1 N1 C27	6.53(12)	C32 C33 C34 C35	0.0(3)
N4 Fe1 N2 C2	-44.26(16)	C32 C33 C34 C37	-179.71(19)
N4 Fe1 N2 C3	73.51(15)	C33 C34 C35 C36	-1.6(3)
N4 C29 C30 N5	37.75(14)	C34 C35 C36 C31	1.4(3)
N4 C29 C30 C38	160.44(13)	C36 C31 C32 C33	-1.8(3)
N4 C29 C44 C45	65.6(2)	C37 C34 C35 C36	178.16(19)
N4 C29 C44 C49	-111.68(18)	C38 C39 C40 C41	-0.2(3)
N5 S2 C31 C32	-85.44(15)	C39 C38 C43 C42	1.2(3)
N5 S2 C31 C36	95.10(15)	C39 C40 C41 C42	0.8(3)
N5 C30 C38 C39	-132.34(16)	C40 C41 C42 C43	-0.4(3)
N5 C30 C38 C43	50.1(2)	C41 C42 C43 C38	-0.6(3)
N6 Fe1 N1 C1	110.68(13)	C43 C38 C39 C40	-0.8(3)
N6 Fe1 N1 C27	-75.10(13)	C44 C29 C30 N5	161.23(14)
N6 Fe1 N2 C2	-126.91(11)	C44 C29 C30 C38	-76.09(18)
N6 Fe1 N2 C3	-9.14(12)	C44 C45 C46 C47	-1.1(3)
N6 Fe1 N4 C28	74.98(11)	C45 C44 C49 C48	0.1(3)
N6 Fe1 N4 C29	-165.28(11)	C45 C46 C47 C48	1.5(3)
N7 Fe1 F1 B1	-56.28(14)	C46 C47 C48 C49	-1.2(3)
N7 Fe1 N2 C2	140.81(11)	C47 C48 C49 C44	0.4(3)
N7 Fe1 N2 C3	-101.43(12)	C49 C44 C45 C46	0.3(3)
N7 Fe1 N4 C28	165.05(11)		

**Table 8 Hydrogen Atom Coordinates ( $\text{\AA} \times 10^4$ ) and Isotropic Displacement Parameters ( $\text{\AA}^2 \times 10^3$ ) for (*R,R*)-20**

Atom	<i>x</i>	<i>y</i>	<i>z</i>	U(eq)
H2	6583	2677	903	17(5)
H2A	7723	2615	1359	16(5)
H3	4416	3034	1278	12(5)
H4	5868	6264	1153	21(5)
H4A	5055	1209	1159	5(4)
H6	8969	1465	1031	20(5)
H7	9254	1185	421	35(6)
H9	6290	-562	428	62(9)
H10	6019	-317	1036	53(8)
H11A	8188	-483	-77	109(14)
H11B	8599	556	-126	84(12)
H11C	7130	273	-156	140(20)
H13	4526	1938	2039	28(6)
H14	2705	1621	2375	34(6)
H15	921	968	2109	37(6)

---

H16	931	671	1495	37(7)
H17	2756	984	1159	15(5)
H19	2452	3021	950	18(5)
H20	1311	2714	429	31(6)
H21	2320	2016	-51	27(6)
H22	4468	1602	-11	27(6)
H23	5610	1901	511	18(5)
H24	6867	2588	2162	27(6)
H25	6637	3792	2567	23(5)
H26	6205	5262	2355	22(5)
H28	4878	5735	1632	4(4)
H29	8153	6002	1464	9(5)
H30	6659	7602	1511	11(5)
H32	5021	8773	1670	24(6)
H33	3548	9333	1260	38(7)
H35	1242	7186	1434	34(6)
H36	2739	6573	1827	34(6)
H37A	1442	8405	806	51(8)
H37B	1407	9348	1018	48(7)
H37C	436	8552	1121	89(12)
H39	8042	8788	1599	21(5)
H40	9786	9456	1890	53(8)
H41	10994	8609	2286	42(7)
H42	10518	7087	2388	27(6)
H43	8792	6405	2094	17(5)
H45	6737	7627	878	34(6)
H46	7653	8068	336	34(6)
H47	9605	7468	159	24(6)
H48	10606	6371	508	48(8)
H49	9690	5916	1046	34(6)
H51A	1547	4968	858	35(6)
H51B	2073	5939	980	40(7)
H51C	1771	5175	1271	44(7)
H53A	6625	5360	-277	109(14)
H53B	7985	5718	-145	98(13)
H53C	6735	6318	-79	117(15)
H55A	1084	3065	1674	69(10)
H55B	-250	2733	1835	60(9)
H55C	868	3057	2096	69(10)
H57A	2057	5113	2504	77(11)
H57B	3558	5048	2577	90(12)



H57C                      2687                      4159                      2608                      71(9)

### 1.3. Fe(OTf)<sub>2</sub>L1(THF) complex (CCDC 945601)

**Table 2 Fractional Atomic Coordinates ( $\times 10^4$ ) and Equivalent Isotropic Displacement Parameters ( $\text{\AA}^2 \times 10^3$ ) for CCDC 945601.  $U_{\text{eq}}$  is defined as 1/3 of of the trace of the orthogonalised  $U_{\text{ij}}$  tensor.**

Atom	<i>x</i>	<i>y</i>	<i>z</i>	$U_{\text{eq}}$
Fe1	5853.2(3)	5853.2(3)	0	17.29(12)
S1	8120.9(6)	7358.5(8)	-928.20(14)	27.77(18)
S2	3671.0(7)	7920.1(7)	213.50(13)	25.30(16)
O3	4538.7(18)	4538.7(18)	0	28.5(7)
N4	7216(2)	7216(2)	0	21.6(7)
O5	4442.0(19)	7202.9(18)	43.7(4)	24.8(4)
O6	8178(2)	8468(2)	-1070.2(4)	36.3(6)
O7	2405(2)	7912(2)	147.4(4)	36.1(5)
F8	3594(3)	10283(2)	281.5(4)	59.2(7)
F9	3959(2)	9735.3(18)	-105.2(4)	44.2(5)
C10	3979(3)	5799(3)	-776.8(6)	26.6(6)
O11	9208(2)	6828(2)	-823.0(4)	37.7(6)
C12	1816(3)	5651(3)	-725.1(6)	32.7(7)
C13	4172(4)	9470(3)	136.6(6)	36.6(8)
N14	6090(2)	6337(2)	-414.2(4)	18.5(5)
F15	5362(2)	9595.2(19)	180.2(5)	52.3(6)
C16	1851(3)	6576(3)	-550.0(6)	31.2(7)
C17	2951(3)	7109(3)	-482.5(5)	24.0(6)
C18	5933(2)	7919(3)	-738.6(5)	19.9(6)
O19	3971(2)	7758(2)	477.8(4)	36.9(5)
N20	7229(2)	7630(2)	-681.4(4)	22.1(5)
C21	7556(3)	7727(3)	220.1(5)	28.5(6)
C22	7356(3)	6269(3)	-1119.8(5)	26.4(6)
C23	6608(3)	4252(3)	-1186.9(6)	34.1(7)
C24	5235(2)	7278(2)	-517.1(5)	17.7(5)
C25	4032(3)	6717(2)	-595.3(5)	18.9(5)
C26	5651(3)	9266(3)	-753.9(5)	25.7(6)
C27	6846(3)	7310(3)	453.6(5)	22.9(6)
C28	6024(3)	4605(3)	-1414.3(6)	32.6(7)
C29	2877(3)	5259(3)	-841.4(6)	31.5(7)
C30	7273(3)	5060(3)	-1041.9(5)	29.6(7)

C31	2928(3)	3285(3)	135.7(8)	43.8(9)
C32	6788(3)	6661(3)	-1340.3(5)	29.8(7)
C33	6141(3)	5820(3)	-1486.4(6)	32.7(7)
C34	4993(4)	11711(3)	-776.8(8)	51.5(10)
C35	5930(4)	11343(3)	-626.3(7)	44.2(8)
C37	5263(4)	3671(3)	-1568.4(7)	46.9(10)
C39	4083(5)	3413(4)	-1423.8(8)	58.7(12)
C40	8431(4)	8634(4)	228.7(6)	43.2(9)
C42	4920(5)	4183(4)	-1830.1(7)	55.5(11)
C44	4726(4)	9644(4)	-909.7(10)	65.3(11)
C48	3443(3)	4565(3)	153.0(8)	42.5(9)
C51	4391(5)	10860(4)	-914.5(11)	76.5(12)
C52	6252(3)	10129(3)	-613.0(7)	38.8(8)
C1	8976(3)	8976(3)	0	53.2(14)
C2	5998(6)	2499(4)	-1606(1)	83.8(19)

**Table 3 Anisotropic Displacement Parameters ( $\text{\AA}^2 \times 10^3$ ) for CCDC 945601. The Anisotropic displacement factor exponent takes the form:  $-2\pi^2 [h^2 a^{*2} U_{11} + \dots + 2hka \times b \times U_{12}]$**

Atom	$U_{11}$	$U_{22}$	$U_{33}$	$U_{23}$	$U_{13}$	$U_{12}$
Fe1	18.77(16)	18.77(16)	14.3(2)	0.49(15)	-0.49(15)	-3.9(2)
S1	17.8(3)	48.1(5)	17.4(3)	6.7(3)	1.1(3)	-4.4(3)
S2	31.2(4)	27.0(4)	17.7(3)	0.8(3)	2.1(3)	1.8(3)
O3	24.6(9)	24.6(9)	36.4(17)	-4.9(10)	4.9(10)	-8.0(11)
N4	24.8(10)	24.8(10)	15.3(15)	5.1(10)	-5.1(10)	-5.6(14)
O5	31.2(11)	20.5(10)	22.6(10)	-0.7(8)	-1.3(8)	4.3(8)
O6	27.5(12)	54.9(16)	26.4(11)	11.1(10)	1.6(9)	-13.7(11)
O7	32.6(12)	45.0(14)	30.9(11)	3.5(10)	2.5(10)	5.9(11)
F8	97(2)	32.4(12)	47.8(13)	-14(1)	11.9(13)	16.3(12)
F9	73.2(16)	29.3(10)	30.2(10)	6.8(8)	3(1)	3.3(10)
C10	20.9(14)	30.4(15)	28.4(15)	-3.1(13)	-2.6(12)	-0.7(12)
O11	18.9(11)	67.7(17)	26.4(11)	6.1(11)	0.1(9)	-1.8(11)
C12	21.0(15)	34.6(18)	42.6(18)	8.5(15)	-9.6(14)	-10.3(13)
C13	54(2)	23.5(16)	32.2(17)	-3.0(13)	0.5(16)	5.2(15)
N14	17.4(12)	22.8(11)	15.4(10)	0.5(9)	-1.8(8)	-3.0(9)
F15	59.5(15)	31.0(11)	66.5(15)	2.4(11)	-11.3(12)	-13.3(10)
C16	18.4(15)	45(2)	30.3(16)	5.8(14)	2.7(12)	-1.7(13)
C17	21.9(14)	30.6(16)	19.6(13)	0.7(12)	-2.0(11)	-1.2(11)
C18	16.5(13)	30.5(15)	12.9(11)	2.3(10)	-4.3(10)	-6.2(11)
O19	40.6(14)	50.4(15)	19.6(10)	3.8(10)	0.5(9)	-0.5(11)

N20	16.9(11)	34.8(13)	14.6(10)	4.8(10)	-3.2(9)	-7(1)
C21	36.3(16)	26.4(15)	22.8(14)	7.7(11)	-9.6(12)	-11.7(12)
C22	21.8(14)	44.7(18)	12.6(12)	-0.3(12)	2.3(11)	2.8(13)
C23	46(2)	33.8(18)	22.0(14)	1.2(14)	0.2(14)	14.2(15)
C24	18.2(13)	19.2(13)	15.8(12)	-1(1)	-1(1)	-3.0(11)
C25	17.3(13)	20.6(13)	18.8(13)	1.7(10)	-1.9(10)	-3.3(10)
C26	28.5(14)	28.0(14)	20.8(13)	8.3(12)	-6.3(11)	-8.7(12)
C27	31.1(15)	20.3(14)	17.3(13)	1.5(11)	-6.2(11)	-3.2(12)
C28	42.3(19)	37.1(17)	18.4(14)	-5.5(12)	-5.7(13)	13.2(14)
C29	32.4(17)	26.7(16)	35.4(17)	-4.6(13)	-9.4(14)	-5.5(13)
C30	33.0(17)	44.0(18)	11.9(13)	3.6(12)	1.0(12)	11.6(14)
C31	28.5(18)	36.2(19)	67(2)	11.7(17)	2.1(17)	-8.5(15)
C32	30.5(17)	39.3(18)	19.6(14)	4.8(13)	0.0(12)	6.5(13)
C33	38.3(18)	38.6(18)	21.2(14)	1.9(13)	-6.0(12)	13.4(15)
C34	71(2)	25.1(16)	59(2)	10.4(16)	-24.8(19)	-6.6(16)
C35	50(2)	35.0(16)	47.7(18)	-15.2(15)	-11.0(16)	-4.4(16)
C37	81(3)	27.4(17)	32.3(18)	-5.0(15)	-19.5(19)	15.3(18)
C39	81(3)	49(2)	47(2)	4.6(19)	-20(2)	-17(2)
C40	62(2)	43.9(18)	24.3(15)	12.3(14)	-19.3(15)	-33.3(16)
C42	91(3)	42(2)	33(2)	-7.0(17)	-28(2)	7(2)
C44	76(2)	34.6(18)	85(3)	9.9(19)	-59(2)	-10.6(18)
C48	35.3(19)	36.6(19)	56(2)	-4.8(17)	12.7(17)	-5.8(15)
C51	94(3)	36.1(19)	99(3)	15(2)	-65(2)	-5(2)
C52	38.7(17)	38.7(17)	39.0(17)	-11.0(14)	-17.4(15)	4.7(14)
C1	64(2)	64(2)	31(2)	17.3(19)	-17.3(19)	-49(3)
C2	138(5)	45(3)	68(3)	-25(2)	-48(3)	45(3)

**Table 4 Bond Lengths for CCDC 945601**

Atom	Atom	Length/Å	Atom	Atom	Length/Å
Fe1	O3	2.042(3)	C18	N20	1.489(3)
Fe1	N4	2.117(3)	C18	C24	1.560(4)
Fe1	O5 <sup>1</sup>	2.157(2)	C18	C26	1.514(4)
Fe1	O5	2.157(2)	N20	C27 <sup>1</sup>	1.476(3)
Fe1	N14 <sup>1</sup>	2.252(2)	C21	C27	1.523(4)
Fe1	N14	2.252(2)	C21	C40	1.385(4)
S1	O6	1.430(2)	C22	C30	1.393(5)
S1	O11	1.438(2)	C22	C32	1.383(4)
S1	N20	1.650(2)	C23	C28	1.409(4)
S1	C22	1.774(3)	C23	C30	1.378(5)

S2	O5	1.460(2)	C24	C25	1.514(4)
S2	O7	1.433(2)	C26	C44	1.368(5)
S2	C13	1.834(3)	C26	C52	1.372(4)
S2	O19	1.436(2)	C27	N14 <sup>1</sup>	1.468(3)
O3	C48	1.447(4)	C27	N20 <sup>1</sup>	1.476(3)
O3	C48 <sup>1</sup>	1.447(4)	C28	C33	1.392(5)
N4	C21 <sup>1</sup>	1.337(3)	C28	C37	1.551(5)
N4	C21	1.337(3)	C31	C31 <sup>1</sup>	1.528(8)
F8	C13	1.333(4)	C31	C48	1.519(5)
F9	C13	1.323(4)	C32	C33	1.395(5)
C10	C25	1.388(4)	C34	C35	1.358(6)
C10	C29	1.390(4)	C34	C51	1.354(6)
C12	C16	1.370(5)	C35	C52	1.381(5)
C12	C29	1.384(5)	C37	C39	1.528(6)
C13	F15	1.334(5)	C37	C42	1.531(5)
N14	C24	1.497(3)	C37	C2	1.532(5)
N14	C27 <sup>1</sup>	1.468(3)	C40	C1	1.393(4)
C16	C17	1.388(4)	C44	C51	1.386(6)
C17	C25	1.395(4)	C1	C40 <sup>1</sup>	1.393(4)

<sup>1</sup>+Y,+X,-Z**Table 5 Bond Angles for CCDC 945601**

Atom	Atom	Atom	Angle/°	Atom	Atom	Atom	Angle/°
O3	Fe1	N4	180.00(3)	N20	C18	C24	103.0(2)
O3	Fe1	O5 <sup>1</sup>	88.73(6)	N20	C18	C26	114.5(2)
O3	Fe1	O5	88.73(6)	C26	C18	C24	112.3(2)
O3	Fe1	N14	104.38(6)	C18	N20	S1	116.60(17)
O3	Fe1	N14 <sup>1</sup>	104.38(6)	C27 <sup>1</sup>	N20	S1	119.6(2)
N4	Fe1	O5 <sup>1</sup>	91.27(6)	C27 <sup>1</sup>	N20	C18	110.2(2)
N4	Fe1	O5	91.27(6)	N4	C21	C27	115.2(3)
N4	Fe1	N14 <sup>1</sup>	75.62(6)	N4	C21	C40	121.6(3)
N4	Fe1	N14	75.62(6)	C40	C21	C27	123.0(3)
O5	Fe1	O5 <sup>1</sup>	177.47(12)	C30	C22	S1	120.5(2)
O5	Fe1	N14 <sup>1</sup>	89.31(8)	C32	C22	S1	118.5(3)
O5 <sup>1</sup>	Fe1	N14 <sup>1</sup>	91.32(8)	C32	C22	C30	120.8(3)
O5	Fe1	N14	91.32(8)	C30	C23	C28	122.1(3)
O5 <sup>1</sup>	Fe1	N14	89.30(8)	N14	C24	C18	105.7(2)
N14	Fe1	N14 <sup>1</sup>	151.24(12)	N14	C24	C25	111.3(2)
O6	S1	O11	120.58(14)	C25	C24	C18	114.2(2)

O6	S1	N20	106.29(14)	C10	C25	C17	118.7(3)
O6	S1	C22	107.48(14)	C10	C25	C24	121.2(3)
O11	S1	N20	105.35(12)	C17	C25	C24	120.1(2)
O11	S1	C22	109.70(15)	C44	C26	C18	118.7(3)
N20	S1	C22	106.60(13)	C44	C26	C52	118.0(3)
O5	S2	C13	101.10(15)	C52	C26	C18	123.2(3)
O7	S2	O5	114.30(13)	N14 <sup>1</sup>	C27	N20 <sup>1</sup>	106.3(2)
O7	S2	C13	104.12(16)	N14 <sup>1</sup>	C27	C21	110.9(2)
O7	S2	O19	117.08(14)	N20 <sup>1</sup>	C27	C21	111.7(2)
O19	S2	O5	112.93(13)	C23	C28	C37	120.3(3)
O19	S2	C13	104.98(16)	C33	C28	C23	116.9(3)
C48	O3	Fe1	125.03(17)	C33	C28	C37	122.8(3)
C48 <sup>1</sup>	O3	Fe1	125.03(17)	C12	C29	C10	119.6(3)
C48 <sup>1</sup>	O3	C48	109.9(3)	C23	C30	C22	119.1(3)
C21 <sup>1</sup>	N4	Fe1	119.62(17)	C48	C31	C31 <sup>1</sup>	101.4(2)
C21	N4	Fe1	119.62(17)	C22	C32	C33	118.9(3)
C21	N4	C21 <sup>1</sup>	120.8(3)	C28	C33	C32	122.2(3)
S2	O5	Fe1	148.48(13)	C51	C34	C35	118.4(4)
C25	C10	C29	120.9(3)	C34	C35	C52	120.7(3)
C16	C12	C29	120.1(3)	C39	C37	C28	108.7(3)
F8	C13	S2	110.7(3)	C39	C37	C42	107.7(4)
F8	C13	F15	107.4(3)	C39	C37	C2	110.8(4)
F9	C13	S2	111.2(2)	C42	C37	C28	110.9(3)
F9	C13	F8	108.4(3)	C42	C37	C2	108.9(3)
F9	C13	F15	108.4(3)	C2	C37	C28	109.8(4)
F15	C13	S2	110.6(2)	C21	C40	C1	117.6(3)
C24	N14	Fe1	116.00(16)	C26	C44	C51	120.0(4)
C27 <sup>1</sup>	N14	Fe1	109.33(16)	O3	C48	C31	104.9(3)
C27 <sup>1</sup>	N14	C24	105.0(2)	C34	C51	C44	121.7(4)
C12	C16	C17	120.6(3)	C26	C52	C35	121.1(3)
C16	C17	C25	120.2(3)	C40	C1	C40 <sup>1</sup>	120.7(4)

<sup>1</sup>+Y,+X,-Z

**Table 6 Hydrogen Atom Coordinates ( $\text{\AA}\times 10^4$ ) and Isotropic Displacement Parameters ( $\text{\AA}^2\times 10^3$ ) for CCDC 945601**

Atom	x	y	z	U(eq)
H10	4691	5541	-856	32
H12	1077	5286	-766	39
H14	6016	5648	-509	22

H16	1133	6849	-476	37
H17	2967	7729	-362	29
H18	5707	7533	-900	24
H20	7519	8354	-623	27
H23	6543	3448	-1133	41
H24	5079	7880	-383	21
H27	6182	7885	487	28
H29	2853	4639	-962	38
H30	7661	4801	-894	36
H31A	2052	3280	158	53
H31B	3299	2748	261	53
H32	6836	7472	-1390	36
H33	5777	6078	-1637	39
H34	4771	12527	-785	62
H35	6359	11915	-531	53
H39A	4273	3144	-1254	88
H39B	3632	2791	-1511	88
H39C	3604	4143	-1415	88
H40	8646	9002	382	52
H42A	4445	4910	-1809	83
H42B	4452	3590	-1922	83
H42C	5646	4371	-1924	83
H44	4322	9084	-1012	78
H48A	2868	5155	86	51
H48B	3630	4774	328	51
H51	3735	11098	-1015	92
H52	6887	9893	-507	47
H1	9574	9574	0	64
H2A	6772	2692	-1681	126
H2B	5560	1958	-1717	126
H2C	6123	2112	-1444	126

#### 1.4. *Cis* 1,1'-peroxydiisochroman (CCDC 945602)

**Table 2 Fractional Atomic Coordinates ( $\times 10^4$ ) and Equivalent Isotropic Displacement Parameters ( $\text{\AA}^2 \times 10^3$ ) for CCDC 945602.  $U_{\text{eq}}$  is defined as 1/3 of the trace of the orthogonalised  $U_{\text{IJ}}$  tensor.**

Atom	x	y	z	U(eq)
O2	-66.2(6)	1766.1(7)	350.5(13)	20.1(3)
C3	1471.6(9)	2354.7(10)	-1489.1(17)	18.9(3)
C4	883.0(8)	3140.2(10)	-920.4(17)	16.7(3)

C5	987.7(9)	4190.1(10)	-1469.7(17)	18.3(3)
C6	116.0(9)	2855.6(10)	274.5(17)	17.3(3)
C7	1348.5(10)	1220.2(11)	-897(2)	24.4(3)
C8	1668.5(9)	4463.2(11)	-2599.8(18)	20.1(3)
C9	2254.7(9)	3681.2(11)	-3185.5(18)	21.9(3)
C10	736.5(9)	1154.9(10)	666(2)	21.4(3)
C11	2156.1(9)	2641.9(11)	-2626.5(18)	22.2(3)
O1	400.3(6)	3282.7(7)	1928.6(12)	18.2(2)

**Table 3 Anisotropic Displacement Parameters ( $\text{\AA}^2 \times 10^3$ ) for CCDC 945602. The Anisotropic displacement factor exponent takes the form:  $-2\pi^2[h^2a^{*2}U_{11}+\dots+2hka \times b \times U_{12}]$**

Atom	U <sub>11</sub>	U <sub>22</sub>	U <sub>33</sub>	U <sub>23</sub>	U <sub>13</sub>	U <sub>12</sub>
O2	19.0(5)	17.7(5)	23.4(5)	-0.2(4)	-2.6(4)	-1.8(3)
C3	20.1(6)	20.8(7)	15.8(7)	-3.7(5)	-3.6(5)	1.1(5)
C4	17.2(6)	19.3(6)	13.6(6)	-2.7(5)	-2.3(5)	0.1(5)
C5	18.8(6)	19.6(6)	16.3(7)	-2.2(5)	-1.6(5)	0.9(5)
C6	18.3(6)	16.3(6)	17.3(7)	-0.3(5)	-2.1(5)	0.5(5)
C7	29.0(8)	18.4(7)	25.6(8)	-4.8(6)	0.0(6)	3.9(6)
C8	20.4(7)	22.2(7)	17.5(7)	0.9(5)	-3.0(5)	-2.4(5)
C9	18.4(7)	30.8(7)	16.4(7)	-1.9(6)	0.5(5)	-2.0(5)
C10	23.1(7)	16.4(6)	24.6(8)	1.0(5)	-2.7(6)	1.2(5)
C11	20.0(7)	27.5(7)	19.1(7)	-5.0(5)	-0.4(6)	3.9(5)
O1	16.6(5)	22.6(5)	15.4(5)	-2.3(3)	4.5(4)	-2.5(3)

**Table 4 Bond Lengths for CCDC 945602.**

Atom	Atom	Length/ $\text{\AA}$	Atom	Atom	Length/ $\text{\AA}$
O2	C6	1.3999(15)	C5	C8	1.3842(18)
O2	C10	1.4416(16)	C6	O1	1.4307(16)
C3	C4	1.3957(18)	C7	C10	1.513(2)
C3	C7	1.5101(19)	C8	C9	1.3946(19)
C3	C11	1.3964(19)	C9	C11	1.385(2)
C4	C5	1.3962(18)	O1	O1 <sup>1</sup>	1.4879(16)
C4	C6	1.5152(17)			

<sup>1</sup>-X,+Y,1/2-Z

**Table 5 Bond Angles for CCDC 945602.**

Atom	Atom	Atom	Angle/°	Atom	Atom	Atom	Angle/°
C6	O2	C10	111.63(10)	O2	C6	O1	112.79(10)
C4	C3	C7	119.87(12)	O1	C6	C4	102.92(10)
C4	C3	C11	118.55(12)	C3	C7	C10	111.34(11)
C11	C3	C7	121.57(12)	C5	C8	C9	119.51(13)
C3	C4	C5	120.29(12)	C11	C9	C8	119.94(13)
C3	C4	C6	120.18(12)	O2	C10	C7	110.37(11)
C5	C4	C6	119.52(11)	C9	C11	C3	121.17(12)
C8	C5	C4	120.53(12)	C6	O1	O1 <sup>1</sup>	106.57(10)
O2	C6	C4	113.91(10)				

<sup>1</sup>-X,+Y,1/2-Z

**Table 6 Hydrogen Atom Coordinates ( $\text{\AA} \times 10^4$ ) and Isotropic Displacement Parameters ( $\text{\AA}^2 \times 10^3$ ) for CCDC 945602.**

Atom	x	y	z	U(eq)
H10A	555(10)	411(12)	910(20)	19(4)
H5	573(10)	4738(12)	-1050(20)	18(4)
H6	-459(10)	3189(11)	-106(19)	12(3)
H9	2741(11)	3882(13)	-3990(20)	26(4)
H8	1720(10)	5208(12)	-2990(20)	19(4)
H7A	1928(11)	899(13)	-560(20)	28(4)
H7B	1094(11)	804(13)	-1870(20)	28(4)
H11	2564(12)	2097(14)	-3020(20)	35(5)
H10B	1040(10)	1430(11)	1740(20)	18(4)

### 1.5. *Trans* 1,1'-peroxydiisochroman (CCDC 945603)

**Table 2 Fractional Atomic Coordinates ( $\times 10^4$ ) and Equivalent Isotropic Displacement Parameters ( $\text{\AA}^2 \times 10^3$ ) for CCDC 945603.  $U_{\text{eq}}$  is defined as 1/3 of the trace of the orthogonalised  $U_{\text{IJ}}$  tensor.**

Atom	x	y	z	U(eq)
O1	10484.6(13)	6206.8(14)	2097.2(4)	18.3(3)
O2	4550.5(13)	4711.4(14)	2888.8(4)	17.1(2)
O3	7548.5(14)	5756.3(14)	2774.7(4)	19.2(3)
C4	8194.8(19)	5965.5(19)	1425.8(5)	14.9(3)



O5	7501.0(14)	5164.2(14)	2239.7(4)	19.2(3)
C6	6737.1(19)	4978.0(19)	3586.3(5)	14.9(3)
C7	5376(2)	5790.6(19)	3872.8(5)	16.7(3)
C8	6502(2)	6451(2)	1224.5(6)	19.8(3)
C9	8618.5(19)	6362.3(19)	1974.4(5)	15.1(3)
C10	8398(2)	4499(2)	3808.2(6)	22.3(3)
C11	5720(2)	6107(2)	4382.6(6)	21.9(3)
C12	6394.8(19)	4568.3(19)	3034.1(5)	15.1(3)
C13	9044(2)	4785(2)	621.5(6)	21.1(3)
C14	11332(2)	4624(2)	1344.8(6)	22.2(4)
C15	3570(2)	6284(2)	3630.8(6)	22.0(4)
C16	6089(2)	6136(2)	722.5(6)	24.1(4)
C17	9498(2)	5124.4(19)	1124.5(5)	16.6(3)
C18	11259(2)	4594(2)	1916.6(6)	22.0(3)
C19	7370(2)	5292(2)	421.1(6)	23.6(4)
C20	3738(2)	6318(2)	3061.4(6)	21.5(3)
C21	8716(2)	4816(2)	4315.1(6)	29.1(4)
C22	7365(2)	5625(2)	4602.5(6)	26.9(4)

**Table 3 Anisotropic Displacement Parameters ( $\text{\AA}^2 \times 10^3$ ) for CCDC 945603. The Anisotropic displacement factor exponent takes the form:  $-2\pi^2[h^2a^{*2}U_{11}+\dots+2hka \times b \times U_{12}]$**

Atom	$U_{11}$	$U_{22}$	$U_{33}$	$U_{23}$	$U_{13}$	$U_{12}$
O1	15.9(5)	19.7(6)	19.4(5)	-1.7(4)	-3.4(4)	-0.3(4)
O2	15.7(5)	17.8(5)	17.9(5)	-1.0(4)	-2.8(4)	0.6(4)
O3	24.7(6)	21.6(6)	11.3(5)	-3.6(4)	2.3(4)	-8.5(5)
C4	16.2(7)	12.4(7)	16.2(7)	0.6(6)	0.6(5)	-2.7(6)
O5	25.5(6)	21.1(6)	11.0(5)	-3.9(4)	2.3(4)	-8.5(4)
C6	16.0(7)	13.3(7)	15.3(7)	2.1(6)	0.5(5)	-1.6(6)
C7	16.6(7)	15.1(7)	18.5(7)	1.1(6)	0.1(6)	-1.2(6)
C8	17.8(7)	20.5(8)	21.0(8)	-0.4(6)	0.5(6)	1.8(6)
C9	15.4(7)	13.6(7)	16.2(7)	1.1(6)	0.8(5)	-2.3(6)
C10	18.9(8)	25.3(9)	22.8(8)	-2.5(7)	-1.3(6)	3.3(6)
C11	23.0(8)	24.0(8)	18.6(8)	-2.3(6)	4.4(6)	-0.8(7)
C12	14.8(7)	14.1(7)	16.5(7)	0.8(6)	-0.2(5)	-0.5(6)
C13	22.0(8)	22.4(8)	18.9(8)	-0.5(6)	5.5(6)	-2.2(6)
C14	17.6(7)	24.3(8)	24.6(8)	-2.5(7)	1.6(6)	4.1(6)
C15	17.9(8)	23.6(8)	24.4(8)	-3.7(7)	-0.8(6)	5.5(6)
C16	19.5(8)	28.8(9)	24.0(8)	2.0(7)	-5.2(6)	-0.1(7)
C17	16.8(7)	14.8(7)	18.3(7)	2.6(6)	1.9(5)	-2.8(6)

C18	19.1(8)	21.7(8)	25.1(8)	0.8(7)	-3.4(6)	5.8(6)
C19	28.4(8)	28.4(9)	13.9(7)	1.5(7)	-1.8(6)	-6.2(7)
C20	19.5(8)	20.0(8)	24.9(8)	-0.2(6)	-5.7(6)	4.9(6)
C21	24.3(8)	37.2(10)	25.6(9)	-0.7(8)	-8.9(7)	5.9(8)
C22	30.2(9)	34.9(10)	15.5(8)	-1.5(7)	-4.7(6)	-1.8(8)

**Table 4 Bond Lengths for CCDC 945603.**

Atom	Atom	Length/Å	Atom	Atom	Length/Å
O1	C9	1.4014(17)	C7	C11	1.395(2)
O1	C18	1.4455(18)	C7	C15	1.509(2)
O2	C12	1.4002(17)	C8	C16	1.385(2)
O2	C20	1.4457(18)	C10	C21	1.384(2)
O3	O5	1.4903(14)	C11	C22	1.381(2)
O3	C12	1.4210(17)	C13	C17	1.397(2)
C4	C8	1.393(2)	C13	C19	1.385(2)
C4	C9	1.517(2)	C14	C17	1.506(2)
C4	C17	1.402(2)	C14	C18	1.518(2)
O5	C9	1.4184(17)	C15	C20	1.516(2)
C6	C7	1.399(2)	C16	C19	1.392(2)
C6	C10	1.392(2)	C21	C22	1.394(2)
C6	C12	1.517(2)			

**Table 5 Bond Angles for CCDC 945603.**

Atom	Atom	Atom	Angle/°	Atom	Atom	Atom	Angle/°
C9	O1	C18	112.09(11)	C21	C10	C6	120.34(15)
C12	O2	C20	111.95(11)	C22	C11	C7	120.95(14)
C12	O3	O5	104.65(9)	O2	C12	O3	112.65(11)
C8	C4	C9	119.32(13)	O2	C12	C6	113.73(12)
C8	C4	C17	120.40(13)	O3	C12	C6	103.79(11)
C17	C4	C9	120.28(13)	C19	C13	C17	121.20(14)
C9	O5	O3	105.23(9)	C17	C14	C18	110.89(12)
C7	C6	C12	120.20(13)	C7	C15	C20	110.73(12)
C10	C6	C7	120.33(14)	C8	C16	C19	119.36(15)
C10	C6	C12	119.45(13)	C4	C17	C14	119.92(13)
C6	C7	C15	119.98(13)	C13	C17	C4	118.20(14)
C11	C7	C6	118.63(14)	C13	C17	C14	121.89(13)
C11	C7	C15	121.38(13)	O1	C18	C14	109.48(12)
C16	C8	C4	120.65(14)	C13	C19	C16	120.17(14)

O1	C9	C4	113.49(12)	O2	C20	C15	109.60(12)
O1	C9	O5	112.80(12)	C10	C21	C22	119.60(15)
O5	C9	C4	103.31(11)	C11	C22	C21	120.16(15)

**Table 6 Hydrogen Atom Coordinates ( $\text{\AA}\times 10^4$ ) and Isotropic Displacement Parameters ( $\text{\AA}^2\times 10^3$ ) for CCDC 945603.**

Atom	<i>x</i>	<i>y</i>	<i>z</i>	U(eq)
H8	5640	6991	1429	24
H9	8210	7547	2051	18
H10	9298	3964	3615	27
H11	4830	6652	4577	26
H12	6816	3382	2965	18
H13	9883	4209	418	25
H14A	12256	5450	1237	27
H14B	11681	3484	1222	27
H15A	3195	7421	3750	26
H15B	2635	5452	3727	26
H16	4967	6486	588	29
H18A	10512	3625	2028	26
H18B	12487	4445	2053	26
H19	7099	5068	84	28
H20A	2533	6463	2910	26
H20B	4497	7292	2960	26
H21	9824	4492	4463	35
H22	7571	5840	4943	32

### 1.6. 1,1'-Oxydiisochroman (CCDC 945604)

**Table 2 Fractional Atomic Coordinates ( $\times 10^4$ ) and Equivalent Isotropic Displacement Parameters ( $\text{\AA}^2\times 10^3$ ) for CCDC 945604.  $U_{\text{eq}}$  is defined as 1/3 of of the trace of the orthogonalised  $U_{\text{IJ}}$  tensor.**

Atom	<i>x</i>	<i>y</i>	<i>z</i>	U(eq)
O1	2423.5(5)	11836.7(19)	935.1(4)	21.5(2)
O2	2500	9005(3)	0	19.5(3)
C3	3729.9(7)	8893(3)	881.8(5)	18.5(3)
C4	2971.3(7)	10852(3)	530.0(5)	19.1(3)
C5	2227.6(7)	9337(3)	1336.3(6)	22.4(3)
C6	3774.4(7)	7754(3)	1508.6(5)	19.6(3)

C7	3042.4(8)	8432(3)	1839.7(6)	22.9(3)
C8	4492.4(7)	5971(3)	1815.2(6)	22.4(3)
C9	5156.8(7)	5347(3)	1502.3(6)	24.7(3)
C10	4394.1(7)	8235(3)	565.2(6)	21.6(3)
C11	5107.6(7)	6479(3)	873.9(6)	24.4(3)

**Table 3 Anisotropic Displacement Parameters ( $\text{\AA}^2 \times 10^3$ ) for CCDC 945604. The Anisotropic displacement factor exponent takes the form:  $-2\pi^2[h^2a^{*2}U_{11}+\dots+2hka \times b \times U_{12}]$**

Atom	U <sub>11</sub>	U <sub>22</sub>	U <sub>33</sub>	U <sub>23</sub>	U <sub>13</sub>	U <sub>12</sub>
O1	19.5(4)	22.3(4)	23.7(4)	-0.6(3)	6.8(3)	2.3(3)
O2	17.2(5)	20.2(6)	18.9(5)	0	-0.1(4)	0
C3	14.1(5)	19.8(6)	20.9(5)	-2.9(4)	2.9(4)	-3.6(4)
C4	17.5(5)	21.0(6)	19.0(6)	-1.8(4)	4.8(4)	-2.4(4)
C5	17.9(6)	26.0(6)	24.9(6)	0.3(5)	8.4(5)	0.7(5)
C6	16.4(5)	21.8(6)	20.3(5)	-3.3(4)	3.6(4)	-3.0(4)
C7	21.9(6)	28.0(6)	20.2(6)	0.5(5)	7.4(5)	1.9(5)
C8	20.0(5)	25.4(6)	20.4(6)	-1.4(5)	1.7(4)	-1.1(5)
C9	16.3(6)	26.8(6)	28.1(6)	-3.2(5)	-0.8(5)	1.7(5)
C10	17.7(5)	25.9(6)	21.7(6)	-1.8(5)	5.2(4)	-4.0(5)
C11	15.2(5)	29.8(7)	29.1(6)	-4.8(5)	7.1(5)	-1.5(5)

**Table 4 Bond Lengths for CCDC 945604.**

Atom	Atom	Length/ $\text{\AA}$	Atom	Atom	Length/ $\text{\AA}$
O1	C4	1.4141(13)	C5	C7	1.5195(16)
O1	C5	1.4400(14)	C6	C7	1.5129(15)
O2	C4 <sup>1</sup>	1.4288(13)	C6	C8	1.3981(17)
O2	C4	1.4288(13)	C8	C9	1.3907(16)
C3	C4	1.5117(16)	C9	C11	1.3934(18)
C3	C6	1.3926(16)	C10	C11	1.3879(17)
C3	C10	1.3983(15)			

<sup>1</sup>1/2-X,+Y,-Z

**Table 5 Bond Angles for CCDC 945604**

Atom	Atom	Atom	Angle/°	Atom	Atom	Atom	Angle/°
C4	O1	C5	112.19(9)	C3	C6	C7	119.50(10)
C4	O2	C4 <sup>1</sup>	112.88(12)	C3	C6	C8	119.07(10)
C6	C3	C4	121.23(10)	C8	C6	C7	121.42(10)
C6	C3	C10	120.11(10)	C6	C7	C5	110.29(9)
C10	C3	C4	118.66(10)	C9	C8	C6	120.74(11)
O1	C4	O2	110.61(8)	C8	C9	C11	119.99(11)
O1	C4	C3	113.55(9)	C11	C10	C3	120.51(11)
O2	C4	C3	106.83(9)	C10	C11	C9	119.58(11)
O1	C5	C7	109.53(9)				

<sup>1</sup>1/2-X,+Y,-Z

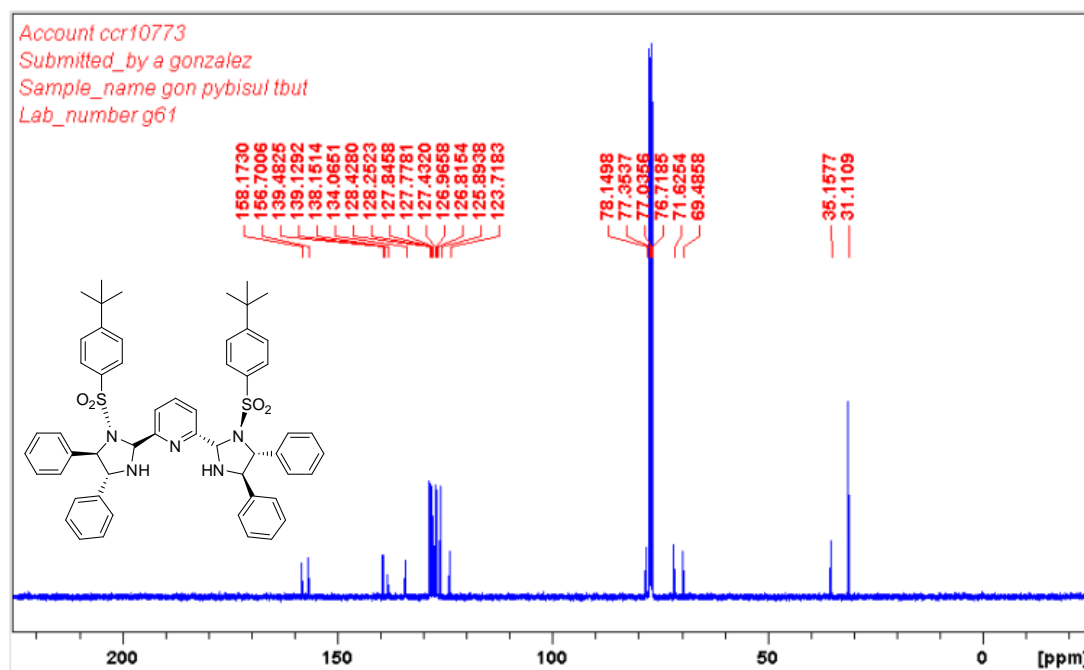
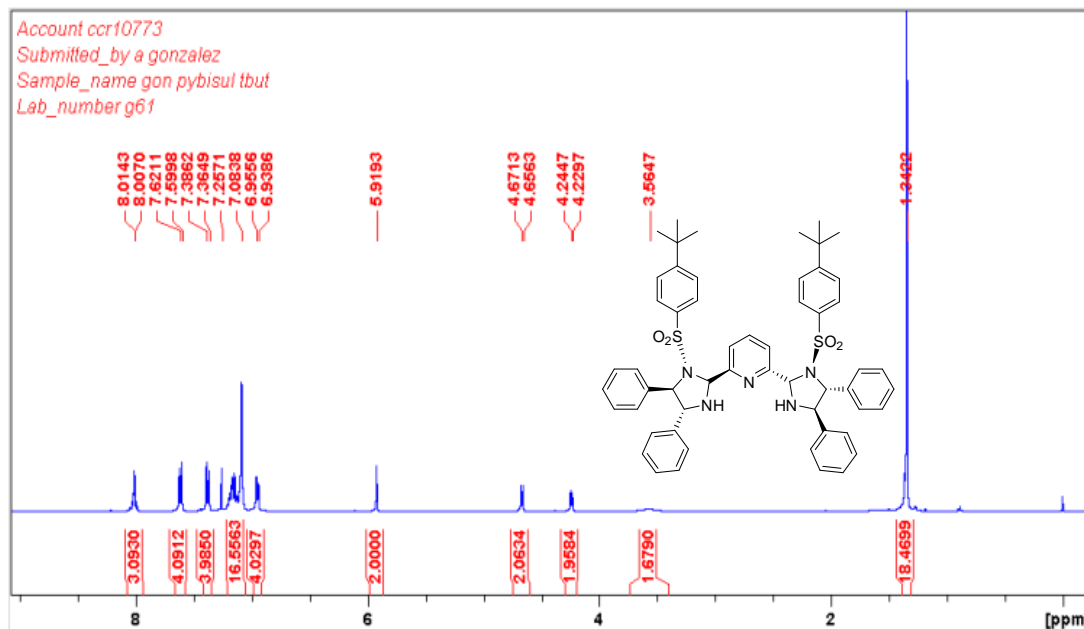
**Table 6 Hydrogen Atom Coordinates ( $\text{\AA}\times 10^4$ ) and Isotropic Displacement Parameters ( $\text{\AA}^2\times 10^3$ ) for CCDC 945604.**

Atom	<i>x</i>	<i>y</i>	<i>z</i>	U(eq)
H5A	1995(9)	7540(30)	1060(6)	21(3)
H7A	3212(9)	10180(40)	2160(7)	28(4)
H7B	2921(9)	6560(30)	2093(7)	26(4)
H4	3171(8)	12760(30)	367(6)	18(3)
H9	5652(10)	4050(40)	1709(7)	28(4)
H5B	1776(9)	10210(30)	1538(6)	23(3)
H11	5567(10)	6040(40)	653(7)	35(4)
H10	4349(9)	9040(30)	120(7)	25(3)
H8	4522(9)	5090(30)	2255(7)	27(3)

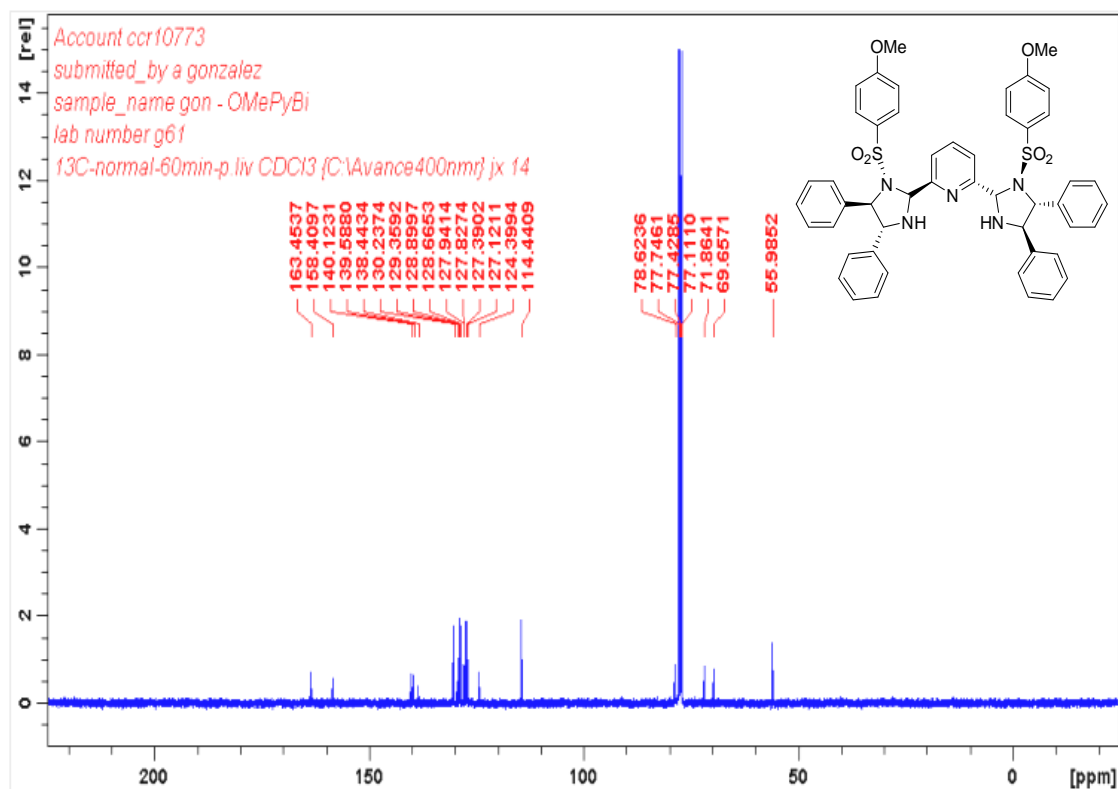
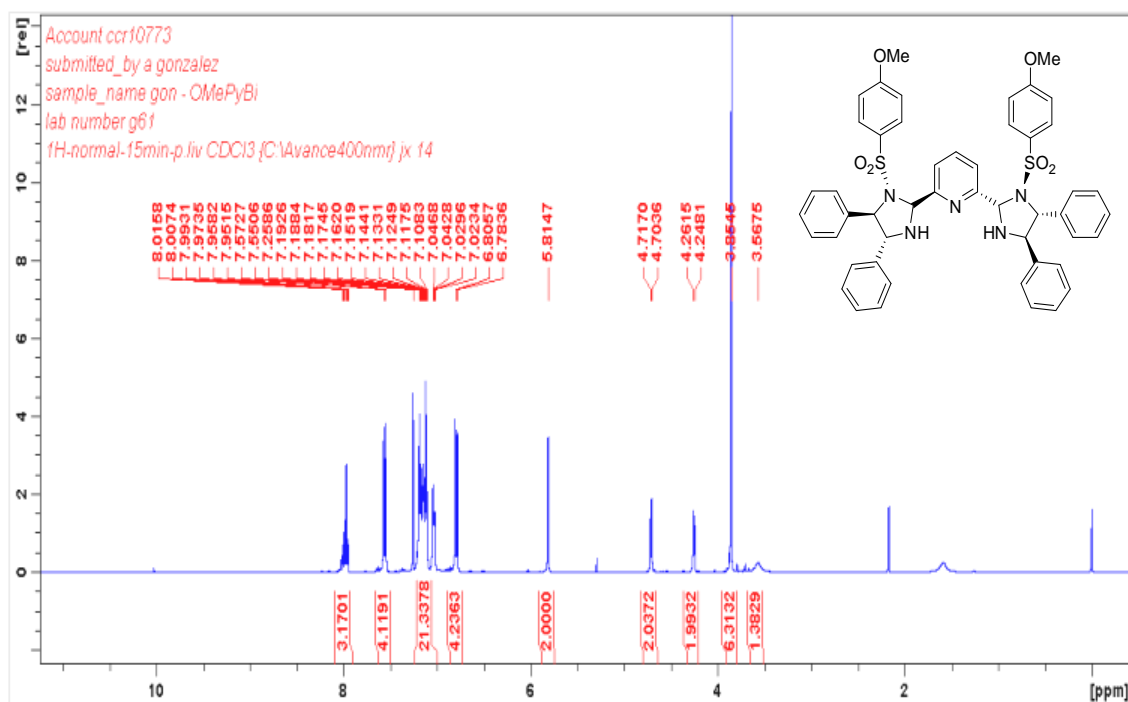
## 2. Chapter 2: additional information

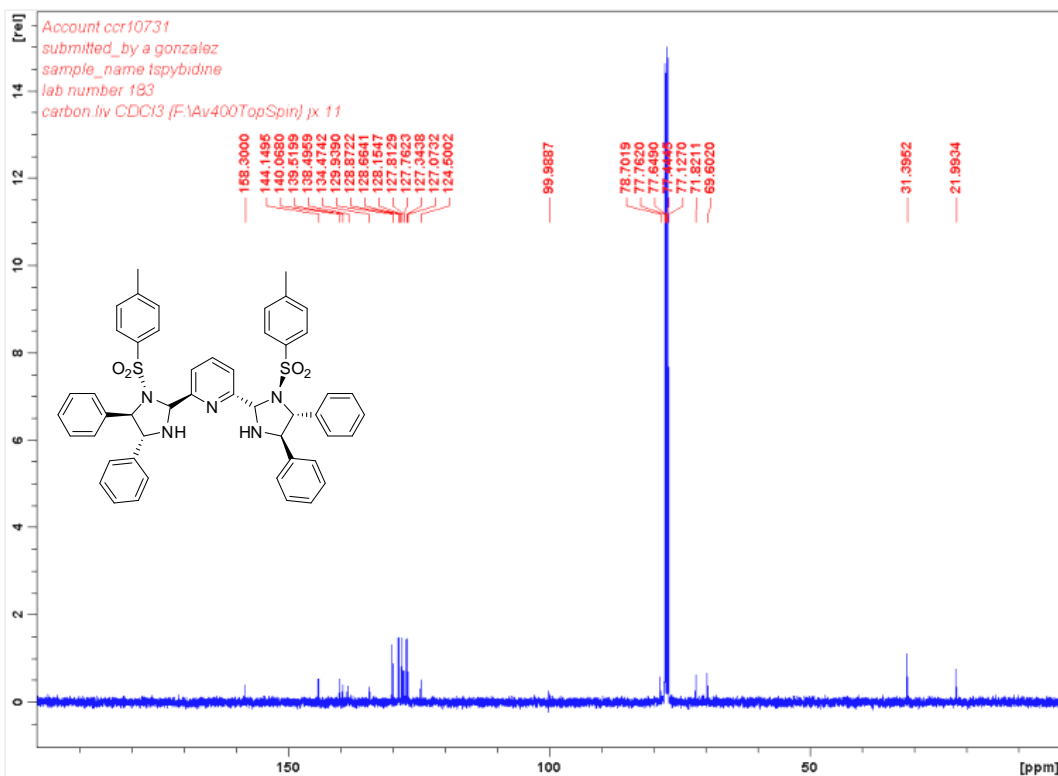
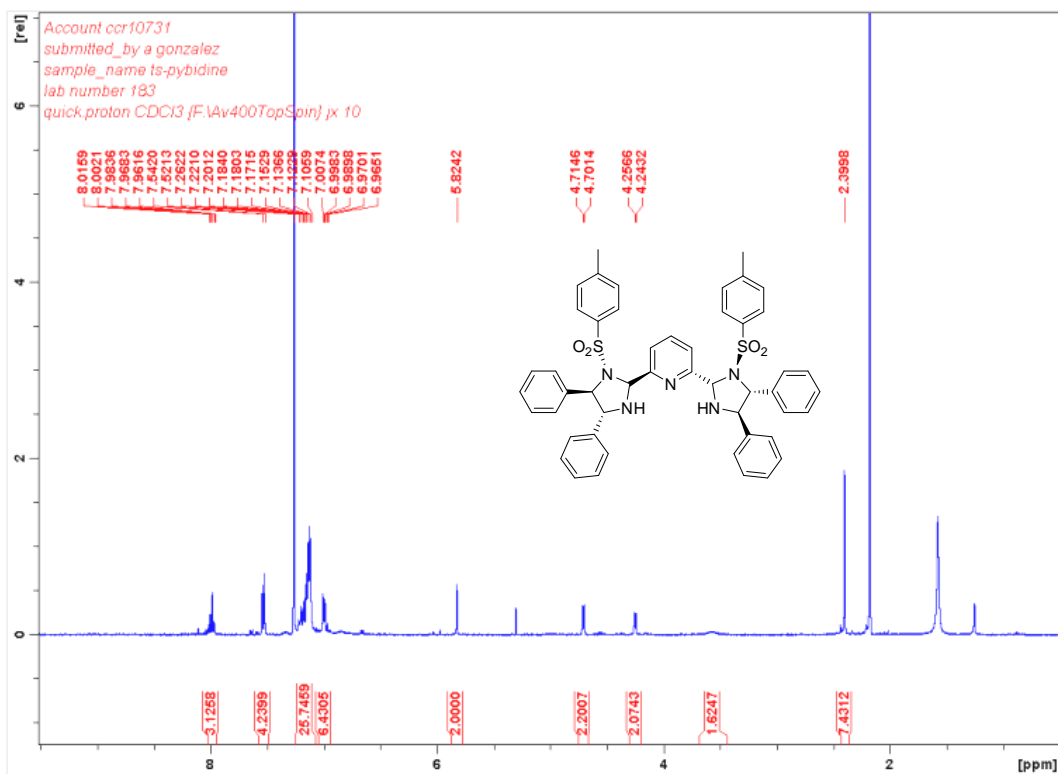
### 2.1. $^1\text{H}$ and $^{13}\text{C}$ NMR of novel PyBisulidine ligands

#### 2-((2R,4R,5R)-1-((4-(*tert*-Butyl)phenyl)sulfonyl)-4,5-diphenylimidazolidin-2-yl)-6-((2S,4R,5R)-1-((4-(*tert*-butyl)phenyl)sulfonyl)-4,5-diphenylimidazolidin-2-yl)pyridine



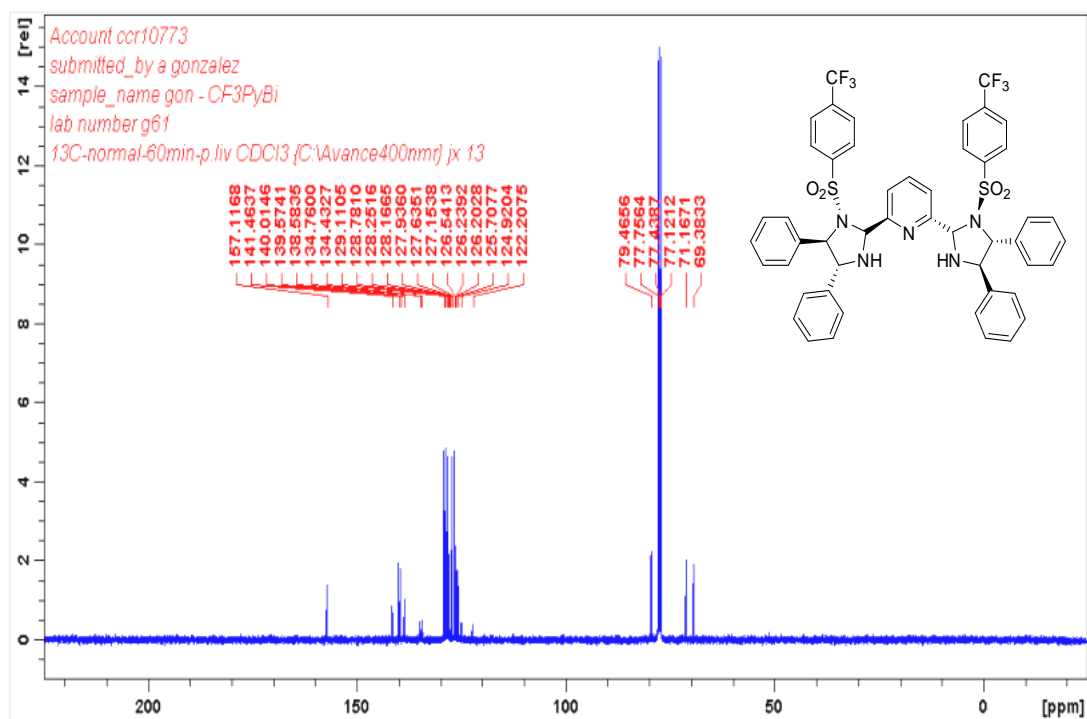
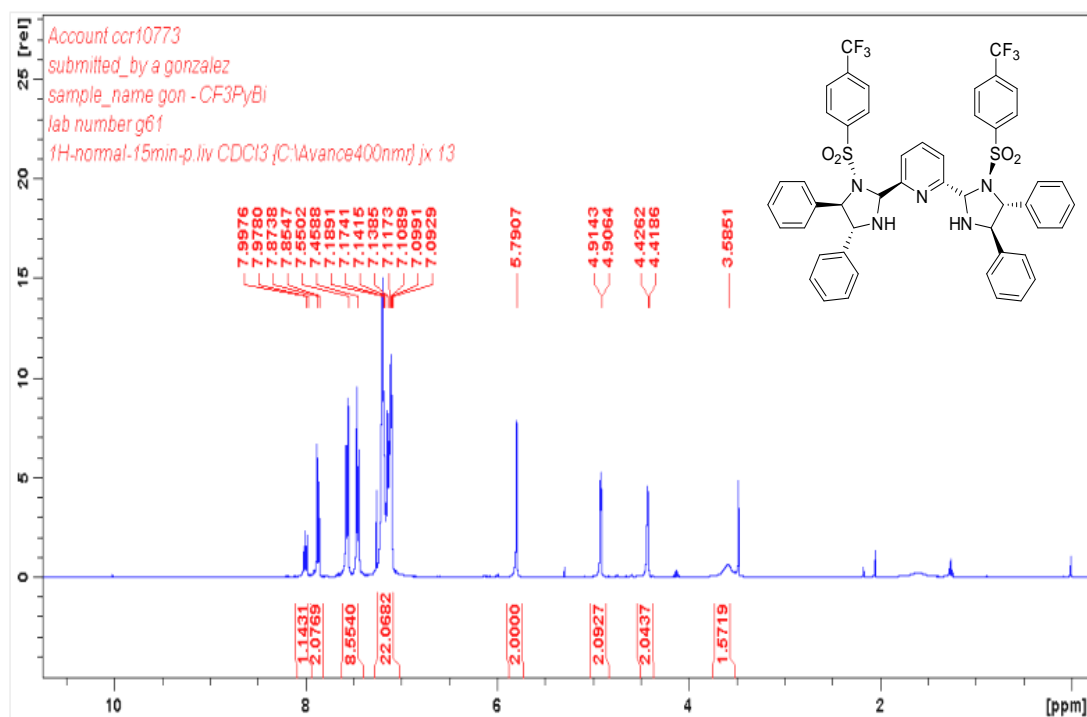
**2-((2R,4R,5R)-1-((4-Methoxyphenyl)sulfonyl)-4,5-diphenylimidazolidin-2-yl)-6-((2S,4R,5R)-1-((4-methoxyphenyl)sulfonyl)-4,5-diphenylimidazolidin-2-yl)pyridine**



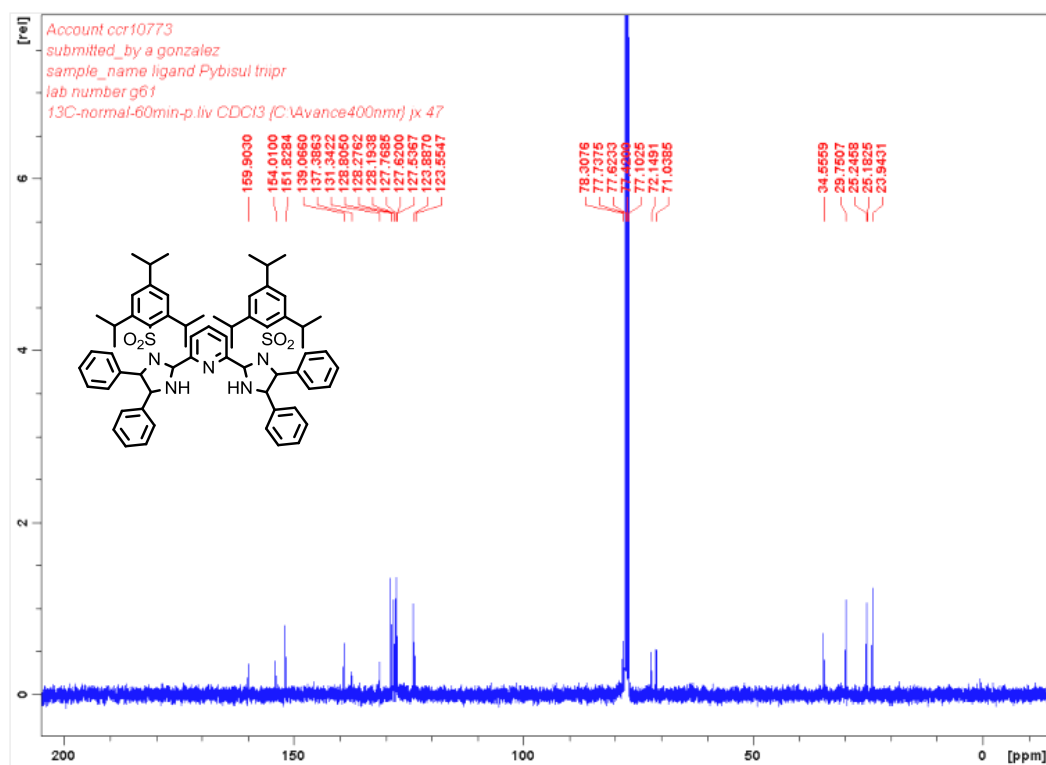
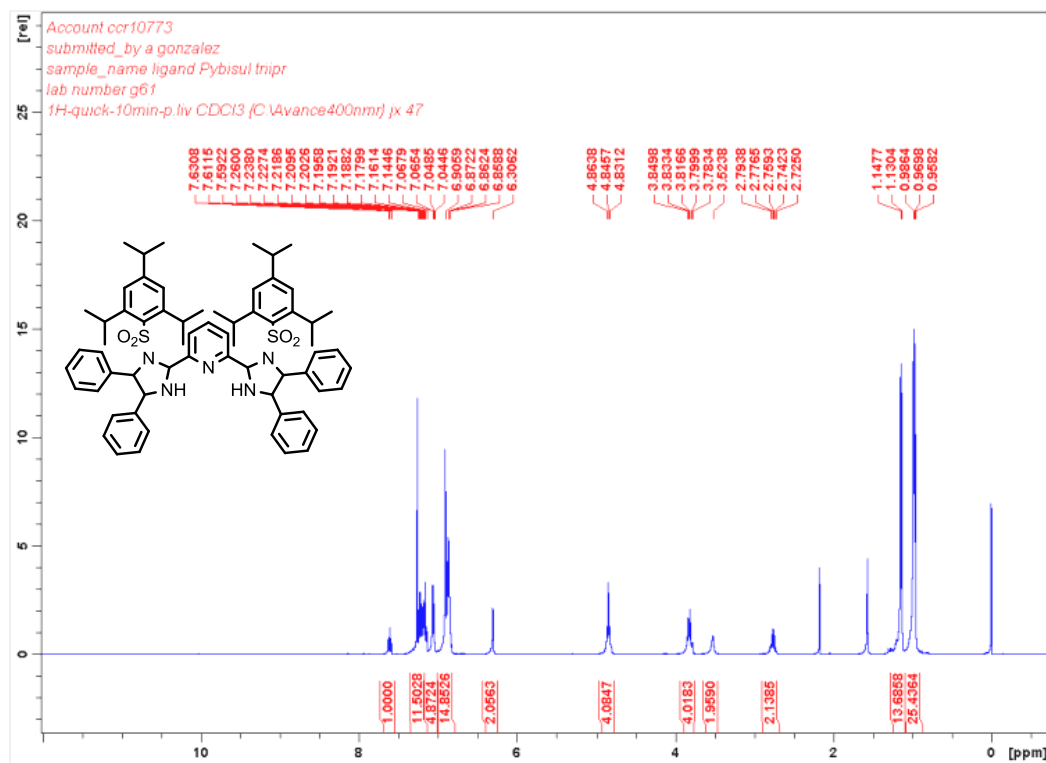
**2-((2R,4R,5R)-4,5-Diphenyl-1-tosylimidazolidin-2-yl)-6-((2S,4R,5R)-4,5-diphenyl-1-tosylimidazolidin-2-yl)pyridine**

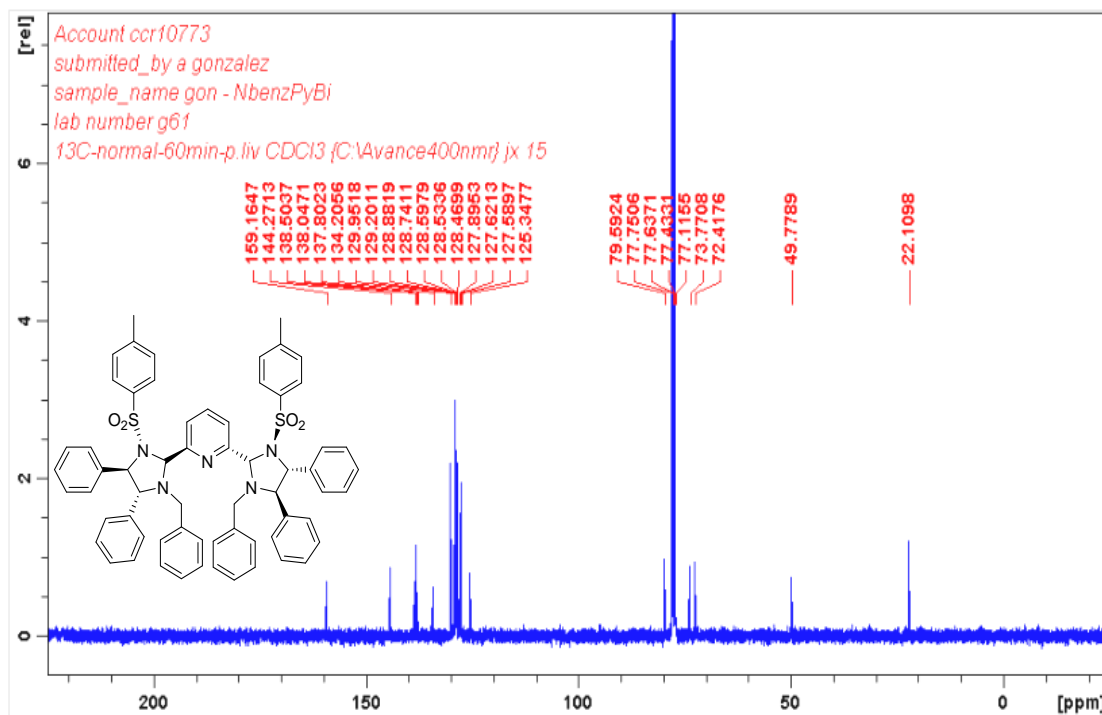
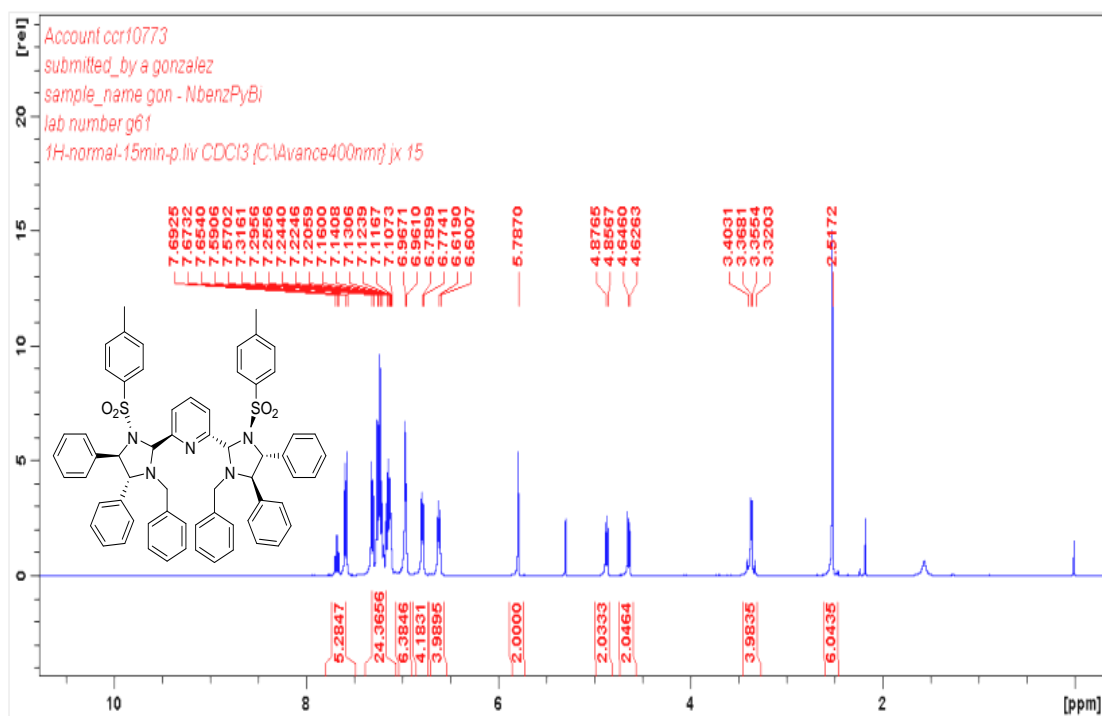


**2-((2R,4R,5R)-4,5-Diphenyl-1-((4-(trifluoromethyl)phenyl)sulfonyl)imidazolidin-2-yl)-6-((2S, 4R,5R)-4,5-diphenyl-1-((4-(trifluoromethyl)phenyl)sulfonyl)imidazolidin-2-yl)pyridine**

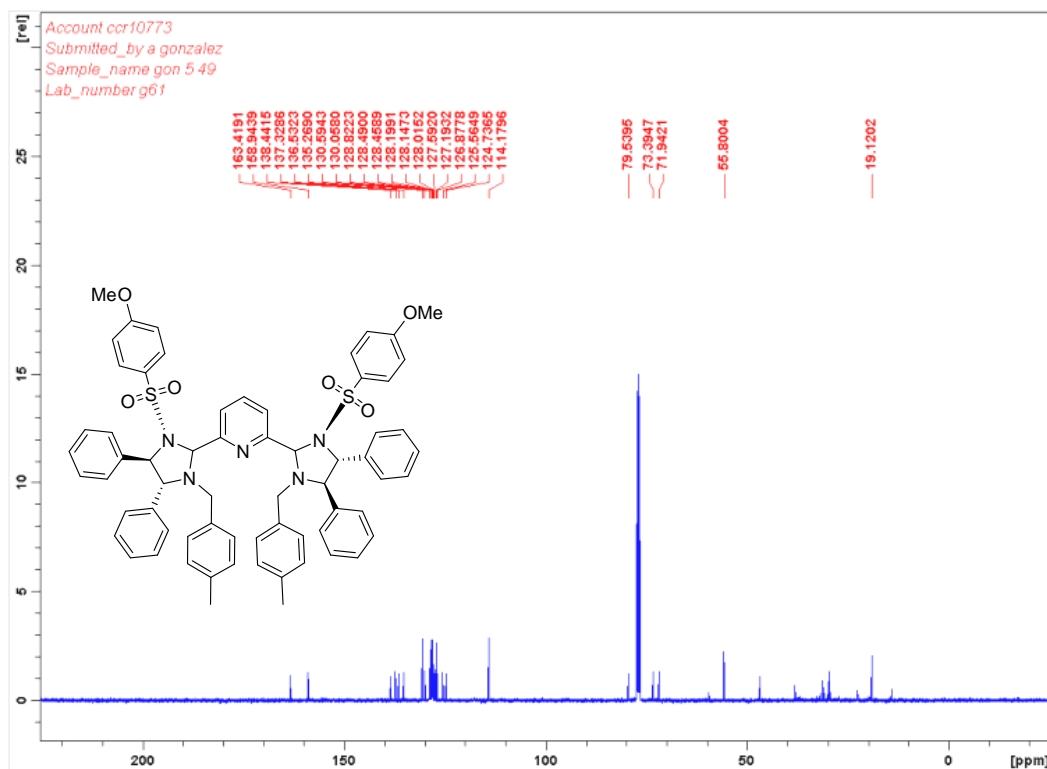
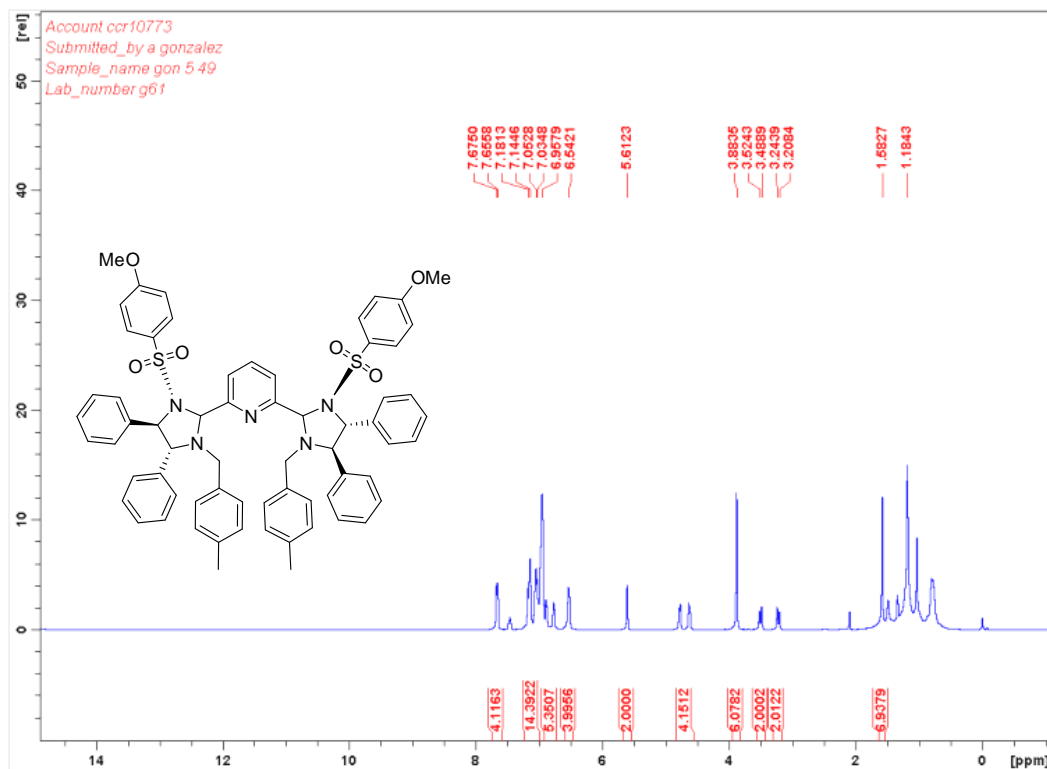


**2-((2R,4R,5R)-4,5-Diphenyl-1-((2,4,6-triisopropylphenyl)sulfonyl)imidazolidin-2-yl)-6-((2S,4R,5R)-4,5-diphenyl-1-((2,4,6-triisopropylphenyl)sulfonyl)imidazolidin-2-yl)pyridine**

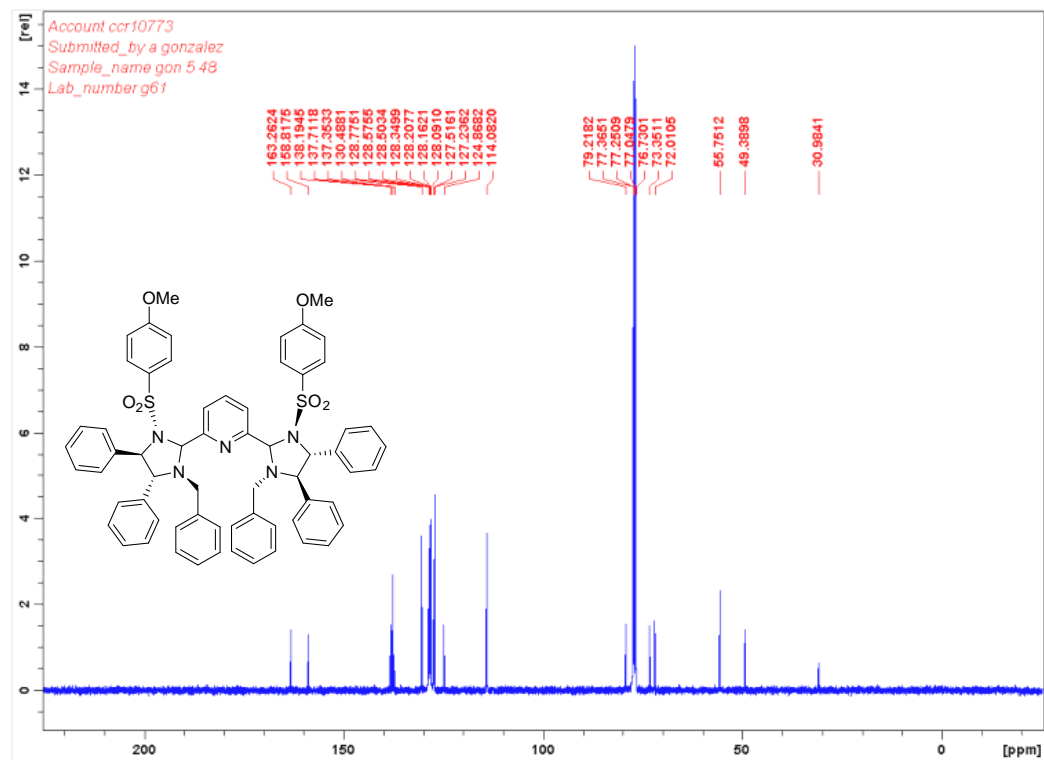
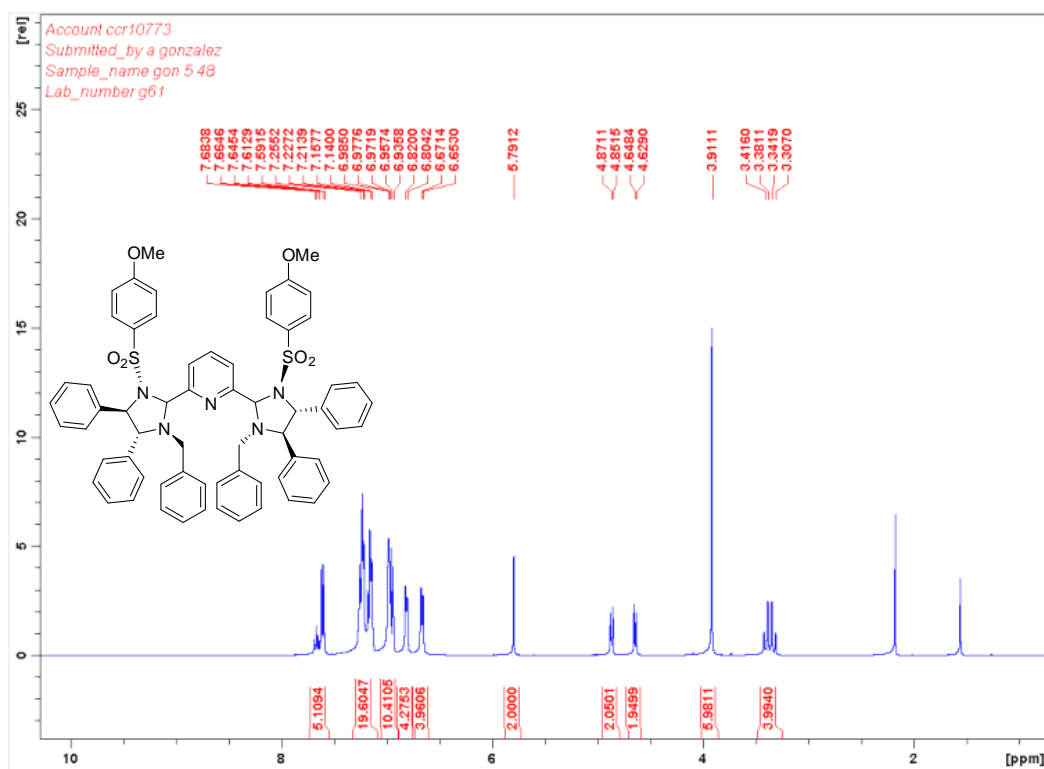


**2-((2R,4R,5R)-1-Benzyl-4,5-diphenyl-3-tosylimidazolidin-2-yl)-6-((2S,4R,5R)-1-benzyl-4,5-diphenyl-3-tosylimidazolidin-2-yl)pyridine**

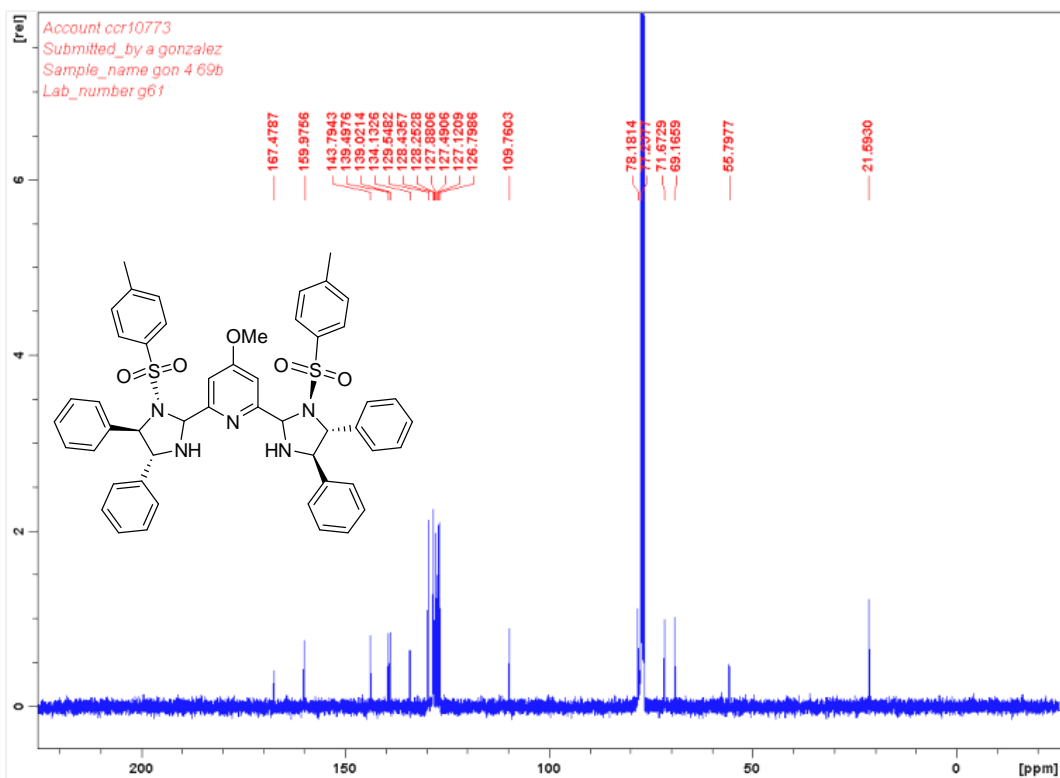
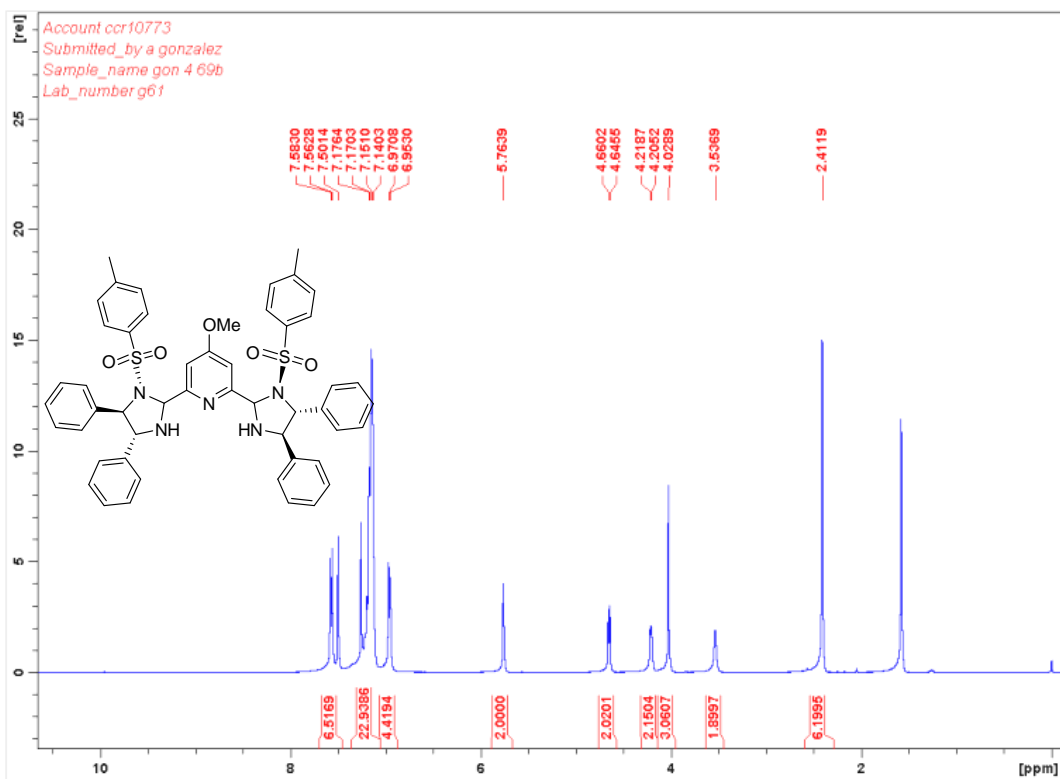
**2-((2*R*,4*S*,5*S*)-1-Benzyl-4,5-diphenyl-3-(methoxyphenyl)imidazolidin-2-yl)-6-((2*S*,4*S*,5*S*)-1-benzyl-4,5-diphenyl-3-(methoxyphenyl)imidazolidin-2-yl)pyridine**



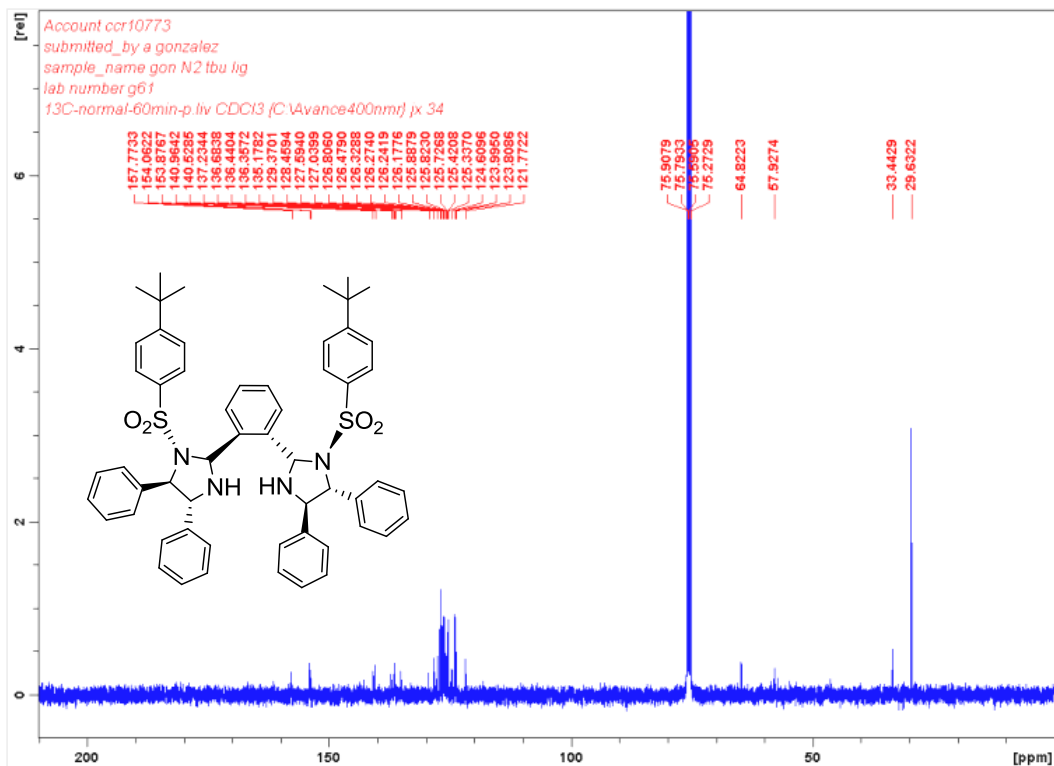
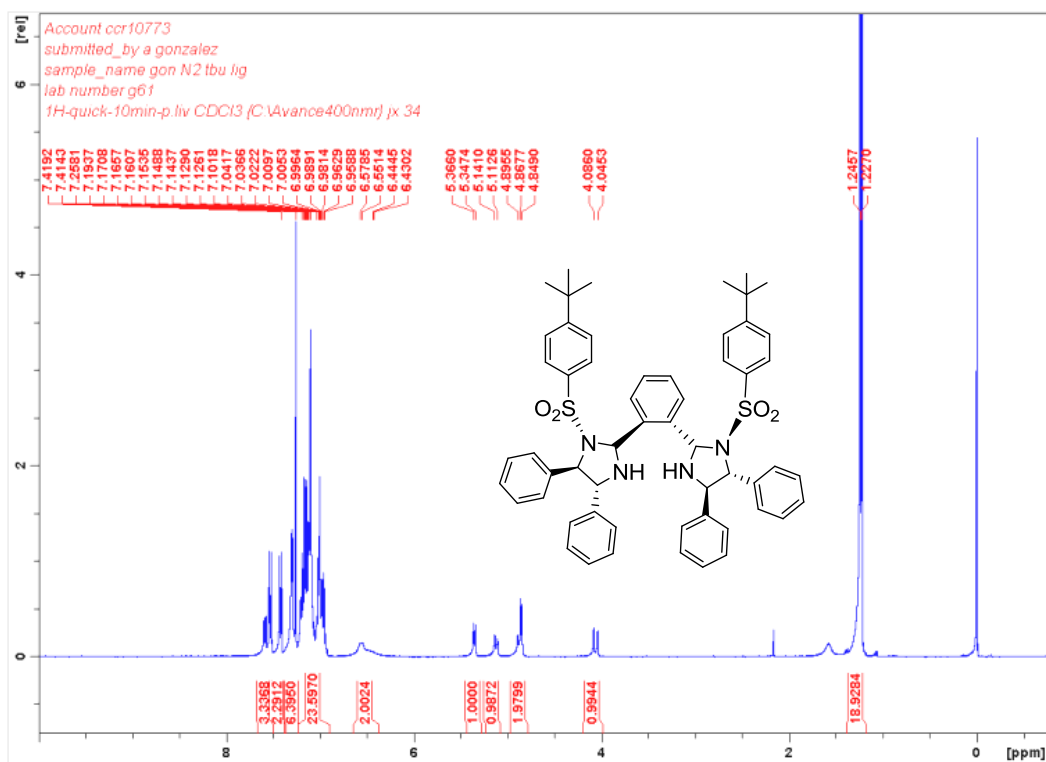
2-((2*R*,4*S*,5*S*)-1-Benzyl-4,5-diphenyl-3-(methoxyphenyl)imidazolidin-2-yl)-6-((2*S*,4*S*,5*S*)-1-benzyl-4,5-diphenyl-3-(methoxyphenyl)imidazolidin-2-yl)pyridine

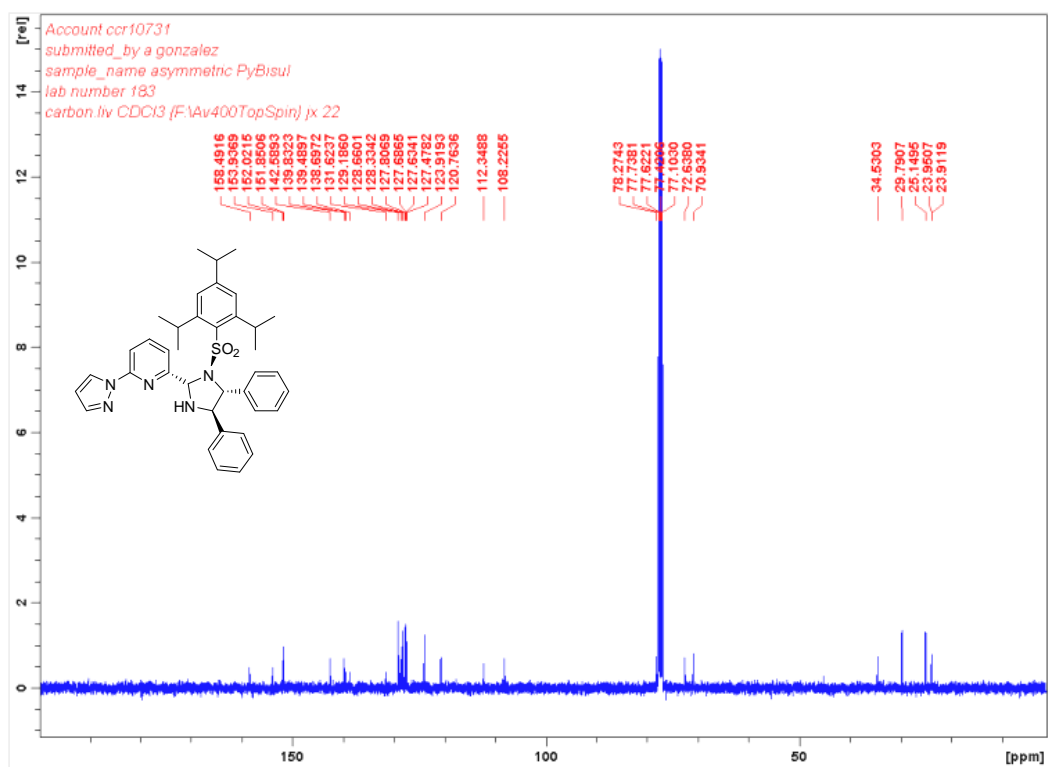
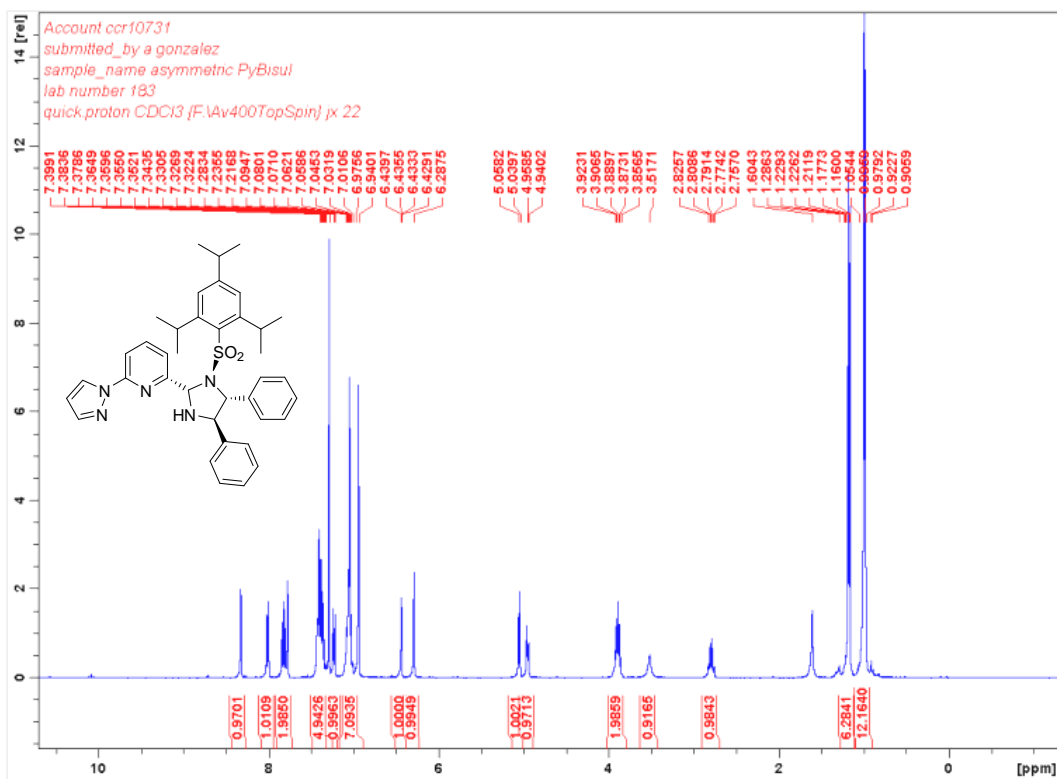


**2-((2*R*,4*R*,5*R*)-4,5-Diphenyl-1-tosylimidazolidin-2-yl)-6-((2*S*,4*R*,5*R*)-4,5-diphenyl-3-tosylpyrrolidin-2-yl)-4-methoxypyridine**



**1-((2*R*,4*R*,5*R*)-1-((4-*tert*-Butyl)phenyl)sulfonyl)-4,5-diphenylimidazolidin-2-yl)-2-((2*S*,4*R*,5*R*)-1-((4-*tert*-butyl)phenyl)sulfonyl)-4,5-diphenylimidazolidin-2-yl)benzene**



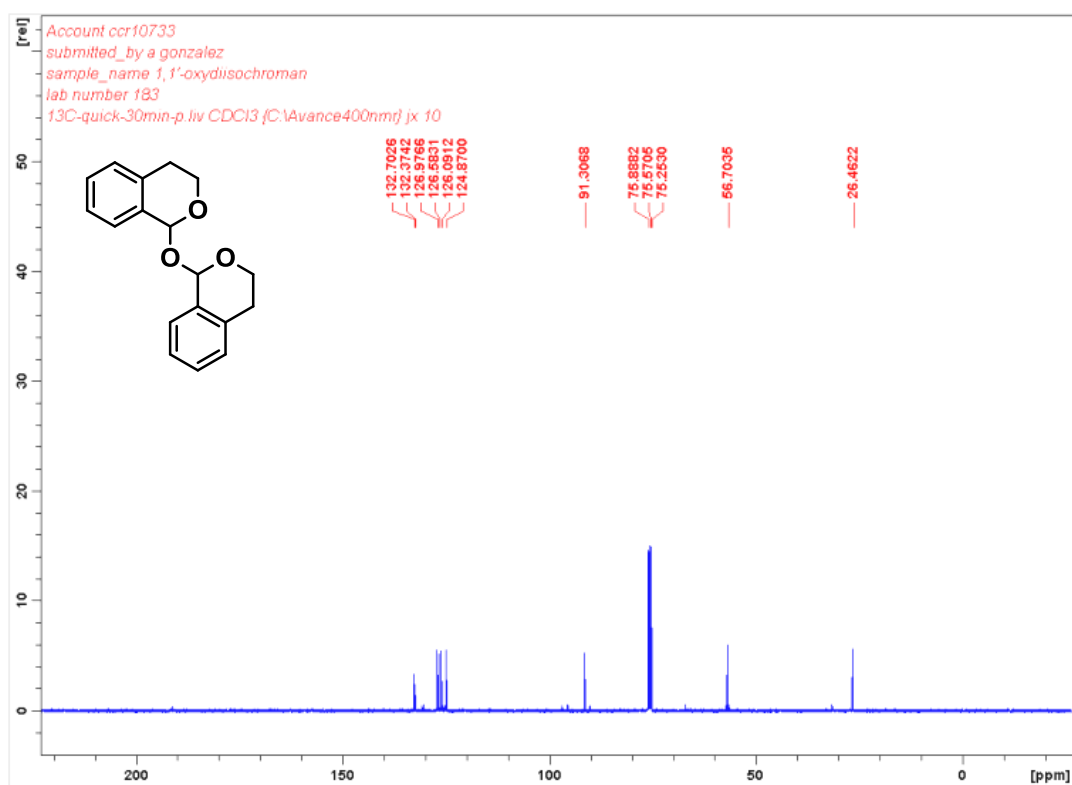
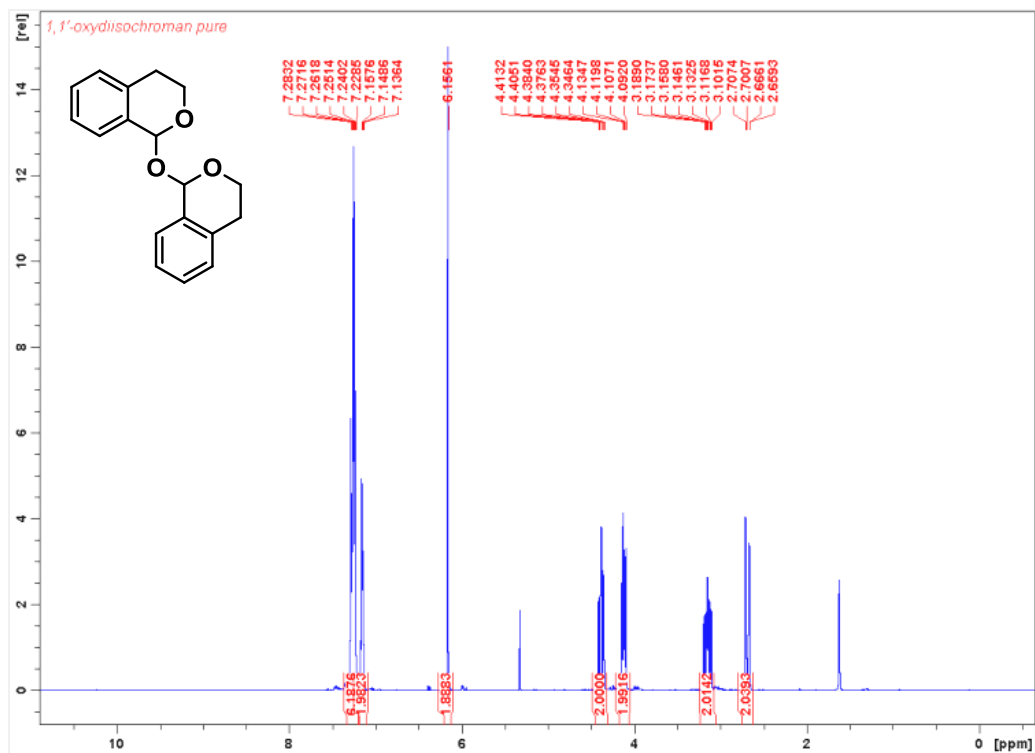
**2-((2S,4R,5R)-4,5-Diphenyl-1-((2,4,6-triisopropylphenyl)sulfonyl)imidazolidin-2-yl)-6-(1H-pyrazol-1-yl)pyridine**



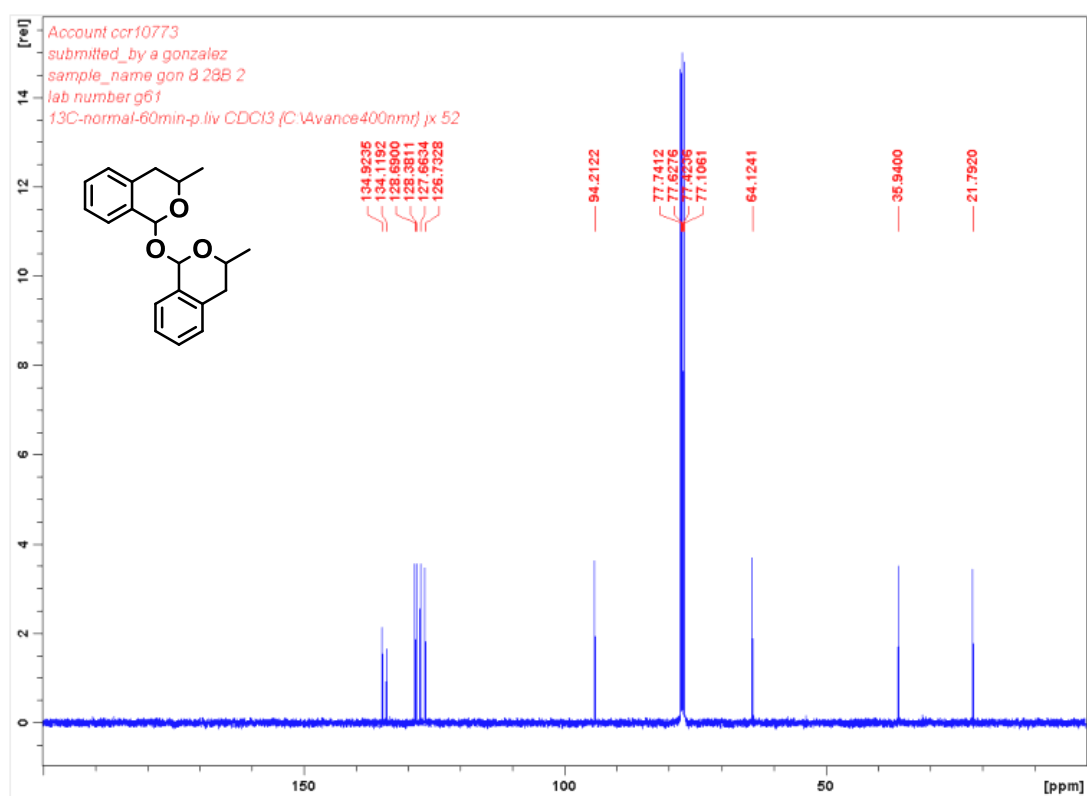
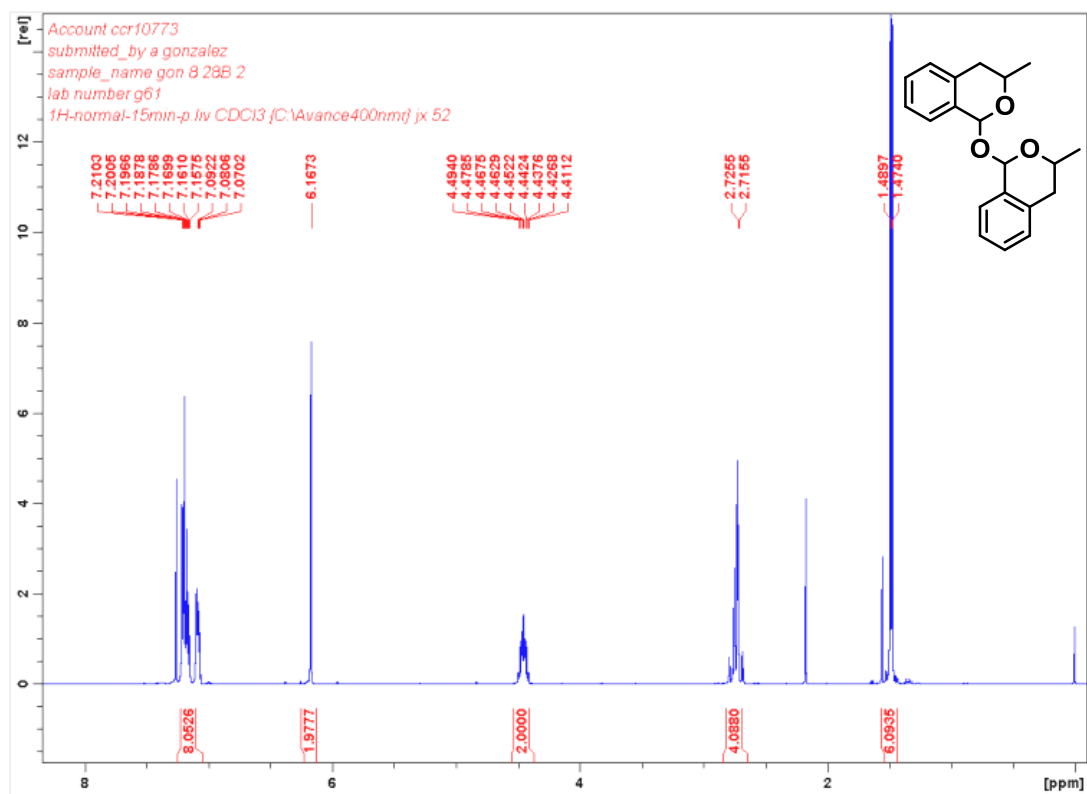
### 3. Chapter 3: additional information

#### 3.1. $^1\text{H}$ and $^{13}\text{C}$ NMR of novel compounds

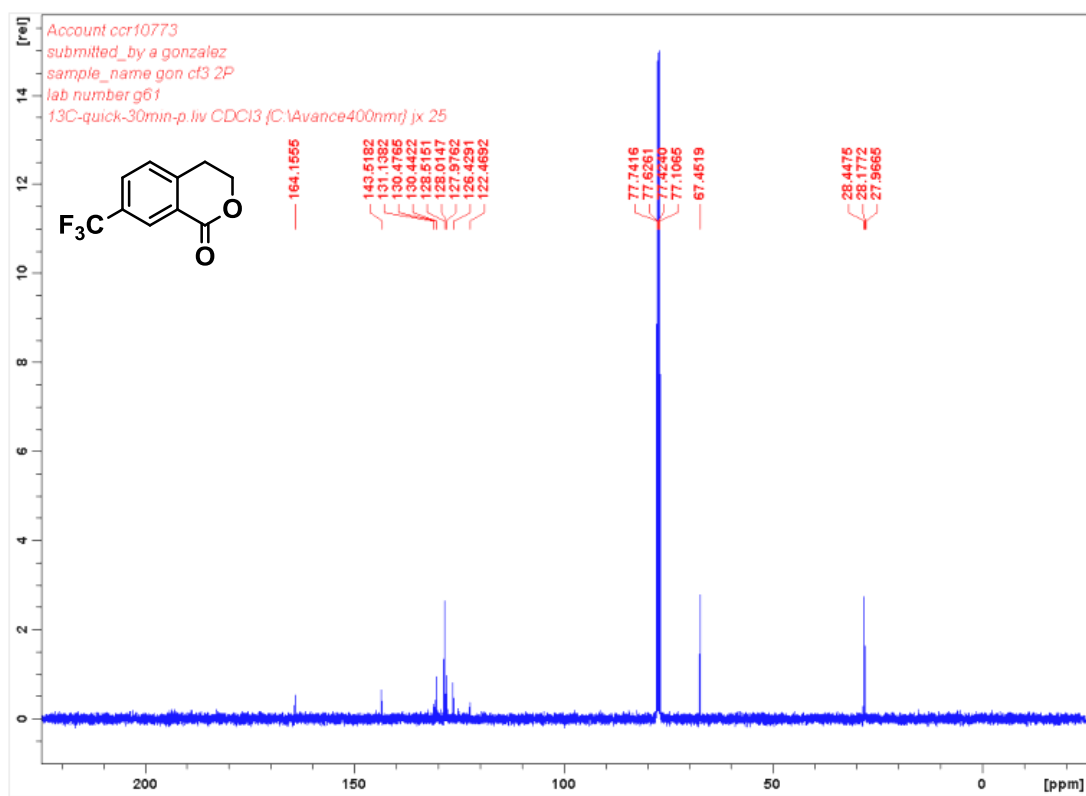
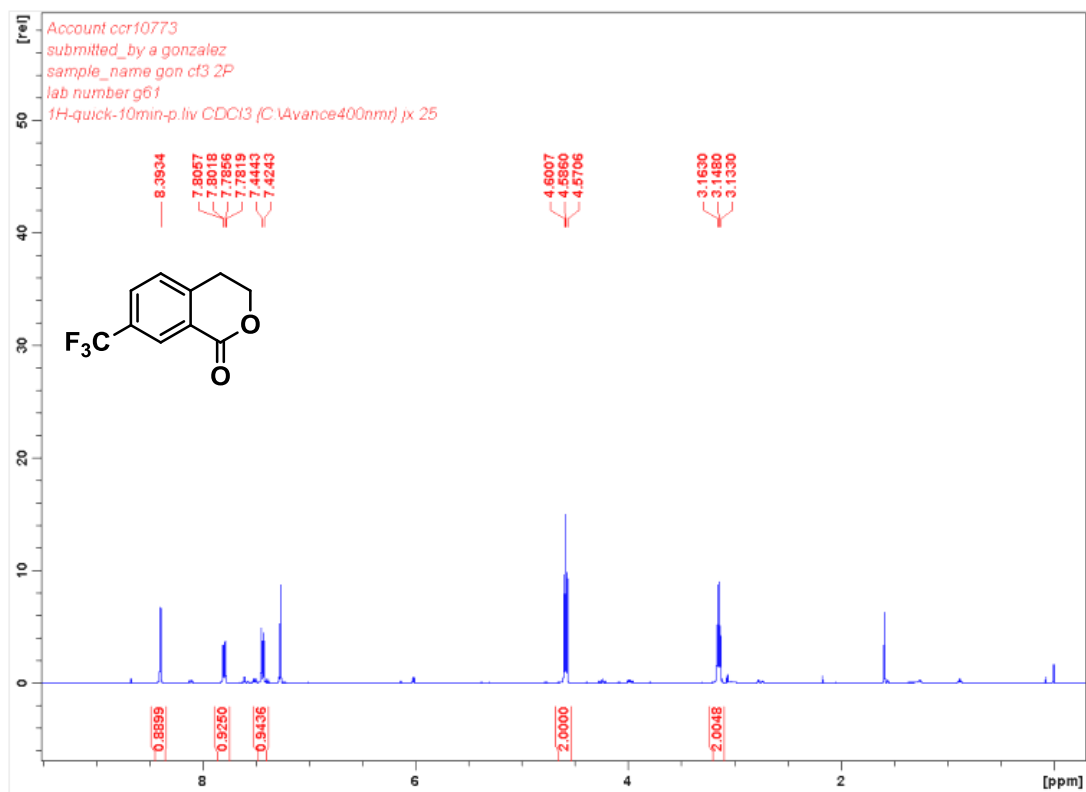
##### 1,1'-Oxydiisochroman



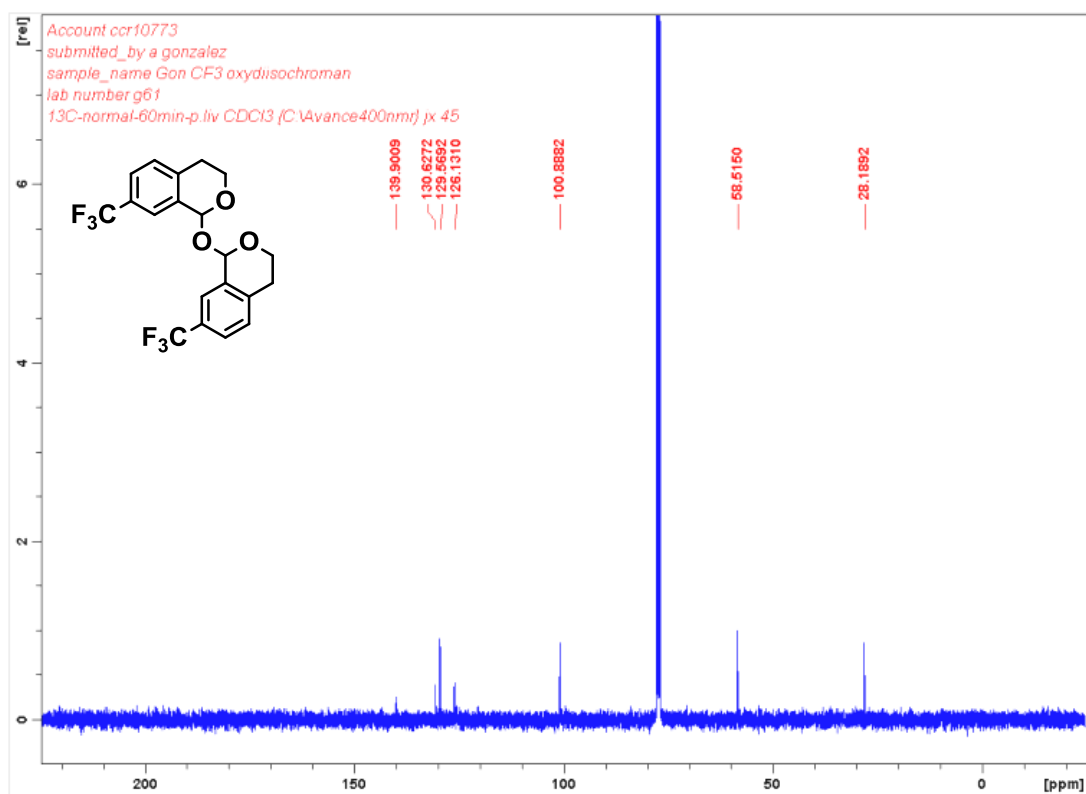
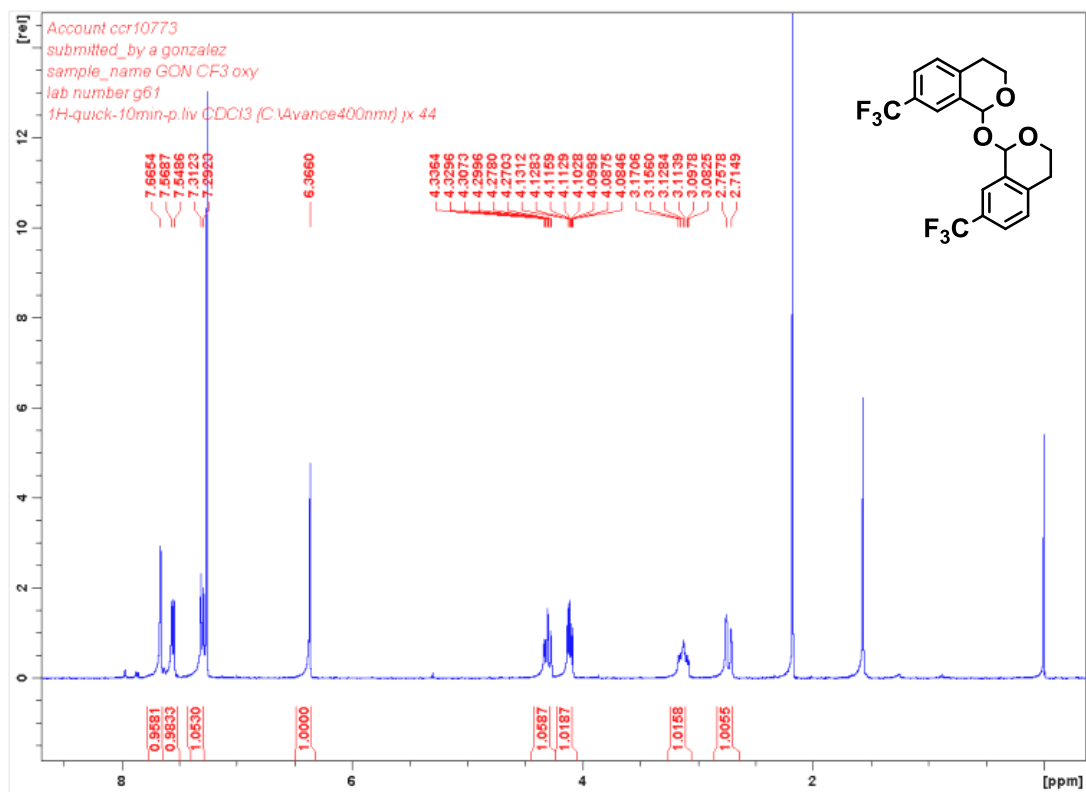
## 1,1'-Oxybis(3-methylisochroman)



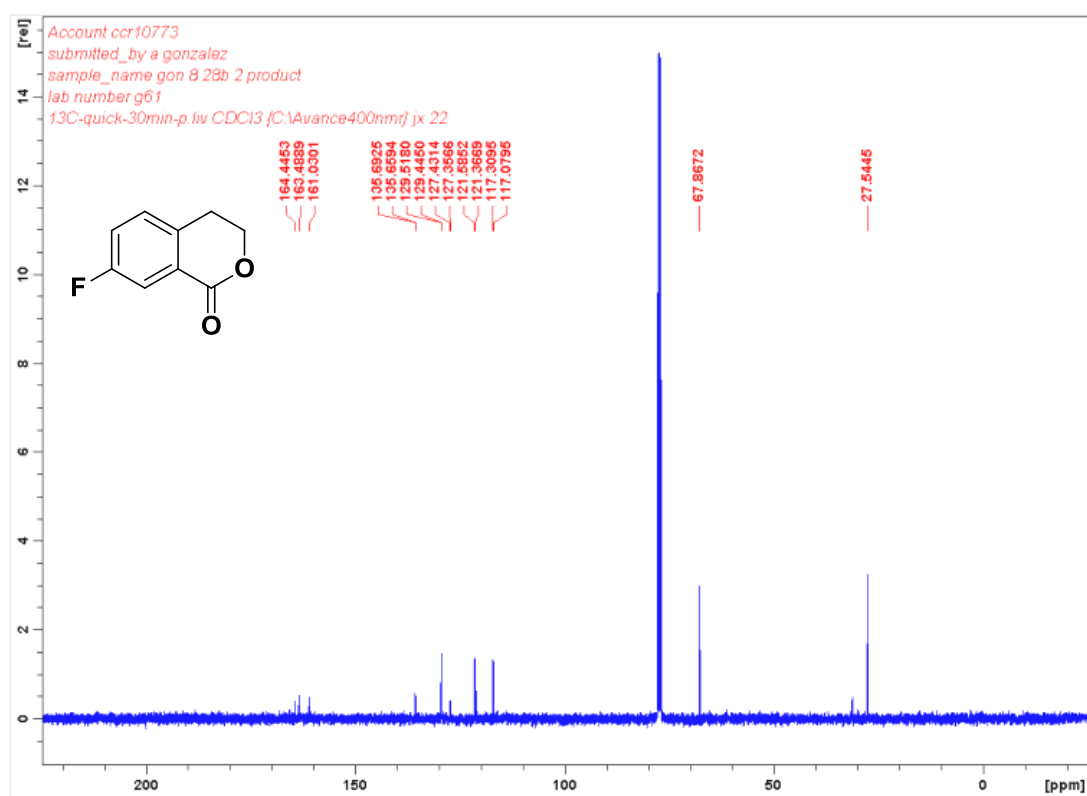
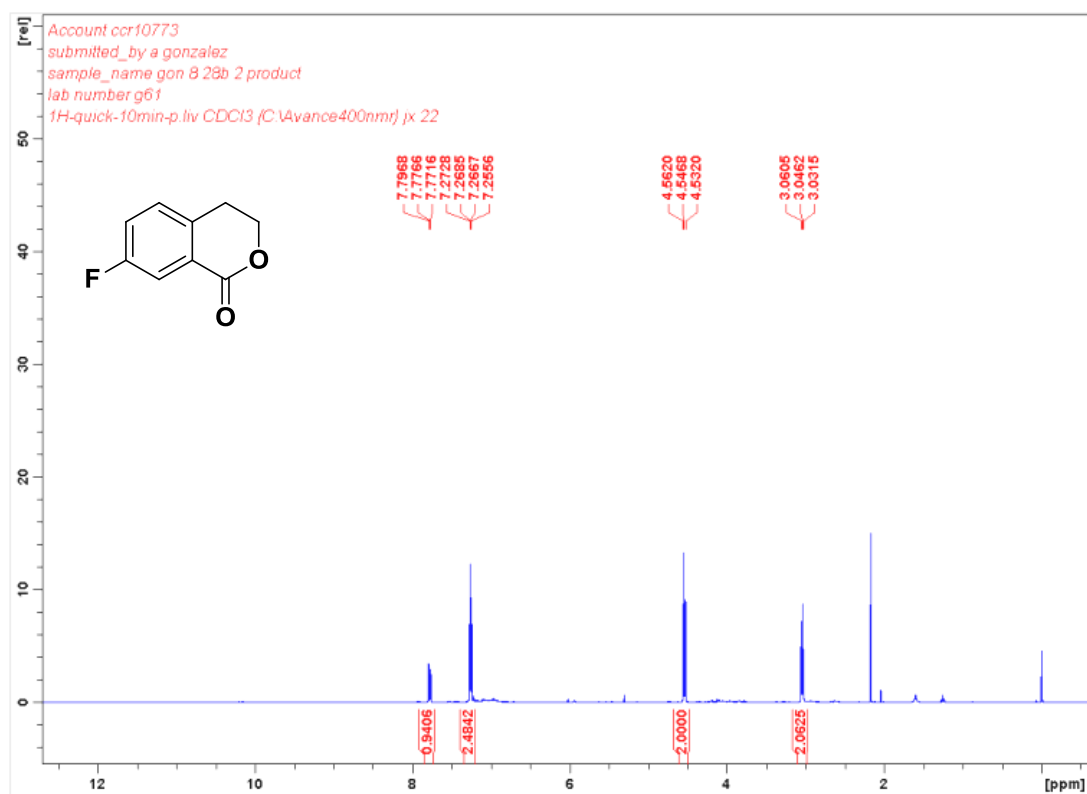
## 7-(Trifluoromethyl)isochroman-1-one

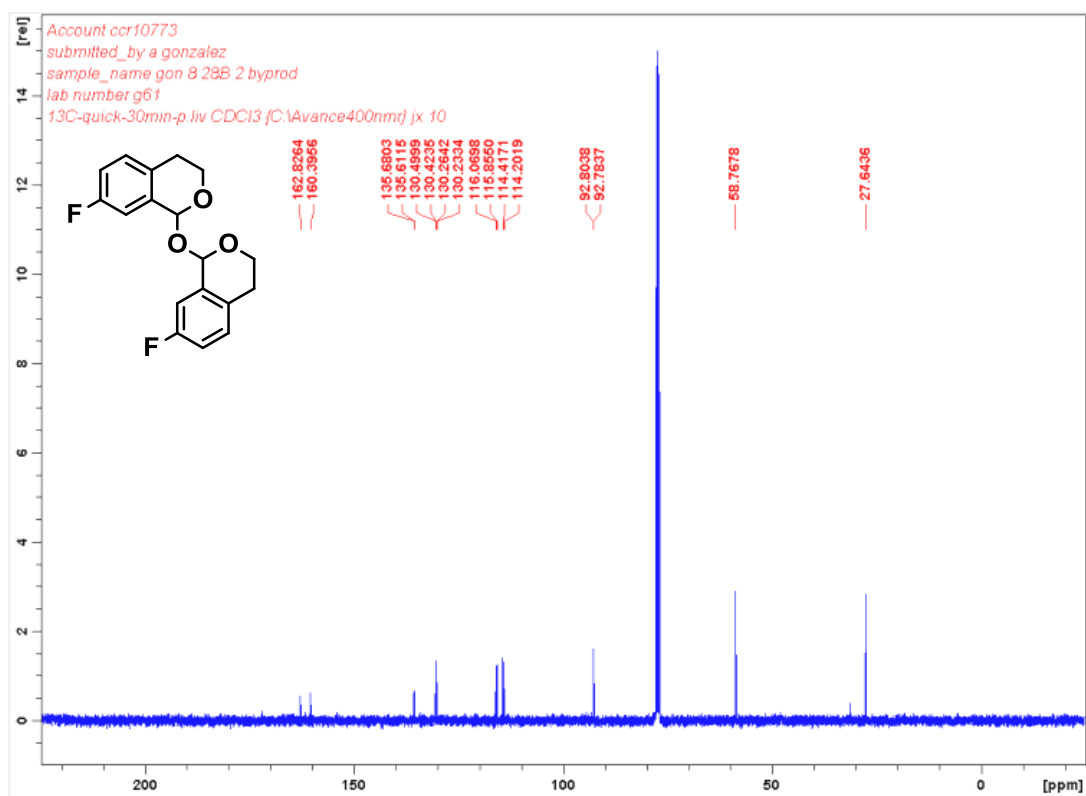
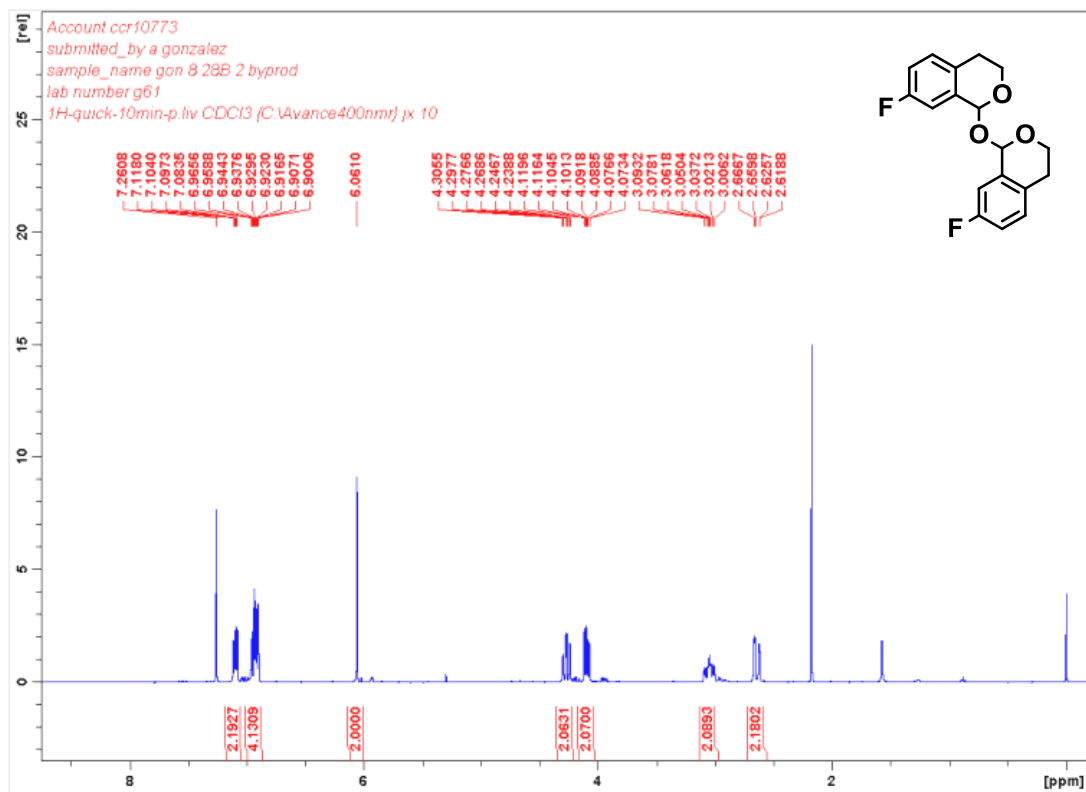


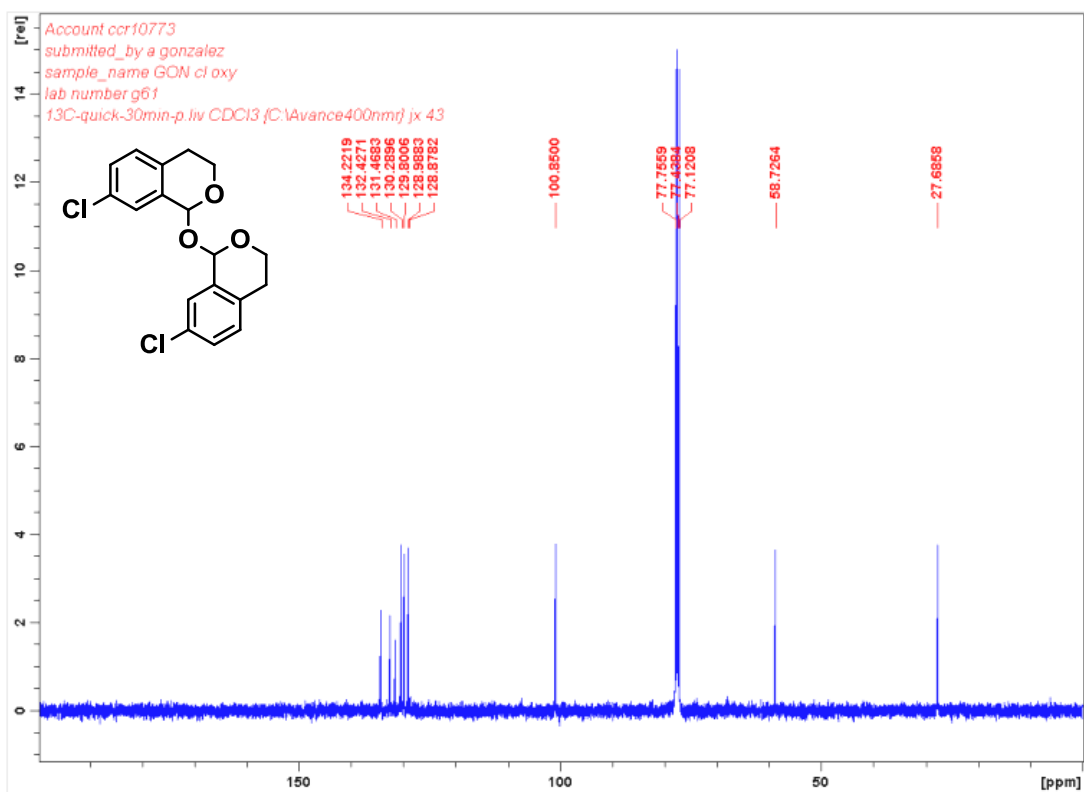
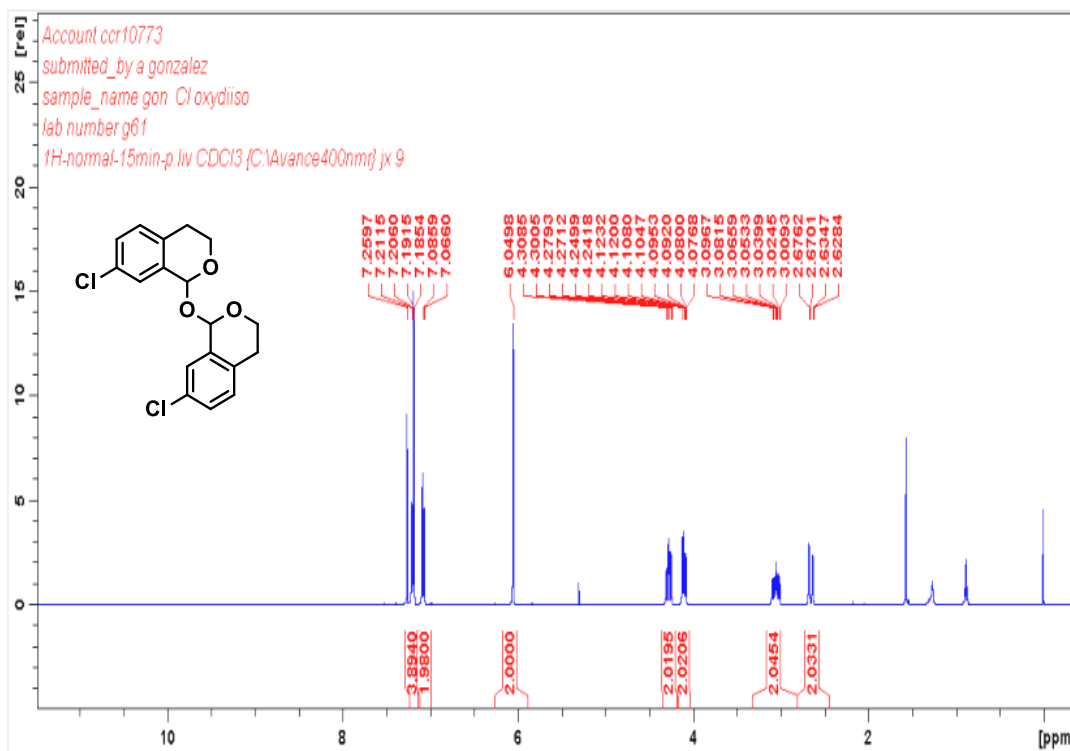
## 1,1'-Oxybis(7-(trifluoromethyl)isochroman)



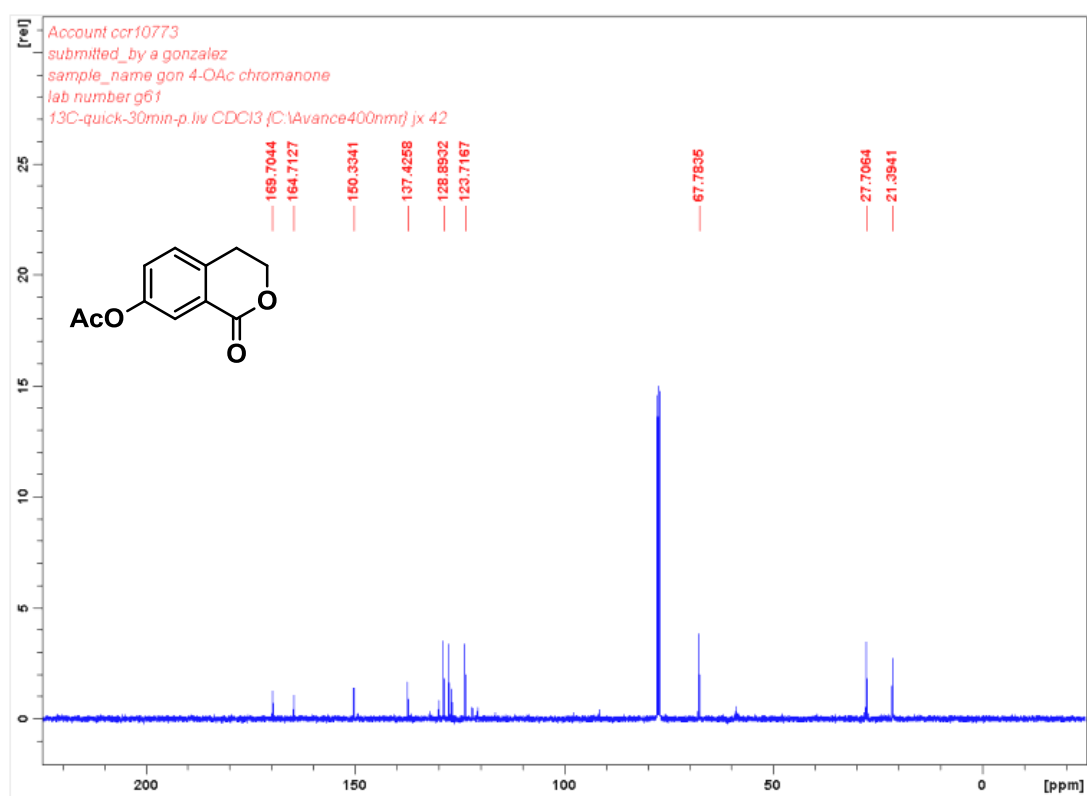
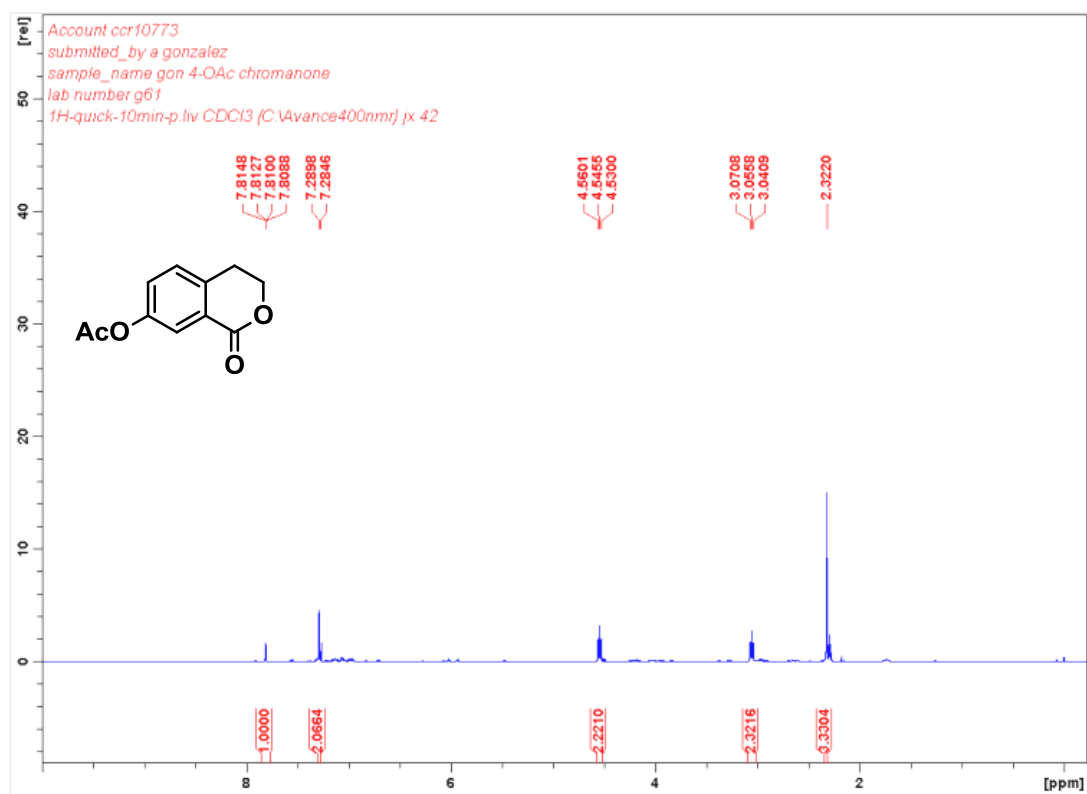
## 7-Fluoroisochroman-1-one



**1,1'-Oxybis(7-fluoroisochroman)**

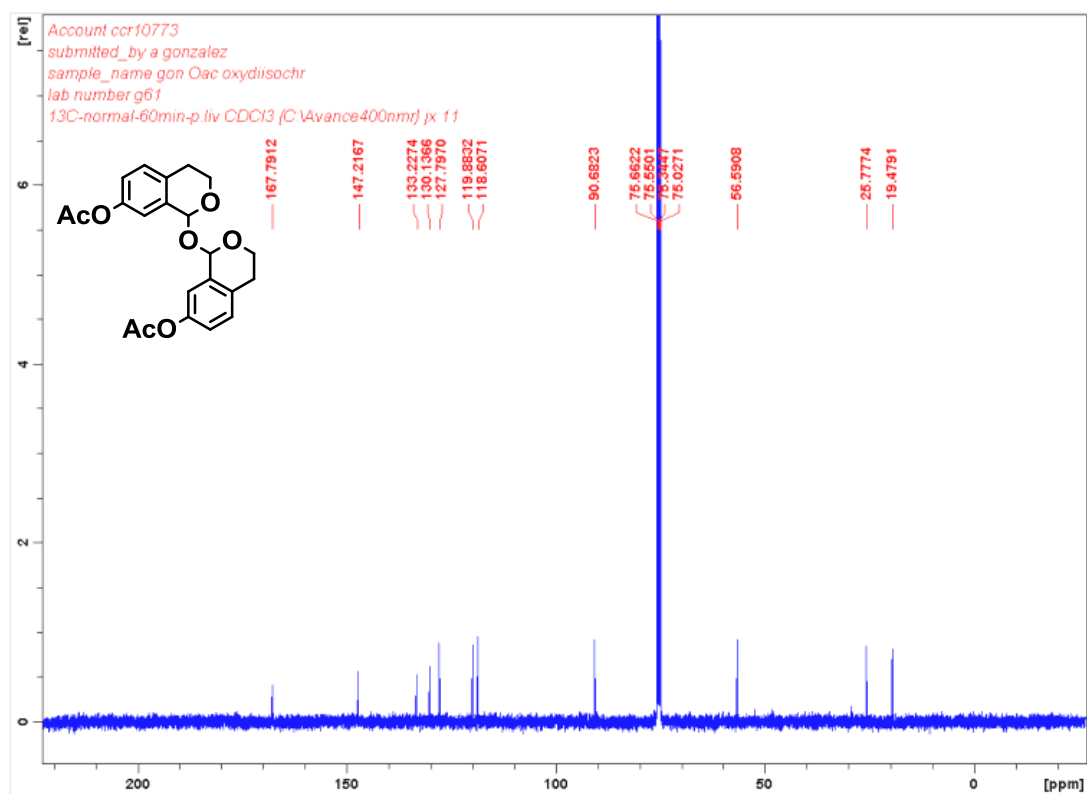
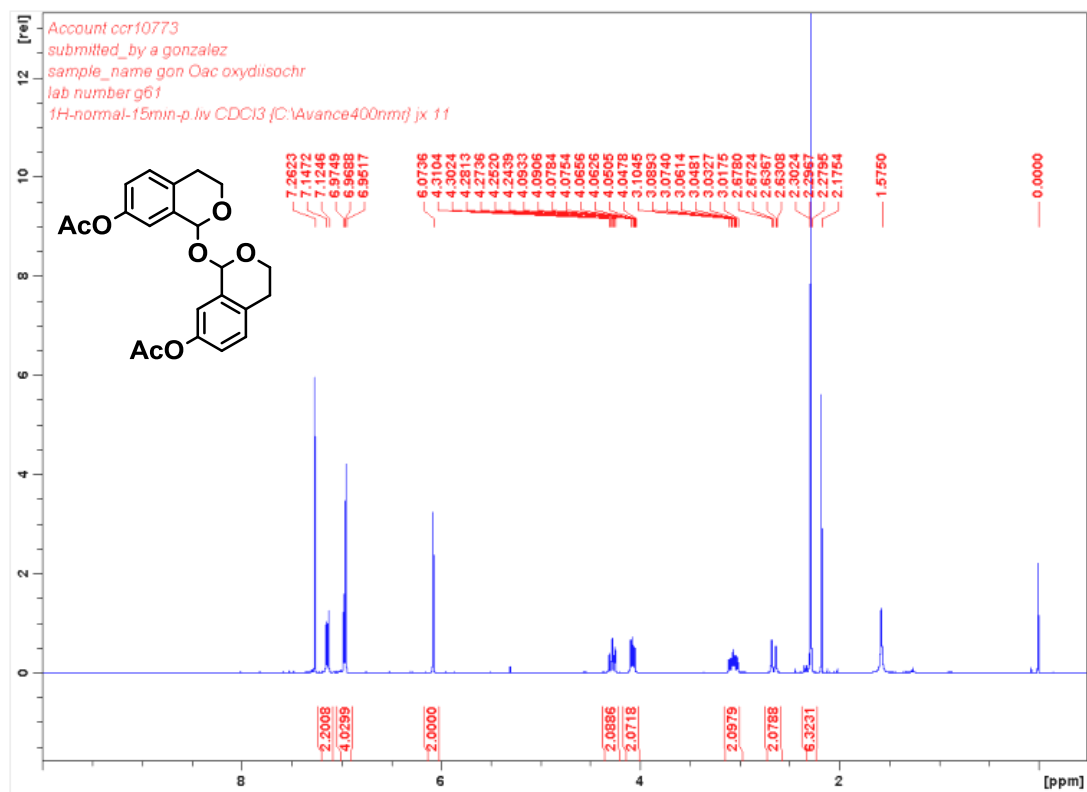
**1,1'-Oxybis(7-chloroisochroman)**

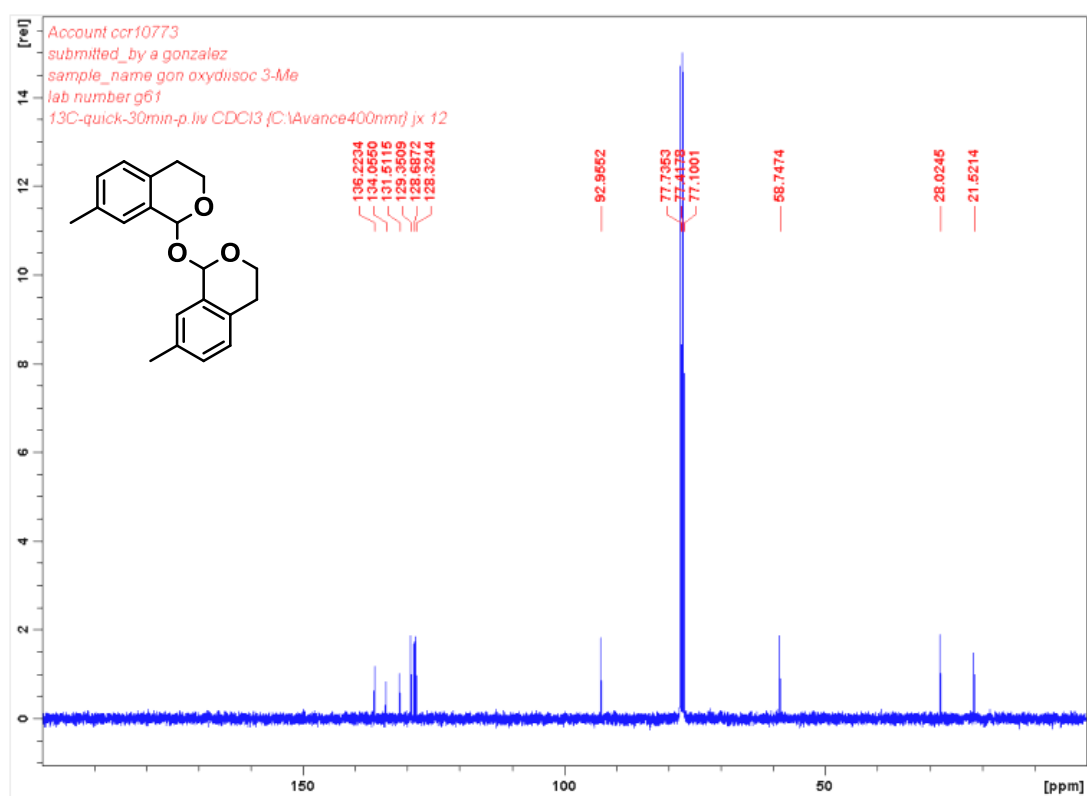
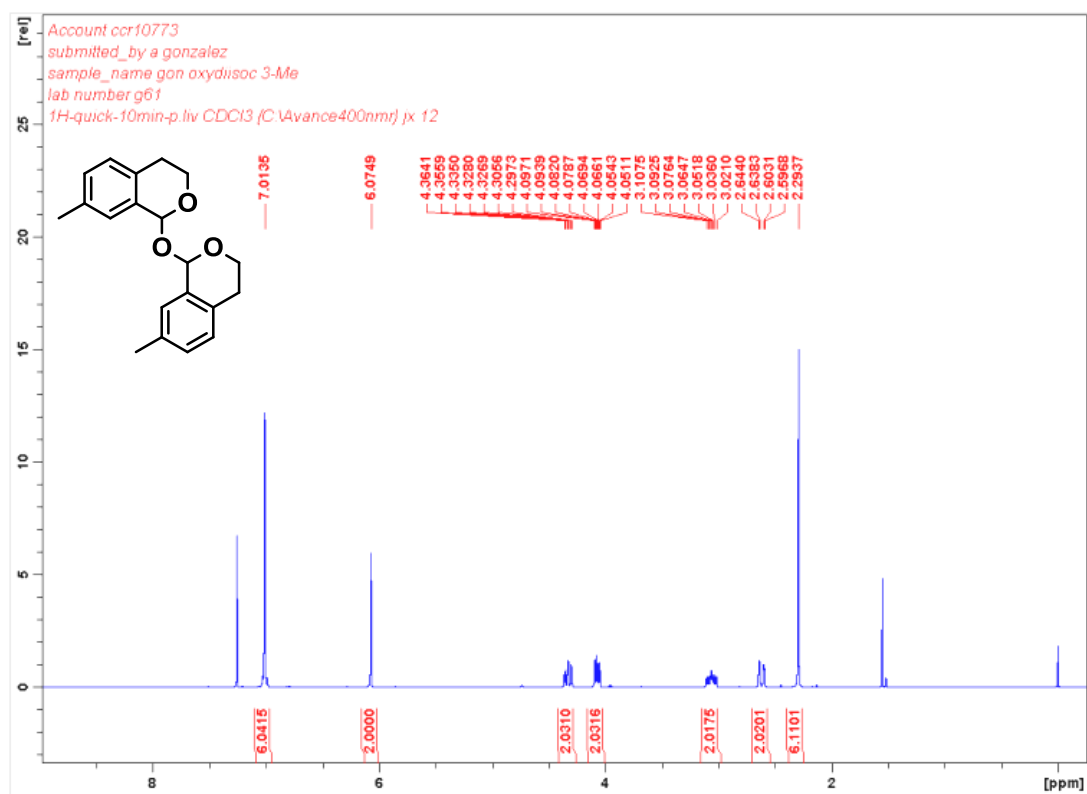
## 1-Oxisochroman-7-yl acetate



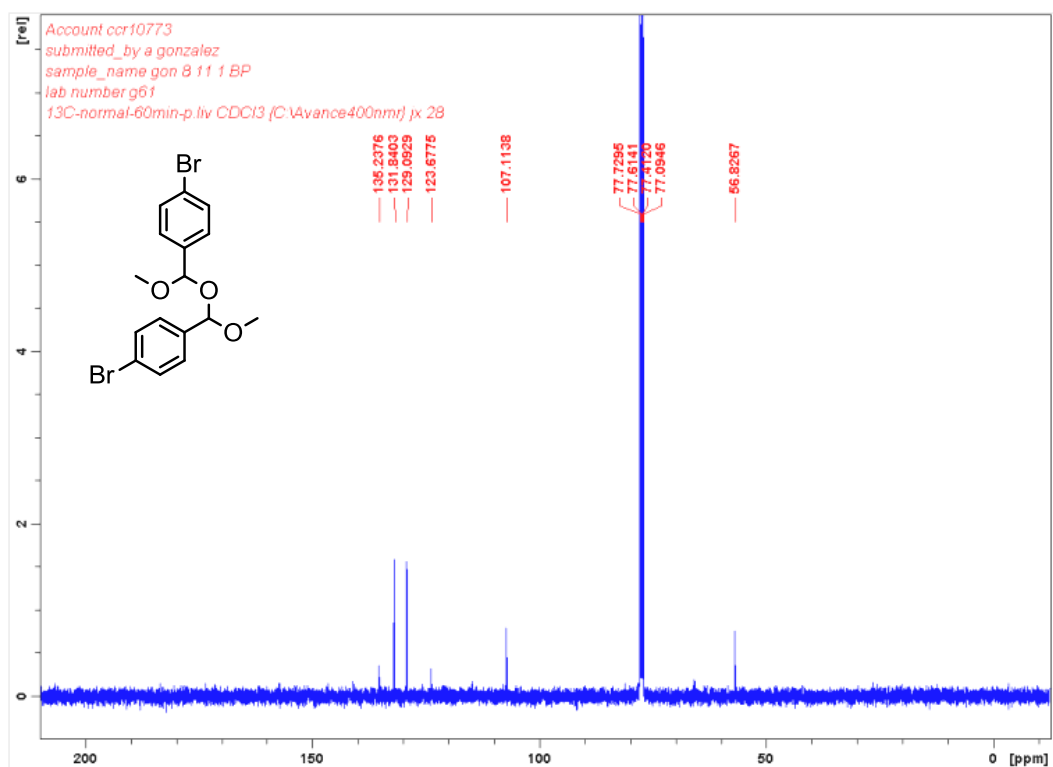
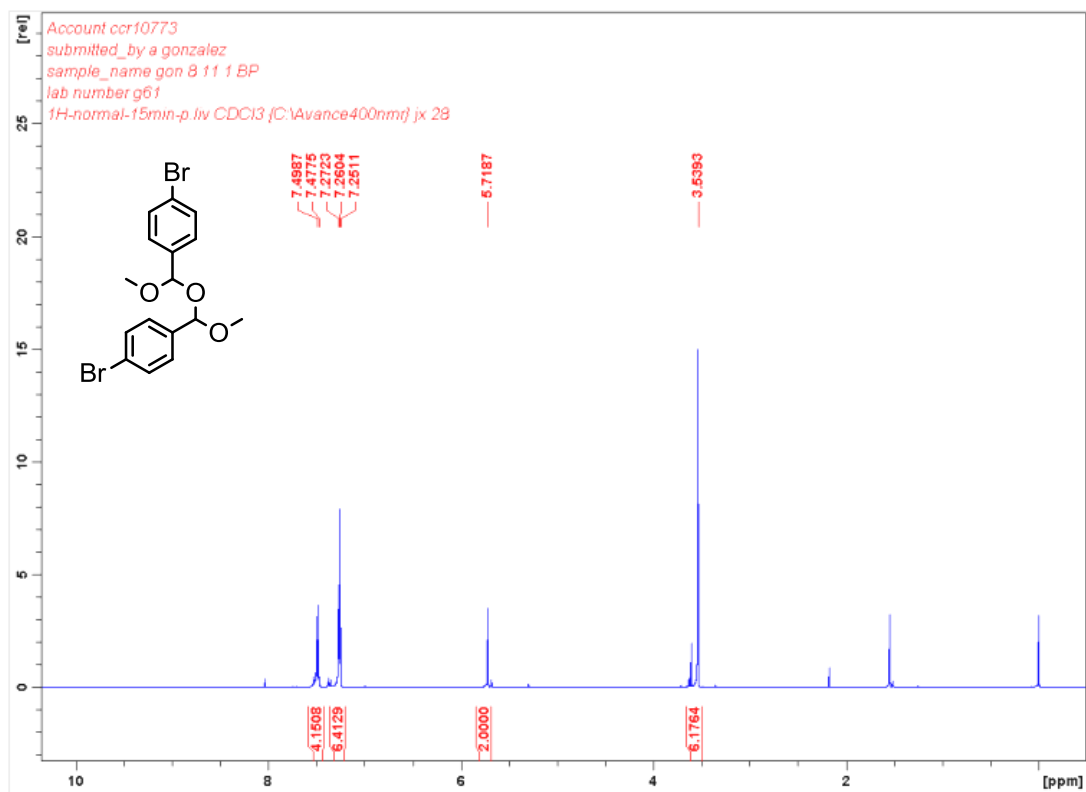


## 1,1'-Oxybis(isochroman-7,1-diyl) acetate



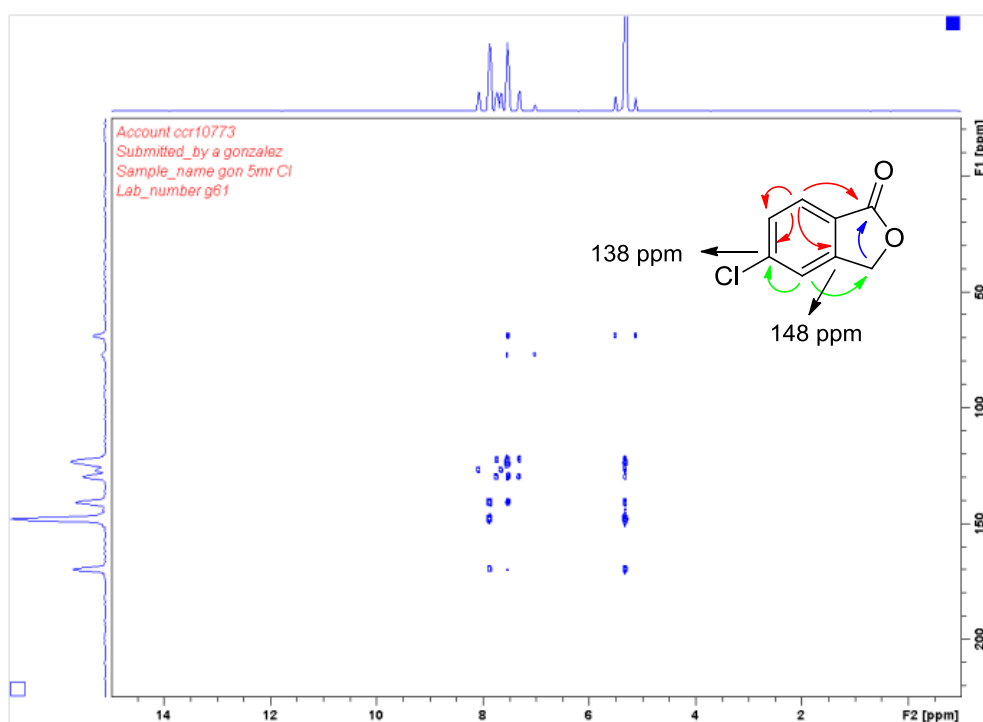
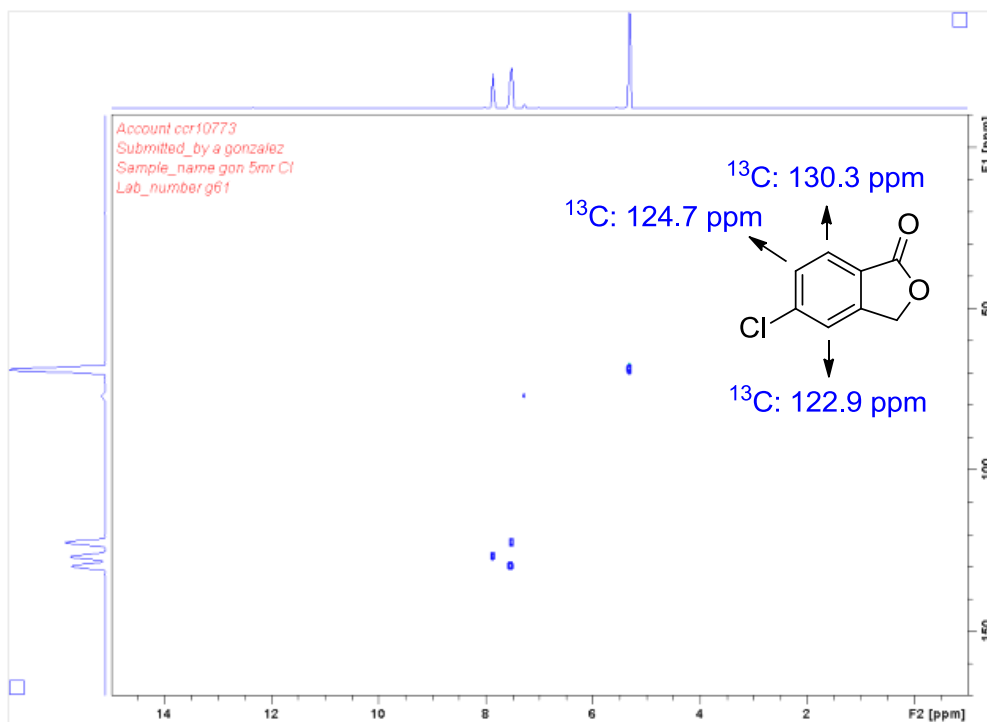
**1,1'-Oxybis(7-methylisochroman)**

## 4,4'-(Oxybis(methoxymethylene))bis(bromobenzene)



### 3.2. Assignment of the regioselectivity in phthalides:

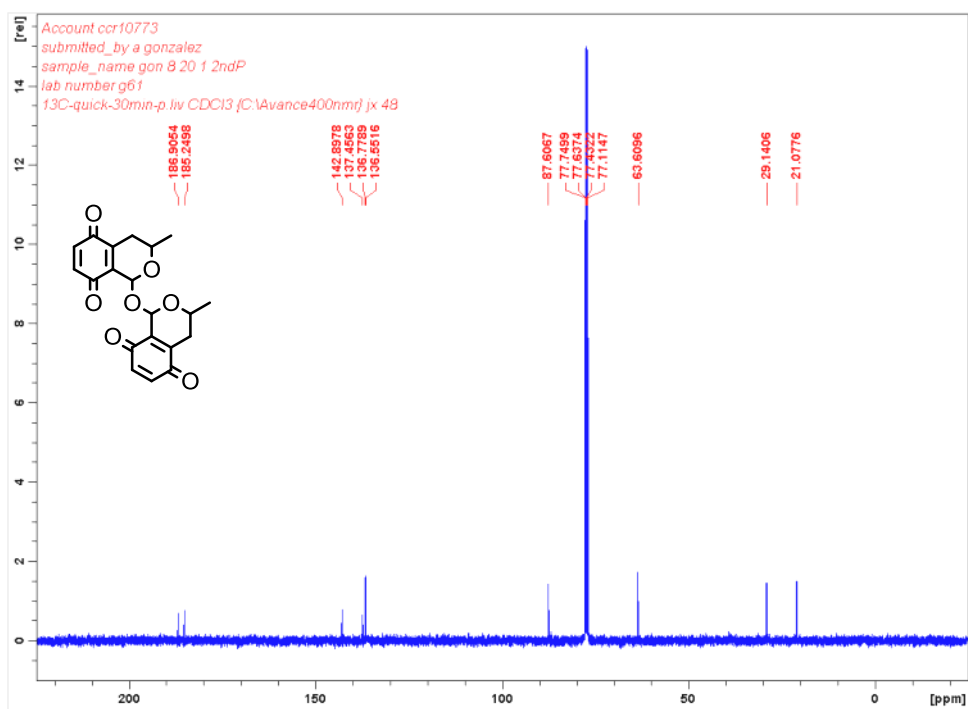
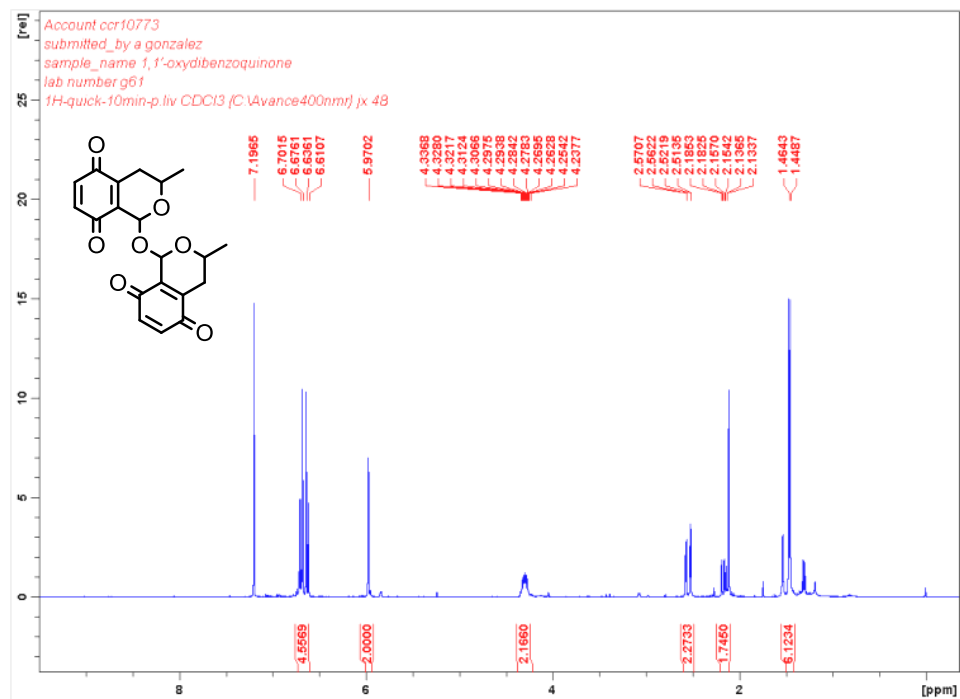
#### Example of 5-chloroisobenzofuran-1(3H)-one:



## 4. Chapter 4: additional data

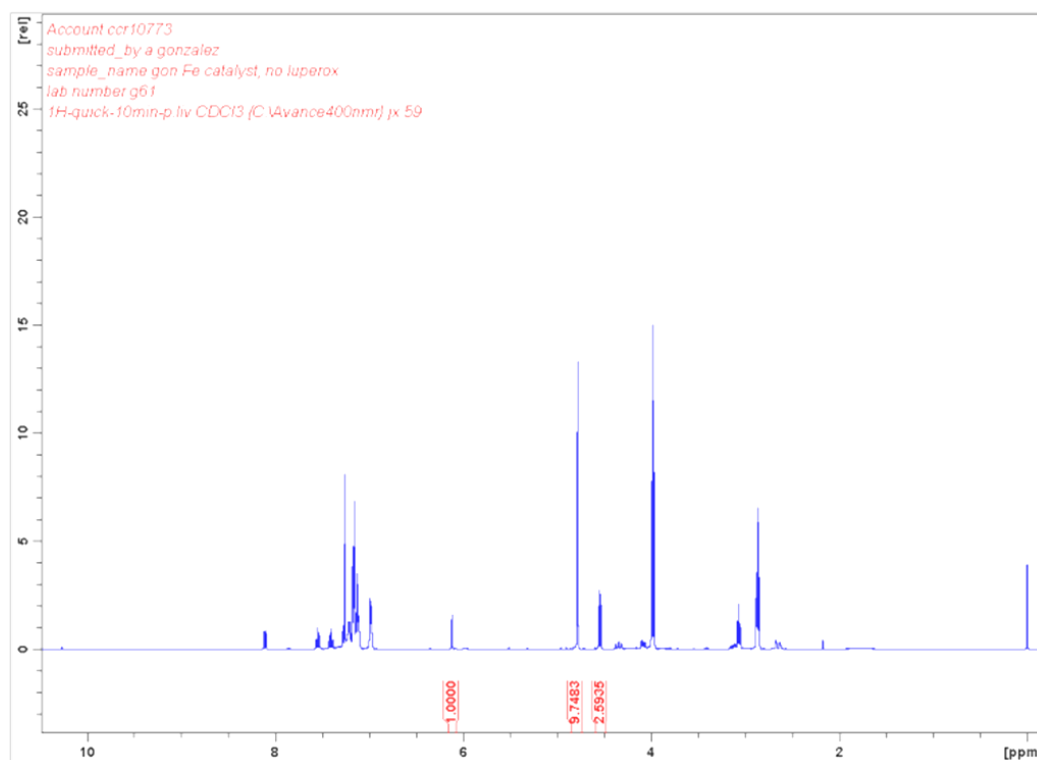
### 4.1. NMR data of the mechanistic investigations of the Fe(OTf)<sub>2</sub>-L1 catalysed aerobic oxidation of ethers.

#### 4.1.1. 1,1'-oxybis(3-methyl-3,4-dihydro-1*H*-isochromene-5,8-dione) (14)

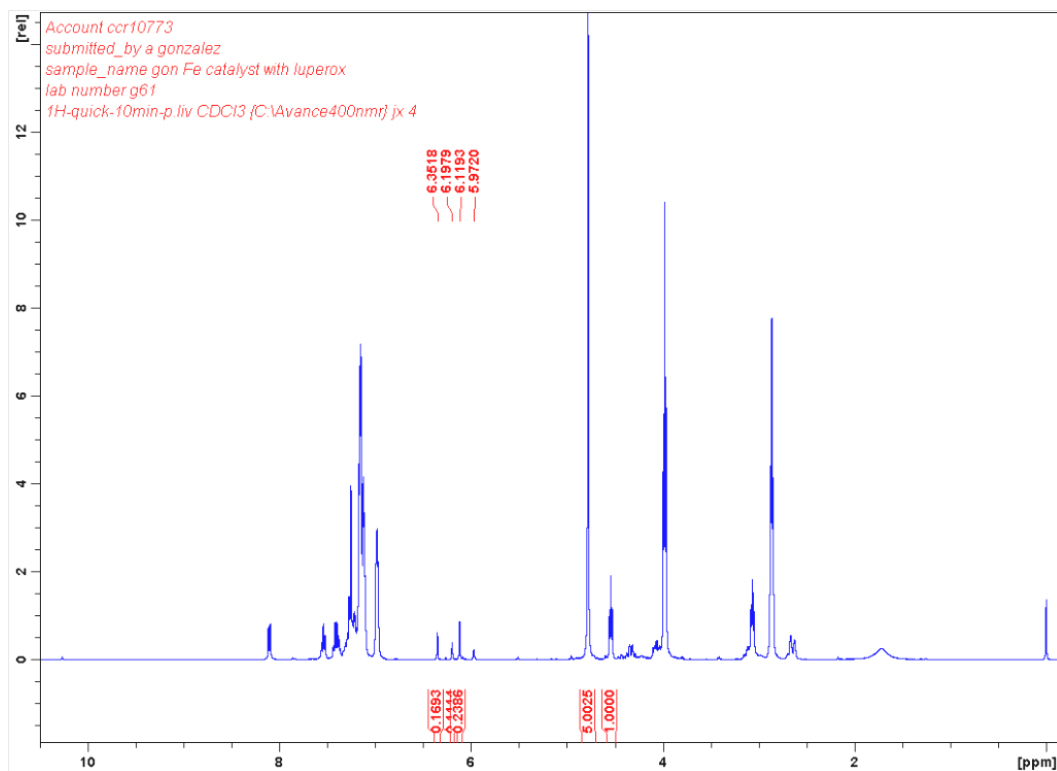


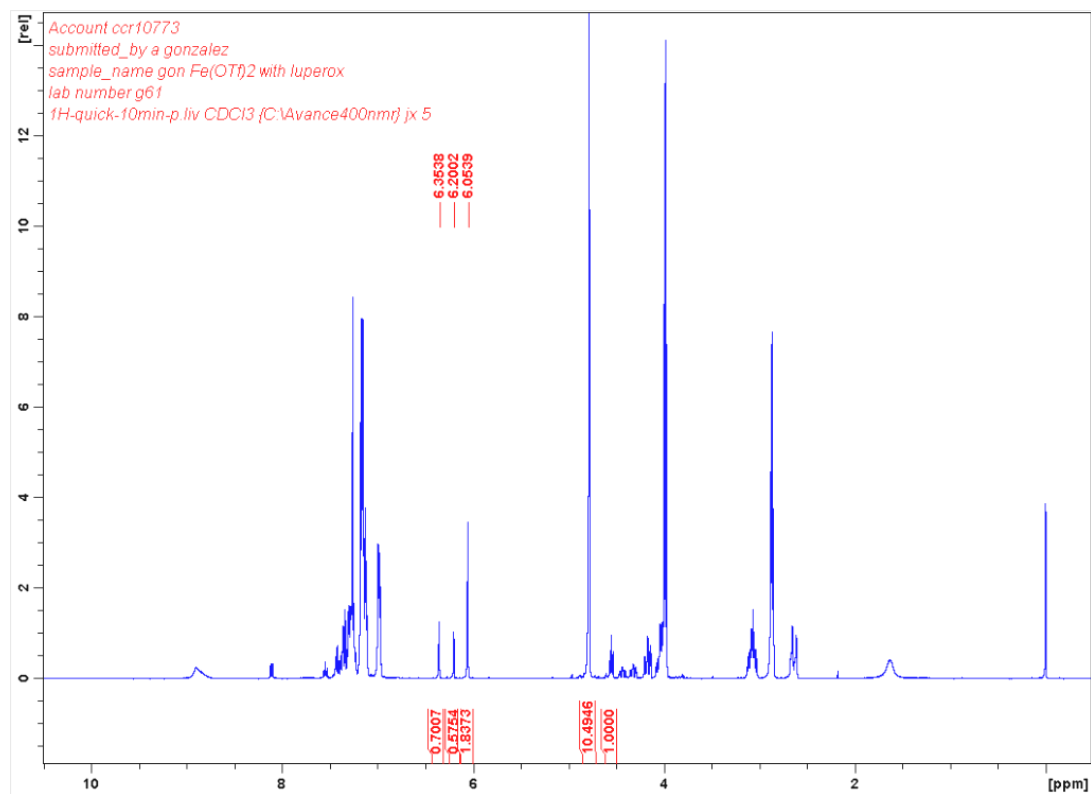
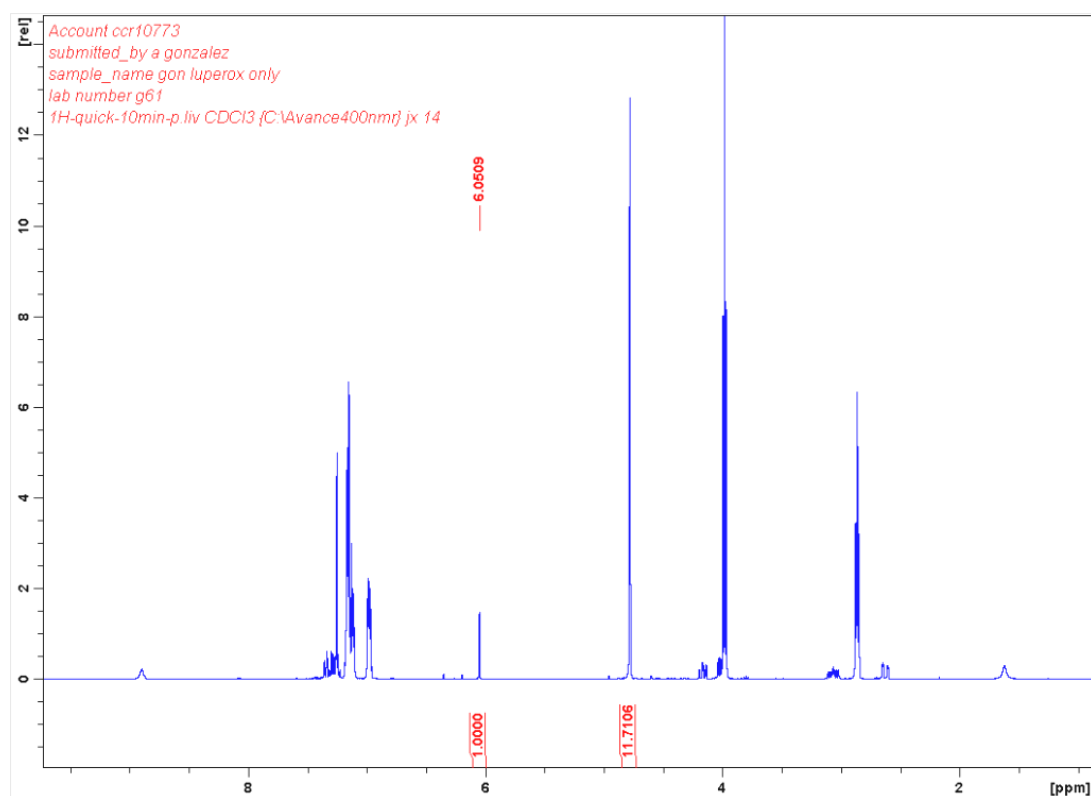
#### 4.1.2. Effect of a radical initiator: enlarged NMR spectra

##### Scheme 4, entry 1: catalyst only

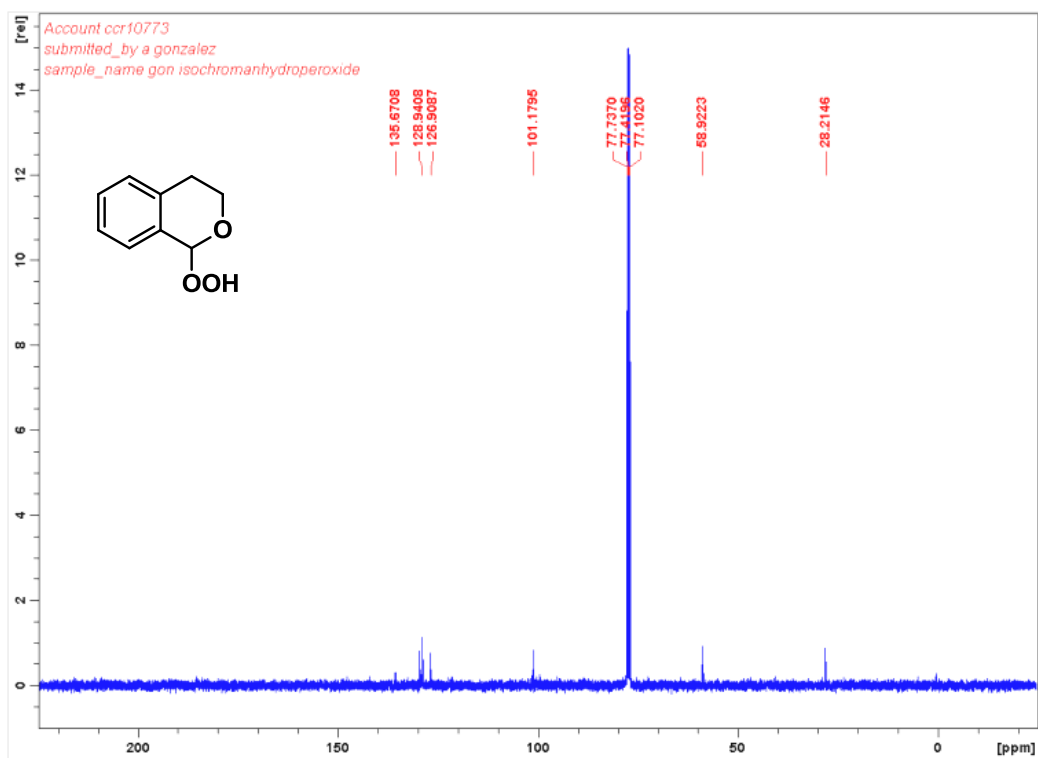
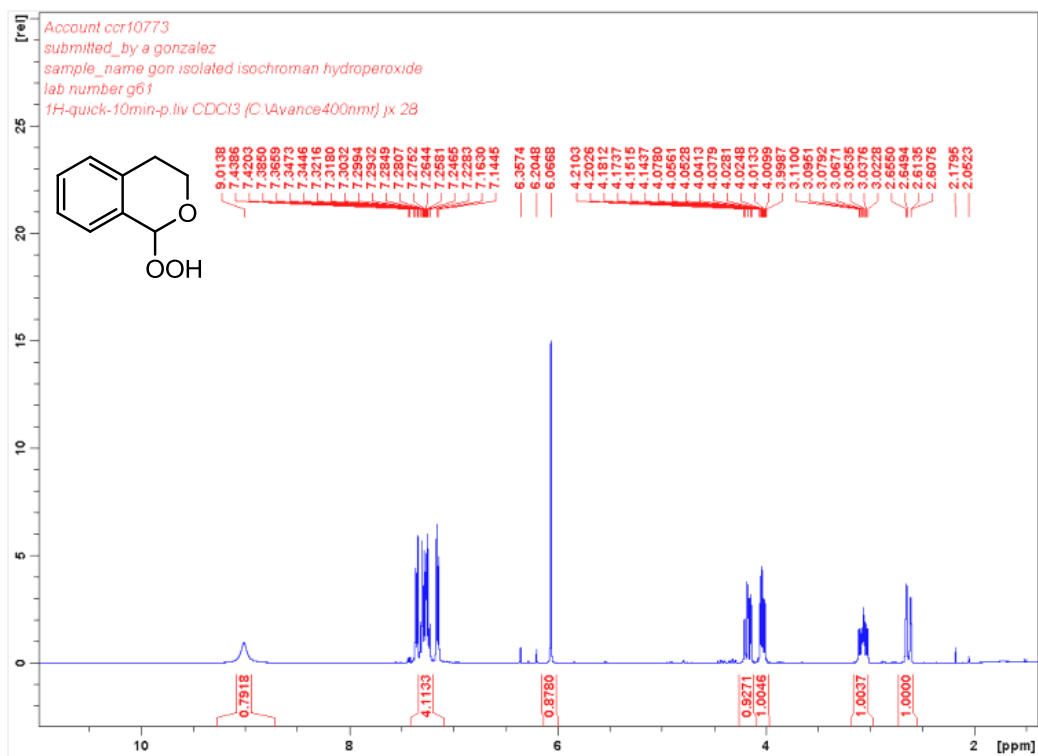


##### Scheme 4, entry 2: catalyst in the presence of Luperox



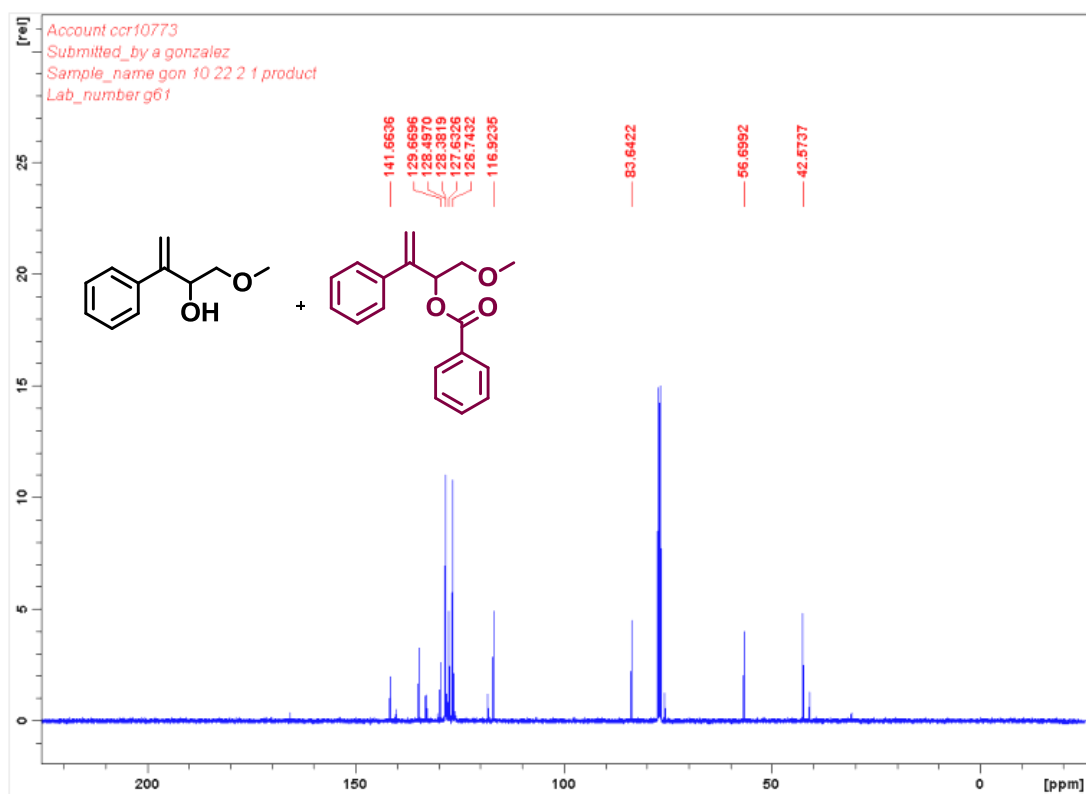
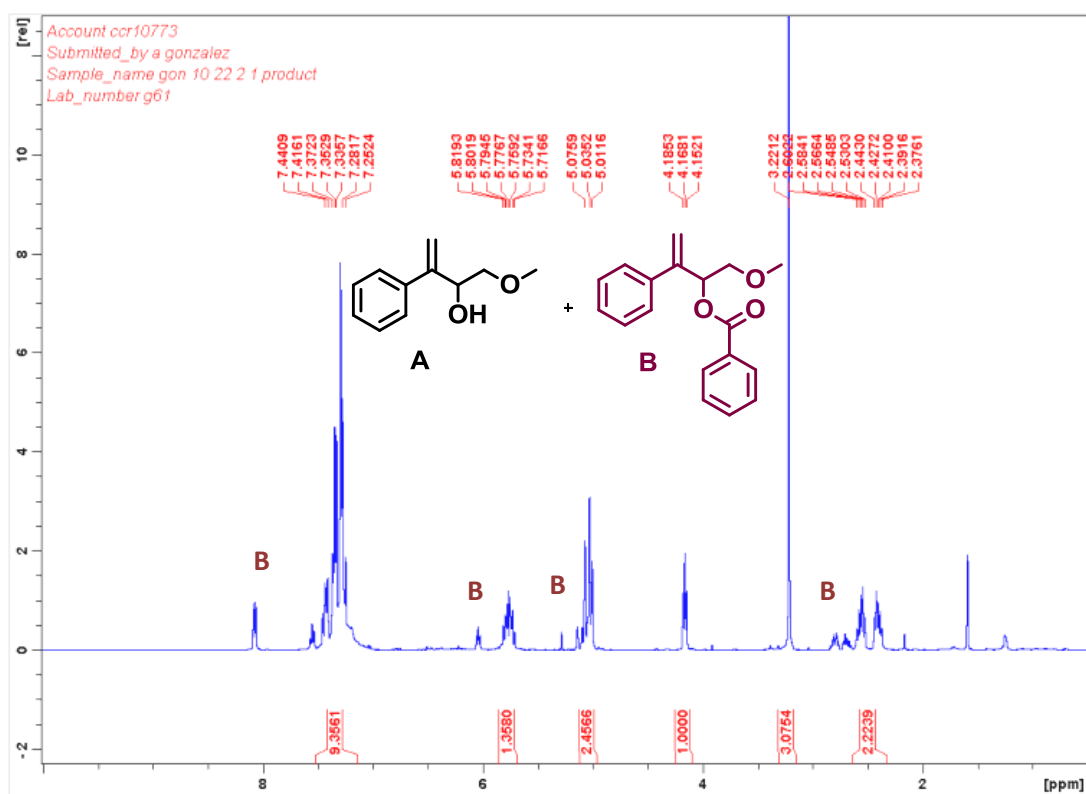
**Scheme 4, entry 3: Fe(OTf)<sub>2</sub> and Luperox****Scheme 4, entry 4: Luperox only**

## 4.1.3. Isochroman hydroperoxide



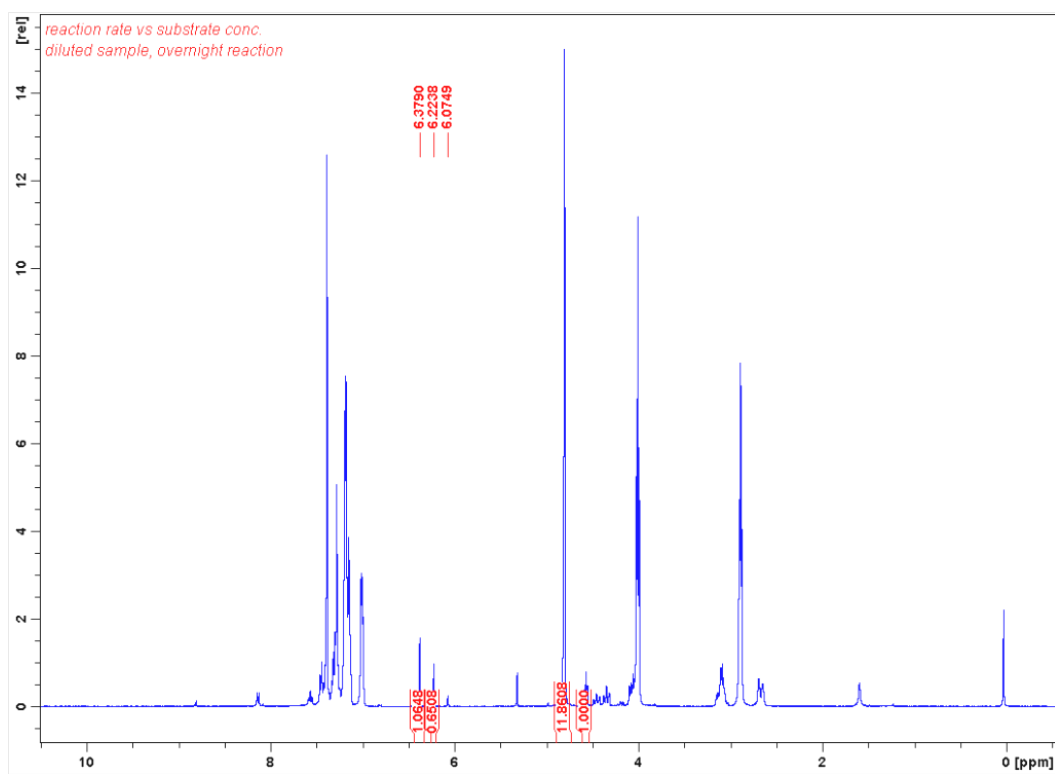


## 4.1.4. Oxidation of the radical clock: NMR of the isolated products

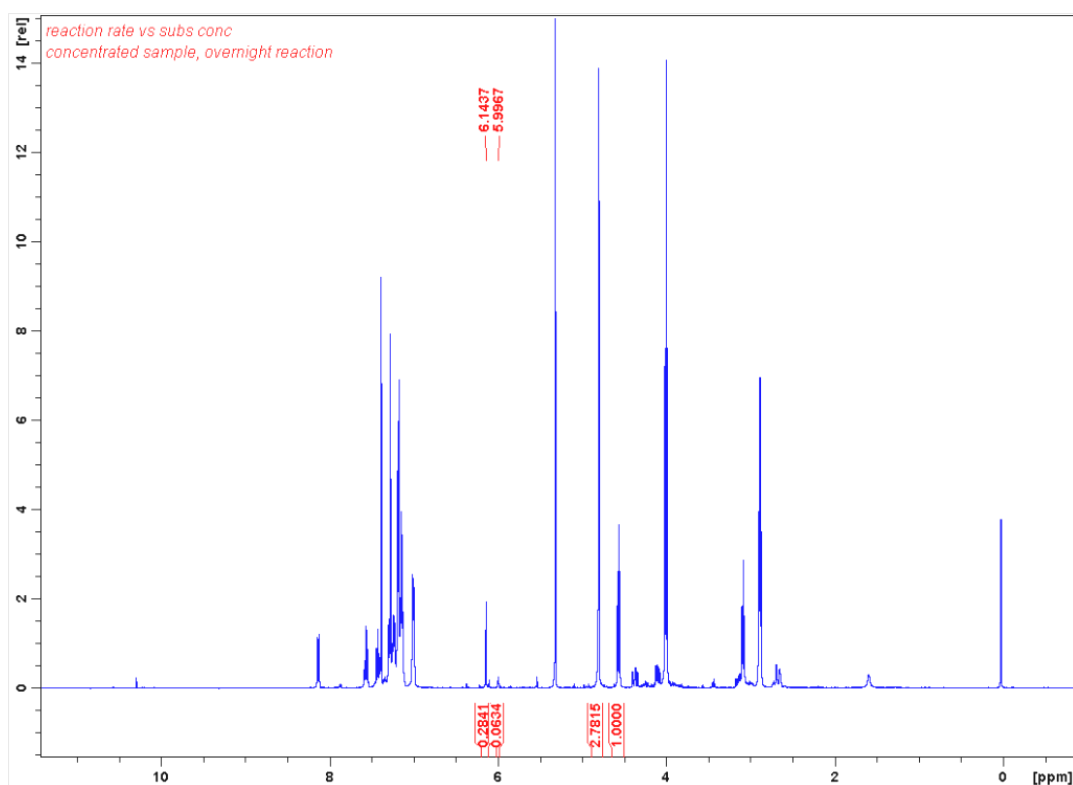


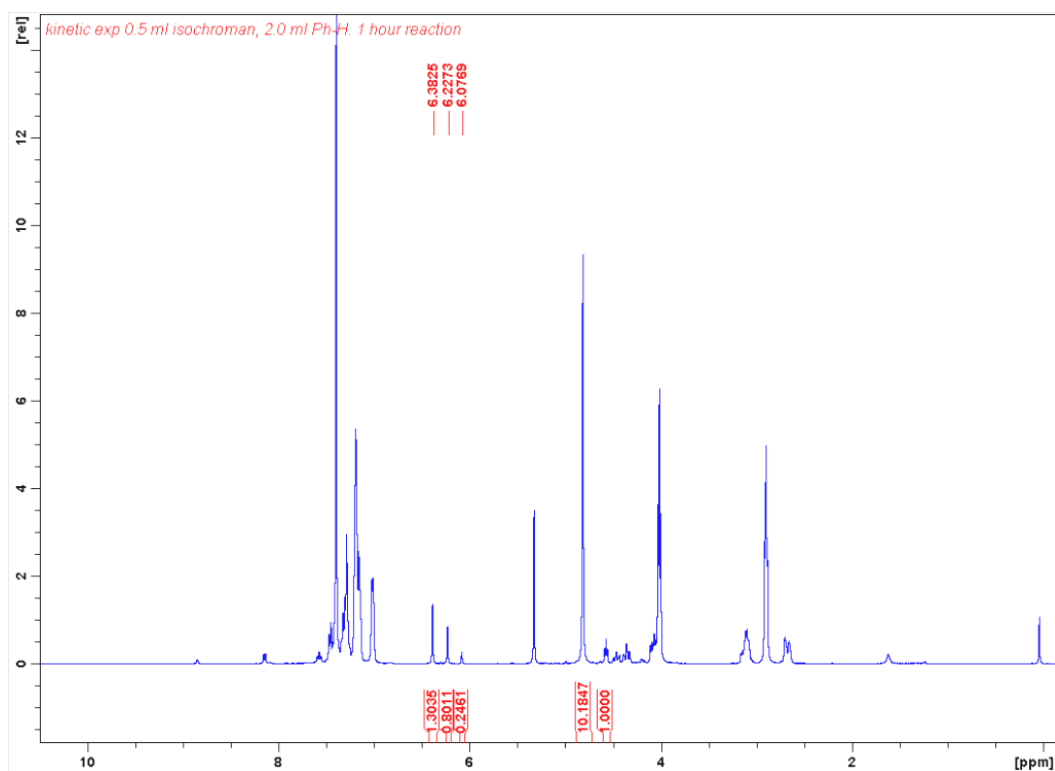
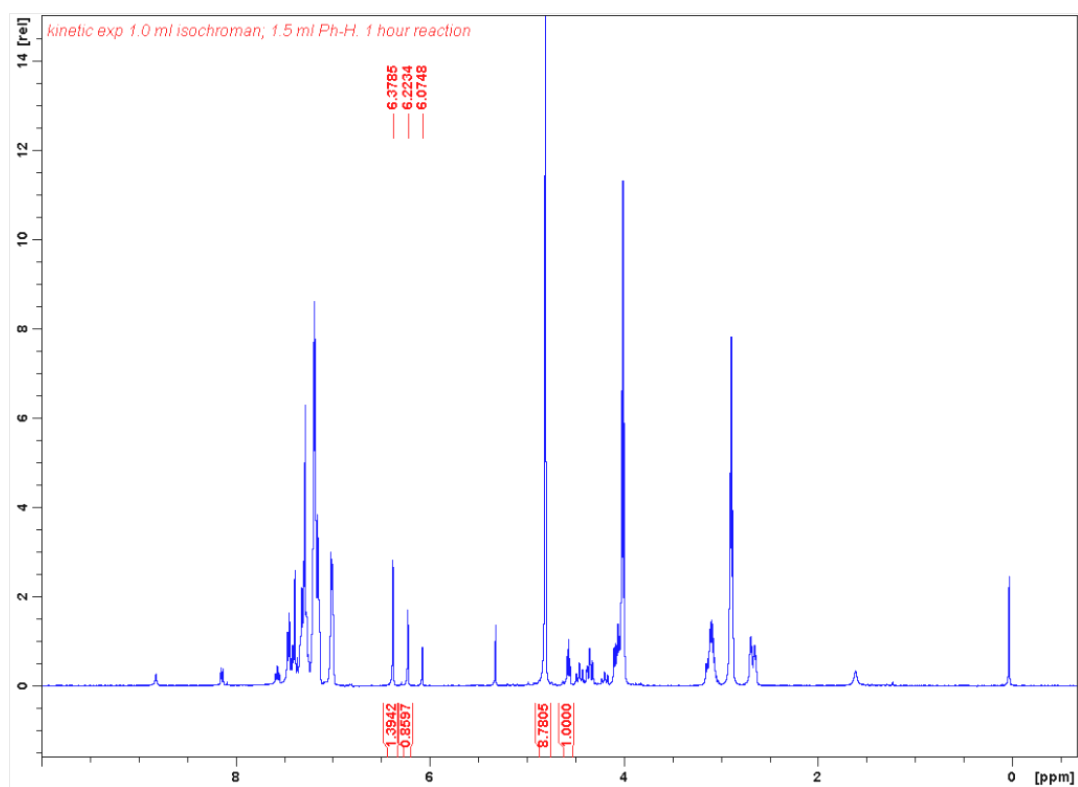
#### 4.1.5. Isolation of the 1,1'-peroxydiisochroman intermediate: enlarged spectra

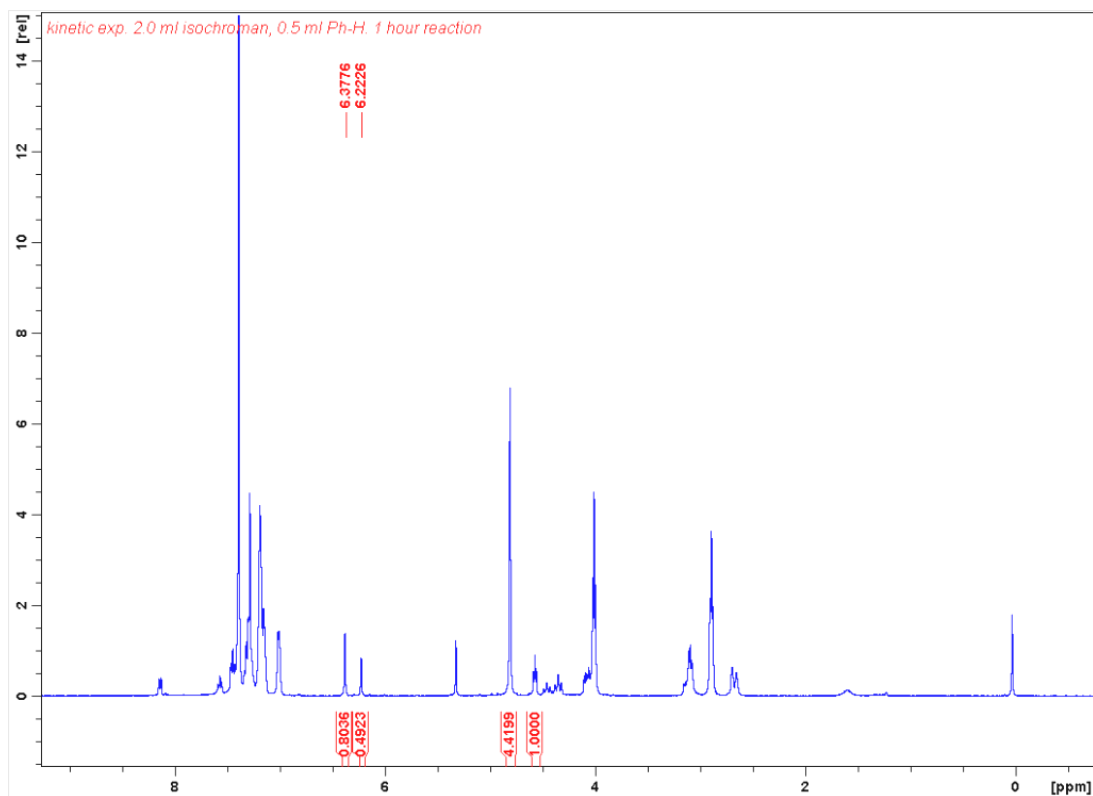
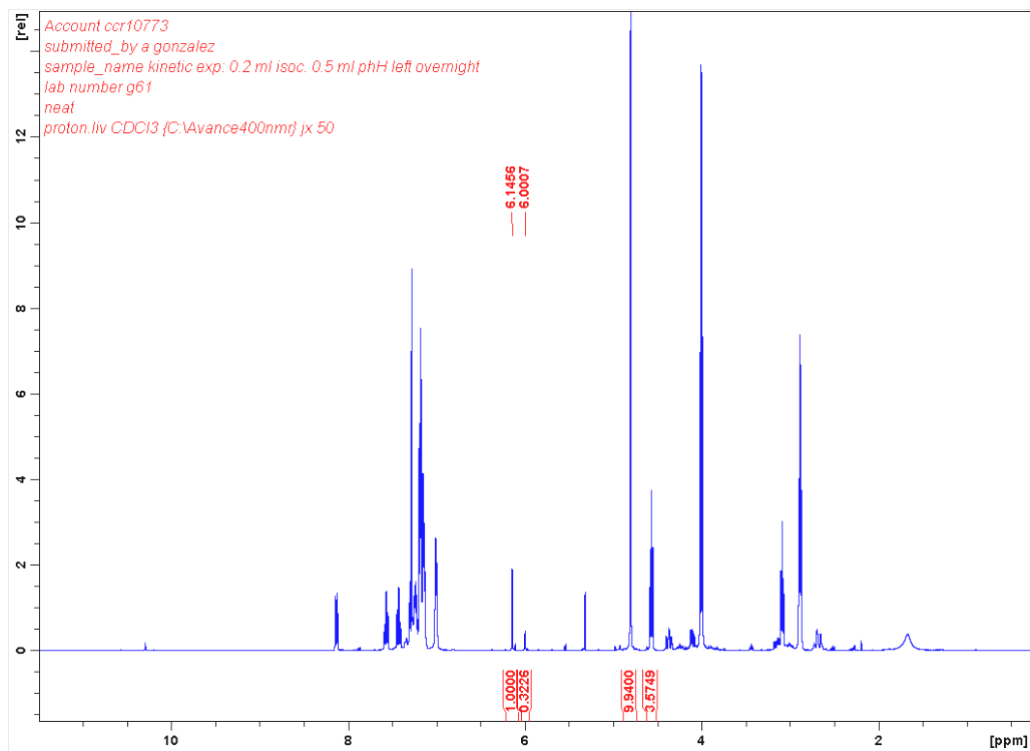
Scheme 6, entry 1: 1.0 ml isochroman in 2.0 ml C<sub>6</sub>H<sub>6</sub>, overnight reaction



Scheme 6, entry 2: 2.0 ml isochroman in 1.0 ml C<sub>6</sub>H<sub>6</sub>, overnight reaction

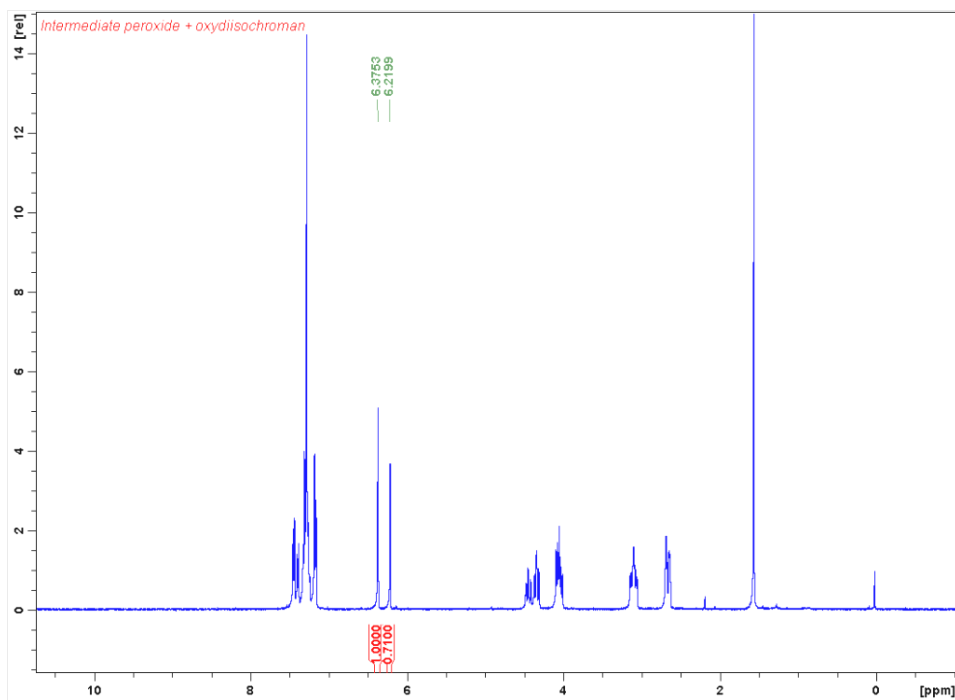


**Scheme 6, entry 3: 0.5 ml isochroman in 2.0 ml C<sub>6</sub>H<sub>6</sub>, 1h reaction****Scheme 6, entry 4: 1.0 ml isochroman in 1.5 ml C<sub>6</sub>H<sub>6</sub>, 1h reaction**

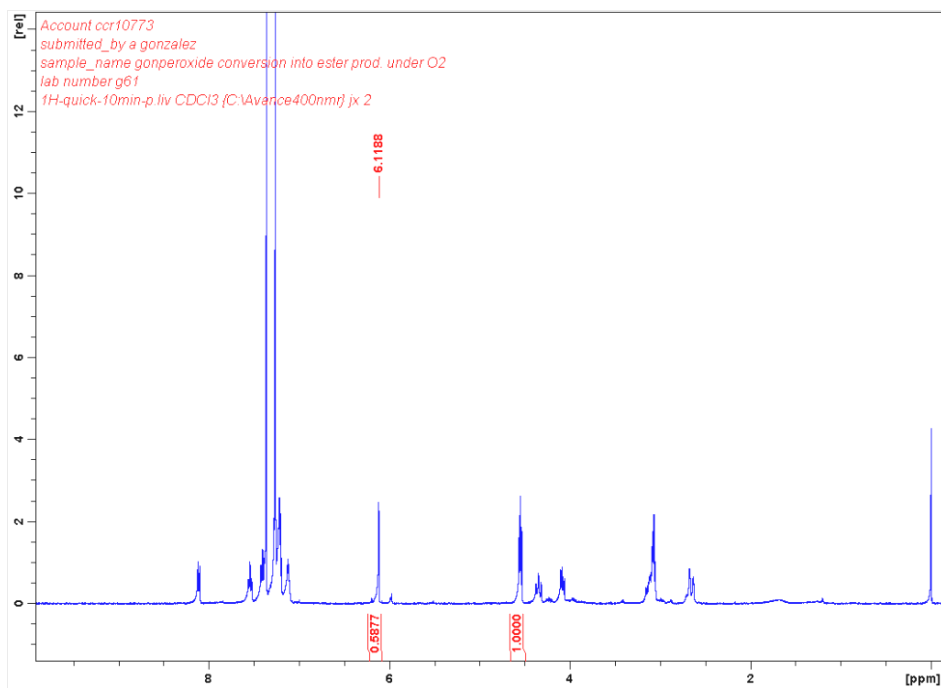
**Scheme 6, entry 5: 2.0 ml isochroman in 0.5 ml C<sub>6</sub>H<sub>6</sub>, 1h reaction****Scheme 6, entry 6: 2.0 ml isochroman in 0.5 ml C<sub>6</sub>H<sub>6</sub>, overnight reaction**

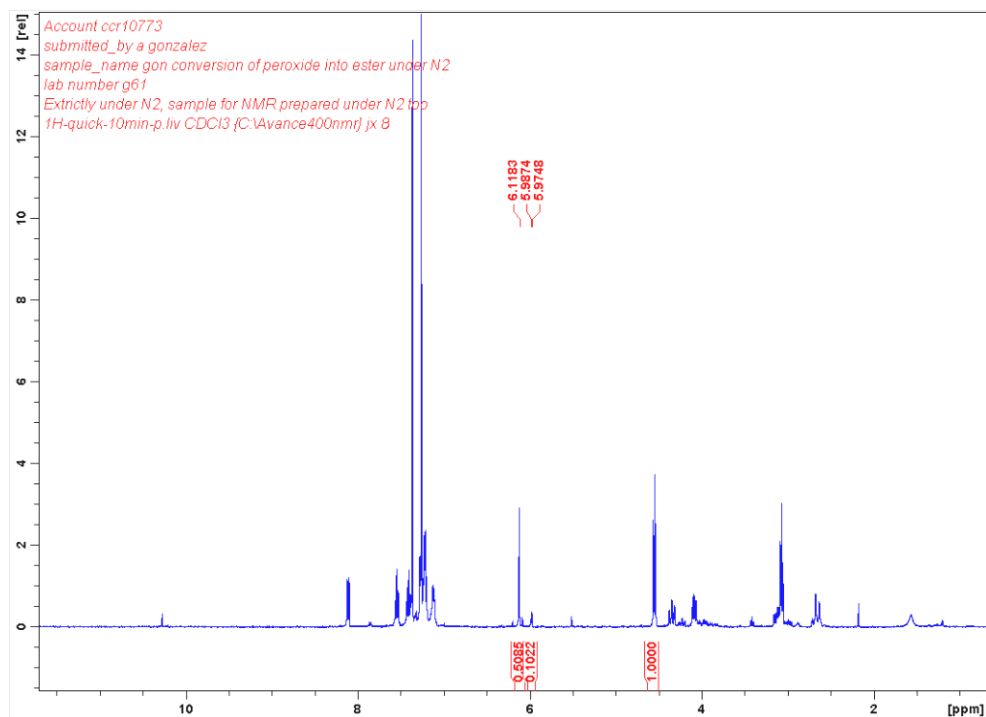
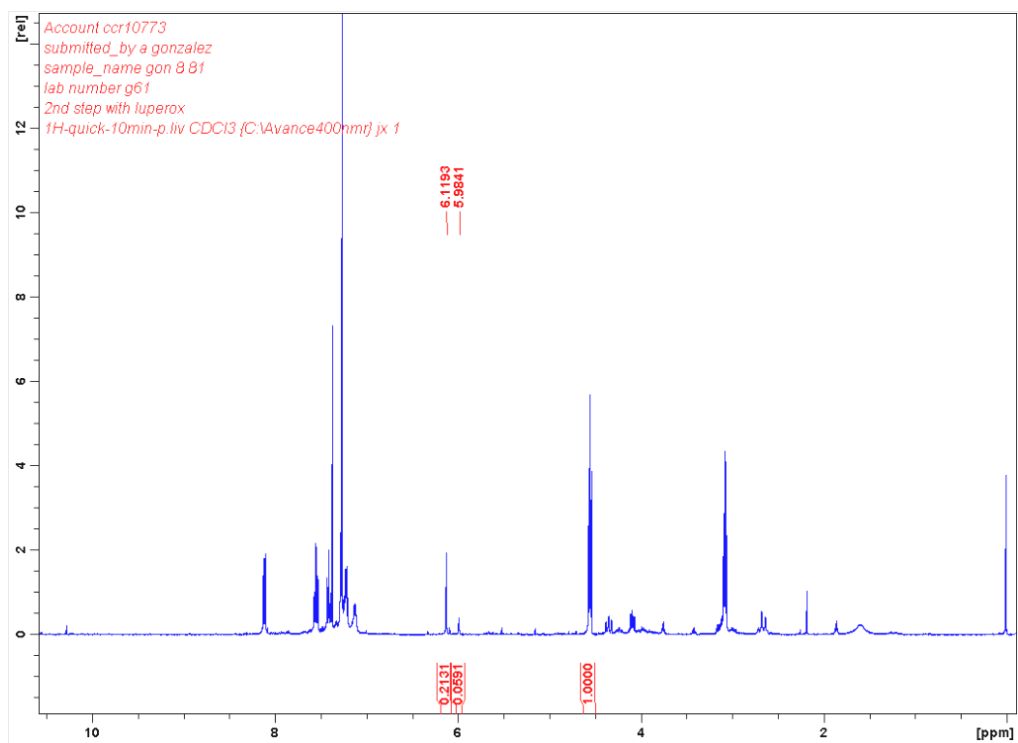
#### 4.1.6. Conversion of 1,1'- peroxyisochroman to chromanone: enlarged spectra

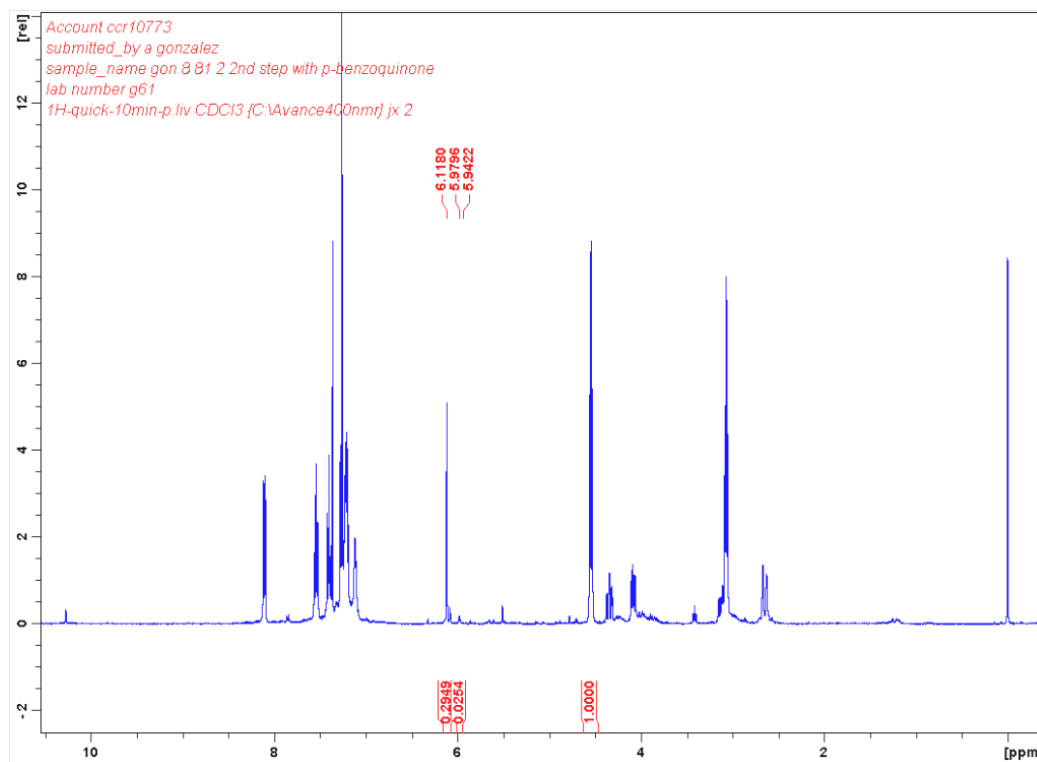
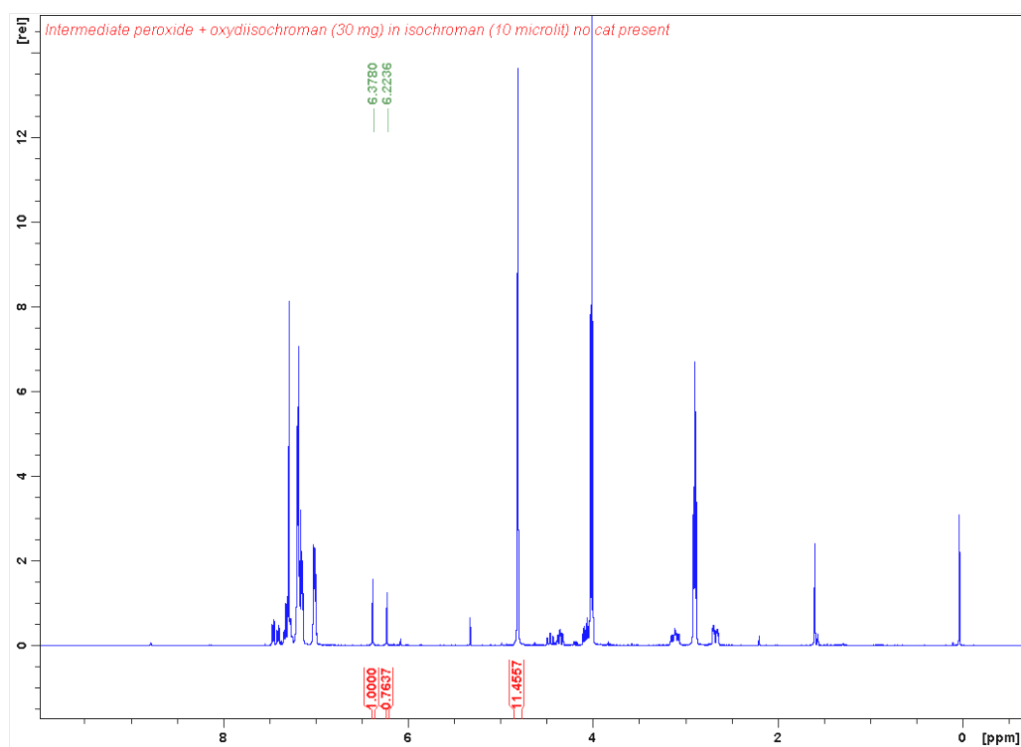
Scheme 8, entry 1: starting mixture of 1,1'- peroxyisochroman and 1,1'-oxydiisochroman

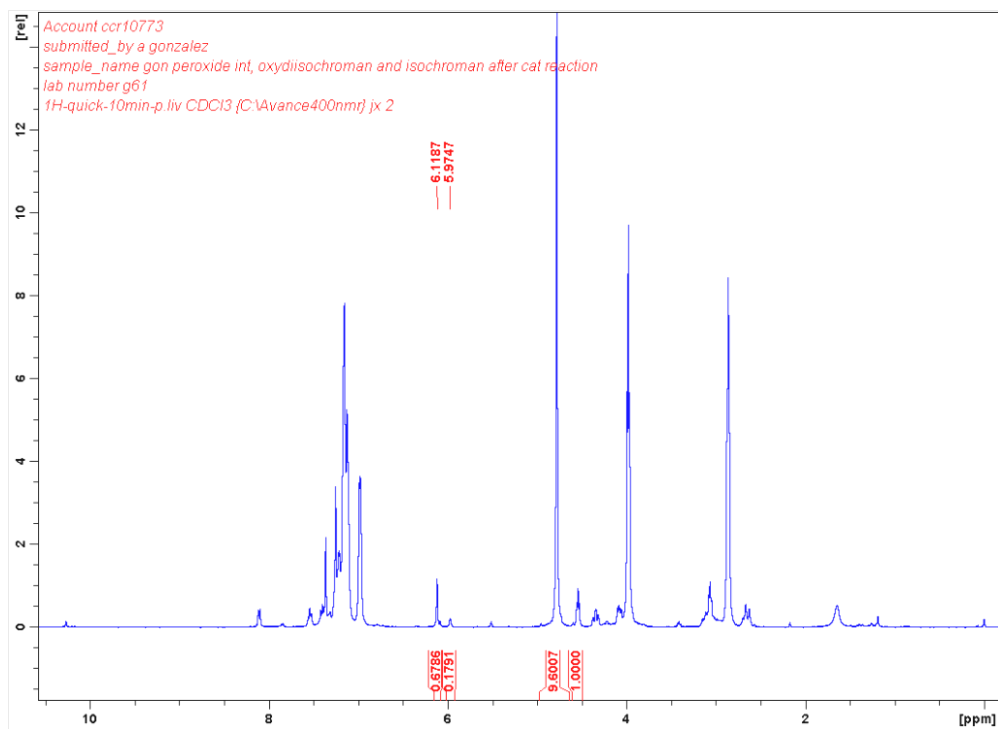
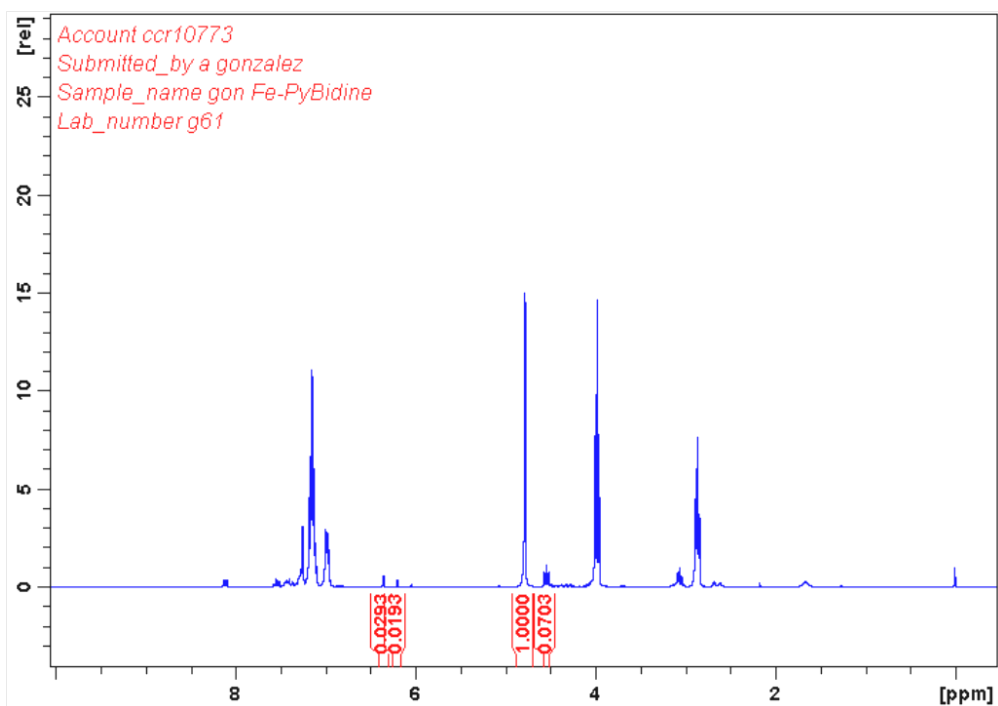


Scheme 8, entry 2: reaction under oxygen atmosphere

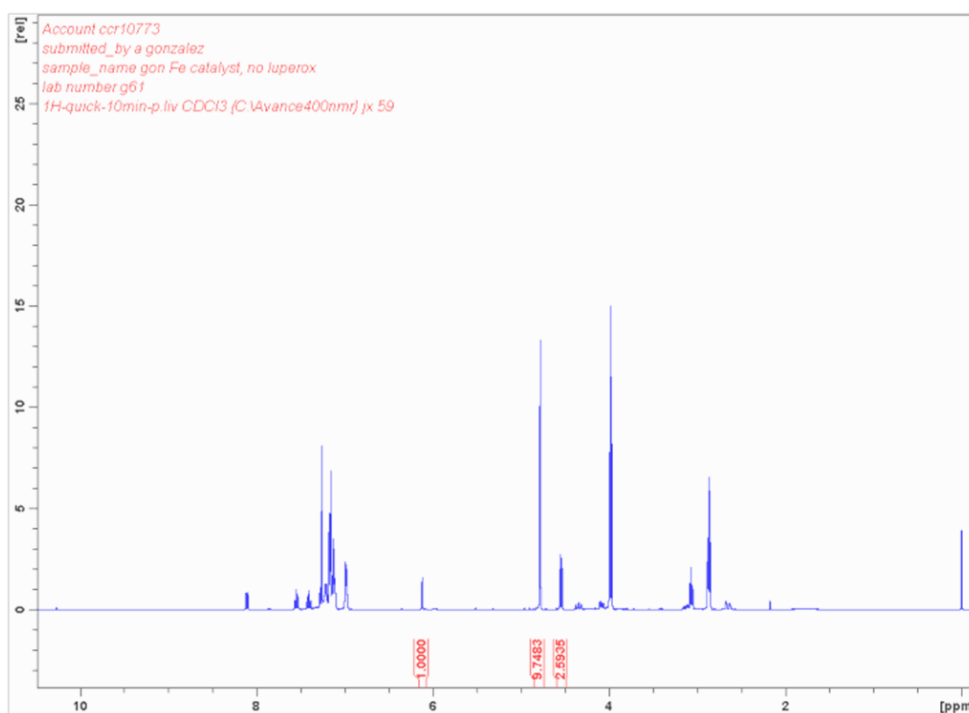
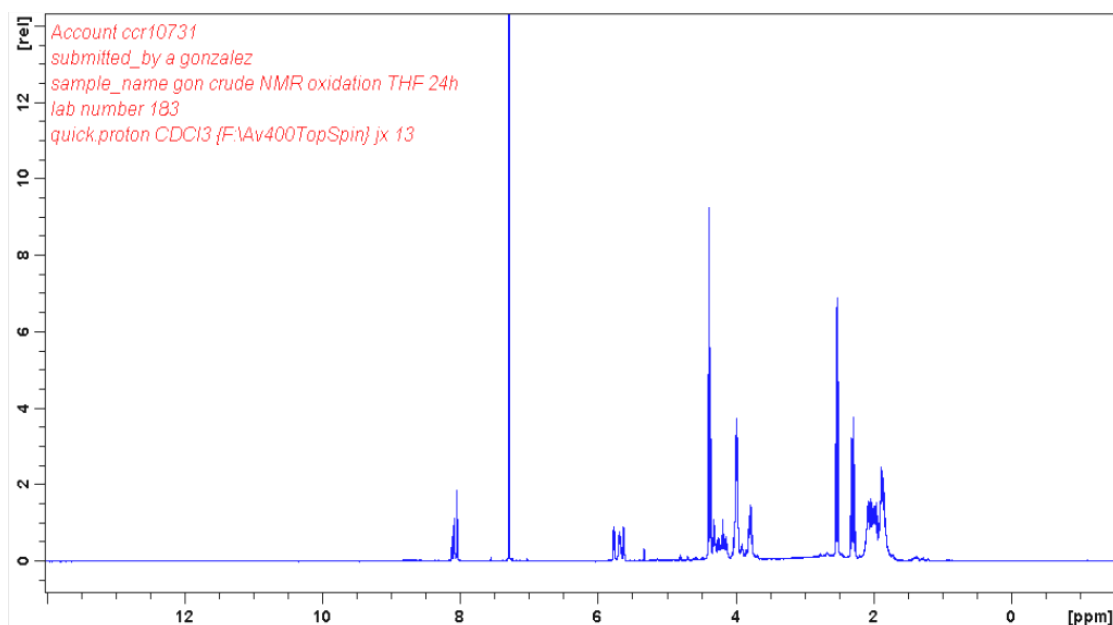


**Scheme 8, entry 3: reaction under N<sub>2</sub> atmosphere****Scheme 9, entry 2: reaction run in the presence of radical initiator Luperox**

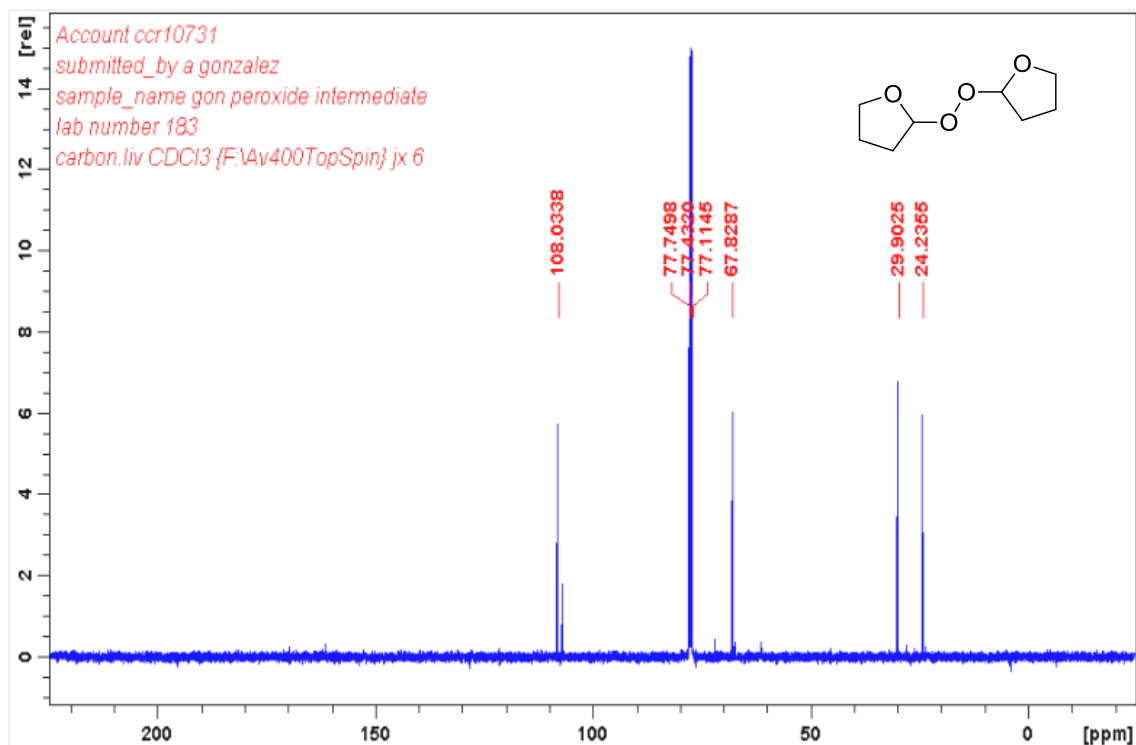
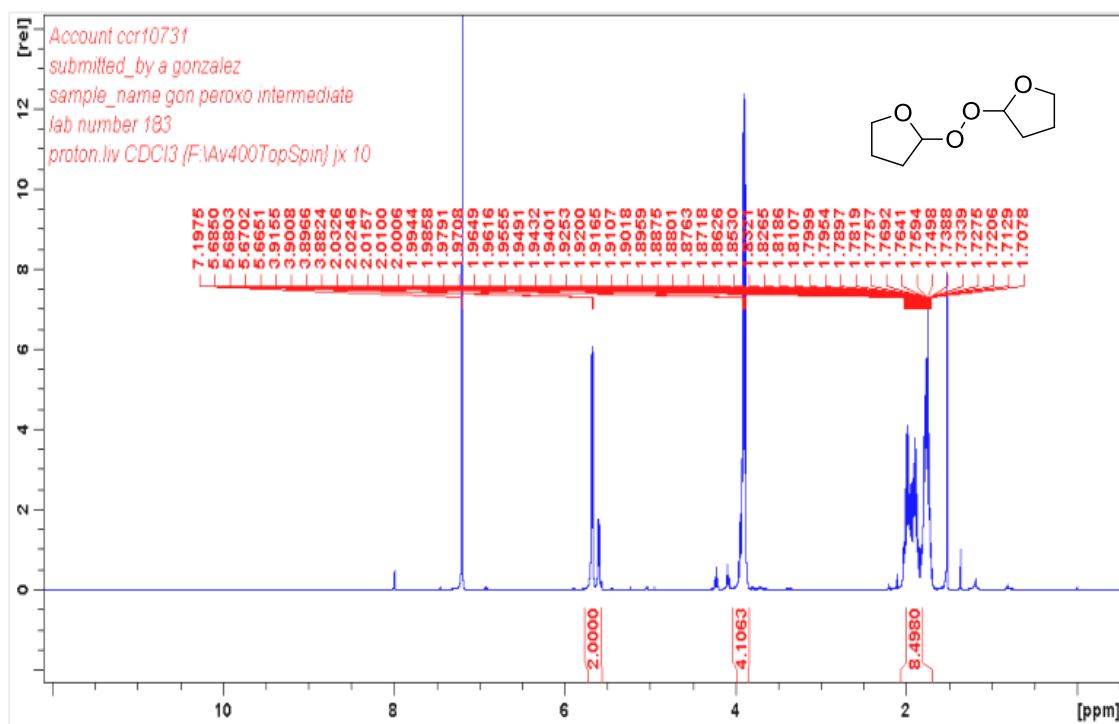
**Scheme 9, entry 3: reaction run in the presence of radical inhibitor p-benzoquinone****Scheme 10, entry 2: starting mixture of isochroman, 1,1'-peroxydiisochroman and 1,1'-oxydiisochroman**

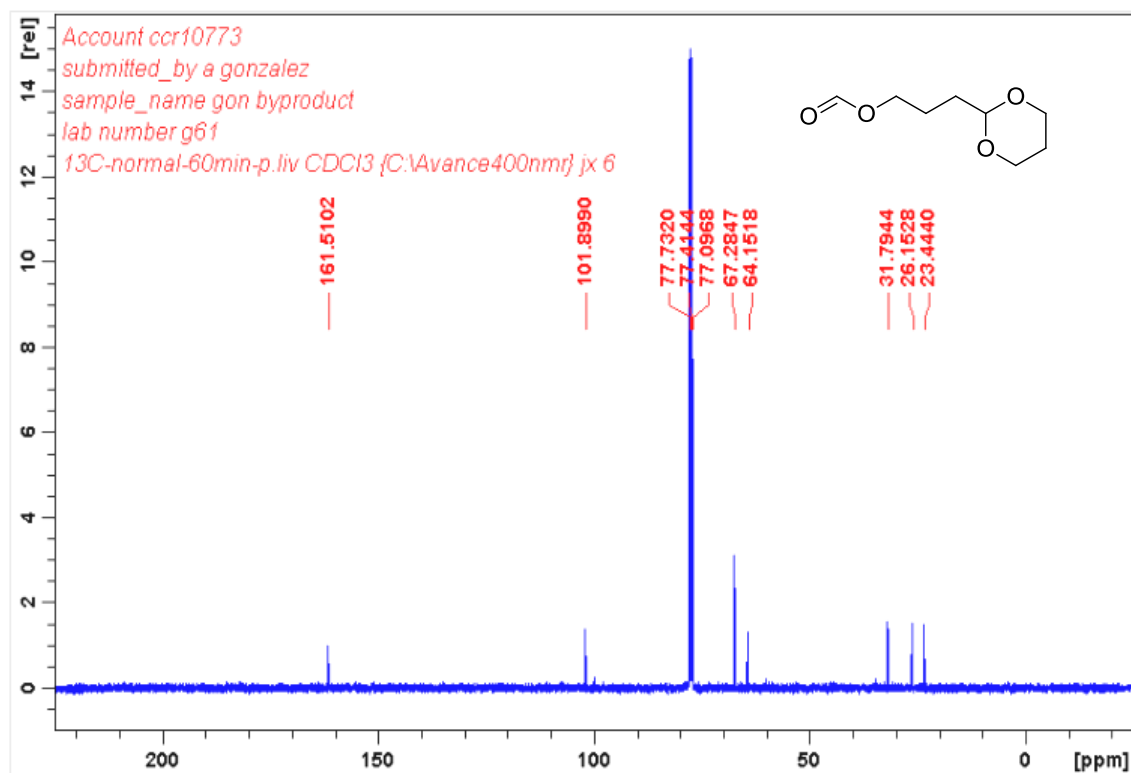
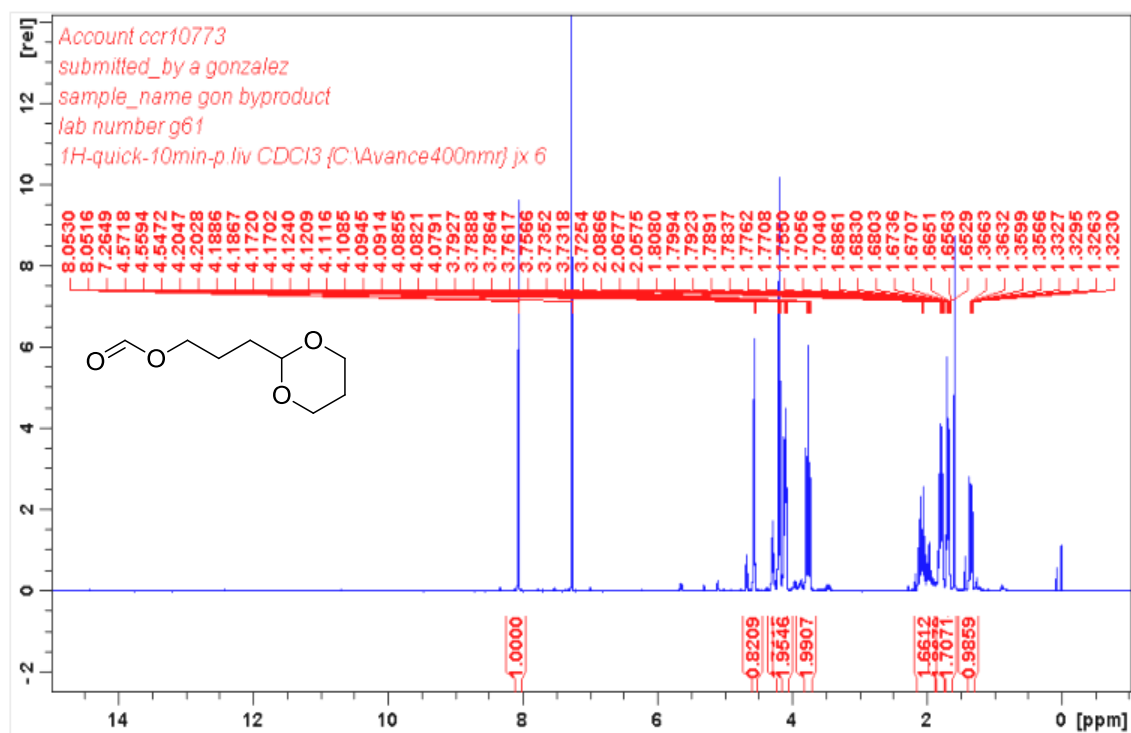
**Scheme 10, entry 3: reaction under N<sub>2</sub> atmosphere****4.1.7. Effect of the sulfonamide: Comparison between Fe(OTf)<sub>2</sub>PyBisulidine and Fe(OTf)<sub>2</sub>PyBidine in isochroman oxidation: NMR spectra****Scheme 11, entry 1: Fe-PyBidine catalyst**



**Scheme 11, entry 2: Fe-PyBisulidine catalyst****4.1.8. Oxidation of THF to  $\gamma$ -butyrolactone: NMR spectra****NMR spectrum of the crude reaction**

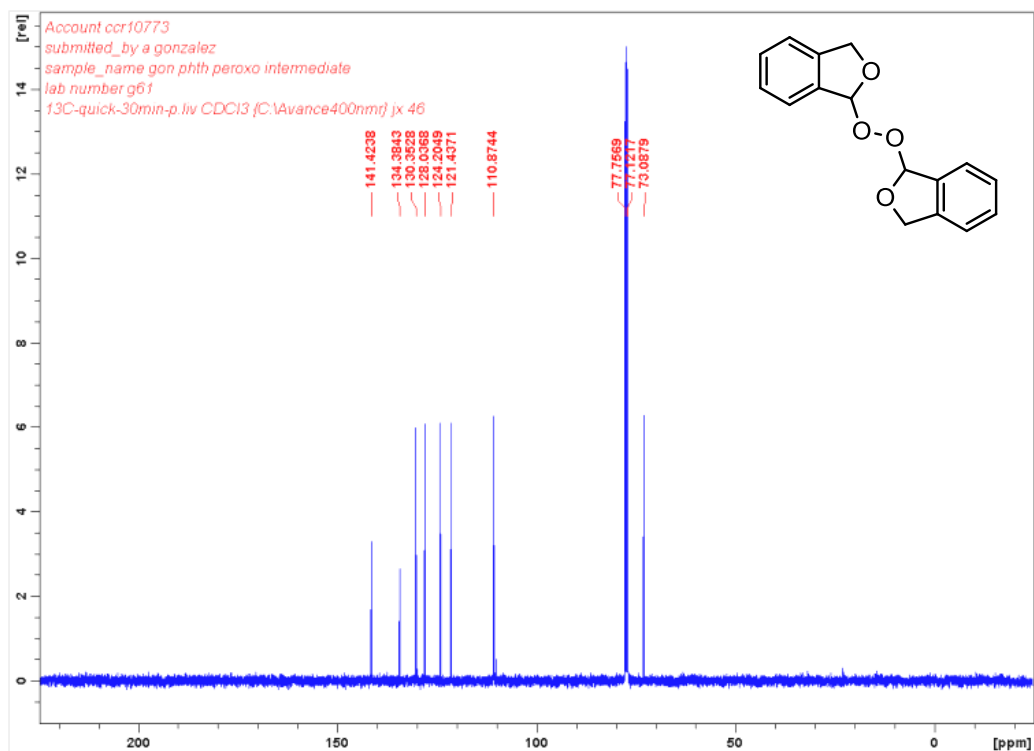
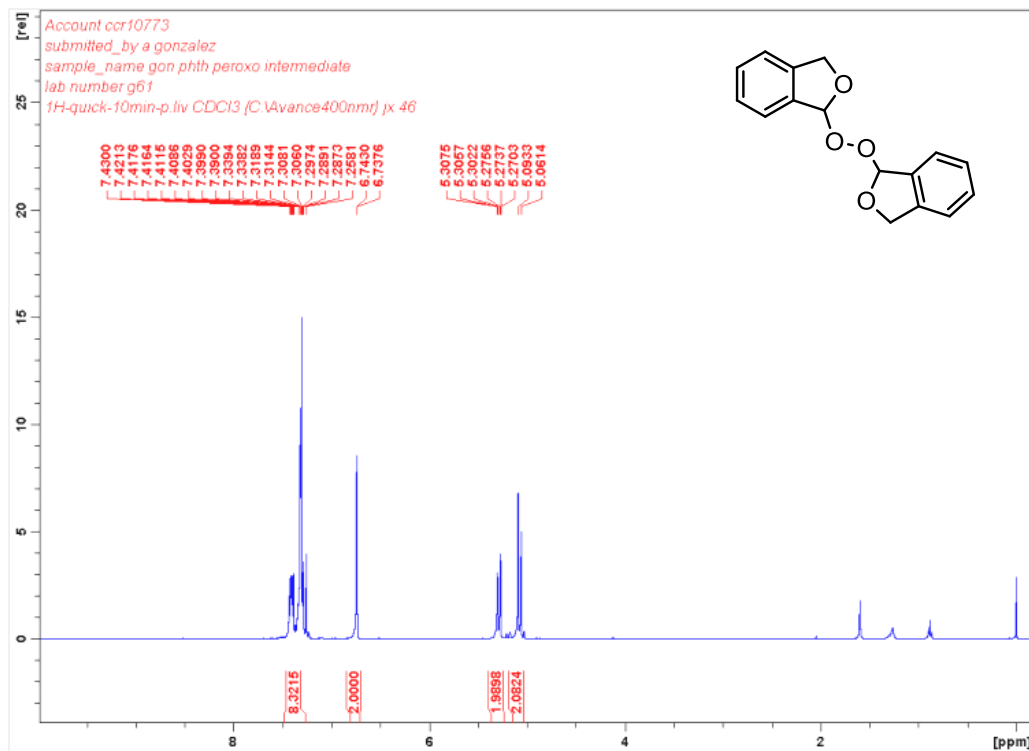
## 2,2'-peroxybis(tetrahydrofuran)

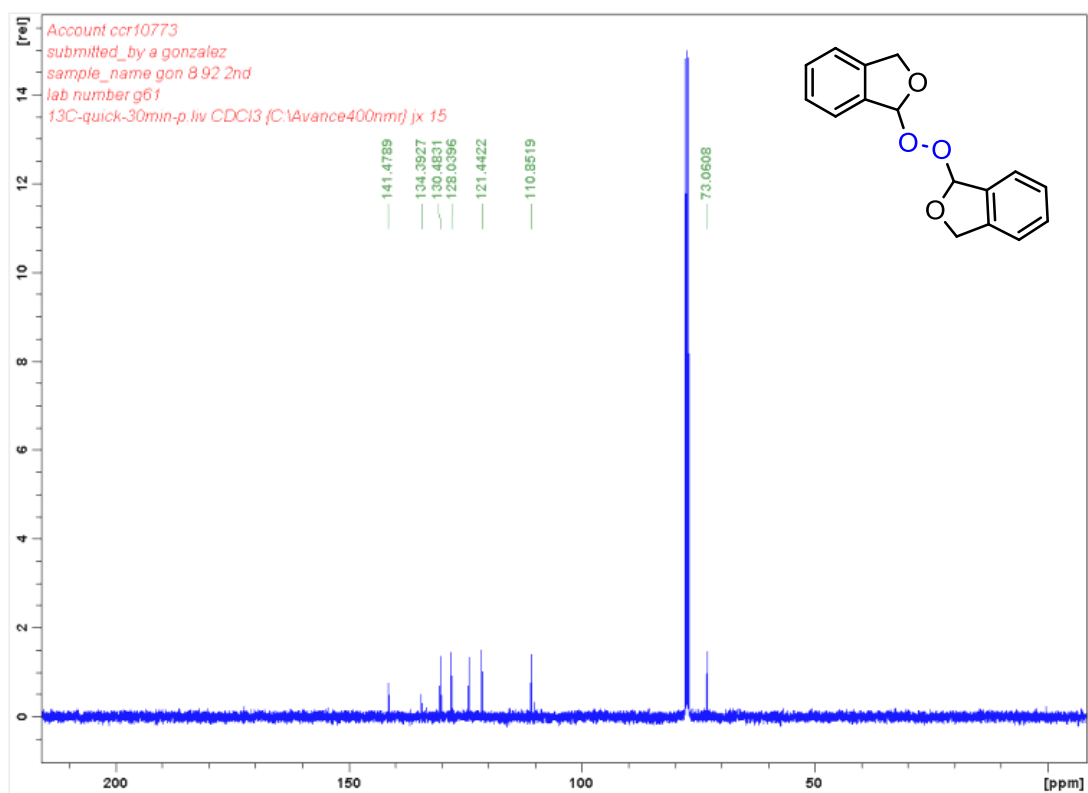
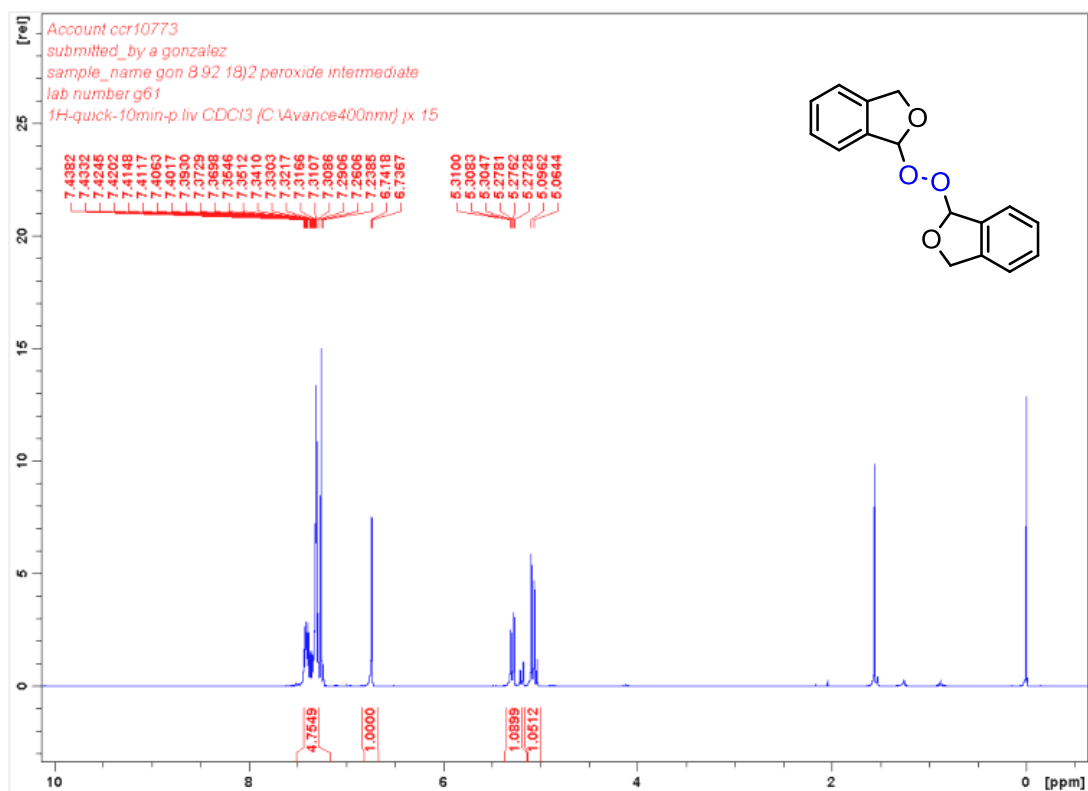


**3-(1,3-dioxan-2-yl)propyl formate**

## 4.1.9. Isotope labelling experiments: NMR of the peroxide species

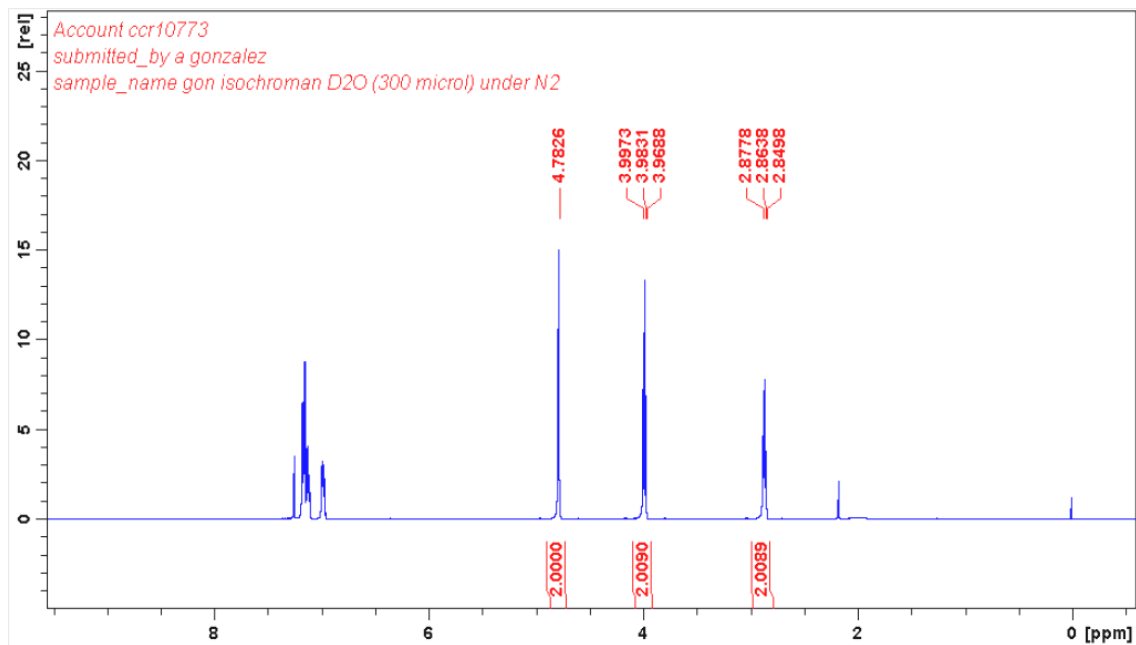
### 4.1.9.1. 1,1-Peroxydiisochroman under $^{16}\text{O}_2$ atmosphere



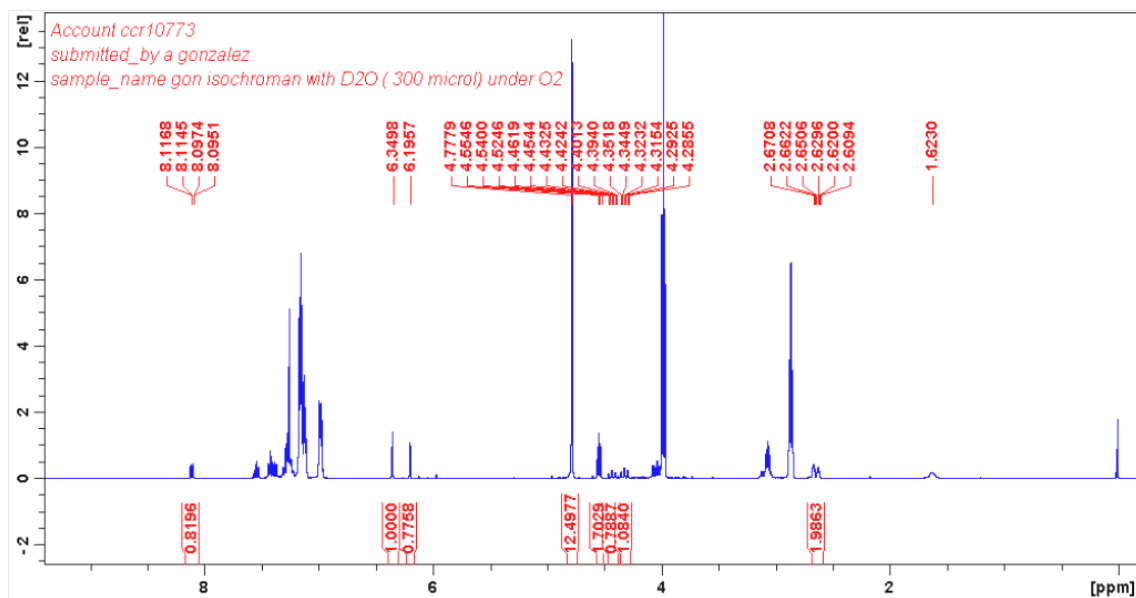
4.1.9.2. 1,1-peroxydiisochroman under  $^{18}\text{O}_2$  atmosphere

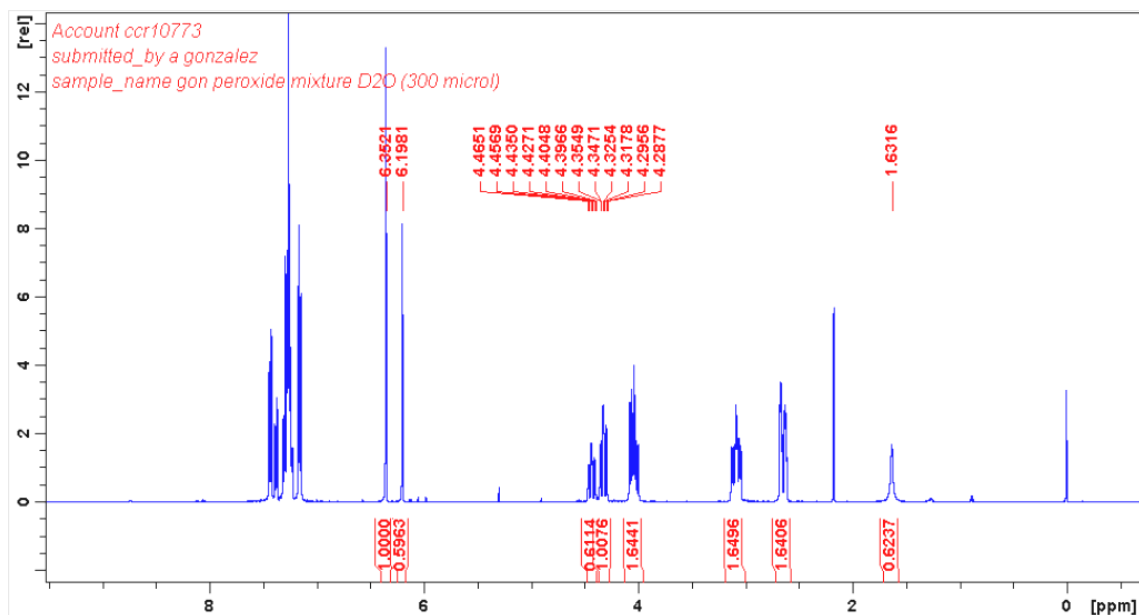
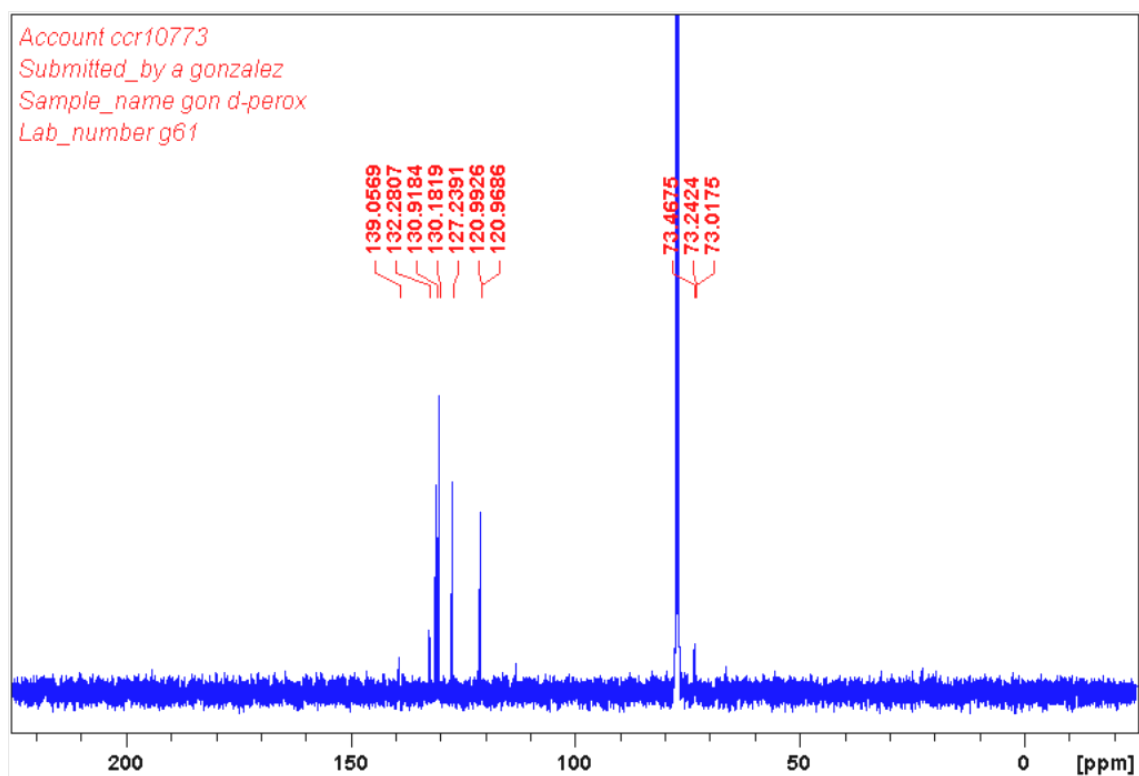
#### 4.1.10. H/D exchange experiments: crude NMR spectra

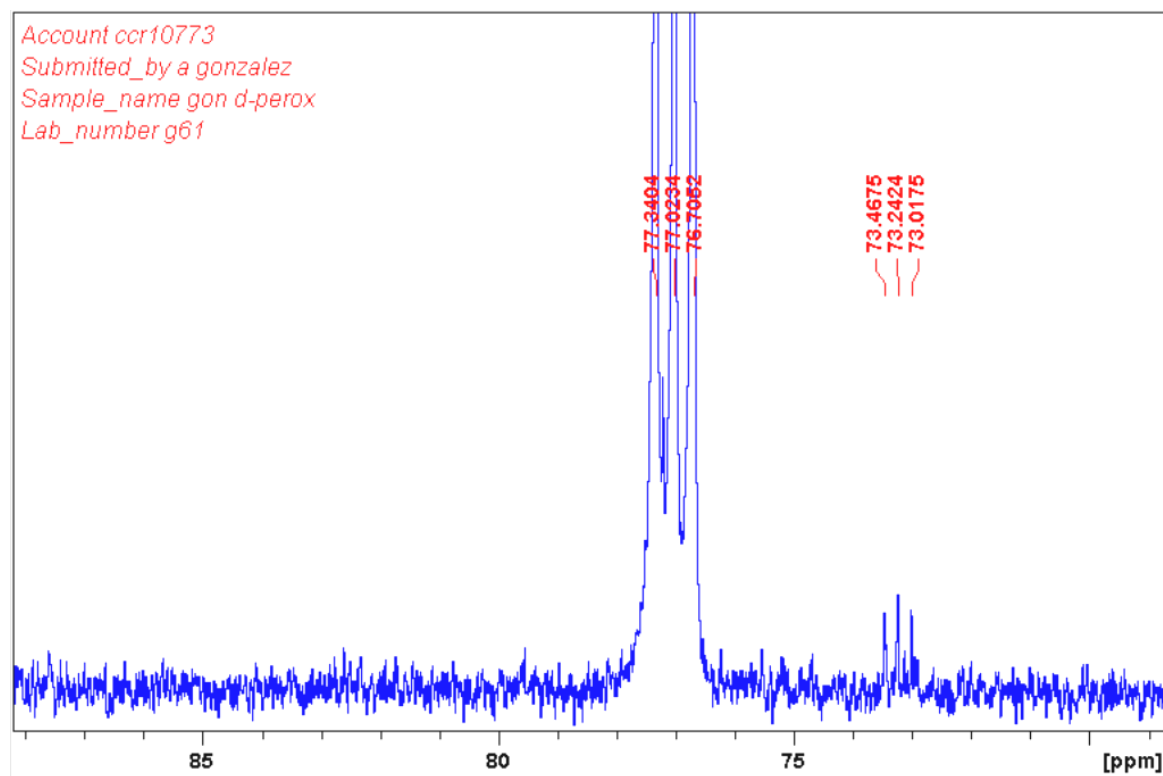
##### Reaction under N<sub>2</sub> atmosphere



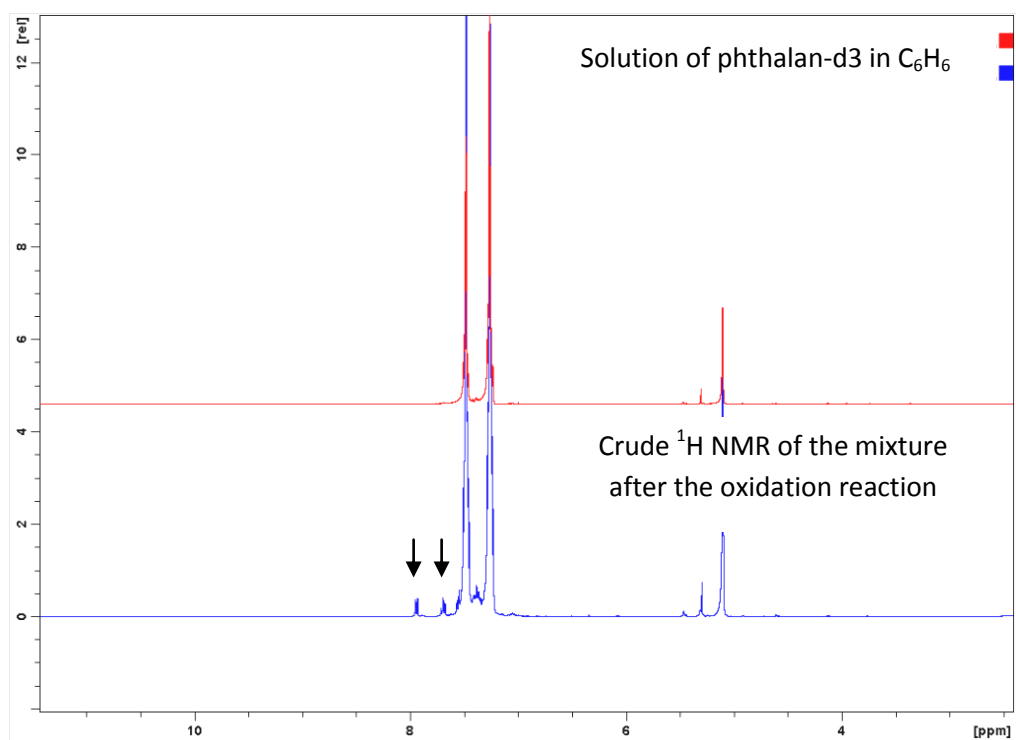
##### Reaction under O<sub>2</sub> atmosphere



**Mixture of peroxide and oxidation dimer****4.1.11. Experiments with  $^2\text{H}$ -labelled peroxides****4.1.11.1.  $^{13}\text{C}$  NMR characterisation of 1,1'-Peroxybis(1,3-dihydroisobenzofuran)-d6:**



**4.1.11.2. Crude  $^1\text{H}$  NMR of the reaction with phthalan-d3.** Oxidation of phthalan-d3 in the Young's tube afforded phthalide-d2 in small amounts. Resonances corresponding to the aromatic protons of the phthalide-d2 are highlighted with a black arrow.





## 4.1.13. Comparison of mass vs gas pressure in samples 10, 9 and 8

sample10.csv		sample9.csv		sample8.csv	
Start	1	Start	1	Start	1
End	50	End	10	End	10
Dwell	20	Dwell	20	Dwell	20
MultVolt	0	MultVolt	0	MultVolt	0
MultGain	1	MultGain	1	MultGain	1
MultProt	1	MultProt	1	MultProt	1
1	2.08E-09	1	6.20E-09	1	6.11E-09
1.1	2.46E-09	1.1	5.73E-09	1.1	5.85E-09
1.2	2.44E-09	1.2	4.71E-09	1.2	4.77E-09
1.3	2.40E-09	1.3	3.64E-09	1.3	3.75E-09
1.4	2.95E-09	1.4	4.31E-09	1.4	4.48E-09
1.6	4.48E-09	1.5	5.47E-09	1.5	5.62E-09
1.7	5.38E-09	<b>1.6</b>	<b>6.61E-09</b>	<b>1.6</b>	<b>6.52E-09</b>
1.8	5.94E-09	<b>1.7</b>	<b>7.68E-09</b>	<b>1.7</b>	<b>7.68E-09</b>
1.9	5.65E-09	<b>1.8</b>	<b>8.73E-09</b>	<b>1.8</b>	<b>8.79E-09</b>
2.1	4.80E-09	<b>1.9</b>	<b>8.44E-09</b>	<b>1.9</b>	<b>8.44E-09</b>
2.2	3.73E-09	<b>2</b>	<b>7.97E-09</b>	<b>2</b>	<b>7.97E-09</b>
2.3	4.09E-10	<b>2.1</b>	<b>7.10E-09</b>	<b>2.1</b>	<b>7.13E-09</b>
2.4	5.41E-11	<b>2.2</b>	<b>5.33E-09</b>	<b>2.2</b>	<b>5.36E-09</b>
2.5	4.55E-11	2.3	6.98E-10	2.3	5.20E-10
2.7	1.32E-10	2.4	6.82E-11	2.4	1.08E-12
2.8	4.55E-11	2.5	1.61E-11	2.5	4.43E-11
2.9	6.28E-11	2.6	1.61E-11	2.6	8.78E-11
3	4.55E-11	2.7	6.82E-11	2.7	1.31E-10
3.2	3.68E-11	2.8	1.03E-10	2.8	1.48E-10
3.3	2.44E-10	2.9	5.96E-11	2.9	7.87E-11
3.4	1.51E-09	3	1.55E-10	3	7.87E-11
3.5	4.39E-09	3.1	1.11E-10	3.1	1.05E-10
3.6	7.97E-09	3.2	4.21E-11	3.2	1.48E-10
<b>3.8</b>	<b>1.30E-08</b>	3.3	2.16E-10	3.3	2.51E-10
<b>3.9</b>	<b>1.20E-08</b>	3.4	1.19E-09	3.4	1.18E-09
<b>4</b>	<b>1.21E-08</b>	3.5	3.13E-09	3.5	3.13E-09
<b>4.1</b>	<b>1.11E-08</b>	3.6	5.70E-09	3.6	5.62E-09
4.3	2.52E-09	<b>3.7</b>	<b>7.63E-09</b>	<b>3.7</b>	<b>7.45E-09</b>
4.4	8.87E-11	<b>3.8</b>	<b>9.02E-09</b>	<b>3.8</b>	<b>8.96E-09</b>
4.5	9.73E-11	<b>3.9</b>	<b>8.50E-09</b>	<b>3.9</b>	<b>8.32E-09</b>
4.6	4.55E-11	<b>4</b>	<b>8.09E-09</b>	<b>4</b>	<b>8.15E-09</b>
4.7	1.08E-11	<b>4.1</b>	<b>7.51E-09</b>	<b>4.1</b>	<b>7.51E-09</b>
4.9	1.00E-14	<b>4.2</b>	<b>5.91E-09</b>	<b>4.2</b>	<b>5.88E-09</b>
5	1.00E-14	<b>4.3</b>	<b>1.71E-09</b>	<b>4.3</b>	<b>1.59E-09</b>
5.1	3.68E-11	4.4	1.00E-14	4.4	1.00E-14
5.2	1.00E-14	4.5	5.96E-11	4.5	3.57E-11
5.4	1.00E-14	4.6	1.00E-14	4.6	1.00E-14

5.5	2.16E-12	4.7	4.21E-11	4.7	9.64E-11
5.6	2.16E-12	4.8	1.00E-14	4.8	1.00E-14
5.7	1.00E-14	4.9	1.00E-14	4.9	1.00E-14
5.9	1.00E-14	5	1.00E-14	5	4.43E-11
6	1.00E-14	5.1	1.61E-11	5.1	1.00E-14
6.1	1.00E-14	5.2	2.49E-11	5.2	9.72E-12
6.2	1.00E-14	5.3	1.61E-11	5.3	9.72E-12
6.3	1.00E-14	5.4	1.61E-11	5.4	5.30E-11
6.5	3.68E-11	5.5	1.00E-14	5.5	1.08E-12
6.6	4.55E-11	5.6	5.09E-11	5.6	2.71E-11
6.7	4.55E-11	5.7	2.49E-11	5.7	1.00E-14
6.8	2.81E-11	5.8	7.56E-12	5.8	1.84E-11
7	7.14E-11	5.9	1.00E-14	5.9	1.08E-12
		6	4.21E-11	6	1.00E-14
		6.1	2.49E-11	6.1	3.57E-11
		6.2	1.61E-11	6.2	1.08E-12
		6.3	1.00E-14	6.3	1.00E-14
		6.4	2.49E-11	6.4	1.08E-12
		6.5	1.00E-14	6.5	1.08E-12
		6.6	1.00E-14	6.6	5.30E-11
		6.7	2.49E-11	6.7	8.78E-11
		6.8	2.49E-11	6.8	6.14E-11
		6.9	1.00E-14	6.9	9.72E-12
		7	1.00E-14	7	8.78E-11

#### 4.1.14. Comparison of mass vs gas pressure in samples 7, 6 and 4.

	sample7.csv		sample6.csv		sample4.csv
Start	1	Start	1	Start	1
End	50	End	10	End	10
Dwell	20	Dwell	20	Dwell	20
MultVolt	0	MultVolt	0	MultVolt	0
MultGain	1	MultGain	1	MultGain	1
MultProt	1	MultProt	1	MultProt	1
1	6.26E-09	1	8.15E-09	1	1.03E-08
1.1	5.53E-09	1.1	8.03E-09	1.1	1.69E-05
1.2	4.57E-09	1.2	6.52E-09	1.2	6.81E-09
1.3	3.75E-09	1.3	3.68E-09	1.3	3.20E-09
1.4	4.54E-09	1.4	4.16E-09	1.4	3.75E-09
1.6	6.78E-09	1.5	5.21E-09	1.5	5.68E-09
<b>1.7</b>	<b>7.97E-09</b>	<b>1.6</b>	<b>6.58E-09</b>	1.6	7.92E-09
<b>1.8</b>	<b>8.91E-09</b>	<b>1.7</b>	<b>8.27E-09</b>	1.7	1.01E-08
<b>1.9</b>	<b>8.56E-09</b>	<b>1.8</b>	<b>9.55E-09</b>	1.8	1.29E-08
<b>2.1</b>	<b>6.96E-09</b>	<b>1.9</b>	<b>9.26E-09</b>	<b>1.9</b>	<b>1.44E-08</b>

<b>2.2</b>	<b>5.18E-09</b>	<b>2</b>	<b>9.02E-09</b>	<b>2</b>	<b>1.36E-08</b>
2.3	4.95E-10	<b>2.1</b>	<b>8.09E-09</b>	<b>2.1</b>	<b>1.16E-08</b>
2.4	3.24E-12	<b>2.2</b>	<b>6.20E-09</b>	2.2	7.92E-09
2.5	6.37E-11	<b>2.3</b>	<b>1.21E-09</b>	2.3	1.43E-09
2.7	9.82E-11	2.4	1.00E-14	2.4	1.96E-10
2.8	1.16E-10	2.5	4.43E-11	2.5	6.91E-10
2.9	7.23E-11	2.6	8.78E-11	2.6	1.57E-09
3	1.85E-10	2.7	1.84E-11	2.7	2.24E-09
3.2	2.91E-11	2.8	8.78E-11	2.8	2.87E-09
3.3	1.33E-10	2.9	3.57E-11	<b>2.9</b>	<b>3.04E-09</b>
3.4	8.84E-10	3	2.71E-11	<b>3</b>	<b>2.79E-09</b>
3.5	2.60E-09	3.1	9.64E-11	<b>3.1</b>	<b>2.39E-09</b>
<b>3.6</b>	<b>4.74E-09</b>	3.2	6.14E-11	3.2	1.88E-09
<b>3.8</b>	<b>7.07E-09</b>	3.3	8.78E-11	3.3	4.04E-10
<b>3.9</b>	<b>6.64E-09</b>	3.4	4.43E-11	3.4	1.11E-10
<b>4</b>	<b>6.58E-09</b>	3.5	9.72E-12	3.5	1.45E-10
<b>4.1</b>	<b>5.68E-09</b>	3.6	1.84E-11	3.6	4.66E-10
<b>4.3</b>	<b>1.10E-09</b>	3.7	4.43E-11	3.7	7.42E-10
4.4	1.07E-10	3.8	9.72E-12	<b>3.8</b>	<b>9.31E-10</b>
4.5	1.19E-11	3.9	1.00E-14	<b>3.9</b>	<b>1.06E-09</b>
4.6	1.00E-14	4	9.72E-12	<b>4</b>	<b>9.53E-10</b>
4.7	9.82E-11	4.1	1.00E-14	<b>4.1</b>	<b>8.29E-10</b>
4.9	3.77E-11	4.2	1.00E-14	4.2	7.17E-10
5	7.23E-11	4.3	1.00E-14	4.3	2.23E-10
5.1	8.96E-11	4.4	1.00E-14	4.4	1.00E-14
5.2	1.00E-14	4.5	1.84E-11	4.5	1.00E-14
5.4	1.00E-14	4.6	1.84E-11	4.6	1.00E-14
5.5	1.00E-14	4.7	1.00E-14	4.7	1.00E-14
5.6	1.00E-14	4.8	1.00E-14	4.8	1.00E-14
5.7	2.91E-11	4.9	1.08E-12	4.9	1.00E-14
5.9	2.06E-11	5	9.72E-12	5	1.00E-14
6	1.00E-14	5.1	4.43E-11	5.1	1.00E-14
6.1	1.00E-14	5.2	1.00E-14	5.2	1.00E-14
6.2	1.00E-14	5.3	2.71E-11	5.3	1.00E-14
6.3	1.00E-14	5.4	1.00E-14	5.4	1.00E-14
6.5	2.91E-11	5.5	5.30E-11	5.5	1.51E-11
6.6	1.19E-11	5.6	1.08E-12	5.6	1.00E-14
6.7	3.77E-11	5.7	9.72E-12	5.7	1.00E-14
6.8	8.96E-11	5.8	1.00E-14	5.8	6.48E-12
7	1.25E-10	5.9	1.08E-12	5.9	1.00E-14
		6	1.08E-12	6	1.51E-11
		6.1	1.00E-14	6.1	1.00E-14
		6.2	1.00E-14	6.2	1.00E-14
		6.3	1.00E-14	6.3	1.00E-14
		6.4	1.00E-14	6.4	6.48E-12
		6.5	1.00E-14	6.5	1.00E-14

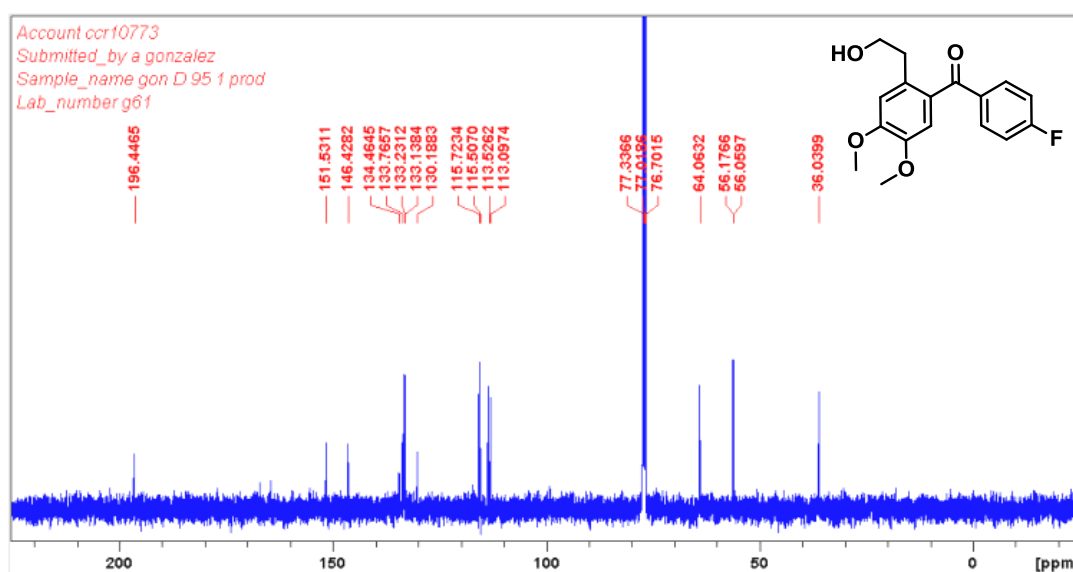
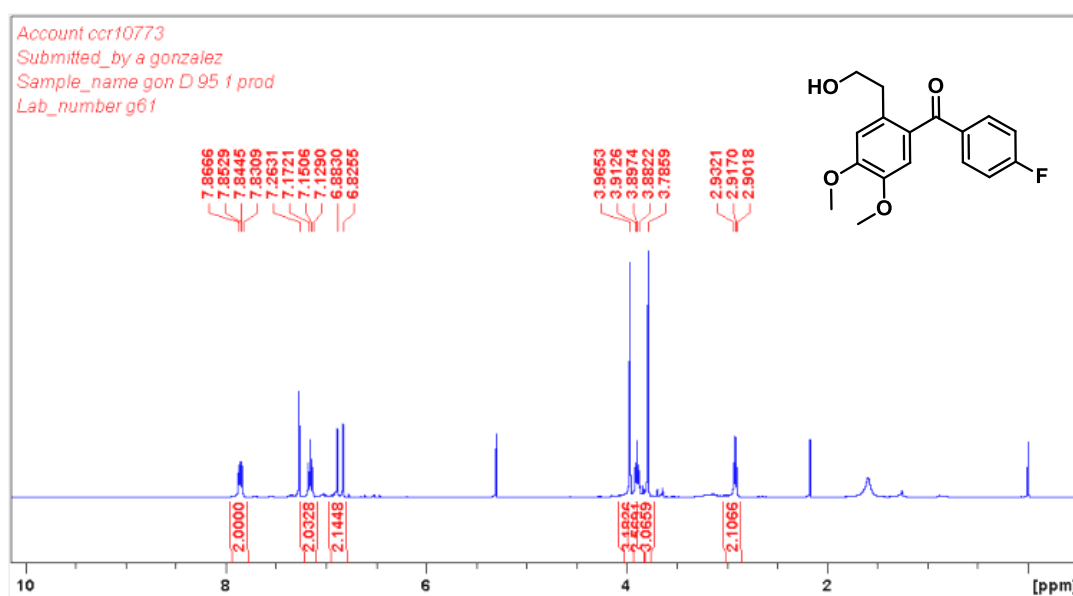
6.6	5.30E-11	6.6	5.82E-11
6.7	2.71E-11	6.7	1.79E-10
6.8	5.30E-11	6.8	2.75E-10
6.9	6.14E-11	6.9	2.91E-10
7	1.84E-11	7	2.49E-10

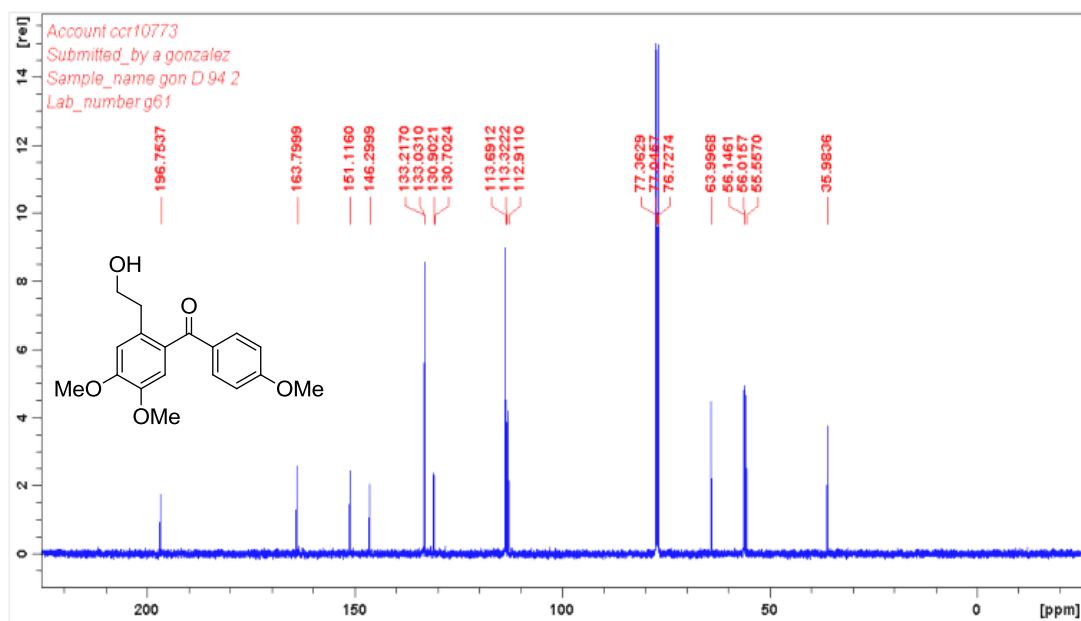
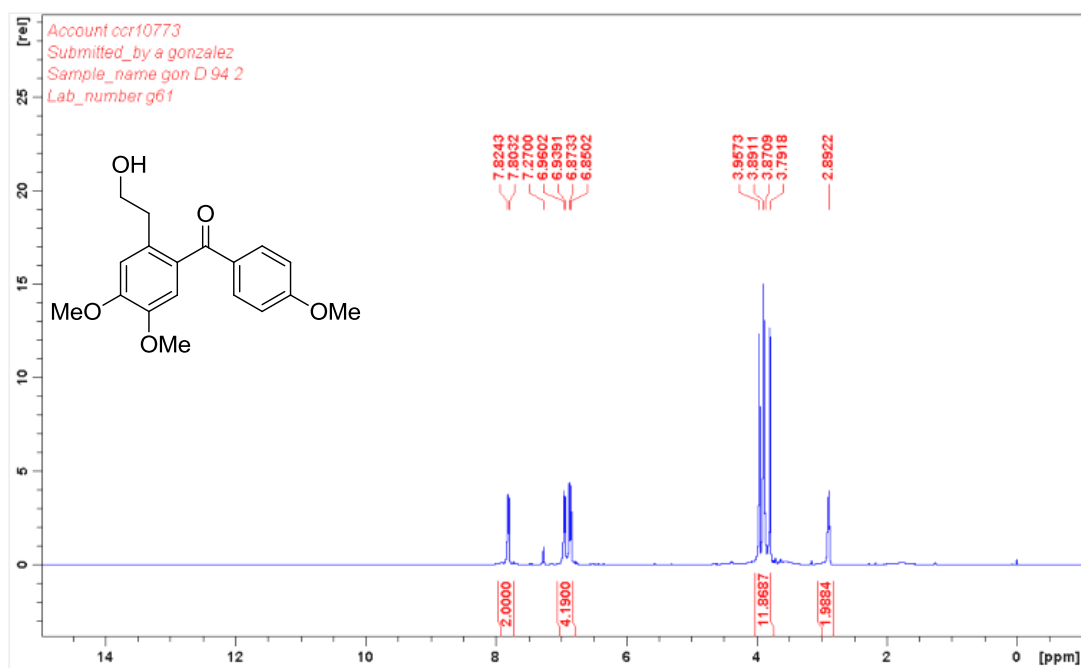
## 5. Chapter 5: additional data

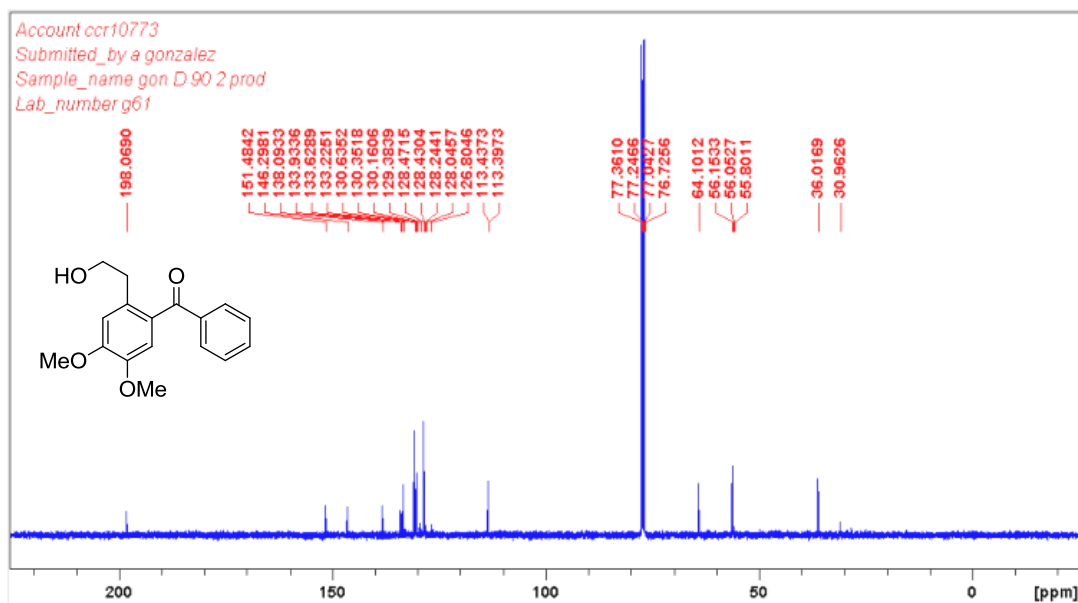
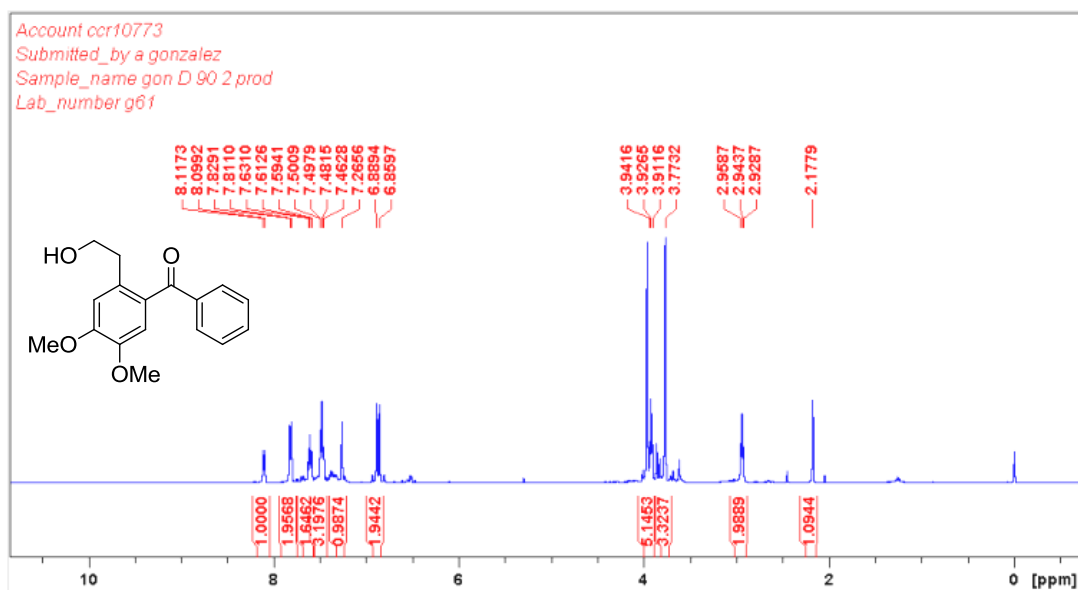
### 5.1. NMR of products

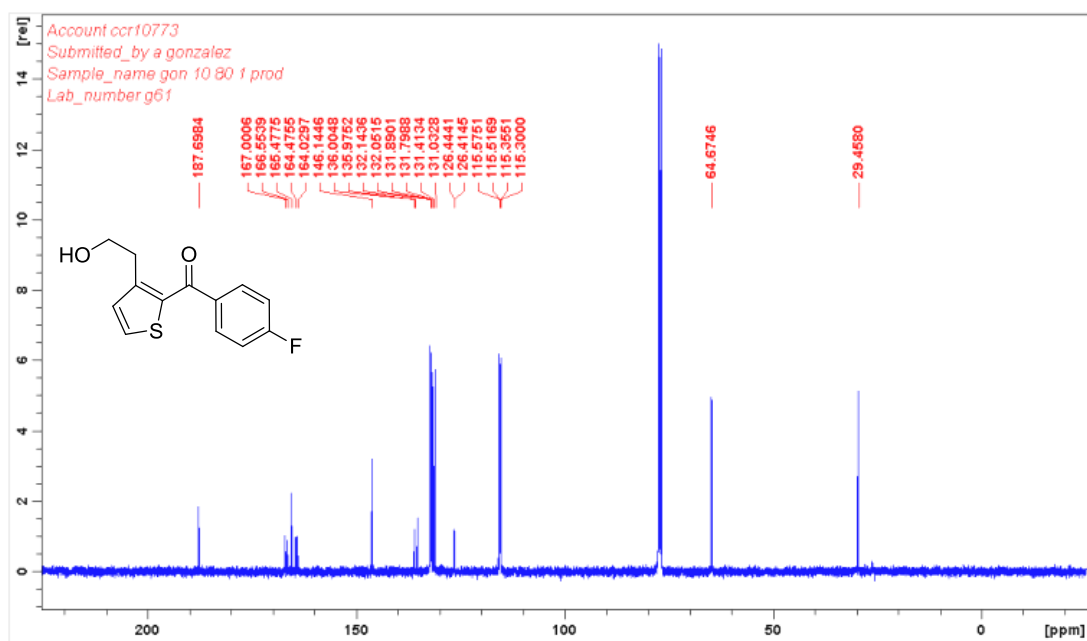
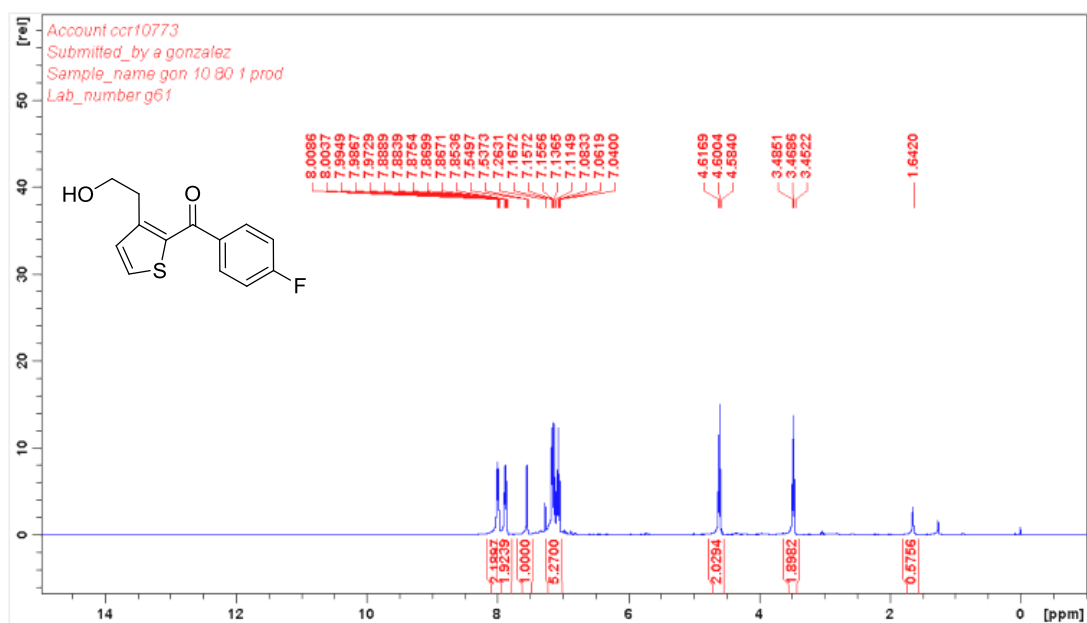
#### 5.1.1. 2-(Hydroxyethyl)benzophenone products from the Csp<sup>3</sup>-O cleavage of 1-arylisochromans

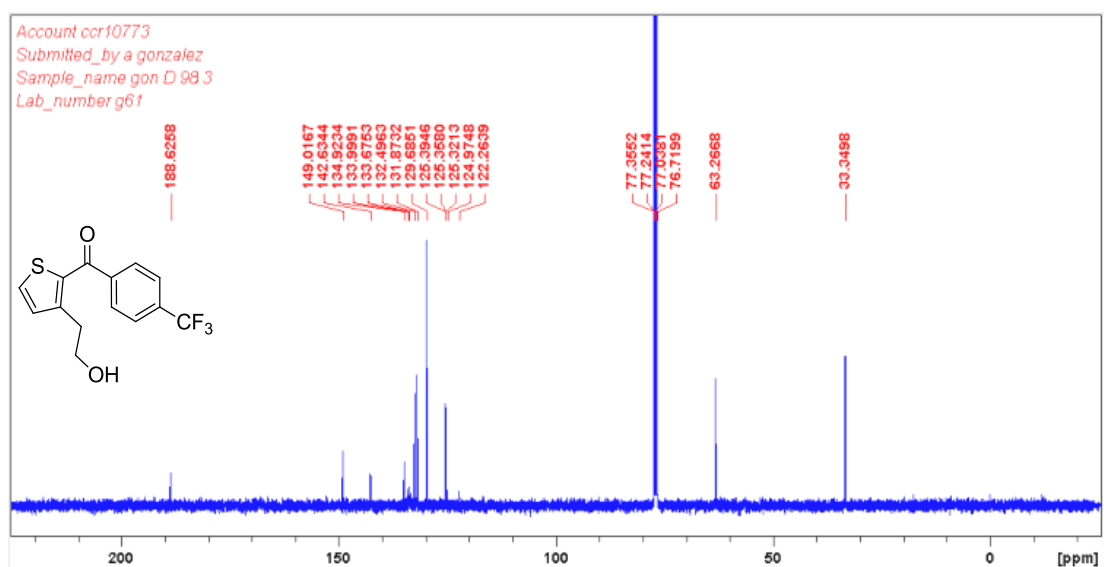
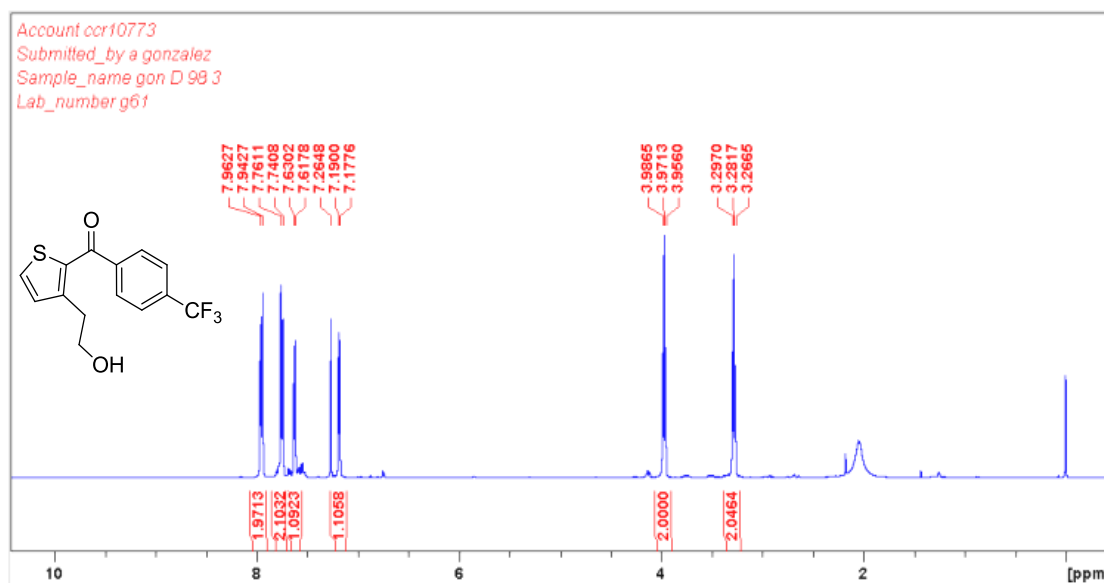
##### (4-Fluorophenyl)(2-(2-hydroxyethyl)-4,5-dimethoxyphenyl)methanone



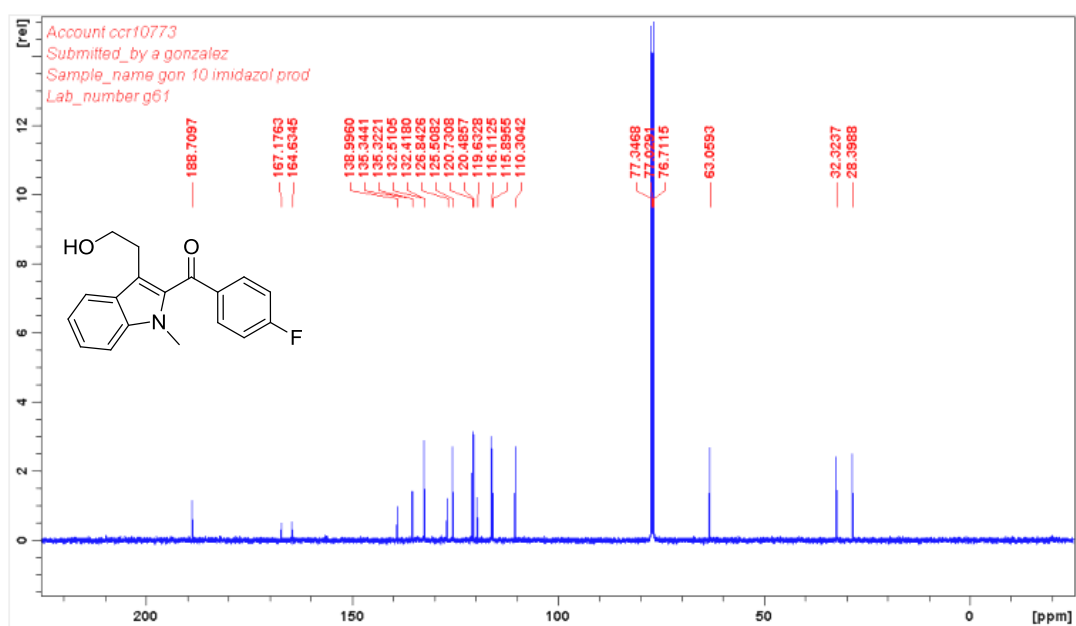
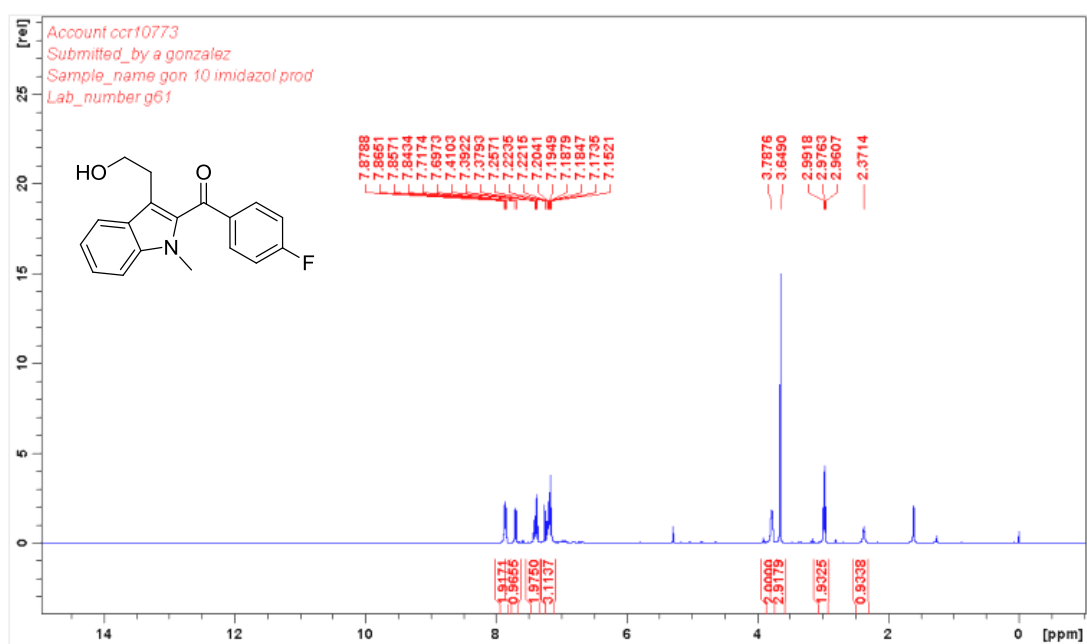
**(2-(2-Hydroxyethyl)-4,5-dimethoxyphenyl)(4-methoxyphenyl)methanone**

**(2-(2-Hydroxyethyl)-4,5-dimethoxyphenyl)(phenyl)methanone**

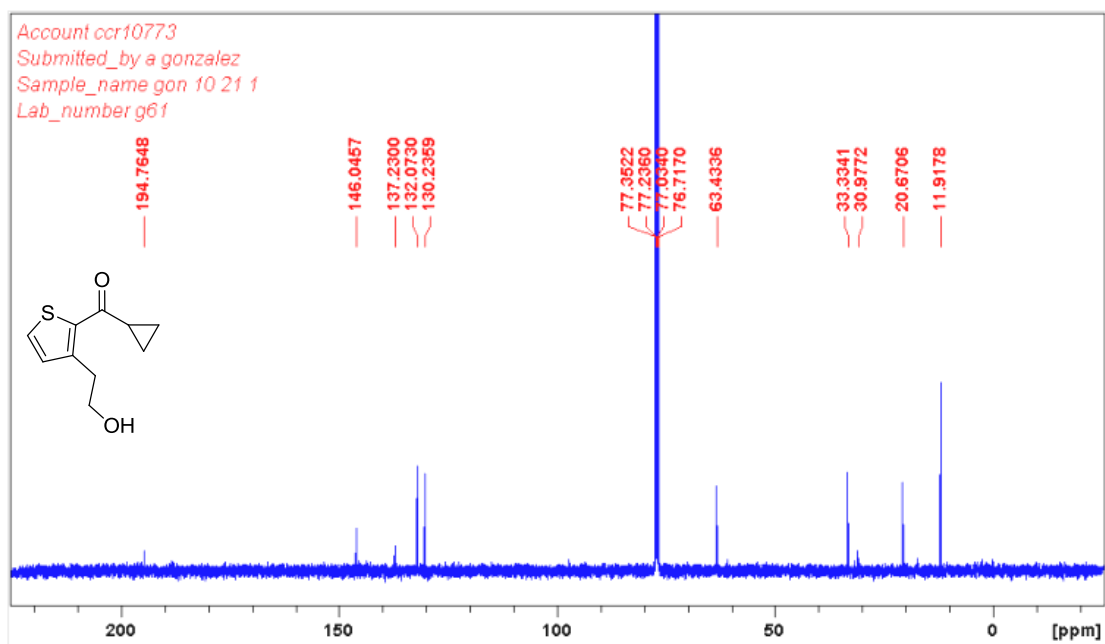
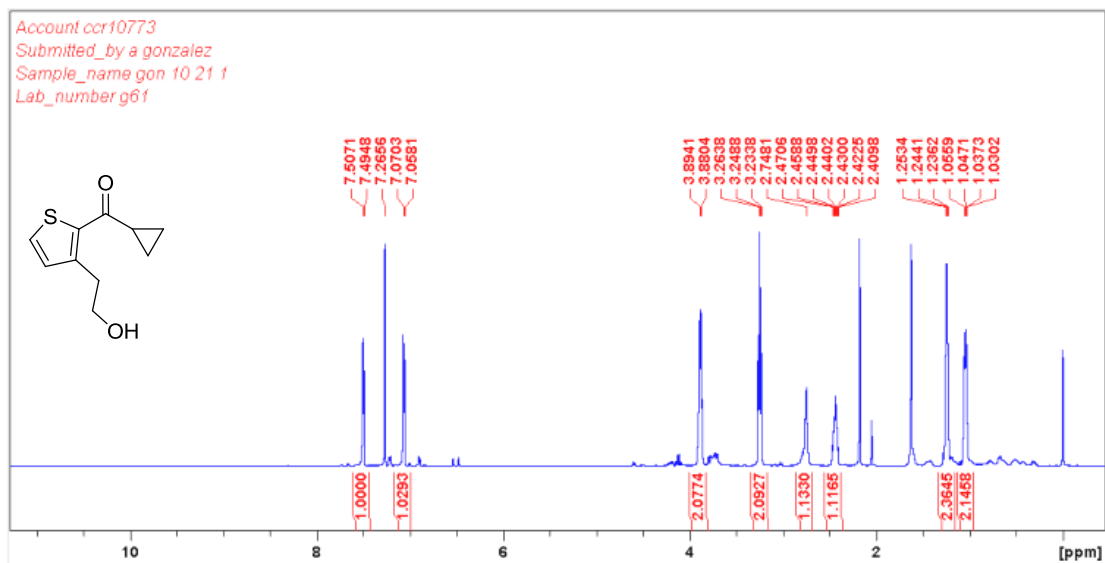
**(4-Fluorophenyl)(3-(2-hydroxyethyl)thiophen-2-yl)methanone**

**(3-(2-Hydroxyethyl)thiophen-2-yl)(4-(trifluoromethyl)phenyl)methanone**



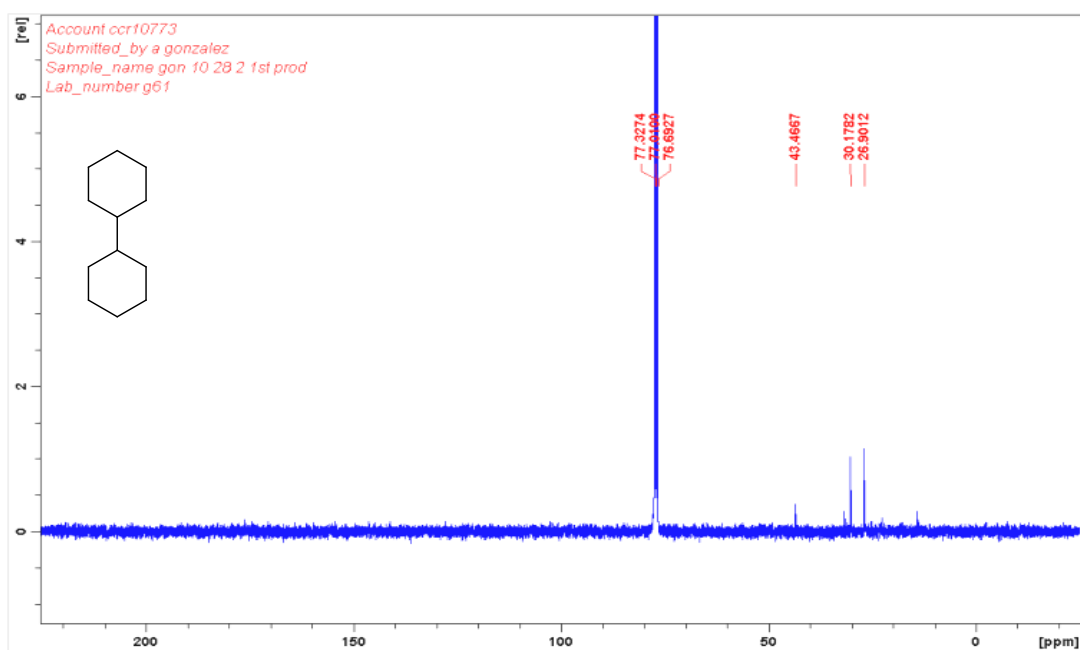
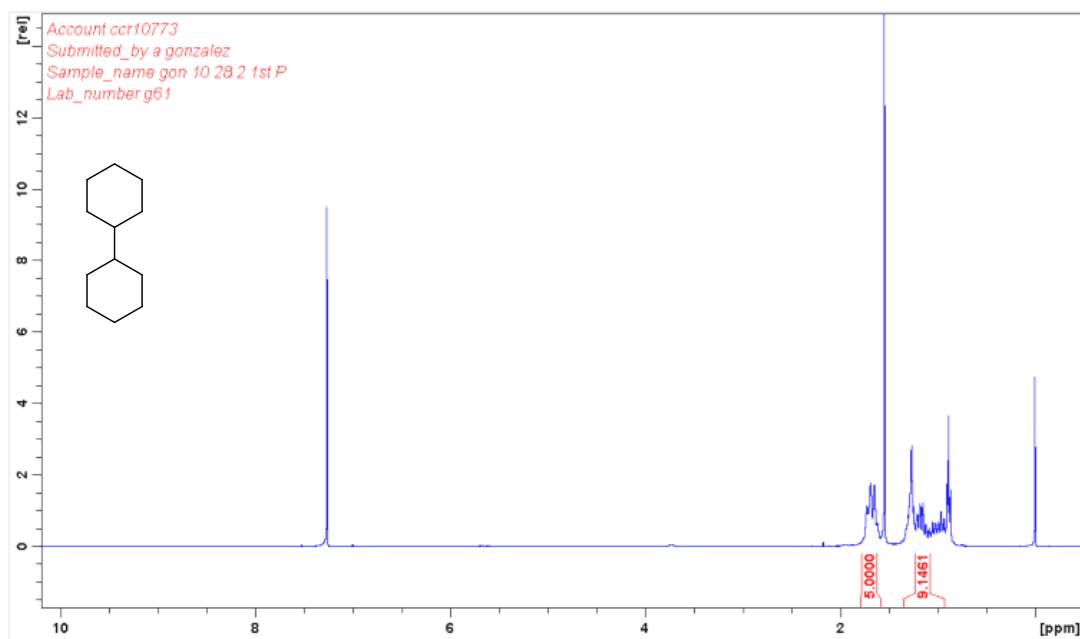
**(4-Fluorophenyl)(3-(2-hydroxyethyl)-1-methyl-1H-indol-2-yl)methanone**

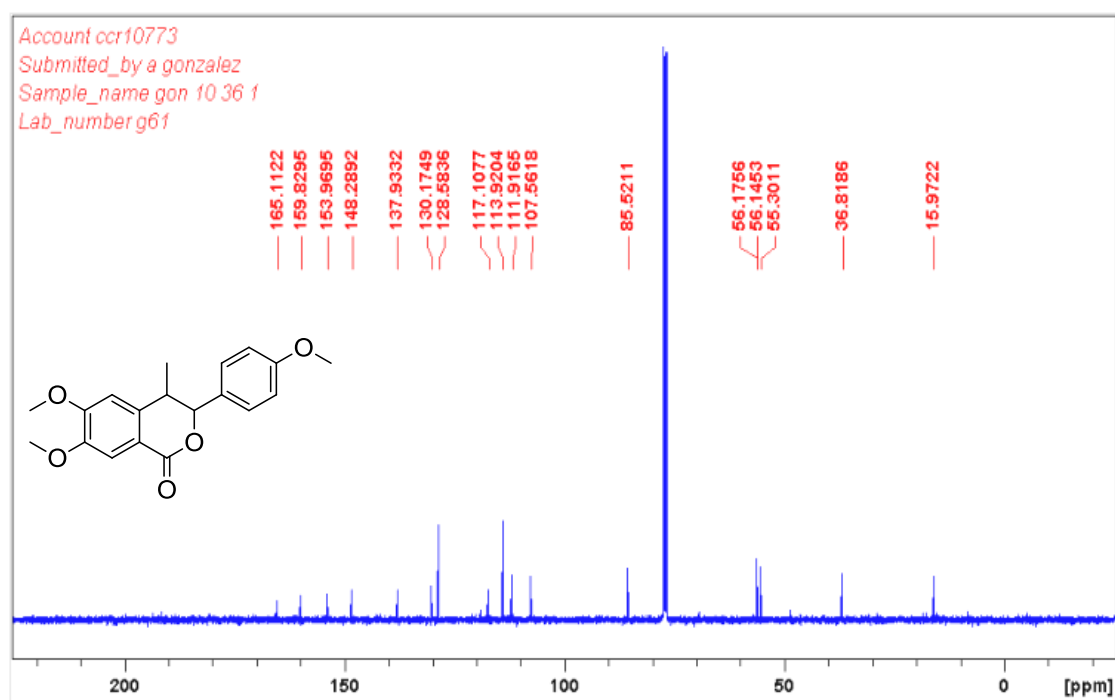
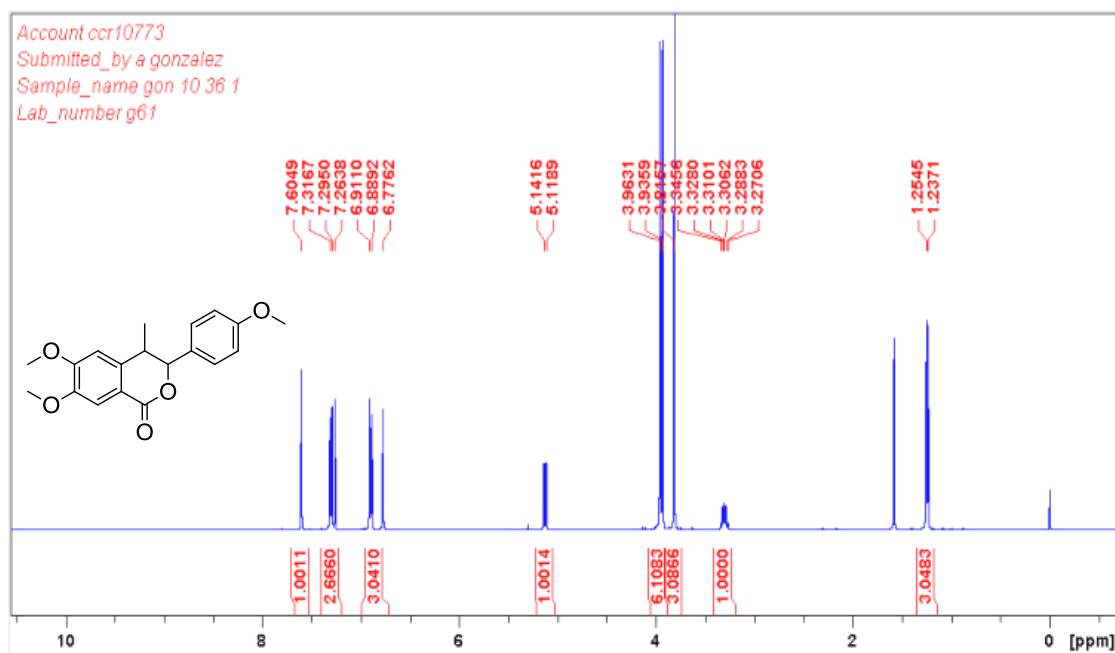
## Cyclopropyl(3-(2-hydroxyethyl)thiophen-2-yl)methanone

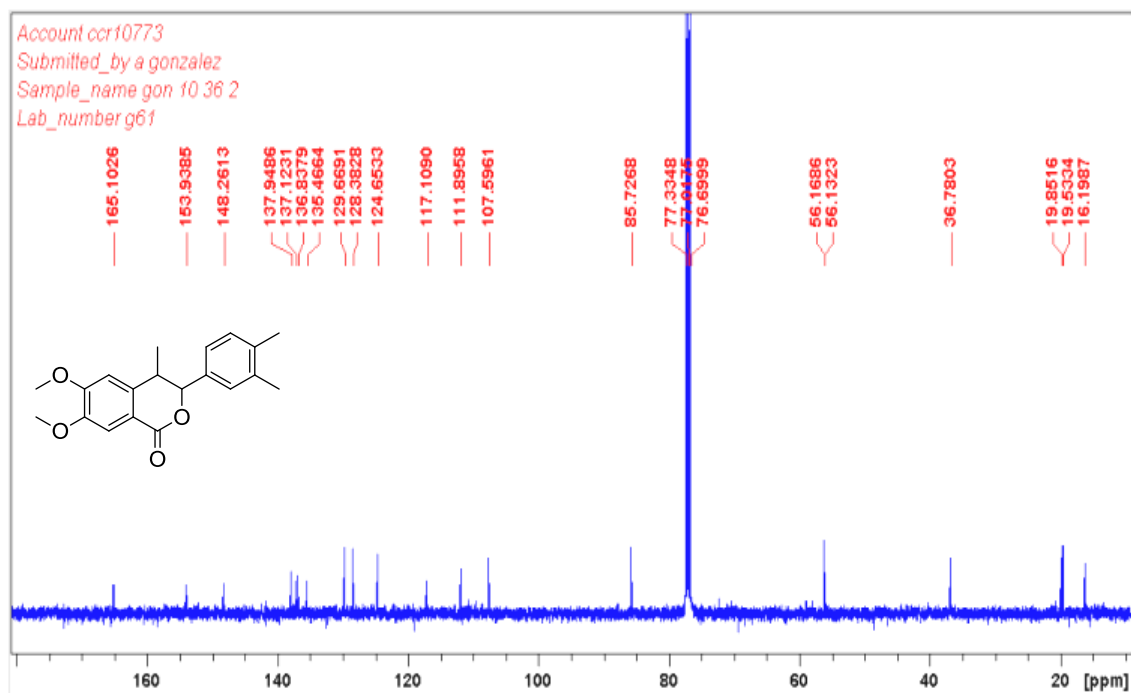
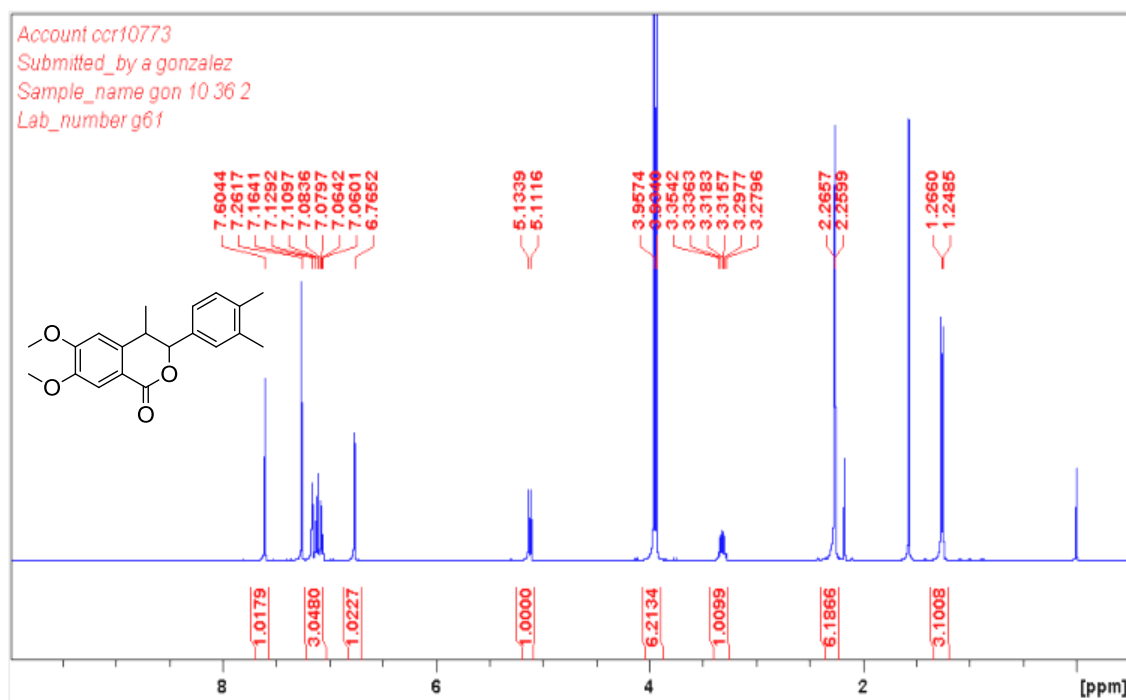


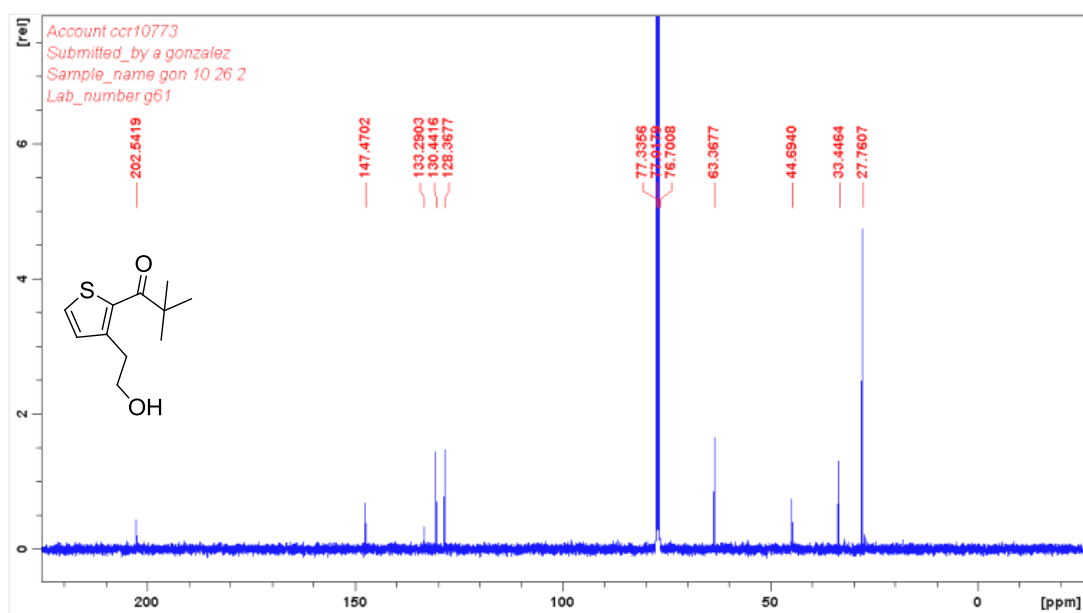
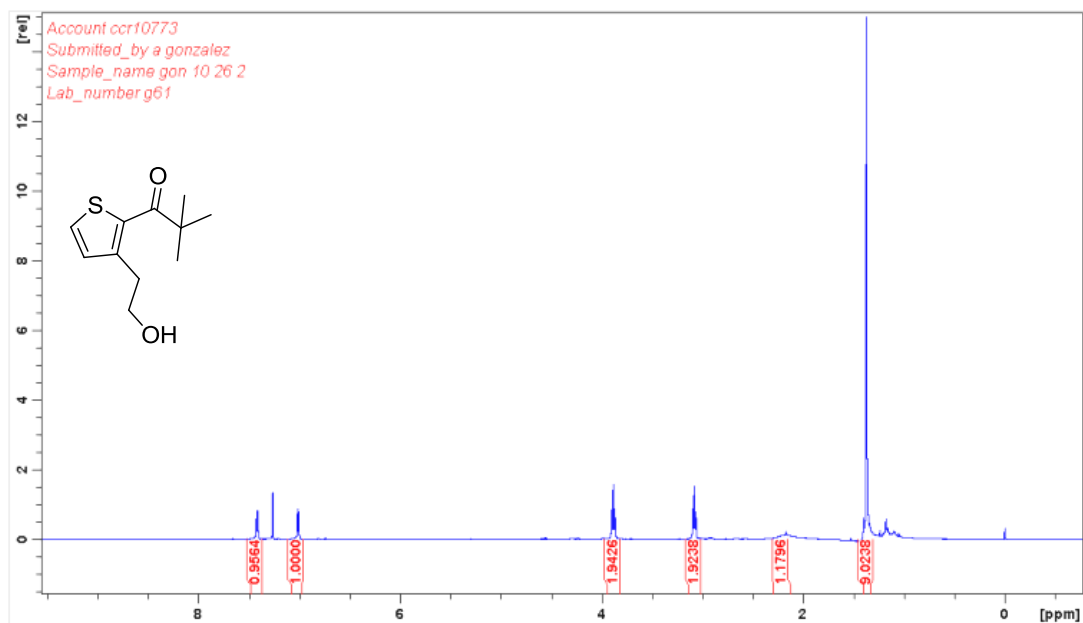
## 5.1.2. Products from the selective Csp<sup>3</sup>-Csp<sup>3</sup> cleavage of 1-alkyl isochromans

### 1,1'-Bi(cyclohexane)



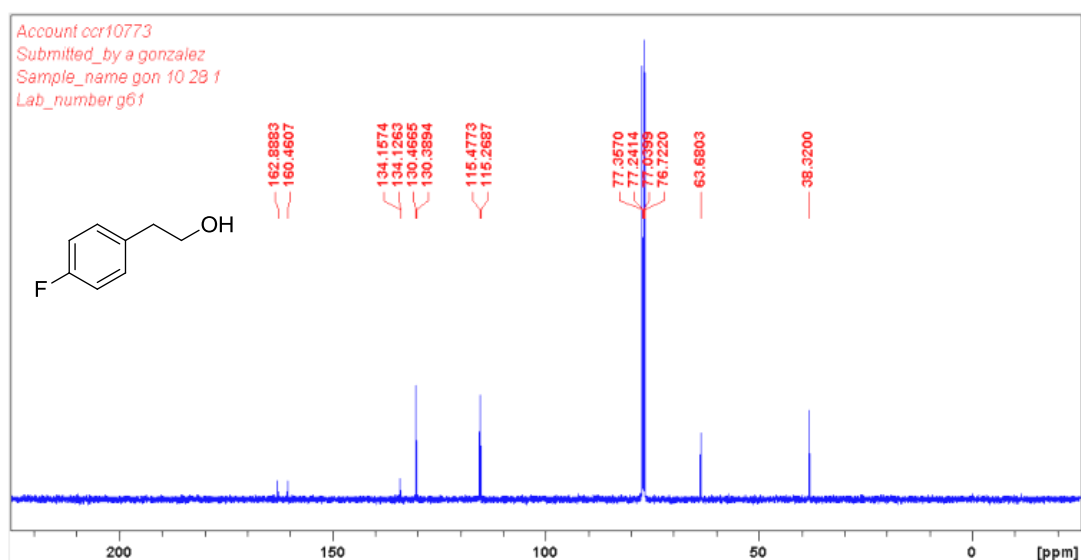
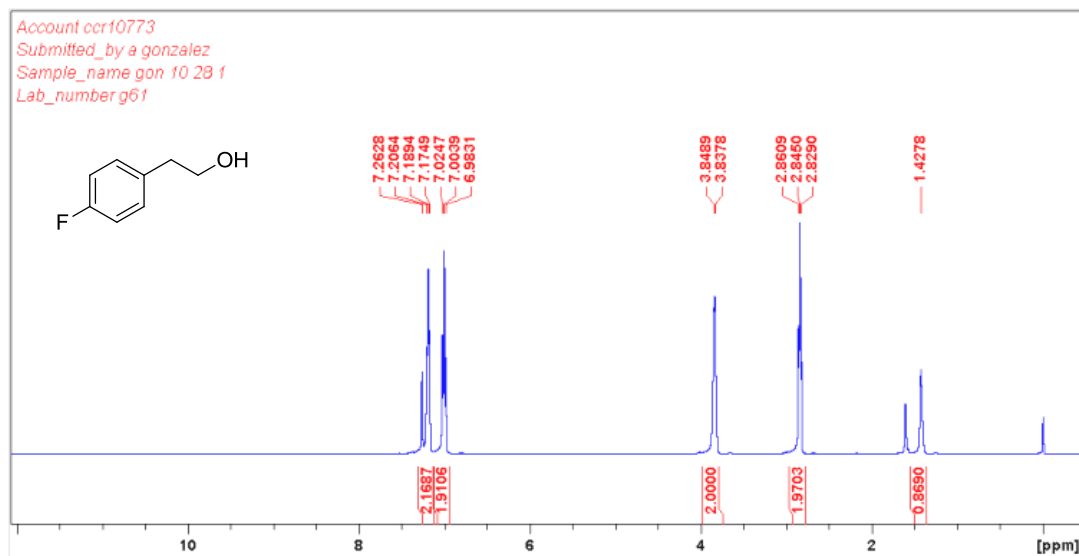
**6,7-Dimethoxy-3-(4-methoxyphenyl)-4-methylisochroman-1-one**

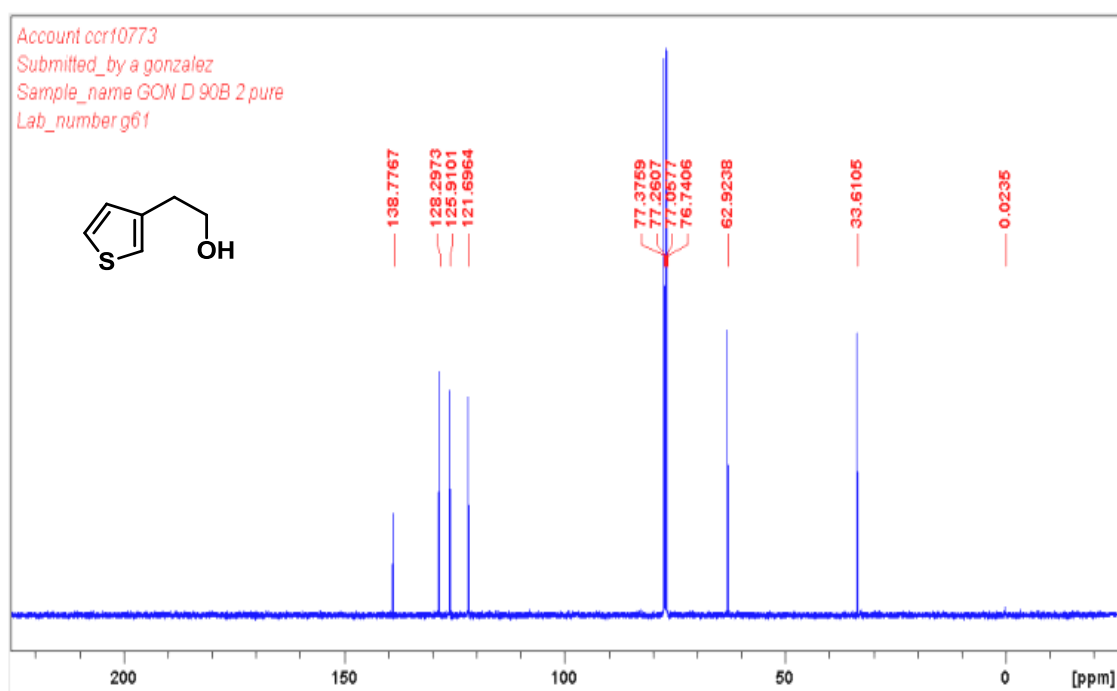
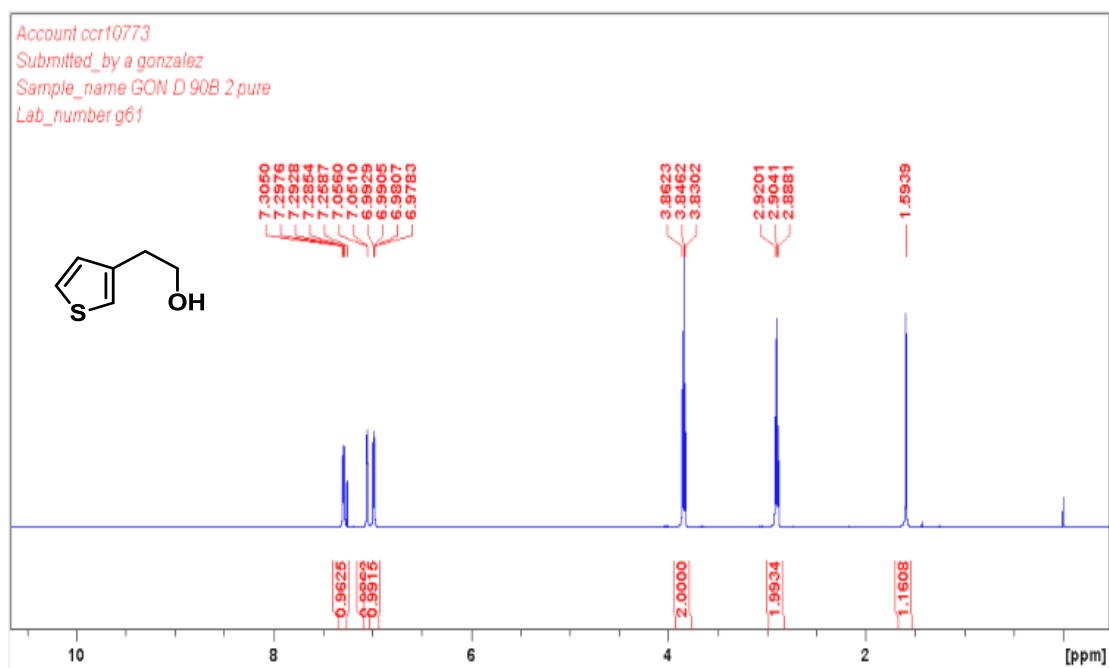
**3-(3,4-Dimethylphenyl)-6,7-dimethoxy-4-methylisochroman-1-one**

**5.1.3. Products from the cleavage of 1-alkyl 5,7-dihydro-4H-thieno[2,3c]pyranes****1-(3-(2-Hydroethyl)thiophen-2-yl)-2,2-dimethylpropan-1-one**

5.1.4. Products from the Csp<sup>2</sup>-Csp<sup>3</sup> and Csp<sup>3</sup>-O cleavage of 1-methylisochromans

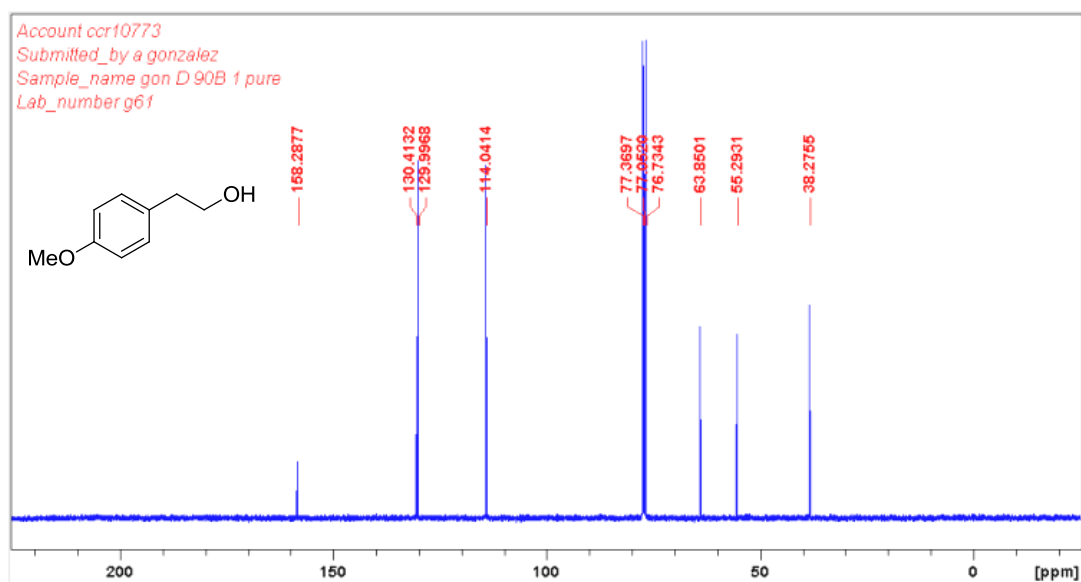
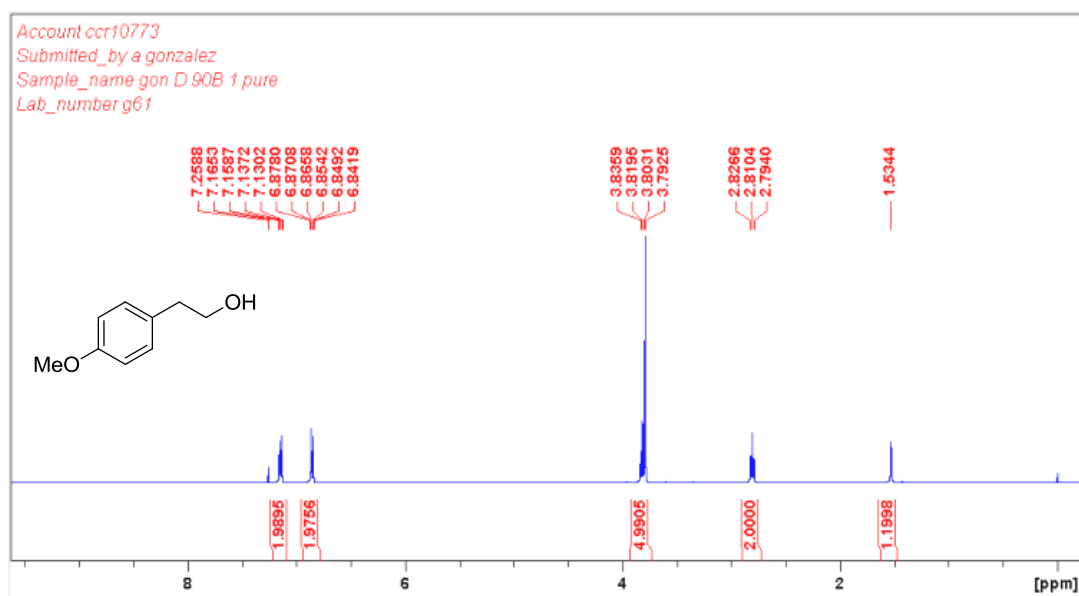
## 2-(4-Fluorophenyl)ethanol

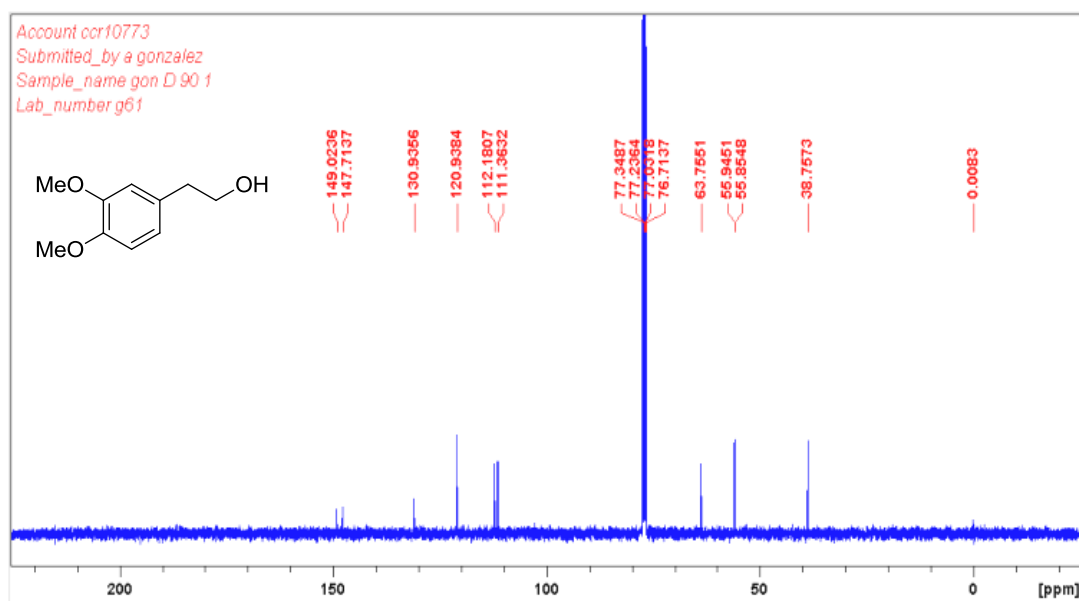
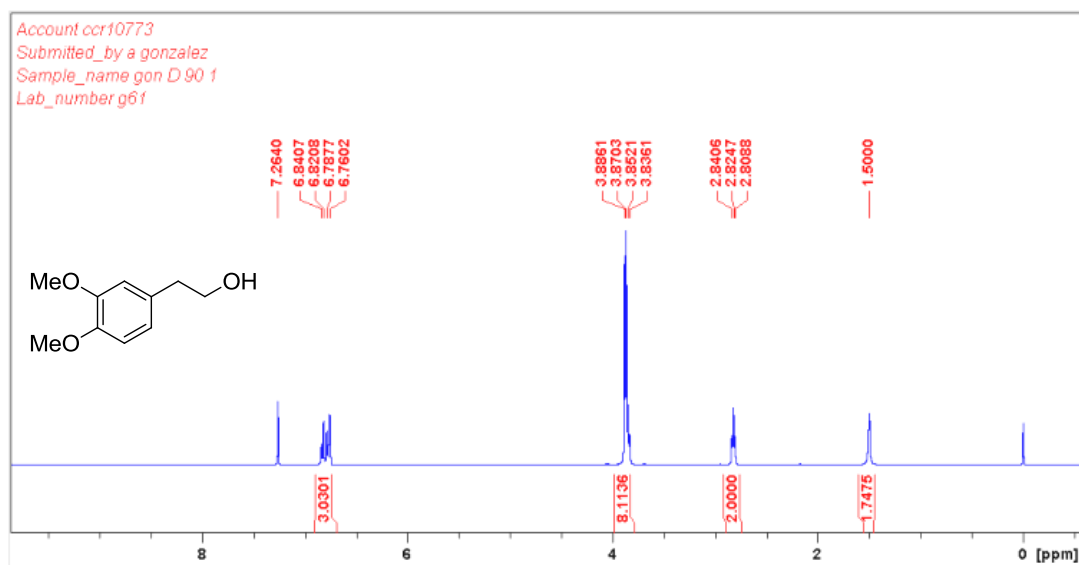


**2-(Thiophen-3-yl)ethanol**



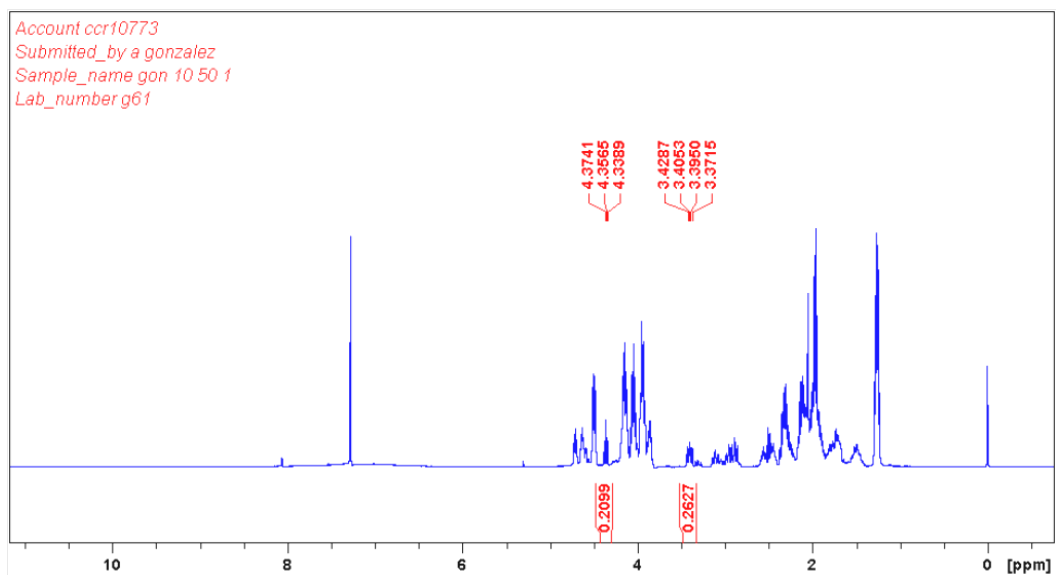
## 2-(4-Methoxyphenyl)ethanol



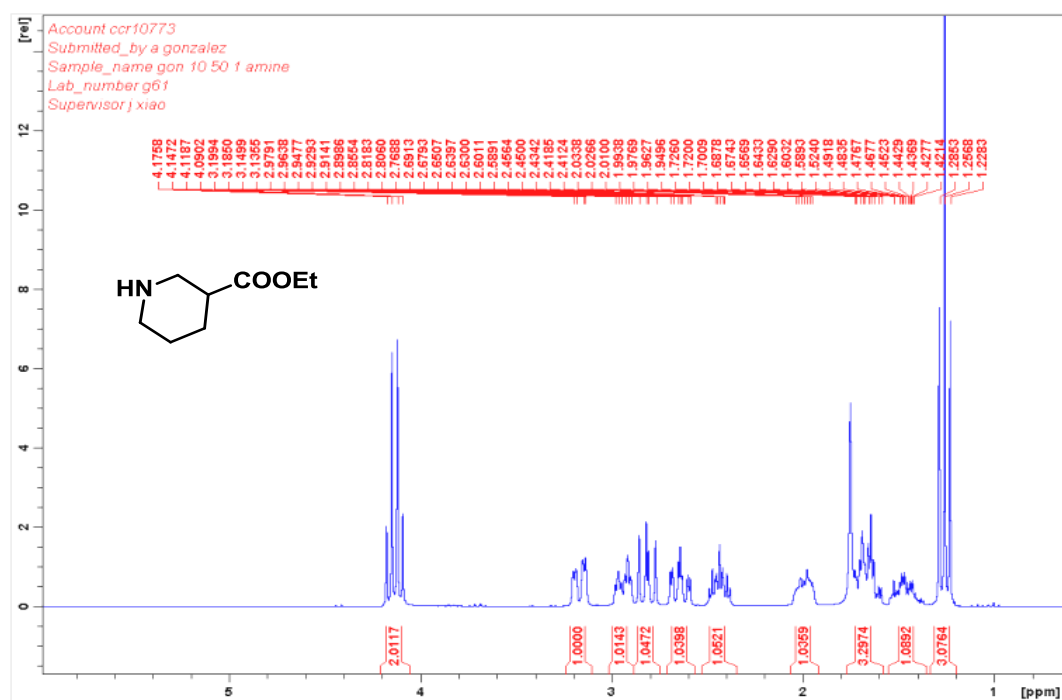
**2-(3,4-Dimethoxyphenyl)ethanol**

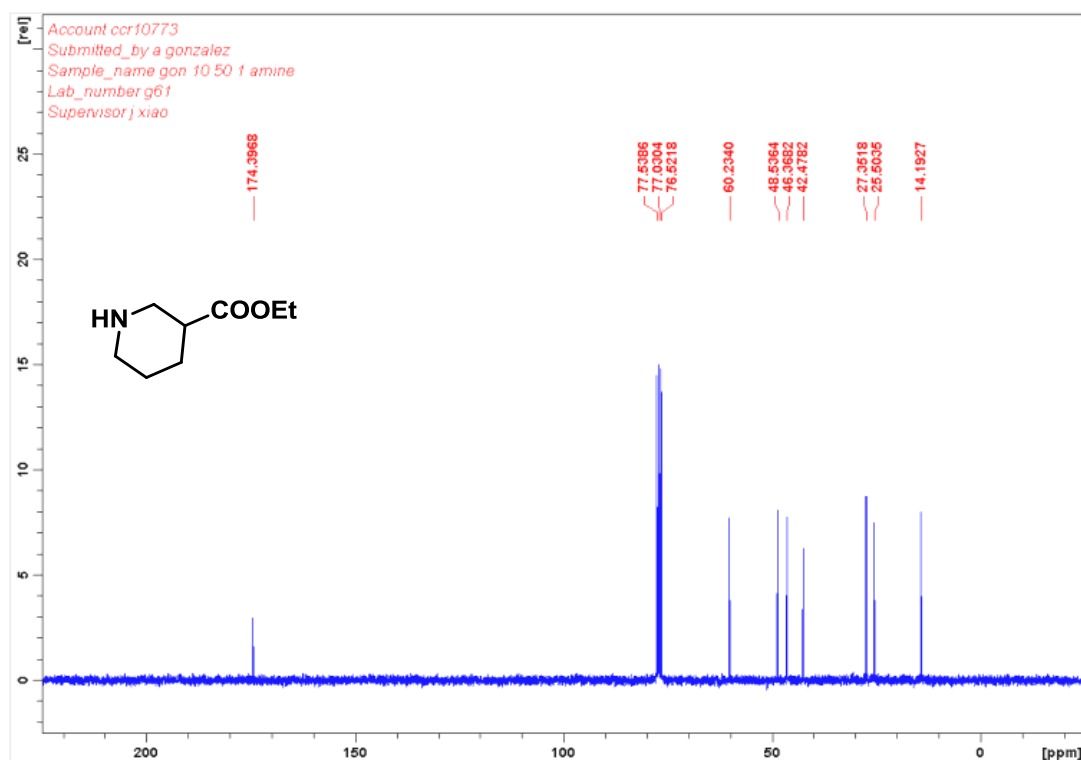
### 5.1.5. Combined Csp<sup>3</sup>-Csp<sup>2</sup> and Csp<sup>2</sup>-N cleavage: example of the decarboxylation of ethyl 1-(tetrahydrofuran-2-carbonyl)piperidine-3-carboxylate

#### Crude <sup>1</sup>H NMR



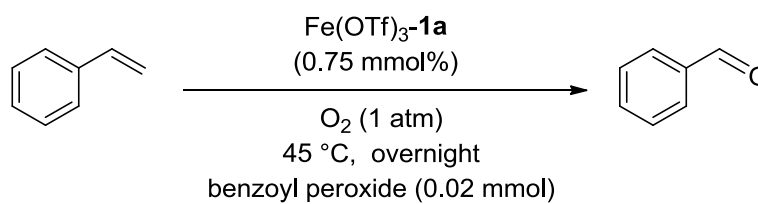
#### Isolated amine



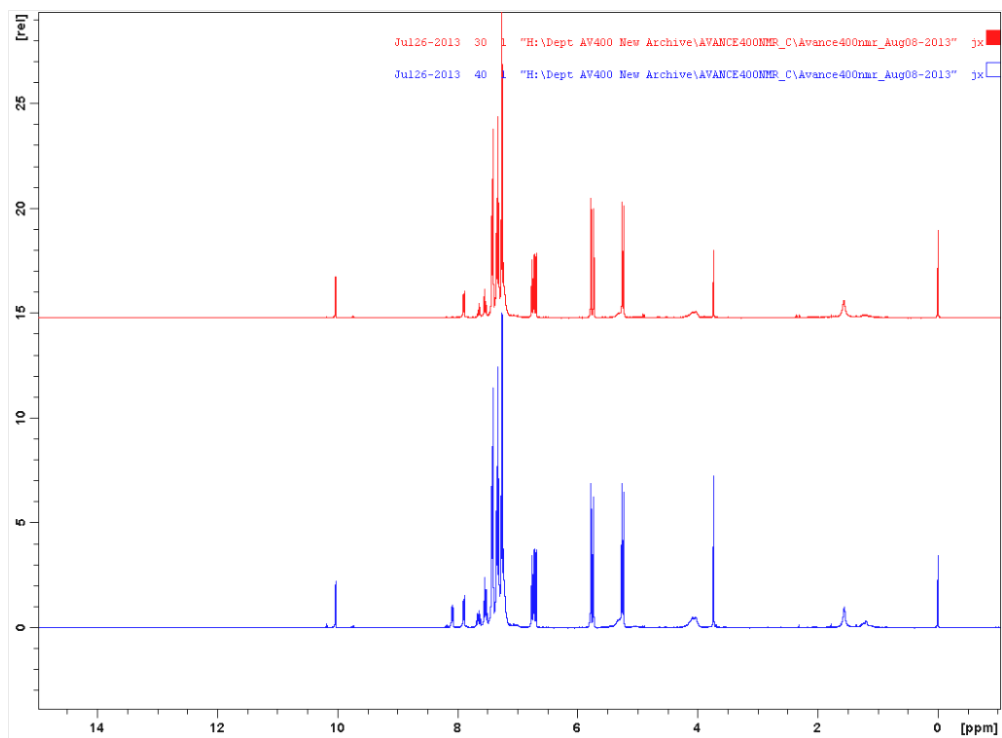


## 6. Chapter 6: additional data

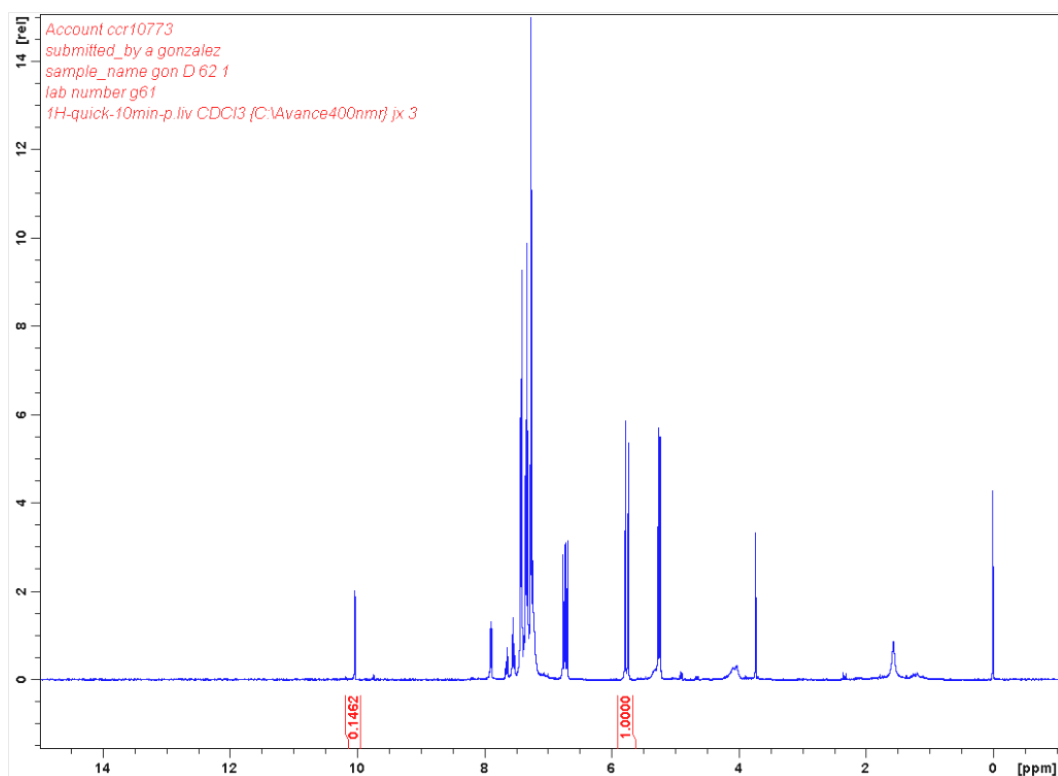
**6.1. Aerobic cleavage of styrene in the presence of a radical initiator.** Crude  $^1\text{H}$  NMR spectra of the aerobic cleavage of styrene in the presence and in the absence of the radical initiator benzoyl peroxide.



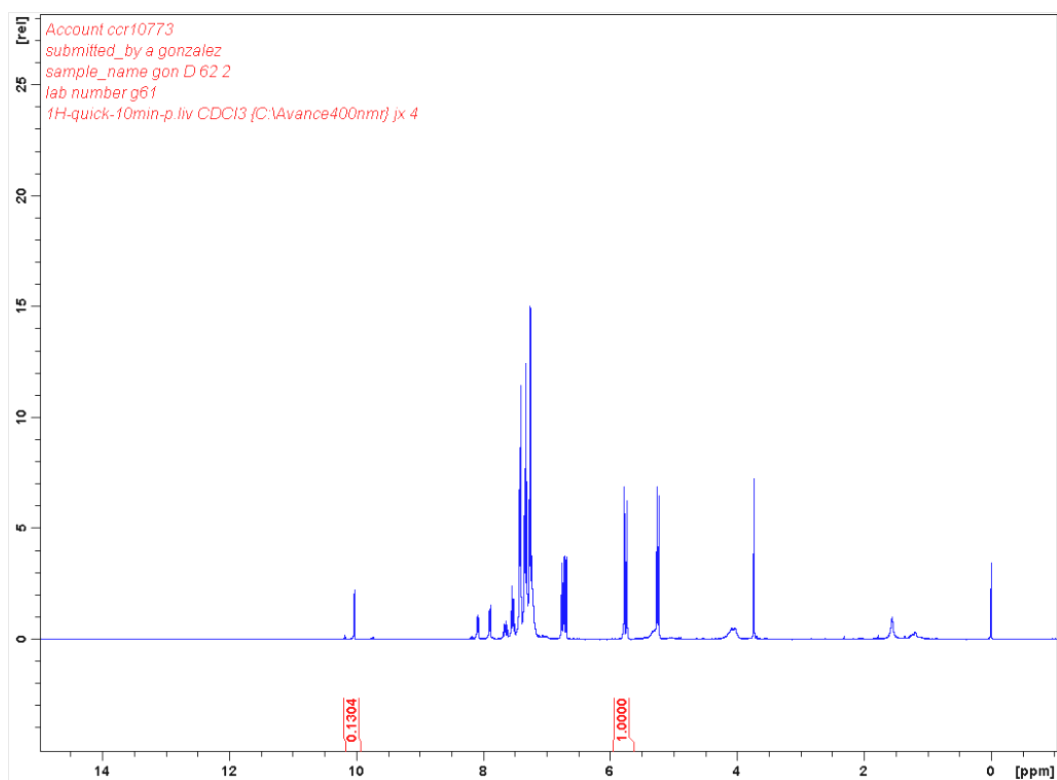
Entry	Catalyst	Benzaldehyde (% yield)
1	$\text{Fe}(\text{OTf})_3\text{L1}$ , no peroxide	13%
2	$\text{Fe}(\text{OTf})_3\text{L1}$	12%



Without initiator, enlarged spectra

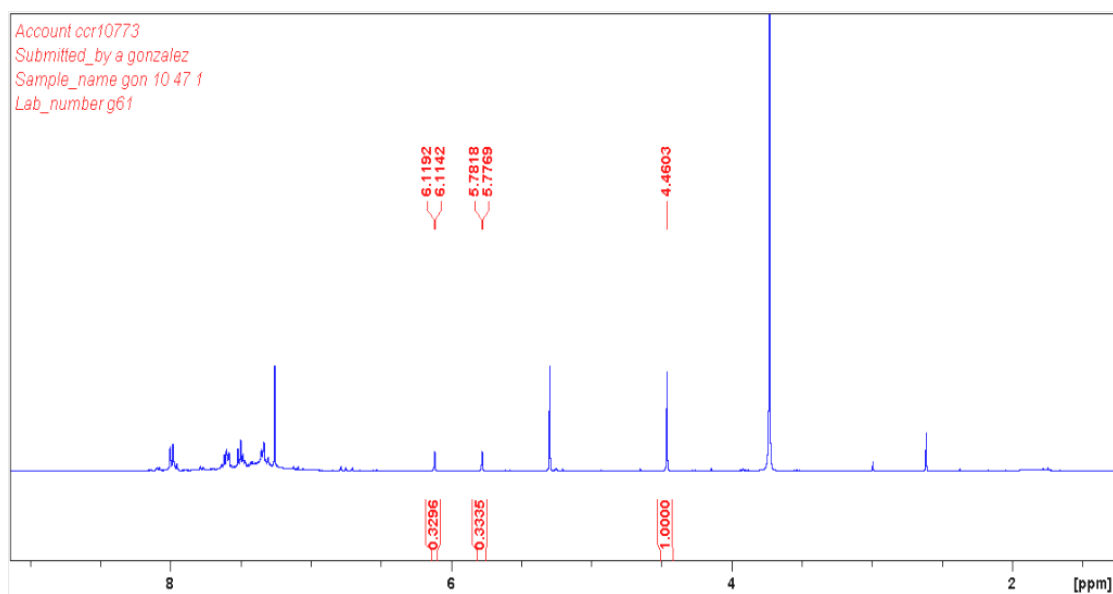


With radical initiator, enlarged spectra

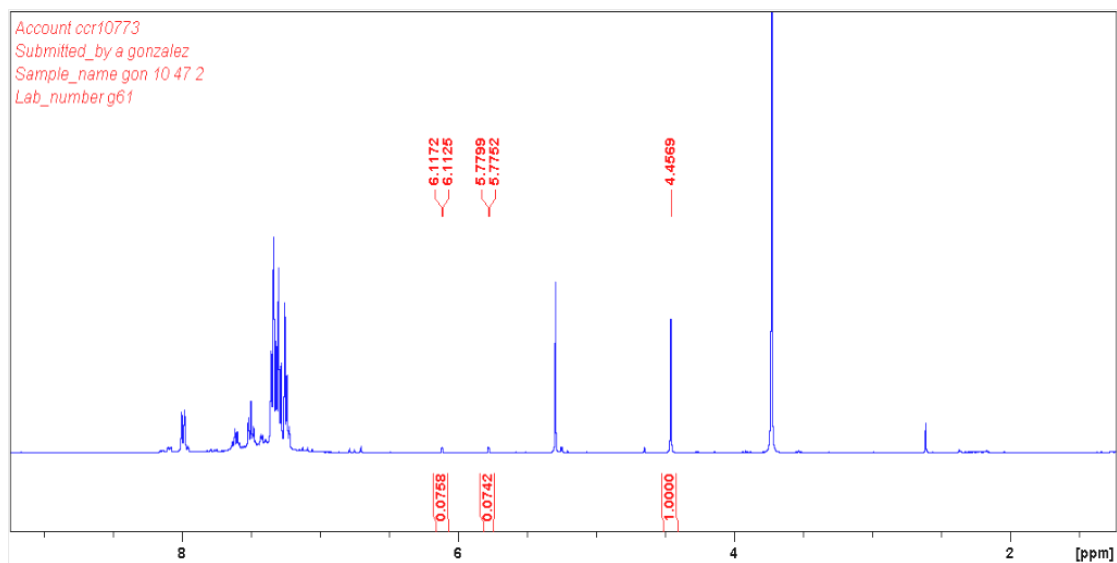


**6.2. Iron catalysed oxidation of vinyl bromide to phenacyl bromide.** Crude  $^1\text{H}$  NMR spectra of the catalytic oxidation of vinyl bromide in the presence and in the absence of diphenyl sulphide.

Crude  $^1\text{H}$  NMR of the  $\text{Fe}(\text{OTf})_3\text{-L1}$  catalysed oxygenation of 1-bromostyrene (no  $\text{Ph}_2\text{S}$ )

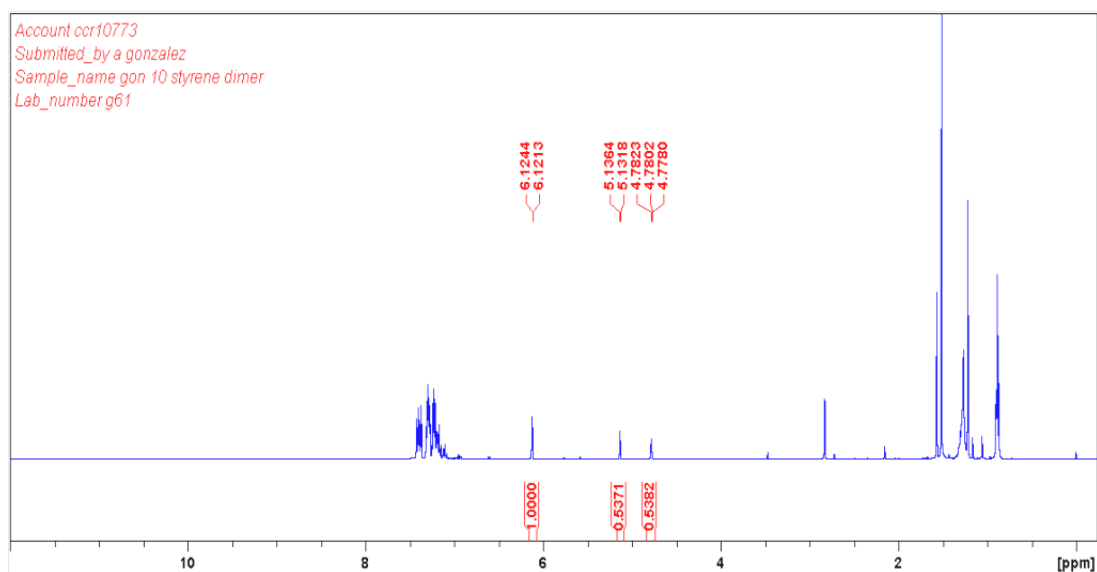


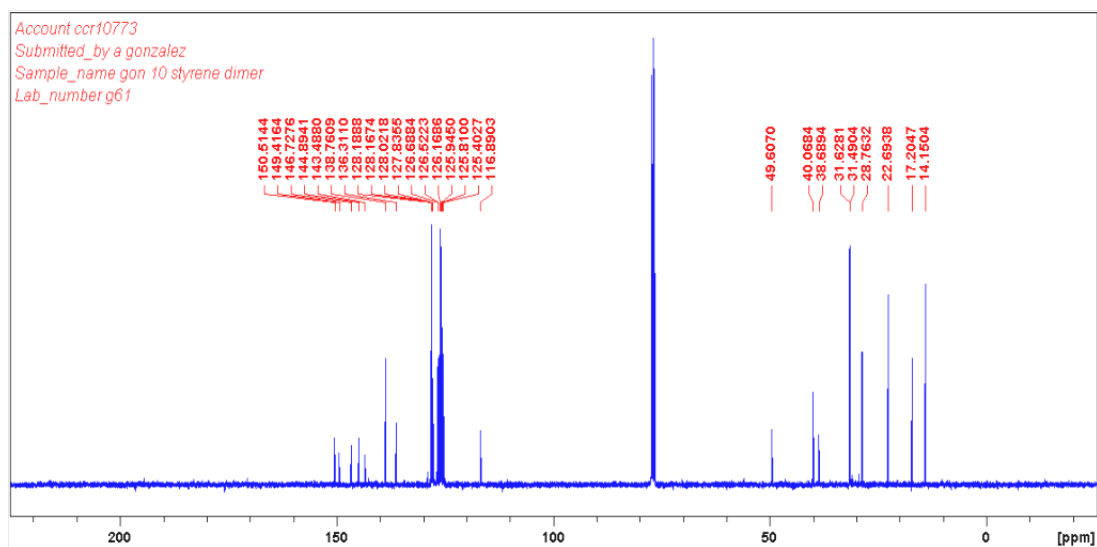
Crude  $^1\text{H}$  NMR of the  $\text{Fe}(\text{OTf})_3\text{-L1}$  catalysed oxygenation of 1-bromostyrene (with 0.5 equiv.  $\text{Ph}_2\text{S}$ )



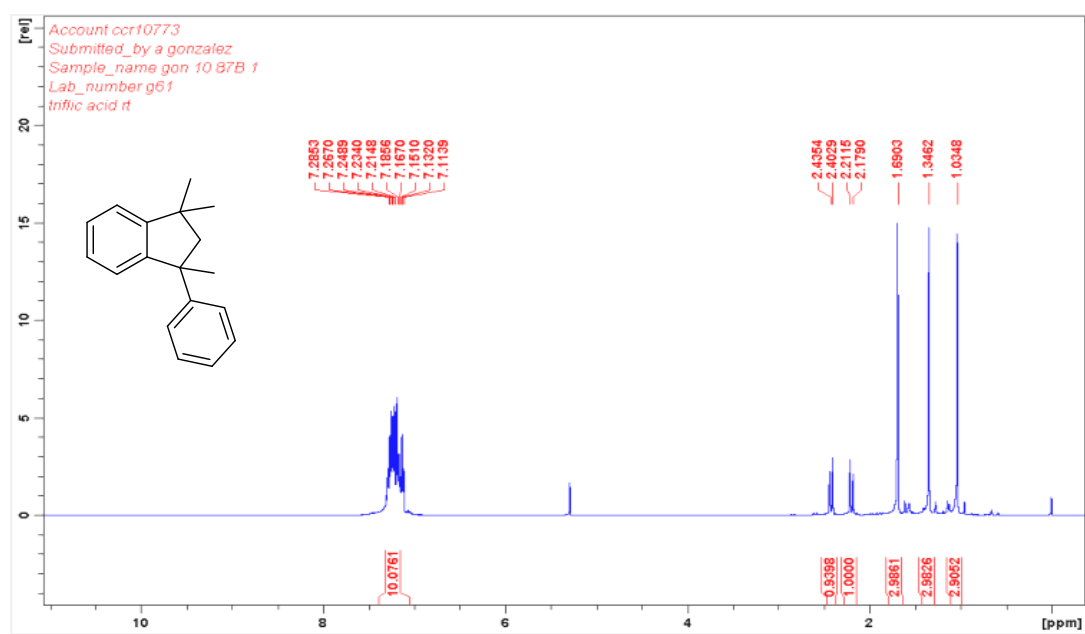
## Chapter 7: additional data

### $\alpha$ -Methylstyrene dimers under thermodynamic conditions

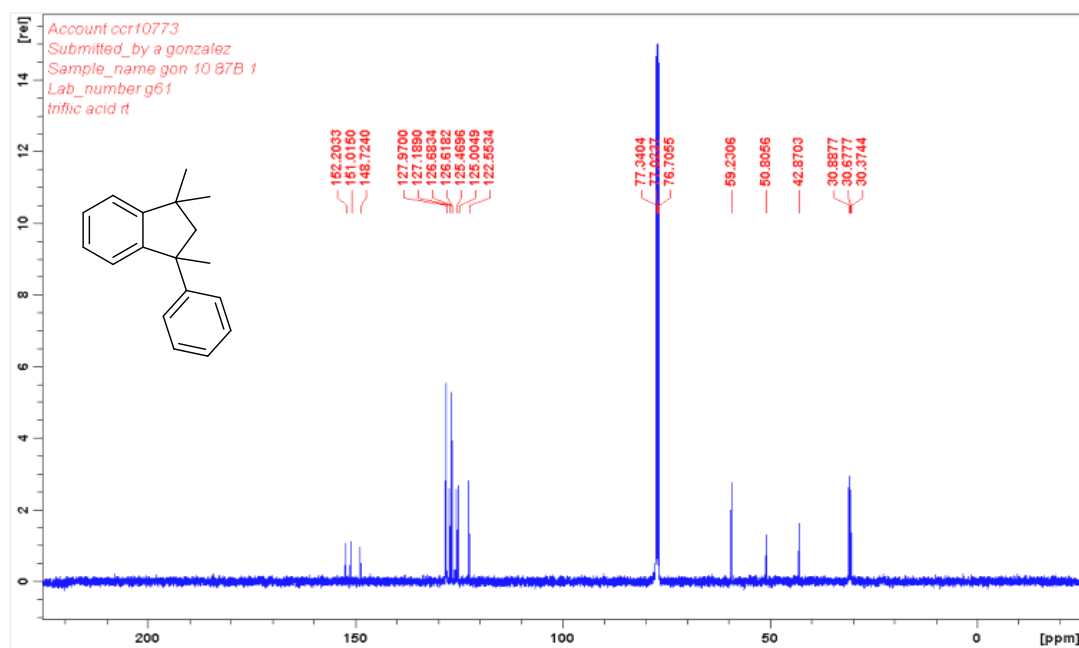




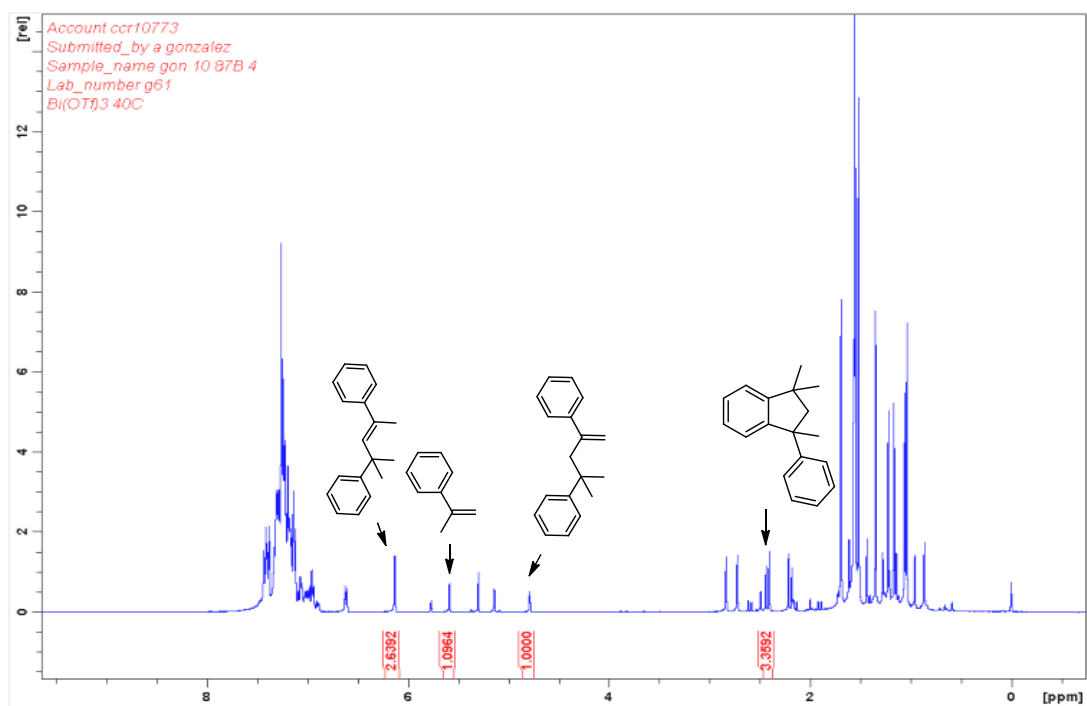
### 1,1,3-Trimethyl-3-phenyl-2,3-dihydro-1H-indene obtained using triflic acid as catalyst







### Product distribution obtained using $\text{Bi}(\text{OTf})_3$ as catalyst



**Example of a very electron rich substrate: 1-methoxy-4-(prop-1-en-2-yl)benzene dimers (integrated signals correspond to the internal olefin product)**

